EFFECTS OF ORGANIC ACIDS AND HEAVY METALS ON THE BIOMINING BACTERIUM: *ACIDITHIOBACILLUS CALDUS* STRAIN BC13

by

John Earl Aston

A dissertation submitted in partial fulfillment

of the requirements for the degree

of

Doctor of Philosophy

in

Engineering

MONTANA STATE UNIVERSITY

Bozeman, Montana

April 2010

©COPYRIGHT

by

John Earl Aston

2010

All Rights Reserved

APPROVAL

of a dissertation submitted by

John Earl Aston

This dissertation has been read by each member of the dissertation committee and has been found to be satisfactory regarding content, English usage, format, citation, bibliographic style, and consistency and is ready for submission to the Division of Graduate Education.

Dr. Brent M. Peyton

Approved for the Department of Chemical and Biological Engineering

Dr. Ron Larsen

Approved for the Division of Graduate Education

Dr. Carl A. Fox

STATEMENT OF PERMISSION TO USE

In presenting this dissertation in partial fulfillment of the requirements for a doctoral degree at Montana State University, I agree that the Library shall make it available to borrowers under rules of the Library. I further agree that copying of this dissertation is allowable only for scholarly purposes, consistent with "fair use" as prescribed in the U.S. Copyright Law. Requests for extensive copying or reproduction of this dissertation should be referred to ProQuest Information and Learning, 300 North Zeeb Road, Ann Arbor, Michigan 48106, to whom I have granted "the exclusive right to reproduce and distribute my dissertation in and from microform along with the non-exclusive right to reproduce and distribute my abstract in any format in whole or in part."

John Earl Aston

April 2010

ACKNOWLEDGEMENTS

I would like to thank my parents Earl and Barbara Aston for, among other things, keeping me alive until I turned 18, but also for teaching by example. I want to thank my Wife's parents, Jack and Becky Millstein, for raising such a wonderful daughter. Speaking of whom, I owe so much gratitude to my wife. Flower – you're basically all-round great, but in the context of graduate school, I especially appreciate your tolerance, patience, and good food … you spoil me.

There are two other people that made this dissertation possible. First, my advisor, Dr. Brent Peyton – among many, many things, you have always made time, been patient, provided honest and straight-forward advice, and taught by example. I also thank Dr. William Apel – you gave me the opportunity to work on this project, and the time I spent at the Idaho National Laboratory was invaluable, but even more so, your constant support and interest in my project was very much appreciated. I consider myself unreasonably fortunate to have the two of you as mentors.

In addition, thanks to Brady Lee for always being willing to contribute ideas and review my work. I also extend thanks to Drs. Robin Gerlach, Ross Carlson, and Abbie Richards for providing advice and assistance when sought. Drs. Matthew Fields, Brian Bothner, and Walid Maaty deserve thanks for mentoring me during IGERT rotations.

The IGERT program deserves special mention. It was a great opportunity and learning experience, namely because of the effort that went into it, so thank you to Drs. William Inskeep and Christine Foreman.

Last but not least, to those that befriended Flower and me in Bozeman … thanks!

TABLE OF CONTENTS

1. INTRODUCTION 1

Outline 1
Acidithiobacilli 3
Classification 3
Natural Habitat 4
Mineral Sulfide Oxidation 5
Applications 6
Acid-Mine Drainage 6
Biomining 7
Acidithiobacillus Caldus 8
Importance of *Acidithiobacillus Caldus* in Acid-Mine Drainage and Biomining 8
Previous Work 8
Scope of Present Work 9
References 11

2. TOXICITY OF SELECT ORGANIC ACIDS TO THE SLIGHTLY THERMOPHILIC ACIDOPHILE, *ACIDITHIOBACILLUS CALDUS* STRAIN BC13 17

Abstract 17
Introduction 17
Materials and Methods 19
Microorganism, Media, and Growth Conditions 19
Determination of Organic Acid Toxicity 20
Organic Acid Analysis 21
PLFA Analysis 21
Cell Imaging 22
Statistical Analyses 23
Results 23
Organic Acid Toxicity 23
Changes to Organic Acid Concentrations 28
PLFA Analysis and Cell Imaging 29
Discussion 31
Organic Acid Toxicity 31
Changing Organic Acid Concentrations 33
PLFA Analysis and Cell Imaging 34
Conclusions 35
References 36

TABLE OF CONTENTS - CONTINUED

3. GROWTH EFFECTS AND ASSIMILATION OF ORGANIC ACIDS IN CHEMOSTAT AND BATCH CULTURES OF *ACIDITHIOBACILLUS CALDUS* STRAIN BC13 39

Abstract 39
Introduction 40
Materials and Methods 41
Microorganism, Media, and Growth Conditions 41
Chemostat Culturing 42
Organic Acid Measurement 43
Dissolved Oxygen and Inorganic Carbon Measurement 44
Dry-Cell Weight and Carbon Composition Measurements 44
Batch Growth with Pyruvate as the Sole Carbon Source 45
Growth Effects of Organic Acids in Batch Cultures 45
16S rRNA Culture Analysis 46
Statistical Analysis 46
Results 47
Test for Heterotrophic Growth 47
Test for Mixotrophic Growth 47
Batch Growth with Pyruvate as the Sole Carbon Source 50
Toxicity of Organic Acids in Batch Cultures 50
Discussion 53
Conclusions 56
References 57

4. LEAD, ZINC, AND COPPER TOXICITY TO *ACIDITHIOBACILLUS CALDUS* STRAIN BC13 60

Abstract 60
Introduction 61
Materials and Methods 62
Microorganism, Media, and Growth Conditions 62
Determining Single Metal Toxicity 63
Determining Combined Metal Toxicity 63
Determining Effects of Previous Metal Exposure 64
Determining Metal Chloride Toxicity 65
Modeling Metal Complexation and Precipitation 65
Results 66

TABLE OF CONTENTS - CONTINUED

Single Metal Toxicity 66
Combined Metal Toxicity 67
Effects of Ferrous Iron on Metal Toxicity 69
Effect of Previous Exposure on Metal Toxicity 70
Comparison of Metal Chloride and Metal Sulfate Toxicity 72
Metal Complexation and Precipitation 74
Discussion 75
Single Toxicity of Lead, Zinc, and Copper 75
Comparisons with Other Acidithiobacilli 76
Effects of Combined Metals 76
Effects of Inoculum History 77
Metal Chloride versus Metal Sulfate Toxicity 78
Conclusions 79
References 80

5. EFFECTS OF CELL CONDITION, PH, AND TEMPERATURE ON LEAD, ZINC, AND COPPER SORPTION TO *ACIDITHIOBACILLUS CALDUS* STRAIN BC13 84

Abstract 84
Introduction 85
Materials and Methods 86
Culture and Cell Preparation 86
Measurement of Aqueous Metal Concentrations 87
Calculation of Sorption Parameters 88
Calculation of the Heat of Sorption 89
Desorption Experiments 89
Mixed Metal Sorption 90
Modeling Metal Speciation 90
Statistical Analysis and Controls 91
Results 91
Effect of pH on Lead, Zinc, and Copper Sorption 91
Temperature Effects 96
Desorption Experiments 96
Mixed Metal Sorption 98
Discussion 100
Sorption of Lead, Zinc, and Copper to BC13 100
Temperature Effects 103
Mixed Metal Sorption 103
Comparisons to Previous Work with Acidithiobacilli 104

TABLE OF CONTENTS – CONTINUED

Conclusions 105
References 107

6. EFFECTS OF ORGANIC ACIDS AND METALS ON PROTEIN EXPRESSION OF *ACIDITHIOBACILLUS CALDUS* STRAIN BC13 110

Abstract 110
Introduction 111
Materials and Methods 112
Microorganism, Media, and Growth Conditions 112
MALDI Analysis 113
Determining the Toxicity of Metals in Spent Medium 114
One-Dimensional Gel Analysis 114
Protein Identification 115
Two-Dimensional Gel Analysis 115
Results 117
MALDI Analysis 117
Gel Analysis 119
Discussion 122
Conclusions 124
References 125

7. SUMMARY 127

Conclusions 127
Future Work 129
References 133

APPENDICES 135

APPENDIX A: Ability of *Acidithiobacillus Caldus* Strain BC13 to Grow Using Various Electron Donor/Acceptor Pairs 136
APPENDIX B: Precipitation of Covellite in the Growth Medium of *Acidithiobacillus Caldus* Strain BC13 149
APPENDIX C: Components of Growth Medium Rates 162
APPENDIX D: Calculating Specific Growth 164
APPENDIX E: Chapter 2 Raw Data 168
APPENDIX F: Chapter 3 Raw Data 226
APPENDIX G: Chapter 4 Raw Data 309

TABLE OF CONTENTS – CONTINUED

APPENDIX H: Chapter 5 Raw Data 408
APPENDIX I: Chapter 6 Raw Data 459
APPENDIX J: Protocols for Protein Separation and Analyses 467
APPENDIX K: 16S Sequence of the Strain Used in Experiments 475

LIST OF TABLES

Table Page

1. PLFA Analysis of BC13 Grown in the Presence of Organic Acids 30

2. Percent of Organic Acids Protonated at the Medium pH 31

3. Percent of Pyruvate Consumed and Converted to Biomass by BC13 50

4. Toxicity of Lead, Zinc, and Copper to BC13 67

5. The Heat of Sorption for Lead, Zinc, and Copper 98

6. Percent of Lead, Zinc, or Copper that Desorbed from BC13 Cells in a 5 mM Nitriloacetic Acid Wash at Equilibrium 99

7. Effects of Organic Acids and Heavy Metals on Protein Expression by BC13 117

LIST OF FIGURES

Figure Page

1. Typical Effect of Various Organic Acid Concentrations on the Growth of BC13 24
2. Effect of Organic Acids on the Specific Growth Rate of BC13 25
3. Acid Strength Plotted versus the Calculated IC_{50}s 26
4. Combined Toxicity of Organic Acids 27
5. Changes in Organic Acid Concentrations during Batch Cultures 28
6. Field Emission Scanning Electron Micrographs of BC13 Cells Exposed to Organic Acids 30
7. Growth of BC13 in a Chemostat Culture under Mixotrophic Conditions 48
8. Oxygen Consumption by BC13 in a Chemostat Reactor under Mixotrophic Conditions 49
9. BC13 Growth Using Pyruvate as the Sole Carbon Source 51
10. Effect of Previous Exposure on the Specific Growth Rate of BC13 52
11. Single Toxicity of Lead, Zinc, and Copper to BC13 66
12. Combined Toxicity of Lead, Zinc, and Copper to BC13 68
13. Effect of Ferrous Iron on the Toxicity of Lead, Zinc, and Copper to BC13 69
14. Effect of Previous Exposure on Metal Toxicity to BC13 71
15. Growth of BC13 Cells Following Exposure to Minimal Inhibitory Concentrations of Lead, Zinc, and Copper 72
16. Comparison of Metal Sulfate and Metal Chloride Toxicity toBC13 73
17. Additive Effects of Metal and Chloride Toxicities 74

LIST OF FIGURES - CONTINUED

Figure Page

18. Lead, Zinc, and Copper Sorption to BC13 92
19. Lineweaver-Burk Plot used to Calculate Sorption Parameters 92
20. Effect of pH on Lead, Zinc, and Copper Sorption to BC13 93
21. Relationship Between pH, Metal Complexation, and Sorption 94
22. Relationship Between pH and Metal Complexation 95
23. Effect of Temperature on Lead, Zinc, and Copper Sorption to BC13 97
24. Mixed Metal Sorption to BC13 100
25. Toxicity of Spent Metal Media 118
26. One-Dimensional Gel of Peripheral Membrane Proteins from Pyruvate Treated Cells 119
27. One-Dimensional Gel of Integral Membrane Proteins from Pyruvate, Lead, Zinc, or Copper Treated Cells 120
28. Two-Dimensional Gel of Soluble Proteins from BC13 121

ABSTRACT

Acidithiobacillus caldus is an important microorganism to biomining and acid-mine formation. However, its degree of characterization is not commensurate to its significance in such systems. Specifically, studies enumerating effects of organic acids and metals on this microorganism are limited. The work presented in this dissertation improves understanding of *At. caldus* with respect to interactions with these compounds. All experiments discussed in this dissertation used *At. caldus* strain BC13.

The organic acids; pyruvate, acetate, 2-ketoglutarate, succinate, fumarate, malate, and oxaloacetate were each toxic to *At. caldus* strain BC13. Depending on the organic acid tested, concentrations between 250 and 5,000 μM completely inhibited the growth of *At. caldus* strain BC13 (chapter two). Subsequent experiments, reported in chapter three, showed that *At. caldus* strain BC13 used pyruvate as a sole carbon source. Chapter four discusses the toxicities of the heavy metals; lead, zinc, and copper to *At. caldus* strain BC13. Lead was by far the most toxic metal tested, with an observed minimum inhibitory concentration of 7.5 mM. Conversely, zinc and copper had minimum inhibitory concentrations of 75 and 250 mM, respectively. The sorption of lead, zinc, and copper was also studied, and is discussed in chapter 5. Between pH 5.5 and 7.0, zinc and copper sorbed to *At. caldus* strain BC13 with similar capacity and affinity as that observed to other acidithiobacilli, however at pH 2.0, significant sorption of zinc and copper to viable cells was observed, whereas previous work did not report sorption of zinc or copper to viable acidithiobacilli cells below pH 3.0. Chapter six reports efforts to qualify changes in protein expression of *At. caldus* strain BC13 when exposed to organic acids or heavy metals. Matrix assisted laser desorption ionization mass spectrometry and one-dimensional gel electrophoresis qualified the up-regulation of an integral membrane protein with a molecular weight of approximately 25 kDa. Efforts to identify up-regulated proteins were not successful, but any proteins that are regulated in response to organic acids or heavy metals in biomining microorganisms would likely be of commercial application.

CHAPTER ONE

INTRODUCTION

Outline

The goal of this dissertation is to further characterize the interactions of organic acids and metals with the biomining bacterium, *Acidithiobacillus caldus*. This work constitutes an important contribution towards understanding this microorganism and its role in microbial communities.

Previous work has suggested that *At. caldus* is important in acid-mine systems, however it is not as well understood as similar microorganisms, even though *At. caldus* may represent a dominant metabolic guild in certain systems. To that end, the experiments reported in this dissertation, using *At. caldus* strain BC13, help to fill gaps in understanding this bacterium, and lay the groundwork for future research with *At. caldus* (from this point on "BC13" will refer specifically to *At. caldus* strain BC13). Chapters two through five summarize journal articles that were submitted for publication. Chapter two discusses the effects of the organic acids pyruvate, acetate, 2-ketoglutarate, succinate, fumarate, malate, and oxaloacetate on the growth of BC13 under batch conditions. Chapter three investigates the ability of BC13 to assimilate these organic acids under both heterotrophic and mixotrophic conditions in a chemostat. In addition, the ability of this bacterium to use pyruvate as a sole carbon source under batch conditions was investigated. Also, the ability of BC13 to adapt to organic acids through subsequent culturing is discussed. Chapter four reports the effects of lead, zinc, and

copper on BC13 growth, including single and combined toxicity studies, as well as a report on the effects of ferrous iron on metal toxicity to BC13. As in chapter three, the effects of subsequent culturing are discussed. Chapter five reports the ability of *At. caldus* to sorb lead, zinc, and copper, examining the effects of cell condition, pH, and temperature. Chapter six builds on the observations made in chapters two through five, and discusses the effect of both organic acids and heavy metals on the expression of proteins by BC13. Because this bacterium has commercial applications, as discussed below, any proteins that can be up-regulated to improve its metabolic activity are of special significance. Finally, the findings and significance of chapters two through six are summarized in chapter seven.

Additional experiments that were not central to the topic of this dissertation are included in the Appendices. Appendix A discusses attempts to culture BC13 anaerobically; and Appendix B discusses the potential biogenically catalyzed precipitation of covellite in the presence of BC13. Each chapter contains an introduction, materials and methods, results, and discussion section relevant to the work discussed. However, to provide better context for the work in this dissertation, the remainder of this chapter introduces topics relevant to *At. caldus*, including a description of the acidithiobacilli genus, natural occurrence, a description of industrial and environmental processes relevant to *At. caldus*, and a description of previous studies on *At. caldus*.

Acidithiobacilli

Classification

The genus acidithiobacilli falls under the γ-proteobacteria class and currently contains four named species: *Acidithiobacillus albertensis* [1], *Acidithiobacillus caldus* [2], *Acidithiobacillus ferrooxidans* [3], and *Acidithiobacillus thiooxidans* [4]. In addition, a fifth species has been proposed, *Acidithiobacillus cuprithermicus*, although its 16S phylogeny is very similar to *At. caldus* [5]. The genus was formed when the former *Thiobacillus* genus was split into the genera *Acidithiobacillus*, *Alothiobacillus* and *Thermithiobacillus*, based on 16S rRNA gene sequencing [6]. The members of the genus are acidophilic, motile, gram-negative rods. *At. albertensis*, *At. ferrooxidans*, and *At. thiooxidans* are mesophilic microorganisms, however *At. caldus* and *At. cuprithermicus* are slightly thermophilic, growing best between 40 and 50°C [2,5]. All of the acidithiobacilli are chemolithotrophic autotrophs that can fix carbon dioxide as a carbon source, and use inorganic compounds as electron donors. Each is capable of oxidizing reduced sulfur compounds [1-5], and in addition, *At. ferrooxidans* can oxidize ferrous iron [3]. *At. ferrooxidans* and *At. thiooxidans* are by far the most studied and best characterized of the acidithiobacilli, particularly *At. ferrooxidans*, which is represented by a number of well characterized strains [7-10]. There is very little work characterizing *At. albertensis* and the potentially new species, *At. cuprithermicus*. The subject of this dissertation is *At. caldus*, which was first characterized by Hallberg and Lindstrom in 1994 [2]. There have been several strains identified, including the type strain, KU, and others [11-15], and although there are serotype variations within these strains [16], there

have not been significant differences identified in the physiology and metabolism from strain to strain.

Natural Habitat

The ability of acidithiobacilli to use various reduced inorganic sulfur compounds or ferrous iron as an electron donor, coupled to their acidophilic properties, make them important organisms in metal sulfide deposits world-wide, associated waste waters, and locally acidic marine environments [17-19]. Only *At. ferrooxidans* has been observed to use a terminal electron acceptor other than oxygen, as it is capable of reducing elemental sulfur and ferric iron [3]. This may relegate *At. thiooxidans*, *At. caldus*, *At. albertensis*, and *At. cuprithermicus* to aerobic environments, and may limit their activity in sub-surface and deep-ore systems.

The ability of this genus to fix carbon dioxide as a sole carbon source allows them to thrive in environments where organic carbon is limited. In fact, the presence of low-molecular weight organic acids has been observed to decrease the catabolic behavior of chemolithotrophic autotrophs in biomining environments [20-24], and a review by Matin documents the toxicity of these compounds to the acidithiobacilli [25]. However, *At. ferrooxidans* and *At. caldus* are capable of mixotrophic growth, providing them with a mechanism to degrade organic carbon [2,26]. This is especially significant as heterotrophic and mixotrophic activity has been reported to increase mineral leaching kinetics in biomining applications [27-31].

Mineral Sulfide Oxidation

Acidithiobacilli are believed to facilitate metal solubilization from mineral sulfides by contributing to mineral oxidation [32-34], for which a direct and an indirect mechanism have been proposed [35,36]. The indirect mechanism suggests that the mineral is oxidized by ferric iron or protons. Subsequently, the ferric iron is reduced to ferrous iron, and the proton is reduced to water or molecular hydrogen. Iron oxidizers, such as *At. ferrooxidans* catalyze oxidation of the mineral surface by replenishing ferric iron; and sulfur oxidizers, such as *At. caldus* catalyze the production of protons by producing sulfuric acid during the oxidation of reduced sulfur compounds [34]. In addition, it has been hypothesized that sulfur oxidizers play an important secondary role by oxidizing solid-sulfur layers from the mineral surface by oxidizing them to soluble sulfur compounds, such as tetrathionate and sulfate [34], making the mineral surface available for ferric iron or proton attack.

Interestingly, Sand et al. [36] and Schippers and Sand [37] proposed a model suggesting that two types of sulfides require two different indirect leaching mechanisms. This model proposes that sulfides with valence bands derived from metal electron orbitals can be oxidized by ferric iron. Examples of such sulfides include molybdenum disulfide, pyrite, and tungstenite. However, sulfides with valence bands derived from metal and sulfur electron orbitals could be oxidized by either ferric iron or proton attack. Covellite, chalcocite, and sphalerite are examples of this type of mineral.

The direct mechanism suggests that microorganisms would oxidize minerals during direct contact, with either secreted enzymes or membrane bound electron carriers.

Applications

The primary interest in acidithiobacilli in industrial and environmental applications relates to their ability to facilitate the solubilization of metals from mineral sulfides, and their ability to produce sulfuric acid. Because of this, acidithiobacilli activity is beneficial to the extraction of valuable metals from sulfide minerals [27-31]. However, this same process contributes to acid-mine formation, which is environmentally detrimental [*i.e.* 38-43]. In addition, *At. ferrooxidans* and *At. thiooxidans* are reported to increase the rate of concrete corrosion fifteen-fold, via the formation of sulfuric acid [44,45]. However, their production of sulfuric acid has at least one medical application. A study using *At. thiooxidans*, showed that these microorganisms may be able to dissolve urinary stones *in vivo* [46].

Acid-Mine Drainage

The oxidation of reduced sulfur compounds leads to the acidification of surface and ground waters, where pH values as low as -3.6 have been observed [38]. This acidification also results in the solubilization of several environmentally harmful metals, including iron, copper, zinc, lead, chromium, and arsenic [38]. Although solubilization may occur abiotically, the presence of sulfur- and iron-oxidizing acidophiles has been observed to increase the rate of acidification over 1,000,000-fold [33].

In general, acid-mine drainage is hazardous to living organisms, as it concentrates heavy metals in an acidic solution. Following exposure to acid-mine effects, species

diversity and abundance in marine and fresh waters decreased and remain lower for several years after remediation [47,48].

Biomining

As described earlier, the oxidation of ferrous iron and reduced sulfur compounds contributes to the leaching of metals in sulfide ores. This process is known as biomining, and although the exact percentage of metals harvested in this manner is unknown, it is believed to contribute significantly to the solubiliztion of economically important metals such as iron, zinc, copper, and gold [49]. This process occurs at many different scales, from incidental (dump-leaching) to highly designed (reactor-leaching) [34]. Typically, dump-leaching is applied to large ore heaps, with undefined and highly variable spatial and temporal properties (*i.e.* temperature, nutrient availability, and pH) [34]. These systems typically contain diverse biotic activity of a complexity too difficult to characterize completely. However, it may be possible to use dominant microorganisms of specific functional guilds to approximate metabolisms important to the system [50]. Efforts to optimize microbial activity in these systems are often limited to general aeration and nutrient inoculation [34]. Conversely, precious metals, such as gold, may be leached in specifically designed reactors using more controlled processes designed to maximize the efficiency of a relatively small, defined microbial community [34].

Acidithiobacillus Caldus

Importance of *Acidithiobacillus Caldus* in Acid-Mine Drainage and Biomining

The harsh conditions found in acid-mine environments limit the diversity of microorganisms that are found in these environments [34]. Studies have enumerated the importance of two genera in particular; the leptospirulii and the acidithiobacilli. Within the acidithiobacilli, *At. caldus*, *At. albertensis*, and *At. curprithermicus* are the least characterized. However; previous work has suggested that *At. caldus* may significantly improve mineral leaching rates when added to microbial cultures already containing iron- and sulfur-oxidizers [27-31]. The incomplete understanding, and potential significance, of this bacterium make it an ideal candidate for further research. In addition, the ability of *At. caldus* to grow at warm temperatures (up to 50°C) make it even more important, as it is a dominant sulfur-oxidizer in many high-temperature ore heaps and reactors [34].

Previous Work

At. caldus was isolated and characterized by Hallberg and Lindstrom in 1994 [2]. The initial characterization, using strain KU, identified *At. caldus* as a chemolithotrophic autotroph capable of oxidizing reduced-sulfur compounds and growing mixotrophically on sulfur or tetrathionate and yeast extract or glucose under aerobic conditions [2]. *At. caldus* was also characterized as a moderately thermophilic acidophile growing at temperatures between 32-50°C (45°C optimum) and from pH 1-4 (2.5 optimum) [2]. Since its initial characterization, *At. caldus* has been isolated from a variety of locations, from natural geothermal springs to bioleaching process systems in Africa [51-54].

Studies of *At. caldus* suggest that it contributes significantly to the biomining of metal sulfides. Its role in arsenopyrite bioleaching was investigated by Dopson and Lindstrom [27], who proposed that *At. caldus* plays three beneficial roles in the process: 1) removal of inhibitory sulfur layers from the mineral surface, 2) facilitation of heterotrophic and /or mixotrophic growth within the microbial community through the release of organic metabolites, and 3) solubilization of solid sulfur via the production of surface wetting agents. Edwards [28] and McGuire [30] observed that *At. caldus* decreased inhibitory sulfur layers on sulfide minerals by over 99%, and increased leaching of arsenopyrite ten-fold when compared to experiments carried out without *At. caldus*. Dopson et al. [55] observed resistance to arsenate, arsenite, and antimony via an inducible, chromosomally encoded resistance mechanism that induced active transport of arsenate and arsenite across the cell membrane against a concentration gradient.

Recently, the genome of *At. caldus* was annotated with a focus on metabolism related genes [56]. Genes consistent with the Calvin-Benson carbon dioxide fixation pathway, an incomplete tricarboxylic acid cycle (lacking 2-ketoglutarate dehydrogenase), hydrogen oxidation, sulfur oxidation (SOX pathway), and iron uptake were identified. Sulfur reduction, ferrous iron oxidation, and nitrogen fixation genes were not identified.

Scope of Present Study

Organic compounds and metals have significant effects on biotic activity in acid-mine environments [20-24,57-60]. Therefore it is surprising that studies examining the interactions of *At. caldus* and organic acids have not been reported, in addition, interactions between *At. caldus* and metals have been largely limited to the metalloid

arsenic [55]. The goal of this dissertation is to elucidate these interactions to increase understanding of the role and potential of *At. caldus* in biomining and remediation applications.

References

1. Bryant, RD, McGroarty KM, Costerton JW, Laishley EJ (1983) Isolation and characterization of a new acidophilic *Thiobacillus* acidophile (*T. albertis*). *Can J Microbiol* 29:1159-1170.

2. Hallberg KB, Lindstrom EB (1994) Characterization of *Thiobacillus caldus* sp. Nov., a moderately thermophilic acidophile. *Microbiology* 140:3451-3456.

3. Temple KL, Colmer AR (1951) The autotrophic oxidation of iron by an new bacterium, *Thiobacillus ferrooxidans*. *J Bacteriol* 62:605-611.

4. Waksman SA, Joffe JS (1922) Microorganisms concerned in the oxidation of sulfur in the soil II. *Thiobacillus thiooxidans*, a new sulfuroxidizing organism isolated from the soil. *J Bacteriol* 7:239-256.

5. Ann Louw L (2009) Analysis of an 18kb accessory region of plasmid pTcM1 from *Acidithiobacillus caldus* MNG. *Stellenbosch Univ*.

6. Kelly DP, Wood AP (2000) Reclassification of some species of *Thiobacillus* to the newly designated genera *Acidithiobacillus* gen. nov., *Halothiobacillus*, gen. nov. and *Thermithiobacillus* gen. nov. *International Journal of Systematic Evolution and Microbiology* 50:511-516.

7. Iwahori K, Kammura K, Sugio T (1998) Isolation and some properties of cytochrome *c* oxidase purified from a bisulfite ion resistant *Thiobacillus ferrooxidans*. *Biosci, Biotechnol, and Biochem* 62:1081-1086.

8. Sugio T, Fujioka A, Tsuchiya M, Shibusawa N, Iwahori K, Kamimura K (1998) Isolation and some properties of a strain of the iron-oxidizing bacterium *Thiobacillus ferrooxidans* resistant to 2,4-dinitrophenol. *J Ferm Bioeng*

9. Sugio T, Kougami T, Tano T, Imai K (1982) Glutathione transport system in *Thiobacillus ferrooxidans* strain AP-44. *Agricul Biolog Chem* 46:2919-2924.

10. Bengrine A, Guiliani N, Appia Ayme C, Jedlicki E, Holmes DS, Chippaux M, Bonnefoy V (1998) Sequence and expression of the rusticyanin structural gene from *Thiobacillus ferrooxidans* ATCC33020 strain. *Biochem Biophys Acta* 1443:99-112.

11. Groot P, Deane SM, Rawlings DE (2003) A transposon-located arsenic resistance mechanism from a strain of *Acidithiobacillus caldus* isolated from commercial, arsenopyrite biooxidation tanks. *Hydrometallurgy* 71:115-123.

12. Kamimura K, Sawada R, Sugio T (2002) Mechanism of oxidation of reduced sulfur compounds by sulfur-grown *Acidithiobacillus caldus* strain GO-1. *Okayama Univ* 91:23-29.

13. Nan DJ, Lin ZR, Jian K, Gui ZC, Ling WX, Zhou QG (2008) Identification and cadmium (II) resistance of strain YN12, *Acidithiobacillus caldus*. *Chinese J Nonferrous Met* 18:342-348.

14. Tuffin M, Groot P, Deane SM, Rawlings DE (2004) Multiple sets of arsenic resistance genes are present within the highly arsenic-resistant industrial strains of the biomining bacterium, *Acidithiobacillus caldus*. *Comp Physiol Biochem* 1275:165-172.

15. Van Zyl LJ, Deane SM, Louw LA, Rawlings DE (2008) Presence of a family of plasmids (29 to 65 kilobases) with a 26-kilobase common region in different strains of the sulfur-oxidizing bacterium *Acidithiobacillus caldus*. *Appl Enviorn Microbiol* 74:4300-4308.

16. Hallberg KB, Lindstrom EB (1996) Multiple serotypes of the moderate thermophile *Thiobacillus caldus*, a limitation of immunological assays for biomining microorganisms. *Appl Environ Microbiol* 62:4243-4246.

17. Karavaiko GI, Turova TP, Kondrat'eva TF, Lysenko AM, Kolganova TV, Ageeva SN, Muntyan LN, Pivovarova TA (2003) Phylogenetic heterogeneity of the species *Acidithiobacillus ferrooxidans*. *Int J Syst Evol Microbiol* 53:113-119.

18. Gonzalez-Toril E, Llobet-Brossa E, Casamayor EO, Amann R, Amils R (2003) Microbial ecology of an extreme acidic environment, the Tinto River. *Appl Environ Microbiol* 69:4853-4865.

19. Kamimura K, Higashino E, Moriya S, Sugio T (2003) Marine acidophilic sulfur-oxidizing bacterium requiring salts for the oxidation of reduced inorganic sulfur compounds. *Extremophiles* 7:95-99.

20. Burckhard SR, Schwab AP, Banks MK (1995) The effects of organic acids on the leaching of heavy metals from mine tailings. J Hazard Mat 41:135-145.

21. Marchland EA, Silverstein J (2003) The role of enhanced heterotrophic bacterial growth on iron oxidation by *Acidithiobacillus ferrooxidans*. *Geomicrobiol J* 20:231–244.

22. Olson GJ, Brierley JA, Brierley CL (2003) Bioleaching review. Part B: Progress in bioleaching: Applications of microbial processes by the mineral industries. *Appl Microbiol Biotechnol* 63:249–257.

23. Gu XY, Wong JWC (2004) Identification of inhibitory substances affecting bioleaching of heavy metals from anaerobically digested sewage sludge. *Eniviron Sci Technol* 38:2934-2939.

24. Gu XY, Wong JWC (2007) Degradation of inhibitory substances by heterotrophic microorganisms during bioleaching of heavy metals from anaerobically digested sewage sludge. *Chemosphere* 69:311–318.

25. Matin A (1978) Organic nutrition of chemolithotrophic bacteria. *Annu Rev Microbiol* 32:433-468.

26. Pronk JT, Mejer WM, Hazeu W, van Dijken JP, Bos P, Kuenen JG (1991) Growth of *Thiobacillus thiooxidans* on formic acid. *Appl Environ Microbiol* 57:2057-2062.

27. Dopson M, Lindstrom EB (1999) Potential role of *Thiobacillus caldus* in arsenopyrite bioleaching. *Appl Environ Microbiol* 65:36-40.

28. Edwards KJ, Bond PL, Banfield JF (2000) Characteristics of attachment and growth of *Thiobacillus caldus* on sulphide minerals: a chemotactic response to sulphur minerals? *Environ Microbiol* 2:324-332.

29. Fu B, Zhou H, Zhang R, Qiu G (2008) Bioleaching of chalcopyrite by pure and mixed cultures of *Acidithiobacillus* spp. and *Leptospirillum ferriphilum*. *Int J Biodeteriat and Biodegrad* 62:109-115.

30. McGuire MM, Edwards KJ, Banfield JF, Hamers RJ (2001) Kinetics, surface chemistry, and structural evolution of microbially mediated sulfide mineral dissolution. *Geochem Cosmochim Acta* 65:1243-1258.

31. Zhou QG, Bo F, Bo ZH, Xi L, Jian G, Fei LF, Hau CH (2007) Isolation of a strain of *Acidithiobacillus caldus* and its role in bioleaching of chalcopyrite. *World J Microbiol Biotechnol* 23:1217-1225.

32. Colmer AR, Hinkle ME (1947) The role of microorganisms in acid mine drainage: A preliminary report. *Science* 106:253-256.

33. Singer PC, Stumm W (1970) Acidic mine drainage: The rate-determining step. *Science* 167:1121-1123.

34. Rawlings DE. (2002) Heavy metal mining using microbes. *Annu Rev Microbiol* 56:65-91.

35. Silverman MP, Ehrlich HL (1964) Microbial formation and degradation of minerals. *Advan Appl Microbiol* 6:153-206.

36. Sand W, Gehrke T, Jozsa PG, Schippers A (2001) (Bio) chemistry of bacterial leaching – direct vs. indirect bioleaching. *Hydrometallurgy* 59:159-175.

37. Schippers A, Sand W (1999) Bacterial leaching of metal sulfides proceeds by two indirect mechanisms via thiosulfate or via polysulfides and sulfur. *Appl Environ Microbiol* 65:319-321.

38. Nordstrom DK, Alpers CN, Ptacek CJ, Blowes DW (2000) Negative pH and extremely acidic mine waters from Iron Mountain, California. *Environ Sci Technol* 34:254-258.

39. Canovas CR, Olias M, Nieto JM, Sarmiento AM, Ceron JC (2007) Hydrogeochemical characteristics of the Tinto and Odiel Rivers (SW Spain). Factors controlling metal contents. *Sci Total Environ* 373:363-382.

40. Lefebvre R, Hockley D, Smolensky J, Gelinas P (2001) Multiphase transfer processes in waste rock piles producing acid mine drainage 1: Conceptual model and system characterization. *J Contam Hydrol* 52:137-164.

41. Lefebvre R, Hockley D, Smolensky J, Lamontagne A (2001) Multiphase transfer processes in waste rock piles producing acid mine drainage 2: Applications of numerical stimulations. *J Contam Hydrol* 52:165-186.

42. Olias M, Nieto JM, Sarmiento AM, Ceron JC, Canovas CR (2004) Seasonal water quality variations in a river affected by acid mine drainage: the Odiel River (South West Spain). *Sci Total Environ* 333:267-281.

43. Vigneault B, Campbell PG, Tessier A, De Vitre R (2001) Geochemical changes in sulfidic mine tailings stored under a shallow water cover. *Water Res* 35:1066-1076.

44. Maeda T, Negishi A, Komoto H, Oshima Y, Kamimura K, Sugio T (1999) Isolation of iron-oxidizing bacteria from corroded concretes of sewage treatment plants. *J Biosci Bioeng* 88:300-305.

45. Sand W (1987) Importance of hydrogen sulfide, thiosulfate, and methylmercaptan for growth of thiobacilli during simulation of concrete corrosion. *Appl Environ Microbiol* 53:1645-1648.

46. Nishio S, Aoki K, Yokoyama M (2003) A new method using a bacterium for dissolution of urinary stones. *Aktuelle Urol* 34:253-255.

47. Demchak J, Skousen J, McDonald LM (2004) Longevity of acid discharges from underground mines located above the regional water table. *J Environ Qual* 33:656-668.

48. Younger PL (1997) The longevity of minewater pollution: a basis for decision-making. *Sci Total Environ* 194:457-466.

49. Rawlings DE, Johnson DB (2007) The microbiology of biomining: development and optimization of mineral-oxidizing consortia. *Microbiology* 153:315-324.

50. Taffs R, Aston JE, Brileya K, Jay Z, Klatt CG, McGlynn S, Mallette N, Montross S, Gerlach R, Inskeep WP, Ward DM, Carson RP (2009) *In silico* approaches to study mass and energy flows in microbial consortia: a syntrophic case study. *BMC Syst Biol* 3: 10.1186/1752-0509-3-114.

51. Burton NP, Norris PR (2000) Microbiology of acidic, geothermal springs of Montserrat: environmental rDNA analysis. *Extremophiles* 4:315-320.

52. Okibe N, Gericke M, Hallberg KB, Johnson DB (2003) Enumeration and characterization of acidophilic microorganisms isolated from a pilot plant-stirred tank bioleaching operation. *Appl Environ Microbiol* 69:1936-1943.

53. Simmons S, Norris PR (2002) Acidophiles of saline water at thermal vents of Vulcano, Italy. *Extremophiles* 6:201-207.

54. Kinnunen PHM, Puhakka JA (2004) Characterization of iron- and sulphide mineral-oxidizing moderately thermophilic acidophilic bacteria from an Indonesian auto-heating copper mine waste heap and a deep South African gold mine. *J Ind Microbiol Biotechnol* 31:409-414.

55. Dopson M, Lindstrom EB, Hallberg KB (2001) Chromosomally encoded arsenical resistance of the moderately thermophilic acidophile *Acidithiobacillus caldus*. *Extremophiles* 5:247-255.

56. Valdes J, Quatrini R, Hallberg K, Dopson M, Valenzuela PDT, Holmes DS (2009) Draft genome sequence of the extremely acidophilic bacterium *Acidithiobacillus caldus* ATCC 51756 reveals metabolic versatility in the genus *Acidithiobacillus*. *J Bact* 191:5877-5878.

57. Dopson M, Baker-Austin C, Koppineedi PR, Bond PL (2003) Growth in sulfidic mineral environments: metal resistance mechanisms in acidophilic micro-organisms. *Microbiology* 149:1959-1970.

58. Soon AO, Chye ES, Poh, EL (2007) Influence of heavy metal on activated sludge activity: DO and SOUR monitoring. *J Eng Res Edu* 4:20-24.

59. Sampson MI, Phillips CV (2001) Influence of base metals on the oxidizing ability of acidophilic bacteria during the oxidation of ferrous sulfate and mineral sulfide concentrates, using mesophiles and moderate thermophiles. *Min Eng* 14:317-340.

60. Nurmi P, Ozkaya B, Kaksonen AH, Tuovinen OH, Puhakka JA (2009) Inhibition kinetics of iron oxidation by *Leptospirillum ferriphilum* in the presence of ferric, nickel, and zinc ions. *Hydrometallurgy* 97:137-145.

CHAPTER TWO

TOXICITY OF SELECT ORGANIC ACIDS TO THE SLIGHTLY THERMOPHILIC ACIDOPHILE, *ACIDITHIOBACILLUS CALDUS* STRAIN BC13

Abstract

At. caldus is a thermophilic acidophile relevant to commercial biomining and acid-mine drainage. Previous work characterized *At. caldus* as a chemolithotrophic autotroph capable of oxidizing reduced sulfur compounds under aerobic conditions. This chapter reports the toxic effects of pyruvate, acetate, 2-ketoglutarate, succinate, fumarate, malate, and oxaloacetate to BC13 under batch conditions. All organic acids tested exhibited some toxic effect. Oxaloacetate was observed to completely inhibit growth at a concentration of 250 μM, whereas other organic acids were completely inhibitory at concentrations between 1,000 μM and 5,000 μM. In these experiments, the measured concentrations of organic acids decreased with time, indicating uptake, transformation, or assimilation by the cells. Phospholipid fatty acid analyses indicated an effect of organic acids on the cellular envelope. Notable differences included an increase in trans fatty acids in the presence of organic acids, indicating possible instability of the cellular envelope. This was supported by field emission scanning electron micrographs that showed sloughing in cells grown in the presence of organic acids.

Introduction

At. caldus is a thermophilic acidophile originally characterized as

Thiobacillus caldus [1], and later reclassified as an acidithiobacilli [2]. Compared to the more commonly studied *At. thiooxidans* [3] and *At. ferrooxidans* [4], relatively little is known about *At. caldus*. As with all acidithiobacilli, *At. caldus* thrives at low pH (optimum 2.0 - 3.0), however, unlike other acidithiobacilli, *At. caldus* grows well at moderately high temperatures with optimum growth at 45°C [1]. *At. caldus* is a chemolithotrophic autotroph capable of oxidizing sulfur and reduced sulfur compounds [1,5,6]. However, *At. caldus* strain KU can grow mixotrophically with sulfur or tetrathionate and either glucose or yeast extract [1].

The conditions at which *At. caldus* thrives, coupled with its ability to oxidize reduced sulfur compounds make it prevalent in acid mine systems [7,8], where it is believed to contribute to metal solubilization. Dopson and Lindstrom [9] proposed that *At. caldus* assists metal leaching by oxidizing sulfur layers from the mineral surface. They also suggested *At. caldus* releases metabolites that facilitate heterotrophic and mixotrophic growth of other community members [9]. In addition, Edwards et al. [10] and McGuire et al. [11] showed *Sulfobacillus thermosulfidooxidans* co-cultured with *At. caldus* removed more sulfur from sulfide mineral surfaces than when grown alone.

The toxicity of small organic acids to microorganisms is well documented. These effects are enhanced at low pH where the acids are highly protonated. In this neutral state, organic acids diffuse into the cytoplasm, where they dissociate and acidify the near-neutral cytoplasm [12], reducing the proton motive force. A loss of integrity in the cellular envelope of acidophilic chemolithotrophs has also been observed in the presence of organic acids [7,13].

The research presented here demonstrates the effect of several relevant organic acids on BC13. The organic acids used in the present study were: pyruvate, acetate, 2-ketoglutarate, succinate, fumarate, malate, and oxaloacetate. These organic acids were chosen because of their presence in spent *At. ferrooxidans* medium, and their toxicity to these microorganisms at low concentrations (< 50 μM) [14-16].

Materials and Methods

Microorganism, Media, and Growth Conditions

BC13 (ATCC 51757) was grown in the basal salts medium used by Hallberg and Lindstrom [1]. Nanopure water (17.4 MΩ) was added to volume and the medium was autoclaved for 15 min at 121°C and 22 psig. After the medium cooled to room temperature, 1 ml L^{-1} of a filter sterilized (0.2 μm) trace element solution [1] was added to the medium. The pH was adjusted to 2.5 using 6N sulfuric acid. Filter sterilized (0.2 μm) potassium tetrathionate was added to a final concentration of 5 mM to provide an electron donor, and ambient carbon dioxide provided a carbon source. Cells preserved at 4°C in nanopure water (17.4 MΩ), with the pH adjusted to 3.0 using 6N sulfuric acid, provided the initial inoculum. An organic acid stock solution in growth medium was prepared daily and filter sterilized (0.2 μm) into the medium to give the desired final organic acid concentration.

Cells were grown in 250-ml Erlenmeyer flasks (100 ml medium volume) fitted with foam stoppers and shaken at 150 rotations per minute (rpm) in a temperature controlled incubator at 45°C. To better replicate *in situ* conditions where microbial

metabolism may expose cells to organic acids continuously; cells were pre-conditioned to organic acids through two transfers (transferred during late exponential growth). After the second transfer, cell concentration measurements were used to calculate specific growth rates. In experiments where organic acid concentrations completely inhibited growth, inoculum was supplied from cells cultured through two transfers at the highest organic acid concentration tested that still allowed for growth.

Determination of Organic Acid Toxicity

Cell concentrations were determined via direct cell counts using a Petroff-Hauser counting chamber and a transmitted-light microscope (Zeiss, Thornwood, NY, U.S.A.). Cell- and substrate-free experiments were used as controls. Experiments were stopped after several consecutive measurements indicated exponential cell growth had ceased. All experiments were carried out in triplicate and average cell concentrations, specific growth rates and 95% confidence intervals were calculated. Linear regressions between the organic acid concentrations that bracketed a concentration that reduced the observed specific growth rates by 50% were used to calculate the half-maximal inhibitory concentrations (IC_{50}s).

In addition to quantifying the toxicity of individual organic acids, it was hypothesized that combinations of organic acids may exhibit an additive effect. In separate experiments, organic acids were mixed to determine if an additive toxic effect would be observed. Concentrations were mixed to give an "effective concentration," C_e, defined as

$$C_e = \sum_i C_I \qquad (2.1)$$

where C_I represents the concentration of the i^{th} organic acid in the mixture and

$$C_I = IC_{50i} / n \qquad (2.2)$$

Where IC_{50i} represents the IC_{50} of the i^{th} organic acid in the experiment and n represents the total number of organic acids added to the mixture. These equations are adapted from similar work focusing on metal toxicity [17]. Concentrations of 0.25, 0.5, 1.0, 1.5, 2.0, and 10.0 times the C_e were tested. In this manner, experiments were carried out with a mixture of all seven organic acids, as well as the pairs: oxaloacetate/2-ketoglutarate and succinate/malate. The observed specific growth rates were compared with a predicted specific growth rate, μ_p, the specific growth rate that would be observed assuming additive toxicity (Equation 2.1) of the individual organic acids.

Organic Acid Analysis

Samples for organic acid quantification were filtered (0.2 μm) and measured using ion chromatography (Dionex DX-500, Sunnyvale, CA, U.S.A.) at 254 nm on a Dionex AS-11 column. Potassium tetraborate (PT) eluent was used in a gradient from 0.35 mM (100% → 40%) to 100 mM (0% → 60%) over 20 minutes. Standards were used to calibrate all measurements.

PLFA Analysis

Cells were grown in the presence of each of the organic acids for phospholipid fatty acid (PLFA) analysis. The initial organic acid concentrations were set to the previously calculated IC_{50} values. Culture samples were collected during late-exponential growth after the second transfer, and 100 ml were sent overnight on ice to

Microbial Insights (Rockford, TN, U.S.A.). Cells were pre-conditioned so that PLFA analysis would reflect adaptations as well as physiological effects of organic acid exposure. Lipids were recovered using a modified Bligh and Dyer method [18]. Extractions were performed using a single-phase chloroform-methanol-buffer extractant. Lipids were recovered in chloroform, then fractionated on disposable silicic acid columns into neutral-, glycol-, and polar-lipid fractions. The polar lipid fraction was trans-esterified under alkaline conditions to recover the PLFA as methyl esters in hexane. The PLFA were then analyzed by gas chromatography with peak confirmation performed by electron impact mass spectrometry.

Cell Imaging

Cells that had been exposed to various concentrations of organic acids were imaged using field emission scanning electron microscopy (FESEM) (Supra 55VP Zeiss, Peabody, MA, U.S.A.). To observe structural effects of organic acid exposure on the cellular envelope, cells were not pre-adapted to the organic acids. The organic acids were added to organic acid-free cultures just as they began exponential growth. After 24 h, during mid-exponential growth, a sample of each culture was syringe-filtered onto a 0.2 μm polycarbonate filter. The filter was placed onto a stub using carbon tape and allowed to dry for 15 min at 45°C. In cases where single cells were imaged, 10 μl was pipeted onto a silica chip and allowed to dry. Samples were coated with iridium for 90 s at 20 mA, placed onto a carousel and viewed with an SE2 detector at an aperture diameter of 30 μm and an accelerating voltage of 1 keV.

Statistical Analyses

With the exception of PLFA analysis, all experiments were carried out in triplicate and average cell concentrations, specific growth rates, and 95% confidence intervals were calculated. The specific growth rates were plotted versus the organic acid concentrations that the cells were exposed to and linear regressions were calculated using Microsoft Excel. From the resulting equation, the organic acid concentration that decreased the specific growth rate by 50% (IC_{50}) and associated 95% confidence intervals were calculated. All error bars and ± values represent 95% confidence intervals. PLFA analyses of cultures exposed to organic acids produced similar results regardless of the acid, with the exception of oxaloacetate. Because of this, PLFA results of cells exposed to pyruvate, acetate, 2-ketoglutarate, succinate, fumarate, and malate were averaged and 95% confidence intervals were calculated. These values were then compared to cells that were not exposed to organic acids and to cells exposed to oxaloacetate.

Results

Organic Acid Toxicity

All organic acids tested exhibited inhibitory effects on BC13. In addition to decreasing the specific growth rate, total cell yields decreased with increasing organic acid concentration. Figures 1a and b illustrate this, using succinate and malate as examples. These growth curves were used to calculate specific growth rate curves, shown in Figure 2, from which IC_{50} values were calculated.

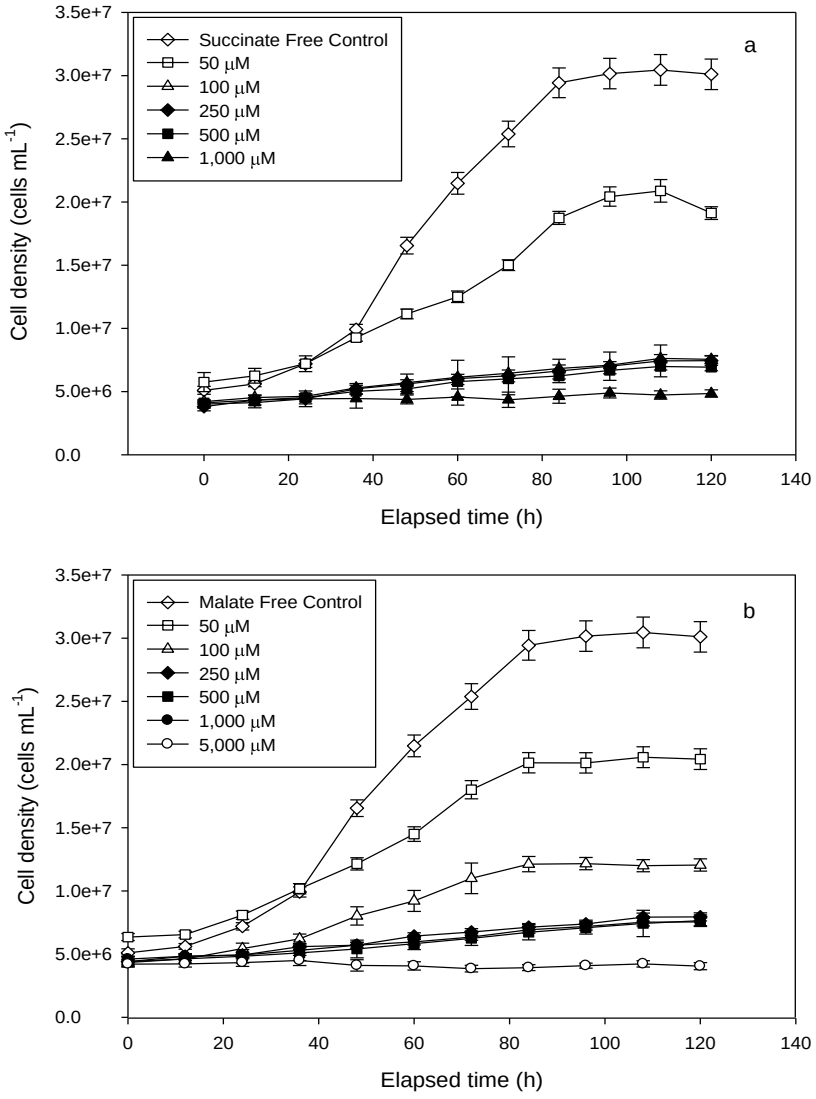


Figure 1. Typical effect of various organic acid concentrations on the growth of *Acidithiobacillus caldus* strain BC13. Organic acids shown are (a) succinate, and (b) malate. Error bars represent 95% confidence intervals.

In general, the specific growth rate decreased rapidly with increasing organic acid concentration up to 200 μM, indicating inhibition. Above 200 μM, changes in the specific growth rate were minimal (Figure 2). The exception to these more general

observations was oxaloacetate, where inhibition was severe at 100 μM and complete at 250 μM.

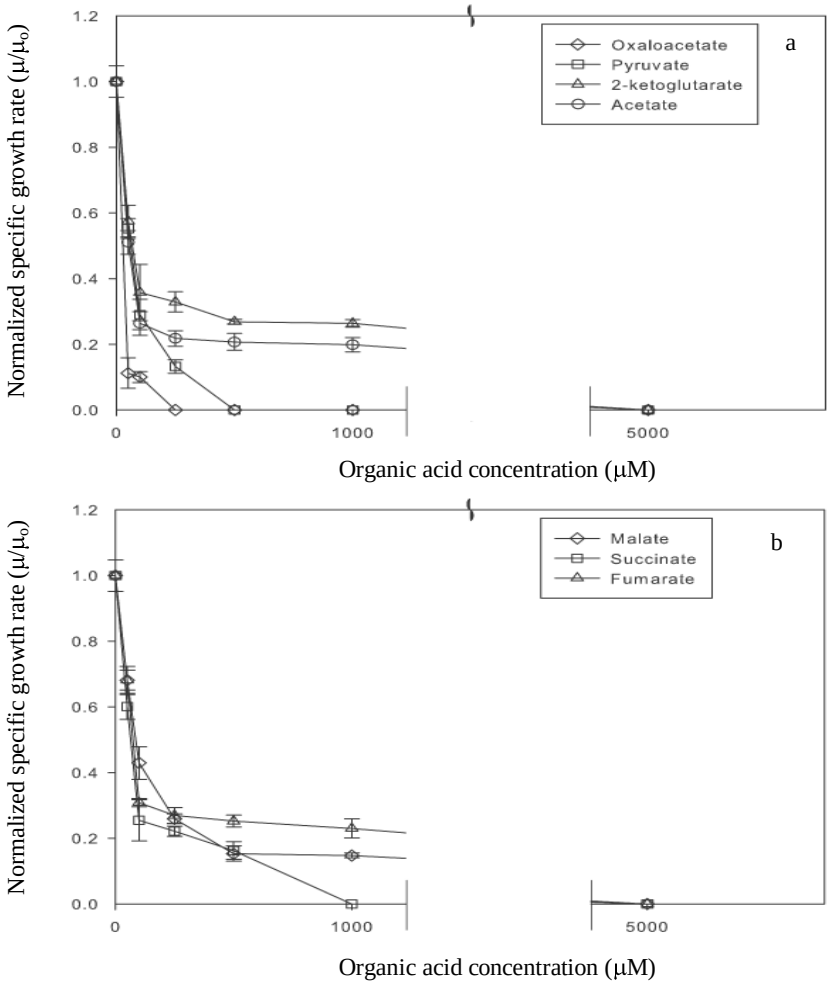


Figure 2. Specific growth rate of *Acidithiobacillus caldus* strain BC13 when exposed to different concentrations of (a) oxaloacetate, pyruvate, 2-ketoglutarate, acetate, and (b) malate, succinate, and fumarate. Changes in the specific growth rate are measured as a ratio of the specific growth rate in the presence of organic acids compared to an acid-free control. Error bars represent 95% confidence intervals.

Oxaloacetate was the most inhibitory acid (pKa = 2.15) used in the present study, with an IC_{50} of 28 ± 1.5 μM. Pyruvate, acetate, 2-ketoglutarate, succinate, fumarate, and

malate had IC_{50} concentrations between 63 and 74 μM and pKa values between 2.5 and 4.75, respectively. Malate, with a pKa of 3.40, had the highest IC_{50} at 84 ± 7.2 μM (Figure 3).

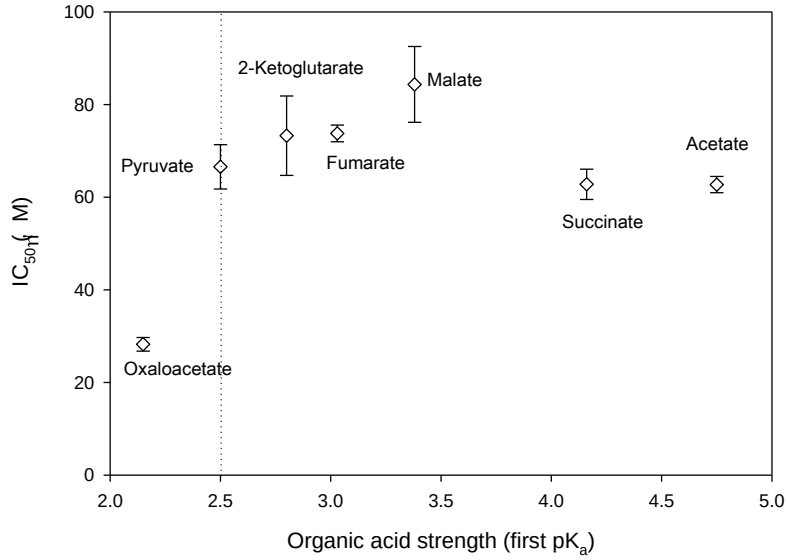


Figure 3. Acid strength plotted versus the calculated IC_{50}s. The dashed vertical line indicates the medium pH. Error bars represent 95% confidence intervals.

As well as being grown in the presence of individual organic acids, several combinations of organic acids were added (Figure 4). The observed specific growth rate was not statistically different than the specific growth rate predicted assuming additive toxic effects of each organic acid (Equations 2.1 and 2.2). This additive effect was observed for all mixtures tested (Appendix E). Substrate- and cell-free controls did not exhibit growth.

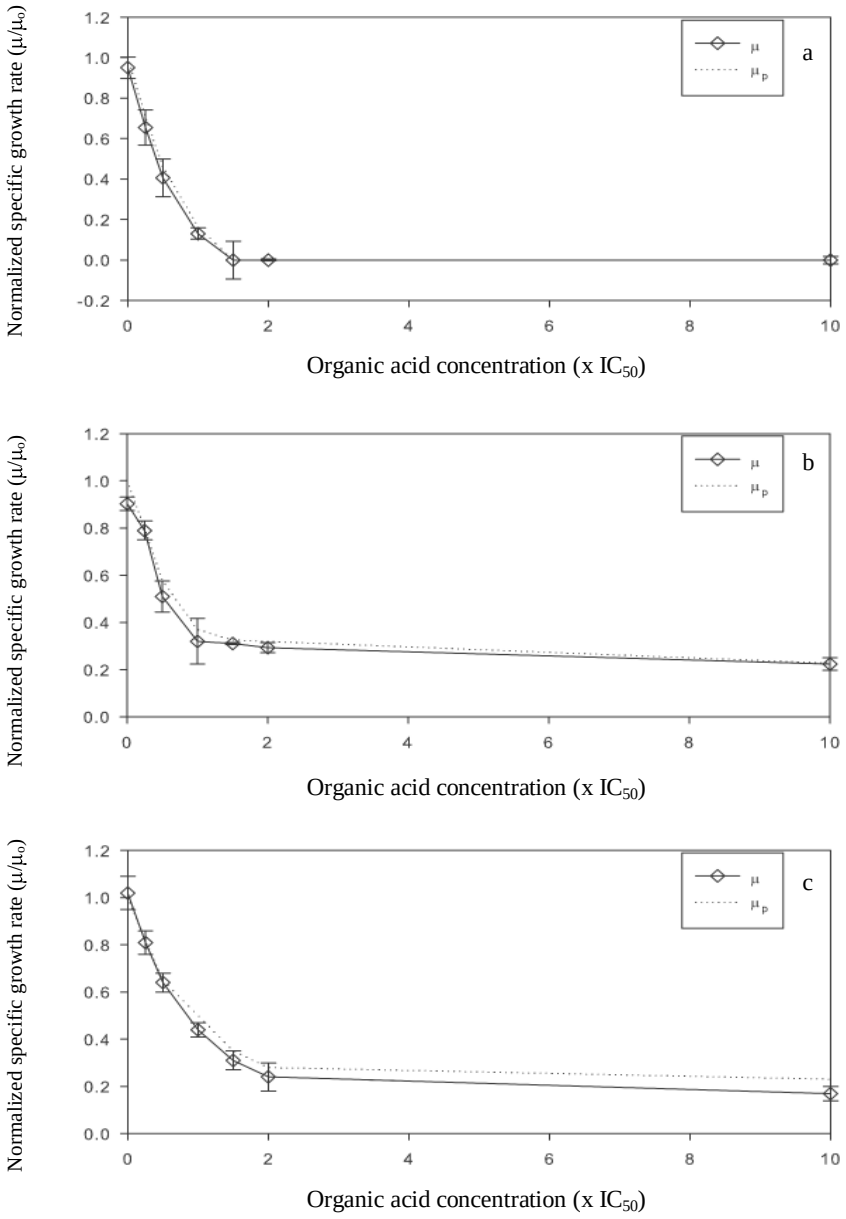


Figure 4. Normalized measured specific growth rates, μ, in mixtures of organic acids compared to normalized predicted specific growth rates, μ_p, predicted by the 'effective concentration' as calculated by Equation 2.2. Mixtures shown here are (a) oxaloacetate and 2-ketoglutarate (b) succinate and malate and (c) all organic acids. Error bars represent 95% confidence intervals.

Changes to Organic Acid Concentrations

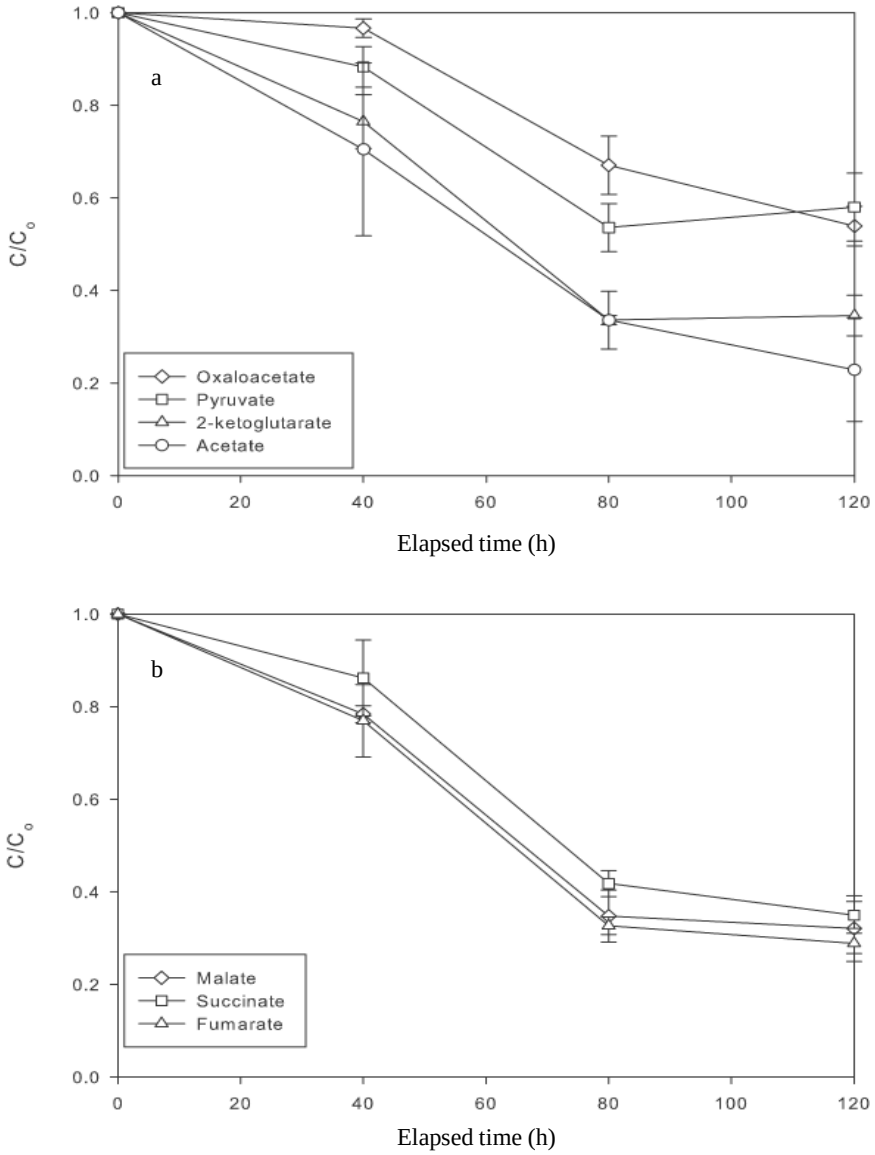


Figure 5. Normalized concentrations of (a) oxaloacetate, pyruvate, 2-ketoglutarate, acetate, and (b) malate, succinate, and fumarate during batch growth of *Acidithiobacillus caldus* strain BC13. C_o equals the concentration at which the specific growth rate was reduced by 50% (IC_{50}) values (oxaloacetate = 28.2 μM, pyruvate = 66.5 μM, 2-ketoglutarate = 73.3μM, acetate = 62.7 μM, malate = 84.3 μM, succinate = 62.8 μM, and fumarate = 73.8 μM). Error bars represent 95% confidence intervals.

As shown in Figures 5a and b, organic acid concentrations decreased in the medium by varying amounts during batch growth. The final concentrations of oxaloacetate and pyruvate were the highest, at over 50% of their initial concentration in the medium (53.9 ± 7.3% and 58.0 ± 4.3% respectively, Figure 5a). 2-ketoglutarate, malate, succinate, and fumarate had final medium concentrations of between 29% and 35% of the initial concentrations. The acetate concentration decreased the most with a final medium concentration of 22.9 ± 11.2% of the starting concentration (Figure 5a). A negligible decrease in organic acid concentrations was observed in cell-free controls over a 120 hour period.

PLFA Analysis and Cell Imaging

PLFA analysis indicated differences between cells grown in the absence and presence of organic acids. Results from an organic acid-free control were compared to the average of results observed from cells grown in the presence of each of the acids individually, and with results from cells grown in the presence of oxaloacetate alone (Table 1). There was no statistically significant variation ($p \leq 0.05$), with the exception of the trans to cis monoenoic fatty acid compositions, and cyclic to straight chained fatty acid ratios.

In addition, FESEM images showed that exposure to organic acid concentrations that completely inhibited growth also resulted in severe physical changes to the cellular envelope (Figure 6). Images of only malate-exposed cells are shown here to facilitate comparison of the effect of changing concentration. However, when other organic acids were used, similar effects were seen.

Table 1. Phospholipid fatty acid (PLFA) analysis of *Acidithiobacillus caldus* strain BC13. Values shown are percent composition. The "Control" column contains PLFA analysis of cells not exposed to organic acids. The "Organic Acids with out Oxaloacetate" is an average of results obtained from cultures grown in the presence of acetate, pyruvate, 2-ketoglutarate, malate, succinate, or fumarate. The ± values represent 95% confidence intervals. The "Oxaloacetate" column contains data from cells grown in the presence of oxaloacetate. All organic acids were added to the IC_{50} concentration.

	Control	Oxaloacetate	Organic acids with out oxaloacetate ± 95%
Terminally branched saturates	4.06	4.55	4.39 ± 1.33
Monoenoic	66.95	68.32	69.22 ± 24.89
Normal saturates	25.80	22.96	19.98 ± 7.84
		Physiological status	
Cyclic/cis	1.54	1.67	1.94 ± 0.21
Trans/cis	0.00	0.32	0.43 ± 0.04

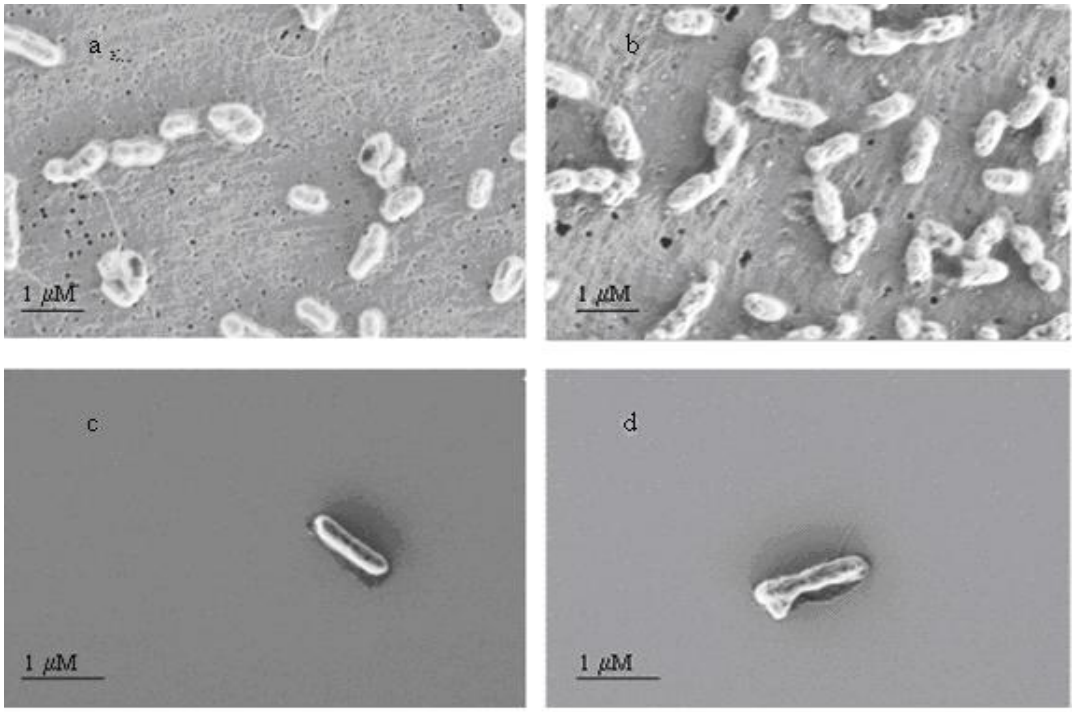


Figure 6. Micrographs of *Acidithiobacillus caldus* strain BC13 cells when grown in (a) the absence of organic acids and (b) 5,000 μM malate. Note the increased roughness of the cells exposed to malate. These cells were filtered through a 0.2 μm carbonate filter. Also shown are individual cells representative of cultures grown in (c) the absence of organic acids, and (d) 5,000 μM malate. Note the sloughing of the cell exposed to malate. These cells were aliquoted onto a silicon wafer where the medium evaporated.

Discussion

Organic Acid Toxicity

Figures 1 and 2 suggest that BC13 is susceptible to inhibition by organic acids, much like other acidophilic chemolithotrophs such as *At. ferrooxidans, At. thiooxidans*, and *L. ferrooxidans* [16]. Oxaloacetate was observed to have the greatest inhibitory effect and was the only organic acid tested with a pKa value (2.15) less than the pH of the growth medium (2.5).

Table 2. Percent of organic acids protonated (by first pKa) at the medium pH, pKa values are bracketed.

Organic Acid (pK_a)	% Protonation at pH 2.50
Oxaloacetate (2.15)	30.9
Pyruvate (2.50)	50.0
2-ketoglutarate (2.80)	66.6
Fumarate (3.03)	77.2
Malate (3.40)	88.8
Succinate (4.16)	97.9
Acetate (4.75)	99.4

At a medium pH of 2.5, there is a relatively large percentage of protonated molecules (Table 2), increasing organic acid flux into the cell and subsequent acidification of the cytoplasm, however the data suggest that stronger acids (less

protonated) are still more toxic than weaker acids (more protonated). Previous studies have also reported that stronger acids are more inhibitory. Xian-Yang and Wong [19] grew *At. ferrooxidans* in anaerobically digested sewage sludge and observed IC_{50} values of 63 and 230 μM for formate and acetate respectively, whereas simple sugars (weak acids) such as fructose and glucose had IC_{50} values of 126 to 491 mM. Similarly, Matin reported that pyruvate was a stronger inhibitor to *At. thiooxidans* then weaker acids [16]. As discussed by Escher and Schwarzenbach [20], the dependence of toxicity on pKa may be due to the protonation of organic acids at lower pH. Greater inhibition by stronger acids may suggest that the extent of de-protonation within the cytoplasm plays a more significant role than the rate of diffusion into the cell. However, for this to be the case, cells could not be inhibited until cytoplasmic pH decreases significantly, as the degree of de-protonation of the organic acids used in these experiments would be within 10% until the cytoplasmic pH drops below 5.5. This paradox is interesting, and warrants future study.

When organic acids were mixed, the specific growth rates matched those predicted by Equation 2.1, which assumes organic acid toxicity is additive when normalized to the IC_{50}. We were unable to find published studies on the additive toxic effects of organic acids, but this may suggest that the organic acids tested inhibit the growth of BC13 through a similar mechanism.

This is the first report of single or combined organic acid toxicity to *At. caldus*. Results reported here are comparable to those of the related bacteria *At. ferrooxidans* and *At. thiooxidans*. *At. thiooxidans*, was completely inhibited at concentrations (in μM) of

pyruvate (40), acetate (100), 2-ketoglutarate (100), succinate (1,000), and malate (100). Concentrations that resulted in complete inhibition of *At. ferrooxidans* for pyruvate, acetate, succinate, fumarate, and oxaloacetate were reported to be 2,000 to 10,000 μM [16]. It appears that *At. caldus* may be somewhat more resistant to organic acids than *At. thiooxidans*, and equally or slightly less resistant than *At. ferrooxidans*.

Changes in Organic Acid Concentrations

During batch experiments, acetate, 2-ketoglutarate, succinate, fumarate, and malate concentrations decreased by varying amounts (Figure 5). Oxaloacetate and pyruvate, the most inhibitory compounds tested, retained the highest relative concentration in the medium throughout batch growth. The diffusion of oxaloacetate and pyruvate into the cells was likely hindered, since they were the strongest acids tested and therefore the least protonated in the medium (Table 2). This may further indicate that the extent of intracellular de-protonation determines inhibition. The ability of BC13 to reduce the concentration of organic acids may be an important benefit to bioleaching microbial communities and warrants further study.

Acidithiobacilli have not been reported to reduce organic acid concentrations under batch conditions, however, *At. ferrooxidans* and *Thiobacillus acidophilus* have been observed to oxidize formate and pyruvate, respectively, in chemostat [21,22] at concentrations ≤ 50 μM. *At. caldus* has not been shown to use carbon compounds under heterotrophic growth conditions; however, it has been reported to grow mixotrophically on glucose and yeast extract in the presence of tetrathionate [1]. The ability for BC13 to

assimilate organic acids is examined in chapter 3, as it has implications in biomining environments. For example, Marchand and Silverstein [23] observed increased iron oxidation by *At. ferrooxidans* in soluble ferrous iron media only after glucose had been largely removed by the heterotroph, *Acidiphilium acidophilum*. Similarly, increased bioleaching kinetics in an anaerobically digested sewage sludge were observed following the removal of acetate and propionate by heterotrophs [24]. In addition, Olson et al. reported that heterotrophic degradation of organic acids was observed to increase pyrite leaching by chemolithotrophic bacteria [25].

PLFA Analysis and Cell Imaging

Given the relatively high inhibition of oxaloacetate when compared to the other organic acids tested, the PLFA data from cells exposed to oxaloacetate were compared to an acid-free control and the average of PLFA results for cells grown with each of the other acids individually. The lack of straight chained trans monoenoic fatty acids in cells not exposed to organic acids compared to cells exposed to organic acids is interesting, since some work has indicated that a high trans/cis ratio may indicate cell wall instability [26]. Direct observation of the cellular membrane using FESEM supports this possibility, as increased roughness and sloughing was seen in cells exposed to organic acids (Figure 6). This has been previously observed using microscopy with *At. ferrooxidans* grown in the presence of organic acids [13]. In addition, the increase in cyclic fatty acids in all cultures exposed to organic acids is not surprising, as high cyclic/cis ratios are indicative of slow/inhibited growth, and have been observed in other extremophiles under high stress conditions [27,28].

The growth inhibition of BC13 observed in the current batch studies may be greater than that observed in natural environments. The growth of cells in planktonic culture on a soluble substrate limits the formation of biofilms, and may have limited the formation of extrapolymeric substances [28], leading to greater exposure of cells to organic acids. Because of this, observations reported here may represent a more intrinsic view of organic acid toxicity to BC13.

Conclusions

Pyruvate, acetate, 2-ketoglutarate, succinate, fumarate, malate, and oxaloacetate were all toxic to BC13 when presented singly. When combined, the toxicities appeared to be additive. The inhibition observed here was similar to that observed in previous work with the acidithiobacilli [15,16]. PLFA analysis suggested membrane instability, and FESEM imaging supported this possibility, as blebbing and sloughing of the cellular envelope was observed when cells were exposed to concentrations of organic acids that completely inhibited growth. Finally, the concentrations of organic acids were observed to decrease with time during batch growth of BC13. As previously discussed, *At. caldus* is prevalent in commercial bioleaching processes [7,8], therefore, any ability of BC13 to transform organic acids in the extracellular environment may benefit biomining communities and indirectly improve leaching kinetics in commercial processes. The work presented here contributes to further understanding of *At. caldus* and lays the ground work for future work to investigate the metabolic capabilities of this important biomining microorganism.

References

1. Hallberg KB, Lindstrom EB (1994) Characterization of *Thiobacillus caldus* sp. Nov., a moderately thermophilic acidophile. *Microbiology* 140:3451-3456.

2. Kelly DP, Wood AP (2000) Reclassification of some species of *Thiobacillus* to the newly designated genera *Acidithiobacillus* gen. nov., *Halothiobacillus*, gen. nov. and *Thermithiobacillus* gen. nov. *Int J Systematic Evol and Microbiol* 50:511-516.

3. Waksman SA, Joffe JS (1922) Microorganisms concerned in the oxidation of sulfur in the soil. II. *Thiobacillus thiooxidans*, a new sulfur-oxidizing organism isolated from the soil. *J Bacteriol* 7:239-256.

4. Temple KL, Colmer AR (1951) The autotrophic oxidation of iron by a new bacterium, *Thiobacillus ferrooxidans*. *J Bacteriol* 62:605-611.

5. Hallberg KB, Lindstrom EB (1996) Multiple serotypes of the moderate thermophile *Thiobacillus caldus*, a limitation of immunological assays for biomining microorganisms. *Appl Environ Microbiol* 62:4243-4246.

6. Dopson M, Lindstrom EB, Hallberg KB (2002) ATP generation during reduced inorganic sulfur compound oxidation by *Acidithiobacillus caldus* is exclusively due to electron transport phosphorylation. *Extremophiles* 6:123-129.

7. Rawlings DE (2002) Heavy metal mining using microbes. *Annu Rev Microbiol* 56:65-91.

8. Okibe N, Gericke M, Hallberg KB, Johnson DB (2003) Enumeration and characterization of acidophilic microorganisms isolated for a pilot plant stirred-tank bioleaching operation. *Appl Environ Microbiol* 69:1936-1943.

9. Dopson, M, Lindstrom EB (1999) Potential role of *Thiobacillus caldus* in arsenopyrite bioleaching. *Appl Environ Microbiol* 65:36-40.

10. Edwards KJ, Bond PL, Banfield JF (2000) Characteristics of attachment and growth of *Thiobacillus caldus* on sulphide minerals: a chemotactic response to sulphur minerals? *Environ Microbiol* 2:324-332.

11. McGuire MM, Edwards KJ, Banfield JF Hamers RJ (2001) Kinetics, surface chemistry, and structural evolution of microbially mediated sulfide mineral dissolution. *Geochem Cosmochim Acta* 65:1243-1258.

12. Ingledew WJ, Poole RK (1982) *Thiobacillus ferrooxidans*: The bioenergetics of an acidophilic chemolithotroph. *Biochem Biophys Acta* 683:89-117.

13. Tuttle JH, Dugan PR, Apel WA (1977) Leakage of cellular material from *Thiobacillus ferrooxidans* in the presence of organic acids. *Appl Environ Microbiol* 33:459-469.

14. Schnaitman C, Lundgren D (1965) Organic compounds in the spent medium of *Ferrobacillus ferrooxidans.* *Can J Microbiol* 1:23-27.

15. Borischewski RM (1967) Keto acids as growth-limiting factors in autotrophic growth of *Thiobacillus thiooxidans*. *J Bacteriol* 93:597-599.

16. Matin A (1978) Organic nutrition of chemolithotrophic bacteria. *Annu Rev Microbiol* 32:433-468.

17. Gikas P (2008) Kinetic responses of activitated sludge to individual and joint Nickel (Ni(II)) and Cobalt (Co(II)): An isobolographic approach. *J. Haz. Mater.* 143:246-256.

18. White DC, Davis WM, Nickels JS, King JD, Bobbie J (1979) Determination of the sedimentary microbial biomass by extractable lipid phosphate. *Oceologia* 40:51-62.

19. Xiang-Yang F, Wong WCJ (2004) Identification of inhibitory substances affecting bioleaching of heavy metals from anaerobically digested sewage sludge. *Environ Sci Technol* 38:2934-2939.

20. Escher BI, Schwarzenbach RP (2002) Mechanistic studies on baseline toxicity and uncoupling of organic compounds as a basis for modeling effective membrane concentrations in aquatic organisms. *Aqua Sci* 64:20-35.

21. Pronk JT, Meijer WM, Van Dijken JP, Kuenen JG (1991) Growth of *Thiobacillus ferrooxidans* on formic acid. *Appl Environ Microbiol* 57:2057-2062.

22. Pronk JT, Meesters Van Dijken JP, Bos P, Kuenen JG (1990) Heterotrophic growth of *Thiobacillus acidophilus* in batch and chemostat cultures. *Arch Microbiol* 153:392-398.

23. Marchand EA, Silverstein J (2003) The role of enhanced heterotrophic bacterial growth on iron oxidation by *Acidithiobacillus ferrooxidans*. *Geomicrobiol J* 20:231-244.

24. Xiang-Yang F, Wong WCJ (2007) Degradation of inhibitory substances by heterotrophic microorganisms during bioleaching of heavy metals from anaerobically digested sewage sludge. *Chemosphere* 69:311-318.

25. Olson GJ, Brierley JA. Brierley CL (2003) Bioleaching review part B: progress in bioleaching: applications of microbial processes by the mineral industries. *Appl Microbiol Biotechnol* 63:249-257.

26. Loffeld B, Keweloh H (1996) *cis/trans* isomerization of unsaturated fatty acids as possible control mechanism of membrane fluidity in *Pseudomonas putida* P8. *Lipids* 31:811-815.

27. Aston JE, Peyton BM (2007) Response of *Halomonas campisalis* to saline stress: changes in growth kinetics, compatible solute production and membrane phospholipid fatty acid analysis. *FEMS Microbiol Lett* 274:196-203.

28. Brown GR, Sutcliffe IC, Bendell D, Cummings SP (2000) The modification of the membrane of *Oceanomonas baumannii* when subjected to both osmotic and organic solvent stress. *FEMS Microbiol Lett* 189:149-154.

29. Neis DH (1999) Microbial heavy-metal resistance. *Appl Microbiol Biotechnol* 51:730-750.

CHAPTER THREE

GROWTH EFFECTS AND ASSIMILATION OF ORGANIC ACIDS IN CHEMOSTAT AND BATCH CULTURES OF *ACIDITHIOBACILLUS CALDUS* STRAIN BC13

Abstract

The ability of BC13 to grow aerobically using pyruvate, acetate, citrate, 2-ketoglutarate, succinate, and malate as either an electron donor and carbon source (heterotrophic growth), or as a carbon source when potassium tetrathionate was added as an electron donor (mixotrophic growth), was tested in chemostat cultures. Under both heterotrophic and mixotrophic conditions, organic acids were added to a sub-lethal concentration (50 μM). Under mixotrophic conditions, potassium tetrathionate was added to an excess concentration (10 mM). No cell growth was observed under heterotrophic conditions; however effluent cell concentrations increased over three-fold when pyruvate was coupled with potassium tetrathionate. Under these conditions, the effluent pyruvate concentration was reduced to below the detection limit (2 μM), and oxygen consumption increased by approximately 100%. Although pyruvate provided a carbon source in these experiments, ambient carbon dioxide was also available to the cells.

To test whether BC13 could grow mixotrophically using pyruvate as a sole carbon source and potassium tetrathionate as an electron donor, cells were batch cultured in a medium free of dissolved inorganic carbon, and with no carbon dioxide in the headspace.

These experiments showed that BC13 converted between 65 ± 8 and 82 ± 15% of the pyruvate carbon to cellular biomass, depending on the initial pyruvate concentrations.

This work is the first to identify a defined organic-carbon source, other than glucose, that *At. caldus* can assimilate. This has important implications, as mixotrophic and heterotrophic activity has been shown to increase mineral leaching in acidic systems.

Introduction

Compared to the more commonly studied *At. thiooxidans* [1] and *At. ferrooxidans* [2], relatively little is known about *At. caldus*. As with all acidithiobacilli, *At. caldus* thrives at low pH (optimum 2.0 - 3.0); however, unlike other acidithiobacilli, *At. caldus* grows well at moderately high temperatures, with optimum growth at 45°C [3]. *At. caldus* oxidizes sulfur and reduced sulfur compounds for energy, and can fix carbon dioxide as a sole carbon source [4,5]. *At. caldus* has also been reported to grow mixotrophically using sulfur or tetrathionate as an electron donor and either glucose or yeast extract as a carbon source [3]. The conditions at which *At. caldus* thrives, coupled with its ability to oxidize reduced sulfur compounds, make it important in many acid-mine systems around the world [6,7], where it may stimulate mineral sulfide leaching [8-12].

There are many considerations affecting the bioleaching of metals in acid-mine environments, one of these is the presence and concentration of organic acids [13-17]. The toxicity of low-molecular weight organic acids to microorganisms is well documented. These effects may increase at low pH where acids are more protonated and

can more easily diffuse across the cell membrane, weakening the proton motive force [18]. In addition, Tuttle et al. observed a loss of integrity in the cellular envelope of acidophilic chemolithotrophs when exposed to inhibitory concentrations of organic acids [19]. Because of these effects, heterotrophic or mixotrophic activity in carbon-limited bioleaching systems can improve leaching efficiency by reducing organic acid concentrations [14-17].

In the present study, the ability of BC13 to use pyruvate, acetate, citrate, 2-ketoglutarate, succinate, and malate as an electron donor and carbon source (heterotrophic growth) and as a carbon source coupled with the inorganic electron donor, potassium tetrathionate (mixotrophic growth), was studied in chemostat and batch cultures. These organic acids were chosen because of their presence in the spent medium of acidophilic sulfur-oxidizing autotrophs [20], and their toxicity to acidithiobacilli [21-23].

Materials and Methods

Microorganism, Media, and Growth Conditions

BC13 (ATCC 51757) was grown in the basal salts medium and trace elements used by Hallberg and Lindstrom [3]. To prepare the medium, nanopure water (17.4 MΩ) was added to the salts to volume, and the medium was autoclaved for 15 min at 121°C and 22 psig. After the medium cooled to room temperature, 1 mL L^{-1} of the filter sterilized (0.2 μm) trace element solution was added [3], and the pH was adjusted to 2.5 using 6N sulfuric acid. Cells preserved at 4°C in nanopure water (17.4 MΩ), with the pH

adjusted to 3.0 using 6N sulfuric acid, provided the initial inoculum. An organic acid stock solution was prepared the same day and filter sterilized (0.2 μm) into the medium to give the desired final organic acid concentration.

Chemostat Culturing

Pronk et al. showed *Thiobacillus acidophilus* could oxidize pyruvate in chemostat cultures, but not in batch cultures [24]. Because of this, chemostat cultures were used in the initial experiments discussed here. Prior to inoculation into a continuous-flow system, BC13 cells were grown in 500-mL serum bottles (350 mL medium volume) fitted with butyl-rubber stoppers. Filter sterilized (0.2 μm) potassium tetrathionate was added to a concentration of 10 mM as the electron donor, and carbon dioxide provided the sole carbon source. The serum bottles were placed in a temperature controlled incubator at 45°C, and shaken at 150 rotations per minute (rpm). During the late-exponential growth phase, pyruvate, acetate, citrate, 2-ketoglutarate, succinate, or malate was added to a concentration of 10 μM to pre-adapt the cells to each organic acid. Cells were harvested using centrifugation (7,000 g) during the late-exponential growth phase, and were washed three times in pH 3.0 nanopure water (17.4 MΩ) to minimize substrate transfer. An aliquot of cells that provided between 5.0×10^7 and 5.5×10^7 cells mL^{-1} was inoculated into 500 mL of fresh growth medium in a continuous-flow SIXFORS reactor (ATR, Columbia, MD, U.S.A.), maintained at 45°C, and agitated using a magnetic stir bar rotating at 200 rpm.

To test for heterotrophic growth, pyruvate, acetate, citrate, 2-ketoglutarate, succinate, or malate were added to the influent to a sub-lethal concentration of 50 μM [21]. To test for mixotrophic growth, parallel experiments were run, using an influent medium containing 10 mM potassium tetrathionate, in addition to the organic acids, to provide an inorganic electron donor. In either case, the influent was added at 5 mL hr^{-1}, setting the dilution rate at 0.01 h^{-1}. An adjacent SIXFORS pump removed the effluent, maintaining a constant medium volume in each chemostat.

Cell concentrations were measured by direct counts using a Petrof-counting chamber (Hausser Scientific, Horsham, PA, U.S.A.), and a phase-contrast microscope at 1,000X (Zeiss, Thornwood, NY, U.S.A.). Cultures were monitored until cell concentrations either reached steady-state, or washed out. Effluent samples were then saved at 4°C for measurement of organic acid concentrations.

Organic Acid Measurement

Samples collected for organic acid measurements were concentrated using a CentriVap Concentrator (LABCONCO, Kansas City, MO, U.S.A.). Concentrations were measured using capillary electrophoresis (CE) (BioRad 4000, Hercules, CA, U.S.A.) against an anion buffer (Agilent, Santa Clara, CA, U.S.A.). A capillary cartridge 104 cm in length, with an inside diameter of 50 μm, was washed with nanopure water (17.4 mΩ) and the buffer solution between each sample run. Samples were injected at 50 mbar for 6 seconds, and run positive to negative at 30 kV. Absorbance was measured at 350 nm.

Dissolved Oxygen and Inorganic Carbon Measurement

The dissolved oxygen concentrations were measured using an HQ40d dissolved oxygen probe (HACH, Loveland, CO, U.S.A.). The probe was calibrated using nanopure water (17.4 MΩ) at 22 and 45ºC. To measure dissolved inorganic carbon, samples were collected using a 3-mL syringe and filtered (0.2 μm) into a 30-mL serum bottle, capped with a butyl-rubber stopper, that had been purged with filter sterilized (0.2 μm) ultra-pure nitrogen gas for 5 minutes to remove ambient carbon dioxide. A 1-mL syringe was then used to transfer the samples to a carbon analyzer (Dohrmann, St. Cloud, MN, U.S.A.). The UV-light apparatus, normally used to cleave organic compounds into dissolved inorganic carbon, was turned off, so that only dissolved inorganic carbon was measured.

Dry-Cell Weight and Carbon Composition Measurement

It was necessary to measure the carbon composition of BC13 cells to determine carbon yield on pyruvate during mixotrophic growth. A 50-mL effluent sample from a chemostat culture at steady state was collected and centrifuged. Cells were dried in a Samdri-795 critical point dryer (Tousimis, Rockville, MD), and then placed in an oven at 80ºC for 48 hours. Dry weights were recorded and correlated with direct-cell counts to calculate a specific dry-cell weight. The cell pellet was re-suspended in 10 mL of nanopure water (17.4 mΩ) and agitated for 30 seconds using a Branson 1020 sonicator (Danbury, CT, U.S.A.). This sample was introduced into the carbon analyzer, with the UV-light apparatus turned on. After the specific dry-cell weight and carbon mass was measured, the percent carbon composition of BC13 was calculated.

Batch Growth with Pyruvate as the Sole Carbon Source

Inorganic carbon was removed from the growth medium by sparging 350 mL of heated (80ºC) medium, in a 500-mL serum bottle fitted with a butyl-rubber stopper, with carbon dioxide-free air for 30 minutes. Because chemostat experiments showed that BC13 could not use pyruvate as a sole electron donor, potassium tetrathionate was added to a concentration of 10 mM and pyruvate was added to a concentration of 5, 10, 15, or 20 μM. Controls showed the dissolved inorganic carbon concentration in the medium was below the detection limit (approximately 1 μM). The medium was then inoculated with cells that were pre-adapted to pyruvate. To adapt the cells to pyruvate, cells were harvested during the late-exponential growth phase of a growth cycle, and washed using the methods described earlier. Cells were then re-inoculated into fresh medium containing the same initial organic acid concentration. This process was repeated a total of three times.

Cell concentrations were measured using direct counts (described earlier) and the specific growth rates were calculated. Samples were collected at the end of the exponential growth phase to measure pyruvate concentrations using the methods described earlier. The growth of these cultures was compared with potassium tetrathionate-free, pyruvate-free, and pyruvate plus carbon dioxide controls.

Growth Effects of Organic Acids in Batch Cultures

In separate experiments, the toxicity of organic acids was determined at concentrations at and below 50 μM. BC13 was grown in 125-mL serum bottles (75 mL

medium volume) fitted with butyl-rubber stoppers. Potassium tetrathionate was added to a concentration of 10 mM as an electron donor. Prior to inoculation, pyruvate, acetate, citrate, 2-ketoglutarate, succinate, or malate was added to a concentration of 5, 10, 20, 30, or 50 μM. Ambient carbon dioxide was also available as a carbon source. Cells preserved at 4°C in pH 3.0 nanopure water (17.4 MΩ) provided the initial inoculum. The serum bottles were placed in a temperature controlled incubator at 45°C and shaken at 150 rpm. To calculate specific growth rates, cell concentrations were measured by direct counts. This experiment was repeated in parallel with cultures that had been pre-adapted to organic acids through subsequent transfers, using the methods described earlier.

16S rRNA Culture Analysis

After chemostat cultures had reached steady-state, and after batch cultures had reached late-log phase growth, DNA was extracted using a DNA soil extraction kit (Promega, Madison, WI, U.S.A.). A polymerase chain reaction (PCR) was carried out in an Eppendorf master cycler gradient thermocycler (New York, NY, U.S.A.) using 8F and 1492R primers, to amplify the 16S rRNA gene, and a PCR master mix from PROMEGA. The amplicons were sequenced at the Bioinformatics laboratory at Idaho State University. The sequence results were analyzed with BLAST software, and had a 99% percent similarity to several uncultured *At. caldus* 16S clones.

Statistical Analysis

All experiments were carried out in triplicate, and average values and 95% confidence intervals are reported. A single carboy was used to supply influent medium to

three continuous-flow reactors, preventing statistical analysis of influent substrate concentrations.

Results

Test for Heterotrophic Growth

When acetate, citrate, 2-ketoglutarate, succinate, or malate were added as a carbon source and sole electron donor, there were no statistically significant differences between effluent cell concentrations and a theoretical washout curve calculated from an unsteady state mass balance that assumed a specific growth rate of zero. The organic acid concentrations were nearly constant between the influent and effluent at steady state. In addition, the dissolved oxygen concentration remained steady between the influent and effluent, at 185 μM. In comparison, when potassium tetrathionate was added as an electron donor, and ambient carbon dioxide provided the sole carbon source, cultures reached steady state between 360 and 412 hours, or 3.60 to 4.12 residence times, at $7.40 \times 10^6 \pm 1.90 \times 10^6$ cells mL^{-1}, and the effluent dissolved oxygen concentration decreased to 139.4 ± 1.8 μM (Appendix F).

Test for Mixotrophic Growth

Figure 7a shows changes in the effluent cell concentrations over time when potassium tetrathionate was present with the organic acid. There was little difference in the steady state effluent cell concentrations between cultures containing acetate, citrate, 2-ketoglutarate, succinate, or malate coupled with potassium tetrathionate, and cultures containing only potassium tetrathionate. These effluent cell concentrations ranged

between 5.60 x 10^6 ± 9.17 x 10^5 (citrate) and 7.67 x 10^6 ± 1.40 x 10^6 cells mL^{-1} (acetate). However, when pyruvate was added, steady state cell concentrations reached 2.07 x 10^7 ± 0.06 x 10^7 cells mL^{-1}.

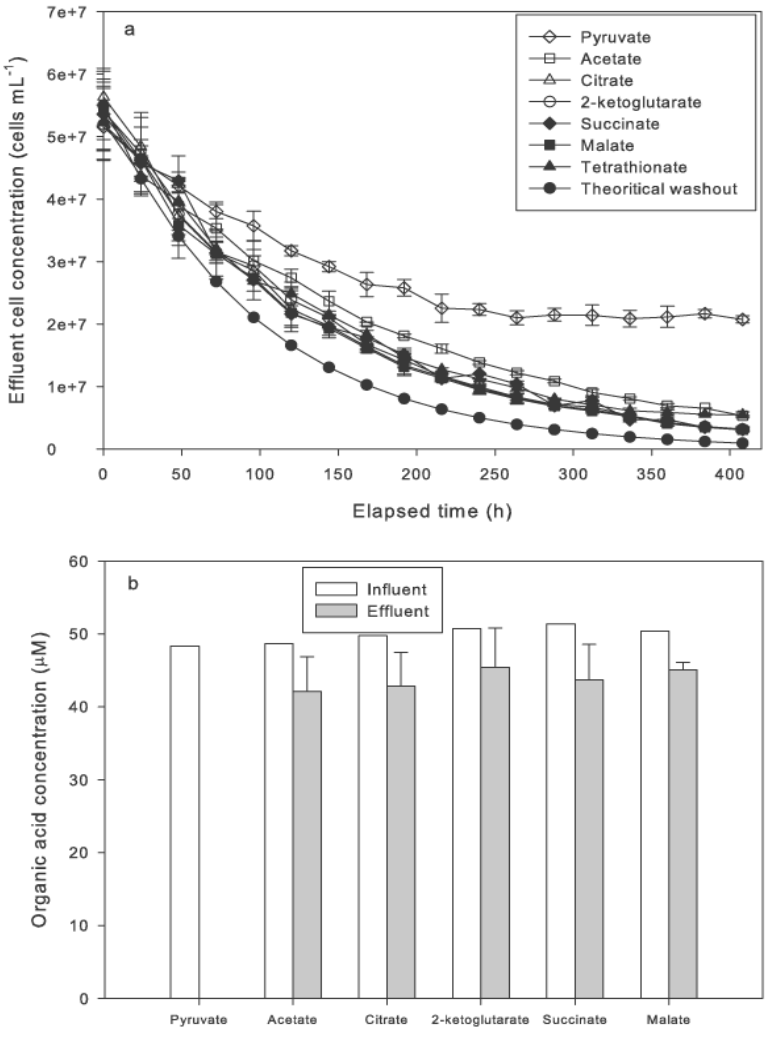


Figure 7. (a) Effluent cell concentrations of *Acidithiobacillus caldus* strain BC13 grown in chemostat under mixotrophic conditions. Each respective organic acid supplied a possible electron donor (50 μM), in addition to potassium tetrathionate (10 mM), and supplemented ambient carbon dioxide as a potential carbon source. A potassium tetrathionate only control and theoretical washout are presented for comparison. It can be seen that the chemostat comes to steady state between 264 and 336 hours. (b) Influent and steady state effluent concentrations of organic acids corresponding to plot (a). Error bars represent 95% confidence intervals.

Figure 7b shows that acetate, citrate, 2-ketoglutarate, succinate, and malate concentrations decreased 10-20% between the influent and effluent at steady state. Conversely, the effluent concentration of pyruvate was below the detection limit (approximately 2 μM) at steady state. Figure 8 shows the dissolved oxygen concentration in cultures grown in the presence of pyruvate was also significantly lower than in cultures grown in the presence of other organic acids, 95.4 ± 3.2 μM compared with a low of 136.5 ± 3.2 μM for 2-ketoglutarate and a high of 147.6 ± 3.3 μM for succinate. The effluent dissolved oxygen concentration in the potassium tetrathionate only control was 139.4 ± 1.8 μM.

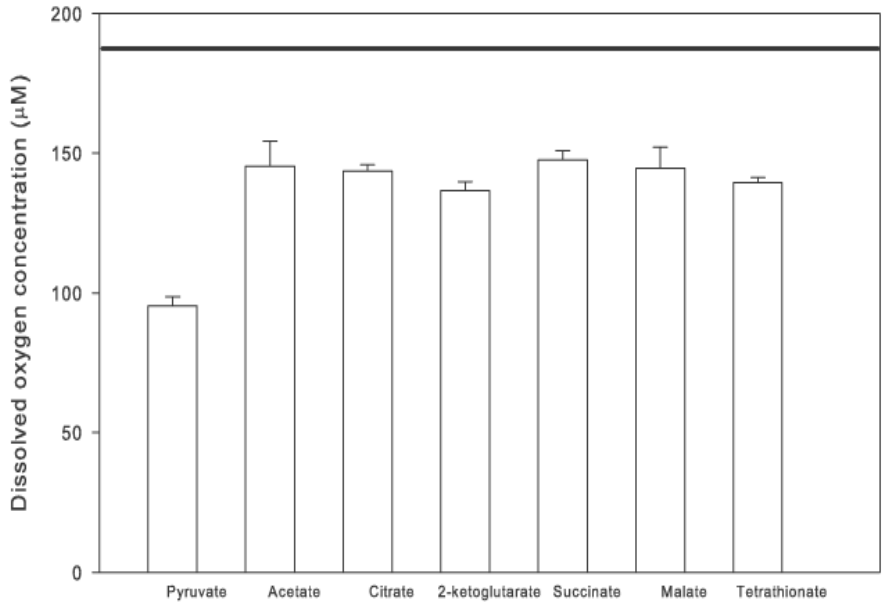


Figure 8. Dissolved oxygen concentration of the chemostat effluent under mixotrophic conditions. The x-axis lists the organic acid supplied with potassium tetrathionate. A potassium tetrathionate only control is shown for comparison. Error bars represent 95% confidence intervals. The horizontal line indicates the theoretical solubility of oxygen in water under the experimental conditions.

Batch Growth with Pyruvate as the Sole Carbon Source

Figure 9 shows BC13 grew mixotrophically in batch cultures when pyruvate provided the sole carbon source and potassium tetrathionate provided an electron donor. When the initial pyruvate concentrations were 5, 10, 15, and 20 μM, 65 ± 8, 77 ± 4, 79 ± 11, and 82 ± 15% of the pyruvate was used anabolically, respectively. Table 3 shows that pyruvate was efficiently converted to biomass. No cell growth was observed in samples where potassium tetrathionate was withheld.

Table 3. Percent of pyruvate consumed and converted to biomass by *Acidithiobacillus caldus* strain BC13, in carbon dioxide free media, at initial concentrations of 5, 10, 15, or 20 μM. Potassium tetrathionate was added to a concentration of 10 mM to provide an inorganic electron donor.

Pyruvate concentration (μM)	Pyruvate uptake (%)	Pyruvate converted to biomass (%)
5	100 ± 0	65 ± 8
10	100 ± 0	77 ± 4
15	74 ± 7	79 ± 11
20	73 ± 4	82 ± 15

Toxicity of Organic Acids in Batch Cultures

Pyruvate, acetate, citrate, 2-ketoglutarate, succinate, and malate each showed a negligible effect on the specific growth rate at a concentration of 5 μM. At concentrations at or above 20 μM, significant inhibitory effects were observed (Figure 10a). When cells were pre-adapted to pyruvate, the specific growth rate increased by 11 ± 3, 13 ± 3, 34 ± 3, 28 ± 1, and 7 ± 1 %, at initial concentrations of 5, 10, 20, 30, and 50 μM, respectively, compared with cells exposed to pyruvate for the first time. When cells

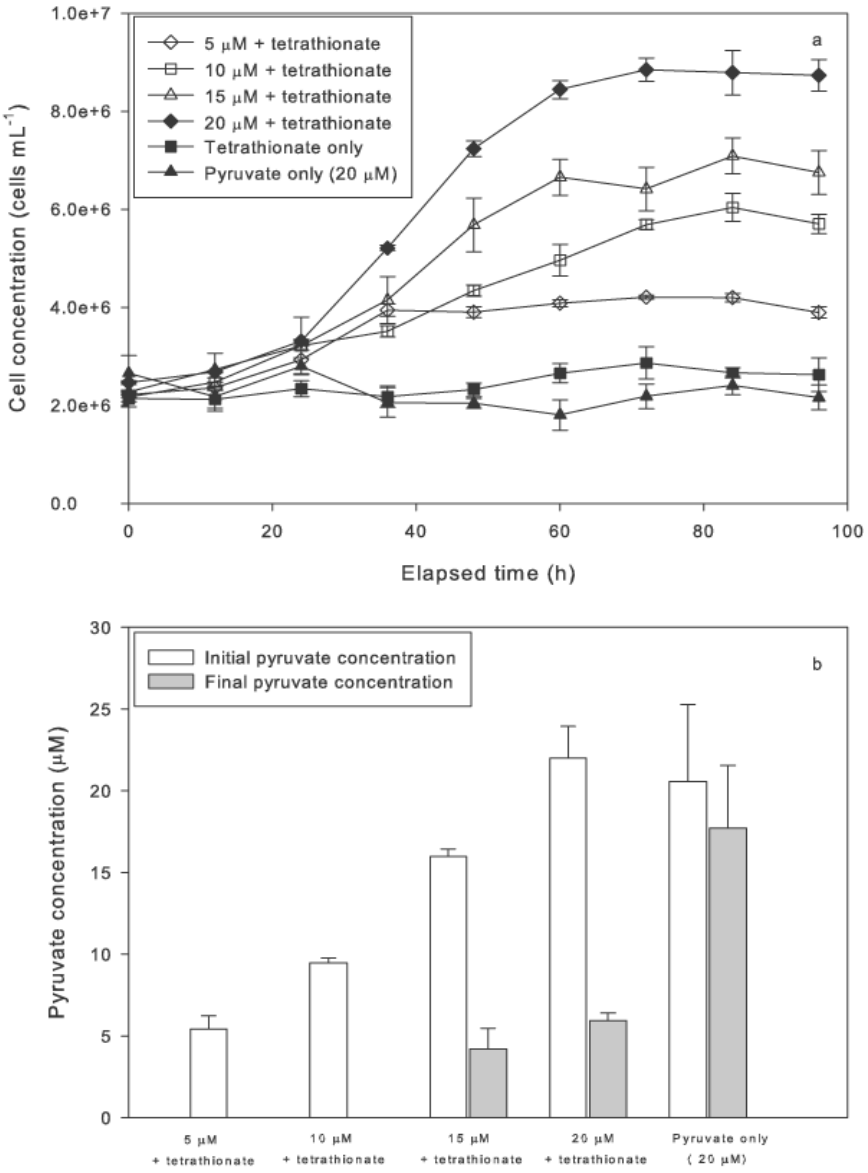


Figure 9. (a) Growth of *Acidithiobacillus caldus* strain BC13 in batch cultures using pyruvate as the sole carbon source and (b) initial and final pyruvate concentrations when provided as the sole carbon source in batch cultures. Potassium tetrathionate was present at a concentration of 10 mM. Error bars represent 95% confidence intervals.

were pre-adapted to acetate, the specific growth rate increased by 4 ± 2 and 10 ± 3 %, when the initial concentration was 5 μM and 10 μM, respectively, compared to un-

adapted cells. No significant increases in specific growth rates were observed after subsequent culturing in the presence of citrate, 2-ketoglutarate, succinate, or malate (Figure 10b).

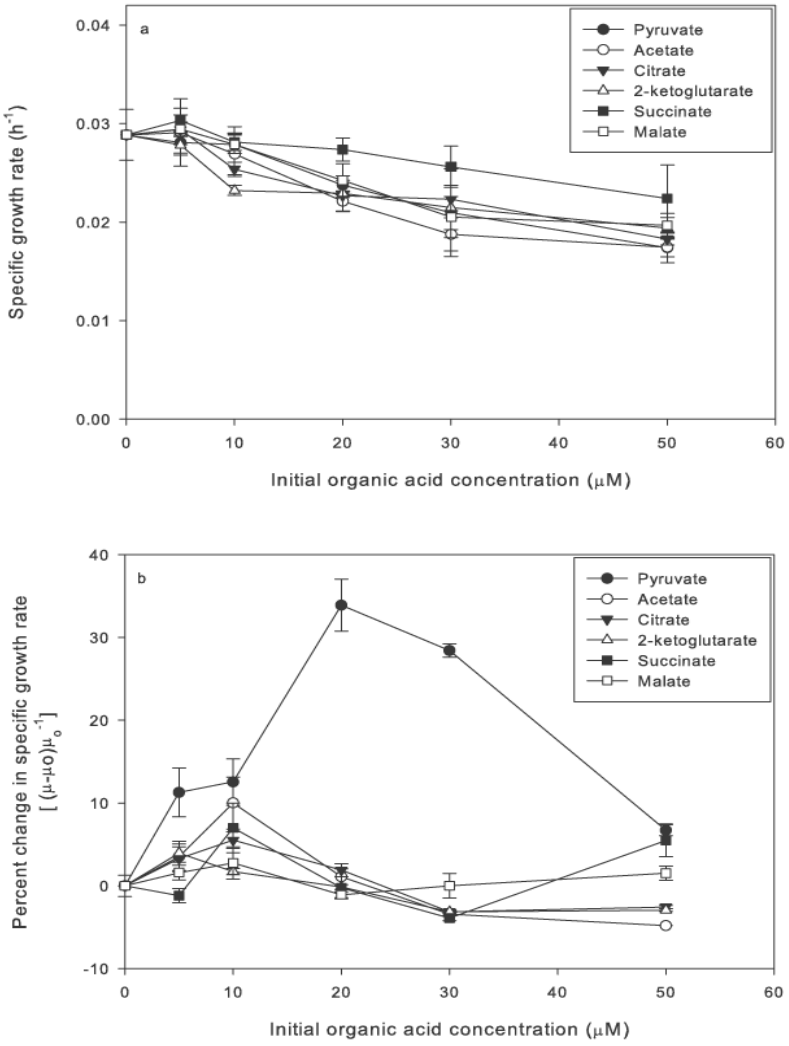


Figure 10. Effect of pyruvate, acetate, citrate, 2-ketoglutarate, succinate, and malate on the specific growth rate of *Acidithiobacillus caldus* strain BC13 during batch growth conditions after (a) no previous exposure to organic acids, and (b) four sequential transfers between identical conditions. μ_o represents the specific growth rate observed without prior exposure to the respective organic acid, and μ represents the specific growth rate observed in cultures with prior exposure to the respective organic acid. Potassium tetrathionate was present at a concentration of 10 mM. Error bars represent 95% confidence intervals.

Discussion

The work presented here shows that BC13 can grow mixotrophically using pyruvate as a carbon source and potassium tetrathionate as an electron donor, under aerobic conditions (Figures 7 and 8). Conversely, acetate, citrate, 2-ketoglutarate, succinate, and malate were not used as a significant carbon source.

Because carbon dioxide was available to the cells in the chemostat experiments, separate experiments were designed to determine whether BC13 is capable of mixotrophic growth on pyruvate in a carbon dioxide limited system. Using media free of dissolved inorganic carbon, we confirmed that BC13 grew while using pyruvate as the sole-carbon source in batch cultures (Figure 10). Coupled with the inability of BC13 to grow in the absence of potassium tetrathionate, this further suggests that pyruvate was primarily used for anabolic growth, rather than being oxidized solely as an electron donor.

This is not the first report of mixotrophic growth by *At. caldus*, as Hallberg and Lindstrom reported that *At. caldus* strain KU could grow using sulfur or potassium tetrathionate and either glucose or yeast extract [3]. However, this work is significant because pyruvate has been identified in the spent medium filtrate of acidophilic chemolithophic autotrophs [20], and is toxic to chemolithotrophic autotrophs at low concentrations under acidic conditions [21,23]. In addition, previous work has shown that removing inhibitory organic acids can significantly increase metal-leaching rates [14-17].

Recent studies may provide clues for how BC13 can assimilate pyruvate as a carbon source. Valdes et al. used whole-genome shotgun sequencing to assemble a draft genome for *At. caldus* strain KU and predict proteins from coding sequences [25,26]. Sequences coding for pyruvate dehydrogenase and phosphoenolpyruvate synthase were identified. Pyruvate dehydrogenase catalyzes the oxidation of pyruvate to carbon dioxide and acetyl-CoA. Carbon dioxide could then be fixed via the Calvin cycle, and acetyl-CoA could be used as a precursor for lipid synthesis, for which the necessary genes were also identified [26]. This mechanism would be similar to the anabolic oxidation of formate by *At. thiooxidans* [27], where formate was oxidized to carbon dioxide, which could then be fixed for anabolic growth. In addition, phosphoenolpyruvate synthase converts pyruvate to phosphoenolpyruvate, and Valdes et al. did predict that *At. caldus* strain KU possesses the necessary enzymes to convert phosphoenolpyruvate into five-carbon sugars important for anabolic growth using gluconeogenesis and the pentose phosphate pathway [26].

In this study, pyruvate in particular showed a significant increase in specific growth rates following adaptation (Figure 10). This suggests that the expression of enzymes that may facilitate pyruvate metabolism, such as those discussed above, or proteins that aid in resisting organic acid toxicity, increased with prior exposure.

Valdes et al. also identified the presence of an incomplete TCA cycle (lacking 2-ketoglutarate dehydrogenase) [25,26]. However, the present study indicates that BC13 does not assimilate external organic acids used in the TCA cycle (citrate, 2-ketoglutarate,

succinate, and malate), suggesting that it may lack the required transport mechanisms, or cannot use the concentrations of these acids tested in this study.

It is interesting that under mixotrophic conditions, the effluent cell concentrations in chemostat cultures containing acetate, 2-ketoglutarate, succinate, or malate did not differ statistically from cultures containing only potassium tetrathionate given that they were not used as a carbon source and are toxic at the concentrations measured in the effluent (Figures 7 and 10). However, the dilution rate used in these chemostat studies (0.01 h^{-1}) was lower than the specific growth rates observed in batch cultures that contained acetate, citrate, 2-ketoglutarate, succinate, or malate (0.016 to 0.023 h^{-1} at 50 μM), and there have been several studies that report a correlation between bacterial growth phase and the toxicity of a given inhibitor [*i.e.* 28,29]. By fixing the specific growth rate in the chemostat at 0.01 h^{-1}, the toxic effect of the organic acids may be reduced, or masked by the already low specific growth rate. A previous study with *Thiobacillus acidophilus* reported a similar effect, where, although no growth was observed in batch cultures containing pyruvate, cells grew and oxidized pyruvate in a chemostat culture [24].

No cell growth was observed when organic acids were supplied as the sole electron donor in either chemostat or batch cultures. Therefore, it is possible that the slight decrease in the concentration of organic acids between the influent and the effluent at steady state (Appendix F) was due to chemiosmosis [18]. It is also possible that a portion of this decrease in organic acids was due to anabolic maintenance, but because the dissolved oxygen concentration remained nearly constant, this would have been an

energetically limited process. These results were not surprising, as no acidithiobacilli have been observed to grow using organic acids as a sole energy source.

Conclusions

The work presented here shows that BC13 can use pyruvate for anabolic growth under mixotrophic conditions. In addition, prior exposure to pyruvate significantly increased the specific growth rate of BC13 when pyruvate was added to batch cultures. However, BC13 could not grow when pyruvate was the sole electron donor, nor could it use acetate, citrate, 2-ketoglutarate, succinate, or malate as energy or carbon sources to a significant extent at the concentrations and dilution rates used in this study. This work is an important contribution towards understanding the metabolic capabilities of *At. caldus*, and its role in microbial communities and industrial and environmental applications.

References

1. Waksman SA, Joffe JS (1922) Microorganisms concerned in the oxidation of sulfur in the soil II. *Thiobacillus thiooxidans*, a new sulfuroxidizing organism isolated from the soil. *J Bacteriol* 7:239-256.

2. Temple KL, Colmer AR (1951) The autotrophic oxidation of iron by an new bacterium, *Thiobacillus ferrooxidans*. *J Bacteriol* 62:605-611.

3. Hallberg KB, Lindstrom EB (1994) Characterization of *Thiobacillus caldus* sp. Nov., a moderately thermophilic acidophile. *Microbiology* 140:3451-3456.

4. Dopson M, Lindstrom EB, Hallberg KB (2002) ATP generation during reduced inorganic sulfur compound oxidation by *Acidithiobacillus caldus* is exclusively due to electron transport phosphorylation. *Extremophiles* 6:123-129.

5. Hallberg KB, Lindstrom EB (1996) Multiple serotypes of the moderate thermophile *Thiobacillus caldus*, a limitation of immunological assays for biomining microorganisms. *Appl Environ Microbiol* 62:4243-4246.

6. Rawlings DE. (2002) Heavy metal mining using microbes. *Annu Rev Microbiol* 56:65-91.

7. Okibe N, Gericke M, Hallberg KB, Johnson DB (2003) Enumeration and characterization of acidophilic microorganisms isolated for a pilot plant stirred-tank bioleaching operation. *Appl Environ Microbiol* 69:1936-1943.

8. Dopson M, Lindstrom EB (1999) Potential role of *Thiobacillus caldus* in arsenopyrite bioleaching. *Appl Environ Microbiol* 65:36-40.

9. Edwards KJ, Bond PL, Banfield JF (2000) Characteristics of attachment and growth of *Thiobacillus caldus* on sulphide minerals: a chemotactic response to sulphur minerals? *Environ Microbiol* 2:324-332.

10. Fu B, Zhou H, Zhang R, Qiu G (2008) Bioleaching of chalcopyrite by pure and mixed cultures of *Acidithiobacillus* spp. and *Leptospirillum ferriphilum*. *Int J Biodeteriat and Biodegrad* 62:109-115.

11. McGuire MM, Edwards KJ, Banfield JF, Hamers RJ (2001) Kinetics, surface chemistry, and structural evolution of microbially mediated sulfide mineral dissolution. *Geochem Cosmochim Acta* 65:1243-1258.

12. Zhou QG, Bo F, Bo ZH, Xi L, Jian G, Fei LF, Hau CH (2007) Isolation of a strain of *Acidithiobacillus caldus* and its role in bioleaching of chalcopyrite. *World J Microbiol Biotechnol* 23:1217-1225.

13. Burckhard SR, Schwab AP, Banks MK (1995) The effects of organic acids on the leaching of heavy metals from mine tailings. J Hazard Mat 41:135-145.

14. Gu XY, Wong JWC (2004) Identification of inhibitory substances affecting bioleaching of heavy metals from anaerobically digested sewage sludge. *Eniviron Sci Technol* 38:2934-2939.

15. Gu XY, Wong JWC (2007) Degradation of inhibitory substances by heterotrophic microorganisms during bioleaching of heavy metals from anaerobically digested sewage sludge. *Chemosphere* 69:311–318.

16. Marchland EA, Silverstein J (2003) The role of enhanced heterotrophic bacterial growth on iron oxidation by *Acidithiobacillus ferrooxidans*. *Geomicrobiol J* 20:231–244.

17. Olson GJ, Brierley JA, Brierley CL (2003) Bioleaching review. Part B: Progress in bioleaching: Applications of microbial processes by the mineral industries. *Appl Microbiol Biotechnol* 63:249–257.

18. Ingledew WJ, Poole RK (1982) *Thiobacillus ferrooxidans*: The bioenergetics of an acidophilic chemolithotroph. *Biochem Biophys Acta* 683:89-117.

19. Tuttle JH, Dugan PR, Apel WA (1977) Leakage of cellular material from *Thiobacillus ferrooxidans* in the presence of organic acids. *Appl Environ Microbiol* 33:459-469.

20. Schnaitman C, Lundgren D 1965 Organic compounds in the spent medium of *Ferrobacillus ferrooxidans.* *Can J Microbiol* 1:23-27.

21. Aston JA, Apel WA, Lee BD, Peyton BM (2009) Toxicity of select organic acids to the slightly thermophilic acidophile *Acidithiobacillus caldus*. *Environ Toxicol Chem* 28:279-286.

22. Borischewski RM (1967) Keto acids as growth-limiting factors in autotrophic growth of *Thiobacillus thiooxidans*. *J Bacteriol* 93:597-599.

24. Matin A (1978) Organic nutrition of chemolithotrophic bacteria. *Annu Rev Microbiol* 32:433-468.

25. Valdes J, Pedroso I, Quatrini R, Holmes DS (2008) Comparative genome analysis of *Acidithiobacillus ferrooxidans, A. thiooxidans* and *A. caldus*: insights into their metabolism and ecophysiology. *Hydrometallurgy* 94:180-184.

26. Valdes J, Quatrini R, Hallberg K, Dopson M, Valenzuela PDT, Holmes DS (2009) Draft genome sequence of the extremely acidophilic bacterium *Acidithiobacillus caldus* ATCC 51756 reveals metabolic versatility in the genus *Acidithiobacillus*. *J Bact* 191:5877-5878.

27. Pronk JT, Mejer WM, Hazeu W, van Dijken JP, Bos P, Kuenen JG (1991) Growth of *Thiobacillus thiooxidans* on formic acid. *Appl Environ Microbiol* 57:2057-2062.

28. Richard HT, Foster JW (2003) Acid resistance in *Escherichia coli*. *Adv Appl Microbiology* 52:167-184.

29. Yilmaz EI (2003) Metal tolerance and biosorption capacity of *Bacillus circulans* strain EB1. *Res Microbiology* 154:409-415.

30. Pronk JT, Meesters PJW, van Dijken JP, Bos P, Kuenen JG (1989) Heterotrophic growth of *Thiobacillus acidophilus* in batch and chemostat cultures. *Microbiology* 153:392-398.

CHAPTER FOUR

LEAD, ZINC, AND COPPER TOXICITY TO *ACIDITHIOBACILLUS CALDUS* STRAIN BC13

Abstract

This study reports the single and combined toxicity of lead, zinc, and copper to BC13. The observed IC_{50}s, ± 95% confidence intervals, for lead, zinc, and copper were 0.9 ± 0.1 mM, 39 ± 0.5 mM, and 120 ± 8 mM, respectively. The observed minimum inhibitory concentrations (MIC) for lead, zinc, and copper were 7.5 mM, 75 mM, and 250 mM, respectively. When metals were presented in binary mixtures, the toxicities were less than additive. For example, when 50% of the lead MIC and 50% of the copper MIC were presented together, the specific growth rate was inhibited by only 59 ± 3%, rather than 100%. In addition, the presence of ferrous iron in the growth media decreased lead and zinc toxicity to BC13.

The importance of inoculum history was evaluated by pre-adapting cultures through subsequent transfers in the presence of lead, zinc, or copper at their respective IC_{50}s. After pre-adaptation, cultures had specific growth rates 39 ± 11, 32 ± 7, and 28 ± 12% higher in the presence of lead, zinc, and copper IC_{50}s, respectively, compared to cultures that had not been pre-adapted. In addition, when cells exposed to the MIC of lead, zinc, or copper were harvested, washed, and re-inoculated into fresh, metal-free medium, they grew at near normal growth rates, showing that the cells remained viable with no observed residual toxicity.

Finally, metal chlorides showed more toxicity than metal sulfates, and studies using sodium chloride or a mixture of metal sulfates and sodium chloride suggested that this was due to an additive combination of the metal and chloride toxicities.

Introduction

At. caldus is a Gram-negative bacterium that oxidizes sulfur and reduced sulfur compounds for energy, and can fix carbon dioxide as a sole carbon source [1-2]. *At. caldus* grows from pH 1-4, with optimal growth between pH 2 and 3, and from 32-50°C, with optimal growth at 45°C [1]. These traits make *At. caldus* well suited for growth in many biomining systems [3-6], where recent studies suggest that it may play a significant role in metal mobilization. McGuire et al. (2001) reported that microbial communities containing *At. caldus* were observed to leach more iron from pyrite, arsenopyrite, and marcasite than communities without *At. caldus* [7]. Dopson and Lindstrom (1999) reported that twice as much iron was leached from arsenopyrite when an iron oxidizer, *Sulfobacillus thermosulfidooxidans*, was co-cultured with *At. caldus*, as compared to when *S. thermosulfidooxidans* was cultured alone [8]. In addition, *At. caldus* was observed to enhance copper recovery by oxidizing sulfur formed during the biomining of chalcopyrite [9]. These studies suggest an important role for *At. caldus* in commercial biomining, yet there have been few direct studies of metal interactions and toxicities to *At. caldus*.

The toxicity of metals to microorganisms has been well documented and there have been several general reviews written covering this subject [*i.e.* 10-15]. Specific to

the work presented here, multiple studies have reported that the related microorganisms, *At. ferrooxidans* and *At. thiooxidans*, have relatively high tolerance to zinc and copper when presented individually [16-21], or combined [18,22]. However, toxicity studies with *At. caldus* have largely been limited to the metalloid arsenic [23-25]. Recent work by Watkin et al. compared iron, copper, zinc, nickel, and cobalt tolerances of several new isolates to those of several known strains, including *At. caldus* strain KU, but in depth inhibition studies were not done [26].

The present study is a comprehensive report on the effects of lead, zinc, and copper on the growth of BC13, including; 1) effects of single versus combined metal toxicity, 2) effects of high ferrous iron concentrations on lead, zinc, and copper toxicity, 3) effects of prior exposure to lead, zinc, and copper, and 4) comparisons of metal sulfate and metal chloride toxicity. This report significantly increases the current understanding of *At. caldus*, an important microorganism to biomining and acid-mine drainage.

Materials and Methods

Microorganism and Growth Conditions

BC13 (ATCC 51757) was grown in a basal salts medium [1]. The medium was autoclaved for 15 minutes at 121°C and 22 psig, and the pH was then adjusted to 2.5 using 6N sulfuric acid. A filter sterilized (0.2 μm) metal sulfate solution (lead, zinc, or copper) was added from a stock solution. The concentrations of metal in the stock solutions were adjusted to ensure that an equal volume could be added to each flask. A filter sterilized (0.2 μm) solution of potassium tetrathionate was then added to a

concentration of 5 mM, as an electron donor, and ambient carbon dioxide provided the sole carbon source. Cells preserved at 4°C in nanopure water (17.4 MΩ), with the pH adjusted to 3.0 using 6N sulfuric acid, provided the initial inoculum. Aliquots that provided initial cell densities of approximately 5×10^7 cells mL^{-1} were used. Cells were cultured in 125-mL Erlenmeyer flasks (75 mL medium volume), fitted with foam stoppers, and shaken at 150 rpm in a temperature controlled incubator at 45°C. Cell concentrations were measured at 12 hour intervals, and each experiment was repeated in triplicate so that average values and 95% confidence intervals could be calculated.

Determining Single Metal Toxicity

Cell concentrations were measured using direct cell counts with a Petroff-counting chamber (Hausser Scientific, Horsham, PA, U.S.A.) and a phase-contrast microscope (Zeiss, Thornwood, N.Y., U.S.A.). The observed specific growth rates were used to quantify inhibition. Linear regressions were used to calculate IC_{50}s and corresponding 95% confidence intervals. In addition, the no observable effect concentration (NOEC), lowest observable effect concentration (LOEC), and MIC were determined graphically.

Determining Combined Metal Toxicity

To determine combined metal toxicity, binary mixtures of lead and zinc, lead and copper, and zinc and copper were prepared. Concentrations were proportional to their respective MICs and, assuming additive toxicities, mixed to produce a total metal concentration proportional to an effective MIC. For example, to produce a mixture

containing lead and zinc equivalent to 50% of an effective MIC, the final growth medium would contain: $0.5 \cdot \left(\frac{MIC_{Pb}}{2} + \frac{MIC_{Zn}}{2} \right)$. Linear regressions were used to calculate expected toxicities using the LINEST function in Microsoft Excel. From these regressions, estimated contributions towards the total effective toxicity from each metal were calculated.

Similar experiments were conducted to determine if ferrous iron affected the toxicity of lead, zinc, or copper to BC13. Each metal was added to a concentration equal to its previously calculated IC_{50}, and ferrous iron sulfate was added to concentrations of 0, 25, 50, 75, or 100 mM. The concentration of ferrous iron in each stock was adjusted so that an equal volume was added to each flask. Lead, zinc, and copper-free controls were performed to determine if ferrous iron alone affected BC13 in the absence of lead, zinc, or copper.

Determining Effects of Previous Metal Exposure

Cells were prepared as described earlier and inoculated into growth medium containing lead, zinc, or copper concentrations equal to the previously calculated IC_{50}. During the late-log growth phase, cells were harvested and washed as previously described, then inoculated into fresh medium containing the same metal concentration. This process was repeated three subsequent times to allow cells to adapt to lead, zinc, or copper. During the fourth growth cycle, cell concentrations were measured using direct counts as described previously, and the specific growth rates were calculated.

Determining Metal Chloride Toxicity

Cells were prepared as described previously, but metal chlorides were used instead of metal sulfates. Chloride salts of lead, zinc, or copper were introduced at initial concentrations equal to the previously calculated IC_{50}s of the respective metal sulfate counterparts. To determine if chloride ions contributed directly to cell inhibition, sodium chloride was added to metal-free growth media at concentrations of 0, 50, 100, and 200 mM. In control experiments, lead, zinc, or copper sulfates were added at the previously calculated IC_{50}s, and sodium chloride was also added to concentrations of 0, 50, 100, 150, or 200 mM. In these experiments, cell concentrations were measured as described previously, and specific growth rates were calculated for comparison.

Modeling Metal Complexation and Precipitation

Visual MINTEQ (version 2.53) software was used to predict complexation and precipitation of media components using activities from the Debye-Huckel Equation and the default MINTEQA2 thermodynamic database. The temperature was set to 45°C and the proton concentration was calculated from the pH, which was set at 2.50. The saturation index (defined as the log of the ion activity divided by the solubility product) was used to predict metal precipitation. Compounds with a positive saturation index were set to infinite saturation, to allow for their precipitation. Each experimental medium condition tested was modeled in this manner.

Results

Single Metal Toxicity

Figure 11a shows the effect of lead concentrations on the specific growth rate of BC13. Similarly, the effects of zinc (Figure 11b) and copper (Figure 11c) are shown.

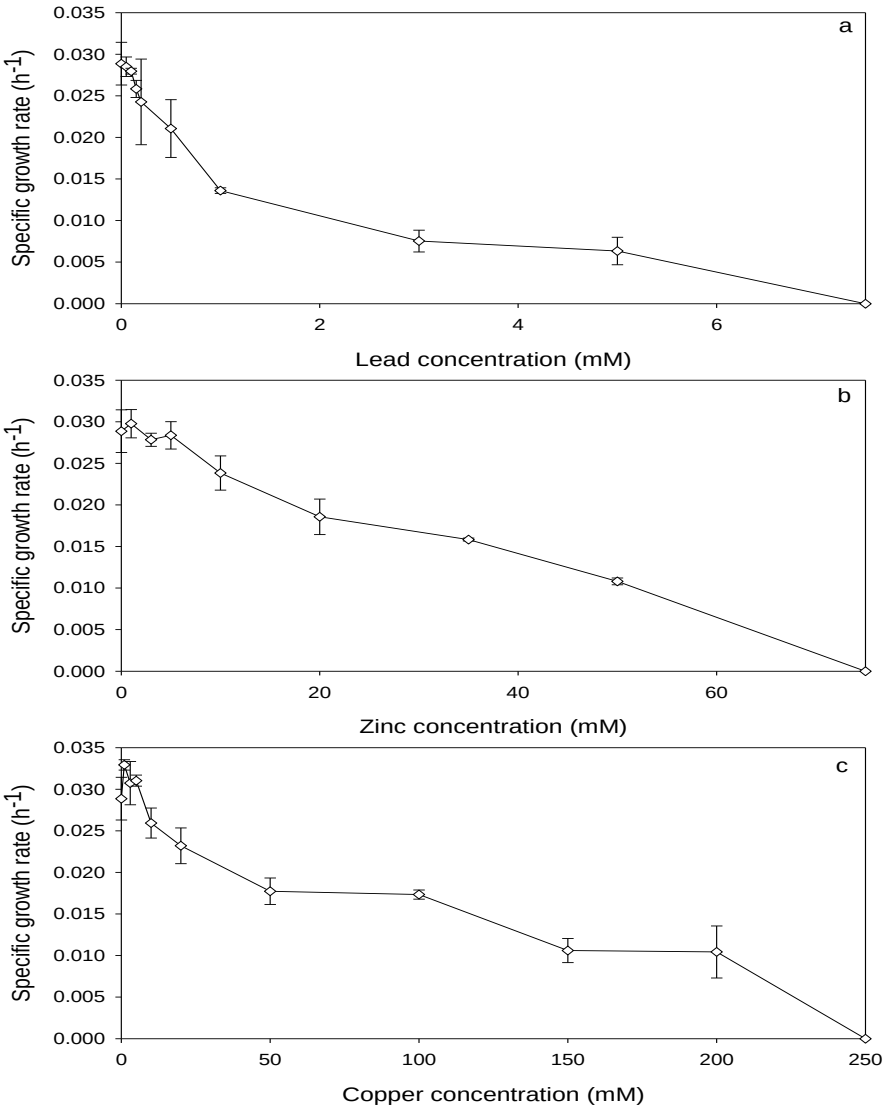


Figure 11. Effect of (a) lead, (b) zinc, and (c) copper sulfate on the specific growth rate of *Acidithiobacillus caldus* strain BC13. Error bars represent 95% confidence intervals.

Lead was the most toxic of the three metals tested with an IC_{50} of 0.94 ± 0.13 mM, and an MIC of 7.5 mM. An IC_{50} and MIC of 39 ± 0.5 mM and 75 mM, respectively, were observed for zinc, while copper was the least inhibitory metal tested with an IC_{50} and MIC of 120 ± 8.2 mM and 250 mM, respectively (Table 4).

Table 4. Toxicity of lead, zinc, and copper sulfates to *Acidithiobacillus caldus* strain BC13 described using the no observable effect concentration (NOEC), lowest observable effect concentration (LOEC), half-maximal inhibitory concentration (IC_{50}), and the minimum inhibitory concentration (MIC). Inhibition was quantified by changes in the specific growth rate in the presence of metals. ± values indicate 95% confidence intervals.

	NOEC (mM)	LOEC (mM)	IC_{50} (mM)	MIC (mM)
Lead	0.1	0.15	0.94 ± 0.13	7.5
Zinc	1	3	39 ± 0.46	75
Copper	5	10	120 ± 8.2	250

Combined Metal Toxicity

To determine the combined toxicity of lead, zinc, and copper, metals were presented in binary mixtures in ratios proportional to their individual IC_{50}s. Binary metal mixtures containing ratios of 12.5%, 25%, 37.5%, and 50% of each metal's respective MIC was used. Assuming additive toxicity when mixed, the effective overall metal concentrations were then 25%, 50%, 75%, and 100% of an effective MIC. However, Figure 12 shows that the toxicities were less than additive. For example, when 25% of the lead MIC was mixed with 25% of the zinc MIC, the observed specific growth rate was 0.016 ± 0.001 h^{-1}, compared to a predicted specific growth rate of 0.012 h^{-1}, calculated assuming additive toxicities (Figure 12a). Similar results were seen when lead and copper, and zinc and copper were mixed (Figures 12b and c).

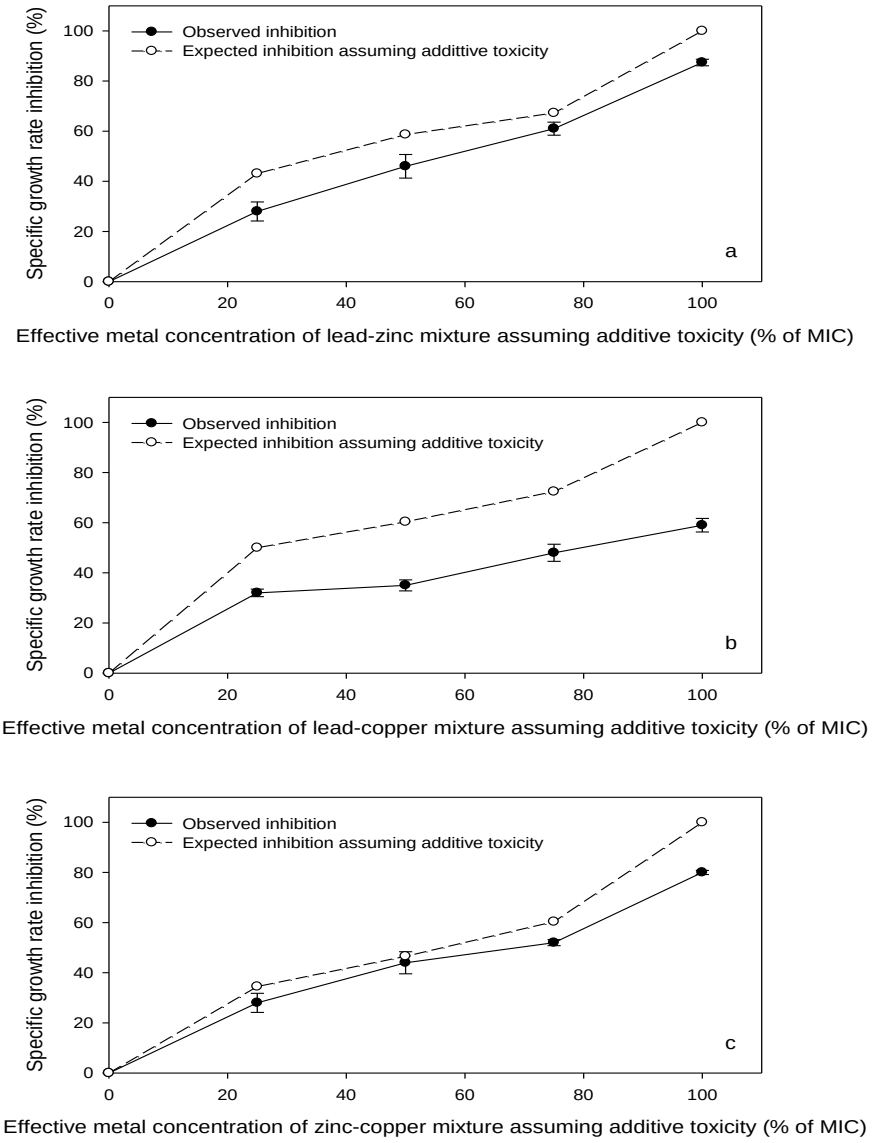


Figure 12. Observed inhibition compared to predicted inhibition, assuming additive toxicity, of binary mixtures of (a) lead and zinc, (b) lead and copper, and (c) zinc and copper to strain *Acidithiobacillus caldus* BC13. The x-axis represents the percentage of the minimum inhibitory concentration (MIC) calculated assuming additive effects. Error bars represent 95% confidence intervals. The MIC concentrations for lead, zinc, and copper were 7.5, 75, and 250 mM, respectively.

Effect of Ferrous Iron on Metal Toxicity

Ferrous iron gave significant protection to BC13 from lead and zinc toxicity. Figure 13 shows that cultures exposed to a concentration of lead equal to the IC_{50}, exhibited specific growth rates of 0.014 ± 0.001, 0.032 ± 0.001, and 0.030 ± 0.001 h^{-1} when ferrous iron was added to concentrations of 0, 50, and 100 mM, respectively. Similarly, the observed specific growth rates of cultures in the presence of the zinc IC_{50} were 0.016 ± 0.001, 0.023 ± 0.001, and 0.028 ± 0.001 h^{-1} when ferrous iron was added to 0, 50, and 100 mM, respectively. However, when this experiment was

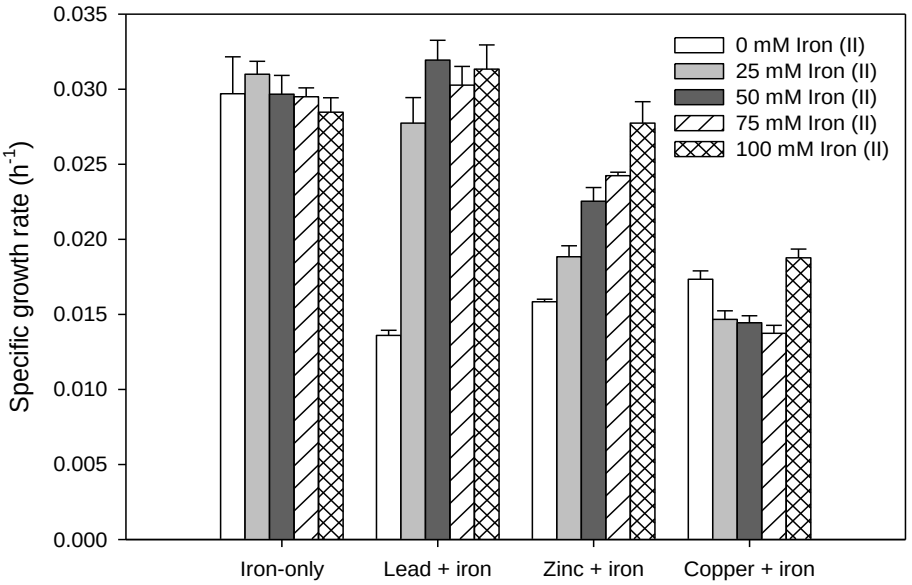


Figure 13. The effect of ferrous iron added to concentrations of 0, 25, 50, 75, or 100 mM on lead, zinc, and copper toxicity to *Acidithiobacillus caldus* strain BC13 when added at concentrations equal to the previously calculated half-maximal inhibition concentrations (0.94 mM, 39 mM, and 120 mM for lead, zinc, and copper, respectively). Error bars represent 95% confidence intervals.

performed using copper, the effect was significantly decreased, as observed specific growth rates were 0.017 ± 0.001, 0.014 ± 0.000, and 0.019 ± 0.001 h^{-1} when ferrous iron was added to concentrations of 0, 50, and 100 mM, respectively (Figure 13). In separate control experiments, ferrous iron was added to concentrations of 0, 50, and 100 mM with no lead, zinc, or copper added. At these concentrations, the observed specific growth rates were 0.030 ± 0.001, 0.030 ± 0.001, and 0.028 ± 0.001 h^{-1}; suggesting that ferrous iron did not significantly affect the growth of BC13 by itself (Figure 13). MINTEQ modeling predicted that over 96% of the iron remained as aqueous ferrous iron at the concentrations used in this study.

Effect of Prior Metal Exposure on Metal Toxicity

Figure 14 shows that the specific growth rate increased 39 ± 11, 32 ± 7, and 28 ± 12% when cultures were pre-adapted, through subsequent transfers, to lead, zinc, or copper, respectively. In addition to increased specific growth rates, the lag phase of cultures pre-adapted to lead, zinc, or copper decreased by 12, 24, and 48 hours, respectively (Appendix G).

Figure 15 shows that cells collected from media containing the MIC of lead, zinc, or copper were able to resuscitate and grow in fresh, metal-free, medium. After being exposed for 120 hours to the MIC of lead, then re-inoculated into fresh, metal-free medium, cultures grew with no residual inhibition, and attained a final cell concentration of 107 ± 7% of the final cell concentration observed for cultures that had not been exposed to lead. However, when cells were collected from medium containing the MIC of zinc or copper after 120 hours of exposure, and re-inoculated into fresh, metal-free

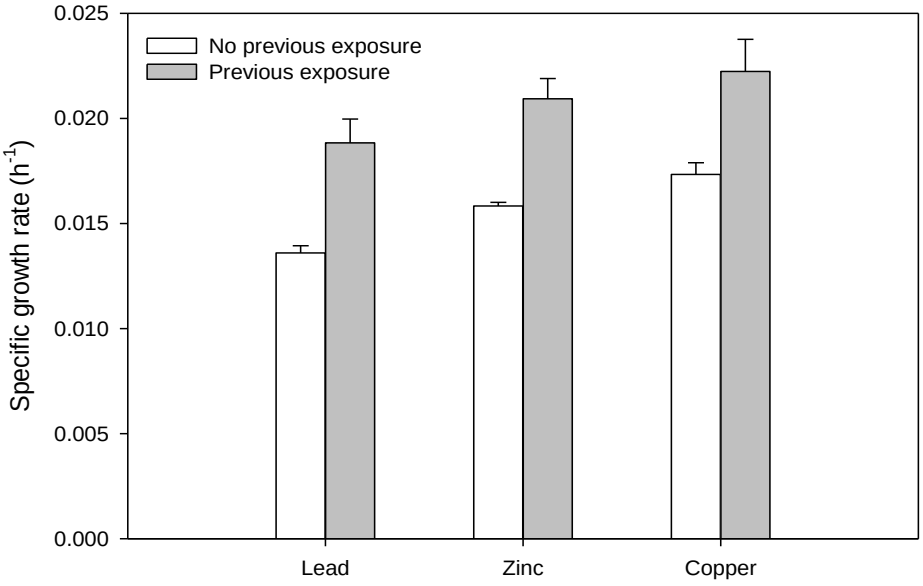


Figure 14. Effect of prior exposure to lead, zinc, and copper on the specific growth rate of *Acidithiobacillus caldus* strain BC13. Cells were adapted through subsequent culturing and transfers in the presence of the half-maximal inhibitory concentrations of lead, zinc, or copper (0.94 mM, 39 mM, and 120 mM, respectively). Error bars represent 95% confidence intervals.

medium, the cultures grew to final cell concentrations of only 83 ± 1% and 83 ± 23% of the final cell concentration observed in cultures with no prior exposure to zinc or copper, respectively. The observed specific growth rates of cells exposed to MICs of lead, zinc, and copper for 120 hours were 0.032 ± 0.003, 0.028 ± 0.002, and 0.030 ± 0.003 h^{-1}, respectively, after being re-inoculated into fresh, metal-free medium. Cells that had not been pre-treated by the MICs of lead, zinc, or copper, exhibited an observed specific growth rate of 0.029 ± 0.003, suggesting that there were no significant residual affects on the observed specific growth rates (Appendix G).

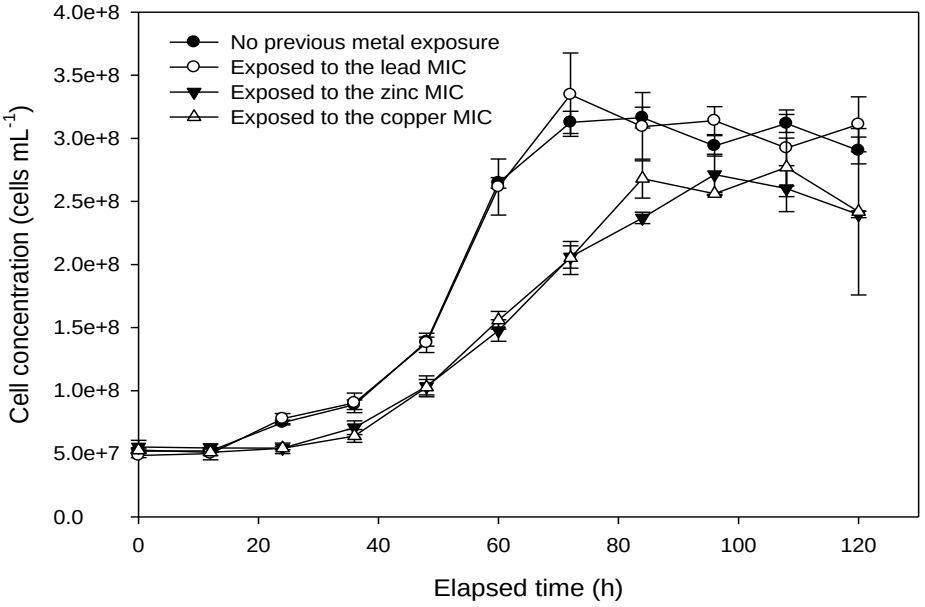


Figure 15. Growth of *Acidithiobacillus caldus* strain BC13 in metal-free cultures after cells were harvested from cultures containing minimum inhibitory concentrations of lead, zinc, or copper, or 7.5, 75, and 250 mM, respectively. Error bars represent 95% confidence intervals.

Comparison of Metal Chloride and Metal Sulfate Toxicity

Figure 16 shows that when lead, zinc, and copper chlorides were added at concentrations equal to the IC_{50}s of their respective sulfates, the observed specific growth rates were lower than those observed for the metal sulfates. For lead, this difference was relatively minor, 0.012 ± 0.001 h^{-1} versus 0.014 ± 0.000 h^{-1}, respectively. However, in the case of zinc and copper, the differences were more pronounced. The specific growth rate observed when zinc chloride was used was 0.012 ± 0.001 h^{-1}, compared to 0.016 ± 0.000 h^{-1} when zinc sulfate was added. Similarly, the specific growth rate observed when copper chloride was added was 0.012 ± 0.000 h^{-1}, compared to 0.017 ± 0.001 h^{-1} when copper sulfate was used.

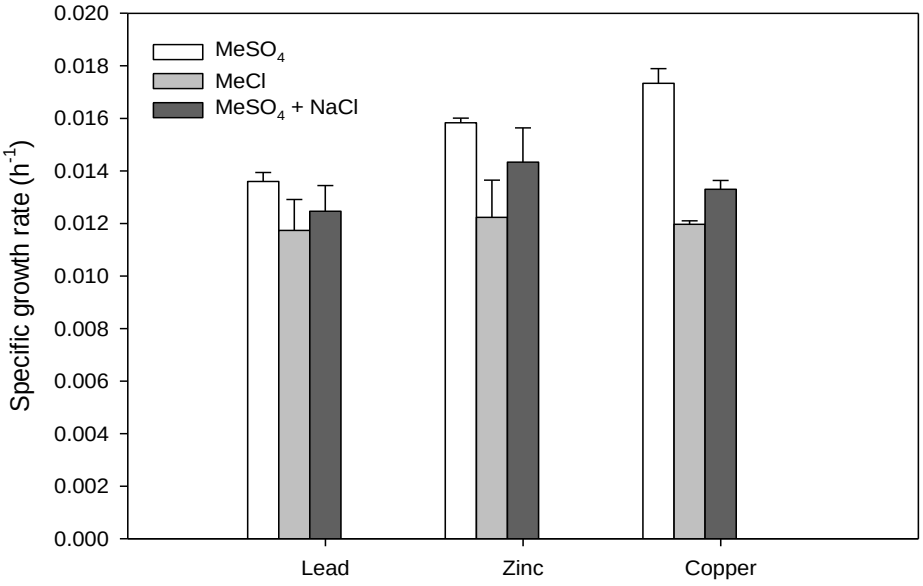


Figure 16. Effect of lead, zinc, and copper on the specific growth rate of *Acidithiobacillus caldus* strain BC13 when added as either metal sulfates, metal chlorides, or as metal sulfates with a corresponding concentration of sodium chloride. In each case, metals were added to concentrations equal to previously calculated half-maximal inhibition concentrations for the corresponding metal sulfates, or 0.94 mM, 39 mM, and 120 mM, for lead, zinc, and copper, respectively. Error bars represent 95% confidence intervals.

The specific growth rate of BC13 also decreased when only sodium chloride was added to metal-free medium. When sodium chloride was added to concentrations of 0, 50, 100, and 200 mM, the specific growth rates were 0.029 ± 0.002, 0.027 ± 0.001, 0.023 ± 0.001, and 0.021 ± 0.001h^{-1}, respectively. In other experiments, lead, zinc, and copper sulfate was added to concentrations equal to their respective IC_{50}s, and the sodium chloride concentration was varied. The inhibition observed in these tests suggested that the metal-chloride toxicity effects are additive (Figure 17).

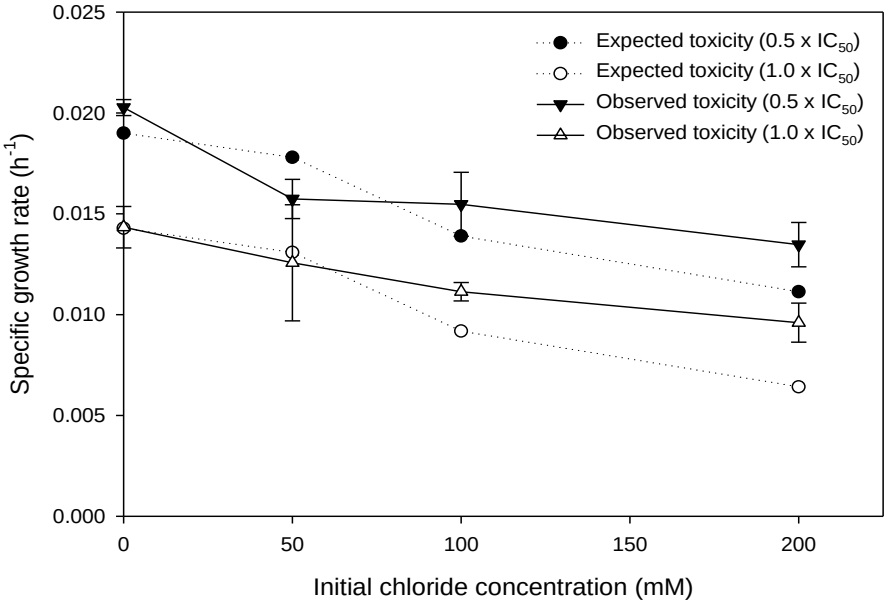


Figure 17. Predicted and observed effect of chloride concentrations on the specific growth rate of *Acidithiobacillus caldus* strain BC13 with zinc sulfate added to a concentration equal to either 50% or 100% of the previously calculated half-maximal inhibition concentration (39 mM). Similar results were observed with lead and copper (Appendix G). Error bars represent 95% confidence intervals.

Metal Complexation and Precipitation

Visual MINTEQ predicted the complexation and potential precipitation of lead, zinc, and copper over the range of concentrations and combinations used in these experiments. The primary dissolved constituents of lead, zinc, and copper were aqueous divalent metal cations and metal sulfates, regardless of whether the metals were added as metal sulfates or metal chlorides. Lead was predicted to remain soluble up to a concentration of 20 μM. Concentrations used in these experiments were beyond this value. No precipitation was predicted for zinc or copper (Appendix G).

MINTEQ modeling results and the multi-variant statistical software MINITAB, and compared against changes in the corresponding observed specific growth rates. Matrix plots and primary component analyses suggested that for all the metals, only changes in the total metal concentrations correlated strongly with changes in observed specific growth rates, and that speciation was not a significant factor (Appendix G).

Discussion

Single toxicity of Lead, Zinc, and Copper

BC13 grew in millimolar concentrations of lead, zinc, and copper, with lead being the most inhibitory metal tested, with an MIC of 7.5 mM. Interestingly, *At. caldus* has not been isolated from environments containing high levels of galena [27]; and results reported here suggest that these environments may contain lead concentrations too high for significant *At.* caldus activity (Figure 11a). BC13 exhibited relatively high tolerances for zinc and copper, with MICs of 75 and 250 mM (Figures 11b and c). This is not surprising as many of the environments where *At. caldus* has been identified have high concentrations of zinc and copper [4,27-29].

Previous work with *At. caldus* strain KU reported MIC values of 65 g L^{-1} (993.9 mM) for zinc, and only 1.5 g L^{-1} (23.6 mM) for copper [26], suggesting a zinc tolerance significantly higher than that observed here, and a copper tolerance significantly lower. The previous work did not report methods for quantifying growth, or describe the growth medium used [26], making a direct comparison difficult. These differences may be due to strain to strain variance in metal tolerance, medium composition, or possibly inoculum

history. Regardless, it is apparent that BC13 and strain KU are quite tolerant to zinc and copper.

Comparisons with Other Acidithiobacilli

High resistance to zinc and copper is not unprecedented among the acidithiobacilli. Aside from previous work with *At. caldus* strain KU [26], *At. ferrooxidans* has been observed to grow on ground sulfur in a medium containing 100 mM copper [30], and can facilitate spalerite leaching in the presence of 25 mM zinc, and chalcopyrite leaching in the presence of 10-25 g L^{-1} of copper (158-397 mM) [18,30]. Barreira et al. [16] and Chen et al. [17] made similar observations while working with *At. thiooxidans*.

With observed MIC values of 75 mM and 250 mM for zinc and copper, respectively, the present study suggests that BC13 has a similar level of tolerance to zinc and copper as *At. ferrooxidans* and *At. thiooxidans*. However, it is important to note key differences between this work and previous work with acidithiobacilli. First, the present study used a soluble substrate (tetrathionate). Conversely, previous work with acidithiobacilli species used solid substrates, which may encourage the formation of biofilms and provide some protection from metals [31]. Secondly, the present study characterized inhibition with respect to cell growth, rather than leaching kinetics.

Effects of Combined Metals

Metals presented in binary mixtures exhibited less than additive toxicity towards BC13, suggesting an aspect of competitive inhibition (Figure 12). In addition, the

apparent dampening effect of ferrous iron on lead, zinc, and copper toxicity (Figure 13) is also quite interesting, given that many environments where *At. caldus* has been isolated from also contain high concentrations of iron, both reduced and oxidized, relevant to the concentrations used in this study [*i.e.* 4,27-29]. This suggests that BC13 may exhibit catabolic activity (*i.e.* leaching) in environments containing lead, zinc, and copper concentrations higher than the respective MIC values reported here. Previous studies have also observed less than additive toxicity effects of binary-metal systems. Gikas et al. observed that nickel(II) and cobalt(II) exhibited similar individual toxicities to microbes growing in an activated sludge, however when presented in combination, their toxicities were significantly reduced [32].

Effect of Inoculum History

One aspect of cell culturing that is often overlooked in toxicity studies is inoculum history. In the current study, pre-adaption to lead, zinc, or copper increased specific growth rates of BC13 significantly when subsequently exposed to heavy metals (Figure 14). Similar results have been observed by others [*i.e.*, 33-35], and may indicate higher tolerances in *in situ* environments where species have had prolonged exposure to metals.

Another aspect of prior metal exposure examined here was the effect of prior exposure to the MIC of lead, zinc, and copper. Cells harvested from these conditions did grow when re-inoculated into fresh, metal-free medium (Figure 15), suggesting that lead, zinc, and copper may simply slow cell growth, perhaps through increased energy requirements. However, when cells were collected from MIC exposures to zinc or

copper, they did not grow as well as cells collected from MIC exposure to lead (Figure 15). This may be due to residual metal strongly bound to the cells. As is discussed in chapter five, BC13 has larger sorption capacities for zinc and copper than lead. The ability of BC13 to adapt to heavy-metals, and be resuscitated from exposure to heavy-metal MICs may suggest that cells are viable and metabolically active in environments containing lead, zinc, or concentrations significantly higher than the MICs observed when these metals are presented individually.

Metal Sulfate versus Metal Chloride Toxicity

Figure 16 shows the increased toxicity of metal chlorides over metal sulfates, and Figure 17 suggests that this is due to additive toxicity, as additional experiments showed that chloride itself was inhibitory to BC13. This may explain why lead chloride toxicity was not significantly different than lead sulfate, as corresponding the chloride concentration would have been only 1.9 mM, which was not observed to be toxic when sodium chloride was added in the absence of lead, zinc, or copper (Appendix G). Conversely, the chloride concentrations associated with zinc and copper chlorides (78 and 240 mM) were toxic even in the absence of metals. This idea is supported by past work that reported chloride inhibition towards the acidithiobacilli [36], and although the chloride concentrations necessary to achieve this effect are not necessarily relevant to natural environments containing *At. caldus* [28,29], these results do emphasize the importance of metal salts chosen for inhibition studies.

Conclusions

This is the first comprehensive report on lead, zinc, or copper toxicity to *At. caldus*, and the first study reporting the toxicity of lead to any acidithiobacilli. The order of toxicity observed here was copper < zinc < lead, and the relatively high tolerance observed to zinc and copper were comparable to those observed in other acidithiobacilli [16-18,30]. Additional studies using binary-metal mixtures and high ferrous iron concentrations were carried out to better relate the single metal toxicity observations to *in situ* realities. Interestingly, these studies suggested that binary-metal mixtures, and the presence of ferrous iron, significantly decreased the toxicity of lead and zinc to BC13. In addition, inoculum history was an important factor in metal tolerance, as cells adapted to lead, zinc, and copper through subsequent culturing showed significantly increased tolerance to these metals. Combined, these results may suggest that BC13 may grow and be metabolically active in *in situ* environments containing lead, zinc, or copper concentrations higher than the MICs observed here when these metals were presented individually.

Finally, a comparison of metal sulfate versus metal chloride toxicity suggested that metal sulfates were much less toxic to BC13, as chloride ions exhibited an inhibitory effect of their own, which was approximately additive with that of lead, zinc, or copper.

Acidophilic chemolithoautotrophs play important roles in acid-mine systems due to their tolerance [37] and mobilization of metals [38,39]. This study improves the understanding of one such microorganism, BC13, and may lead the way for future research of specific toxicity mechanisms and metal-regulated protein expression.

References

1. Hallberg KB, Lindstrom EB (1994) Characterization of *Thiobacillus caldus* sp. nov., a moderately thermophilic acidophile. *Microbiology* 140:3451-3456.

2. Dopson M, Lindstrom EB, Hallberg KB (2002) ATP generation during reduced inorganic sulfur compound oxidation by *Acidithiobacillus caldus* is exclusively due to electron transport phosphorylation. *Extremophiles* 6:123-129.

3. Burton NP, Norris PR (2000) Microbiology of acidic, geothermal springs of Montserrat: environmental rDNA analysis. *Extremophiles* 4:315-320.

4. Druschel GK, Baker BJ, Gihiring TM, Banfield JF (2004) Acid mine drainage biogeochemistry at Iron Mountain, California. *Geochem Trans* 5:12-32.

5. Goebel BM, Stackebrandt E (1994) Cultural and phylogenetic analysis of mixed microbial populations found in natural and commercial bioleaching environments. *Appl Environ Microbiol* 60:1614-1621.

6. Okibe N, Gericke M, Hallberg KB, Johnson DB (2003) Enumeration and characterization of acidophilic microorganisms isolated for a pilot plant stirred-tank bioleaching operation. *Appl Environ Microbiol* 69:1936-1943.

7. McGuire MM, Edwards KJ, Banfield JF, Hamers RJ (2001) Kinetics, surface chemistry, and structural evolution of microbially mediated sulfide mineral dissolution. *Geochem Geophys Geosyst* 65:1243-1258.

8. Dopson M, Lindstrom EB (1999) Potential role of *Thiobacillus caldus* in arsenopyrite bioleaching. *Appl Environ Microbiol* 65:36-40.

9. Zhou QG, Bo F, Bo ZH, Xi L, Jian G, Fei LF, Hau CH (2007) Isolation of a strain of *Acidithiobacillus caldus* and its role in bioleaching of chalcopyrite. *World J Microbiol Biotechnol* 23:1217-1225.

10. Gadd GM, Griffiths AT (1978) Microorganisms and heavy metal toxicity. *Microb Ecol* 4:303-317.

11. Nies DH (1999) Microbial heavy-metal resistance. *Appl Microbiol Biotechnol* 51:730-750.

12. Nies DH (2000) Heavy metal-resistant bacteria as extremophiles: molecular physiology and biotechnological use of Ralstonia sp CH34. *J Bacteriol* 182:1390-1398.

13. Nies DH (2003) Efflux-mediated heavy metal resistance in prokaryotes. *FEMS Microbiol Rev* 23:313-339.

14. Silver S (1996) Bacterial resistance to toxic ions - a review. *Gene* 179:9-19.

15. Wood JM, Wang HK (1983) Microbial resistance to heavy metals. *Environ Sci Technol* 17:582-590.

16. Barreira RPR, Villar LD, Garcia O (2005) Tolerance to copper and zinc of *Acidithiobacillus thiooxidans* isolated from sewage sludge. *World J Microbiol Biotechnol* 21:89-91.

17. Chen BY, Chen YW, Wu DJ, Cheng YC (2003) Metal toxicity assessment upon indigenous *Thiobacillus thiooxidans* BC1. *Environ Eng Sci* 20:375-385.

18. Das A, Modak JM, Natarajan KA (1997) Studies on multi-metal ion tolerance of *Thiobacillus ferrooxidans*. *Miner Eng* 10:743-749.

19. Leduc LG, Ferroni GD, Trevors JT (1997) Resistance to heavy metals in different strains of *Thiobacillus Ferrooxidans*. *World J Microbiol Biotechnol* 13:453-455.

20. Natarajan KA, Sudeesha K, Rao GR (1994) Stability of copper tolerance in *Thiobacillus ferrooxidans*. *Antonie van Leeuwenhoek* 66:303-306.

21. Tuovinen OH (1974) Studies on the growth of *Thiobacillus ferrooxidans*. II. Toxicity of uranium to growing cultures and tolerance conferred by mutation, other metal cations and EDTA. *Arch Microbiol* 95:153.

22. Hong-mei L, Jia-jun K (2001) Influence of Ni^{2+} and Mg^{2+} on the growth and activity of Cu^{2+}-adapted *Thiobacillus ferrooxidans*. *Hydrometallurgy* 61:151-156.

23. Dopson M, Lindstrom EB, Hallberg KB (2001) Chromosomally encoded arsenical resistance of the moderately thermophilic acidophile *Acidithiobacillus caldus*. *Extremophiles* 5:247-255.

24. Kotze AA, Tuffin IM, Deane SM, Rawlings DE (2006) Cloning and characterization of the chromosomal arsenic resistance genes from *Acidithiobacillus caldus* and enhanced arsenic resistance on conjugal transfer of *ars* genes located on transposon Tn*AtsArs*. M*icrobiology* 152:3551-3560.

25. Tuffin M, Hector SB, Deane SM, Rawlings DE (2006) Resistance determinants of a highly arsenic-resistant strain of *Leptospirillum feriphilum* isolated from a commercial biooxidation tank. *Appl Environ Microbiol* 72:2247-2253.

26. Watkin ELJ, Keeling SE, Perrot FA, Shiers DW, Palmer ML, Watling HR (2009) Metals tolerance in moderately thermophilic isolates from a spent copper sulfide heap, closely related to *Acidithiobacillus caldus*, *Acidimicrobium ferrooxidans* and *Sulfobacillus thermosulfidooxidans*. *J Ind Microbiol Biotechnol* 36:461-465.

27. Rawlings DE (2002) Heavy metal mining using microbes. *Ann Rev Microbiol* 56:65-91.

28. Banks D, Younger PL, Arnesen RT, Iversen ER Banks SB (1997) Mine-water chemistry: the good, the bad and the ugly. *Environ Geology* 32:157-174.

29. Benner SG, Blowes DW, Gould WD, Herbert RB, Ptacek CJ (1999) Geochemistry of a permeable reactive barrier for metals and acid mine drainage. *Environ Sci Technol* 33:2793-2799.

30. Alvarez S, Jerez C (2004) Copper ions stimulate polyphosphate degradation and phosphate efflux in *Acidithiobacillus ferrooxidans*. *Appl Environ Microbiol* 70:5177-5182.

31. Xu KD, McFeters GA, Stewart PS (2000) Biofilm resistance to antimicrobial agents. *Microbiology* 146:547-549.

32. Gikas P (2007) Kinetic response of activated sludge to individual and joint nickel (Ni(II)) and cobalt (Co(II)): an isobolographic approach. *J Haz Mat* 143:246-256.

33. Oorts KK (2006) Discrepancy of the microbial response to elevated copper between freshly spiked and long-term contaminated soils. *Environ Toxicol Chem* 25:845-853.

34. Oorts KK (2007) Leaching and aging decrease nickel toxicity to soil microbial processes in soils freshly spiked with nickel chloride. *Environ Toxicol Chem* 26:1130-1138.

35. Maderova L, Dawson JJC, Paton GI (2009) Cu and Ni mobility and bioavailability in sequentially conditioned soils. *Water Air Soil Pollut* DOI 10.1007/s11270-009-0224-4

36. Kawabe Y, Chihiro I, Tadashi C (2000) Relaxation of chloride inhibition on the biochemical activity of *Thiobacillus ferrooxidans* by Diatomaceous Earths. *J Mining and Mat Process Inst of Japan* 116:198-202.

37. Dopson M, Baker-Austin C, Koppineedi PR, Bond PL (2003) Growth in sulfidic mineral environments: metal resistance mechanisms in acidophilic microorganisms. *Microbiol* 149:1959-1970.

38. Gadd GM (2000) Bioremedial potential of microbial mechanisms of metal mobilization and immobilization. *Cur Opin Biotech* 11:271-279.

39. Veglio F, Beolchini F (1997) Removal of metals by biosorption: a review. *Hydrometallurgy* 44:301-316.

CHAPTER 5

EFFECTS OF CELL CONDITION, PH, AND TEMPERATURE ON LEAD, ZINC, AND COPPER SORPTION TO *ACIDITHIOBACILLUS CALDUS* STRAIN BC13

Abstract

This study describes the effects of cell condition, pH, and temperature on lead, zinc, and copper sorption to BC13 with a Langmuir model. Copper exhibited the highest loading capacity, 4.76 ± 0.28 mmol g^{-1}, to viable cells at pH 5.5. The highest binding-site affinity observed was 61.2 ± 3.0 L $mmol^{-1}$ to dehydrated cells at pH 4.0. The pHs that maximized loading capacities and binding-site affinities were generally between 4.0 and 5.5, where the sum of free proton and complexed metal concentrations was near a minimum. Of additional importance, lead, zinc, and copper sorbed to viable cells at pH values as low as 1.5. Previous studies with other acidithiobacilli did not measure viable-cell sorption below pH 4.0. In separate experiments, desorption studies showed that far less copper was recovered from viable cells than any other metal or cell condition, suggesting that uptake may play an important role in copper sorption by BC13. To reflect an applied system, the sorption of metal mixtures was also studied. In these experiments, lead, zinc, and copper sorption from a tertiary mixture were 40.2 ± 4.3, 28.7 ± 3.8, and 91.3 ± 3.0%, respectively, of that sorbed in single metal systems.

Introduction

At. caldus is a thermophilic acidophile that oxidizes reduced sulfur compounds, fixes carbon dioxide [1], has been isolated from several acidic environments [2-4], and is believed to be important for leaching metals from mineral sulfides in acid-mine environments [5-9]. Despite its important interactions with metals in such systems there have been no metal sorption studies published to date with this organism.

Microbial sorption has been used as a relatively inexpensive tool for the immobilization of heavy metals from many types of contaminated systems [10]. Relevant to the work presented here, studies have shown that *At. thiooxidans* and *At. ferrooxidans* can remove heavy metals from contaminated soil and sewage systems [11-13]. In addition, zinc and copper sorption to *At. thiooxidans* and *At. ferrooxidans* has been studied by several researchers [14-17], and are important in metal mobilization and transport [18]. However, these organisms are typically found at temperatures below 35°C, whereas *At. caldus* grows optimally at 45° [1]. This suggests that a metal sorption study using *At. caldus* is very relevant to warmer systems.

Here, the sorption of lead, zinc, and copper to BC13 is described with a Langmuir model. In contrast to most prior research, experiments were carried out using viable cells, between pH 1.5 and 7.0, and from 25 to 45C°. Tests were also carried out with dehydrated cells for comparison to previous work [14-17]. The effects of proton competition and metal speciation were investigated with changing pH. In addition, temperature effects were used to calculate the heat of sorption for lead, zinc, and copper to BC13 . Finally, the sorption of metal mixtures to BC13 was measured to determine

how the presence of competing metals affected the sorption capacity of lead, zinc, and copper. The use of viable cells and mixed metal systems provides an important fundamental link between past results and the mixed metal systems found in acid-mine drainage and many remediation applications. This study increases the understanding of *At. caldus*' role in the fate and mobilization of metals and may lead the way for more applied studies with this organism.

Materials and Methods

Culture and Cell Preparation

A basal salts medium [1] was prepared and autoclaved for 15 minutes at 121°C and 22 psig, and allowed to cool to room temperature. A trace element solution [1] was then added to a concentration of 1 mL L^{-1}, and a filter sterilized (0.2 μm) potassium tetrathionate was added to a concentration of 5 mM to provide an electron donor. The medium pH was adjusted to 2.5 using 6N sulfuric acid, aliquoted into 500-mL serum bottles (350 mL medium volume), and capped with butyl-rubber stoppers. A 20:80 mixture of carbon dioxide:nitrogen gas was sparged into the medium to a headspace pressure of 5 psig to provide a carbon source. BC13 (ATCC 51757) cells preserved at 4°C in nanopure water (17.4 MΩ, with the pH adjusted to 3.0 using 6N sulfuric acid), provided the initial inoculum). Cultures were grown aerobically at 45°C and shaken at 150 rotations per minute (rpm). Cells were harvested via centrifugation during the mid-exponential growth phase and washed using the pH 3.0 nanopure water. This wash was repeated three times to remove residual potassium tetrathionate.

Cell pellets for use in viable-cell sorption studies were re-suspended in a small aliquot of the basal salts medium at a concentration of 1 g dry-cell weight L^{-1}. Cell pellets for use in dehydrated-cell sorption studies were dried in a Samdri-795 critical point dryer (Tousimis, Rockville, MD). Sorption experiments were done immediately to avoid potential effects of cell storage.

The sorption experiments were carried out in the same basal salts medium, but without potassium tetrathionate. A filter sterilized (0.2 μm) metal solution (lead, zinc, or copper sulfates) was added from a stock solution prepared in the medium. The pH was adjusted to 1.5, 2.5, 4.0, 5.5, or 7.0, using either 6N sulfuric acid or 10N sodium hydroxide. Following cell preparation, aliquots that provided an initial cell density of 100 mg dry-cell weight L^{-1} were added to 125-mL Erlenmeyer flasks (75 mL medium volume) fitted with foam stoppers. Samples were shaken at 150 rpm at 25, 35, or 45°C in a temperature controlled incubator.

Measurement of Aqueous Metal Concentrations

Filter sterilized (0.2 μm) samples were taken and preserved at 4°C for analysis. Inductively coupled plasma mass spectrometry (ICP-MS) (Agilent 7500ce ORS, Foster City, CA, U.S.A.) using an Octopole Reaction System and a MicroMist glass concentric nebulizer was used to measure metal concentrations. The sample temperature was set at 2°C and the radio frequency power was set to 1500 W. Argon was used as the carrier gas, at a flow rate of 0.64 L min^{-1}. The nebulizer pump was operated at 0.15 rotations per second (rps) and the sample pump was set to 0.1 rps. Measurements were compared with

standards to calculate metal concentrations. Germanium and indium were used as internal standards to correct for drift over a series of runs.

Calculation of Sorption Parameters

The Langmuir Equation (Equation 5.1) is derived for monolayer sorption onto a surface with a finite number of homogenous binding sites, where the occupation of one site does not affect the binding affinity of adjacent sites.

$$Q_e = \frac{Q_o k_L C_e}{1 + k_L C_e} \qquad (5.1)$$

Where Q_e is the concentration of sorbed metal at equilibrium, Q_o is the maximum amount of metal per unit sorbent required for a complete monolayer (loading capacity), C_e is the equilibrium metal concentration in solution, and k_L describes binding-site affinity by Equation 5.2:

$$k_L = \frac{\Phi}{(1-\Phi)C_e} \qquad (5.2)$$

where Φ is defined as the percent coverage of binding-sites.

Equation 5.1 may be re-written in the linear form:

$$\frac{1}{Q_e} = \frac{1}{Q_o k_L C_e} + \frac{1}{Q_o} \qquad (5.3)$$

Lineweaver-Burk plots of $\frac{1}{Q_e}$ versus $\frac{1}{C_e}$ were used to calculate values for Q_o and k_L.

Calculation of the Heat of Sorption

The Arrhenius Equation (Equation 5.4) was used to calculate the heat of lead, zinc, and copper sorption to BC13.

$$k_L = Ae^{[-E_a(RT)^{-1}]} \qquad (5.4)$$

where A is the Arrhenius pre-exponential factor, E_a is the activation energy, R is the universal gas constant, and T is the absolute temperature. Because this is an equilibrium calculation, E_a represents the difference between the activation energy required for sorption to occur, and the activation energy required for desorption to occur. This difference is equal to the enthalpy of sorption ($\Delta H_{sorption}$), assuming the thermal expansivity of the solution is negligible. Therefore:

$$E_a = \Delta H_{sorption} \qquad (5.5)$$

Because Equation 5.4 may be re-written in the linear form:

$$\ln(k_L) = \ln(A) - \frac{\Delta H_{sorption}}{RT} \qquad (5.6)$$

A plot of $\ln(k_L)$ versus $\frac{1}{RT}$ has a slope equal to the negative heat of sorption, and a y-intercept equal to the natural logarithm of the Arrhenius pre-exponential factor.

Desorption Experiments

Separate sorption experiments were done at 45ºC and either pH 1.5, 4.0, or 7.0. At equilibrium, cells were collected via centrifugation, and re-suspended in fresh basal salts medium containing 5 mM nitrilotriacetic acid (NTA). This solution was placed in a

temperature controlled incubator at 45ºC and shaken at 150 rpm until the system equilibrated. Filter sterilized (0.2 μm) samples were taken and preserved at 4°C for analysis using ICP-MS. In these experiments, results were compared between whole and lysed cells. To lyse cells, cultures were autoclaved for 15 minutes at 121°C and 22 psig, then sonicated for one minute with a Bronson 1020 sonicator (Danbury, CT, U.S.A.). Cell lysis was confirmed visually using a transmitted-light microscopy (Zeiss, Thornwood, NY, U.S.A.).

Mixed Metal Sorption

Mixed metal sorption was studied with viable cells at physiologically relevant conditions (pH 2.5 and 45°C) using the same techniques for cell preparation, experimental design, and measurement of aqueous metal concentrations described earlier. The initial concentrations of lead, zinc, and copper were 0.24, 0.92, and 1.57 mM. For direct comparison with single metal systems, these concentrations were equal to the highest initial metal concentrations used in the individual sorption studies.

Modeling Metal Speciation

Visual MINTEQ (version 2.53) was used to predict the speciation of metal using activities from the Debye-Huckel Equation, and the default MINTEQA2 thermodynamic database. The temperature was set to 45°C and the free-proton concentration was calculated from the pH, which was fixed at 1.5, 2.5, 4.0, 5.5, or 7.0. The lead, zinc, and copper concentrations used were 0.24, 0.92, and 1.57 mM, respectively, to match the highest metal concentrations used in the sorption experiments.

Statistical Analysis and Controls

In separate experiments, cells were cultured in the basal salts growth medium described earlier, with the pH adjusted to 1.5, 2.5, or 4.0 at 45°C, covering the pH range over which *At. caldus* grows well [1]. These cells were then prepared for sorption experiments at the same pH they were grown at. The results were not statistically different from those observed when the growth medium pH differed from the sorption medium pH (Appendix H).

All experiments were performed in triplicate, and average values and 95% confidence intervals were calculated. Langmuir and Arrhenius parameters, and corresponding 95% confidence intervals, were calculated with multiple linear regressions using the LINEST function in Microsoft Excel.

Results

Effect of pH on Lead, Zinc, and Copper Sorption

Figure 18 shows the sorption of lead, zinc, and copper to viable and dehydrated cells over time, at pH 2.5 and 45°C. It can be seen that viable-cell systems equilibrated more slowly than dehydrated-cell systems. Using equilibrium concentrations, Lineweaver-Burk plots were used to calculate loading capacities and binding-site affinities. Figure 19 shows the Lineweaver-Burk plot for the sorption of zinc to viable BC13 cells, at pH 2.5 and 45°C. Results for all conditions tested for lead, zinc, and copper sorption are not shown, but showed similar trends and variances. R^2 values for these plots varied between 0.88 and 0.98 (Appendix H).

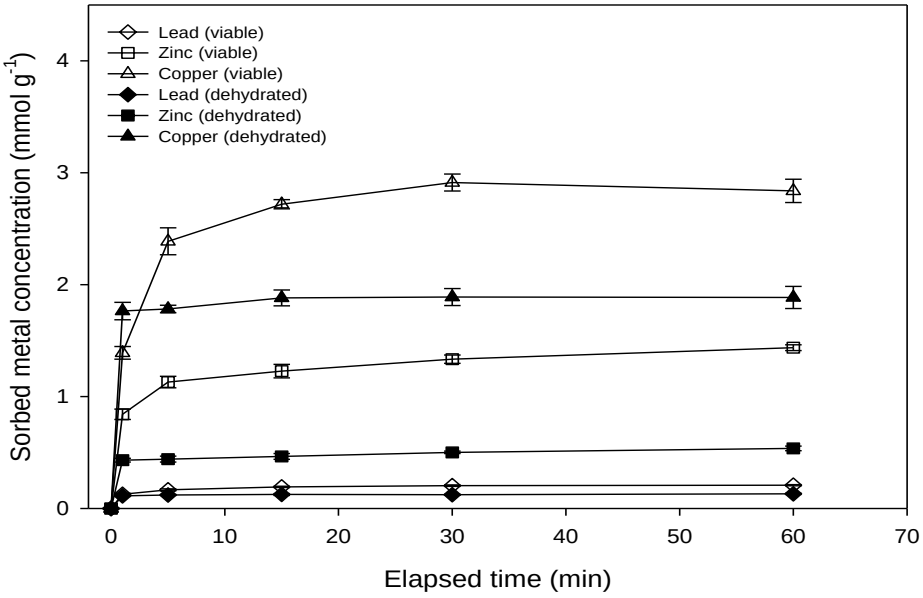


Figure 18. Change in sorbed lead, zinc, and copper concentrations to viable and dehydrated *Acidithiobacillus caldus* strain BC13 cells with time at pH 2.5 and 45°C. Error bars represent 95% confidence intervals.

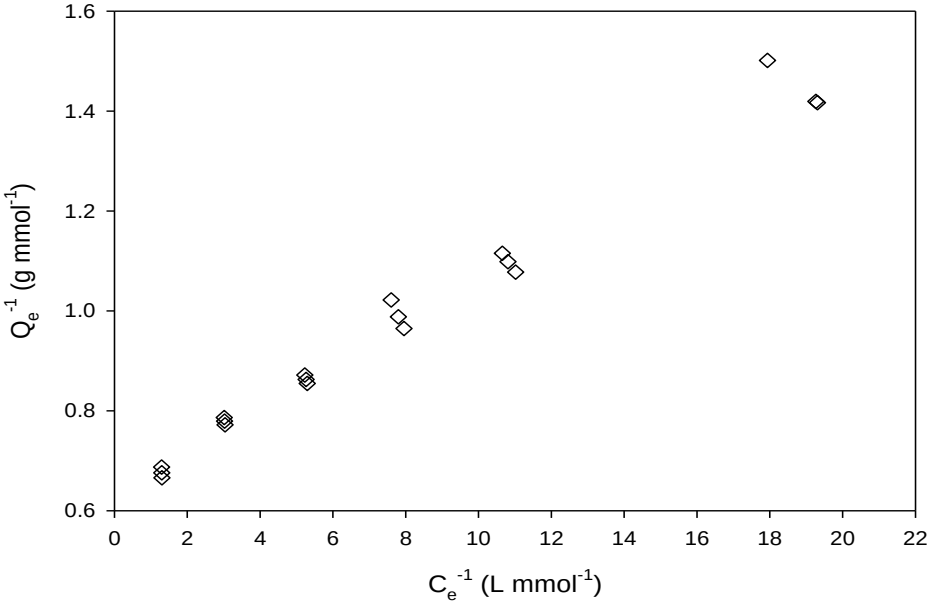


Figure 19. A Lineweaver-Burk plot of the linearized Langmuir Equation. Here, the sorption of zinc to viable *Acidithiobacillus caldus* strain BC13 cells, at pH 2.5 and 45°C, is represented. The plotted values are the inverse of metal sorbed, Q_e^{-1}, and metal in solution, C_e^{-1}, at equilibrium.

Figure 20 shows the effect of pH on the loading capacities and binding-site affinities for lead, zinc, and copper to viable and dehydrated cells at 45°C. Viable cells were observed to

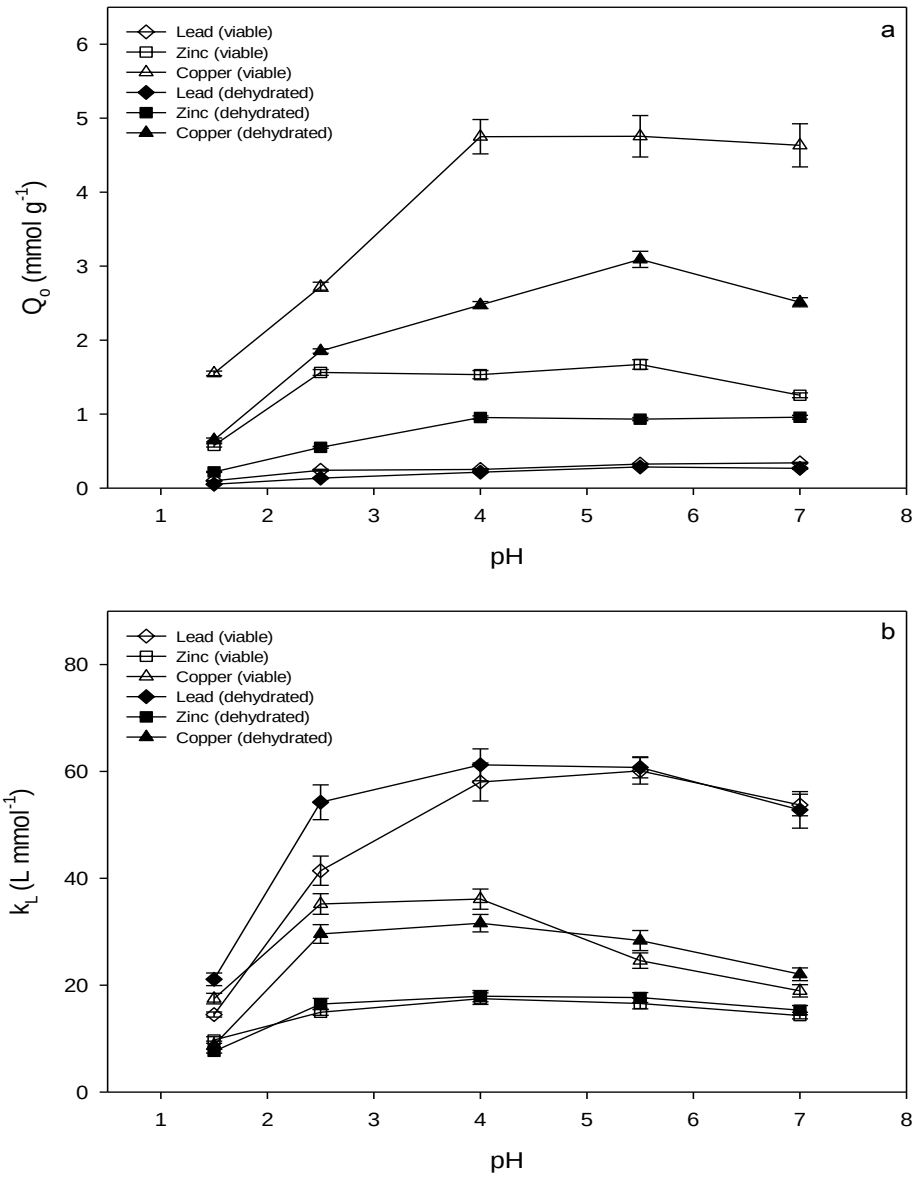


Figure 20. The effect of pH on the (a) loading capacity (Q_o), and (b) binding-site affinity (k_L) for the sorption of lead, zinc, and copper to viable and dehydrated *Acidithiobacillus caldus* strain BC13 cells. Error bars represent 95% confidence intervals.

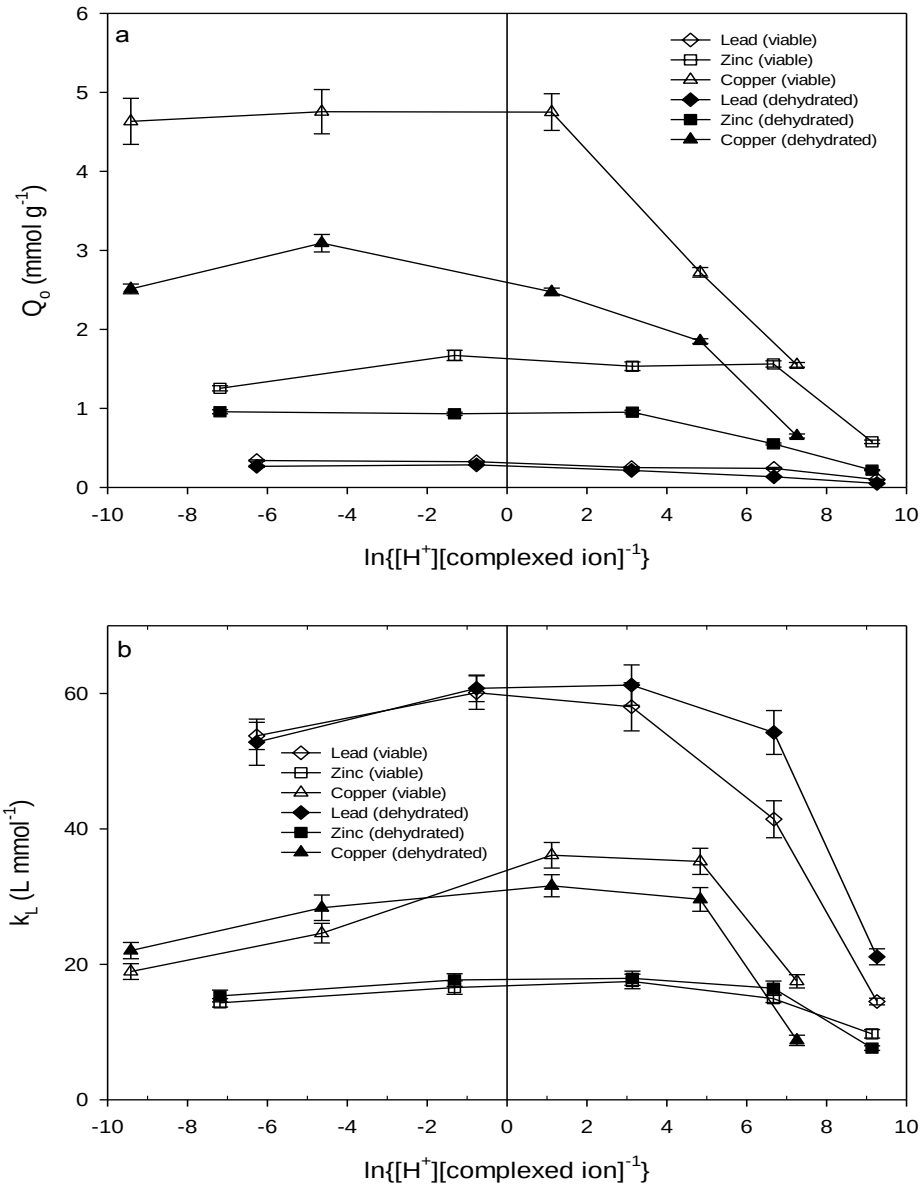


Figure 21. The relationship between the free-proton and complexed lead, zinc, or copper concentrations on the (a) loading capacity (Q_o), and (b) binding-site affinity (k_L) for the sorption of lead, zinc, and copper to viable and dehydrated *Acidithiobacillus caldus* strain BC13 cells. Complexed ions are any ions other than monoatomic divalent lead, zinc, and copper. Concentrations of 0.24, 0.92, and 1.57 mM for lead, zinc, and copper, respectively, were used to model speciation. These were the highest aqueous concentrations used in this study, and represent conditions where each binding site could theoretically interact with a metal molecule. Error bars represent 95% confidence intervals.

have higher loading capacities, for zinc and copper, than dehydrated cells. However, in the case of lead, the loading capacities for viable and dehydrated cells were very close. Copper exhibited the highest loading capacity, 4.76 ± 0.28 and 3.09 ± 0.11 mmol g^{-1} to viable and dehydrated cells, respectively, at pH 5.5 (Figure 20a). The highest binding-site affinities observed were for lead, 60.1 ± 2.5 L $mmol^{-1}$ at pH 5.5, and 61.2 ± 3.0 L $mmol^{-1}$ at pH 4.0, for viable and dehydrated cells, respectively (Figure 20b).

The ratios of free-proton to complexed metal concentrations are plotted on a natural logarithm scale against loading capacity (Figure 21a) and binding-site affinity (Figure 21b). A vertical line at y = 0 represents the pH where the free-proton

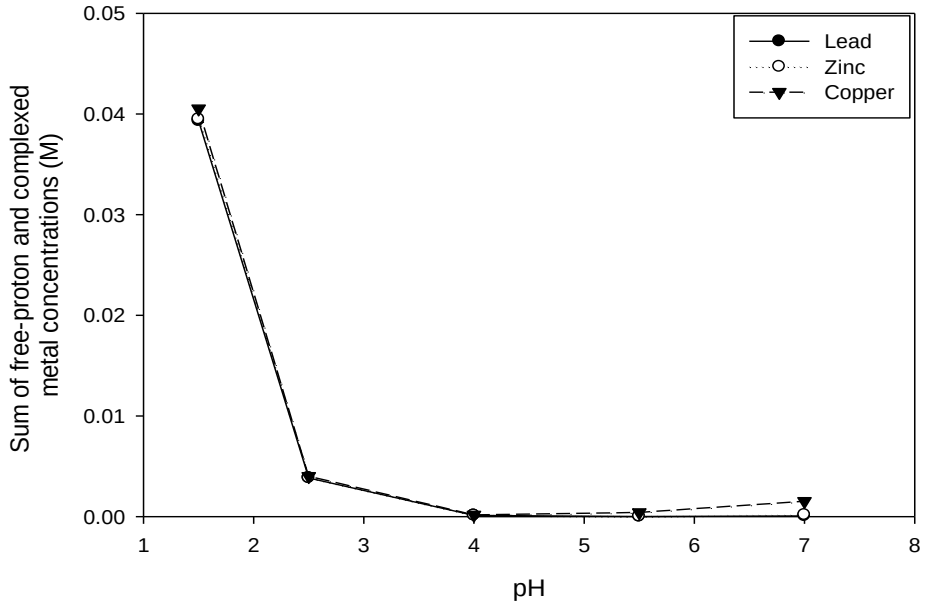


Figure 22. Sum of the free-proton and complexed-metal concentrations, representing two sources of competition for metal sorption onto a cellular binding-site. Concentrations of 0.24, 0.92, and 1.57 mM for lead, zinc, and copper, respectively, were used to model speciation. These were the highest aqueous concentrations used in this study, and represent conditions where each binding site could theoretically interact with a metal molecule.

concentration is equal to the complexed-metal concentration. The ratio at which the loading capacity is maximized varied among lead, zinc, and copper, and between viable and dehydrated cells. However, Figure 21b shows that, for each metal and cell condition, the binding-site affinity was maximized when the free proton concentration is higher than the complexed metal concentration. The sum of the free proton and complexed metal concentrations is shown with pH in Figure 22.

Temperature Effects

At pH 2.5, the loading capacities of lead and zinc onto viable and dehydrated cells were not significantly dependent on temperature, neither was the loading capacity of copper onto dehydrated cells. However, the loading capacity of copper onto viable cells decreased from 3.2 ± 0.1 mmol g^{-1}, at 35ºC, to 2.7 ± 0.06 mmol g^{-1} at 45ºC (Figure 23a). Conversely, binding-site affinities for lead, zinc, and copper sorption to viable and dehydrated cells consistently decreased with increasing temperature. The largest decrease was observed for the sorption of lead to dehydrated cells, where the binding-site affinities were 104.9 ± 6.5, 74.5 ± 5.6, and 54.2 ± 3.2 L $mmol^{-1}$ at 25, 35, and 45ºC, respectively (Figure 23b). From Equation 5.6, heats of sorption were calculated and are shown in Table 5.

Desorption Experiments

For each cell condition tested, at pH 2.5, 4.0, and 7.0, between 94.6 and 99.5% of lead and zinc desorbed from cellular surfaces in an NTA wash. However, at each pH, much less copper desorbed from viable cells than any of the other cell conditions tested.

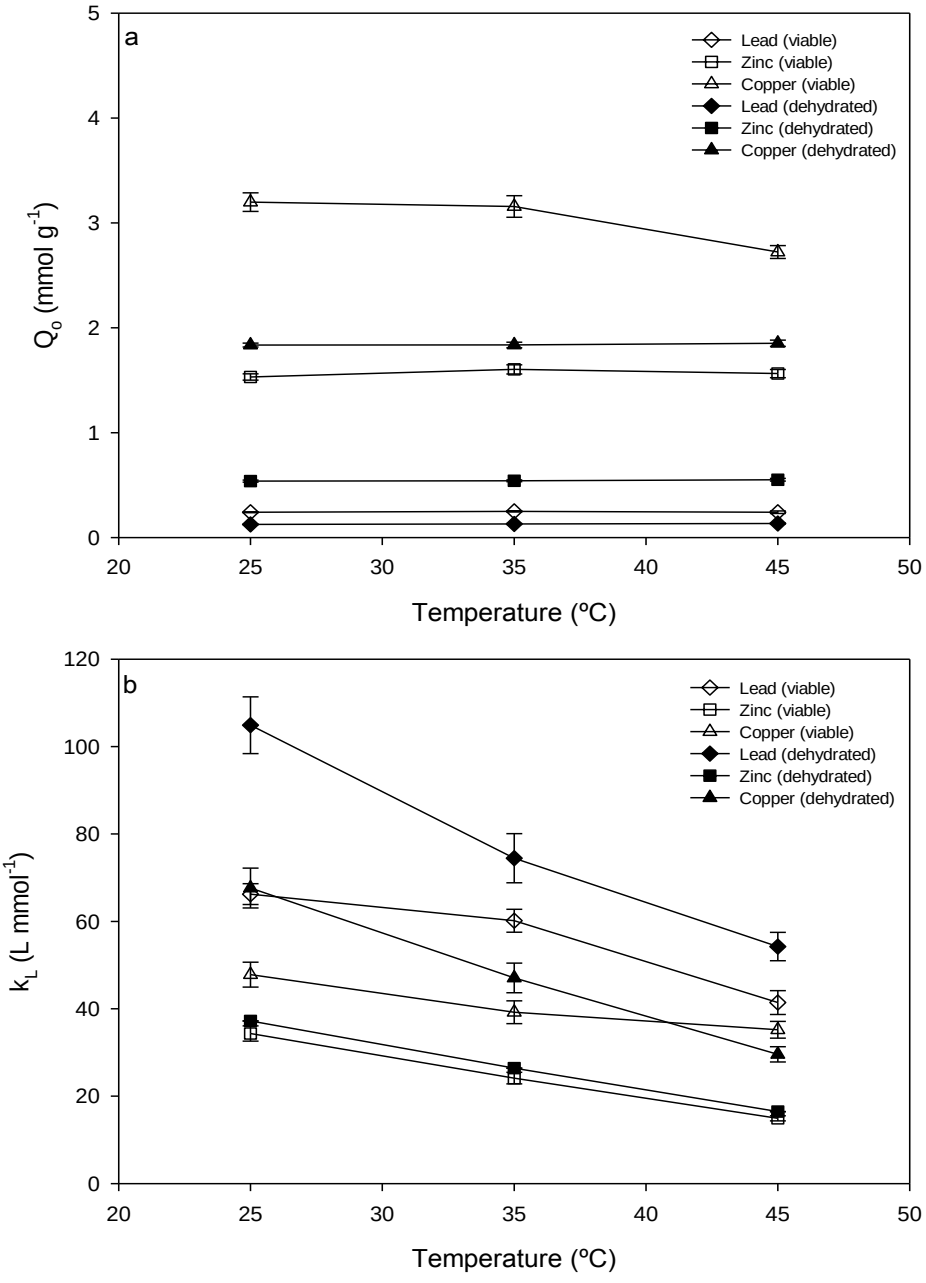


Figure 23. The effect of temperature on the (a) loading capacity (Q_o), and (b) binding-site affinity (k_L) for the sorption of lead, zinc, and copper to viable and dehydrated *Acidithiobacillus caldus* strain BC13 cells. Error bars represent 95% confidence intervals.

Table 5. The heat of sorption ($\Delta H_{sorption}$) for lead, zinc, and copper to viable and dehydrated *Acidithiobacillus caldus* strain BC13 cells, calculated from an Arrhenius plot. The Arrhenius factor (A) and R^2 value (indicating goodness of fit) are also shown.

	$\Delta H_{sorption}$ (J mmol^{-1})	A (L mmol^{-1})	R^2
Lead (viable)	-18.4	6.8×10^{-2}	0.884
Zinc (viable)	-32.8	6.4×10^{-5}	0.989
Copper (viable)	-12.1	3.6×10^{-1}	0.978
Lead (dehydrated)	-26.0	2.9×10^{-3}	0.998
Zinc (dehydrated)	-32.1	9.1×10^{-5}	0.988
Copper (dehydrated)	-32.5	1.4×10^{-4}	0.992

For example, at pH 2.5, only 78.4 ± 2.8% of the copper desorbed from viable cells, whereas 94.6 ± 1.7, 95.8 ± 0.4, and 95.6 ± 2.4% desorbed from dehydrated, lysed-viable, and lysed-dehydrated cells, respectively (Table 6).

Mixed Metal Sorption

Figure 24 shows that lead and zinc sorption decreased significantly when present in a mixture containing copper. In contrast however, the presence of lead or zinc did not significantly reduce the sorption of copper. When metals were presented individually, at the highest concentrations used in the previously described experiments, 95.3 ± 2.3, 92.7 ± 5.6, and 94.8 ± 2.6% of the lead, zinc, and copper sorbed, respectively. However, when combined with copper, only 46.5 ± 2.8 and 33.8 ± 5.5% of lead and zinc sorbed to BC13. Conversely, 96.0 ± 2.7 and 97.0 ± 2.9% of the copper sorbed when combined with either lead or zinc, respectively. When lead and zinc were mixed there was not a significant effect, as 93.6 ± 3.3 and 95.6 ± 3.2% of the lead and zinc sorbed, respectively.

When all three metals were mixed, 40.2 ± 4.3, 28.7 ± 3.8, and 91.3 ± 3.0% of the lead, zinc, and copper sorbed, respectively.

Table 6. Percent of lead, zinc, or copper that desorbed from *Acidithiobacillus caldus* strain BC13 cells in a 5 mM nitriloacetic acid (NTA) wash at equilibrium. ± values represent 95% confidence intervals.

	Percent of sorbed metal removed in NTA wash		
	Lead	Zinc	Copper
		pH 1.5	
Viable cells	96.4 ± 3.1	94.2 ± 1.3	78.4 ± 2.8
Dehydrated cells	98.1 ± 1.7	98.1 ± 1.0	94.6 ± 1.7
Lysed-viable cells	96.3 ± 0.8	96.5 ± 0.9	95.8 ± 0.4
Lysed-dehydrated cells	96.8 ± 0.6	97.5 ± 1.2	95.6 ± 2.4
		pH 4.0	
Viable cells	95.4 ± 0.6	94.6 ± 1.5	83.1 ± 3.3
Dehydrated cells	97.6 ± 0.6	96.0 ± 2.8	97.4 ± 1.3
Lysed-viable cells	98.2 ± 2.0	97.5 ± 1.3	94.5 ± 2.4
Lysed-dehydrated cells	99.0 ± 1.2	97.4 ± 1.6	95.3 ± 1.3
		pH 7.0	
Viable cells	98.3 ± 1.0	98.0 ± 0.4	90.5 ± 0.8
Dehydrated cells	99.5 ± 0.5	98.4 ± 1.1	96.9 ± 0.4
Lysed-viable cells	97.0 ± 0.5	97.7 ± 2.2	94.4 ± 3.1
Lysed-dehydrated cells	97.4 ± 1.0	97.4 ± 1.2	96.2 ± 1.0

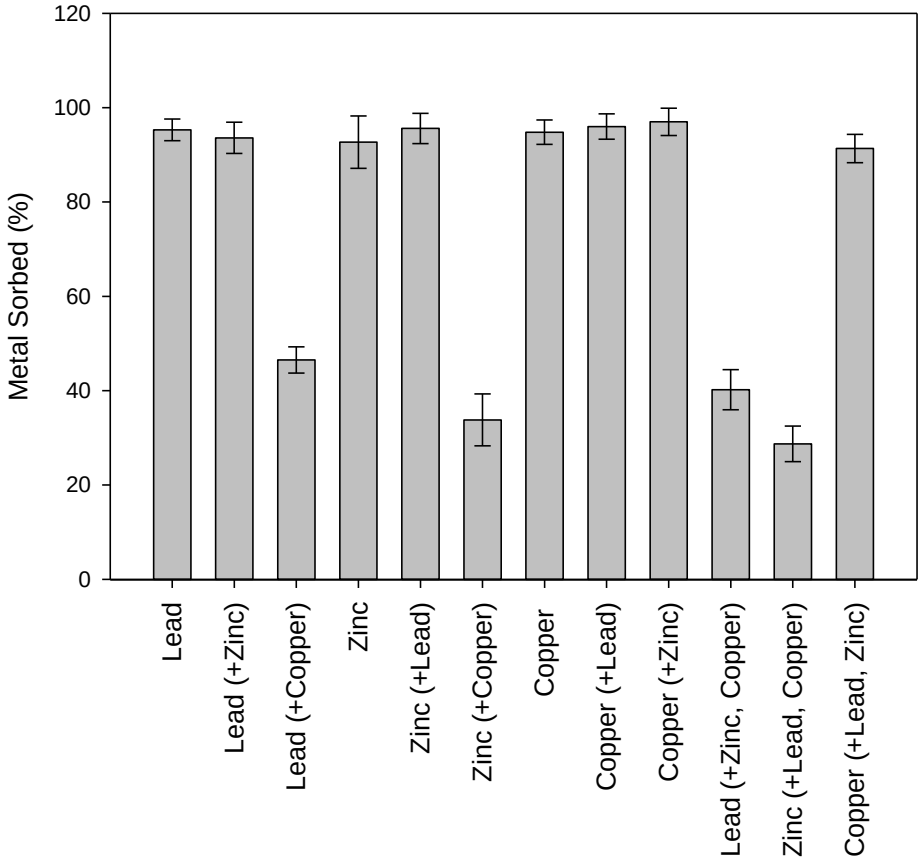


Figure 24. Effect of lead, zinc, and copper mixtures on metal sorption by *Acidithiobacillus caldus* strain BC13. The initial concentration of each metal was 0.24, 0.92, and 1.57 mM for lead, zinc, and copper respectively. These were the highest aqueous concentrations used in this study, and represent conditions where each binding site could theoretically interact with a metal molecule. X-axis labels indicate the metals present. The values are reported for the un-parenthesized label. Error bars represent 95% confidence intervals.

Discussion

Sorption of Lead, Zinc, and Copper to BC13

Although various authors have suggested metal properties that effect binding-site affinity, the literature suggests that the relative affinities of metals are specific to the

organism used. In the present study, the order of binding-site affinity was lead > copper > zinc. This matches the order of binding-site affinity for these metals to *Pseudomonas putida* as observed by Pardo et al. [19].

Ferris and Beveridge [20] suggested that a higher metal charge density contributes to greater affinity. However, the ionic radii of lead, copper and zinc are 133 pm, 87 pm, and 74 pm, respectively, so in the present case, it appears that other factors are greater contributors to sorption affinity than charge density. It has also been suggested that metal acidity is an important factor [21]. In the present study, the metal acidities of lead, zinc, and copper, as represented by the stability constant of the first hydroxyl-metal complex, were calculated to be 6.2, 6.0, and 4.4 at pH 4.0, respectively. This corresponds with the order of binding-site affinities observed here, suggesting that metal acidity may be important in the affinity for metal sorption to BC13.

Several studies have reported significant differences in metal sorption to viable versus non-viable biota [*i.e.* 22-24]. In the present study, copper exhibited the highest loading capacity to both viable and dehydrated cells, while lead had the lowest. In the case of zinc and copper, a significantly higher loading capacity was observed for viable cells as compared to dehydrated cells. This suggests that changes to zinc and copper binding sites during the dehydrating process significantly affected zinc and copper sorption.

Figure 18 suggests that the sorption kinetics also differ between viable and dehydrated cells. Only 48% of the copper sorption to viable cells occurred before the first time point, compared to 93% of the sorption to dehydrated cells. These calculations

were made for lead (61 versus 86%) and zinc (59 versus 80%). Interestingly, the data in Table 6 shows that far less copper is recovered in an NTA wash of viable cells than lead and zinc. However, recoveries of copper from dehydrated, lysed-viable, and lysed-dehydrated cells were all similar. This may indicate that more copper had absorbed into the viable cells, rather than adsorbing to the surface. Alvarez and Jerez [25] suggested that *At. ferrooxidans* possesses a copper efflux system that requires polyphosphate kinase activity. If BC13 possesses a similar mechanism, electron-donor starved cells would likely lack the energy to pump phosphate-metal complexes out of the cell. Although, there is no evidence in this report, this may explain the difference between copper sorption kinetics to viable versus dehydrated cells, and the lower amount of copper that desorbed from viable cells in the NTA wash.

For viable and dehydrated cells, the loading capacities and binding-site affinities were also dependent on pH (Figure 20). In general, both increased to a plateau with increasing pH, and then decreased slightly. A review by Febrianto et al. [26] reported many studies that observed significant increases in the loading capacity with increasing pH, and in many cases, a subsequent decrease in the loading capacity with further increases in pH. Specific to bacteria, this observation has been reported by several researchers [21,27-29].

In many systems, there are two competing factors that affect metal sorption. First, the metal must compete with proton sorption at the binding site [30], especially at low pH. Secondly, metal speciation increases with pH, possibly reducing the biological availability of the metal [31]. Figure 21 shows how these factors affect the loading

capacity and binding-site affinity. The binding-site affinities were maximized between pH 4.0 and 5.5, where, interestingly, the sum of the free protons and complexed ions was near a minimum for solutions containing lead, zinc, and copper, respectively (Figure 22).

Temperature Effects

Many published studies have reported an increase in loading capacities of metals with increasing temperature [16,17,32,33]. However, in the present report, temperature did not significantly affect the loading capacity of lead, zinc, or copper to viable or dehydrated cells. Conversely, the loading capacity of copper on viable cells did decrease slightly between 35 and 45ºC (Figure 23). Similar observations were made of zinc sorption to several species of *Pseudomonas* [34].

Binding-site affinities decreased with increasing temperature suggesting, by LeChatelier's principle, that the sorption of these metals is an exothermic reaction and is dominated by reversible (physical) mechanisms [23]. Copper sorption was the less exothermic than lead or zinc sorption (Table 5), indicating a more irreversible aspect to its binding mechanism, such as absorption. This may also support observations from the desorption experiments.

Mixed Metal Sorption

Because of its higher calculated specific loading capacity, copper appeared to out-compete lead and zinc for cellular binding sites in mixed-metal environments containing high concentrations of copper. This is strongly supported by the results shown in Figure 24. These results are especially significant in the context of an applied system, where

mixtures of metals are likely to be present. The ability of BC13 to sorb relatively high amounts of copper, even in the presence of other metals, suggests an especially important role in copper transport in acidic environments. Conversely, the sharp decrease in lead and zinc sorption in the presence of copper suggests that BC13 may play a more limited role in lead and zinc transport in systems containing high concentrations of copper. Interestingly, even a relatively high concentration of zinc did not significantly affect the sorption of either lead or copper. This is important as many acid-mine drainages and metal contaminated sites contain very high zinc concentrations [3,35,36].

Comparisons to Previous Work with Acidithiobacilli

Previous metal sorption studies using *At. thiooxidans* and *At. ferrooxidans* have reported loading capacities for zinc and copper. To facilitate a comparison with the results presented here, the units for loading capacity in previous reports were converted from mg L^{-1} to mmol g^{-1}.

Liu et al. [16] used a Langmuir model to describe the sorption of zinc (at pH 2.0, 4.0, and 6.0) and copper (at pH 4.0 and 5.0) to viable *At. thiooxidans* cells at 25ºC. In contrast to the sorption of zinc to BC13 observed here, Liu et al. did not observe any sorption of zinc to viable cells below pH 6.0. At pH 6.0 a loading capacity of 0.661 ± 0.014 mmol g^{-1} was reported, compared to 1.67 ± 0.065 mmol g^{-1}, in the present study at pH 5.5 at 45ºC. However, when Liu et al. pre-treated the cells with sodium hydroxide, rendering them non-viable, sorption occurred at pH 2.0 (0.577 ± 0.019 mmol g^{-1}), pH 4.0 (0.832 ± 0.034 mmol g^{-1}), and pH 6.0 (1.46 ± 0.055 mmol g^{-1}). These values are over three-fold higher than those reported here for dehydrated BC13 cells at similar pH. The

same study reported loading capacities for copper for both viable and non-viable cells that are significantly lower than those reported here, for BC13. This comparison suggests that viable BC13 cells may be capable of sorbing greater amounts of zinc and copper than *At. thiooxidans*, especially below pH 4.0.

In another study, Ruiz-Manriquez et al. [17] reported a loading capacity of 3.14 mmol g^{-1} for copper sorption to *At. ferrooxidans* cells treated with sodium hydroxide at pH 6.0 and 37°C, this is very close to the 3.09 mmol g^{-1} reported for dehydrated BC13 cells, at pH 5.5 and 45°C, in the present study. However, when viable cells were used, Ruiz-Manriquez et al. observed loading capacities of copper lower than those observed for viable BC13 cells in the present study. The ability of viable BC13 to sorb relatively high amounts of lead, zinc, and copper below pH 4.0 may suggest that it could play a significant role in the fate and mobility of these metals, especially in low pH environments such as acid-mine drainages. In addition, *At. caldus* may play an especially important role in the immobilization of copper at low pH as copper sorption did not decrease significantly when present in a mixture containing lead and zinc.

Conclusions

This is the first report on the effects of cell condition, pH, or temperature on lead, zinc, or copper sorption to *At. caldus*. This is also the first study of these effects on the sorption of lead to any organism of the acidithiobacilli genus. Lead, zinc, and copper sorption was observed to be highly dependent on pH, with the greatest sorption occurring between pH 4.0 and 5.5. Temperature did not affect the loading capacities of lead, zinc, and copper significantly; however, the binding-site affinities decreased significantly with

increasing temperature, suggesting that lead, zinc, and copper sorption to BC13 is an exothermic reaction.

Because experiments were not carried out identically, it is difficult to make an exact comparison with previous work by [16,17]; however it appears that viable BC13 cells are excellent sorbents of zinc and copper at low pH compared to viable *At. thiooxidans* and *At. ferrooxidans* cells. In addition, mixed sorption studies showed the presence of lead and zinc did not significantly decrease copper sorption from metal mixtures. This suggests that *At. caldus* may be especially important to the fate and transport of copper in acid-mine drainages, and may suggest a role in copper remediation. This comprehensive study of sorption of mixtures of lead, zinc, and copper to viable BC13 cultures contributes to understanding the role, and possible applications, of this microorganism in the fate and transport of heavy metals in acid-mine environments. In addition, its relatively high accumulation of zinc and copper identify *At. caldus* as a potential sorbent for these metals in other acidic systems.

References

1. Hallberg KB, Lindstrom EB (1994) Characterization of *Thiobacillus caldus* sp. Nov., a moderately thermophilic acidophile. *Microbiology* 140:3451-3456.

2. Burton NP, Norris PR (2000) Microbiology of acidic, geothermal springs of Montserrat: environmental rDNA analysis. *Extremophiles* 4:315-320.

3. Druschel GK, Baker BJ, Gihiring TM, Banfield JF (2004) Acid mine drainage biogeochemistry at Iron Mountain, California. *Geochem Trans* 5:12-32.

4. Okibe N, Gericke M, Hallberg KB, Johnson DB (2003) Enumeration and characterization of acidophilic microorganisms isolated for a pilot plant stirred-tank bioleaching operation. *Appl Environ Microbiol* 69:1936-1943.

5. Dopson M, Lindstrom EB (1999) Potential role of *Thiobacillus caldus* in arsenopyrite bioleaching. *Appl Environ Microbiol* 65:36-40.

6. Edwards KJ, Bond PL, Banfield JF (2000) Characteristics of attachment and growth of *Thiobacillus caldus* on sulphide minerals: a chemotactic response to sulphur minerals?. *Environ Microbiol* 2:324-332.

7. Fu B, Zhou H, Zhang R, Qiu G (2008) Bioleaching of chalcopyrite by pure and mixed cultures of *Acidithiobacillus* spp. and *Leptospirillum ferriphilum*. *Int J Biodeterior and Biodegrad* 62:109-115.

8. McGuire MM, Edwards KJ, Banfield JF, Hamers RJ (2001) Kinetics, surface chemistry, and structural evolution of microbially mediated sulfide mineral dissolution. *Geochem Geophys Geosyst* 65:1243-1258.

9. Zhou QG, Bo F, Bo ZH, Xi L, Jian G, Fei LF, Hau CH (2007) Isolation of a strain of *Acidithiobacillus caldus* and its role in bioleaching of chalcopyrite. *World J Microbiol Biotechnol* 23:1217-1225.

10. Vijayaraghavan K, Yun YS (2008) Bacterial biosorbents and biosorption. *Biotechnol Adv* 26:266-291.

11. Gomez C, Bosecker K (1999) Leaching heavy metals from contaminated soil using *Thiobacillus ferrooxidans* or *Thiobacillus thiooxidans*. *J Geomicrobiol* 16:233-244.

12. Nareshkumar R, Nagendran R, Parvathi K (2008) Bioleaching of heavy metals from contaminated soil using *Acidithiobacillus ferrooxidans*: effect of sulfur/soil ratio. *World J Microbiol Biotechnol* 24:1539-1546.

13. Ryu HW, Moon HS, Lee EY, Cho KS, Choi H (2003) Leaching characteristics of heavy metals from sewage sludge by *Acidithiobacillus thiooxidans*. *Met J Environ Qual* 32:751-759.

14. Celeya RJ, Noriega JA, Yeomans JH, Ortega LJ, Ruiz-Manriquez A (2000) Biosorption of Zinc(II) by *Thiobacillus ferrooxidans*. *Bioprocess Eng* 22:539-542.

15. Hossain SM, Anantharaman N (2005) Studies on copper(II) biosorption using *Thiobacillus ferrooxidans*. *J Univ Chem Technol Metall* 40:227-234.

16. Liu HL, Chen BY, Lan YW, Cheng YC (2004) Biosorption of Zn(II) and Cu(II) by the indigenous *Thiobacillus thiooxidans*. *Chem Eng J* 97:195-201.

17. Ruiz-Manriquez A, Magana PI, Lopez V, Guzman R (1997) Biosorption of Cu by *Thiobacillus ferrooxidans*. *Bioprocess Eng* 18:113-118.

18. Rawlings DE (2002) Heavy metal mining using microbes. *Annu Rev Microbiol* 56:65-91.

19. Pardo R, Herguedas M, Barrado E, Vega M (2003) Biosorption of cadmium, copper, lead and zinc by inactive biomass of *Pseudomonas putida*. *Anal Bioanal Chem* 376:26-32.

20. Ferris FG, Beveridge TJ (1986) Site specificity of metallic ion binding in *Escherichia coli* K-12 lipopolysaccharide. *Can J Microbiol* 32:52-55.

21. Pagnanelli F, Esposito A, Toro L, Veglio F (2003) Metal speciation and pH effect on Pb, Cu, Zn and Cd biosorption onto *Sphaerotilus natans*: Langmuir-type empirical model. *Water Res* 37:627-633.

22. Sandau E, Sandau P, Pulz O (1996) Heavy metal sorption by microalgae. *Acta Biotechnol* 16:227-235.

23. Hawari AH, Mulligan CN (2006) Biosorption of lead(II), cadmium(II), copper(II) and nickel(II) by anaerobic granular biomass. *Bioresource Technol* 97:692-700.

24. San, Tuzen M (2007) Biosorption of Pb(II) and Cd(II) from aqueous solution using green alga (*Ulva lactuca*) biomass. *J Haz Mat* 152:302-308.

25. Alvarez S, Jerez C (2004) Copper ions stimulate polyphosphate degradation and phosphate efflux in *Acidithiobacillus ferrooxidans*. *Appl Environ Microbiol* 70:5177-5182.

26. Febrianto J, Kosasih AN, Sunarso J, Ju YH, Indraswati N, Ismadji S (2009) Equilibrium and kinetic studies in adsorption of heavy metals using biosorbent: a summary of recent studies. *J Haz Mat* 162:616-645.

27. Akzu Z (2001) Equilibrium and kinetic modeling of cadmium(II) biosorption by *C. vulgaris* in a batch system: effect of temperature. *Sep Purif Technol* 21:285-294.

28. Ledin M, Pedersen K, Allard B (1997) Effects of pH and ionic strength on the adsorption of Cs, Sr, Eu, Zn, Cd and Hg by *Pseudomonas putida*. *Water Air Soil Poll* 93:367-381.

29. Ozdemir G, Ceyhan N, Ozturk T, Akirmak F, Cosar T (2004) Biosorption of chromium(VI), cadmium(II) and copper(II) by Pantoea sp. TEM18. *Chem Eng J* 102:249-253.

30. Crist RH, Oberholser K, Shenk N, Nguyen M (1981) Nature of bonding between metallic ions and algal cell walls. *Environ Sci Technol* 15:1212-1217.

31. Tubbing DMJ, Amdiraal W, Cleven RFMJ, Iqbal M, Van De Ment D, Verweij W (1994) The contribution of complexed copper to the metabolic inhibition of algae and bacteria in synthetic media and river water. *Water Res* 28:37-44.

32. Deng L, Zhu X, Wang X, Su Y, Su H (2007) Biosorption of copper(II) from aqueous solutions by green alga *Cladophora fascicularis*. *Biodegradation* 18:393-402.

33. Green-Ruiz C, Rodriguez-Tirado V, Gomez-Gil B (2008) Cadmium and zinc removal from aqueous solutions by *Bacillus jeotgali*: pH, salinity and temperature effects. *Bioresource Technol* 99:750-762.

34. Shaker MA (2007) Thermodynamic profile of some heavy metal ions adsorption onto biomaterial surfaces. *Am J Appl Sci* 4:605-612.

35. Banks D, Younger PL, Arnesen RT, Banks SB (1997) Mine-water chemistry: the good, the bad and the ugly. *Environ Geol* 32:157-174.

36. Benner SG, Blowes DW, Gould WD, Herbert RB, Ptacek CJ (1999) Geochemistry of a permeable reactive barrier for metals and acid mine drainage. *Environ Sci Technol* 33:2793-2799.

CHAPTER SIX
EFFECTS OF ORGANIC ACIDS AND METALS ON PROTEIN EXPRESSION BY *ACIDITHIOBACILLUS CALDUS* STRAIN BC13

Abstract

Matrix assisted laser desorption ionization mass spectrometry (MALDI-MS) was used to identify changes in expression of surface and secreted proteins when BC13 was exposed to the organic acids; pyruvate, acetate, 2-ketoglutarate, succinate, fumarate, malate, oxaloacetate, and the metals; lead, zinc, and copper. A membrane protein of approximately 25.9 kDa was up-expressed in the presence of 0.25 x IC_{50} concentration of organic acids, and of at least 1.0 x IC_{50} of heavy metals. In addition, two secreted proteins of approximately 7.8 and 11.5 kDa were observed only when copper was present.

One-dimensional gels were used to separate proteins (by molecular weight) collected from fractions containing either soluble cytoplasmic proteins, peripheral-membrane proteins, or integral-membrane proteins. No up-regulation was observed in proteins in the soluble fraction. Protein bands at 45, 60, 80, and 100 kDa consistently up-regulated in the peripheral fraction from cells that were allowed to adapt to pyruvate through subsequent culturing. In addition, protein bands at approximately 10 and 25 kDa consistently up-regulated in the presence of organic acids and heavy metals. It is possible that these proteins are the same as those observed using MALDI-MS. Finally, two-dimensional gels were used to separate proteins, by pI and molecular weight, however a method was not developed that allowed for a full representation of the BC13 proteome.

These preliminary results suggest that BC13 can regulate protein expression in response to the organic acids and metals tested here. Proteins that are up-regulated may play a role in resistance mechanisms of this microorganism, and would be of commercial interest in biomining and acid-mine remediation applications.

Introduction

At. caldus is considered an important biomining microorganism [1], especially in warmer environments (32-50°C) [2], where its thermophilic properties make it an important member of the autotrophic sulfur oxidizing guild [2]. The studies presented in chapters two and three are the first reporting the toxicity and assimilation of organic acids with *At. caldus*, despite previous reports indicating the important roles of organic acid toxicity and mixotrophic and/or heterotrophic activity in many biomining environments, especially acid-mine drainages, metal-leaching bioreactors, and acidic industrial waste streams [3-5]. Similarly, prior to the work presented in chapter 4 of this dissertation, metal toxicity studies with *At. caldus* were largely limited to the metalloid arsenic [6-9], and the sorption studies reported in chapter five are the first using this microorganism. Also, there have been no studies on the effects of organic acids on protein regulation in *At. caldus*, and metal-induced protein regulation studies have been limited to the metalloid arsenic, which induces the expression of TetB and several Ars family proteins, which appear to infer arsenic and antimony resistance [3,5].

This chapter is a preliminary report on the effects of organic acids and metals on protein expression by BC13. MALDI-MS was used to identify surface and secreted

proteins in the presence of varying concentrations of organic acids (pyruvate, acetate, 2-ketoglutarate, succinate, fumarate, malate, and oxaloacetate) and metals (lead, zinc, and copper). In addition, cells cultured in the presence of pyruvate, lead, zinc, or copper were fractionated and the proteins were separated using one- and two-dimensional gels, and then identified using Liquid chromatography – mass spectrometry (LC-MS). Protein expression was compared between cells exposed to pyruvate, lead, zinc, or copper for the first time, and those adapted to these compounds through subsequent culturing.

Materials and Methods

Microorganism, Media, and Growth Conditions

BC13 (ATCC 51757) was grown in a basal salts medium [1]. The medium was autoclaved for 15 minutes at 121°C and 22 psig and allowed to cool to room temperature. A trace metal solution [1] was then added to a concentration of 1 mL L^{-1} and the pH was adjusted to 2.5 using 6N sulfuric acid. A filter sterilized (0.2 μm) solution of potassium tetrathionate was then added to a concentration of 5 mM, as an electron donor, and ambient carbon dioxide provided a carbon source. A filter sterilized (0.2 μm) solution containing either metal sulfates (lead, zinc, or copper), or a sodium organic acid salt (pyruvate, acetate, 2-ketoglutarate, succinate, fumarate, malate, or oxaloacetate) was added from a stock solution to a concentration equal to the previously calculated IC_{50}s. The concentrations of organic acids and metals in the stock solutions, and salts in the medium were adjusted to ensure that the final medium salt compositions were equal. Cells preserved at 4°C in nanopure water (17.4 MΩ), with the pH adjusted to 3.0 using

6N sulfuric acid, provided the initial inoculum. Aliquots that provided initial cell densities of approximately 5 x 10^7 cells mL^{-1} were used. Cells were cultured in 500-mL Erlenmeyer flasks (350 mL medium volume), fitted with foam stoppers, and shaken at 150 rpm in a temperature controlled incubator at 45°C.

Cell concentrations were measured using direct cell counts with a Petroff-counting chamber (Hausser Scientific, Horsham, PA, U.S.A.) and a phase-contrast microscope (Zeiss, Thornwood, N.Y., U.S.A.). For each proteomic analysis, cells were harvested during the late-exponential growth phase. To adapt cultures to pyruvate, lead, zinc, or copper, cells were transferred to into identical, fresh, medium during the late-exponential growth phase. Cells were washed via centrifugation and nanopure water (17.4 MΩ), with the pH adjusted to 3.0 using 6N sulfuric acid, between each transfer. This was repeated three times.

MALDI Analysis

During late-exponential growth an aliquot of each sample was mixed with an α-cyano-4-hydroxycinnamic acid matrix and spotted onto MALDI plates. The remaining medium was centrifuged to separate the cells. Any secreted proteins present in the supernatant were concentrated with ultra-filtration through 1 kDa filters using nitrogen gas at 40 psig. The filter paper was washed with 1 x TAE Buffer. The buffer solution was then mixed with a sinapinic acid matrix and spotted onto MALDI plates. An Agilent MALDI-MS (Foster City, CA, U.S.A.) was used to analyze spots. Laser power and frequency were optimized for maximum detection.

Determining the Toxicity of Metals in Spent Medium

In separate experiments, all cells were removed from cultures during the late-exponential growth phase via filtration (0.2 μm) during the late-exponential growth phase. The medium filtrate was then re-inoculated with fresh BC13 cells. Prior to re-inoculation, using methods previously described in chapter 4, ICP-MS was used to measure metal concentrations in the medium filtrate. The specific growth rate of the fresh culture was then determined using direct cell counts. For comparison, a separate culture was grown with lead, zinc, or copper added to a concentration equal to that measured in the spent medium filtrate.

One-Dimensional Gel Analysis

Because BC13 grew mixotrophically using potassium tetrathionate and pyruvate (chapter 3, Figures 7-9), one-and two-dimensional gel analyses focused on cells exposed to pyruvate, as well as those exposed to lead, zinc, and copper. Cells were harvested during late-exponential growth via centrifugation and washed three times using a phosphate buffer (Appendix J). Proteins were collected from different cell fractions using the protocol described in Appendix J. The protein concentrations in the resultant solution were measured using a Bradford assay kit (Bio-Rad, Hercules, CA, U.S.A.), and were then diluted to approximately 10 $\mu g\ \mu L^{-1}$ in a denaturing buffer (Appendix J). A 5 μL aliquot of the final solution was run on a precast 4-20% gradient acrylamide gel (Bio-Rad) that was placed into a Bio-Rad MiniFormat gel box at 80 volts for 2 hours and 15

minutes. The gels were then dyed using coomasie blue (Appendix J) overnight, and de-stained with nanopure water (17.4 MΩ).

Protein Identification

JQuant software was used to measure band intensities to determine protein bands that were up-regulated in the presence of pyruvate, lead, zinc, or copper. These bands were cut from the gel and subjected to the trypsin digest described in Appendix J.

Samples were then centrifuged for 10 minutes at 10,000 rpm. A 10 μL aliquot of supernatant was placed into a sample vial. An Agilent 6340 ion trap LC-MS (Foster City, CA, U.S.A.) was used to separate and identify peptide products of the trypsin digest. A gradient of two solvents containing (A) 95% HPLC grade water, 5% HPLC acetonitrile, and 0.1% formic acid; and (B) 95% HPLC grade acetonitrile, 5% HPLC grade water, and 0.1% formic acid was used. A sample injection of 3 μL was used. A capillary flow rate of 4 uL min^{-1} and a column flow rate of 0.6 uL min^{-1} were used. The capillary and column pumps were run following the gradients described in Appendix J. A drying temperature of 325°C was used during electron transfer dissociation. MASCOT software was used to compare the identified peptides against a library of known proteins.

Two-Dimensional Gel Analysis

Cells were collected via centrifugation and washed three times using a phosphate buffer (Appendix J). Soluble proteins were then extracted, and re-suspended in a rehydration buffer (Appendix J). Protein concentrations were measured using a Bradford

assay kit (Bio-Rad). Several method variations were tested in an attempt to obtain a more complete representation of the soluble proteome. These are described briefly below.

Proteins were loaded onto either 18 or 24 cm iso-electric focusing strips (Bio-Rad), and focused onto a Bio-Rad protein IEF cell. Strips with pH 3 → 11 gradients, and a combination of pH 3 → 7 and pH 7 → 11 gel strips were also tested. The amount of protein loaded onto each strip was varied between 50 and 600 μg. In addition, proteins were subjected to ultra-filtration (50 kDa, 40 psig nitrogen gas) in an attempt to separate proteins that appeared to dominate the proteome. Finally, different dyes with various levels of sensitivity were used, including coomasie (Appendix J), Sypro (Bio-Rad), CY-dyes (Amersham, Louisville, CO, U.S.A.), and Z-dyes (Zdye, Bozeman, MT, U.S.A.).

Following isolectric focusing, gel strips were placed in an equilibration solution (Appendix J). The gel strips were then placed into an acylamide gel prepared following the directions given in Appendix J. A recA molecular weight marker (Bio-rad) was placed into the acrylamide gel, and the gel was placed into an Ettan Dalttwelve System gel electrophoresis box (General Electric, Fairfield, CT, U.S.A.). The voltage was set to 4 volts per gel, and the current was applied until the bromophenol blue migrated the length of the gel. This typically required between 16 and 28 hours, with variances possibly due to inconsistent cooling of the gel box.

Results

MALDI Analysis

Table 7 shows that pyruvate, acetate, 2-ketoglutarate, succinate, fumarate, malate, and oxaloacetate increased expression of a membrane protein with a molecular weight of approximately 25.9 kDa. This was observed when BC13 was cultured in the presence of 0.25 x, 0.5 x, and 1.0 x IC_{50} of each organic acid tested. In addition, this protein was identified when BC13 was cultured in the presence of 1.0 x IC_{50} of lead, zinc, or copper; however it was not observed when concentrations of 0.25 x and 0.50 x IC_{50} of these heavy metals were added (Table 7). Also, this protein was not observed when BC13 was cultured in the absence of organic acids or heavy metals. Using MALDI analysis, no other membrane proteins were observed to up-regulate in the presence of organic acids or metals. Two secreted proteins were identified with molecular weights of

Table 7. Specific intensity (counts per second per cell) of proteins from *Acidithiobacillus caldus* strain BC13 grown in varying concentrations of pyruvate, lead, zinc, or copper proportional to the respective half-maximal inhibitory concentrations (IC_{50}s). Proteins are denoted by their molecular weight within quotation marks. Results from pyruvate exposure are shown here; other organic acids were tested (acetate, 2-ketoglutarate, succinate, fumarate, malate, and oxaloacetate), however they did not produce results significantly different than pyruvate.

	Secreted proteins (counts s^{-1} $cell^{-1}$)			Membrane protein '25,961' (counts s^{-1} $cell^{-1}$)		
	'7,820'	'11,501'		0.25 x IC_{50}	0.50 x IC_{50}	1.0 x IC_{50}
Lead	-	-	Lead	-	-	48
Zinc	-	-	Zinc	-	-	96
Copper	10.16	6.17	Copper	-	-	105
Pyruvate	-	-	Pyruvate	54	58	66
Control	-	-	Control	Protein not identified		

approximately 7.8 and 11.5 kDa, respectively, when BC13 was exposed to copper (Table 7). No secreted proteins were observed in the presence of organic acids, lead, zinc, or organic acid and heavy metal free controls.

To determine whether the proteins '7,820' and '11,501' may serve to detoxify copper in the growth medium, spent medium from previous BC13 cultures containing the copper IC_{50} was inoculated with fresh cells. These cultures exhibited higher specific growth rates ($0.022 \pm 0.001\ h^{-1}$) than those inoculated into medium with the same copper concentration, but without previous exposure to BC13 cells ($0.016 \pm 0.002\ h^{-1}$, Figure 25).

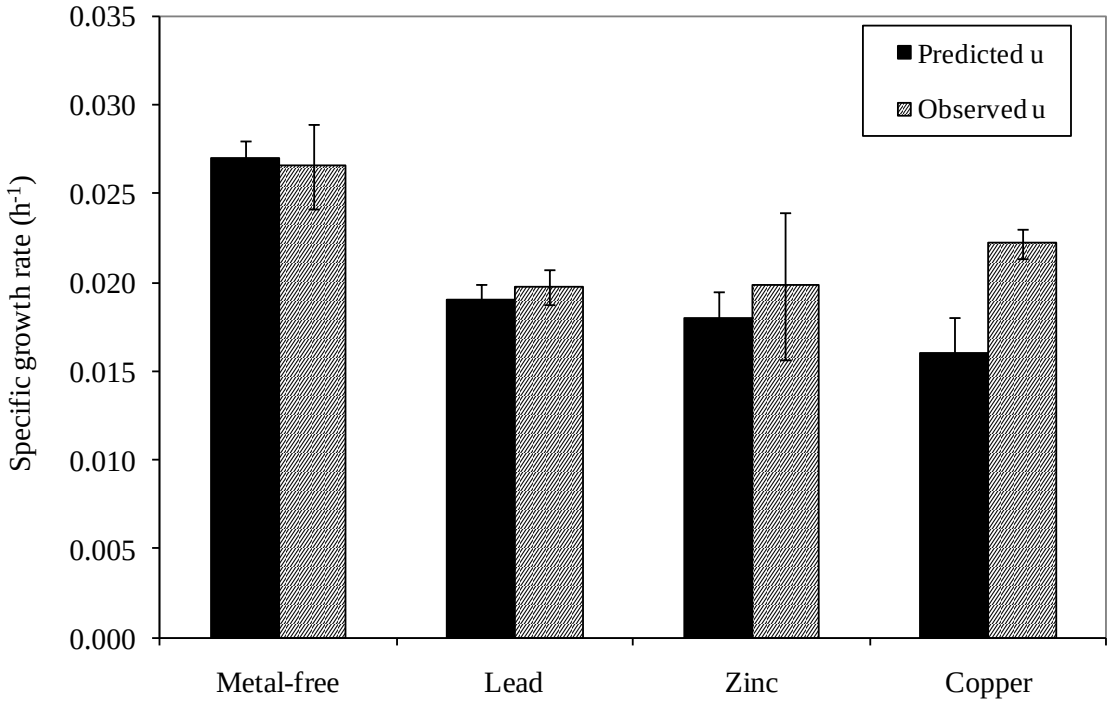


Figure 25. Specific growth rates of cells inoculated in medium filtrate previously exposed to *Acidithiobacillus caldus* strain BC13 compared to cells inoculated into spent medium with no previous exposure to *At. caldus* strain BC13. The spent medium contained lead, zinc, copper, or a heavy metal free control.

Gel Analysis

No significant, repeatable, up-regulation in protein bands from the soluble fraction was observed when BC13 was exposed to pyruvate, lead, zinc, or copper, compared to an organic acid and heavy metal free control. In addition, no changes in protein band expression were observed between soluble fractions collected from cultures exposed to pyruvate, lead, zinc, or copper for the first time, and those that were subsequently adapted to these compounds.

Similarly, no differences were observed in proteins peripheral to the cell membrane when exposed to pyruvate for the first time, or after subsequent culturing. However, Figure 26 shows that protein bands from the peripheral-membrane fraction with molecular weights of 45, 60, 80, and 120 kDa were up-regulated after BC13 was adapted to pyruvate.

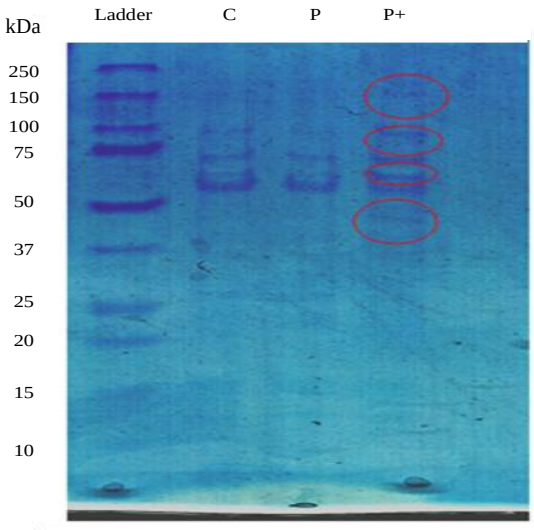


Figure 26. One-dimensional, coomassie stained, gel showing peripheral protein bands from *Acidithiobacillus caldus* strain BC13 in the absence of pyruvate (C), when exposed to pyruvate for the first time (P), and when adapted to pyruvate through subsequent culturing (P+).

Conversely, no up-regulation of peripheral-membrane proteins was observed when cells were exposed to lead, zinc, or copper.

Figure 27 shows that integral-membrane proteins with molecular weights of 10 and 25 kDa were up-regulated when exposed to pyruvate, lead, zinc, or copper for the first time. No additional changes were observed in the integral-membrane proteins when the cultures were allowed to adapt to these compounds through subsequent culturing.

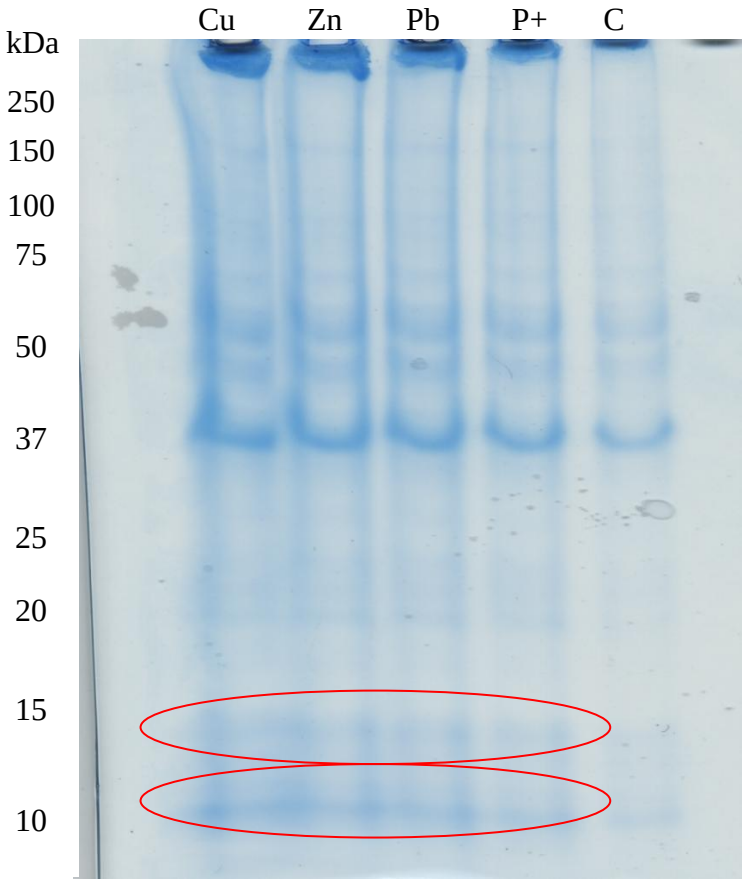


Figure 27. Effect of copper (Cu), zinc (Zn), lead (Pb), and pyruvate (P+) on the up- and down- regulation of *Acidithiobacillus caldus* strain BC13 proteins integral to the cellular membranes and separated on a one-dimensional, coomassie stained, gel. An organic acid and heavy metal free control (C) is shown for comparison.

Figure 28 shows a two-dimensional gel of the soluble protein fraction of BC13 that was not exposed to organic acids or metals. The gel shown in Figure 28 is representative of several replicates, and the lack of spots may suggest that the proteome is not entirely represented using the methods tested, as previous work has predicted that *At. caldus* strain KU possesses 2,821 protein coding genes [10]. It may indicate that relatively few individual proteins are expressed to a great degree, or that the majority of the proteome could not be visualized using a two-dimensional gel without overloading the isoelectric focusing gels used in the first dimension of separation. More sensitive fluorescent dyes were tested without success.

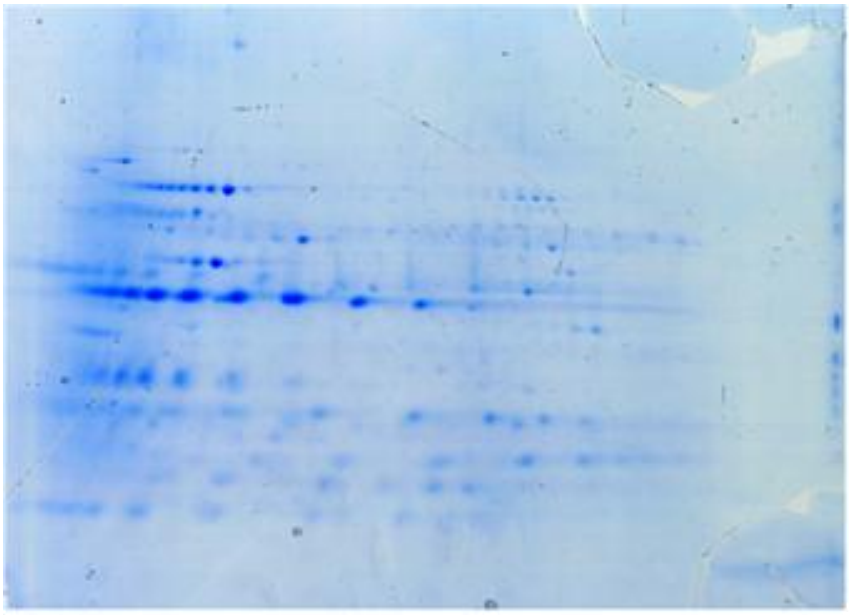


Figure 28. Two-dimensional, coomassie stained, gel of soluble proteins from *Acidithiobacillus caldus* strain BC13.

Discussion

The inability to detect membrane protein '25,961' in the organic acid and heavy metal free controls using MALDI-MS may suggest that this protein is related to cell stress. It appeared that a metal concentration greater than 0.5 x IC_{50} was required for this protein to be detected (Table 7). However, exposure to organic acid concentrations greater than 0.25 x IC_{50} caused increased expression of this protein.

Figure 26 shows that copper present in the spent medium was not as toxic as copper in medium with no previous exposure to BC13. This experiment was repeated with lead and zinc, however the same phenomenon was not observed. Given that secreted proteins unique to cells grown in the presence of copper were identified (Table 7), it is possible that BC13 employs extracellular protein activity to detoxify aqueous copper. Previous researchers have identified metal chelating proteins [11], and researchers, too numerous to fairly cite, have identified proteins secreted as a stress response [*i.e.* 12]. Future work to explore a possible mechanism for this de-toxicification by secreted proteins would be of value. However, it is also possible that BC13 may degrade internal polyphosphate stores and efflux inorganic phosphate that would bind to copper, using a mechanism similar to that employed by the closely related *At. ferrooxidans* [13].

Many metabolic proteins important to the central carbon metabolism are found in the cytoplasm [14], and would be found in the soluble protein fraction using the methods used here. The lack of up-regulation observed in this fraction may suggest that any enzymes used for pyruvate metabolism are not highly up-regulated by the pyruvate

concentration, and did not increase through subsequent adaptations in the presence of pyruvate. This may also suggest that increases in the specific growth rate observed after subsequent adaptations to pyruvate, lead, zinc, and copper (chapters 3 and 4; Figures 10, 14, and 15) may be due to the regulation of proteins peripheral or integral to the membrane. However, it is important to note that a single discernable band may constitute several proteins, since only one dimension of separation was used. Because of this, changes in protein expression can occur without being detected by changes in the band intensity. For this reason, no firm conclusions can be drawn regarding a lack of protein up-regulation. Figures 26 and 27 suggest that pyruvate, lead, zinc, and copper affect the expression of peripheral- and integral-membrane proteins. Interestingly, Figure 27 indicates the up-regulation of a protein band from the integral-membrane fraction at about 25 kDa, this supports results from the MALDI-MS analysis. The secreted proteins identified in the presence of copper using MALDI-MS may have originated as proteins peripheral to the membrane [14], or in the soluble fraction of the cytoplasm or periplasm [14]. However, no proteins of this size were observed to be up-regulated from these fractions on one-dimensional gels. Conversely, there was an up-regulated protein of approximately 10 kDa in the integral-membrane fraction (Figure 27). Typically, integral proteins are not secreted [14], however it is conceivable that some peripheral proteins may not elute in the salt wash used to extract these proteins from the membrane (Appendix J), instead remaining in the integral fraction.

Conclusions

The results presented here strongly suggest that BC13 can modify the expression of proteins to adapt to stresses of organic acids and heavy metals. These changes in protein expression may be related to the increased specific growth rates described in chapters 3 and 4 when BC13 was pre-adapted to organic acids and heavy metals, respectively (Figures 10 and 14). If this is the case, these proteins, and the regulatory systems that govern their expression would have significant importance in microbial activity in biomining environments.

Although the results presented here do not completely elucidate the effects of organic acids and heavy metals on the proteome of BC13, they indicate that proteins up-regulated in response to organic acids and heavy metals. Given the importance of this microorganism in biomining and remediation, any proteins that are up-regulated in response to organic acid or metal stress may be of commercial interest. These results lay the foundation for future work, including the identification of up-regulated proteins, and determination of organic acid and heavy metal tolerance mechanisms employed by *At. caldus*.

References

1. Hallberg KB, Lindstrom EB (1994) Characterization of *Thiobacillus caldus* sp. Nov., a moderately thermophilic acidophile. *Microbiology* 140:3451-3456.

2. Rawlings DE (2002) Heavy metal mining using microbes. *Annu Rev Microbiol* 56:65-91.

3. Gu XY, Wong JWC (2007) Degradation of inhibitory substances by heterotrophic microorganisms during bioleaching of heavy metals from anaerobically digested sewage sludge. *Chemosphere* 69:311–318.

4. Marchland EA, Silverstein J (2003) The role of enhanced heterotrophic bacterial growth on iron oxidation by *Acidithiobacillus ferrooxidans*. *Geomicrobiol J* 20:231–244.

5. Olson GJ, Brierley JA, Brierley CL (2003) Bioleaching review. Part B: Progress in bioleaching: Applications of microbial processes by the mineral industries. *Appl Microbiol Biotechnol* 63:249–257.

6. Dopson M, Lindstrom EB, Hallberg KB (2001) Chromosomally encoded arsenical resistance of the moderately thermophilic acidophile *Acidithiobacillus caldus*. *Extremophiles* 5:247-255.

7. Kotze AA, Tuffin IM, Deane SM, Rawlings DE (2006) Cloning and characterization of the chromosomal arsenic resistance genes from *Acidithiobacillus caldus* and enhanced arsenic resistance on conjugal transfer of *ars* genes located on transposon Tn*AtsArs*. M*icrobiology* 152:3551-3560.

8. Tuffin M, Hector SB, Deane SM, Rawlings DE (2006) Resistance determinants of a highly arsenic-resistant strain of *Leptospirillum feriphilum* isolated from a commercial biooxidation tank. *Appl Environ Microbiol* 72:2247-2253.

9. Van Zyl LJ, van Munster JM, Rawlings DE (2008) Construction of *ArsH* and *TetH* mutants of the sulfur-oxidizing bacterium *Acidithiobacillus caldus* by marker exchange. *App Environ Microbiol* 74:5686-5694.

10. Valdes J, Quatrini R, Hallberg K, Dopson M, Valenzuela PDT, Holmes DS (2009) Draft genome sequence of the extremely acidophilic bacterium *Acidithiobacillus caldus* ATCC 51756 reveals metabolic versatility in the genus *Acidithiobacillus*. *J Bact* 191:5877-5878.

11. Goldenberg DM, Griffiths GL, Hansen HJ (1998) Detection and therapy of lesions with biotin/advetin-metal chelating protein. U.S. patent application # 5,736,119.

12. Martin CA, Kurkowski DL, Valentino AM, Santiago-Schwarz F (2009) Increased intracellular, cell surface, and secreted inducible heat shock protein 70 responses are triggered during the monocyte to dendritic cell (DC) transition by cytokines independently of heat stress and infection and may positively regulate DC growth. *J Immunol* 183:388-399.

13. Alvarez S, Jerez C (2004) Copper ions stimulate polyphosphate degradation and phosphate efflux in *Acidithiobacillus ferrooxidans*, *Appl Enviro. Microbiol* 70:5177-5182.

14. White D (2007) The Physiology and Biochemistry of Prokaryotes, 3rd Edition. Oxford University Press, Indiana University 1-45.

CHAPTER SEVEN

SUMMARY

Conclusions

At. caldus is an important, yet relatively uncharacterized bacterium in acid-mine environments. Several papers have suggested that *At. caldus* plays an important role in metal solubilization and acid-mine formation [1-5], however studies of intrinsic interactions with compounds relevant to acid-mine environments, organic acids and heavy metals, have been limited.

For the first time, the effects of organic acids on *At. caldus* were studied in detail. Pyruvate, acetate, 2-ketoglutarate, succinate, fumarate, malate, and oxaloacetate have all been identified in the spent medium of chemolithoautotrophic acidophiles [6], and each exhibited toxic effects towards BC13. Oxaloacetate was observed to inhibit growth completely at a concentration of 250 μM, whereas other organic acids were completely inhibitory at concentrations between 1,000 and 5,000 μM. In these experiments, the measured concentrations of organic acids decreased with time, indicating uptake, transformation, or assimilation by the cells. PLFA analysis indicated an effect of organic acids on the cellular envelope. Notable differences included an increase in cyclic fatty acids, indicating possible instability of the cellular envelope. This was supported by FESEM images showing sloughing in cells grown in the presence of organic acids.

To determine whether the decrease in organic acid concentrations in batch cultures was due to catabolic oxidation or anabolic assimilation, the ability of BC13 to

grow using several different organic acids was tested under heterotrophic and mixotrophic conditions. No cell growth was observed under heterotrophic conditions; however, effluent cell concentrations increased over three-fold when pyruvate was presented with potassium tetrathionate compared to cultures containing only potassium tetrathionate or potassium tetrathionate and any of the other organic acids tested. In addition, the pyruvate concentration of the effluent decreased to below the detection limit and oxygen consumption increased by approximately 100%, compared to chemostat cultures supplied with other organic acids and potassium tetrathionate or only potassium tetrathionate. Batch experiments confirmed that BC13 grew using pyruvate as a sole carbon source. This is significant, as the presence of mixotrophic activity can significantly increase leaching kinetics in acid-mine environments [7-10].

The single and combined toxicities of lead, zinc, and copper under batch conditions suggest that BC13 is at least as tolerant of metals as other acidithiobacilli. Direct comparisons are difficult as previous studies with *At. ferrooxidans* and *At. thiooxidans* did not use direct cell quantification or a soluble substrate [*i.e.*, 11,12]. In addition, the importance of inoculum history was tested by pre-adapting cultures to lead, zinc, and copper via subsequent transfers. These cultures had specific growth rates that were 39 ± 11, 32 ± 7, and 28 ± 12% higher in the presence of lead, zinc, or copper IC_{50}s, respectively, compared to cultures that had not been pre-adapted. Similar results were observed using organic acids.

To further investigate the role of *At. caldus* in metal transport, and to evaluate it as a candidate for metal remediation in acidic waste streams, the effects of pH and

temperature on lead, zinc, and copper sorption to viable and dehydrated BC13 cells were studied using a Langmuir model. Copper exhibited the highest loading capacity, 4.76 ± 0.28 mmol g^{-1}, to viable cells at pH 5.5. The pHs that maximized loading capacities and affinities were generally between 4.0 and 5.5, where the sum of the free proton and complexed metal concentrations was near a minimum. Of additional importance, lead, zinc, and copper sorbed to viable cells at pH values as low as 1.5. Previous studies with other acidithiobacilli did not measure viable-cell sorption below pH 3.0, indicating that *At. caldus* may be important in metal fate and transport in acidic environments.

Finally, results suggest that BC13 modifies the expression of proteins to adapt to the stresses of the organic acids; pyruvate, acetate, 2-ketoglutarate, succinate, fumarate, malate, and oxaloacetate, and the metals; lead, zinc, and copper. These changes in protein expression may be related to the increased specific growth rates observed when BC13 was pre-adapted to organic acids or metals through subsequent culturing, compared to un-adapted cultures. If this is the case, these proteins, and the regulatory systems that control their expression are important to microbial activity in acid-mine environments.

This dissertation improves the characterization of *At. caldus*, and has laid the foundation for future work with this important biomining microorganism.

Future Work

Results in chapter two show that oxaloacetate was the most toxic organic acid tested. Oxaloacetate was also the only organic acid with a pKa below the medium pH (2.15 compared to 2.5). This would suggest that oxaloacetate protonates to a lesser degree than the other organic acids, and would therefore diffuse into the cell less readily.

Within the near pH-neutral cytoplasm, the organic acids tested would de-protonate to virtually identical extents, as all have a pKa below 5.5. This would suggest that the weaker acids should be more toxic, as they may more readily diffuse into the cell. However, if the toxic effects are not manifested until intracellular pH decreases to below 6.0, oxaloacetate may then de-protonate to a more significant extent, explaining its higher toxicity. Another plausible explanation is that the toxic effects of organic acids are manifested in the periplasmic space, disrupting the pH gradient, and subsequently the proton motive force, that exists between the cellular surface and the cytoplasm. To this end, pH homeostasis studies would be useful to correlate intracellular pH changes with organic acid uptake. In addition, tests with other organic acids with low pKa values would help support or contradict this hypothesis.

Chapter three presented strong empirical evidence that BC13 assimilated pyruvate under mixotrophic conditions. This work would be further supported by experiments using C^{14}-labeled pyruvate. The use of a scintillation counter to close the C^{14} mass balance across culture fractions could confirm the assimilation of pyruvate into cellular material. This approach could also suggest a mechanism for pyruvate assimilation. For example, C^{14} detected in the headspace would indicate that the pyruvate is oxidized to carbon dioxide, and then fixed via autotrophic pathways, such as the Calvin cycle. In addition, enzyme assays, coupled with quantitative-PCR analysis could help to identify an exact mechanism by which BC13 uses pyruvate.

BC13 was not observed to use acetate, 2-ketoglutarate, succinate, fumarate, malate, or oxaloacetate, even though some of the proteins necessary for their metabolism

were predicted from the partial genome of *At. caldus* strain KU [13]. Additional chemostat experiments using various influent concentrations and dilution rates would be useful to determine if measurable assimilation may be observed at different concentrations and growth rates.

The results presented in chapter six are preliminary, although they strongly suggest that BC13 regulated protein expression to adapt to organic acid and metal exposure. Proteins that affect the activity of this important biomining bacterium in the presence of relevant compounds may be of commercial interest. Identifying proteins from one-dimensional gels carries the difficulty of several proteins possibly having similar molecular weights. Ideally, proteins could be separated on a two-dimensional gel; however BC13 appears to express a select few proteins to a relatively high degree, making it difficult to fully represent the proteome without saturating the isoelectric focusing gel. Further efforts should be made to separate the proteome into sub fractions prior to two-dimensional gel separation. For example, one possible solution is to use ultra-centrifugation to separate fractions by molecular weight. In addition, varying the ampholyte concentration during iso-electric focusing may facilitate focusing of heavier protein loads, and allow for the enumeration of more dilute proteins during two-dimensional gel electrophoresis. Finally, given the recently annotated genome of *At. caldus* strain KU [13], a genome-wide protein array may be useful for initially qualifying up and down-regulation of protein translation in the presence of heavy metals and organic acids [14].

The completion of these suggested tasks would compliment the results presented here, and contribute further to not only the understanding of *At. caldus*, but the acidithiobacilli genus, and microbial activity in acid-mine environments in general.

References

1. Goebel BM, Stackebrandt E (1994) Cultural and phylogenetic analysis of mixed microbial populations found in natural and commercial bioleaching environments. *Appl Environ Microbiol* 60:1614-1621.

2. Okibe N, Gericke M, Hallberg KB, Johnson DB (2003) Enumeration and characterization of acidophilic microorganisms isolated for a pilot plant stirred-tank bioleaching operation. *Appl Environ Microbiol* 69:1936-1943.

3. McGuire MM, Edwards KJ, Banfield JF, Hamers RJ (2001) Kinetics, surface chemistry, and structural evolution of microbially mediated sulfide mineral dissolution. *Geochem Geophys Geosyst* 65:1243-1258.

4. Dopson M, Lindstrom EB (1999) Potential role of *Thiobacillus caldus* in arsenopyrite bioleaching. *Appl Environ Microbiol* 65:36-40.

5. Zhou QG, Bo F, Bo ZH, Xi L, Jian G, Fei LF, Hau CH (2007) Isolation of a strain of *Acidithiobacillus caldus* and its role in bioleaching of chalcopyrite. *World J Microbiol Biotechnol* 23:1217-1225.

6. Schnaitman C, Lundgren D (1965) Organic compounds in the spent medium of *Ferrobacillus ferrooxidans.* *Can J Microbiol* 1:23-27.

7. Dopson M, Lindstrom EB (1999) Potential role of *Thiobacillus caldus* in arsenopyrite bioleaching. *Appl Environ Microbiol* 65:36-40.

8. Edwards KJ, Bond PL, Banfield JF (2000) Characteristics of attachment and growth of *Thiobacillus caldus* on sulphide minerals: a chemotactic response to sulphur minerals? *Environ Microbiol* 2:324-332.

9. Fu B, Zhou H, Zhang R, Qiu G (2008) Bioleaching of chalcopyrite by pure and mixed cultures of *Acidithiobacillus* spp. and *Leptospirillum ferriphilum*. *Int J Biodeteriat and Biodegrad* 62:109-115.

10. McGuire MM, Edwards KJ, Banfield JF, Hamers RJ (2001) Kinetics, surface chemistry, and structural evolution of microbially mediated sulfide mineral dissolution. *Geochem Cosmochim Acta* 65:1243-1258.

11. Barreira RPR, Villar LD, Garcia O (2005) Tolerance to copper and zinc of *Acidithiobacillus thiooxidans* isolated from sewage sludge. *World J Microbiol Biotechnol* 21:89-91.

12. Chen BY, Chen YW, Wu DJ, Cheng YC (2003) Metal toxicity assessment upon indigenous *Thiobacillus thiooxidans* BC1. *Environ Eng Sci* 20:375-385.

13. Valdes J, Quatrini R, Hallberg K, Dopson M, Valenzuela PDT, Holmes DS (2009) Draft genome sequence of the extremely acidophilic bacterium *Acidithiobacillus caldus* ATCC 51756 reveals metabolic versatility in the genus *Acidithiobacillus*. *J Bact* 191:5877-5878.

14. MacBeath G (2002) Protein microarrays and proteomics. *Nature* 32:526-532.

APPENDICES

APPENDIX A

ABILITY OF *ACIDITHIOBACILLUS CALDUS* STRAIN BC13 TO GROW USING VARIOUS ELECTRON DONOR/ACCEPTOR PAIRS

Abstract

The results reported in this Appendix suggest that BC13 is not able to grow anaerobically when ferric iron was available as the electron acceptor coupled to the oxidation of either molecular hydrogen or reduced sulfur compounds, as cell concentrations did not increase significantly, and the concentration of ferric iron in the growth medium did not decrease. In addition, BC13 was not able to grow when molecular hydrogen was available as an electron donor and tetrathionate or elemental sulfur were available as electron accepters, as cell concentrations were not observed to increase. Also, when ferrous iron was supplied as an electron donor under aerobic conditions, no cell growth was observed, and ferrous iron concentrations did not decrease. However, cells concentrations did increase when molecular hydrogen was supplied as an electron donor under aerobic conditions, suggesting that BC13 is capable of oxidizing molecular hydrogen. These results suggest that the activity of BC13 may be limited in anoxic regions, such as subsurface and deep-ore environments.

Introduction

At. caldus is a chemolithotrophic autotroph that is capable of oxidizing reduced sulfur compounds, including elemental sulfur, sulfide, tetrathionate, and thiosulfate as energy sources under aerobic conditions. In addition, *At. caldus* strain KU can oxidize molecular hydrogen aerobically [1]. *At. caldus* has not been observed to grow using organic compounds as sole electron donors, however it has been observed to use glucose and yeast extract [1], and as reported in chapter 3, pyruvate as carbon sources under

mixotrophic growth conditions. To date, *At. caldus* has not been observed to grow in anaerobic environments, however, the closely related *At. ferrooxidans* can oxidize sulfur anaerobically, using ferric iron as an electron acceptor [2].

The metabolic traits described above, coupled to the ability of *At. caldus* to thrive at low pH (optimal growth between pH 2.0 and 3.0) and warm temperatures (optimal growth at 45°C) [1] contribute to its prevalence in biomining environments [3-6], where it is believed to play an important role in mineral leaching [7-9]. The results presented in the body of this dissertation have significantly improved the characterization of this important microorganism, however the lack of studies with *At. caldus* in anaerobic environments has lead to an incomplete understanding of this microorganism's potential, specifically in subsurface and deep-ore environments, where anoxic conditions may exist [10].

The work presented in this Appendix summarizes experiments that further characterize the metabolic flexibility of *At. caldus*, specifically its ability to reduce ferric iron under anaerobic conditions, and oxidize ferrous iron and molecular hydrogen was tested. Although, the following report does not represent a comprehensive study of possible catabolic activity, it does improve the general understanding of this microorganism's metabolic capabilities, and provides important information for future researchers who may expand on this work.

Materials and Methods

Microorganism, Media, and Growth Conditions

BC13 (ATCC 51757) was grown in a basal salts medium [1]. The medium was autoclaved for 15 minutes at 121°C and 22 psig and allowed to cool to room temperature. A trace element solution [1] was then added to a concentration of 1 mL L^{-1}, and the pH was then adjusted to 2.5 using 6N sulfuric acid. Solid electron donors and acceptors were added via a filter sterilized (0.2 μm) solution to a concentration of 5 mM. Table 8 lists electron donor/acceptor pairs tested. The media were aliquoted into 125-mL serum bottles (50 mL medium volume), and capped with butyl-rubber stoppers. Anaerobic samples were purged with filter sterilized (0.2 μm) nitrogen gas for 30 minutes. Each sample was then pressurized to 5 atm using a filter sterilized (0.2 μm), 80:20 mixture of nitrogen and carbon dioxide gas. The carbon dioxide provided the sole carbon source. If molecular hydrogen was used as the electron donor, the serum bottles were pressurized an additional 5 atm using a filter sterilized (0.2 μm) 95:5 mixture of nitrogen and hydrogen gas. Cells preserved at 4°C in nanopure water (17.4 MΩ), with the pH adjusted to 3.0 using 6N sulfuric acid, provided the initial inoculum. Aliquots that provided initial cell densities of approximately 2.5×10^6 cells mL^{-1} were used. The serum bottles were shaken at 150 rpm in a temperature controlled incubator at 45°C. Cell concentrations were measured at regular time intervals using direct cell counts with a Petroff-counting chamber (Hausser Scientific, Horsham, PA, U.S.A.) and a transmitted-light microscope (Zeiss, Thornwood, N.Y., U.S.A.). In experiments where ferrous or ferric iron were used

as an electron donor or acceptor, FerroZine® kits (Hach Company, Loveland, CO, U.S.A.) were used to measure changes in their respective concentrations. Each experiment was repeated in triplicate so that average values and 95% confidence intervals could be calculated.

Table 8. Pairs of electron donor/acceptors tested for growth.

Electron donor	Electron acceptor
Tetrathionate	Ferric iron
Sulfur	Ferric iron
Ferrous iron	Oxygen
Hydrogen	Tetrathionate
Hydrogen	Sulfur
Hydrogen	Ferric iron
Hydrogen	Oxygen

Results

Figure 29 shows that BC13 did not grow over a period of 350 hours when any of the electron donor/acceptor pairs were used with the exception of hydrogen/oxygen. When hydrogen was supplied as an electron donor under aerobic conditions cell concentrations increased from $2.83 \pm 0.29 \times 10^6$ cells mL^{-1}, at time 0, to $6.58 \pm 0.65 \times 10^6$ cells mL^{-1}, after 169 hours. The cell concentration then remained relatively steady between 169 and 350 hours. A lag time of between 96 and 138 hours was observed prior to growth (Figure 29). No significant changes in the ferrous or ferric iron concentrations were observed in any of the experiments (see raw data, following text).

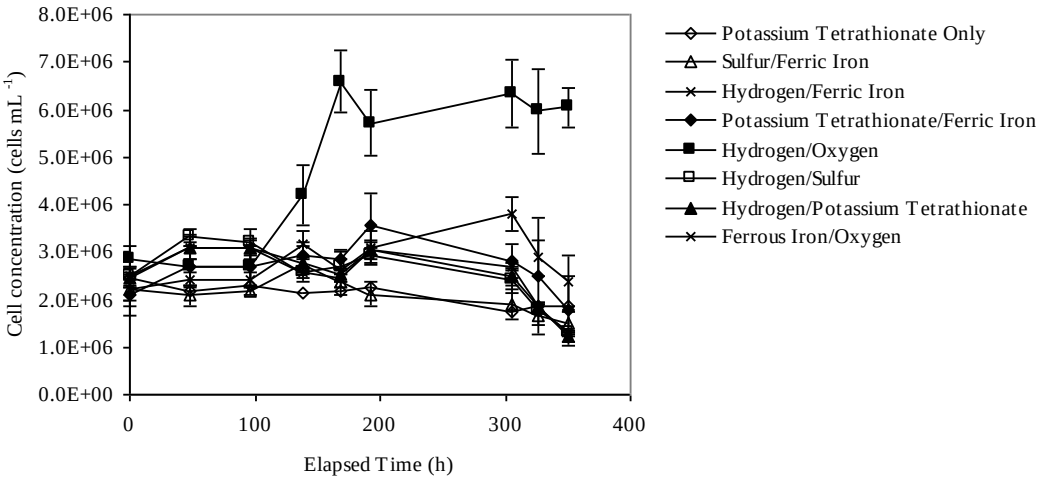


Figure 29. Changes in *Acidithiobacillus caldus* strain BC13 cell concentrations when grown using various electron donor/acceptor pairs. Error bars represent 95% confidence intervals.

Discussion

The results presented in this Appendix suggest that BC13 is not able to use ferric iron as a terminal electron acceptor, as no growth was observed on this substrate when several different reduced sulfur compounds and molecular hydrogen were tested as corresponding electron donors. This indicates that BC13 is unlikely to grow using any electron donor coupled to ferric iron, as past reports have reported growth of *At. caldus* when reduced sulfur compounds or molecular hydrogen were coupled with oxygen [1]. For similar reasons, it is unlikely that BC13 can oxidize ferrous iron, as it was not observed to in these experiments when coupled with oxygen. However, Figure 29 shows that BC13 can grow when molecular hydrogen was supplied as the sole electron donor under aerobic conditions. This was also observed by Hallberg and Lindstrom using strain

KU [1]. The experimental observations reported in this Appendix have been supported by the subsequent publication of the genome for *At. caldus* strain KU by Valdez et al., where the genes necessary for hydrogen oxidation were predicted, however those necessary for iron oxidation and reduction were not [11,12].

References

1. Hallberg KB, Lindstrom EB (1994) Characterization of *Thiobacillus caldus* sp. Nov., a moderately thermophilic acidophile. *Microbiology* 140:3451-3456.

2. Pronk JT, Bos BP, Kuenen JG (1992) Anaerobic growth of *Thiobacillus ferrooxidans*. *App Environ Microbiol* 58:2227-2230.

3. Burton NP, Norris PR (2000) Microbiology of acidic, geothermal springs of Montserrat: environmental rDNA analysis. *Extremophiles* 4:315-320.

4. Druschel GK, Baker BJ, Gihiring TM, Banfield JF (2004) Acid mine drainage biogeochemistry at Iron Mountain, California. *Geochem Trans* 5:12-32.

5. Goebel BM, Stackebrandt E (1994) Cultural and phylogenetic analysis of mixed microbial populations found in natural and commercial bioleaching environments. *Appl Environ Microbiol* 60:1614-1621.

6. Okibe N, Gericke M, Hallberg KB, Johnson DB (2003) Enumeration and characterization of acidophilic microorganisms isolated for a pilot plant stirred-tank bioleaching operation. *Appl Environ Microbiol* 69:1936-1943.

7. McGuire MM, Edwards KJ, Banfield JF, Hamers RJ (2001) Kinetics, surface chemistry, and structural evolution of microbially mediated sulfide mineral dissolution. *Geochem Geophys Geosyst* 65:1243-1258.

8. Dopson M, Lindstrom EB (1999) Potential role of *Thiobacillus caldus* in arsenopyrite bioleaching. *Appl Environ Microbiol* 65:36-40.

9. Zhou QG, Bo F, Bo ZH, Xi L, Jian G, Fei LF, Hau CH (2007) Isolation of a strain of *Acidithiobacillus caldus* and its role in bioleaching of chalcopyrite. *World J Microbiol Biotechnol* 23:1217-1225.

10. Stromberg B, Banwart S (1994) Kinetic modeling of geochemical processes at the Aitik mining waste rock site in Northern Sweden. *App Geochem* 9:583-595.

11. Valdes J, Pedroso I, Quatrini R, Holmes DS (2008) Comparative genome analysis of *Acidithiobacillus ferrooxidans, A. thiooxidans* and *A. caldus*: insights into their metabolism and ecophysiology. *Hydrometallurgy* 94:180-184.

12. Valdes J, Quatrini R, Hallberg K, Dopson M, Valenzuela PDT, Holmes DS (2009) Draft genome sequence of the extremely acidophilic bacterium *Acidithiobacillus caldus* ATCC 51756 reveals metabolic versatility in the genus *Acidithiobacillus*. *J Bact* 191:5877-5878.

Raw Data

Table A.1. BC13 cell concentrations when various electron donor/acceptor pairs were provided. Experiments were repeated in triplicate and average values, standard deviations (STDEV), and 95% confidence intervals (95% CI) are shown. Concentrations are given in cells mL^{-1}.

Potassium Tetrathionate Only

Elapsed Time (h)	Trial 1
0	2.44E+06
48	2.19E+06
96	2.31E+06
138	2.13E+06
169	2.19E+06
192	2.25E+06
305	1.75E+06
326	1.88E+06
350	1.88E+06

Sulfur/Ferric Iron

Elapsed Time (h)	Trial 1	Trial 2	Trial 3	Average	STDEV	95% CI
0	2.00E+06	2.38E+06	2.25E+06	2.21E+06	1.91E+05	2.16E+05
48	1.88E+06	2.13E+06	2.25E+06	2.08E+06	1.91E+05	2.16E+05
96	2.13E+06	2.13E+06	2.25E+06	2.17E+06	7.22E+04	8.17E+04
138	2.38E+06	2.88E+06	3.00E+06	2.75E+06	3.31E+05	3.74E+05
169	2.13E+06	2.38E+06	2.63E+06	2.38E+06	2.50E+05	2.83E+05
192	1.88E+06	2.13E+06	2.35E+06	2.12E+06	2.38E+05	2.69E+05
305	1.63E+06	1.88E+06	2.19E+06	1.90E+06	2.82E+05	3.19E+05
326	1.50E+06	1.66E+06	1.88E+06	1.68E+06	1.88E+05	2.13E+05
350	1.25E+06	1.56E+06	1.66E+06	1.49E+06	2.15E+05	2.43E+05

Hydrogen/Ferric Iron

Elapsed Time (h)	Trial 1	Trial 2	Trial 3	Average	STDEV	95% CI
0	1.88E+06	2.25E+06	2.50E+06	2.21E+06	3.15E+05	3.56E+05
48	2.25E+06	2.50E+06	2.50E+06	2.42E+06	1.44E+05	1.63E+05
96	2.25E+06	2.50E+06	2.50E+06	2.42E+06	1.44E+05	1.63E+05
138	2.88E+06	3.38E+06	3.25E+06	3.17E+06	2.60E+05	2.94E+05
169	2.25E+06	2.88E+06	2.75E+06	2.63E+06	3.31E+05	3.74E+05
192	2.75E+06	3.13E+06	3.38E+06	3.08E+06	3.15E+05	3.56E+05
305	3.50E+06	3.75E+06	4.13E+06	3.79E+06	3.15E+05	3.56E+05
326	3.00E+06	2.50E+06	3.13E+06	2.88E+06	3.31E+05	3.74E+05
350	2.50E+06	1.88E+06	2.81E+06	2.40E+06	4.77E+05	5.40E+05

Potassium Tetrathionate/Ferric Iron

Elapsed Time (h)	Trial 1	Trial 2	Trial 3	Average	STDEV	95% CI
0	2.50E+06	1.88E+06	1.88E+06	2.08E+06	3.61E+05	4.08E+05
48	3.13E+06	2.50E+06	2.50E+06	2.71E+06	3.61E+05	4.08E+05
96	3.13E+06	2.50E+06	2.50E+06	2.71E+06	3.61E+05	4.08E+05
138	2.63E+06	3.00E+06	3.13E+06	2.92E+06	2.60E+05	2.94E+05
169	2.63E+06	3.00E+06	2.88E+06	2.83E+06	1.91E+05	2.16E+05
192	3.00E+06	3.63E+06	4.13E+06	3.58E+06	5.64E+05	6.38E+05
305	2.50E+06	2.81E+06	3.13E+06	2.81E+06	3.13E+05	3.54E+05
326	1.88E+06	1.88E+06	3.75E+06	2.50E+06	1.08E+06	1.22E+06
350	1.25E+06	1.56E+06	2.50E+06	1.77E+06	6.51E+05	7.36E+05

Hydrogen/Potassium Tetrathionate

Elapsed Time (h)	Trial 1	Trial 2	Trial 3	Average	STDEV	95% CI
0	2.26E+06	2.61E+06	2.54E+06	2.47E+06	1.84E+05	2.09E+05
48	3.14E+06	3.27E+06	2.85E+06	3.08E+06	2.13E+05	2.41E+05
96	2.85E+06	3.13E+06	3.24E+06	3.07E+06	1.97E+05	2.23E+05
138	2.68E+06	2.74E+06	2.85E+06	2.76E+06	8.29E+04	9.39E+04
169	2.55E+06	2.63E+06	2.39E+06	2.52E+06	1.24E+05	1.41E+05
192	3.07E+06	3.20E+06	2.94E+06	3.07E+06	1.29E+05	1.46E+05
305	2.43E+06	2.36E+06	2.67E+06	2.49E+06	1.65E+05	1.87E+05
326	1.94E+06	1.83E+06	1.77E+06	1.84E+06	8.42E+04	9.52E+04
350	1.17E+06	1.17E+06	1.30E+06	1.21E+06	7.46E+04	8.44E+04

Hydrogen/Sulfur

Elapsed Time (h)	Trial 1	Trial 2	Trial 3	Average	STDEV	95% CI
0	2.58E+06	2.57E+06	2.30E+06	2.49E+06	1.60E+05	1.81E+05
48	3.41E+06	3.42E+06	3.19E+06	3.34E+06	1.31E+05	1.49E+05
96	2.93E+06	3.29E+06	3.37E+06	3.20E+06	2.38E+05	2.69E+05
138	2.56E+06	2.56E+06	2.55E+06	2.56E+06	5.87E+03	6.65E+03
169	2.56E+06	2.85E+06	2.69E+06	2.70E+06	1.44E+05	1.63E+05
192	2.78E+06	2.92E+06	3.06E+06	2.92E+06	1.37E+05	1.55E+05
305	2.68E+06	2.26E+06	2.31E+06	2.42E+06	2.31E+05	2.61E+05
326	1.74E+06	1.75E+06	1.91E+06	1.80E+06	9.64E+04	1.09E+05
350	1.25E+06	1.35E+06	1.31E+06	1.30E+06	5.44E+04	6.16E+04

Hydrogen/Oxygen

Elapsed Time (h)	Trial 1	Trial 2	Trial 3	Average	STDEV	95% CI
0	2.63E+06	3.13E+06	2.75E+06	2.83E+06	2.60E+05	2.94E+05
48	3.13E+06	2.50E+06	2.50E+06	2.71E+06	3.61E+05	4.08E+05
96	3.13E+06	2.50E+06	2.50E+06	2.71E+06	3.61E+05	4.08E+05
138	4.25E+06	4.75E+06	3.63E+06	4.21E+06	5.64E+05	6.38E+05
169	6.25E+06	7.25E+06	6.25E+06	6.58E+06	5.77E+05	6.53E+05
192	5.00E+06	6.00E+06	6.13E+06	5.71E+06	6.17E+05	6.98E+05
305	6.88E+06	6.50E+06	5.63E+06	6.33E+06	6.41E+05	7.26E+05
326	6.88E+06	5.41E+06	5.63E+06	5.97E+06	7.90E+05	8.94E+05
350	6.25E+06	6.25E+06	5.63E+06	6.04E+06	3.61E+05	4.08E+05

Ferrous Iron/Oxygen

Elapsed Time (h)	Trial 1	Trial 2	Trial 3	Average	STDEV	95% CI
0	2.28E+06	2.67E+06	2.53E+06	2.49E+06	1.93E+05	2.18E+05
48	3.28E+06	2.86E+06	3.18E+06	3.11E+06	2.19E+05	2.48E+05
96	3.17E+06	2.97E+06	3.17E+06	3.10E+06	1.19E+05	1.34E+05
138	2.46E+06	2.62E+06	2.65E+06	2.58E+06	1.01E+05	1.14E+05
169	2.43E+06	2.53E+06	2.38E+06	2.45E+06	7.79E+04	8.82E+04
192	2.86E+06	3.18E+06	3.15E+06	3.06E+06	1.80E+05	2.03E+05
305	2.71E+06	2.74E+06	2.61E+06	2.69E+06	6.85E+04	7.75E+04
326	1.93E+06	1.78E+06	1.75E+06	1.82E+06	9.81E+04	1.11E+05
350	1.30E+06	1.32E+06	1.36E+06	1.33E+06	2.86E+04	3.23E+04

Table A.2. Change in ferrous or ferric iron concentrations when supplied as either the electron donor or acceptor, respectively. Experiments were repeated in triplicate and average values, standard deviations (STDEV), and 95% confidence intervals (95% CI) are shown. Concentrations are given in millimolar units. The initial time point was taken at 0 hours, the final time point was taken at 350 hours.

Ferric Iron Concentration
Sulfur/Ferric Iron

	Trial 1	Trial 2	Trial 3	Average	STDEV	95%
Initial	5.02	5.04	5.11	5.06	0.05	0.05
Final	5.22	4.54	4.53	4.76	0.40	0.45

Ferric Iron Concentration
Hydrogen/Ferric Iron

	Trial 1	Trial 2	Trial 3	Average	STDEV	95%
Initial	4.87	4.65	5.55	5.02	0.47	0.53
Final	4.66	5.04	5.11	4.94	0.24	0.27

Ferric Iron Concentration
Potassium Tetrathionate/Ferric Iron

	Trial 1	Trial 2	Trial 3	Average	STDEV	95%
Initial	5.33	5.16	5.22	5.24	0.09	0.10
Final	4.99	5.31	4.85	5.05	0.24	0.27

Ferrous Iron Concentrations
Ferrous Iron/Oxygen

	Trial 1	Trial 2	Trial 3	Average	STDEV	95%
Initial	5.04	4.95	4.86	4.95	0.09	0.10
Final	5.09	5.11	4.98	5.06	0.07	0.08

APPENDIX B

PRECIPITATION OF COVELLITE IN THE GROWTH MEDIUM OF *ACIDITHIOBACILLUS CALDUS* STRAIN BC13

Abstract

This Appendix describes the precipitation of covellite during *in vitro* culturing of BC13. Covellite was observed to precipitate during the late-exponential growth phase when copper sulfate was added to concentrations of at least 20 mM. This precipitate was not observed in abiotic controls, and MINTEQ thermodynamic modeling did not predict the formation of covellite, and predicted that total precipitation would be ≤ 1.0 mg L^{-1}. However, (± 95% confidence intervals) 56 ± 17 mg L^{-1} of precipitate was measured. A spot scan of the precipitate using energy-dispersive x-ray spectroscopy (EDX) detected only copper and sulfur, with a copper to sulfur ratio of 0.83. Powder X-ray diffraction (p-XRD) analysis suggested that the precipitate was comprised of elemental sulfur and covellite. *At. caldus* is believed to increase metal solubilization, contributing towards acid-mine drainage formation, making these observations particularly interesting, as they suggest that under the experimental conditions used here, this microorganism may also facilitate the mineralization of copper.

Introduction

At. caldus is a gram negative bacterium that oxidizes sulfur and reduced sulfur compounds for energy, and can fix carbon dioxide as a sole carbon source [1-2]. *At. caldus* grows from pH 1-4, with optimal growth between pH 2 and 3, and from 32-50°C, with optimal growth at 45°C [1]. These traits make *At. caldus* well suited for growth in many biomining systems [3-6], where recent studies suggest that it may play a significant role in metal mobilization [7-9].

The purpose of this study was to identify a precipitate that formed in the growth medium of BC13 when copper sulfate was added to concentrations of at least 20 mM. This precipitate was not predicted by the thermodynamic modeling software, MINTEQ. Any biogenic mineralization involving *At. caldus* is interesting as it is an important microorganism in acid-mine environments, where mineralization and solubilization of metals are important to biomining and bioremediation.

Methods and Approach

Microorganism, Media, and Growth Conditions

BC13 (ATCC 51757) was grown in a basal salts medium [1]. The medium was autoclaved for 15 minutes at 121°C and 22 psig and allowed to cool to room temperature. A trace element solution [1] was then added to a concentration of 1 mL L^{-1}, and the pH was adjusted to 2.5 using 6N sulfuric acid. A filter sterilized (0.2 μm) solution of potassium tetrathionate was then added to a concentration of 5 mM, as an electron donor, and ambient carbon dioxide provided the sole carbon source. A filter sterilized (0.2 μm) copper sulfate solution was added to a concentration of 20 mM. Cells preserved at 4°C in nanopure water (17.4 MΩ), with the pH adjusted to 3.0 using 6N sulfuric acid, provided the initial inoculum. Aliquots that provided initial cell densities of approximately 5×10^7 cells mL^{-1} were used. Cells were cultured in 500-mL Erlenmeyer flasks (350 mL medium volume), fitted with foam stoppers, and shaken at 150 rpm in a temperature controlled incubator at 45°C (Barnstead 4000Q, Dubuque, IA, U.S.A.). To determine the coincidence of precipitation with a specific part of the growth cycle, cell concentrations

were measured using direct cell counts with a Petroff-counting chamber (Hausser Scientific, Horsham, PA, U.S.A.) and a phase-contrast microscope (Zeiss, Thornwood, N.Y., U.S.A.). Sacrificial sampling was used to quantify precipitation with time. Precipitate samples were collected via centrifugation and dried in a model 40 GC lab oven (Quincy Lab, Chicago, Il, U.S.A.) at 80°C for 12 hours. Dry weight measurements were then recorded. Experiments were repeated in triplicate, and average values and 95% confidence intervals were calculated.

Sample Preparation and Analysis

After 144 hours, the precipitate was collected via centrifugation, and washed using nanopure water (17.4 MΩ). This process was repeated three times to remove medium salts. The sample was re-suspended to a concentration of approximately 50 g L^{-1} in nanopure water (17.4 MΩ). An aliquot of 10 μL was pipetted onto a silica chip and allowed to dry for 1 hour at 45°C in a temperature controlled incubator. The silica chips were fixed onto a carousal stub using carbon tape, and imaged using FESEM (Supra 55VP, Zeiss, Peabody, MA, USA). An accelerating voltage of 1 keV, and aperture diameter of 30 μm were used. A secondary electron detector was used to image the precipitate. To quantify the elemental composition, the accelerating voltage was increased to 20 keV, and an EDX detector was used to measure x-ray emission.

For p-XRD analysis, a sample was collected and dried as described above. All of the powder collected (approximately 100 mg) was poured into a p-XRD sample holder to facilitate a random orientation of crystal structures. The sample was then analyzed using

a Syntag X1 powder diffractometer (Cupertino, CA, U.S.A.). The incidence of diffraction was varied from 5 to 65°, in 0.5° increments, by adjusting the goniometer. An electron beam, with an accelerating voltage of 1 keV, enumerated x-rays from a copper kα source. Raw data was compared to a standard library using PCPDFWIN™ software.

Results

Figure 30 shows that precipitation did not form until the late-exponential/early-stationary growth phase, and then occurred within a period of 24 hours. Measurements showed that the

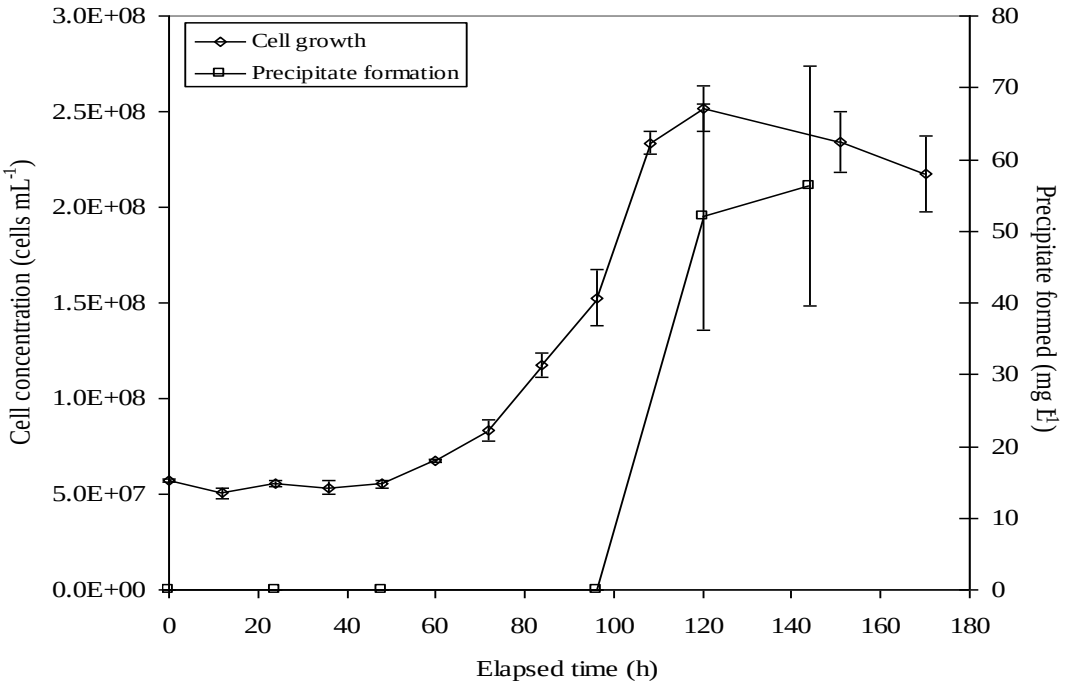


Figure 30. Correlation of cell growth in *Acidithiobacillus caldus* strain BC13 cultures (left axis) and the formation of the precipitate (right axis).

culture pH decreased from 2.5 to 1.9 ± 0.2 (see raw data, following text). Because of this, MINTEQ was used to model experimental conditions from pH 1.5 to 7.0, since previous reports suggest that environments local to acidithiobacilli surfaces may be pH 4.0-5.5, and intracellular pH is approximately 6.7 [10].

Table 9. Predicted precipitation using MINTEQ thermodynamic modeling of the experimental conditions with the pH varied from 1.5 to 7.0. These pH values encompass a range from the final growth medium pH (1.85 ± 0.17) to the maximum pH measured within the cytoplasm of acidithiobacilli (6.7).

pH	Copper molybdenate ($CuMoO_4$)	Brochantite (Cu_4SO_4)	Cupric Ferrite ($CuFe_2$)	Tenorite (Cu)
1.5	0.43 mg L^{-1}	-		-
2.5	0.43 mg L^{-1}	-		-
3.5	0.43 mg L^{-1}	-	3.06 mg L^{-1}	-
5.0	0.43 mg L^{-1}	5.43 mg L^{-1}	2.82 mg L^{-1}	-
7.0	0.43 mg L^{-1}	6.1 mg L^{-1}	3.54 mg L^{-1}	0.11 mg L^{-1}

The results from this modeling are shown in Table 9, and indicate that no significant precipitation was predicted, further suggesting that the precipitation was catalyzed via biogenic mechanisms. Figure 31 shows EDX elemental analysis that corresponds to the accompanying image. The detection of silicon is likely due to the silica chip that the sample was placed on. The copper to sulfur ratio of the spot scan shown in Figure 32 is 0.83. These data may suggest the presence of a copper sulfide, although the relative amount of sulfur is higher than that observed in most copper sulfides (Table 10). The ratio observed using EDX is closest to that of covellite, however it

should be noted that covellite is often copper rich due to the presence of oxidized copper, which increases the copper to sulfur ratio.

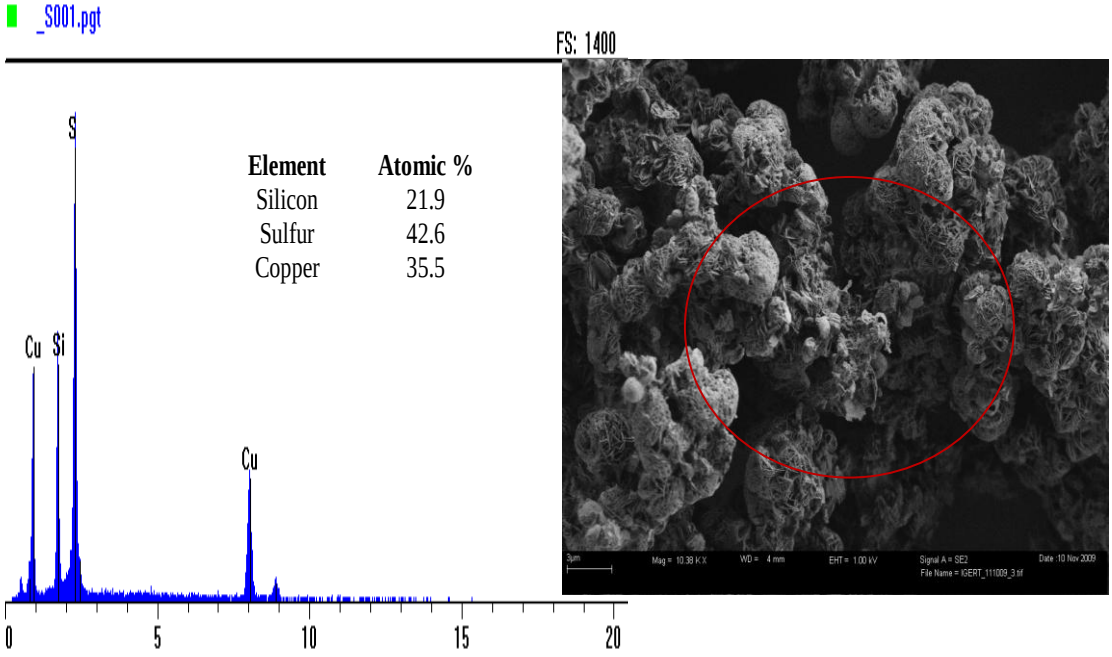


Figure 31. Elemental analysis from an energy dispersive x-ray spectroscopy spot scan. The red circle approximates the area over which the spot-scan sampled, given an accelerating voltage of 20 keV.

Table 10. Approximate copper to sulfur ratios of several copper sulfide minerals.

Mineral	Cu:S
Anilite	1.75
Covellite	1.0
Chalcocite	2
Digenite	1.8
Djurleite	1.96
Geerite	1.6
Spionkopite	1.39

Figure 32 shows that scattered x-rays from p-XRD analysis suggest the precipitate contains sulfur and covellite. The presence of elemental sulfur in the precipitate may explain the relatively low ratio of copper to sulfur measured using EDX. A slight offset in the standard peaks from the raw data can be seen in Figure 32, for both the covellite standard

and sulfur standard (green). This may be due to instrument to instrument variation in the angle settings of the goniometer, or errors in calibrating the angle of the goniometer.

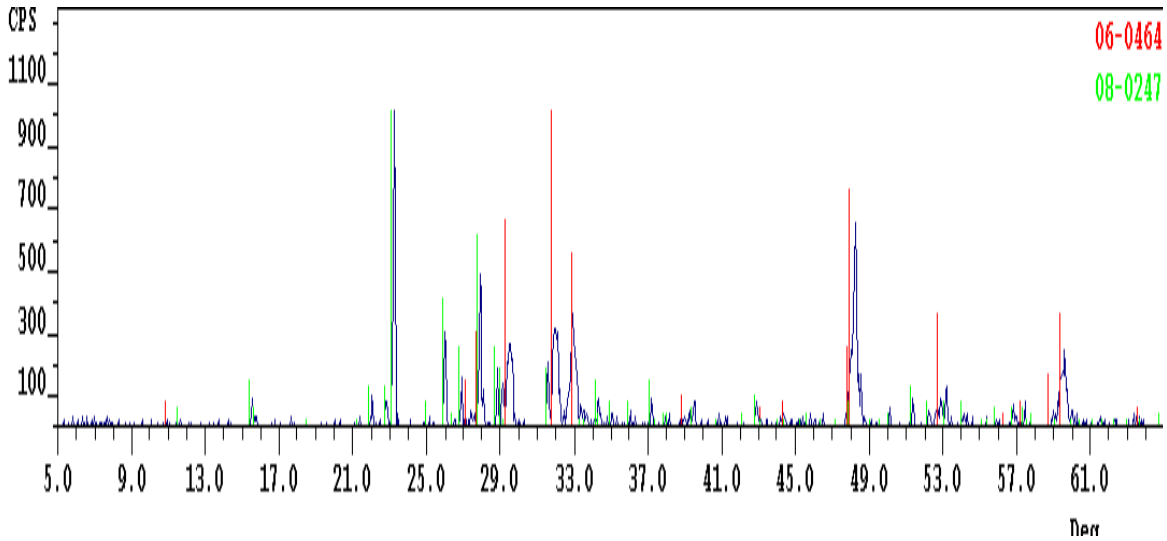


Figure 32. Raw data from powder x-ray diffraction analysis with overlays from an elemental sulfur standard (green) and a covellite standard (red). The reference card numbers are given in the upper right corner.

In summary, the EDX analysis suggests that the precipitate is comprised of copper and sulfur, and the p-XRD analysis supports this, as the crystalline structures for elemental sulfur and covellite were detected. These results are further supported by visual observations, as covellite has a dark grey to black, sooty appearance when moist [11], similar to the precipitate visually observed in the growth medium.

Conclusions and Future Directions

The precipitate formed during the exponential growth phase of BC13 cultures is likely composed of covellite and elemental sulfur. These are interesting results with

implications in biomining and the remediation of acid-mine environments. Many previous researchers have described the ability of *At. caldus* and similar microorganisms to facilitate the dissolution of metals from minerals, especially mineral sulfides [*i.e.* 7-9]. The observations reported here suggest that, under the experimental conditions described, an opposite effect is also possible. These results warrant further study to determine the source of the sulfide required for this mineral formation, and to elucidate a specific mechanism for this formation.

Both elemental sulfur and sulfide may be formed in the periplasm of *At. caldus* during the oxidation of tetrathionate via the SOX pathway, and possibly extracellularly during the oxidation of sulfur via sulfur dehydrogenase [12]. It may be useful to measure sulfide concentrations at various stages throughout batch growth, and possibly in various cell fractions. Past work has shown that BC13 can oxidize molecular hydrogen [1]. Therefore, experiments using it as an electron donor, in place of a reduced sulfur compound, could determine whether the sulfate salts present in the medium may be a primary source for the sulfide generation. However, no acidithiobacilli have been observed to use sulfate as an electron acceptor, and it is unlikely that assimilatory sulfate reduction would result in the amount of sulfide necessary for the precipitation measured here. Finally, as the precipitation was only observed during the late-exponential/early-stationary phase of batch growth, chemostat experiments with varying dilution rates would be interesting to determine if steady state covellite precipitation could be elucidated at various growth rates.

References

1. Hallberg KB, Lindstrom EB (1994) Characterization of *Thiobacillus caldus* sp. Nov., a moderately thermophilic acidophile. *Microbiology* 140:3451-3456.

2. Dopson M, Lindstrom EB, Hallberg KB (2002) ATP generation during reduced inorganic sulfur compound oxidation by *Acidithiobacillus caldus* is exclusively due to electron transport phosphorylation. *Extremophiles* 6:123-129.

3. Burton NP, Norris PR (2000) Microbiology of acidic, geothermal springs of Montserrat: environmental rDNA analysis. *Extremophiles* 4:315-320.

4. Druschel GK, Baker BJ, Gihiring TM, Banfield JF (2004) Acid mine drainage biogeochemistry at Iron Mountain, California. *Geochem Trans* 5:12-32.

5. Goebel BM, Stackebrandt E (1994) Cultural and phylogenetic analysis of mixed microbial populations found in natural and commercial bioleaching environments. *Appl Environ Microbiol* 60:1614-1621.

6. Okibe N, Gericke M, Hallberg KB, Johnson DB (2003) Enumeration and characterization of acidophilic microorganisms isolated for a pilot plant stirred-tank bioleaching operation. *Appl Environ Microbiol* 69:1936-1943.

7. McGuire MM, Edwards KJ, Banfield JF, Hamers RJ (2001) Kinetics, surface chemistry, and structural evolution of microbially mediated sulfide mineral dissolution. *Geochem Geophys Geosyst* 65:1243-1258.

8. Dopson M, Lindstrom EB. 1999. Potential role of *Thiobacillus caldus* in arsenopyrite bioleaching. *Appl Environ Microbiol* 65:36-40.

9. Zhou QG, Bo F, Bo ZH, Xi L, Jian G, Fei LF, Hau CH (2007) Isolation of a strain of *Acidithiobacillus caldus* and its role in bioleaching of chalcopyrite. *World J Microbiol Biotechnol* 23:1217-1225.

10. Matin A, Wilson B, Zynchlinski E, Matin M (1982) Proton motive force and physiological basis of delta pH maintenance in *Thiobacillus acidophilus*. *J Bact* 150:582-591.

11. Klein C, Hurlbut CS (1977) Manual of Mineralogy. John Wiley & Sons. 361.

12. Valdes J, Quatrini R, Hallberg K, Dopson M, Valenzuela PDT, Holmes DS (2009) Draft genome sequence of the extremely acidophilic bacterium *Acidithiobacillus caldus* ATCC 51756 reveals metabolic versatility in the genus *Acidithiobacillus*. *J Bact* 191:5877-5878.

Raw Data

Table B.1. BC13 cell concentrations during growth. This experiment was repeated in triplicate and average values, standard deviations (STDEV), and 95% confidence intervals (95% CI) are shown. Concentrations are in cells mL^{-1}, and time is in hours.

Elapsed Time (h)	Trial 1	Trial 2	Trial 3	Average	STDEV	95% CI
0	5.63E+07	5.65E+07	5.76E+07	5.68E+07	7.07E+05	8.00E+05
12	5.33E+07	4.93E+07	4.93E+07	5.06E+07	2.34E+06	2.64E+06
24	5.70E+07	5.63E+07	5.42E+07	5.58E+07	1.43E+06	1.61E+06
36	4.98E+07	5.47E+07	5.56E+07	5.34E+07	3.12E+06	3.53E+06
48	5.41E+07	5.71E+07	5.44E+07	5.52E+07	1.67E+06	1.89E+06
60	6.78E+07	6.82E+07	6.69E+07	6.76E+07	6.77E+05	7.66E+05
72	7.86E+07	8.27E+07	8.83E+07	8.32E+07	4.87E+06	5.51E+06
84	1.13E+08	1.23E+08	1.15E+08	1.17E+08	5.46E+06	6.18E+06
96	1.40E+08	1.54E+08	1.65E+08	1.53E+08	1.27E+07	1.44E+07
108	2.37E+08	2.36E+08	2.28E+08	2.34E+08	5.16E+06	5.84E+06
120	2.39E+08	2.58E+08	2.57E+08	2.51E+08	1.05E+07	1.19E+07
151	2.18E+08	2.39E+08	2.45E+08	2.34E+08	1.39E+07	1.58E+07
170	2.35E+08	2.16E+08	2.01E+08	2.17E+08	1.73E+07	1.95E+07

Table B.2. Change in concentration of precipitate during batch growth of BC13. Experiments were repeated in triplicate and average values, standard deviations (STDEV), and 95% confidence intervals (95% CI) are shown. Concentrations are given in mg L^{-1}.

Elapsed Time (h)	Trial 1	Trial 2	Trial 3	Average	STDEV	95% CI
0	0	0	0	0	0	0
24	0	0	0	0	0	0
48	0	0	0	0	0	0
96	0	0	0	0	0	0
120	43	68	45	52	14	16
144	51	73	45	56	15	17

Table B.3. Change in medium pH during batch growth of BC13. Experiments were repeated in triplicate and average values, standard deviations (STDEV), and 95% confidence intervals (95% CI) are shown.

	pH					
Elapsed Time (h)	Trial 1	Trial 2	Trial 3	Average	STDEV	95% CI
0	2.50	2.50	2.50	2.50	0.00	0.00
24	2.41	2.29	2.45	2.38	0.08	0.09
48	2.04	2.06	2.13	2.08	0.05	0.05
96	1.90	1.82	2.11	1.94	0.15	0.17
120	1.85	1.73	2.02	1.87	0.15	0.16
144	1.76	1.77	2.03	1.85	0.15	0.17

APPENDIX C

COMPONENTS OF GROWTH MEDIUM

Table C.1. Concentrations of base media components used in all experiments. Concentrations of organic acids or metals added to toxicity or sorption experiments are described in the text of the dissertation.

Media component	Concentration (g $L^{-1)}$
$(NH_4)_2SO_4$	3.00
$Na_2SO_4 \cdot 10H_20$	3.20
KCl	0.10
K_2HPO_4	0.05
$MgSO_4 \cdot 7H_2O$	0.50
$Ca(NO_3)_2$	0.010
$FeCl_3 \cdot 6H_2O$	0.011
$CuSO_4 \cdot 5H_2O$	0.0005
HBO_3	0.0020
$MnSO_4 \cdot H_2O$	0.0020
$Na_2MoO_4 \cdot 2H_2O$	0.0008
$CoCl_2 \cdot 6H_2O$	0.0006
$ZnSO_4 \cdot 7H_2O$	0.0009

APPENDIX D

CALCULATION OF SPECIFIC GROWTH RATES

Specific growth rates were calculated for two systems in the experiments discussed in this dissertation 1) batch systems and 2) chemostat systems. In each case the specific growth rates were determined from a cell-mass balance calculation.

Calculation of Specific Growth Rates in Batch Cultures

With respect to cells:

$$Accumulation = Flow_{in} - Flow_{out} + Generation \qquad \text{Equation D.1}$$

May be represented as:

$$\frac{dX}{dt} = F_{X_o} - F_X + \int^{V} r_X dV \qquad \text{Equation D.2}$$

Where X represents the number of cells in a control volume, V, t represents time, F_{X_o} represents the flow of cells into V, F_X represents the flow out of V, and r_X represents the reaction rate of cells.

During batch culturing there is no flow in or out of the system, and the system is assumed to be well mixed, so Equation D.2 may be re-written as:

$$\frac{dX}{dt} = r_X V \qquad \text{Equation D.3}$$

Also:

$$X = C_X V \qquad \text{Equation D.4}$$

$$r_X = \mu C_X \qquad \text{Equation D.5}$$

where C_X is the cell concentration and μ is the specific growth rate. Therefore, for a constant volume system, Equation D.4 may be re-written as:

$$\frac{dC_X}{dt} = \mu C_X \qquad \text{Equation D.6}$$

Separation and integration gives the following solution:

$$\ln(C_X) = \mu t + \ln(C_{X_o}) \qquad \text{Equation D.7}$$

where C_{X_o} is the initial cell concentration. It can be seen that a plot of the natural logarithm of the cell concentration against elapsed time will have a slope equal to the specific growth rate.

Calculation of Specific Growth Rates in Chemostat Cultures

With respect to cells:

$$Accumulation = Flow_{in} - Flow_{out} + Generation \qquad \text{Equation D.1}$$

May be represented as:

$$\frac{dX}{dt} = F_{X\,o} - F_X + \int^{V} r_X \, dV \qquad \text{Equation D.2}$$

The chemostat cultures described in this dissertation were well mixed, so the reaction rate can be assumed to be independent of location within the chemostat. Also, there were no cells present in the influent. Substituting in Equations D.4 and D.5, Equation D.2 can be re-written as:

$$\frac{dC_X}{dt} = \frac{-F_X}{V} + \mu C_X \qquad \text{Equation D.8}$$

for a chemostat reactor. At steady state, this Equation D.8 can be simplified to:

$$\frac{F_X}{V} = \mu C_X \qquad \text{Equation D.9}$$

because,

$$F_X = \nu C_X \qquad \text{Equation D.10}$$

where ν is the volumetric flow rate, Equation D.11 may be re-written as:

$$\mu = \frac{\nu}{V} \qquad \text{Equation D.11}$$

Or by definition:

$$\mu = D \qquad \text{Equation D.12}$$

where D is the dilution rate.

APPENDIX E

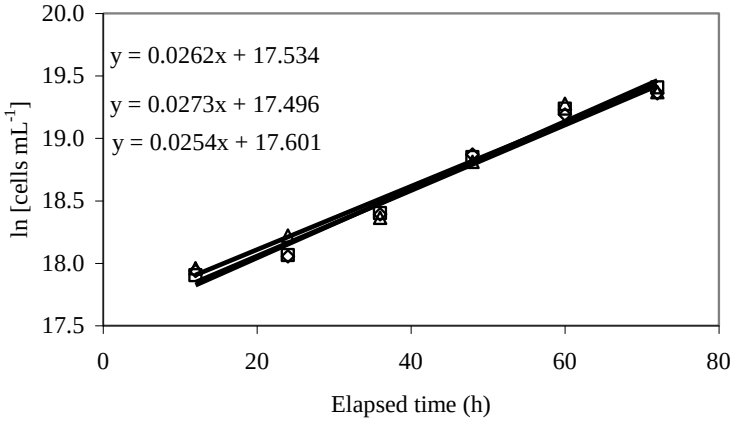
CHAPTER TWO RAW DATA

Organic Acid Free Control

BC13 cell concentrations with time when grown in the absence of organic acids. Experiments were repeated in triplicate and average values, standard deviations (STDEV), and 95% confidence intervals (95% CI) are shown. Specific growth rates are calculated using linear regressions and are shown along with the corresponding STDEV and 95% CI to the right of the plots.

Table E.1. BC13 growth in the absence of organic acids.

	Cells mL^{-1}						ln (Cells mL^{-1})		
Elapsed Time (h)	Trial 1	Trial 2	Trial 3	Average	STDEV	95% CI	Trial 1	Trial 2	Trial 3
0	5.00E+07	5.25E+07	5.10E+07	5.12E+07	1.25E+06	1.42E+06	17.73	17.78	17.75
12	6.17E+07	5.96E+07	6.30E+07	6.15E+07	1.70E+06	1.93E+06	17.94	17.90	17.96
24	6.93E+07	7.00E+07	8.20E+07	7.38E+07	7.12E+06	8.06E+06	18.05	18.06	18.22
36	9.71E+07	9.81E+07	9.44E+07	9.65E+07	1.93E+06	2.18E+06	18.39	18.40	18.36
48	1.57E+08	1.54E+08	1.48E+08	1.53E+08	4.55E+06	5.15E+06	18.87	18.85	18.81
60	2.16E+08	2.26E+08	2.35E+08	2.26E+08	9.76E+06	1.10E+07	19.19	19.24	19.28
72	2.56E+08	2.68E+08	2.58E+08	2.61E+08	6.50E+06	7.35E+06	19.36	19.41	19.37
84	2.86E+08	2.93E+08	2.81E+08	2.87E+08	5.71E+06	6.46E+06	19.47	19.49	19.45
96	3.26E+08	3.59E+08	3.01E+08	3.29E+08	2.93E+07	3.31E+07	19.60	19.70	19.52
108	3.54E+08	3.89E+08	3.23E+08	3.56E+08	3.31E+07	3.75E+07	19.68	19.78	19.59
120	3.62E+08	3.06E+08	3.34E+08	3.34E+08	2.78E+07	3.15E+07	19.71	19.54	19.63



Specific growth rate (h^{-1})

Trial 1	0.026
Trial 2	0.027
Trial 3	0.025
Average	0.026
STDEV	0.001
95% CI	0.001

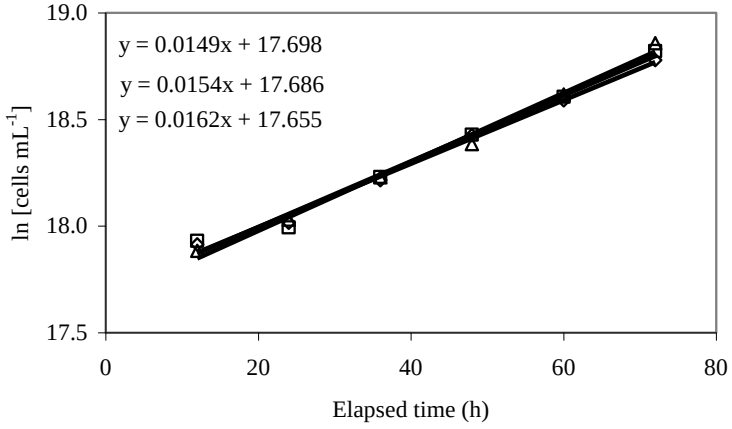
Figure E.1. Specific growth rate calculations for Trial 1 (open circles), Trial 2 (open squares), and Trial 3 (open triangles).

Toxicity of Organic Acids When Presented Singly

BC13 cell concentrations with time when grown in the presence of varying concentrations of different organic acids. Experiments were repeated in triplicate and average values, standard deviations (STDEV), and 95% confidence intervals (95% CI) are shown. Specific growth rates were calculated using linear regressions and are shown along with the corresponding STDEV and 95% CI to the right of the plots. Elapsed time is given in hours

Table E.2. BC13 growth in the presence of 50 μM pyruvate.

	Cells mL^{-1}						ln (Cells mL^{-1})		
Elapsed Time (h)	Trial 1	Trial 2	Trial 3	Average	STDEV	95% CI	Trial 1	Trial 2	Trial 3
0	5.18E+07	5.58E+07	5.10E+07	5.28E+07	2.57E+06	2.91E+06	17.76	17.84	17.75
12	6.03E+07	6.13E+07	5.85E+07	6.00E+07	1.42E+06	1.60E+06	17.91	17.93	17.88
24	6.67E+07	6.52E+07	6.77E+07	6.65E+07	1.24E+06	1.40E+06	18.02	17.99	18.03
36	8.14E+07	8.27E+07	8.25E+07	8.22E+07	6.81E+05	7.71E+05	18.22	18.23	18.23
48	1.00E+08	1.01E+08	9.64E+07	9.92E+07	2.42E+06	2.73E+06	18.43	18.43	18.38
60	1.18E+08	1.20E+08	1.22E+08	1.20E+08	1.72E+06	1.94E+06	18.59	18.61	18.62
72	1.43E+08	1.49E+08	1.55E+08	1.49E+08	5.93E+06	6.71E+06	18.78	18.82	18.86
84	1.62E+08	1.54E+08	1.55E+08	1.57E+08	4.31E+06	4.88E+06	18.90	18.85	18.86
96	1.71E+08	1.76E+08	1.71E+08	1.73E+08	3.06E+06	3.47E+06	18.96	18.99	18.95
108	1.56E+08	1.44E+08	1.48E+08	1.49E+08	5.73E+06	6.49E+06	18.86	18.79	18.82
120	1.62E+08	1.59E+08	1.69E+08	1.63E+08	5.35E+06	6.05E+06	18.90	18.88	18.95

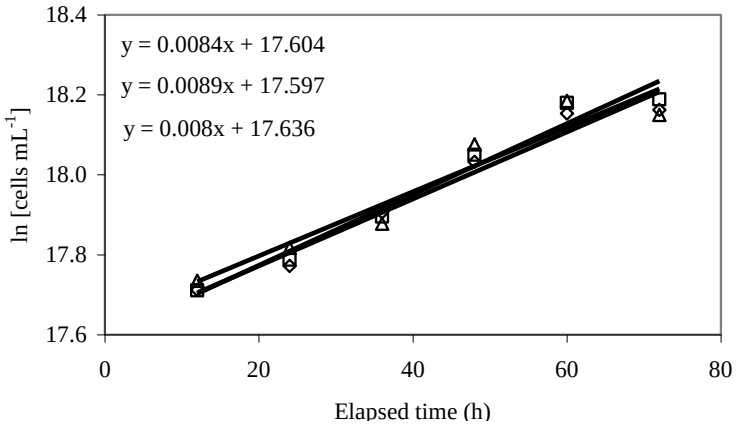


Specific growth rate (h^{-1})	
Trial 1	0.015
Trial 2	0.015
Trial 3	0.016
Average	0.016
STDEV	0.001
95% CI	0.001

.Figure E.2. Specific growth rate calculations for Trial 1 (open circles), Trial 2 (open squares), and Trial 3 (open triangles).

Table E.3. BC13 growth in the presence of 100 μM pyruvate.

	Cells mL^{-1}						ln (Cells mL^{-1})		
Elapsed Time (h)	Trial 1	Trial 2	Trial 3	Average	STDEV	95% CI	Trial 1	Trial 2	Trial 3
0	5.15E+07	5.35E+07	5.36E+07	5.29E+07	1.17E+06	1.32E+06	17.76	17.80	17.80
12	4.92E+07	4.92E+07	5.04E+07	4.96E+07	6.78E+05	7.67E+05	17.71	17.71	17.74
24	5.23E+07	5.31E+07	5.47E+07	5.34E+07	1.24E+06	1.41E+06	17.77	17.79	17.82
36	5.98E+07	5.91E+07	5.81E+07	5.90E+07	8.36E+05	9.46E+05	17.91	17.90	17.88
48	6.78E+07	6.90E+07	7.08E+07	6.92E+07	1.52E+06	1.72E+06	18.03	18.05	18.08
60	7.65E+07	7.86E+07	7.90E+07	7.80E+07	1.33E+06	1.50E+06	18.15	18.18	18.18
72	7.72E+07	7.93E+07	7.63E+07	7.76E+07	1.54E+06	1.74E+06	18.16	18.19	18.15
84	7.95E+07	7.70E+07	7.41E+07	7.68E+07	2.70E+06	3.06E+06	18.19	18.16	18.12
96	8.80E+07	9.02E+07	9.12E+07	8.98E+07	1.61E+06	1.82E+06	18.29	18.32	18.33
108	9.60E+07	9.58E+07	1.01E+08	9.76E+07	2.92E+06	3.31E+06	18.38	18.38	18.43
120	8.44E+07	8.27E+07	8.29E+07	8.33E+07	9.11E+05	1.03E+06	18.25	18.23	18.23

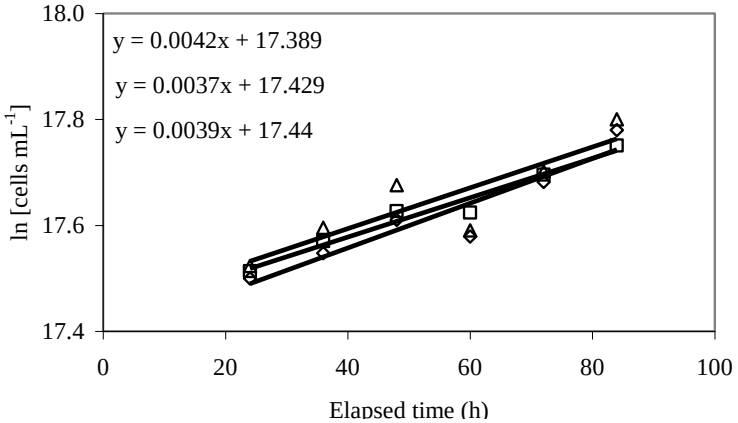


Specific growth rate (h^{-1})	
Trial 1	0.008
Trial 2	0.009
Trial 3	0.008
Average	0.008
STDEV	0.000
95% CI	0.001

Figure E.3. Specific growth rate calculations for Trial 1 (open circles), Trial 2 (open squares), and Trial 3 (open triangles).

Table E.4. BC13 growth in the presence of 250 μM pyruvate.

	Cells mL^{-1}						ln (Cells mL^{-1})		
Elapsed Time (h)	Trial 1	Trial 2	Trial 3	Average	STDEV	95% CI	Trial 1	Trial 2	Trial 3
0	3.93E+07	4.07E+07	3.87E+07	3.96E+07	9.90E+05	1.12E+06	17.49	17.52	17.47
12	4.02E+07	4.21E+07	4.47E+07	4.23E+07	2.25E+06	2.55E+06	17.51	17.55	17.61
24	3.98E+07	4.04E+07	4.08E+07	4.03E+07	4.69E+05	5.30E+05	17.50	17.51	17.52
36	4.18E+07	4.27E+07	4.38E+07	4.28E+07	1.03E+06	1.16E+06	17.55	17.57	17.60
48	4.45E+07	4.52E+07	4.75E+07	4.57E+07	1.57E+06	1.78E+06	17.61	17.63	17.68
60	4.31E+07	4.51E+07	4.36E+07	4.39E+07	1.03E+06	1.16E+06	17.58	17.62	17.59
72	4.78E+07	4.84E+07	4.87E+07	4.83E+07	4.99E+05	5.65E+05	17.68	17.70	17.70
84	5.27E+07	5.12E+07	5.38E+07	5.25E+07	1.31E+06	1.48E+06	17.78	17.75	17.80
96	5.06E+07	5.19E+07	5.10E+07	5.11E+07	6.55E+05	7.41E+05	17.74	17.76	17.75
108	4.82E+07	4.54E+07	4.55E+07	4.64E+07	1.61E+06	1.82E+06	17.69	17.63	17.63
120	4.96E+07	4.76E+07	4.66E+07	4.79E+07	1.55E+06	1.76E+06	17.72	17.68	17.66

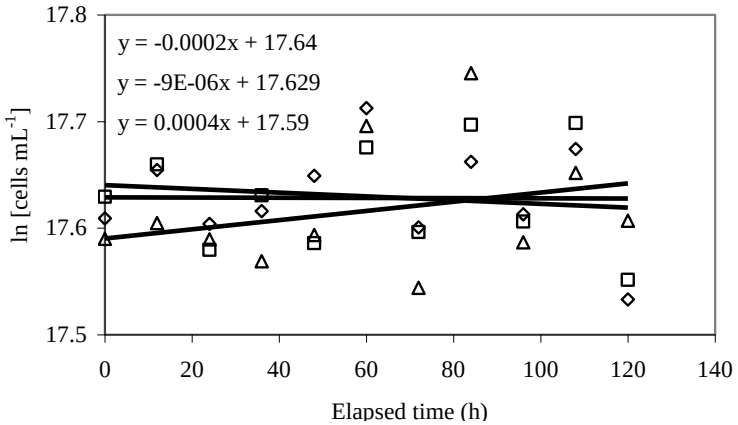


Specific growth rate (h^{-1})	
Trial 1	0.004
Trial 2	0.004
Trial 3	0.004
Average	0.004
STDEV	0.000
95% CI	0.000

Figure E.4. Specific growth rate calculations for Trial 1 (open circles), Trial 2 (open squares), and Trial 3 (open triangles).

Table E.5. BC13 growth in the presence of 500 μM pyruvate.

	Cells mL^{-1}						ln (Cells mL^{-1})		
Elapsed Time (h)	Trial 1	Trial 2	Trial 3	Average	STDEV	95% CI	Trial 1	Trial 2	Trial 3
0	4.44E+07	4.53E+07	4.36E+07	4.44E+07	8.79E+05	9.95E+05	17.61	17.63	17.59
12	4.65E+07	4.67E+07	4.42E+07	4.58E+07	1.38E+06	1.56E+06	17.65	17.66	17.60
24	4.42E+07	4.31E+07	4.36E+07	4.36E+07	5.37E+05	6.08E+05	17.60	17.58	17.59
36	4.47E+07	4.54E+07	4.27E+07	4.43E+07	1.42E+06	1.60E+06	17.62	17.63	17.57
48	4.62E+07	4.34E+07	4.37E+07	4.45E+07	1.54E+06	1.75E+06	17.65	17.59	17.59
60	4.92E+07	4.75E+07	4.84E+07	4.84E+07	8.93E+05	1.01E+06	17.71	17.68	17.70
72	4.40E+07	4.38E+07	4.16E+07	4.32E+07	1.34E+06	1.52E+06	17.60	17.60	17.54
84	4.68E+07	4.85E+07	5.09E+07	4.87E+07	2.04E+06	2.31E+06	17.66	17.70	17.75
96	4.46E+07	4.43E+07	4.34E+07	4.41E+07	5.97E+05	6.75E+05	17.61	17.61	17.59
108	4.74E+07	4.86E+07	4.64E+07	4.74E+07	1.11E+06	1.26E+06	17.67	17.70	17.65
120	4.12E+07	4.19E+07	4.43E+07	4.25E+07	1.64E+06	1.86E+06	17.53	17.55	17.61



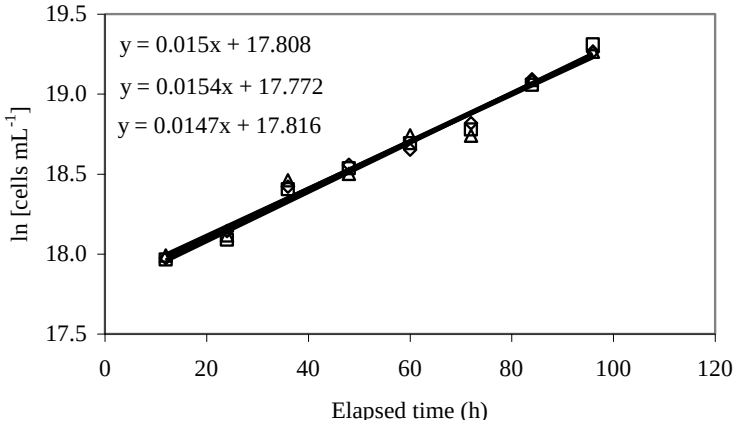
Specific growth rate (h^{-1})	
Trial 1	0.000
Trial 2	0.000
Trial 3	0.000
Average	0.000
STDEV	0.000
95% CI	0.000

Figure E.5. Specific growth rate calculations for Trial 1 (open circles), Trial 2 (open squares), and Trial 3 (open triangles).

Acetate

Table E.6. BC13 growth in the presence of 50 μM acetate.

	Cells mL^{-1}						ln (Cells mL^{-1})		
Elapsed Time (h)	Trial 1	Trial 2	Trial 3	Average	STDEV	95% CI	Trial 1	Trial 2	Trial 3
0	6.11E+07	5.98E+07	6.12E+07	6.07E+07	8.06E+05	9.12E+05	17.93	17.91	17.93
12	6.40E+07	6.34E+07	6.50E+07	6.41E+07	8.23E+05	9.32E+05	17.97	17.97	17.99
24	7.58E+07	7.18E+07	7.37E+07	7.38E+07	1.98E+06	2.24E+06	18.14	18.09	18.12
36	1.00E+08	9.84E+07	1.04E+08	1.01E+08	2.93E+06	3.31E+06	18.42	18.40	18.46
48	1.15E+08	1.12E+08	1.08E+08	1.12E+08	3.21E+06	3.63E+06	18.56	18.54	18.50
60	1.26E+08	1.31E+08	1.38E+08	1.32E+08	5.96E+06	6.74E+06	18.65	18.69	18.74
72	1.49E+08	1.43E+08	1.38E+08	1.43E+08	5.61E+06	6.35E+06	18.82	18.78	18.74
84	1.96E+08	1.89E+08	1.95E+08	1.93E+08	3.75E+06	4.24E+06	19.09	19.06	19.09
96	2.33E+08	2.43E+08	2.33E+08	2.36E+08	6.15E+06	6.96E+06	19.27	19.31	19.27
108	2.24E+08	2.33E+08	2.30E+08	2.29E+08	4.54E+06	5.14E+06	19.23	19.27	19.25
120	2.50E+08	2.62E+08	2.56E+08	2.56E+08	5.71E+06	6.47E+06	19.34	19.38	19.36



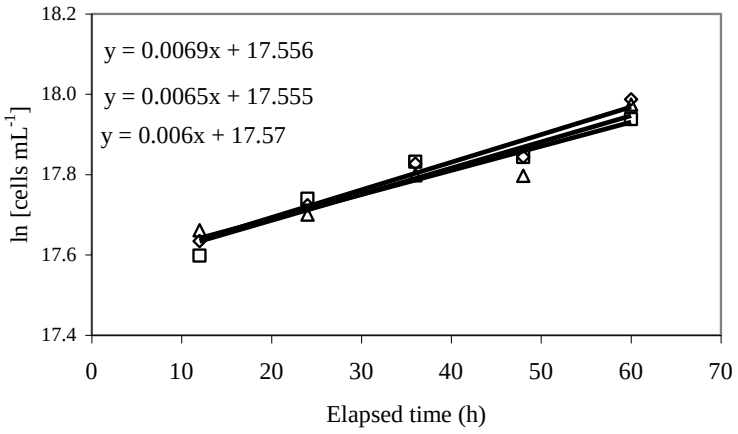
Specific growth rate (h^{-1})

Trial 1	0.015
Trial 2	0.015
Trial 3	0.015
Average	0.015
STDEV	0.000
95% CI	0.000

Figure E.6. Specific growth rate calculations for Trial 1 (open circles), Trial 2 (open squares), and Trial 3 (open triangles).

Table E.7. BC13 growth in the presence of 100 μM acetate.

	Cells mL^{-1}						ln (Cells mL^{-1})		
Elapsed Time (h)	Trial 1	Trial 2	Trial 3	Average	STDEV	95% CI	Trial 1	Trial 2	Trial 3
0	4.59E+07	4.59E+07	4.87E+07	4.69E+07	1.61E+06	1.82E+06	17.64	17.64	17.70
12	4.56E+07	4.39E+07	4.68E+07	4.54E+07	1.44E+06	1.63E+06	17.63	17.60	17.66
24	4.98E+07	5.06E+07	4.87E+07	4.97E+07	9.74E+05	1.10E+06	17.72	17.74	17.70
36	5.53E+07	5.55E+07	5.37E+07	5.48E+07	9.80E+05	1.11E+06	17.83	17.83	17.80
48	5.62E+07	5.61E+07	5.36E+07	5.53E+07	1.48E+06	1.68E+06	17.84	17.84	17.80
60	6.48E+07	6.17E+07	6.40E+07	6.35E+07	1.60E+06	1.81E+06	17.99	17.94	17.97
72	6.23E+07	5.93E+07	6.00E+07	6.05E+07	1.54E+06	1.75E+06	17.95	17.90	17.91
84	7.14E+07	7.05E+07	6.68E+07	6.96E+07	2.43E+06	2.75E+06	18.08	18.07	18.02
96	7.04E+07	6.99E+07	6.61E+07	6.88E+07	2.33E+06	2.63E+06	18.07	18.06	18.01
108	7.59E+07	8.06E+07	7.84E+07	7.83E+07	2.34E+06	2.65E+06	18.15	18.21	18.18
120	7.87E+07	7.91E+07	8.38E+07	8.05E+07	2.82E+06	3.19E+06	18.18	18.19	18.24

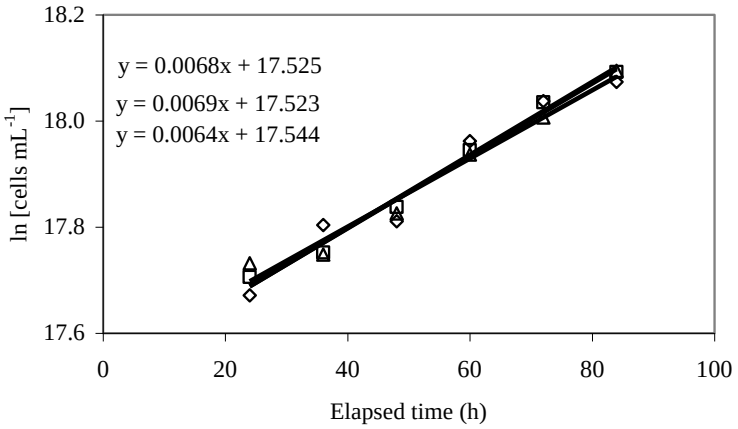


Specific growth rate (h^{-1})	
Trial 1	0.007
Trial 2	0.007
Trial 3	0.006
Average	0.006
STDEV	0.000
95% CI	0.001

Figure E.7. Specific growth rate calculations for Trial 1 (open circles), Trial 2 (open squares), and Trial 3 (open triangles).

Table E.8. BC13 growth in the presence of 250 μM acetate.

	Cells mL^{-1}						ln (Cells mL^{-1})		
Elapsed Time (h)	Trial 1	Trial 2	Trial 3	Average	STDEV	95% CI	Trial 1	Trial 2	Trial 3
0	4.68E+07	4.85E+07	4.81E+07	4.78E+07	8.91E+05	1.01E+06	17.66	17.70	17.69
12	4.63E+07	4.83E+07	4.91E+07	4.79E+07	1.45E+06	1.64E+06	17.65	17.69	17.71
24	4.73E+07	4.89E+07	5.02E+07	4.88E+07	1.48E+06	1.67E+06	17.67	17.71	17.73
36	5.40E+07	5.13E+07	5.10E+07	5.21E+07	1.62E+06	1.83E+06	17.80	17.75	17.75
48	5.44E+07	5.58E+07	5.52E+07	5.51E+07	7.42E+05	8.40E+05	17.81	17.84	17.83
60	6.32E+07	6.22E+07	6.16E+07	6.23E+07	8.00E+05	9.06E+05	17.96	17.95	17.94
72	6.81E+07	6.80E+07	6.61E+07	6.74E+07	1.14E+06	1.29E+06	18.04	18.04	18.01
84	7.07E+07	7.20E+07	7.22E+07	7.16E+07	8.23E+05	9.32E+05	18.07	18.09	18.09
96	7.61E+07	7.41E+07	7.11E+07	7.38E+07	2.52E+06	2.85E+06	18.15	18.12	18.08
108	7.89E+07	7.93E+07	8.38E+07	8.07E+07	2.69E+06	3.04E+06	18.18	18.19	18.24
120	7.40E+07	7.59E+07	7.51E+07	7.50E+07	9.82E+05	1.11E+06	18.12	18.15	18.13

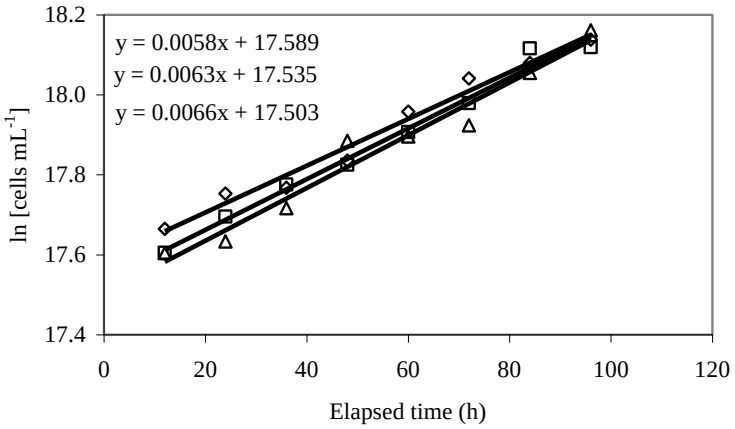


Specific growth rate (h^{-1})	
Trial 1	0.007
Trial 2	0.007
Trial 3	0.006
Average	0.007
STDEV	0.000
95% CI	0.000

Figure E.8. Specific growth rate calculations for Trial 1 (open circles), Trial 2 (open squares), and Trial 3 (open triangles).

Table E.9. BC13 growth in the presence of 500 μM acetate.

	Cells mL^{-1}						ln (Cells mL^{-1})		
Elapsed Time (h)	Trial 1	Trial 2	Trial 3	Average	STDEV	95% CI	Trial 1	Trial 2	Trial 3
0	4.82E+07	4.59E+07	4.52E+07	4.64E+07	1.53E+06	1.73E+06	17.69	17.64	17.63
12	4.70E+07	4.42E+07	4.42E+07	4.51E+07	1.58E+06	1.79E+06	17.66	17.60	17.60
24	5.13E+07	4.84E+07	4.55E+07	4.84E+07	2.88E+06	3.26E+06	17.75	17.70	17.63
36	5.20E+07	5.25E+07	4.95E+07	5.13E+07	1.63E+06	1.84E+06	17.77	17.78	17.72
48	5.57E+07	5.51E+07	5.85E+07	5.65E+07	1.83E+06	2.07E+06	17.84	17.83	17.89
60	6.29E+07	5.98E+07	5.92E+07	6.06E+07	2.02E+06	2.28E+06	17.96	17.91	17.90
72	6.84E+07	6.43E+07	6.08E+07	6.45E+07	3.80E+06	4.30E+06	18.04	17.98	17.92
84	7.11E+07	7.38E+07	6.94E+07	7.14E+07	2.21E+06	2.50E+06	18.08	18.12	18.06
96	7.54E+07	7.40E+07	7.72E+07	7.55E+07	1.61E+06	1.83E+06	18.14	18.12	18.16
108	7.41E+07	7.15E+07	7.59E+07	7.38E+07	2.22E+06	2.51E+06	18.12	18.08	18.14
120	7.53E+07	8.01E+07	7.49E+07	7.68E+07	2.88E+06	3.26E+06	18.14	18.20	18.13



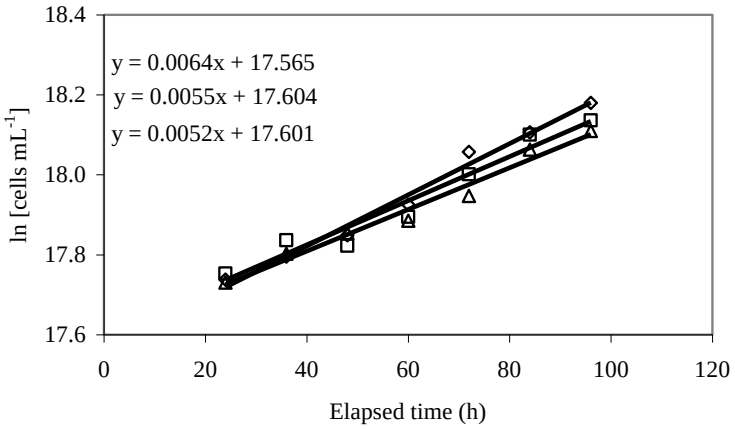
Specific growth rate (h^{-1})

Trial 1	0.006
Trial 2	0.006
Trial 3	0.007
Average	0.006
STDEV	0.000
95% CI	0.000

Figure E.9. Specific growth rate calculations for Trial 1 (open circles), Trial 2 (open squares), and Trial 3 (open triangles).

Table E.10. BC13 growth in the presence of 1,000 μM acetate.

	Cells mL^{-1}						ln (Cells mL^{-1})		
Elapsed Time (h)	Trial 1	Trial 2	Trial 3	Average	STDEV	95% CI	Trial 1	Trial 2	Trial 3
0	4.89E+07	5.01E+07	4.72E+07	4.87E+07	1.48E+06	1.67E+06	17.70	17.73	17.67
12	4.99E+07	5.00E+07	5.01E+07	5.00E+07	9.27E+04	1.05E+05	17.73	17.73	17.73
24	5.05E+07	5.13E+07	5.02E+07	5.07E+07	5.89E+05	6.66E+05	17.74	17.75	17.73
36	5.35E+07	5.58E+07	5.39E+07	5.44E+07	1.20E+06	1.36E+06	17.80	17.84	17.80
48	5.64E+07	5.50E+07	5.68E+07	5.61E+07	9.64E+05	1.09E+06	17.85	17.82	17.85
60	6.09E+07	5.91E+07	5.86E+07	5.95E+07	1.24E+06	1.41E+06	17.93	17.89	17.89
72	6.95E+07	6.57E+07	6.23E+07	6.58E+07	3.61E+06	4.09E+06	18.06	18.00	17.95
84	7.30E+07	7.26E+07	6.99E+07	7.18E+07	1.67E+06	1.89E+06	18.11	18.10	18.06
96	7.86E+07	7.52E+07	7.33E+07	7.57E+07	2.69E+06	3.04E+06	18.18	18.14	18.11
108	7.82E+07	7.93E+07	6.71E+07	7.49E+07	6.74E+06	7.62E+06	18.18	18.19	18.02
120	7.81E+07	7.34E+07	7.02E+07	7.39E+07	3.97E+06	4.50E+06	18.17	18.11	18.07

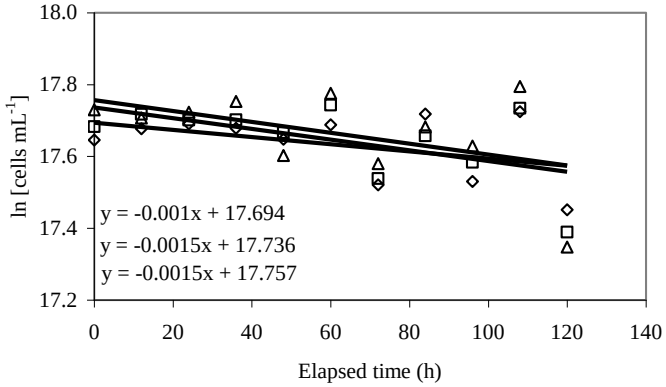


Specific growth rate (h^{-1})	
Trial 1	0.006
Trial 2	0.006
Trial 3	0.005
Average	0.006
STDEV	0.001
95% CI	0.001

Figure E.10. Specific growth rate calculations for Trial 1 (open circles), Trial 2 (open squares), and Trial 3 (open triangles).

Table E.11. BC13 growth in the presence of 5,000 μM acetate.

	Cells mL^{-1}						ln (Cells mL^{-1})		
Elapsed Time (h)	Trial 1	Trial 2	Trial 3	Average	STDEV	95% CI	Trial 1	Trial 2	Trial 3
0	4.61E+07	4.78E+07	5.01E+07	4.80E+07	2.02E+06	2.29E+06	17.65	17.68	17.73
12	4.75E+07	4.95E+07	4.90E+07	4.87E+07	1.02E+06	1.16E+06	17.68	17.72	17.71
24	4.82E+07	4.87E+07	4.98E+07	4.89E+07	7.98E+05	9.03E+05	17.69	17.70	17.72
36	4.76E+07	4.87E+07	5.13E+07	4.92E+07	1.88E+06	2.13E+06	17.68	17.70	17.75
48	4.62E+07	4.70E+07	4.41E+07	4.58E+07	1.49E+06	1.69E+06	17.65	17.67	17.60
60	4.81E+07	5.08E+07	5.25E+07	5.04E+07	2.21E+06	2.51E+06	17.69	17.74	17.78
72	4.07E+07	4.14E+07	4.31E+07	4.17E+07	1.27E+06	1.44E+06	17.52	17.54	17.58
84	4.95E+07	4.66E+07	4.78E+07	4.80E+07	1.46E+06	1.65E+06	17.72	17.66	17.68
96	4.10E+07	4.33E+07	4.53E+07	4.32E+07	2.13E+06	2.41E+06	17.53	17.58	17.63
108	4.98E+07	5.03E+07	5.35E+07	5.12E+07	1.97E+06	2.23E+06	17.72	17.73	17.79
120	3.79E+07	3.57E+07	3.42E+07	3.59E+07	1.88E+06	2.13E+06	17.45	17.39	17.35



Specific growth rate (h^{-1})

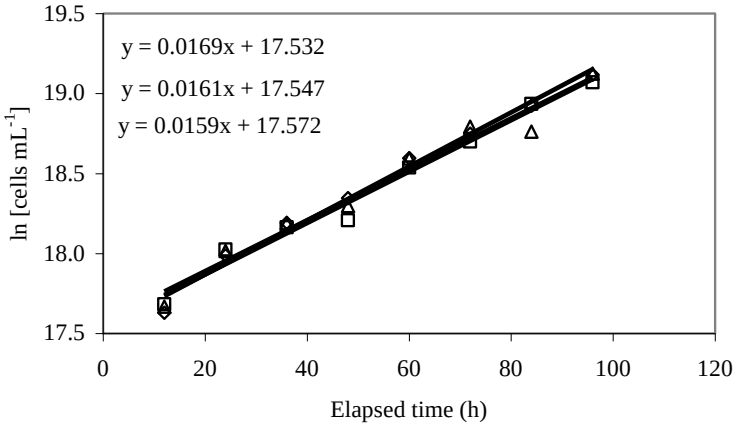
Trial 1	0.000
Trial 2	0.000
Trial 3	0.000
Average	0.000
STDEV	0.000
95% CI	0.000

Figure E.11. Specific growth rate calculations for Trial 1 (open circles), Trial 2 (open squares), and Trial 3 (open triangles).

2-ketoglutarate

Table E.12. BC13 growth in the presence of 50 μM 2-ketoglutarate.

	Cells mL^{-1}						ln (Cells mL^{-1})		
Elapsed Time (h)	Trial 1	Trial 2	Trial 3	Average	STDEV	95% CI	Trial 1	Trial 2	Trial 3
0	4.76E+07	4.57E+07	4.68E+07	4.67E+07	9.64E+05	1.09E+06	17.68	17.64	17.66
12	4.54E+07	4.78E+07	4.71E+07	4.67E+07	1.26E+06	1.42E+06	17.63	17.68	17.67
24	6.50E+07	6.73E+07	6.67E+07	6.63E+07	1.22E+06	1.38E+06	17.99	18.02	18.02
36	7.94E+07	7.73E+07	7.94E+07	7.87E+07	1.23E+06	1.39E+06	18.19	18.16	18.19
48	9.28E+07	8.08E+07	8.83E+07	8.73E+07	6.09E+06	6.89E+06	18.35	18.21	18.30
60	1.19E+08	1.12E+08	1.19E+08	1.17E+08	3.79E+06	4.29E+06	18.60	18.54	18.59
72	1.39E+08	1.32E+08	1.45E+08	1.39E+08	6.41E+06	7.25E+06	18.75	18.70	18.79
84	1.65E+08	1.67E+08	1.41E+08	1.58E+08	1.49E+07	1.69E+07	18.92	18.94	18.76
96	2.01E+08	1.91E+08	2.02E+08	1.98E+08	5.89E+06	6.66E+06	19.12	19.07	19.12
108	1.87E+08	1.98E+08	2.04E+08	1.96E+08	8.71E+06	9.86E+06	19.04	19.10	19.13
120	1.77E+08	1.72E+08	1.74E+08	1.74E+08	2.32E+06	2.62E+06	18.99	18.96	18.98



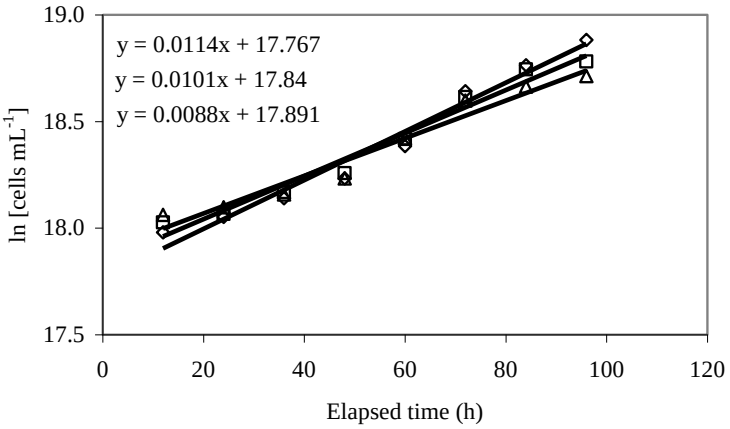
Specific growth rate (h^{-1})

Trial 1	0.017
Trial 2	0.016
Trial 3	0.016
Average	0.016
STDEV	0.001
95% CI	0.001

Figure E.12. Specific growth rate calculations for Trial 1 (open circles), Trial 2 (open squares), and Trial 3 (open triangles).

Table E.13. BC13 growth in the presence of 100 μM 2-ketoglutarate.

	Cells mL^{-1}						ln (Cells mL^{-1})		
Elapsed Time (h)	Trial 1	Trial 2	Trial 3	Average	STDEV	95% CI	Trial 1	Trial 2	Trial 3
0	5.52E+07	6.42E+07	6.25E+07	6.06E+07	4.80E+06	5.44E+06	17.83	17.98	17.95
12	6.43E+07	6.74E+07	6.98E+07	6.72E+07	2.75E+06	3.12E+06	17.98	18.03	18.06
24	6.92E+07	7.01E+07	7.24E+07	7.06E+07	1.63E+06	1.84E+06	18.05	18.07	18.10
36	7.55E+07	7.78E+07	7.68E+07	7.67E+07	1.12E+06	1.26E+06	18.14	18.17	18.16
48	8.29E+07	8.49E+07	8.29E+07	8.36E+07	1.16E+06	1.31E+06	18.23	18.26	18.23
60	9.65E+07	9.96E+07	1.00E+08	9.87E+07	1.96E+06	2.22E+06	18.38	18.42	18.42
72	1.25E+08	1.21E+08	1.19E+08	1.22E+08	2.75E+06	3.11E+06	18.64	18.61	18.60
84	1.41E+08	1.38E+08	1.27E+08	1.35E+08	7.07E+06	8.00E+06	18.76	18.74	18.66
96	1.59E+08	1.43E+08	1.34E+08	1.45E+08	1.25E+07	1.41E+07	18.88	18.78	18.71
108	1.67E+08	1.43E+08	1.41E+08	1.51E+08	1.42E+07	1.61E+07	18.93	18.78	18.77
120	1.62E+08	1.56E+08	1.59E+08	1.59E+08	2.98E+06	3.37E+06	18.91	18.87	18.89



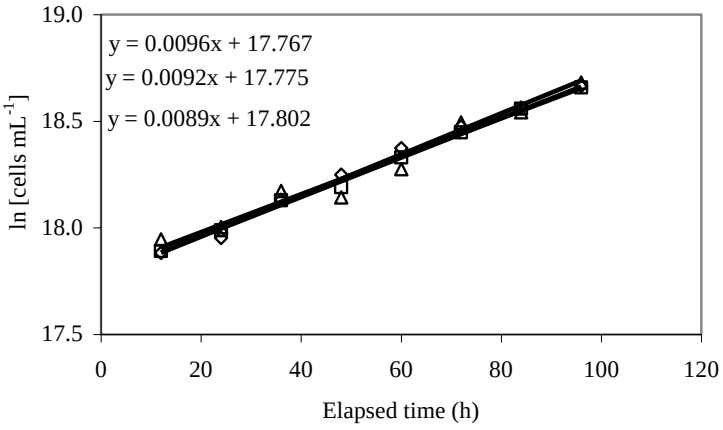
Specific growth rate (h^{-1})

Trial 1	0.011
Trial 2	0.010
Trial 3	0.009
Average	0.010
STDEV	0.001
95% CI	0.001

Figure E.13. Specific growth rate calculations for Trial 1 (open circles), Trial 2 (open squares), and Trial 3 (open triangles).

Table E.14. BC13 growth in the presence of 250 μM 2-ketoglutarate.

	Cells mL^{-1}						ln (Cells mL^{-1})		
Elapsed Time (h)	Trial 1	Trial 2	Trial 3	Average	STDEV	95% CI	Trial 1	Trial 2	Trial 3
0	5.51E+07	5.35E+07	5.37E+07	5.41E+07	8.60E+05	9.73E+05	17.82	17.80	17.80
12	5.84E+07	5.89E+07	6.22E+07	5.98E+07	2.06E+06	2.34E+06	17.88	17.89	17.95
24	6.26E+07	6.49E+07	6.58E+07	6.45E+07	1.66E+06	1.88E+06	17.95	17.99	18.00
36	7.49E+07	7.47E+07	7.80E+07	7.59E+07	1.84E+06	2.08E+06	18.13	18.13	18.17
48	8.42E+07	7.94E+07	7.57E+07	7.98E+07	4.27E+06	4.83E+06	18.25	18.19	18.14
60	9.54E+07	9.13E+07	8.64E+07	9.10E+07	4.48E+06	5.06E+06	18.37	18.33	18.27
72	1.06E+08	1.03E+08	1.08E+08	1.05E+08	2.43E+06	2.75E+06	18.48	18.45	18.49
84	1.15E+08	1.15E+08	1.13E+08	1.14E+08	1.27E+06	1.43E+06	18.56	18.56	18.54
96	1.28E+08	1.27E+08	1.30E+08	1.28E+08	1.56E+06	1.77E+06	18.67	18.66	18.68
108	1.36E+08	1.31E+08	1.25E+08	1.31E+08	5.20E+06	5.88E+06	18.73	18.69	18.65
120	1.38E+08	1.45E+08	1.37E+08	1.40E+08	4.23E+06	4.79E+06	18.74	18.79	18.74

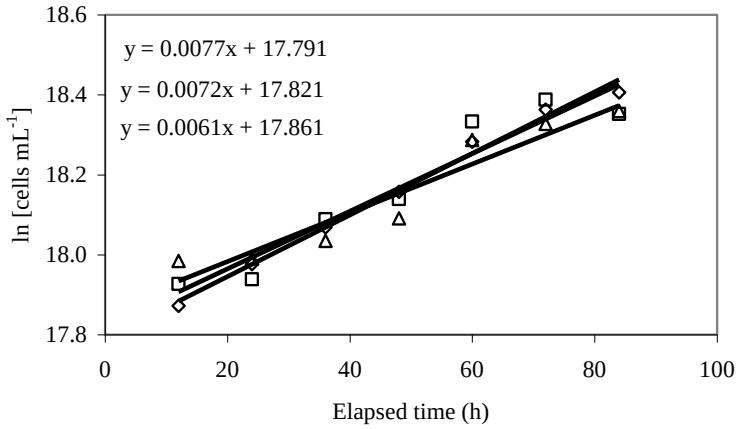


Specific growth rate (h^{-1})	
Trial 1	0.010
Trial 2	0.009
Trial 3	0.009
Average	0.009
STDEV	0.000
95% CI	0.000

Figure E.14. Specific growth rate calculations for Trial 1 (open circles), Trial 2 (open squares), and Trial 3 (open triangles).

Table E.15. BC13 growth in the presence of 500 μM 2-ketoglutarate.

	Cells mL^{-1}						ln (Cells mL^{-1})		
Elapsed Time (h)	Trial 1	Trial 2	Trial 3	Average	STDEV	95% CI	Trial 1	Trial 2	Trial 3
0	5.67E+07	5.38E+07	5.34E+07	5.46E+07	1.83E+06	2.07E+06	17.85	17.80	17.79
12	5.78E+07	6.10E+07	6.47E+07	6.12E+07	3.43E+06	3.89E+06	17.87	17.93	17.98
24	6.41E+07	6.18E+07	6.51E+07	6.37E+07	1.71E+06	1.94E+06	17.98	17.94	17.99
36	7.03E+07	7.18E+07	6.80E+07	7.00E+07	1.91E+06	2.16E+06	18.07	18.09	18.03
48	7.69E+07	7.54E+07	7.19E+07	7.47E+07	2.54E+06	2.88E+06	18.16	18.14	18.09
60	8.71E+07	9.16E+07	8.75E+07	8.87E+07	2.52E+06	2.85E+06	18.28	18.33	18.29
72	9.44E+07	9.68E+07	9.11E+07	9.41E+07	2.84E+06	3.22E+06	18.36	18.39	18.33
84	9.85E+07	9.34E+07	9.40E+07	9.53E+07	2.81E+06	3.18E+06	18.41	18.35	18.36
96	1.10E+08	1.15E+08	1.09E+08	1.11E+08	3.08E+06	3.48E+06	18.52	18.56	18.51
108	1.19E+08	1.25E+08	1.20E+08	1.22E+08	2.99E+06	3.38E+06	18.60	18.64	18.61
120	1.21E+08	1.22E+08	1.27E+08	1.23E+08	3.00E+06	3.39E+06	18.61	18.62	18.66



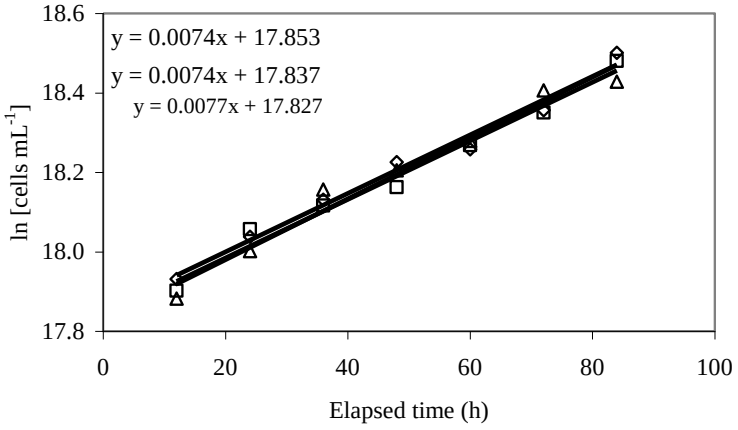
Specific growth rate (h^{-1})

Trial 1	0.008
Trial 2	0.007
Trial 3	0.006
Average	0.007
STDEV	0.001
95% CI	0.001

Figure E.15. Specific growth rate calculations for Trial 1 (open circles), Trial 2 (open squares), and Trial 3 (open triangles).

Table E.16. BC13 growth in the presence of 1,000 μM 2-ketoglutarate.

	Cells mL^{-1}						ln (Cells mL^{-1})		
Elapsed Time (h)	Trial 1	Trial 2	Trial 3	Average	STDEV	95% CI	Trial 1	Trial 2	Trial 3
0	5.88E+07	6.21E+07	6.32E+07	6.13E+07	2.27E+06	2.57E+06	17.89	17.94	17.96
12	6.13E+07	5.95E+07	5.84E+07	5.97E+07	1.48E+06	1.67E+06	17.93	17.90	17.88
24	6.82E+07	6.95E+07	6.58E+07	6.78E+07	1.89E+06	2.13E+06	18.04	18.06	18.00
36	7.48E+07	7.38E+07	7.68E+07	7.51E+07	1.54E+06	1.75E+06	18.13	18.12	18.16
48	8.23E+07	7.73E+07	8.06E+07	8.00E+07	2.55E+06	2.89E+06	18.23	18.16	18.21
60	8.50E+07	8.58E+07	8.68E+07	8.59E+07	9.39E+05	1.06E+06	18.26	18.27	18.28
72	9.37E+07	9.32E+07	9.86E+07	9.52E+07	2.97E+06	3.36E+06	18.36	18.35	18.41
84	1.08E+08	1.06E+08	1.01E+08	1.05E+08	3.89E+06	4.41E+06	18.50	18.48	18.43
96	1.07E+08	1.05E+08	9.99E+07	1.04E+08	3.83E+06	4.33E+06	18.49	18.47	18.42
108	1.08E+08	1.02E+08	9.72E+07	1.03E+08	5.62E+06	6.36E+06	18.50	18.44	18.39
120	1.09E+08	1.15E+08	1.11E+08	1.12E+08	3.12E+06	3.53E+06	18.51	18.56	18.52

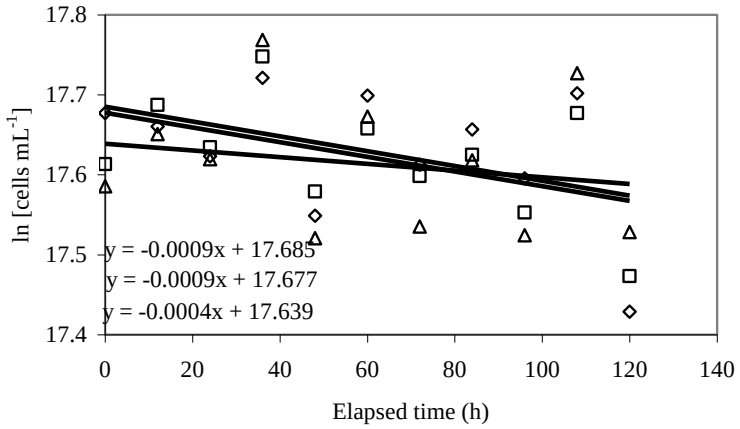


Specific growth rate (h^{-1})	
Trial 1	0.007
Trial 2	0.007
Trial 3	0.008
Average	0.008
STDEV	0.000
95% CI	0.000

Figure E.16. Specific growth rate calculations for Trial 1 (open circles), Trial 2 (open squares), and Trial 3 (open triangles).

Table E.17. BC13 growth in the presence of 5,000 μM 2-ketoglutarate.

	Cells mL^{-1}						ln (Cells mL^{-1})		
Elapsed Time (h)	Trial 1	Trial 2	Trial 3	Average	STDEV	95% CI	Trial 1	Trial 2	Trial 3
0	4.75E+07	4.46E+07	4.34E+07	4.52E+07	2.14E+06	2.42E+06	17.68	17.61	17.59
12	4.67E+07	4.80E+07	4.63E+07	4.70E+07	8.93E+05	1.01E+06	17.66	17.69	17.65
24	4.50E+07	4.55E+07	4.49E+07	4.52E+07	3.52E+05	3.98E+05	17.62	17.63	17.62
36	4.97E+07	5.10E+07	5.21E+07	5.09E+07	1.21E+06	1.37E+06	17.72	17.75	17.77
48	4.18E+07	4.31E+07	4.07E+07	4.19E+07	1.22E+06	1.38E+06	17.55	17.58	17.52
60	4.86E+07	4.66E+07	4.73E+07	4.75E+07	9.89E+05	1.12E+06	17.70	17.66	17.67
72	4.46E+07	4.39E+07	4.13E+07	4.33E+07	1.75E+06	1.99E+06	17.61	17.60	17.54
84	4.66E+07	4.51E+07	4.48E+07	4.55E+07	9.39E+05	1.06E+06	17.66	17.62	17.62
96	4.38E+07	4.20E+07	4.08E+07	4.22E+07	1.52E+06	1.72E+06	17.60	17.55	17.52
108	4.87E+07	4.75E+07	5.00E+07	4.88E+07	1.22E+06	1.38E+06	17.70	17.68	17.73
120	3.71E+07	3.88E+07	4.10E+07	3.89E+07	1.94E+06	2.20E+06	17.43	17.47	17.53



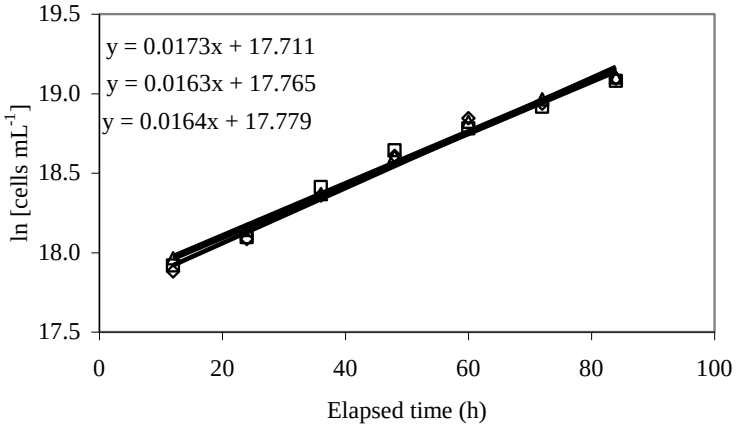
Specific growth rate (h^{-1})	
Trial 1	0.000
Trial 2	0.000
Trial 3	0.000
Average	0.000
STDEV	0.000
95% CI	0.000

Figure E.17. Specific growth rate calculations for Trial 1 (open circles), Trial 2 (open squares), and Trial 3 (open triangles).

Succinate

Table E.18. BC13 growth in the presence of 50 μM succinate.

	Cells mL^{-1}						ln (Cells mL^{-1})		
Elapsed Time (h)	Trial 1	Trial 2	Trial 3	Average	STDEV	95% CI	Trial 1	Trial 2	Trial 3
0	5.53E+07	5.79E+07	5.52E+07	5.62E+07	1.52E+06	1.72E+06	17.83	17.87	17.83
12	5.83E+07	6.05E+07	6.34E+07	6.07E+07	2.54E+06	2.88E+06	17.88	17.92	17.96
24	7.15E+07	7.23E+07	7.57E+07	7.32E+07	2.21E+06	2.50E+06	18.09	18.10	18.14
36	9.40E+07	9.92E+07	9.48E+07	9.60E+07	2.78E+06	3.15E+06	18.36	18.41	18.37
48	1.21E+08	1.25E+08	1.20E+08	1.22E+08	2.71E+06	3.06E+06	18.61	18.64	18.60
60	1.53E+08	1.43E+08	1.49E+08	1.48E+08	4.83E+06	5.46E+06	18.84	18.78	18.82
72	1.68E+08	1.64E+08	1.72E+08	1.68E+08	4.02E+06	4.54E+06	18.94	18.92	18.96
84	1.96E+08	1.93E+08	1.98E+08	1.96E+08	2.21E+06	2.50E+06	19.09	19.08	19.10
96	2.02E+08	2.03E+08	1.97E+08	2.01E+08	3.42E+06	3.87E+06	19.12	19.13	19.10
108	2.21E+08	2.15E+08	2.22E+08	2.19E+08	3.95E+06	4.47E+06	19.21	19.18	19.22
120	1.91E+08	2.01E+08	1.89E+08	1.94E+08	6.37E+06	7.21E+06	19.07	19.12	19.06



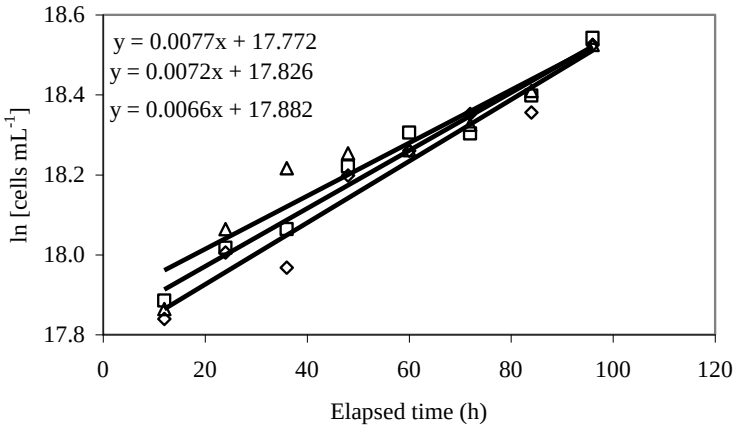
Specific growth rate (h^{-1})

Trial 1	0.017
Trial 2	0.016
Trial 3	0.016
Average	0.017
STDEV	0.001
95% CI	0.001

Figure E.18. Specific growth rate calculations for Trial 1 (open circles), Trial 2 (open squares), and Trial 3 (open triangles).

Table E.19. BC13 growth in the presence of 100 μM succinate.

	Cells mL^{-1}						ln (Cells mL^{-1})		
Elapsed Time (h)	Trial 1	Trial 2	Trial 3	Average	STDEV	95% CI	Trial 1	Trial 2	Trial 3
0	5.30E+07	5.58E+07	5.32E+07	5.40E+07	1.52E+06	1.72E+06	17.79	17.84	17.79
12	5.59E+07	5.86E+07	5.73E+07	5.73E+07	1.33E+06	1.50E+06	17.84	17.89	17.86
24	6.60E+07	6.68E+07	7.00E+07	6.76E+07	2.09E+06	2.37E+06	18.01	18.02	18.06
36	6.36E+07	7.00E+07	8.15E+07	7.17E+07	9.10E+06	1.03E+07	17.97	18.06	18.22
48	8.00E+07	8.19E+07	8.46E+07	8.22E+07	2.31E+06	2.61E+06	18.20	18.22	18.25
60	8.52E+07	8.91E+07	8.53E+07	8.65E+07	2.23E+06	2.53E+06	18.26	18.31	18.26
72	9.33E+07	8.89E+07	9.09E+07	9.11E+07	2.21E+06	2.50E+06	18.35	18.30	18.33
84	9.37E+07	9.78E+07	9.89E+07	9.68E+07	2.73E+06	3.09E+06	18.36	18.40	18.41
96	1.11E+08	1.13E+08	1.11E+08	1.12E+08	1.15E+06	1.30E+06	18.52	18.54	18.52
108	1.17E+08	1.16E+08	1.11E+08	1.15E+08	3.56E+06	4.03E+06	18.58	18.57	18.52
120	1.16E+08	1.18E+08	1.17E+08	1.17E+08	1.01E+06	1.14E+06	18.57	18.58	18.58



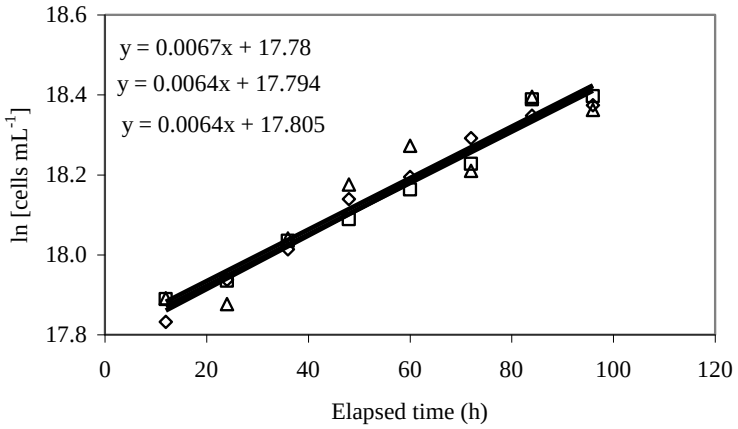
Specific growth rate (h^{-1})

Trial 1	0.008
Trial 2	0.007
Trial 3	0.007
Average	0.007
STDEV	0.001
95% CI	0.001

Figure E.19. Specific growth rate calculations for Trial 1 (open circles), Trial 2 (open squares), and Trial 3 (open triangles).

Table E.20. BC13 growth in the presence of 250 μM succinate.

	Cells mL^{-1}						ln (Cells mL^{-1})		
Elapsed Time (h)	Trial 1	Trial 2	Trial 3	Average	STDEV	95% CI	Trial 1	Trial 2	Trial 3
0	5.45E+07	5.28E+07	4.97E+07	5.23E+07	2.45E+06	2.77E+06	17.81	17.78	17.72
12	5.55E+07	5.88E+07	5.89E+07	5.77E+07	1.93E+06	2.18E+06	17.83	17.89	17.89
24	6.17E+07	6.15E+07	5.80E+07	6.04E+07	2.06E+06	2.33E+06	17.94	17.94	17.88
36	6.66E+07	6.80E+07	6.84E+07	6.76E+07	9.48E+05	1.07E+06	18.01	18.03	18.04
48	7.55E+07	7.18E+07	7.82E+07	7.52E+07	3.26E+06	3.69E+06	18.14	18.09	18.18
60	7.98E+07	7.73E+07	8.62E+07	8.11E+07	4.60E+06	5.20E+06	18.19	18.16	18.27
72	8.79E+07	8.24E+07	8.10E+07	8.38E+07	3.63E+06	4.11E+06	18.29	18.23	18.21
84	9.30E+07	9.68E+07	9.75E+07	9.58E+07	2.42E+06	2.74E+06	18.35	18.39	18.39
96	9.54E+07	9.76E+07	9.43E+07	9.58E+07	1.66E+06	1.88E+06	18.37	18.40	18.36
108	1.24E+08	1.26E+08	1.22E+08	1.24E+08	1.66E+06	1.88E+06	18.63	18.65	18.62
120	1.12E+08	1.13E+08	1.16E+08	1.13E+08	1.97E+06	2.23E+06	18.53	18.54	18.57

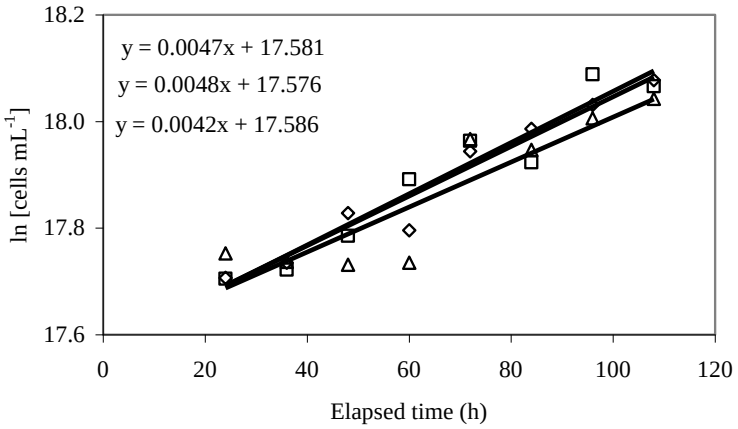


Specific growth rate (h^{-1})	
Trial 1	0.007
Trial 2	0.006
Trial 3	0.006
Average	0.007
STDEV	0.000
95% CI	0.000

Figure E.20. Specific growth rate calculations for Trial 1 (open circles), Trial 2 (open squares), and Trial 3 (open triangles).

Table E.21. BC13 growth in the presence of 500 μM succinate.

	Cells mL^{-1}						ln (Cells mL^{-1})		
Elapsed Time (h)	Trial 1	Trial 2	Trial 3	Average	STDEV	95% CI	Trial 1	Trial 2	Trial 3
0	4.50E+07	4.78E+07	4.88E+07	4.72E+07	1.93E+06	2.19E+06	17.62	17.68	17.70
12	4.77E+07	4.49E+07	4.35E+07	4.54E+07	2.13E+06	2.41E+06	17.68	17.62	17.59
24	4.90E+07	4.89E+07	5.13E+07	4.97E+07	1.35E+06	1.53E+06	17.71	17.70	17.75
36	5.04E+07	4.97E+07	5.05E+07	5.02E+07	4.02E+05	4.54E+05	17.73	17.72	17.74
48	5.53E+07	5.30E+07	5.02E+07	5.28E+07	2.55E+06	2.89E+06	17.83	17.79	17.73
60	5.35E+07	5.89E+07	5.04E+07	5.43E+07	4.31E+06	4.88E+06	17.80	17.89	17.73
72	6.21E+07	6.33E+07	6.35E+07	6.30E+07	7.87E+05	8.91E+05	17.94	17.96	17.97
84	6.48E+07	6.08E+07	6.23E+07	6.26E+07	2.00E+06	2.26E+06	17.99	17.92	17.95
96	6.77E+07	7.17E+07	6.60E+07	6.85E+07	2.92E+06	3.31E+06	18.03	18.09	18.01
108	7.09E+07	7.01E+07	6.85E+07	6.99E+07	1.23E+06	1.39E+06	18.08	18.07	18.04
120	6.77E+07	6.40E+07	6.04E+07	6.40E+07	3.65E+06	4.13E+06	18.03	17.97	17.92

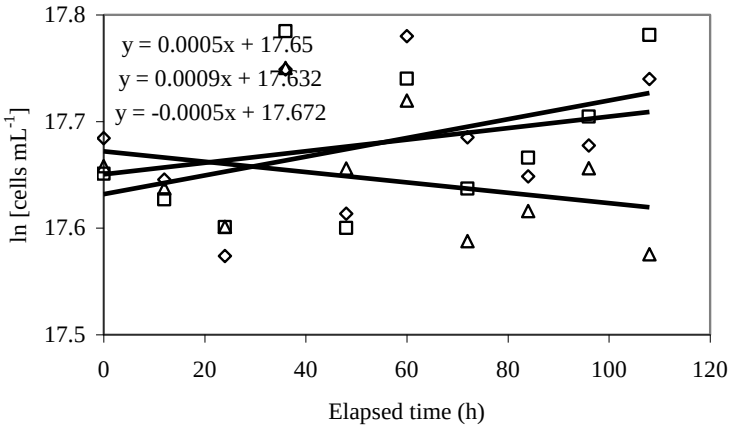


Specific growth rate (h^{-1})	
Trial 1	0.005
Trial 2	0.005
Trial 3	0.004
Average	0.005
STDEV	0.000
95% CI	0.000

Figure E.21. Specific growth rate calculations for Trial 1 (open circles), Trial 2 (open squares), and Trial 3 (open triangles).

Table E.22. BC13 growth in the presence of 1,000 μM succinate.

	Cells mL^{-1}						ln (Cells mL^{-1})		
Elapsed Time (h)	Trial 1	Trial 2	Trial 3	Average	STDEV	95% CI	Trial 1	Trial 2	Trial 3
0	4.79E+07	4.63E+07	4.66E+07	4.69E+07	8.27E+05	9.36E+05	17.68	17.65	17.66
12	4.61E+07	4.52E+07	4.57E+07	4.56E+07	4.25E+05	4.81E+05	17.65	17.63	17.64
24	4.29E+07	4.41E+07	4.41E+07	4.37E+07	6.80E+05	7.70E+05	17.57	17.60	17.60
36	5.11E+07	5.29E+07	5.12E+07	5.17E+07	1.06E+06	1.20E+06	17.75	17.78	17.75
48	4.46E+07	4.40E+07	4.65E+07	4.51E+07	1.32E+06	1.49E+06	17.61	17.60	17.66
60	5.27E+07	5.06E+07	4.96E+07	5.10E+07	1.57E+06	1.78E+06	17.78	17.74	17.72
72	4.79E+07	4.57E+07	4.35E+07	4.57E+07	2.22E+06	2.51E+06	17.69	17.64	17.59
84	4.62E+07	4.70E+07	4.47E+07	4.60E+07	1.16E+06	1.31E+06	17.65	17.67	17.62
96	4.76E+07	4.89E+07	4.65E+07	4.77E+07	1.16E+06	1.31E+06	17.68	17.70	17.66
108	5.06E+07	5.27E+07	4.30E+07	4.88E+07	5.15E+06	5.83E+06	17.74	17.78	17.58
120	3.96E+07	3.77E+07	3.73E+07	3.82E+07	1.21E+06	1.37E+06	17.49	17.44	17.44



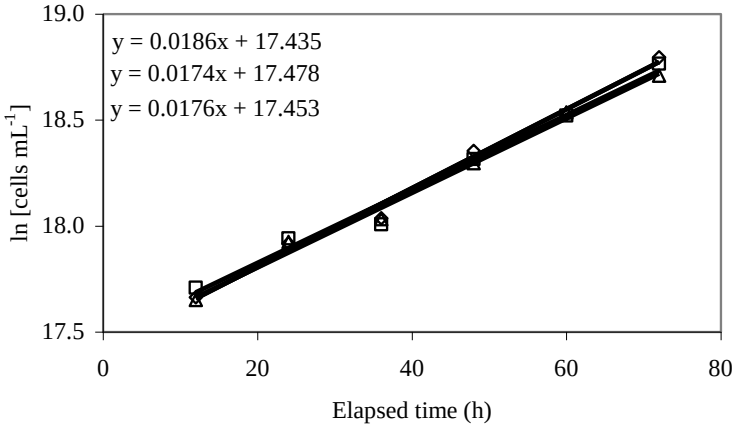
Specific growth rate (h^{-1})	
Trial 1	0.001
Trial 2	0.001
Trial 3	0.000
Average	0.000
STDEV	0.000
95% CI	0.001

Figure E.22. Specific growth rate calculations for Trial 1 (open circles), Trial 2 (open squares), and Trial 3 (open triangles).

Fumarate

Table E.23. BC13 growth in the presence of 50 μM fumarate.

	Cells mL^{-1}						ln (Cells mL^{-1})		
Elapsed Time (h)	Trial 1	Trial 2	Trial 3	Average	STDEV	95% CI	Trial 1	Trial 2	Trial 3
0	4.59E+07	4.60E+07	4.55E+07	4.58E+07	2.99E+05	3.39E+05	17.64	17.65	17.63
12	4.69E+07	4.91E+07	4.63E+07	4.74E+07	1.47E+06	1.66E+06	17.66	17.71	17.65
24	6.05E+07	6.20E+07	6.10E+07	6.11E+07	7.31E+05	8.27E+05	17.92	17.94	17.93
36	6.81E+07	6.61E+07	6.79E+07	6.74E+07	1.08E+06	1.23E+06	18.04	18.01	18.03
48	9.36E+07	9.01E+07	8.83E+07	9.07E+07	2.70E+06	3.06E+06	18.35	18.32	18.30
60	1.11E+08	1.11E+08	1.12E+08	1.11E+08	8.39E+05	9.49E+05	18.53	18.52	18.54
72	1.46E+08	1.41E+08	1.34E+08	1.40E+08	6.11E+06	6.91E+06	18.80	18.77	18.71
84	1.50E+08	1.45E+08	1.44E+08	1.46E+08	3.24E+06	3.67E+06	18.83	18.79	18.78
96	1.62E+08	1.58E+08	1.58E+08	1.59E+08	2.58E+06	2.92E+06	18.90	18.88	18.87
108	1.69E+08	1.66E+08	1.56E+08	1.64E+08	7.07E+06	8.00E+06	18.95	18.93	18.86
120	1.82E+08	1.79E+08	1.70E+08	1.77E+08	6.06E+06	6.86E+06	19.02	19.00	18.95

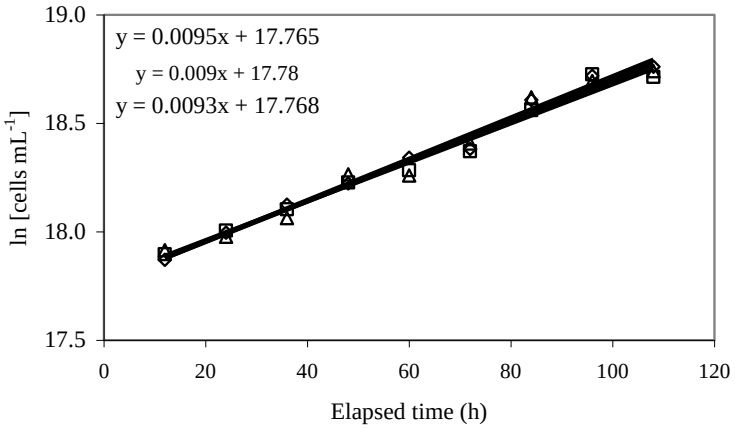


Specific growth rate (h^{-1})	
Trial 1	0.019
Trial 2	0.017
Trial 3	0.018
Average	0.018
STDEV	0.001
95% CI	0.001

Figure E.23. Specific growth rate calculations for Trial 1 (open circles), Trial 2 (open squares), and Trial 3 (open triangles).

Table E.24. BC13 growth in the presence of 100 μM fumarate.

	Cells mL^{-1}						ln (Cells mL^{-1})		
Elapsed Time (h)	Trial 1	Trial 2	Trial 3	Average	STDEV	95% CI	Trial 1	Trial 2	Trial 3
0	5.66E+07	5.83E+07	5.98E+07	5.82E+07	1.57E+06	1.77E+06	17.85	17.88	17.91
12	5.77E+07	5.92E+07	6.03E+07	5.91E+07	1.30E+06	1.47E+06	17.87	17.90	17.92
24	6.54E+07	6.60E+07	6.42E+07	6.52E+07	9.15E+05	1.03E+06	18.00	18.00	17.98
36	7.44E+07	7.28E+07	6.99E+07	7.24E+07	2.26E+06	2.56E+06	18.12	18.10	18.06
48	8.21E+07	8.24E+07	8.55E+07	8.33E+07	1.91E+06	2.16E+06	18.22	18.23	18.26
60	9.24E+07	8.71E+07	8.52E+07	8.82E+07	3.75E+06	4.25E+06	18.34	18.28	18.26
72	9.61E+07	9.52E+07	9.87E+07	9.67E+07	1.82E+06	2.06E+06	18.38	18.37	18.41
84	1.21E+08	1.15E+08	1.22E+08	1.19E+08	3.71E+06	4.20E+06	18.61	18.56	18.62
96	1.35E+08	1.36E+08	1.31E+08	1.34E+08	2.19E+06	2.48E+06	18.72	18.73	18.69
108	1.41E+08	1.34E+08	1.38E+08	1.37E+08	3.26E+06	3.69E+06	18.76	18.71	18.74
120	1.46E+08	1.44E+08	1.44E+08	1.45E+08	1.32E+06	1.49E+06	18.80	18.79	18.78

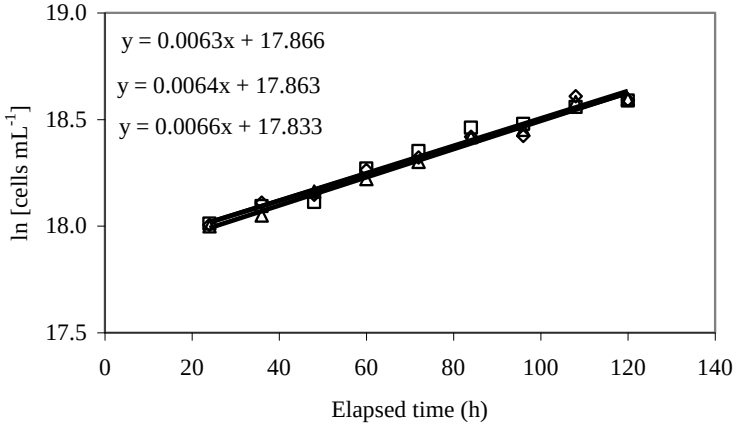


Specific growth rate (h^{-1})	
Trial 1	0.010
Trial 2	0.009
Trial 3	0.009
Average	0.009
STDEV	0.000
95% CI	0.000

Figure E.24. Specific growth rate calculations for Trial 1 (open circles), Trial 2 (open squares), and Trial 3 (open triangles).

Table E.25. BC13 growth in the presence of 250 μM fumarate.

	Cells mL^{-1}						ln (Cells mL^{-1})		
Elapsed Time (h)	Trial 1	Trial 2	Trial 3	Average	STDEV	95% CI	Trial 1	Trial 2	Trial 3
0	5.71E+07	5.72E+07	5.46E+07	5.63E+07	1.45E+06	1.64E+06	17.86	17.86	17.82
12	6.33E+07	6.28E+07	6.19E+07	6.27E+07	7.03E+05	7.96E+05	17.96	17.96	17.94
24	6.61E+07	6.64E+07	6.56E+07	6.60E+07	3.93E+05	4.45E+05	18.01	18.01	18.00
36	7.32E+07	7.21E+07	6.90E+07	7.15E+07	2.19E+06	2.48E+06	18.11	18.09	18.05
48	7.60E+07	7.35E+07	7.72E+07	7.56E+07	1.86E+06	2.11E+06	18.15	18.11	18.16
60	8.55E+07	8.60E+07	8.18E+07	8.44E+07	2.28E+06	2.58E+06	18.26	18.27	18.22
72	9.06E+07	9.34E+07	8.87E+07	9.09E+07	2.36E+06	2.67E+06	18.32	18.35	18.30
84	9.99E+07	1.04E+08	9.97E+07	1.01E+08	2.55E+06	2.89E+06	18.42	18.46	18.42
96	1.00E+08	1.06E+08	1.03E+08	1.03E+08	2.89E+06	3.27E+06	18.42	18.48	18.45
108	1.21E+08	1.15E+08	1.17E+08	1.18E+08	3.02E+06	3.42E+06	18.61	18.56	18.58
120	1.19E+08	1.18E+08	1.19E+08	1.19E+08	3.78E+05	4.28E+05	18.59	18.59	18.60

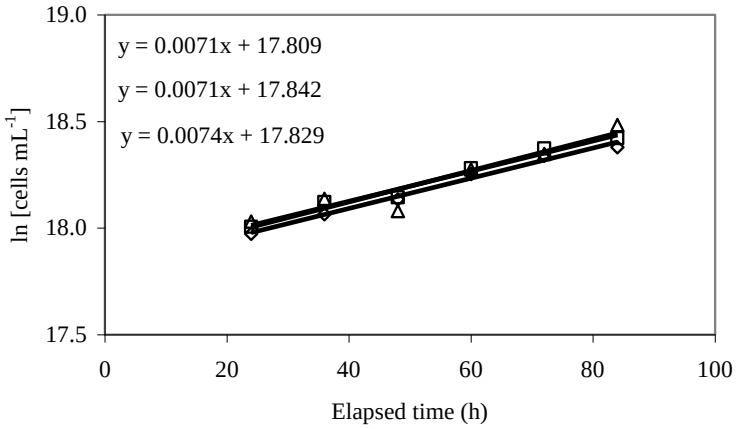


Specific growth rate (h^{-1})	
Trial 1	0.006
Trial 2	0.006
Trial 3	0.007
Average	0.006
STDEV	0.000
95% CI	0.000

Figure E.25. Specific growth rate calculations for Trial 1 (open circles), Trial 2 (open squares), and Trial 3 (open triangles).

Table E.26. BC13 growth in the presence of 500 μM fumarate.

	Cells mL^{-1}						ln (Cells mL^{-1})		
Elapsed Time (h)	Trial 1	Trial 2	Trial 3	Average	STDEV	95% CI	Trial 1	Trial 2	Trial 3
0	5.71E+07	6.03E+07	6.01E+07	5.92E+07	1.77E+06	2.00E+06	17.86	17.91	17.91
12	5.93E+07	5.63E+07	5.50E+07	5.69E+07	2.18E+06	2.47E+06	17.90	17.85	17.82
24	6.40E+07	6.60E+07	6.77E+07	6.59E+07	1.87E+06	2.12E+06	17.97	18.01	18.03
36	7.00E+07	7.42E+07	7.53E+07	7.32E+07	2.80E+06	3.17E+06	18.06	18.12	18.14
48	7.52E+07	7.58E+07	7.11E+07	7.40E+07	2.52E+06	2.85E+06	18.14	18.14	18.08
60	8.46E+07	8.69E+07	8.65E+07	8.60E+07	1.23E+06	1.39E+06	18.25	18.28	18.28
72	9.22E+07	9.54E+07	9.30E+07	9.36E+07	1.69E+06	1.91E+06	18.34	18.37	18.35
84	9.59E+07	1.00E+08	1.06E+08	1.01E+08	5.27E+06	5.96E+06	18.38	18.42	18.48
96	9.83E+07	1.03E+08	1.04E+08	1.02E+08	2.86E+06	3.24E+06	18.40	18.45	18.46
108	9.47E+07	9.99E+07	9.68E+07	9.71E+07	2.60E+06	2.95E+06	18.37	18.42	18.39
120	9.99E+07	1.02E+08	1.06E+08	1.03E+08	3.23E+06	3.65E+06	18.42	18.44	18.48

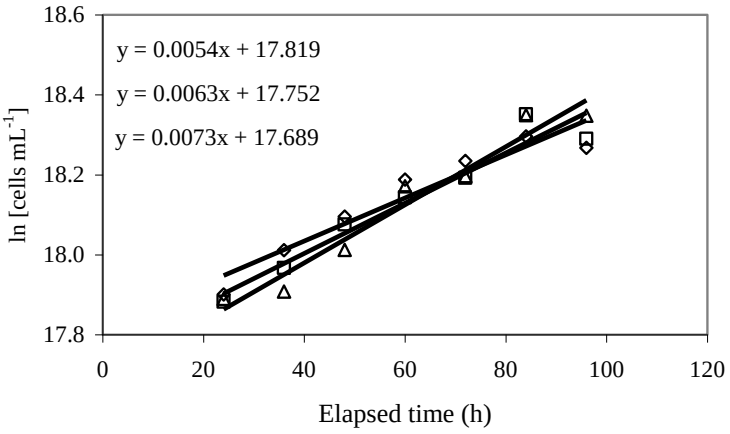


Specific growth rate (h^{-1})	
Trial 1	0.007
Trial 2	0.007
Trial 3	0.007
Average	0.007
STDEV	0.000
95% CI	0.000

Figure E.26. Specific growth rate calculations for Trial 1 (open circles), Trial 2 (open squares), and Trial 3 (open triangles).

Table E.27. BC13 growth in the presence of 1,000 μM fumarate.

	Cells mL^{-1}						ln (Cells mL^{-1})		
Elapsed Time (h)	Trial 1	Trial 2	Trial 3	Average	STDEV	95% CI	Trial 1	Trial 2	Trial 3
0	5.67E+07	5.53E+07	5.68E+07	5.63E+07	8.58E+05	9.71E+05	17.85	17.83	17.86
12	5.73E+07	5.48E+07	5.58E+07	5.60E+07	1.28E+06	1.45E+06	17.86	17.82	17.84
24	5.95E+07	5.84E+07	5.88E+07	5.89E+07	5.45E+05	6.16E+05	17.90	17.88	17.89
36	6.64E+07	6.35E+07	5.99E+07	6.33E+07	3.29E+06	3.72E+06	18.01	17.97	17.91
48	7.22E+07	7.08E+07	6.65E+07	6.98E+07	3.00E+06	3.40E+06	18.10	18.08	18.01
60	7.92E+07	7.58E+07	7.79E+07	7.77E+07	1.73E+06	1.96E+06	18.19	18.14	18.17
72	8.30E+07	7.96E+07	7.99E+07	8.08E+07	1.90E+06	2.15E+06	18.23	18.19	18.20
84	8.83E+07	9.33E+07	9.31E+07	9.16E+07	2.83E+06	3.20E+06	18.30	18.35	18.35
96	8.58E+07	8.78E+07	9.30E+07	8.89E+07	3.72E+06	4.21E+06	18.27	18.29	18.35
108	9.06E+07	9.43E+07	9.49E+07	9.33E+07	2.35E+06	2.65E+06	18.32	18.36	18.37
120	8.69E+07	8.29E+07	7.82E+07	8.27E+07	4.37E+06	4.94E+06	18.28	18.23	18.17

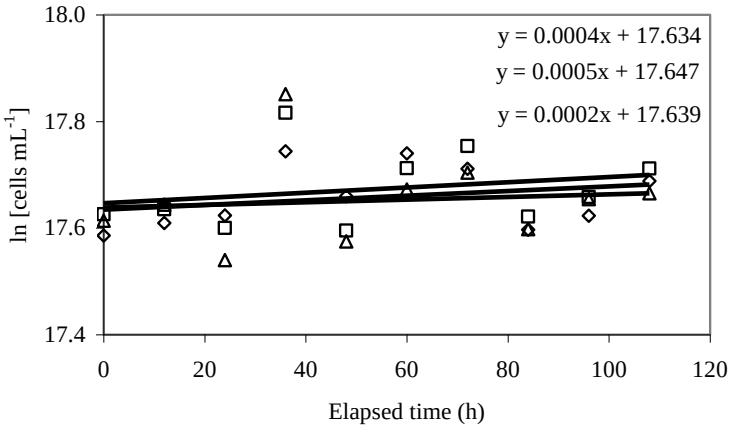


Specific growth rate (h^{-1})	
Trial 1	0.005
Trial 2	0.006
Trial 3	0.007
Average	0.006
STDEV	0.001
95% CI	0.001

Figure E.27. Specific growth rate calculations for Trial 1 (open circles), Trial 2 (open squares), and Trial 3 (open triangles).

Table E.28. BC13 growth in the presence of 5,000 μM fumarate.

	Cells mL^{-1}						ln (Cells mL^{-1})		
Elapsed Time (h)	Trial 1	Trial 2	Trial 3	Average	STDEV	95% CI	Trial 1	Trial 2	Trial 3
0	4.34E+07	4.52E+07	4.46E+07	4.44E+07	9.06E+05	1.03E+06	17.59	17.63	17.61
12	4.44E+07	4.56E+07	4.60E+07	4.53E+07	8.16E+05	9.24E+05	17.61	17.64	17.64
24	4.51E+07	4.40E+07	4.14E+07	4.35E+07	1.86E+06	2.11E+06	17.62	17.60	17.54
36	5.08E+07	5.46E+07	5.66E+07	5.40E+07	2.93E+06	3.32E+06	17.74	17.82	17.85
48	4.67E+07	4.38E+07	4.29E+07	4.45E+07	1.98E+06	2.24E+06	17.66	17.60	17.58
60	5.06E+07	4.92E+07	4.73E+07	4.91E+07	1.67E+06	1.89E+06	17.74	17.71	17.67
72	4.92E+07	5.13E+07	4.89E+07	4.98E+07	1.36E+06	1.53E+06	17.71	17.75	17.70
84	4.39E+07	4.50E+07	4.39E+07	4.43E+07	6.28E+05	7.11E+05	17.60	17.62	17.60
96	4.50E+07	4.67E+07	4.65E+07	4.61E+07	8.85E+05	1.00E+06	17.62	17.66	17.65
108	4.81E+07	4.92E+07	4.70E+07	4.81E+07	1.11E+06	1.26E+06	17.69	17.71	17.67
120	3.75E+07	3.92E+07	3.70E+07	3.79E+07	1.17E+06	1.32E+06	17.44	17.49	17.43



Specific growth rate (h^{-1})

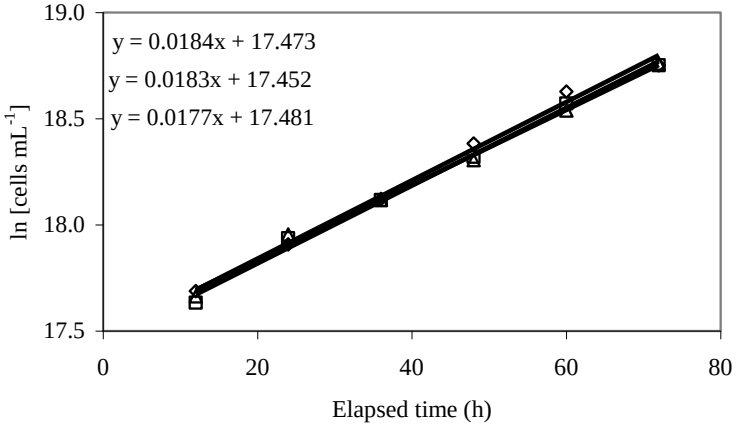
Trial 1	0.000
Trial 2	0.001
Trial 3	0.000
Average	0.000
STDEV	0.000
95% CI	0.000

Figure E.28. Specific growth rate calculations for Trial 1 (open circles), Trial 2 (open squares), and Trial 3 (open triangles).

Malate

Table E.29. BC13 growth in the presence of 50 μM malate.

	Cells mL^{-1}						ln (Cells mL^{-1})		
Elapsed Time (h)	Trial 1	Trial 2	Trial 3	Average	STDEV	95% CI	Trial 1	Trial 2	Trial 3
0	4.75E+07	4.49E+07	4.74E+07	4.66E+07	1.47E+06	1.66E+06	17.68	17.62	17.67
12	4.81E+07	4.55E+07	4.69E+07	4.68E+07	1.29E+06	1.46E+06	17.69	17.63	17.66
24	5.99E+07	6.16E+07	6.28E+07	6.14E+07	1.45E+06	1.64E+06	17.91	17.94	17.96
36	7.42E+07	7.38E+07	7.37E+07	7.39E+07	2.68E+05	3.04E+05	18.12	18.12	18.12
48	9.63E+07	9.04E+07	8.90E+07	9.19E+07	3.85E+06	4.36E+06	18.38	18.32	18.30
60	1.23E+08	1.16E+08	1.12E+08	1.17E+08	5.33E+06	6.03E+06	18.63	18.57	18.54
72	1.39E+08	1.39E+08	1.40E+08	1.40E+08	7.19E+05	8.13E+05	18.75	18.75	18.76
84	1.56E+08	1.50E+08	1.43E+08	1.50E+08	6.85E+06	7.75E+06	18.87	18.83	18.78
96	1.47E+08	1.41E+08	1.38E+08	1.42E+08	4.48E+06	5.07E+06	18.80	18.76	18.74
108	1.85E+08	1.86E+08	1.95E+08	1.88E+08	5.86E+06	6.63E+06	19.03	19.04	19.09
120	1.66E+08	1.65E+08	1.68E+08	1.66E+08	1.42E+06	1.60E+06	18.93	18.92	18.94



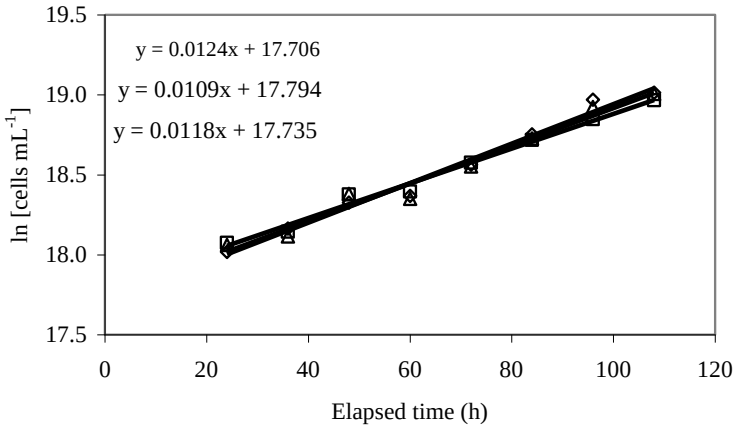
Specific growth rate (h^{-1})

Trial 1	0.018
Trial 2	0.018
Trial 3	0.018
Average	0.018
STDEV	0.000
95% CI	0.000

Figure E.29. Specific growth rate calculations for Trial 1 (open circles), Trial 2 (open squares), and Trial 3 (open triangles).

Table E.30. BC13 growth in the presence of 100 μM malate.

	Cells mL^{-1}						ln (Cells mL^{-1})		
Elapsed Time (h)	Trial 1	Trial 2	Trial 3	Average	STDEV	95% CI	Trial 1	Trial 2	Trial 3
0	5.00E+07	5.03E+07	5.91E+07	5.31E+07	5.16E+06	5.84E+06	17.73	17.73	17.89
12	6.86E+07	6.48E+07	6.60E+07	6.65E+07	1.93E+06	2.19E+06	18.04	17.99	18.01
24	6.69E+07	7.07E+07	6.98E+07	6.92E+07	2.01E+06	2.27E+06	18.02	18.07	18.06
36	7.74E+07	7.57E+07	7.36E+07	7.56E+07	1.88E+06	2.12E+06	18.16	18.14	18.11
48	9.10E+07	9.57E+07	9.61E+07	9.42E+07	2.85E+06	3.23E+06	18.33	18.38	18.38
60	9.48E+07	9.75E+07	9.31E+07	9.52E+07	2.19E+06	2.48E+06	18.37	18.40	18.35
72	1.15E+08	1.17E+08	1.14E+08	1.15E+08	1.34E+06	1.52E+06	18.56	18.58	18.55
84	1.39E+08	1.35E+08	1.36E+08	1.37E+08	2.42E+06	2.74E+06	18.75	18.72	18.73
96	1.73E+08	1.53E+08	1.65E+08	1.64E+08	1.01E+07	1.14E+07	18.97	18.85	18.92
108	1.81E+08	1.72E+08	1.80E+08	1.78E+08	4.61E+06	5.22E+06	19.01	18.97	19.01
120	1.59E+08	1.68E+08	1.60E+08	1.62E+08	5.12E+06	5.79E+06	18.88	18.94	18.89

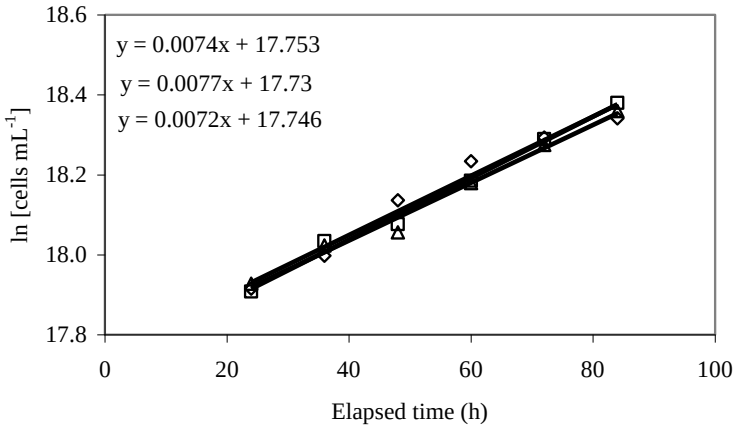


Specific growth rate (h^{-1})	
Trial 1	0.012
Trial 2	0.011
Trial 3	0.012
Average	0.012
STDEV	0.001
95% CI	0.001

Figure E.30. Specific growth rate calculations for Trial 1 (open circles), Trial 2 (open squares), and Trial 3 (open triangles).

Table E.31. BC13 growth in the presence of 250 μM malate.

	Cells mL^{-1}						ln (Cells mL^{-1})		
Elapsed Time (h)	Trial 1	Trial 2	Trial 3	Average	STDEV	95% CI	Trial 1	Trial 2	Trial 3
0	5.92E+07	5.68E+07	5.53E+07	5.71E+07	1.99E+06	2.25E+06	17.90	17.86	17.83
12	6.04E+07	5.94E+07	6.28E+07	6.09E+07	1.77E+06	2.00E+06	17.92	17.90	17.96
24	6.03E+07	5.99E+07	6.11E+07	6.04E+07	6.05E+05	6.85E+05	17.92	17.91	17.93
36	6.55E+07	6.79E+07	6.72E+07	6.69E+07	1.23E+06	1.39E+06	18.00	18.03	18.02
48	7.53E+07	7.09E+07	6.95E+07	7.19E+07	3.03E+06	3.43E+06	18.14	18.08	18.06
60	8.29E+07	7.90E+07	7.85E+07	8.02E+07	2.41E+06	2.73E+06	18.23	18.19	18.18
72	8.80E+07	8.77E+07	8.64E+07	8.74E+07	8.49E+05	9.61E+05	18.29	18.29	18.27
84	9.23E+07	9.60E+07	9.41E+07	9.41E+07	1.82E+06	2.06E+06	18.34	18.38	18.36
96	9.00E+07	8.97E+07	8.77E+07	8.91E+07	1.24E+06	1.40E+06	18.31	18.31	18.29
108	9.50E+07	9.86E+07	9.30E+07	9.55E+07	2.85E+06	3.23E+06	18.37	18.41	18.35
120	9.45E+07	9.29E+07	9.32E+07	9.36E+07	8.71E+05	9.85E+05	18.36	18.35	18.35

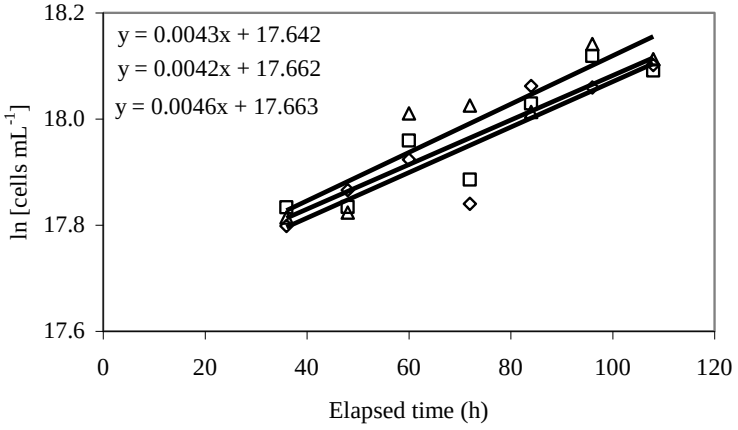


Specific growth rate (h^{-1})	
Trial 1	0.007
Trial 2	0.008
Trial 3	0.007
Average	0.007
STDEV	0.000
95% CI	0.000

Figure E.31. Specific growth rate calculations for Trial 1 (open circles), Trial 2 (open squares), and Trial 3 (open triangles).

Table E.32. BC13 growth in the presence of 500 μM malate.

	Cells mL^{-1}						ln (Cells mL^{-1})		
Elapsed Time (h)	Trial 1	Trial 2	Trial 3	Average	STDEV	95% CI	Trial 1	Trial 2	Trial 3
0	4.65E+07	4.38E+07	4.31E+07	4.45E+07	1.78E+06	2.02E+06	17.66	17.59	17.58
12	4.92E+07	4.65E+07	4.51E+07	4.69E+07	2.12E+06	2.40E+06	17.71	17.66	17.62
24	5.20E+07	5.51E+07	5.44E+07	5.38E+07	1.59E+06	1.80E+06	17.77	17.82	17.81
36	5.37E+07	5.56E+07	5.45E+07	5.46E+07	9.75E+05	1.10E+06	17.80	17.83	17.81
48	5.74E+07	5.56E+07	5.50E+07	5.60E+07	1.23E+06	1.40E+06	17.87	17.83	17.82
60	6.08E+07	6.31E+07	6.63E+07	6.34E+07	2.77E+06	3.13E+06	17.92	17.96	18.01
72	5.59E+07	5.86E+07	6.73E+07	6.06E+07	5.97E+06	6.76E+06	17.84	17.89	18.03
84	6.99E+07	6.76E+07	6.65E+07	6.80E+07	1.70E+06	1.92E+06	18.06	18.03	18.01
96	6.97E+07	7.39E+07	7.56E+07	7.31E+07	3.05E+06	3.45E+06	18.06	18.12	18.14
108	7.27E+07	7.19E+07	7.35E+07	7.27E+07	7.78E+05	8.80E+05	18.10	18.09	18.11
120	6.72E+07	6.58E+07	6.56E+07	6.62E+07	8.48E+05	9.60E+05	18.02	18.00	18.00

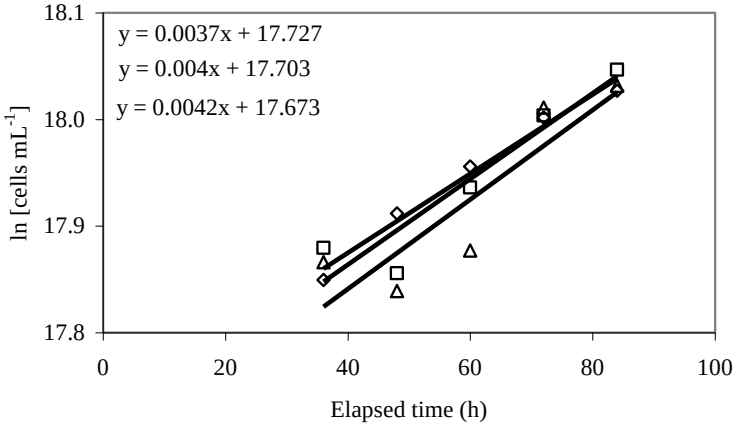


Specific growth rate (h^{-1})	
Trial 1	0.004
Trial 2	0.004
Trial 3	0.005
Average	0.004
STDEV	0.000
95% CI	0.000

Figure E.32. Specific growth rate calculations for Trial 1 (open circles), Trial 2 (open squares), and Trial 3 (open triangles).

Table E.33. BC13 growth in the presence of 1,000 μM malate.

	Cells mL^{-1}						ln (Cells mL^{-1})		
Elapsed Time (h)	Trial 1	Trial 2	Trial 3	Average	STDEV	95% CI	Trial 1	Trial 2	Trial 3
0	5.30E+07	5.04E+07	5.17E+07	5.17E+07	1.30E+06	1.47E+06	17.79	17.74	17.76
12	5.23E+07	5.09E+07	5.12E+07	5.15E+07	7.60E+05	8.60E+05	17.77	17.74	17.75
24	5.48E+07	5.76E+07	5.81E+07	5.69E+07	1.79E+06	2.03E+06	17.82	17.87	17.88
36	5.65E+07	5.82E+07	5.74E+07	5.74E+07	8.61E+05	9.74E+05	17.85	17.88	17.87
48	6.01E+07	5.68E+07	5.59E+07	5.76E+07	2.22E+06	2.51E+06	17.91	17.86	17.84
60	6.28E+07	6.16E+07	5.81E+07	6.08E+07	2.47E+06	2.79E+06	17.96	17.94	17.88
72	6.58E+07	6.59E+07	6.64E+07	6.60E+07	3.24E+05	3.67E+05	18.00	18.00	18.01
84	6.74E+07	6.88E+07	6.78E+07	6.80E+07	7.01E+05	7.93E+05	18.03	18.05	18.03
96	6.69E+07	6.54E+07	6.77E+07	6.67E+07	1.20E+06	1.36E+06	18.02	18.00	18.03
108	7.32E+07	7.50E+07	7.77E+07	7.53E+07	2.22E+06	2.51E+06	18.11	18.13	18.17
120	7.14E+07	7.46E+07	7.15E+07	7.25E+07	1.85E+06	2.09E+06	18.08	18.13	18.08

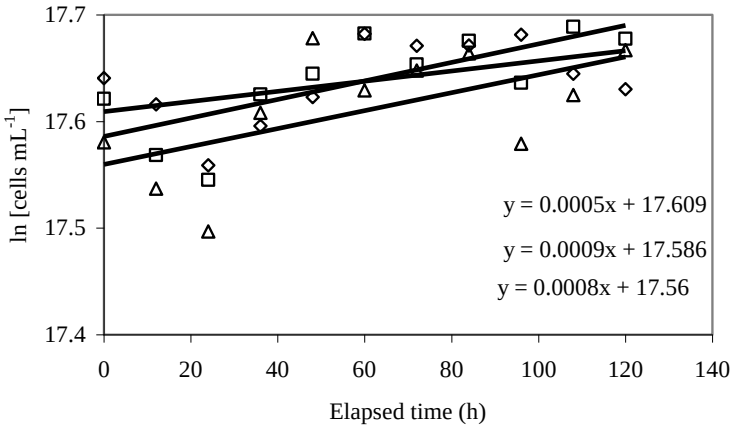


Specific growth rate (h^{-1})	
Trial 1	0.004
Trial 2	0.004
Trial 3	0.004
Average	0.004
STDEV	0.000
95% CI	0.000

Figure E.33. Specific growth rate calculations for Trial 1 (open circles), Trial 2 (open squares), and Trial 3 (open triangles).

Table E.34. BC13 growth in the presence of 5,000 μM malate.

	Cells mL^{-1}						ln (Cells mL^{-1})		
Elapsed Time (h)	Trial 1	Trial 2	Trial 3	Average	STDEV	95% CI	Trial 1	Trial 2	Trial 3
0	4.58E+07	4.50E+07	4.32E+07	4.47E+07	1.37E+06	1.55E+06	17.64	17.62	17.58
12	4.47E+07	4.26E+07	4.13E+07	4.29E+07	1.71E+06	1.93E+06	17.62	17.57	17.54
24	4.22E+07	4.17E+07	3.97E+07	4.12E+07	1.33E+06	1.50E+06	17.56	17.55	17.50
36	4.38E+07	4.51E+07	4.44E+07	4.44E+07	6.62E+05	7.49E+05	17.60	17.63	17.61
48	4.50E+07	4.60E+07	4.76E+07	4.62E+07	1.28E+06	1.45E+06	17.62	17.64	17.68
60	4.78E+07	4.78E+07	4.53E+07	4.70E+07	1.43E+06	1.62E+06	17.68	17.68	17.63
72	4.72E+07	4.64E+07	4.62E+07	4.66E+07	5.64E+05	6.39E+05	17.67	17.65	17.65
84	4.73E+07	4.75E+07	4.69E+07	4.72E+07	2.76E+05	3.13E+05	17.67	17.68	17.66
96	4.77E+07	4.56E+07	4.31E+07	4.55E+07	2.32E+06	2.63E+06	17.68	17.64	17.58
108	4.60E+07	4.81E+07	4.51E+07	4.64E+07	1.53E+06	1.73E+06	17.64	17.69	17.62
120	4.54E+07	4.76E+07	4.71E+07	4.67E+07	1.16E+06	1.31E+06	17.63	17.68	17.67



Specific growth rate (h^{-1})

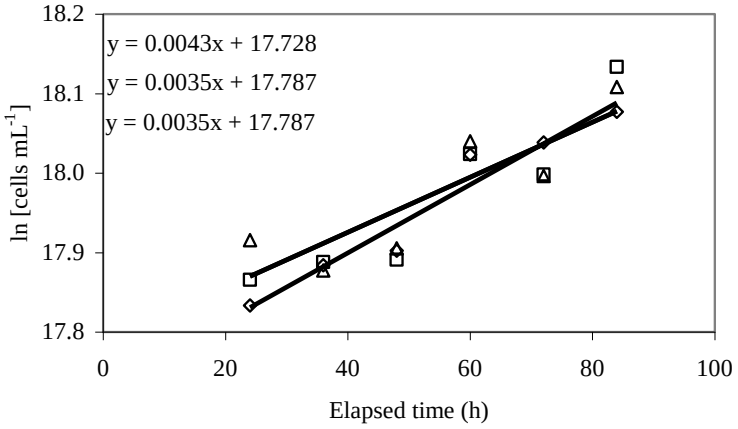
Trial 1	0.001
Trial 2	0.001
Trial 3	0.001
Average	0.001
STDEV	0.000
95% CI	0.000

Figure E.34. Specific growth rate calculations for Trial 1 (open circles), Trial 2 (open squares), and Trial 3 (open triangles).

Oxaloacetate

Table E.35. BC13 growth in the presence of 50 μM oxaloacetate.

	Cells mL^{-1}						ln (Cells mL^{-1})		
Elapsed Time (h)	Trial 1	Trial 2	Trial 3	Average	STDEV	95% CI	Trial 1	Trial 2	Trial 3
0	5.60E+07	5.54E+07	5.77E+07	5.64E+07	1.15E+06	1.30E+06	17.84	17.83	17.87
12	5.56E+07	5.50E+07	5.42E+07	5.50E+07	6.92E+05	7.83E+05	17.83	17.82	17.81
24	5.56E+07	5.74E+07	6.04E+07	5.78E+07	2.41E+06	2.73E+06	17.83	17.87	17.92
36	5.85E+07	5.87E+07	5.81E+07	5.84E+07	3.20E+05	3.62E+05	17.88	17.89	17.88
48	5.95E+07	5.89E+07	5.97E+07	5.94E+07	4.42E+05	5.00E+05	17.90	17.89	17.91
60	6.72E+07	6.72E+07	6.83E+07	6.76E+07	6.44E+05	7.29E+05	18.02	18.02	18.04
72	6.82E+07	6.55E+07	6.54E+07	6.64E+07	1.59E+06	1.80E+06	18.04	18.00	18.00
84	7.09E+07	7.50E+07	7.32E+07	7.30E+07	2.06E+06	2.33E+06	18.08	18.13	18.11
96	7.07E+07	6.71E+07	6.87E+07	6.88E+07	1.81E+06	2.04E+06	18.07	18.02	18.04
108	6.88E+07	6.80E+07	6.47E+07	6.72E+07	2.16E+06	2.45E+06	18.05	18.03	17.99
120	7.67E+07	8.08E+07	8.06E+07	7.93E+07	2.32E+06	2.63E+06	18.15	18.21	18.20

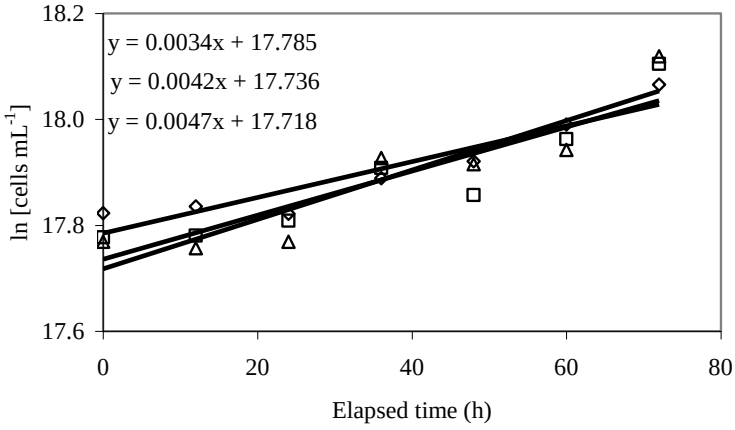


Specific growth rate (h^{-1})	
Trial 1	0.004
Trial 2	0.004
Trial 3	0.004
Average	0.004
STDEV	0.000
95% CI	0.001

Figure E.35. Specific growth rate calculations for Trial 1 (open circles), Trial 2 (open squares), and Trial 3 (open triangles).

Table E.36. BC13 growth in the presence of 100 μM oxaloacetate.

	Cells mL^{-1}						ln (Cells mL^{-1})		
Elapsed Time (h)	Trial 1	Trial 2	Trial 3	Average	STDEV	95% CI	Trial 1	Trial 2	Trial 3
0	5.50E+07	5.26E+07	5.21E+07	5.32E+07	1.56E+06	1.77E+06	17.82	17.78	17.77
12	5.57E+07	5.27E+07	5.15E+07	5.33E+07	2.17E+06	2.46E+06	17.84	17.78	17.76
24	5.49E+07	5.42E+07	5.21E+07	5.38E+07	1.47E+06	1.67E+06	17.82	17.81	17.77
36	5.88E+07	5.99E+07	6.10E+07	5.99E+07	1.14E+06	1.29E+06	17.89	17.91	17.93
48	6.07E+07	5.69E+07	6.03E+07	5.93E+07	2.08E+06	2.35E+06	17.92	17.86	17.92
60	6.50E+07	6.33E+07	6.20E+07	6.34E+07	1.52E+06	1.72E+06	17.99	17.96	17.94
72	7.01E+07	7.29E+07	7.40E+07	7.23E+07	2.00E+06	2.26E+06	18.07	18.10	18.12
84	6.77E+07	6.51E+07	6.24E+07	6.51E+07	2.68E+06	3.04E+06	18.03	17.99	17.95
96	7.06E+07	6.65E+07	6.96E+07	6.89E+07	2.14E+06	2.42E+06	18.07	18.01	18.06
108	6.46E+07	6.19E+07	6.57E+07	6.41E+07	1.95E+06	2.20E+06	17.98	17.94	18.00
120	6.68E+07	6.65E+07	6.45E+07	6.59E+07	1.24E+06	1.40E+06	18.02	18.01	17.98

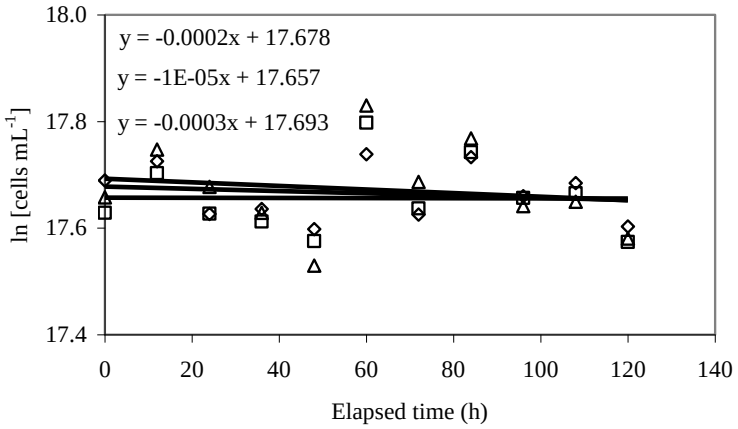


Specific growth rate (h^{-1})	
Trial 1	0.003
Trial 2	0.004
Trial 3	0.005
Average	0.004
STDEV	0.001
95% CI	0.001

Figure E.36. Specific growth rate calculations for Trial 1 (open circles), Trial 2 (open squares), and Trial 3 (open triangles).

Table E.37. BC13 growth in the presence of 250 μM oxaloacetate.

	Cells mL^{-1}						ln (Cells mL^{-1})		
Elapsed Time (h)	Trial 1	Trial 2	Trial 3	Average	STDEV	95% CI	Trial 1	Trial 2	Trial 3
0	4.81E+07	4.53E+07	4.66E+07	4.67E+07	1.42E+06	1.60E+06	17.69	17.63	17.66
12	4.99E+07	4.88E+07	5.10E+07	4.99E+07	1.11E+06	1.26E+06	17.73	17.70	17.75
24	4.52E+07	4.52E+07	4.75E+07	4.60E+07	1.35E+06	1.53E+06	17.63	17.63	17.68
36	4.56E+07	4.46E+07	4.53E+07	4.52E+07	5.40E+05	6.11E+05	17.64	17.61	17.63
48	4.39E+07	4.30E+07	4.10E+07	4.26E+07	1.47E+06	1.67E+06	17.60	17.58	17.53
60	5.06E+07	5.36E+07	5.54E+07	5.32E+07	2.45E+06	2.77E+06	17.74	17.80	17.83
72	4.52E+07	4.57E+07	4.80E+07	4.63E+07	1.51E+06	1.71E+06	17.63	17.64	17.69
84	5.03E+07	5.07E+07	5.21E+07	5.10E+07	9.39E+05	1.06E+06	17.73	17.74	17.77
96	4.67E+07	4.66E+07	4.59E+07	4.64E+07	4.59E+05	5.19E+05	17.66	17.66	17.64
108	4.79E+07	4.70E+07	4.63E+07	4.70E+07	8.19E+05	9.26E+05	17.68	17.67	17.65
120	4.41E+07	4.29E+07	4.32E+07	4.34E+07	6.59E+05	7.46E+05	17.60	17.57	17.58



Specific growth rate (h^{-1})

Trial 1	0.000
Trial 2	0.000
Trial 3	0.000
Average	0.000
STDEV	0.000
95% CI	0.000

Figure E.37. Specific growth rate calculations for Trial 1 (open circles), Trial 2 (open squares), and Trial 3 (open triangles).

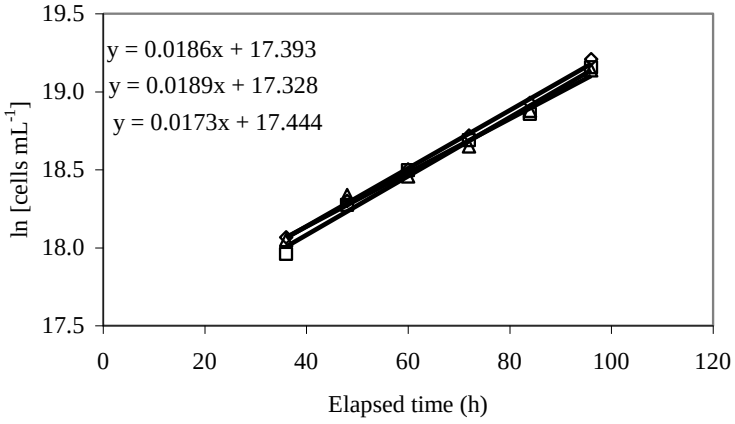
Toxicity of Organic Acids when Combined

2-ketoglutarate and Oxaloacetate

Effective Organic Acid Concentration Equal to 0.25 x IC_{50}

Table E.38. BC13 growth in the presence of 0.125 x IC_{50} of oxaloacetate mixed with 0.125 x IC_{50} of 2-ketoglutarate.

	Cells mL^{-1}						ln (Cells mL^{-1})		
Elapsed Time (h)	Trial 1	Trial 2	Trial 3	Average	STDEV	95% CI	Trial 1	Trial 2	Trial 3
0	5.20E+07	4.98E+07	4.60E+07	4.93E+07	3.02E+06	3.42E+06	17.77	17.72	17.64
12	5.09E+07	5.00E+07	5.00E+07	5.03E+07	5.09E+05	5.76E+05	17.75	17.73	17.73
24	6.06E+07	6.27E+07	5.85E+07	6.06E+07	2.08E+06	2.35E+06	17.92	17.95	17.88
36	7.02E+07	6.31E+07	6.89E+07	6.74E+07	3.80E+06	4.30E+06	18.07	17.96	18.05
48	8.87E+07	8.64E+07	9.19E+07	8.90E+07	2.79E+06	3.16E+06	18.30	18.27	18.34
60	1.08E+08	1.08E+08	1.04E+08	1.07E+08	2.60E+06	2.94E+06	18.50	18.50	18.46
72	1.35E+08	1.31E+08	1.26E+08	1.30E+08	4.60E+06	5.21E+06	18.72	18.69	18.65
84	1.66E+08	1.55E+08	1.58E+08	1.60E+08	5.89E+06	6.66E+06	18.93	18.86	18.88
96	2.20E+08	2.08E+08	2.05E+08	2.11E+08	7.91E+06	8.95E+06	19.21	19.16	19.14
108	2.03E+08	2.17E+08	2.23E+08	2.14E+08	1.07E+07	1.21E+07	19.13	19.19	19.22
120	1.96E+08	1.88E+08	1.79E+08	1.88E+08	8.59E+06	9.72E+06	19.10	19.05	19.00



Specific growth rate (h^{-1})

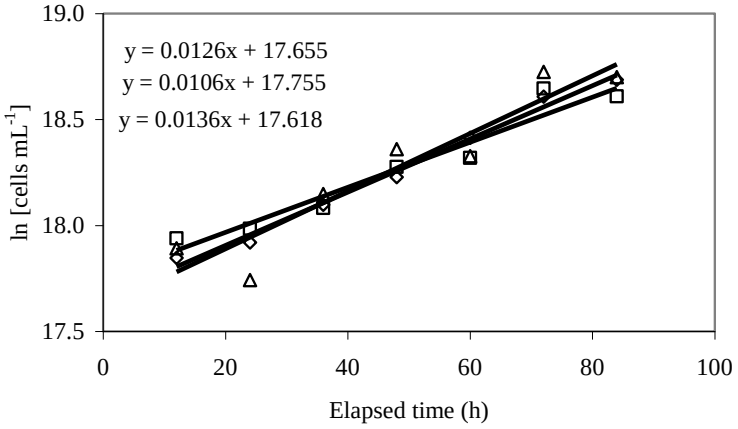
Trial 1	0.019
Trial 2	0.019
Trial 3	0.017
Average	0.018
STDEV	0.001
95% CI	0.001

Figure E.38. Specific growth rate calculations for Trial 1 (open circles), Trial 2 (open squares), and Trial 3 (open triangles).

Effective Organic Acid Concentration Equal to 0.50 x IC_{50}

Table E.39. BC13 cell concentrations during growth in the presence of 0.25 x IC_{50} of oxaloacetate mixed with 0.25 x IC_{50} of 2-ketoglutarate.

	Cells mL^{-1}						ln (Cells mL^{-1})		
Elapsed Time (h)	Trial 1	Trial 2	Trial 3	Average	STDEV	95% CI	Trial 1	Trial 2	Trial 3
0	5.43E+07	5.13E+07	4.83E+07	5.13E+07	3.02E+06	3.41E+06	17.81	17.75	17.69
12	5.63E+07	6.18E+07	5.90E+07	5.90E+07	2.73E+06	3.09E+06	17.85	17.94	17.89
24	6.06E+07	6.46E+07	5.07E+07	5.87E+07	7.15E+06	8.09E+06	17.92	17.98	17.74
36	7.24E+07	7.13E+07	7.62E+07	7.33E+07	2.58E+06	2.92E+06	18.10	18.08	18.15
48	8.25E+07	8.66E+07	9.41E+07	8.77E+07	5.89E+06	6.67E+06	18.23	18.28	18.36
60	9.93E+07	9.03E+07	9.11E+07	9.36E+07	5.01E+06	5.67E+06	18.41	18.32	18.33
72	1.21E+08	1.25E+08	1.36E+08	1.27E+08	7.70E+06	8.72E+06	18.61	18.65	18.73
84	1.31E+08	1.21E+08	1.32E+08	1.28E+08	6.24E+06	7.06E+06	18.69	18.61	18.70
96	1.53E+08	1.62E+08	1.51E+08	1.55E+08	5.81E+06	6.57E+06	18.84	18.90	18.83
108	1.61E+08	1.69E+08	1.68E+08	1.66E+08	4.57E+06	5.17E+06	18.90	18.95	18.94
120	1.61E+08	1.59E+08	1.74E+08	1.65E+08	8.14E+06	9.21E+06	18.90	18.89	18.97



Specific growth rate (h^{-1})

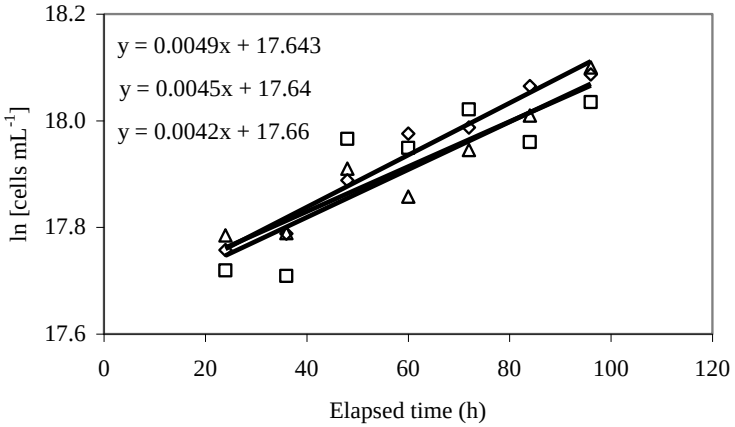
Trial 1	0.013
Trial 2	0.011
Trial 3	0.014
Average	0.012
STDEV	0.002
95% CI	0.002

Figure E.39. Specific growth rate calculations for Trial 1 (open circles), Trial 2 (open squares), and Trial 3 (open triangles).

Effective Organic Acid Concentration Equal to 1.00 x IC_{50}

Table E.40. BC13 cell concentrations during growth in the presence of 0.50 x IC_{50} of oxaloacetate mixed with 0.50 x IC_{50} of 2-ketoglutarate.

	Cells mL^{-1}						ln (Cells mL^{-1})		
Elapsed Time (h)	Trial 1	Trial 2	Trial 3	Average	STDEV	95% CI	Trial 1	Trial 2	Trial 3
0	4.96E+07	4.50E+07	4.73E+07	4.73E+07	2.30E+06	2.60E+06	17.72	17.62	17.67
12	4.93E+07	5.26E+07	5.43E+07	5.20E+07	2.53E+06	2.86E+06	17.71	17.78	17.81
24	5.15E+07	4.96E+07	5.30E+07	5.14E+07	1.69E+06	1.91E+06	17.76	17.72	17.79
36	5.31E+07	4.91E+07	5.32E+07	5.18E+07	2.35E+06	2.66E+06	17.79	17.71	17.79
48	5.87E+07	6.34E+07	6.00E+07	6.07E+07	2.45E+06	2.77E+06	17.89	17.97	17.91
60	6.41E+07	6.24E+07	5.69E+07	6.11E+07	3.74E+06	4.23E+06	17.98	17.95	17.86
72	6.48E+07	6.70E+07	6.22E+07	6.47E+07	2.44E+06	2.76E+06	17.99	18.02	17.95
84	7.01E+07	6.31E+07	6.63E+07	6.65E+07	3.51E+06	3.97E+06	18.07	17.96	18.01
96	7.16E+07	6.80E+07	7.26E+07	7.07E+07	2.41E+06	2.72E+06	18.09	18.04	18.10
108	7.30E+07	7.03E+07	6.91E+07	7.08E+07	2.03E+06	2.30E+06	18.11	18.07	18.05
120	7.51E+07	7.98E+07	8.50E+07	8.00E+07	4.98E+06	5.63E+06	18.13	18.20	18.26



Specific growth rate (h^{-1})

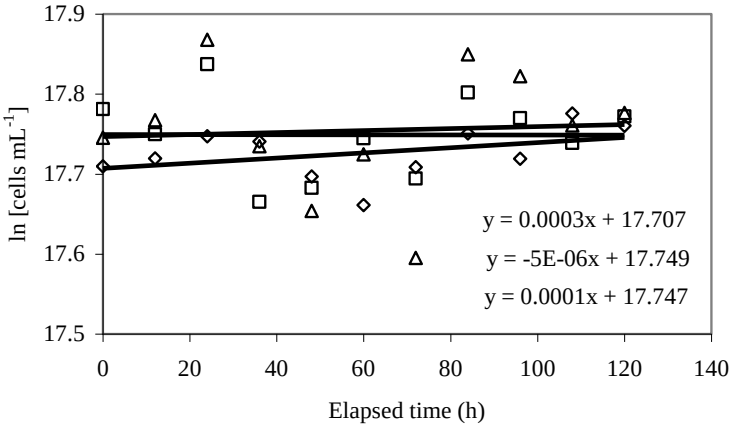
Trial 1	0.005
Trial 2	0.005
Trial 3	0.004
Average	0.005
STDEV	0.000
95% CI	0.000

Figure E.40. Specific growth rate calculations for Trial 1 (open circles), Trial 2 (open squares), and Trial 3 (open triangles).

Effective Organic Acid Concentration Equal to 1.50 x IC_{50}

Table E.41. BC13 cell concentrations during growth in the presence of 0.75 x IC_{50} of oxaloacetate mixed with 0.75 x IC_{50} of 2-ketoglutarate.

	Cells mL^{-1}						ln (Cells mL^{-1})		
Elapsed Time (h)	Trial 1	Trial 2	Trial 3	Average	STDEV	95% CI	Trial 1	Trial 2	Trial 3
0	4.91E+07	5.27E+07	5.09E+07	5.09E+07	1.82E+06	2.06E+06	17.71	17.78	17.75
12	4.96E+07	5.11E+07	5.20E+07	5.09E+07	1.23E+06	1.39E+06	17.72	17.75	17.77
24	5.10E+07	5.58E+07	5.75E+07	5.48E+07	3.40E+06	3.84E+06	17.75	17.84	17.87
36	5.07E+07	4.70E+07	5.04E+07	4.93E+07	2.04E+06	2.31E+06	17.74	17.67	17.73
48	4.85E+07	4.78E+07	4.64E+07	4.76E+07	1.04E+06	1.18E+06	17.70	17.68	17.65
60	4.68E+07	5.09E+07	4.99E+07	4.92E+07	2.12E+06	2.40E+06	17.66	17.74	17.72
72	4.91E+07	4.84E+07	4.38E+07	4.71E+07	2.86E+06	3.24E+06	17.71	17.69	17.60
84	5.12E+07	5.39E+07	5.65E+07	5.38E+07	2.65E+06	3.00E+06	17.75	17.80	17.85
96	4.96E+07	5.22E+07	5.50E+07	5.22E+07	2.70E+06	3.05E+06	17.72	17.77	17.82
108	5.25E+07	5.06E+07	5.17E+07	5.16E+07	9.54E+05	1.08E+06	17.78	17.74	17.76
120	5.17E+07	5.23E+07	5.25E+07	5.21E+07	4.33E+05	4.90E+05	17.76	17.77	17.78



Specific growth rate (h^{-1})

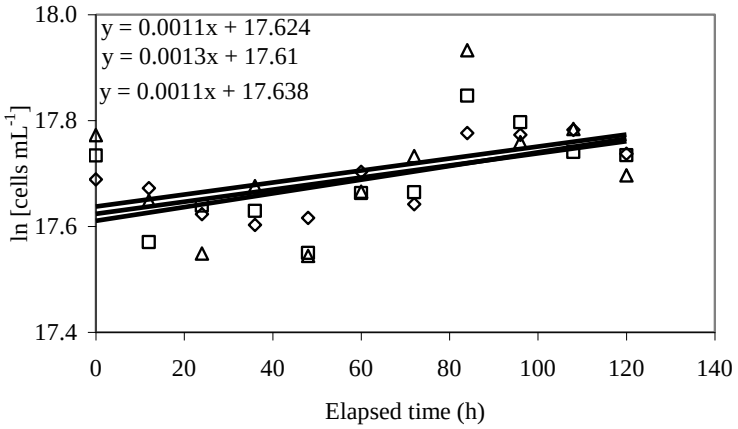
Trial 1	0.000
Trial 2	0.000
Trial 3	0.000
Average	0.000
STDEV	0.000
95% CI	0.000

Figure E.41. Specific growth rate calculations for Trial 1 (open circles), Trial 2 (open squares), and Trial 3 (open triangles).

Effective Organic Acid Concentration Equal to 2.00 x IC_{50}

Table E.42. BC13 cell concentrations during growth in the presence of 1.00 x IC_{50} of oxaloacetate mixed with 1.00 x IC_{50} of 2-ketoglutarate.

	Cells mL^{-1}						ln (Cells mL^{-1})		
Elapsed Time (h)	Trial 1	Trial 2	Trial 3	Average	STDEV	95% CI	Trial 1	Trial 2	Trial 3
0	4.81E+07	5.03E+07	5.23E+07	5.02E+07	2.10E+06	2.38E+06	17.69	17.73	17.77
12	4.73E+07	4.27E+07	4.62E+07	4.54E+07	2.39E+06	2.71E+06	17.67	17.57	17.65
24	4.50E+07	4.58E+07	4.18E+07	4.42E+07	2.10E+06	2.37E+06	17.62	17.64	17.55
36	4.41E+07	4.53E+07	4.75E+07	4.56E+07	1.70E+06	1.92E+06	17.60	17.63	17.68
48	4.47E+07	4.19E+07	4.16E+07	4.27E+07	1.73E+06	1.95E+06	17.62	17.55	17.54
60	4.88E+07	4.69E+07	4.70E+07	4.75E+07	1.07E+06	1.21E+06	17.70	17.66	17.67
72	4.59E+07	4.69E+07	5.03E+07	4.77E+07	2.28E+06	2.58E+06	17.64	17.66	17.73
84	5.25E+07	5.63E+07	6.14E+07	5.67E+07	4.45E+06	5.04E+06	17.78	17.85	17.93
96	5.23E+07	5.36E+07	5.16E+07	5.25E+07	1.01E+06	1.14E+06	17.77	17.80	17.76
108	5.28E+07	5.07E+07	5.29E+07	5.21E+07	1.27E+06	1.44E+06	17.78	17.74	17.78
120	5.05E+07	5.03E+07	4.85E+07	4.98E+07	1.12E+06	1.27E+06	17.74	17.73	17.70



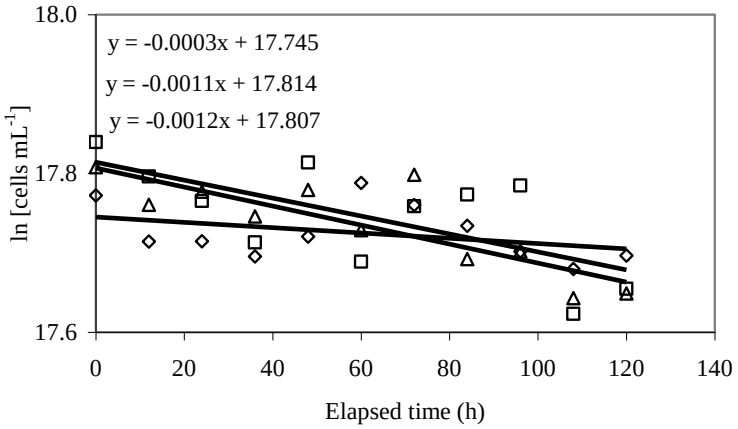
Specific growth rate (h^{-1})	
Trial 1	0.001
Trial 2	0.001
Trial 3	0.001
Average	0.001
STDEV	0.000
95% CI	0.000

Figure E.42. Specific growth rate calculations for Trial 1 (open circles), Trial 2 (open squares), and Trial 3 (open triangles).

Effective Organic Acid Concentration Equal to 10.00 x IC_{50}

Table E.43. BC13 cell concentrations during growth in the presence of 2.00 x IC_{50} of oxaloacetate mixed with 2.00 x IC_{50} of 2-ketoglutarate.

	Cells mL^{-1}						ln (Cells mL^{-1})		
Elapsed Time (h)	Trial 1	Trial 2	Trial 3	Average	STDEV	95% CI	Trial 1	Trial 2	Trial 3
0	5.23E+07	5.59E+07	5.42E+07	5.41E+07	1.83E+06	2.07E+06	17.77	17.84	17.81
12	4.93E+07	5.35E+07	5.17E+07	5.15E+07	2.11E+06	2.39E+06	17.71	17.80	17.76
24	4.94E+07	5.19E+07	5.25E+07	5.13E+07	1.68E+06	1.90E+06	17.71	17.77	17.78
36	4.84E+07	4.93E+07	5.09E+07	4.95E+07	1.27E+06	1.43E+06	17.70	17.71	17.75
48	4.96E+07	5.45E+07	5.27E+07	5.23E+07	2.45E+06	2.78E+06	17.72	17.81	17.78
60	5.31E+07	4.81E+07	5.01E+07	5.04E+07	2.53E+06	2.86E+06	17.79	17.69	17.73
72	5.17E+07	5.16E+07	5.37E+07	5.23E+07	1.18E+06	1.34E+06	17.76	17.76	17.80
84	5.03E+07	5.24E+07	4.83E+07	5.03E+07	2.04E+06	2.31E+06	17.73	17.77	17.69
96	4.87E+07	5.29E+07	4.87E+07	5.01E+07	2.44E+06	2.76E+06	17.70	17.78	17.70
108	4.77E+07	4.50E+07	4.59E+07	4.62E+07	1.33E+06	1.50E+06	17.68	17.62	17.64
120	4.85E+07	4.65E+07	4.62E+07	4.71E+07	1.23E+06	1.39E+06	17.70	17.65	17.65



Specific growth rate (h^{-1})	
Trial 1	0.000
Trial 2	0.000
Trial 3	0.000
Average	0.000
STDEV	0.000
95% CI	0.000

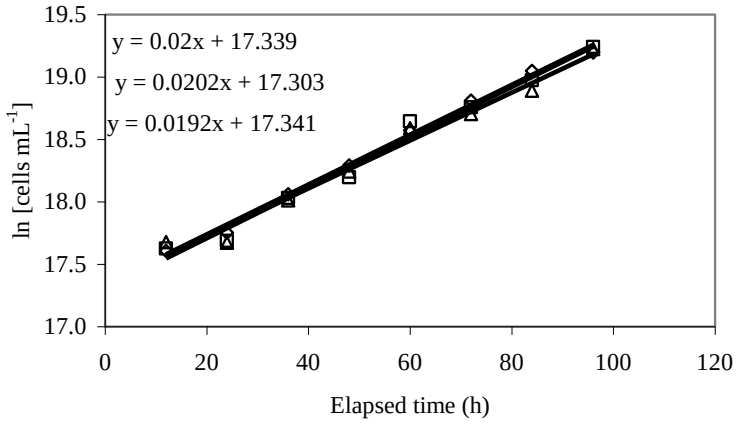
Figure E.43. Specific growth rate calculations for Trial 1 (open circles), Trial 2 (open squares), and Trial 3 (open triangles).

Succinate and Malate

Effective Organic Acid Concentration Equal to 0.25 x IC_{50}

Table E.44. BC13 cell concentrations during growth in the presence of 0.125 x IC_{50} of succinate mixed with 0.125 x IC_{50} of malate.

	Cells mL^{-1}						ln (Cells mL^{-1})		
Elapsed Time (h)	Trial 1	Trial 2	Trial 3	Average	STDEV	95% CI	Trial 1	Trial 2	Trial 3
0	4.53E+07	4.87E+07	4.51E+07	4.64E+07	2.02E+06	2.28E+06	17.63	17.70	17.62
12	4.43E+07	4.52E+07	4.76E+07	4.57E+07	1.69E+06	1.91E+06	17.61	17.63	17.68
24	5.12E+07	4.80E+07	4.73E+07	4.89E+07	2.10E+06	2.37E+06	17.75	17.69	17.67
36	6.98E+07	6.78E+07	6.64E+07	6.80E+07	1.72E+06	1.94E+06	18.06	18.03	18.01
48	8.79E+07	7.99E+07	8.37E+07	8.38E+07	4.03E+06	4.56E+06	18.29	18.20	18.24
60	1.16E+08	1.25E+08	1.18E+08	1.20E+08	4.67E+06	5.28E+06	18.57	18.65	18.59
72	1.48E+08	1.40E+08	1.33E+08	1.40E+08	7.51E+06	8.50E+06	18.81	18.76	18.70
84	1.88E+08	1.74E+08	1.60E+08	1.74E+08	1.39E+07	1.58E+07	19.05	18.97	18.89
96	2.17E+08	2.27E+08	2.23E+08	2.22E+08	4.93E+06	5.57E+06	19.20	19.24	19.22
108	2.01E+08	1.93E+08	1.89E+08	1.94E+08	6.13E+06	6.94E+06	19.12	19.08	19.06
120	1.91E+08	1.90E+08	2.07E+08	1.96E+08	9.74E+06	1.10E+07	19.07	19.06	19.15



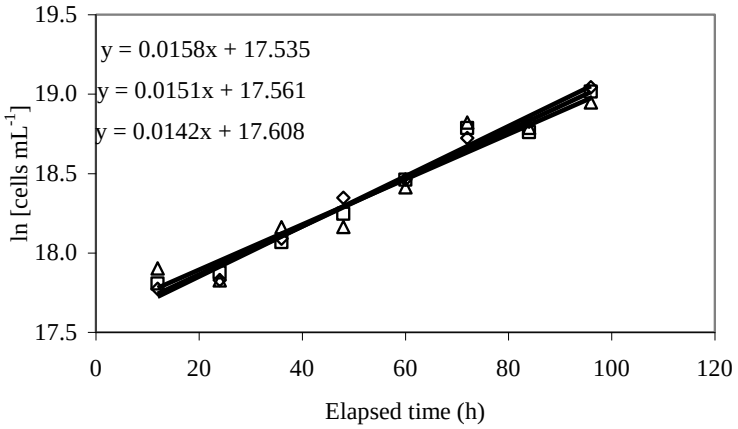
Specific growth rate (h^{-1})	
Trial 1	0.020
Trial 2	0.020
Trial 3	0.019
Average	0.020
STDEV	0.001
95% CI	0.001

Figure E.44. Specific growth rate calculations for Trial 1 (open circles), Trial 2 (open squares), and Trial 3 (open triangles).

Effective Organic Acid Concentration Equal to 0.50 x IC_{50}

Table E.45. BC13 cell concentrations during growth in the presence of 0.25 x IC_{50} of succinate mixed with 0.25 x IC_{50} of malate.

	Cells mL^{-1}						ln (Cells mL^{-1})		
Elapsed Time (h)	Trial 1	Trial 2	Trial 3	Average	STDEV	95% CI	Trial 1	Trial 2	Trial 3
0	5.11E+07	5.08E+07	5.27E+07	5.15E+07	1.01E+06	1.14E+06	17.75	17.74	17.78
12	5.23E+07	5.41E+07	5.95E+07	5.53E+07	3.74E+06	4.23E+06	17.77	17.81	17.90
24	5.53E+07	5.81E+07	5.52E+07	5.62E+07	1.62E+06	1.84E+06	17.83	17.88	17.83
36	7.18E+07	7.03E+07	7.71E+07	7.31E+07	3.55E+06	4.02E+06	18.09	18.07	18.16
48	9.28E+07	8.40E+07	7.73E+07	8.47E+07	7.76E+06	8.78E+06	18.35	18.25	18.16
60	1.04E+08	1.04E+08	9.92E+07	1.02E+08	2.88E+06	3.26E+06	18.46	18.46	18.41
72	1.35E+08	1.44E+08	1.49E+08	1.43E+08	6.90E+06	7.81E+06	18.72	18.79	18.82
84	1.50E+08	1.40E+08	1.44E+08	1.45E+08	4.86E+06	5.50E+06	18.83	18.76	18.79
96	1.86E+08	1.81E+08	1.69E+08	1.79E+08	8.75E+06	9.90E+06	19.04	19.02	18.95
108	2.01E+08	2.12E+08	2.24E+08	2.13E+08	1.18E+07	1.34E+07	19.12	19.17	19.23
120	1.78E+08	1.66E+08	1.71E+08	1.71E+08	5.85E+06	6.62E+06	18.99	18.93	18.95



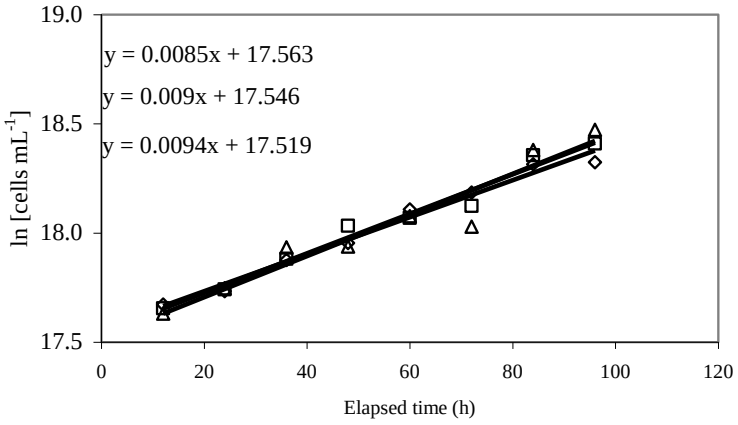
Specific growth rate (h^{-1})	
Trial 1	0.016
Trial 2	0.015
Trial 3	0.014
Average	0.015
STDEV	0.001
95% CI	0.001

Figure E.45. Specific growth rate calculations for Trial 1 (open circles), Trial 2 (open squares), and Trial 3 (open triangles).

Effective Organic Acid Concentration Equal to 1.00 x IC_{50}

Table E.46. BC13 cell concentrations during growth in the presence of 0.50 x IC_{50} of succinate mixed with 0.50 x IC_{50} of malate.

	Cells mL^{-1}						ln (Cells mL^{-1})		
Elapsed Time (h)	Trial 1	Trial 2	Trial 3	Average	STDEV	95% CI	Trial 1	Trial 2	Trial 3
0	4.75E+07	4.80E+07	4.83E+07	4.80E+07	4.04E+05	4.58E+05	17.68	17.69	17.69
12	4.73E+07	4.65E+07	4.54E+07	4.64E+07	9.54E+05	1.08E+06	17.67	17.66	17.63
24	5.03E+07	5.07E+07	5.10E+07	5.07E+07	3.23E+05	3.66E+05	17.73	17.74	17.75
36	5.80E+07	5.84E+07	6.15E+07	5.93E+07	1.92E+06	2.17E+06	17.88	17.88	17.93
48	6.27E+07	6.79E+07	6.17E+07	6.41E+07	3.30E+06	3.73E+06	17.95	18.03	17.94
60	7.32E+07	7.03E+07	7.09E+07	7.15E+07	1.50E+06	1.69E+06	18.11	18.07	18.08
72	7.91E+07	7.43E+07	6.76E+07	7.37E+07	5.74E+06	6.50E+06	18.19	18.12	18.03
84	8.99E+07	9.38E+07	9.61E+07	9.33E+07	3.10E+06	3.51E+06	18.31	18.36	18.38
96	9.08E+07	9.89E+07	1.05E+08	9.83E+07	7.24E+06	8.19E+06	18.32	18.41	18.47
108	9.54E+07	8.69E+07	7.98E+07	8.74E+07	7.84E+06	8.87E+06	18.37	18.28	18.19
120	9.82E+07	1.01E+08	1.04E+08	1.01E+08	3.09E+06	3.50E+06	18.40	18.43	18.46



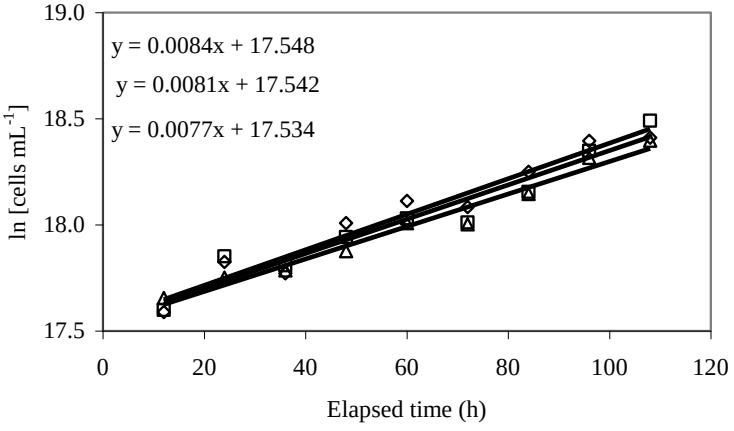
Specific growth rate (h^{-1})	
Trial 1	0.009
Trial 2	0.009
Trial 3	0.009
Average	0.009
STDEV	0.000
95% CI	0.001

Figure E.46. Specific growth rate calculations for Trial 1 (open circles), Trial 2 (open squares), and Trial 3 (open triangles).

Effective Organic Acid Concentration Equal to 1.50 x IC_{50}

Table E.47. BC13 cell concentrations during growth in the presence of 0.75 x IC_{50} of succinate mixed with 0.75 x IC_{50} of malate.

	Cells mL^{-1}						ln (Cells mL^{-1})		
Elapsed Time (h)	Trial 1	Trial 2	Trial 3	Average	STDEV	95% CI	Trial 1	Trial 2	Trial 3
0	4.50E+07	4.55E+07	4.65E+07	4.57E+07	7.69E+05	8.70E+05	17.62	17.63	17.66
12	4.35E+07	4.40E+07	4.65E+07	4.47E+07	1.61E+06	1.82E+06	17.59	17.60	17.66
24	5.52E+07	5.66E+07	5.12E+07	5.43E+07	2.81E+06	3.18E+06	17.83	17.85	17.75
36	5.23E+07	5.43E+07	5.30E+07	5.32E+07	9.91E+05	1.12E+06	17.77	17.81	17.79
48	6.62E+07	6.20E+07	5.80E+07	6.21E+07	4.07E+06	4.60E+06	18.01	17.94	17.88
60	7.35E+07	6.77E+07	6.62E+07	6.91E+07	3.84E+06	4.34E+06	18.11	18.03	18.01
72	7.14E+07	6.64E+07	6.58E+07	6.79E+07	3.09E+06	3.50E+06	18.08	18.01	18.00
84	8.44E+07	7.67E+07	7.59E+07	7.90E+07	4.66E+06	5.28E+06	18.25	18.16	18.15
96	9.75E+07	9.31E+07	9.01E+07	9.36E+07	3.72E+06	4.21E+06	18.40	18.35	18.32
108	9.89E+07	1.07E+08	9.77E+07	1.01E+08	5.15E+06	5.83E+06	18.41	18.49	18.40
120	9.70E+07	9.39E+07	9.13E+07	9.41E+07	2.87E+06	3.25E+06	18.39	18.36	18.33



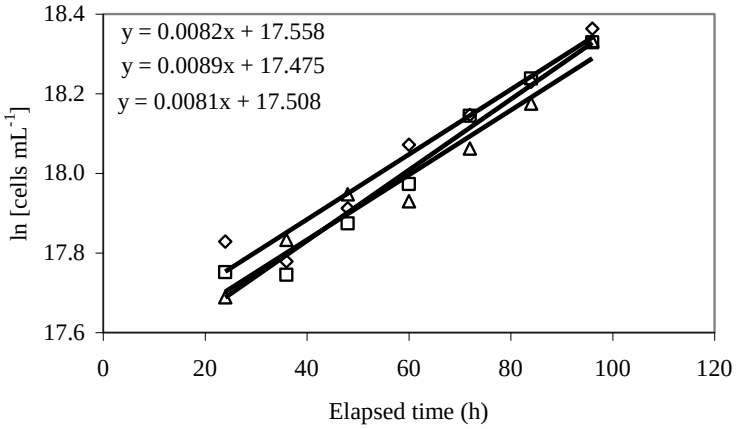
Specific growth rate (h^{-1})	
Trial 1	0.008
Trial 2	0.008
Trial 3	0.008
Average	0.008
STDEV	0.000
95% CI	0.000

Figure E.47. Specific growth rate calculations for Trial 1 (open circles), Trial 2 (open squares), and Trial 3 (open triangles).

Effective Organic Acid Concentration Equal to 2.00 x IC_{50}

Table E.48. BC13 cell concentrations during growth in the presence of 1.00 x IC_{50} of succinate mixed with 1.00 x IC_{50} of malate.

	Cells mL^{-1}						ln (Cells mL^{-1})		
Elapsed Time (h)	Trial 1	Trial 2	Trial 3	Average	STDEV	95% CI	Trial 1	Trial 2	Trial 3
0	5.21E+07	4.83E+07	4.42E+07	4.82E+07	3.96E+06	4.48E+06	17.77	17.69	17.60
12	5.33E+07	5.68E+07	5.56E+07	5.52E+07	1.79E+06	2.03E+06	17.79	17.85	17.83
24	5.53E+07	5.12E+07	4.81E+07	5.15E+07	3.61E+06	4.09E+06	17.83	17.75	17.69
36	5.26E+07	5.09E+07	5.55E+07	5.30E+07	2.35E+06	2.66E+06	17.78	17.75	17.83
48	6.01E+07	5.79E+07	6.23E+07	6.01E+07	2.18E+06	2.47E+06	17.91	17.87	17.95
60	7.06E+07	6.39E+07	6.12E+07	6.52E+07	4.81E+06	5.44E+06	18.07	17.97	17.93
72	7.60E+07	7.58E+07	6.99E+07	7.39E+07	3.50E+06	3.97E+06	18.15	18.14	18.06
84	8.27E+07	8.33E+07	7.82E+07	8.14E+07	2.76E+06	3.12E+06	18.23	18.24	18.18
96	9.44E+07	9.13E+07	9.16E+07	9.24E+07	1.73E+06	1.96E+06	18.36	18.33	18.33
108	1.06E+08	1.02E+08	9.22E+07	1.00E+08	7.10E+06	8.03E+06	18.48	18.44	18.34
120	9.80E+07	9.78E+07	1.04E+08	1.00E+08	3.78E+06	4.28E+06	18.40	18.40	18.46



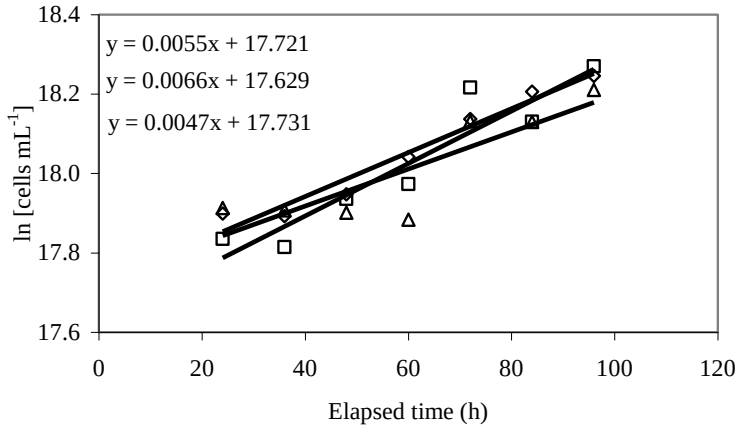
Specific growth rate (h^{-1})	
Trial 1	0.008
Trial 2	0.009
Trial 3	0.008
Average	0.008
STDEV	0.000
95% CI	0.000

Figure E.48. Specific growth rate calculations for Trial 1 (open circles), Trial 2 (open squares), and Trial 3 (open triangles).

Effective Organic Acid Concentration Equal to 10.00 x IC_{50}

Table E.49. BC13 cell concentrations during growth in the presence of 5.00 x IC_{50} of succinate mixed with 5.00 x IC_{50} of malate.

	Cells mL^{-1}						ln (Cells mL^{-1})		
Elapsed Time (h)	Trial 1	Trial 2	Trial 3	Average	STDEV	95% CI	Trial 1	Trial 2	Trial 3
0	5.51E+07	5.84E+07	5.56E+07	5.64E+07	1.80E+06	2.04E+06	17.82	17.88	17.83
12	5.74E+07	5.55E+07	5.31E+07	5.53E+07	2.18E+06	2.47E+06	17.87	17.83	17.79
24	5.93E+07	5.57E+07	6.02E+07	5.84E+07	2.41E+06	2.72E+06	17.90	17.83	17.91
36	5.90E+07	5.45E+07	5.98E+07	5.78E+07	2.83E+06	3.21E+06	17.89	17.81	17.91
48	6.23E+07	6.16E+07	5.95E+07	6.11E+07	1.46E+06	1.66E+06	17.95	17.94	17.90
60	6.84E+07	6.39E+07	5.85E+07	6.36E+07	4.99E+06	5.65E+06	18.04	17.97	17.88
72	7.53E+07	8.15E+07	7.49E+07	7.72E+07	3.71E+06	4.20E+06	18.14	18.22	18.13
84	8.07E+07	7.48E+07	7.47E+07	7.67E+07	3.40E+06	3.85E+06	18.21	18.13	18.13
96	8.39E+07	8.60E+07	8.10E+07	8.37E+07	2.51E+06	2.84E+06	18.25	18.27	18.21
108	8.46E+07	9.04E+07	8.37E+07	8.63E+07	3.65E+06	4.13E+06	18.25	18.32	18.24
120	8.49E+07	8.16E+07	8.45E+07	8.37E+07	1.81E+06	2.05E+06	18.26	18.22	18.25



Specific growth rate (h^{-1})	
Trial 1	0.006
Trial 2	0.007
Trial 3	0.005
Average	0.006
STDEV	0.001
95% CI	0.001

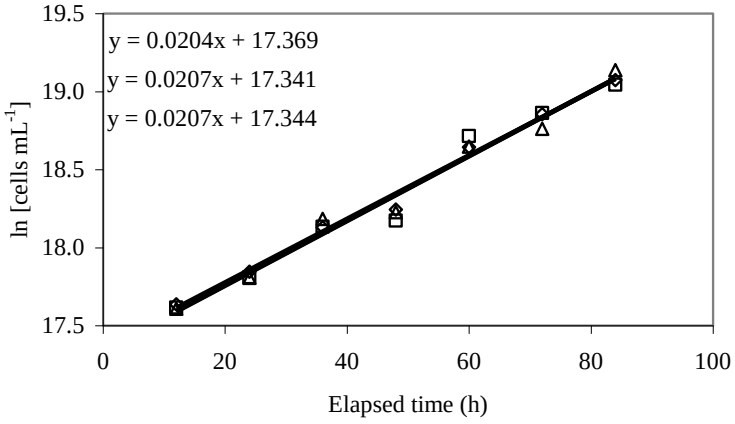
Figure E.49. Specific growth rate calculations for Trial 1 (open circles), Trial 2 (open squares), and Trial 3 (open triangles).

Mixture of all organic acids tested

Effective Organic Acid Concentration Equal to 0.25 x IC_{50}

Table E.50. BC13 cell concentrations during growth in the presence of 0.036 x IC_{50} of pyruvate, acetate, 2-ketoglutarate, succinate, fumarate, malate, and oxaloacetate.

	Cells mL^{-1}						ln (Cells mL^{-1})		
Elapsed Time (h)	Trial 1	Trial 2	Trial 3	Average	STDEV	95% CI	Trial 1	Trial 2	Trial 3
0	4.46E+07	4.65E+07	4.56E+07	4.56E+07	9.47E+05	1.07E+06	17.61	17.66	17.64
12	4.57E+07	4.47E+07	4.44E+07	4.49E+07	6.76E+05	7.65E+05	17.64	17.62	17.61
24	5.62E+07	5.44E+07	5.41E+07	5.49E+07	1.17E+06	1.32E+06	17.85	17.81	17.81
36	7.48E+07	7.51E+07	7.89E+07	7.63E+07	2.30E+06	2.60E+06	18.13	18.13	18.18
48	8.38E+07	7.81E+07	8.24E+07	8.14E+07	2.97E+06	3.36E+06	18.24	18.17	18.23
60	1.25E+08	1.34E+08	1.25E+08	1.28E+08	5.20E+06	5.89E+06	18.64	18.72	18.65
72	1.54E+08	1.56E+08	1.41E+08	1.50E+08	8.35E+06	9.45E+06	18.86	18.86	18.76
84	1.92E+08	1.87E+08	2.05E+08	1.95E+08	9.40E+06	1.06E+07	19.07	19.04	19.14
96	2.09E+08	2.17E+08	2.29E+08	2.18E+08	1.00E+07	1.14E+07	19.16	19.19	19.25
108	2.01E+08	2.07E+08	2.07E+08	2.05E+08	3.35E+06	3.79E+06	19.12	19.15	19.15
120	2.02E+08	1.95E+08	1.84E+08	1.94E+08	8.77E+06	9.93E+06	19.12	19.09	19.03



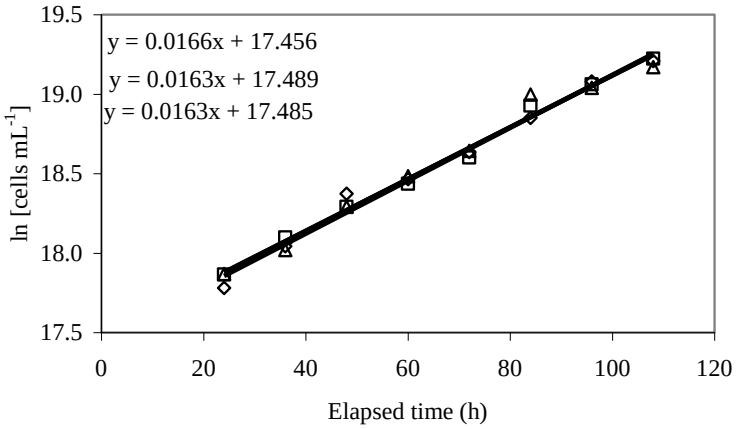
Specific growth rate (h^{-1})	
Trial 1	0.020
Trial 2	0.021
Trial 3	0.021
Average	0.021
STDEV	0.000
95% CI	0.000

Figure E.50. Specific growth rate calculations for Trial 1 (open circles), Trial 2 (open squares), and Trial 3 (open triangles).

Effective Organic Acid Concentration Equal to 0.50 x IC_{50}

Table E.51. BC13 cell concentrations during growth in the presence of 0.071 x IC_{50} of pyruvate, acetate, 2-ketoglutarate, succinate, fumarate, malate, and oxaloacetate.

	Cells mL^{-1}						ln (Cells mL^{-1})		
Elapsed Time (h)	Trial 1	Trial 2	Trial 3	Average	STDEV	95% CI	Trial 1	Trial 2	Trial 3
0	5.05E+07	5.23E+07	5.01E+07	5.09E+07	1.19E+06	1.35E+06	17.74	17.77	17.73
12	5.09E+07	5.41E+07	5.78E+07	5.43E+07	3.45E+06	3.91E+06	17.74	17.81	17.87
24	5.28E+07	5.74E+07	5.76E+07	5.59E+07	2.73E+06	3.09E+06	17.78	17.86	17.87
36	6.85E+07	7.24E+07	6.69E+07	6.93E+07	2.81E+06	3.18E+06	18.04	18.10	18.02
48	9.54E+07	8.79E+07	8.79E+07	9.04E+07	4.34E+06	4.92E+06	18.37	18.29	18.29
60	1.05E+08	1.02E+08	1.06E+08	1.04E+08	2.46E+06	2.79E+06	18.47	18.44	18.48
72	1.24E+08	1.20E+08	1.25E+08	1.23E+08	2.77E+06	3.13E+06	18.64	18.60	18.64
84	1.54E+08	1.66E+08	1.78E+08	1.66E+08	1.21E+07	1.37E+07	18.85	18.93	19.00
96	1.93E+08	1.90E+08	1.86E+08	1.90E+08	3.89E+06	4.40E+06	19.08	19.06	19.04
108	2.20E+08	2.23E+08	2.11E+08	2.18E+08	5.97E+06	6.75E+06	19.21	19.22	19.17
120	1.94E+08	1.96E+08	1.82E+08	1.91E+08	7.37E+06	8.34E+06	19.08	19.09	19.02



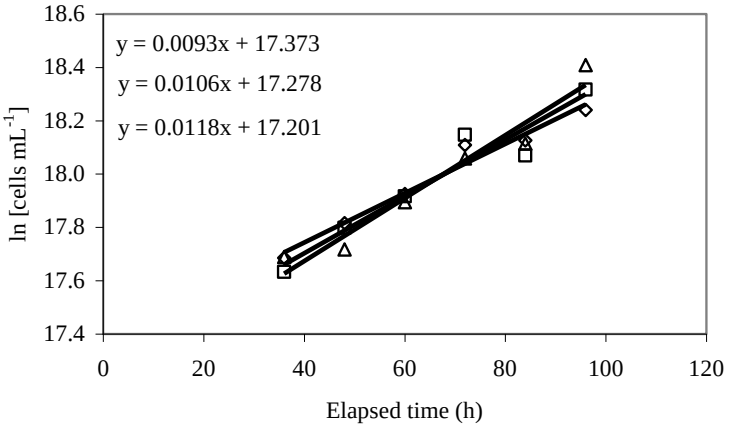
Specific growth rate (h^{-1})	
Trial 1	0.017
Trial 2	0.016
Trial 3	0.016
Average	0.016
STDEV	0.000
95% CI	0.000

Figure E.51. Specific growth rate calculations for Trial 1 (open circles), Trial 2 (open squares), and Trial 3 (open triangles).

Effective Organic Acid Concentration Equal to 1.00 x IC_{50}

Table E.52. BC13 cell concentrations during growth in the presence of 0.143 x IC_{50} of pyruvate, acetate, 2-ketoglutarate, succinate, fumarate, malate, and oxaloacetate.

	Cells mL^{-1}						ln (Cells mL^{-1})		
Elapsed Time (h)	Trial 1	Trial 2	Trial 3	Average	STDEV	95% CI	Trial 1	Trial 2	Trial 3
0	4.91E+07	5.21E+07	4.88E+07	5.00E+07	1.82E+06	2.06E+06	17.71	17.77	17.70
12	4.98E+07	5.02E+07	5.52E+07	5.17E+07	2.98E+06	3.37E+06	17.72	17.73	17.83
24	5.04E+07	4.61E+07	4.38E+07	4.68E+07	3.32E+06	3.76E+06	17.73	17.65	17.60
36	4.79E+07	4.55E+07	4.81E+07	4.72E+07	1.47E+06	1.66E+06	17.69	17.63	17.69
48	5.46E+07	5.36E+07	4.95E+07	5.26E+07	2.72E+06	3.07E+06	17.82	17.80	17.72
60	6.09E+07	6.04E+07	5.91E+07	6.01E+07	9.51E+05	1.08E+06	17.93	17.92	17.89
72	7.32E+07	7.61E+07	6.96E+07	7.30E+07	3.26E+06	3.69E+06	18.11	18.15	18.06
84	7.45E+07	7.04E+07	7.36E+07	7.28E+07	2.15E+06	2.44E+06	18.13	18.07	18.11
96	8.35E+07	9.02E+07	9.88E+07	9.08E+07	7.69E+06	8.71E+06	18.24	18.32	18.41
108	8.62E+07	9.10E+07	9.47E+07	9.06E+07	4.23E+06	4.79E+06	18.27	18.33	18.37
120	8.71E+07	9.00E+07	8.93E+07	8.88E+07	1.49E+06	1.69E+06	18.28	18.32	18.31



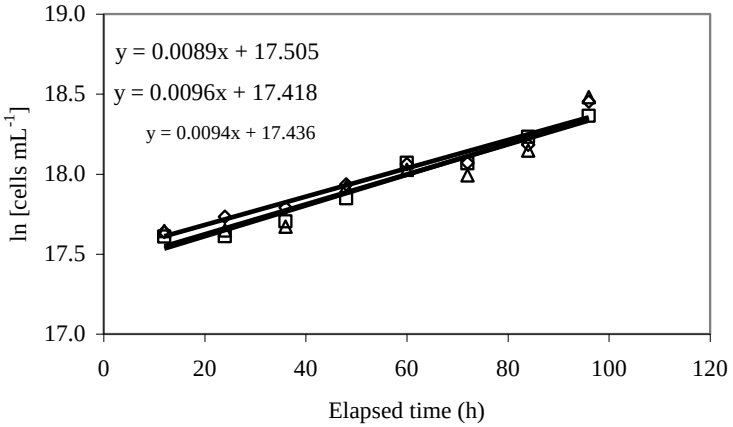
Specific growth rate (h^{-1})	
Trial 1	0.009
Trial 2	0.011
Trial 3	0.012
Average	0.011
STDEV	0.001
95% CI	0.001

Figure E.52. Specific growth rate calculations for Trial 1 (open circles), Trial 2 (open squares), and Trial 3 (open triangles).

Effective Organic Acid Concentration Equal to 1.50 x IC_{50}

Table E.53. BC13 cell concentrations during growth in the presence of 0.214 x IC_{50} of pyruvate, acetate, 2-ketoglutarate, succinate, fumarate, malate, and oxaloacetate.

	Cells mL^{-1}						ln (Cells mL^{-1})		
Elapsed Time (h)	Trial 1	Trial 2	Trial 3	Average	STDEV	95% CI	Trial 1	Trial 2	Trial 3
0	4.14E+07	4.83E+07	4.03E+07	4.33E+07	4.35E+06	4.93E+06	17.54	17.69	17.51
12	4.57E+07	4.44E+07	4.60E+07	4.54E+07	8.60E+05	9.73E+05	17.64	17.61	17.64
24	5.03E+07	4.45E+07	4.61E+07	4.70E+07	2.99E+06	3.39E+06	17.73	17.61	17.65
36	5.31E+07	4.88E+07	4.73E+07	4.97E+07	3.05E+06	3.45E+06	17.79	17.70	17.67
48	6.15E+07	5.64E+07	6.06E+07	5.95E+07	2.73E+06	3.09E+06	17.93	17.85	17.92
60	6.99E+07	7.05E+07	6.74E+07	6.93E+07	1.63E+06	1.84E+06	18.06	18.07	18.03
72	7.04E+07	7.02E+07	6.51E+07	6.86E+07	2.99E+06	3.38E+06	18.07	18.07	17.99
84	7.88E+07	8.29E+07	7.61E+07	7.93E+07	3.40E+06	3.85E+06	18.18	18.23	18.15
96	1.03E+08	9.44E+07	1.06E+08	1.01E+08	6.12E+06	6.92E+06	18.45	18.36	18.48
108	1.04E+08	9.75E+07	9.41E+07	9.86E+07	5.15E+06	5.82E+06	18.46	18.40	18.36
120	1.07E+08	1.11E+08	1.13E+08	1.10E+08	3.39E+06	3.84E+06	18.48	18.53	18.54



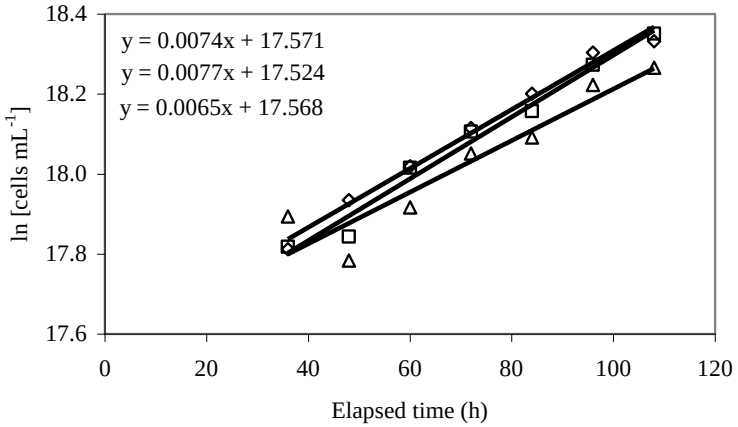
Specific growth rate (h^{-1})	
Trial 1	0.009
Trial 2	0.010
Trial 3	0.009
Average	0.009
STDEV	0.000
95% CI	0.000

Figure E.53. Specific growth rate calculations for Trial 1 (open circles), Trial 2 (open squares), and Trial 3 (open triangles).

Effective Organic Acid Concentration Equal to 2.00 x IC_{50}

Table E.54. BC13 cell concentrations during growth in the presence of 0.286 x IC_{50} of pyruvate, acetate, 2-ketoglutarate, succinate, fumarate, malate, and oxaloacetate.

	Cells mL^{-1}						ln (Cells mL^{-1})		
Elapsed Time (h)	Trial 1	Trial 2	Trial 3	Average	STDEV	95% CI	Trial 1	Trial 2	Trial 3
0	5.05E+07	5.52E+07	5.23E+07	5.27E+07	2.39E+06	2.70E+06	17.74	17.83	17.77
12	5.49E+07	5.32E+07	5.12E+07	5.31E+07	1.86E+06	2.10E+06	17.82	17.79	17.75
24	5.47E+07	5.87E+07	6.24E+07	5.86E+07	3.88E+06	4.39E+06	17.82	17.89	17.95
36	5.44E+07	5.47E+07	5.91E+07	5.61E+07	2.59E+06	2.94E+06	17.81	17.82	17.89
48	6.15E+07	5.62E+07	5.29E+07	5.69E+07	4.34E+06	4.92E+06	17.93	17.84	17.78
60	6.69E+07	6.67E+07	6.04E+07	6.47E+07	3.70E+06	4.19E+06	18.02	18.02	17.92
72	7.36E+07	7.30E+07	6.91E+07	7.19E+07	2.46E+06	2.78E+06	18.11	18.11	18.05
84	8.03E+07	7.68E+07	7.20E+07	7.64E+07	4.18E+06	4.73E+06	18.20	18.16	18.09
96	8.89E+07	8.63E+07	8.21E+07	8.58E+07	3.46E+06	3.92E+06	18.30	18.27	18.22
108	9.15E+07	9.33E+07	8.56E+07	9.01E+07	3.99E+06	4.51E+06	18.33	18.35	18.27
120	9.72E+07	9.29E+07	8.93E+07	9.31E+07	3.94E+06	4.46E+06	18.39	18.35	18.31



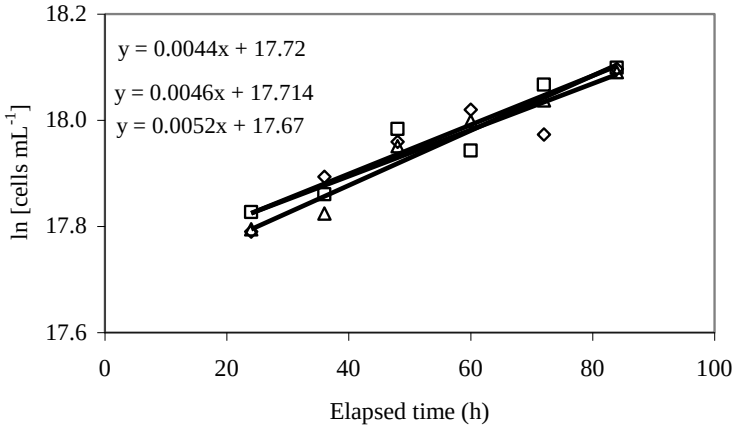
Specific growth rate (h^{-1})	
Trial 1	0.007
Trial 2	0.008
Trial 3	0.007
Average	0.007
STDEV	0.001
95% CI	0.001

Figure E.54. Specific growth rate calculations for Trial 1 (open circles), Trial 2 (open squares), and Trial 3 (open triangles).

Effective Organic Acid Concentration Equal to 10.00 x IC_{50}

Table E.55. BC13 cell concentrations during growth in the presence of 1.429 x IC_{50} of pyruvate, acetate, 2-ketoglutarate, succinate, fumarate, malate, and oxaloacetate.

	Cells mL^{-1}						ln (Cells mL^{-1})		
Elapsed Time (h)	Trial 1	Trial 2	Trial 3	Average	STDEV	95% CI	Trial 1	Trial 2	Trial 3
0	5.10E+07	5.53E+07	5.51E+07	5.38E+07	2.44E+06	2.76E+06	17.75	17.83	17.83
12	5.13E+07	5.64E+07	5.23E+07	5.33E+07	2.71E+06	3.06E+06	17.75	17.85	17.77
24	5.32E+07	5.52E+07	5.35E+07	5.40E+07	1.08E+06	1.23E+06	17.79	17.83	17.79
36	5.90E+07	5.71E+07	5.51E+07	5.71E+07	1.99E+06	2.25E+06	17.89	17.86	17.82
48	6.30E+07	6.46E+07	6.25E+07	6.34E+07	1.07E+06	1.21E+06	17.96	17.98	17.95
60	6.70E+07	6.20E+07	6.56E+07	6.48E+07	2.54E+06	2.87E+06	18.02	17.94	18.00
72	6.39E+07	7.02E+07	6.81E+07	6.74E+07	3.21E+06	3.64E+06	17.97	18.07	18.04
84	7.23E+07	7.25E+07	7.19E+07	7.22E+07	3.05E+05	3.46E+05	18.10	18.10	18.09
96	7.10E+07	7.32E+07	6.91E+07	7.11E+07	2.08E+06	2.35E+06	18.08	18.11	18.05
108	7.08E+07	7.14E+07	7.24E+07	7.15E+07	8.03E+05	9.08E+05	18.08	18.08	18.10
120	7.25E+07	7.73E+07	7.79E+07	7.59E+07	2.94E+06	3.33E+06	18.10	18.16	18.17



Specific growth rate (h^{-1})	
Trial 1	0.004
Trial 2	0.005
Trial 3	0.005
Average	0.005
STDEV	0.000
95% CI	0.000

Figure E.55. Specific growth rate calculations for Trial 1 (open circles), Trial 2 (open squares), and Trial 3 (open triangles).

Changes in Organic Acid Concentrations during Batch Growth of BC13

Table E.56. Organic acid concentrations (μM) with time during batch culturing of BC13. Initial concentrations equal to the previously calculated IC_{50} values.

Pyruvate						
Elapsed Time (h)	Trial 1	Trial 2	Trial 3	Average	STDEV	95% CI
0	66.54	66.54	66.54	66.54	0.00	0.00
40	61.42	56.23	58.62	58.76	2.60	2.94
80	39.19	34.07	33.74	35.67	3.06	3.46
120	35.67	36.67	43.52	38.62	4.27	4.84

Acetate						
Elapsed Time (h)	Trial 1	Trial 2	Trial 3	Average	STDEV	95% CI
0	62.70	62.70	62.70	62.70	0.00	0.00
40	46.78	32.79	52.99	44.19	10.34	11.70
80	23.51	17.12	22.51	21.05	3.44	3.89
120	7.27	17.12	18.69	14.36	6.19	7.00

2-ketoglutarate						
Elapsed Time (h)	Trial 1	Trial 2	Trial 3	Average	STDEV	95% CI
0	73.27	73.27	73.27	73.27	0.00	0.00
40	60.23	54.96	52.98	56.05	3.75	4.24
80	25.35	24.11	24.40	24.62	0.65	0.74
120	24.77	22.79	28.43	25.33	2.86	3.24

Succinate						
Elapsed Time (h)	Trial 1	Trial 2	Trial 3	Average	STDEV	95% CI
0	62.78	62.78	62.78	62.78	0.00	0.00
40	56.63	48.90	56.88	54.14	4.53	5.13
80	27.94	24.99	25.74	26.22	1.53	1.73
120	23.54	20.34	22.10	21.99	1.60	1.81

Fumarate						
Elapsed Time (h)	Trial 1	Trial 2	Trial 3	Average	STDEV	95% CI
0	73.76	73.76	73.76	73.76	0.00	0.00
40	61.59	51.48	57.38	56.82	5.08	5.74
80	25.52	23.23	23.60	24.12	1.23	1.39
120	22.28	19.69	21.98	21.32	1.41	1.60

Malate						
Elapsed Time (h)	Trial 1	Trial 2	Trial 3	Average	STDEV	95% CI
0	84.33	84.33	84.33	84.33	0.00	0.00
40	65.61	67.64	65.02	66.09	1.37	1.55
80	25.72	28.50	33.90	29.38	4.16	4.71
120	21.25	28.17	31.71	27.04	5.32	6.02

Oxaloacetate						
Elapsed Time (h)	Trial 1	Trial 2	Trial 3	Average	STDEV	95% CI
0	28.24	28.24	28.24	28.24	0.00	0.00
40	26.91	27.87	27.16	27.31	0.50	0.56
80	17.28	19.14	20.41	18.95	1.58	1.78
120	16.43	14.77	14.43	15.21	1.07	1.21

Summary of Phospholipid Fatty Acid Analysis

Table E.57. Percent composition of BC13 PLFA in an organic acid free control, when exposed to all organic acids other than oxaloacetate, and when exposed to oxaloacetate. BC13 was exposed to organic acids concentrations equal to the previously calculated IC50 values.

	Control	Organic Acids W/out Oxaloacetate	95% CI	Oxaloacetate
Terminally Branched Saturates				
i14:0	0.00	0.04	0.02	0.00
i15:0	0.24	0.13	0.03	0.00
a15:0	0.28	0.15	0.10	0.00
i16:0	1.52	1.18	0.23	0.88
i17:0	0.05	0.06	0.02	0.00
a17:0	1.97	3.01	1.16	3.51
Total	**4.06**	**4.55**	**1.33**	**4.39**
Monoenoic				
15:1w6c	0.05	0.03	0.02	0.00
16:1w9c	0.05	0.11	0.05	0.00
16:1w7c	0.44	0.58	0.13	0.48
16:1w7t	0.19	0.16	0.06	0.00
16:1w5c	0.07	0.17	0.04	0.00
cy17:0	0.61	0.78	0.13	0.69
18:1w9c	0.84	0.91	0.54	2.49
18:1w7c	51.39	43.83	13.37	43.37
18:1w5c	0.39	0.38	0.12	0.40
cy19:0	12.92	21.36	7.99	21.79
Total	**66.95**	**68.32**	**24.89**	**69.22**
Branched Monoenoic				
i17:1w7c	0.02	0.01	0.01	0.00
br19:1a	0.80	1.60	0.36	1.34
Total	**0.82**	**1.61**	**0.36**	**1.34**
Mid-Chain Branched Saturate				
10me16:0	0.22	0.18	0.05	0.00
12me16:0	0.00	0.01	0.00	0.00
10me18:0	0.04	0.01	0.00	0.00
Total	**0.26**	**0.19**	**0.05**	**0.00**
Normal Saturates				
14:0	0.33	0.29	0.07	0.00
15:0	0.57	0.39	0.10	0.51
16:0	14.99	11.57	3.72	15.22
17:0	1.86	1.54	0.32	1.39
18:0	2.53	1.92	0.69	1.90
20:0	5.52	7.24	2.34	0.96
Total	**25.80**	**22.96**	**7.84**	**19.98**
18:2w6	1.66	2.03	1.15	5.07
20:4w6	0.46	0.34	0.12	0.00
	2.12	**2.37**	**1.18**	**5.07**
Metabolic Status: (Ratio)				
(cy17:0/16:1w7c)	1.39	1.14	0.30	1.44
(cy19:0/18:1w7c)	0.25	0.53	0.22	0.50
Total	**1.64**	**1.67**	**0.53**	**1.94**
(16:1w7t/16:1w7c)	0.43	0.32	0.14	0.00
(18:1w7t/18:1w7c)	0.00	0.00	0.00	0.00
Total	**0.43**	**0.32**	**0.14**	**0.00**

APPENDIX F

CHAPTER THREE RAW DATA

Cell Growth and Substrate Concentrations in Chemostat Cultures

BC13 cell and substrate concentrations in the influent and effluent of chemostat reactors. Experiments were repeated in triplicate and average values, standard deviations (STDEV), and 95% confidence intervals (95% CI) are shown.

Table F.1. BC13 cell concentrations (cells mL^{-1}) on 10 mM potassium tetrathionate and ambient carbon dioxide. Predicted cell concentrations were calculated assuming zero growth and are included for comparison (theoretical washout).

Elapsed Time (h)	Trial 1	Trial 2	Trial 3	Average	STDEV	95% CI	Theoritical Washout Calculation
0	5.22E+07	5.16E+07	5.10E+07	5.16E+07	6.00E+05	6.79E+05	5.50E+07
24	4.36E+07	4.28E+07	4.38E+07	4.34E+07	5.29E+05	5.99E+05	4.33E+07
48	3.90E+07	3.70E+07	4.14E+07	3.91E+07	2.20E+06	2.49E+06	3.40E+07
72	3.24E+07	3.32E+07	3.30E+07	3.29E+07	4.16E+05	4.71E+05	2.68E+07
96	2.70E+07	2.82E+07	2.78E+07	2.77E+07	6.11E+05	6.91E+05	2.11E+07
120	2.50E+07	2.60E+07	2.60E+07	2.57E+07	5.77E+05	6.53E+05	1.66E+07
144	2.18E+07	2.28E+07	2.06E+07	2.17E+07	1.10E+06	1.25E+06	1.30E+07
168	1.88E+07	1.96E+07	2.02E+07	1.95E+07	7.02E+05	7.95E+05	1.03E+07
192	1.48E+07	1.60E+07	1.64E+07	1.57E+07	8.33E+05	9.42E+05	8.06E+06
216	1.28E+07	1.42E+07	1.46E+07	1.39E+07	9.45E+05	1.07E+06	6.34E+06
240	1.10E+07	1.26E+07	1.30E+07	1.22E+07	1.06E+06	1.20E+06	4.99E+06
264	9.80E+06	1.14E+07	1.00E+07	1.04E+07	8.72E+05	9.86E+05	3.92E+06
288	8.00E+06	9.60E+06	1.04E+07	9.33E+06	1.22E+06	1.38E+06	3.09E+06
312	7.00E+06	8.80E+06	9.60E+06	8.47E+06	1.33E+06	1.51E+06	2.43E+06
336	6.20E+06	8.20E+06	8.80E+06	7.73E+06	1.36E+06	1.54E+06	1.91E+06
360	5.80E+06	8.20E+06	8.90E+06	7.63E+06	1.63E+06	1.84E+06	1.50E+06
384	5.60E+06	8.40E+06	8.60E+06	7.53E+06	1.68E+06	1.90E+06	1.18E+06
408	5.50E+06	8.00E+06	8.70E+06	7.40E+06	1.68E+06	1.90E+06	9.30E+05

Table F.2. BC13 cell concentrations (cells mL^{-1}) during heterotrophic growth on 50 μM pyruvate and ambient carbon dioxide.

Elapsed Time (h)	Trial 1	Trial 2	Trial 3	Average	STDEV	95% CI
0	5.26E+07	5.10E+07	5.00E+07	5.12E+07	1.31E+06	1.48E+06
24	4.04E+07	4.34E+07	4.00E+07	4.13E+07	1.86E+06	2.10E+06
48	3.46E+07	3.30E+07	3.40E+07	3.39E+07	8.08E+05	9.15E+05
72	2.64E+07	2.40E+07	2.66E+07	2.57E+07	1.45E+06	1.64E+06
96	2.20E+07	2.38E+07	2.50E+07	2.36E+07	1.51E+06	1.71E+06
120	1.74E+07	1.90E+07	1.50E+07	1.71E+07	2.01E+06	2.28E+06
144	1.26E+07	1.36E+07	1.40E+07	1.34E+07	7.21E+05	8.16E+05
168	9.80E+06	1.10E+07	1.00E+07	1.03E+07	6.43E+05	7.28E+05
192	7.40E+06	6.60E+06	7.00E+06	7.00E+06	4.00E+05	4.53E+05
216	6.40E+06	5.60E+06	6.00E+06	6.00E+06	4.00E+05	4.53E+05
240	4.60E+06	5.00E+06	5.00E+06	4.87E+06	2.31E+05	2.61E+05
264	3.60E+06	4.00E+06	4.00E+06	3.87E+06	2.31E+05	2.61E+05
288	3.20E+06	3.20E+06	3.70E+06	3.37E+06	2.89E+05	3.27E+05
312	2.50E+06	2.00E+06	3.00E+06	2.50E+06	5.00E+05	5.66E+05
336	1.90E+06	2.00E+06	2.20E+06	2.03E+06	1.53E+05	1.73E+05
360	1.60E+06	1.50E+06	1.90E+06	1.67E+06	2.08E+05	2.36E+05
384	1.10E+06	1.00E+06	1.20E+06	1.10E+06	1.00E+05	1.13E+05
408	1.00E+06	6.60E+05	1.34E+06	1.00E+06	3.40E+05	3.85E+05

Table F.3. BC13 cell concentrations (cells mL^{-1}) during heterotrophic growth on 50 μM acetate and ambient carbon dioxide.

Elapsed Time (h)	Trial 1	Trial 2	Trial 3	Average	STDEV	95% CI
0	5.10E+07	4.90E+07	5.06E+07	5.02E+07	1.06E+06	1.20E+06
24	4.00E+07	4.44E+07	4.30E+07	4.25E+07	2.25E+06	2.54E+06
48	3.80E+07	3.64E+07	3.30E+07	3.58E+07	2.55E+06	2.89E+06
72	2.80E+07	2.66E+07	2.66E+07	2.71E+07	8.08E+05	9.15E+05
96	2.10E+07	2.30E+07	2.24E+07	2.21E+07	1.03E+06	1.16E+06
120	1.80E+07	1.88E+07	1.86E+07	1.85E+07	4.16E+05	4.71E+05
144	1.34E+07	1.20E+07	1.30E+07	1.28E+07	7.21E+05	8.16E+05
168	1.00E+07	9.00E+06	8.00E+06	9.00E+06	1.00E+06	1.13E+06
192	6.60E+06	7.00E+06	8.00E+06	7.20E+06	7.21E+05	8.16E+05
216	6.00E+06	5.60E+06	6.20E+06	5.93E+06	3.06E+05	3.46E+05
240	5.00E+06	4.40E+06	5.00E+06	4.80E+06	3.46E+05	3.92E+05
264	3.00E+06	3.40E+06	2.80E+06	3.07E+06	3.06E+05	3.46E+05
288	2.60E+06	2.80E+06	3.00E+06	2.80E+06	2.00E+05	2.26E+05
312	2.00E+06	2.40E+06	2.20E+06	2.20E+06	2.00E+05	2.26E+05
336	1.60E+06	1.50E+06	1.30E+06	1.47E+06	1.53E+05	1.73E+05
360	1.10E+06	1.24E+06	1.18E+06	1.17E+06	7.02E+04	7.95E+04
384	1.00E+06	9.00E+05	1.00E+06	9.67E+05	5.77E+04	6.53E+04
408	8.00E+05	7.60E+05	8.20E+05	7.93E+05	3.06E+04	3.46E+04

Table F.4. BC13 cell concentrations (cells mL^{-1}) during heterotrophic growth on 50 μM citrate and ambient carbon dioxide.

Elapsed Time (h)	Trial 1	Trial 2	Trial 3	Average	STDEV	95% CI
0	5.00E+07	5.16E+07	5.04E+07	5.07E+07	8.33E+05	9.42E+05
24	4.16E+07	4.10E+07	4.20E+07	4.15E+07	5.03E+05	5.70E+05
48	3.12E+07	3.34E+07	2.96E+07	3.14E+07	1.91E+06	2.16E+06
72	2.70E+07	2.78E+07	2.56E+07	2.68E+07	1.11E+06	1.26E+06
96	2.30E+07	2.00E+07	2.10E+07	2.13E+07	1.53E+06	1.73E+06
120	1.54E+07	1.66E+07	1.34E+07	1.51E+07	1.62E+06	1.83E+06
144	1.30E+07	1.14E+07	1.08E+07	1.17E+07	1.14E+06	1.29E+06
168	1.04E+07	1.08E+07	9.60E+06	1.03E+07	6.11E+05	6.91E+05
192	7.00E+06	6.80E+06	7.00E+06	6.93E+06	1.15E+05	1.31E+05
216	7.00E+06	6.80E+06	6.00E+06	6.60E+06	5.29E+05	5.99E+05
240	4.20E+06	3.80E+06	3.40E+06	3.80E+06	4.00E+05	4.53E+05
264	3.20E+06	3.00E+06	2.88E+06	3.03E+06	1.62E+05	1.83E+05
288	2.60E+06	2.80E+06	3.00E+06	2.80E+06	2.00E+05	2.26E+05
312	2.40E+06	2.20E+06	2.30E+06	2.30E+06	1.00E+05	1.13E+05
336	1.80E+06	1.76E+06	1.72E+06	1.76E+06	4.00E+04	4.53E+04
360	1.48E+06	1.40E+06	1.36E+06	1.41E+06	6.11E+04	6.91E+04
384	1.04E+06	9.00E+05	8.40E+05	9.27E+05	1.03E+05	1.16E+05
408	7.60E+05	6.40E+05	7.60E+05	7.20E+05	6.93E+04	7.84E+04

.

Table F.5. BC13 cell concentrations (cells mL^{-1}) during heterotrophic growth on 50 μM 2-ketoglutarate and ambient carbon dioxide.

Elapsed Time (h)	Trial 1	Trial 2	Trial 3	Average	STDEV	95% CI
0	5.50E+07	5.34E+07	5.30E+07	5.38E+07	1.06E+06	1.20E+06
24	4.20E+07	4.30E+07	4.40E+07	4.30E+07	1.00E+06	1.13E+06
48	3.60E+07	3.66E+07	3.50E+07	3.59E+07	8.08E+05	9.15E+05
72	2.90E+07	2.74E+07	2.64E+07	2.76E+07	1.31E+06	1.48E+06
96	2.20E+07	2.50E+07	2.10E+07	2.27E+07	2.08E+06	2.36E+06
120	1.64E+07	1.70E+07	1.56E+07	1.63E+07	7.02E+05	7.95E+05
144	1.40E+07	1.10E+07	1.10E+07	1.20E+07	1.73E+06	1.96E+06
168	9.00E+06	1.04E+07	9.00E+06	9.47E+06	8.08E+05	9.15E+05
192	7.00E+06	6.60E+06	8.60E+06	7.40E+06	1.06E+06	1.20E+06
216	6.00E+06	5.80E+06	8.40E+06	6.73E+06	1.45E+06	1.64E+06
240	5.00E+06	4.60E+06	7.20E+06	5.60E+06	1.40E+06	1.58E+06
264	3.20E+06	2.80E+06	6.80E+06	4.27E+06	2.20E+06	2.49E+06
288	2.80E+06	2.20E+06	5.00E+06	3.33E+06	1.47E+06	1.67E+06
312	2.40E+06	1.76E+06	3.20E+06	2.45E+06	7.21E+05	8.16E+05
336	1.50E+06	1.54E+06	2.40E+05	1.09E+06	7.39E+05	8.37E+05
360	1.20E+06	1.12E+06	2.00E+06	1.44E+06	4.87E+05	5.51E+05
384	1.00E+06	7.60E+05	1.40E+06	1.05E+06	3.23E+05	3.66E+05
408	6.60E+05	6.00E+05	1.08E+06	7.80E+05	2.62E+05	2.96E+05

Table F.6. BC13 cell concentrations (cells mL^{-1}) during heterotrophic growth on 50 μM succinate and ambient carbon dioxide.

Elapsed Time (h)	Trial 1	Trial 2	Trial 3	Average	STDEV	95% CI
0	5.50E+07	5.66E+07	4.86E+07	5.34E+07	4.23E+06	4.79E+06
24	4.44E+07	4.50E+07	4.16E+07	4.37E+07	1.81E+06	2.05E+06
48	3.86E+07	3.58E+07	3.30E+07	3.58E+07	2.80E+06	3.17E+06
72	3.04E+07	2.80E+07	2.54E+07	2.79E+07	2.50E+06	2.83E+06
96	2.60E+07	2.50E+07	2.06E+07	2.39E+07	2.87E+06	3.25E+06
120	2.14E+07	1.92E+07	1.60E+07	1.89E+07	2.72E+06	3.07E+06
144	1.66E+07	1.48E+07	1.28E+07	1.47E+07	1.90E+06	2.15E+06
168	1.38E+07	1.24E+07	9.20E+06	1.18E+07	2.36E+06	2.67E+06
192	1.14E+07	1.02E+07	6.00E+06	9.20E+06	2.84E+06	3.21E+06
216	1.04E+07	1.10E+07	4.00E+06	8.47E+06	3.88E+06	4.39E+06
240	8.60E+06	7.60E+06	3.60E+06	6.60E+06	2.65E+06	2.99E+06
264	7.60E+06	4.80E+06	2.80E+06	5.07E+06	2.41E+06	2.73E+06
288	7.20E+06	4.60E+06	2.20E+06	4.67E+06	2.50E+06	2.83E+06
312	4.40E+06	5.00E+06	1.88E+06	3.76E+06	1.66E+06	1.87E+06
336	2.30E+06	1.66E+06	1.46E+06	1.81E+06	4.39E+05	4.97E+05
360	2.00E+06	1.00E+06	1.00E+06	1.33E+06	5.77E+05	6.53E+05
384	1.50E+06	6.40E+05	8.60E+05	1.00E+06	4.47E+05	5.06E+05
408	1.20E+06	4.00E+05	1.04E+06	8.80E+05	4.23E+05	4.79E+05

Table F.7. BC13 cell concentrations (cells mL^{-1}) during heterotrophic growth on 50 μM malate and ambient carbon dioxide.

Elapsed Time (h)	Trial 1	Trial 2	Trial 3	Average	STDEV	95% CI
0	4.90E+07	4.66E+07	5.10E+07	4.89E+07	2.20E+06	2.49E+06
24	3.96E+07	4.10E+07	4.24E+07	4.10E+07	1.40E+06	1.58E+06
48	3.70E+07	3.50E+07	3.30E+07	3.50E+07	2.00E+06	2.26E+06
72	2.42E+07	2.70E+07	2.68E+07	2.60E+07	1.56E+06	1.77E+06
96	1.84E+07	1.98E+07	2.24E+07	2.02E+07	2.03E+06	2.30E+06
120	1.28E+07	1.54E+07	1.78E+07	1.53E+07	2.50E+06	2.83E+06
144	1.02E+07	1.08E+07	1.30E+07	1.13E+07	1.47E+06	1.67E+06
168	8.60E+06	8.00E+06	1.02E+07	8.93E+06	1.14E+06	1.29E+06
192	6.40E+06	7.60E+06	9.80E+06	7.93E+06	1.72E+06	1.95E+06
216	5.60E+06	4.60E+06	6.80E+06	5.67E+06	1.10E+06	1.25E+06
240	3.40E+06	2.80E+06	4.20E+06	3.47E+06	7.02E+05	7.95E+05
264	2.60E+06	1.80E+06	3.00E+06	2.47E+06	6.11E+05	6.91E+05
288	2.20E+06	1.48E+06	2.20E+06	1.96E+06	4.16E+05	4.70E+05
312	2.04E+06	9.20E+05	1.60E+06	1.52E+06	5.64E+05	6.39E+05
336	1.30E+06	6.20E+05	1.08E+06	1.00E+06	3.47E+05	3.93E+05
360	1.00E+06	4.40E+05	6.00E+05	6.80E+05	2.88E+05	3.26E+05
384	8.20E+05	4.20E+05	3.40E+05	5.27E+05	2.57E+05	2.91E+05
408	6.60E+05	4.00E+05	2.66E+05	4.42E+05	2.00E+05	2.27E+05

Table F.8. Steady state concentrations of organic acids (μM) during heterotrophic growth of BC13 in the presence of ambient carbon dioxide.

	Influent		Effluent				
	Trial 1	Trial 1	Trial 2	Trial 3	AVERAGE	STDEV	95% CI
Pyruvate	50.1	48.6	50.7	43.0	47.4	4.0	4.5
Acetate	51.5	33.1	40.3	44.0	39.1	5.5	6.3
Citrate	48.6	42.6	40.9	47.5	43.7	3.5	3.9
2-ketoglutarate	52.3	45.5	43.7	50.8	46.6	3.7	4.2
Succinate	49.7	44.6	48.6	41.8	45.0	3.4	3.9
Malate	50.1	51.8	45.6	44.0	47.1	4.1	4.7

Table F.9. Steady state concentrations of dissolved oxygen (μM) during heterotrophic growth of BC13 on 50 μM of various organic acids and ambient carbon dioxide.

	Influent		Effluent				
	Trial 1	Trial 1	Trial 2	Trial 3	AVERAGE	STDEV	95% CI
Pyruvate	183.1	184.7	183.4	181.9	183.3	1.4	1.6
Acetate	183.8	180.6	181.2	179.6	180.5	0.8	0.9
Citrate	184.1	183.8	184.4	182.7	183.6	0.8	1.0
2-ketoglutarate	184.1	180.9	180.3	179.8	180.4	0.6	0.6
Succinate	184.4	184.1	184.4	182.3	183.6	1.1	1.3
Malate	184.7	182.8	183.1	180.6	182.2	1.4	1.6
Tetrathionate	184.7	141.3	138.5	138.5	139.4	1.6	1.8

Table F.10. BC13 cell concentrations (cells mL^{-1}) during mixotrophic growth on 50 μM pyruvate, 10 mM potassium tetrathionate, and ambient carbon dioxide.

Elapsed Time (h)	Trial 1	Trial 2	Trial 3	Average	STDEV	95% CI
0	5.06E+07	5.50E+07	4.90E+07	5.15E+07	3.11E+06	3.52E+06
24	4.66E+07	4.62E+07	4.60E+07	4.63E+07	3.06E+05	3.46E+05
48	4.28E+07	4.26E+07	4.10E+07	4.21E+07	9.87E+05	1.12E+06
72	3.80E+07	3.90E+07	3.70E+07	3.80E+07	1.00E+06	1.13E+06
96	3.40E+07	3.52E+07	3.80E+07	3.57E+07	2.05E+06	2.32E+06
120	3.10E+07	3.18E+07	3.24E+07	3.17E+07	7.02E+05	7.95E+05
144	2.90E+07	3.00E+07	2.86E+07	2.92E+07	7.21E+05	8.16E+05
168	2.64E+07	2.80E+07	2.46E+07	2.63E+07	1.70E+06	1.92E+06
192	2.58E+07	2.70E+07	2.46E+07	2.58E+07	1.20E+06	1.36E+06
216	2.10E+07	2.18E+07	2.48E+07	2.25E+07	2.00E+06	2.27E+06
240	2.26E+07	2.30E+07	2.14E+07	2.23E+07	8.33E+05	9.42E+05
264	2.00E+07	2.10E+07	2.20E+07	2.10E+07	1.00E+06	1.13E+06
288	2.04E+07	2.20E+07	2.20E+07	2.15E+07	9.24E+05	1.05E+06
312	2.02E+07	2.10E+07	2.30E+07	2.14E+07	1.44E+06	1.63E+06
336	2.00E+07	2.22E+07	2.04E+07	2.09E+07	1.17E+06	1.33E+06
360	1.96E+07	2.26E+07	2.12E+07	2.11E+07	1.50E+06	1.70E+06
384	2.10E+07	2.20E+07	2.20E+07	2.17E+07	5.77E+05	6.53E+05
408	2.12E+07	2.08E+07	2.02E+07	2.07E+07	5.03E+05	5.70E+05

Table F.11. BC13 cell concentrations (cells mL^{-1}) during mixotrophic growth on 50 μM acetate, 10 mM potassium tetrathionate, and ambient carbon dioxide.

Elapsed Time (h)	Trial 1	Trial 2	Trial 3	Average	STDEV	95% CI
0	5.40E+07	5.36E+07	5.30E+07	5.35E+07	5.03E+05	5.70E+05
24	4.80E+07	4.70E+07	4.60E+07	4.70E+07	1.00E+06	1.13E+06
48	3.92E+07	3.62E+07	3.86E+07	3.80E+07	1.59E+06	1.80E+06
72	3.50E+07	3.72E+07	3.30E+07	3.51E+07	2.10E+06	2.38E+06
96	2.90E+07	3.02E+07	3.18E+07	3.03E+07	1.40E+06	1.59E+06
120	2.84E+07	2.60E+07	2.60E+07	2.68E+07	1.39E+06	1.57E+06
144	2.38E+07	2.30E+07	2.16E+07	2.28E+07	1.11E+06	1.26E+06
168	1.88E+07	1.96E+07	2.22E+07	2.02E+07	1.78E+06	2.01E+06
192	1.58E+07	1.60E+07	1.64E+07	1.61E+07	3.06E+05	3.46E+05
216	1.48E+07	1.42E+07	1.46E+07	1.45E+07	3.06E+05	3.46E+05
240	1.30E+07	1.26E+07	1.50E+07	1.35E+07	1.29E+06	1.46E+06
264	1.18E+07	1.14E+07	1.22E+07	1.18E+07	4.00E+05	4.53E+05
288	1.04E+07	1.16E+07	1.10E+07	1.10E+07	6.00E+05	6.79E+05
312	9.00E+06	1.08E+07	9.60E+06	9.80E+06	9.17E+05	1.04E+06
336	8.20E+06	8.20E+06	8.80E+06	8.40E+06	3.46E+05	3.92E+05
360	7.80E+06	8.20E+06	8.90E+06	8.30E+06	5.57E+05	6.30E+05
384	7.60E+06	7.40E+06	8.60E+06	7.87E+06	6.43E+05	7.28E+05
408	6.30E+06	8.00E+06	8.70E+06	7.67E+06	1.23E+06	1.40E+06

Table F.12. BC13 cell concentrations (cells mL^{-1}) during mixotrophic growth on 50 μM citrate, 10 mM potassium tetrathionate, and ambient carbon dioxide.

Elapsed Time (h)	Trial 1	Trial 2	Trial 3	Average	STDEV	95% CI
0	5.62E+07	5.56E+07	5.50E+07	5.56E+07	6.00E+05	6.79E+05
24	4.76E+07	4.88E+07	4.78E+07	4.81E+07	6.43E+05	7.28E+05
48	3.70E+07	3.80E+07	3.90E+07	3.80E+07	1.00E+06	1.13E+06
72	3.24E+07	2.92E+07	3.30E+07	3.15E+07	2.04E+06	2.31E+06
96	2.70E+07	2.82E+07	2.98E+07	2.83E+07	1.40E+06	1.59E+06
120	2.10E+07	2.60E+07	2.00E+07	2.23E+07	3.21E+06	3.64E+06
144	1.88E+07	1.80E+07	2.06E+07	1.91E+07	1.33E+06	1.51E+06
168	1.88E+07	1.66E+07	1.60E+07	1.71E+07	1.47E+06	1.67E+06
192	1.28E+07	1.10E+07	1.64E+07	1.34E+07	2.75E+06	3.11E+06
216	1.28E+07	1.32E+07	1.20E+07	1.27E+07	6.11E+05	6.91E+05
240	1.08E+07	1.22E+07	1.20E+07	1.17E+07	7.57E+05	8.57E+05
264	9.00E+06	1.04E+07	9.40E+06	9.60E+06	7.21E+05	8.16E+05
288	7.20E+06	8.20E+06	1.00E+07	8.47E+06	1.42E+06	1.61E+06
312	5.60E+06	6.80E+06	7.60E+06	6.67E+06	1.01E+06	1.14E+06
336	4.20E+06	6.20E+06	6.80E+06	5.73E+06	1.36E+06	1.54E+06
360	5.00E+06	6.60E+06	5.20E+06	5.60E+06	8.72E+05	9.86E+05
384	5.40E+06	6.00E+06	5.00E+06	5.47E+06	5.03E+05	5.70E+05
408	5.60E+06	5.80E+06	5.80E+06	5.73E+06	1.15E+05	1.31E+05

Table F.13. BC13 cell concentrations (cells mL^{-1}) during mixotrophic growth on 50 μM 2-ketoglutarate, 10 mM potassium tetrathionate, and ambient carbon dioxide.

Elapsed Time (h)	Trial 1	Trial 2	Trial 3	Average	STDEV	95% CI
0	5.42E+07	5.36E+07	5.00E+07	5.26E+07	2.27E+06	2.57E+06
24	4.56E+07	4.48E+07	4.28E+07	4.44E+07	1.44E+06	1.63E+06
48	4.30E+07	4.00E+07	4.04E+07	4.11E+07	1.63E+06	1.84E+06
72	3.04E+07	3.52E+07	3.20E+07	3.25E+07	2.44E+06	2.77E+06
96	2.50E+07	3.02E+07	2.68E+07	2.73E+07	2.64E+06	2.99E+06
120	2.30E+07	2.80E+07	2.50E+07	2.53E+07	2.52E+06	2.85E+06
144	2.38E+07	2.48E+07	1.96E+07	2.27E+07	2.76E+06	3.12E+06
168	1.68E+07	2.16E+07	1.92E+07	1.92E+07	2.40E+06	2.72E+06
192	1.28E+07	1.80E+07	1.54E+07	1.54E+07	2.60E+06	2.94E+06
216	1.08E+07	1.62E+07	1.36E+07	1.35E+07	2.70E+06	3.06E+06
240	9.00E+06	1.46E+07	1.20E+07	1.19E+07	2.80E+06	3.17E+06
264	7.80E+06	1.34E+07	9.00E+06	1.01E+07	2.95E+06	3.34E+06
288	7.00E+06	1.16E+07	9.40E+06	9.33E+06	2.30E+06	2.60E+06
312	6.00E+06	1.08E+07	8.60E+06	8.47E+06	2.40E+06	2.72E+06
336	5.20E+06	9.20E+06	7.80E+06	7.40E+06	2.03E+06	2.30E+06
360	4.80E+06	8.40E+06	7.60E+06	6.93E+06	1.89E+06	2.14E+06
384	4.60E+06	7.40E+06	7.40E+06	6.47E+06	1.62E+06	1.83E+06
408	4.40E+06	7.00E+06	7.60E+06	6.33E+06	1.70E+06	1.92E+06

Table F.14. BC13 cell concentrations (cells mL^{-1}) during mixotrophic growth on 50 μM succinate, 10 mM potassium tetrathionate, and ambient carbon dioxide.

Elapsed Time (h)	Trial 1	Trial 2	Trial 3	Average	STDEV	95% CI
0	5.32E+07	5.36E+07	5.34E+07	5.34E+07	2.00E+05	2.26E+05
24	4.56E+07	4.48E+07	4.58E+07	4.54E+07	5.29E+05	5.99E+05
48	4.24E+07	4.32E+07	4.28E+07	4.28E+07	4.00E+05	4.53E+05
72	3.10E+07	3.18E+07	3.16E+07	3.15E+07	4.16E+05	4.71E+05
96	3.00E+07	3.12E+07	3.08E+07	3.07E+07	6.11E+05	6.91E+05
120	2.20E+07	2.30E+07	2.24E+07	2.25E+07	5.03E+05	5.70E+05
144	1.98E+07	2.10E+07	1.90E+07	1.99E+07	1.01E+06	1.14E+06
168	1.68E+07	1.80E+07	1.80E+07	1.76E+07	6.93E+05	7.84E+05
192	1.42E+07	1.54E+07	1.52E+07	1.49E+07	6.43E+05	7.28E+05
216	1.06E+07	1.16E+07	1.22E+07	1.15E+07	8.08E+05	9.15E+05
240	1.00E+07	1.14E+07	1.20E+07	1.11E+07	1.03E+06	1.16E+06
264	9.60E+06	1.10E+07	9.60E+06	1.01E+07	8.08E+05	9.15E+05
288	7.00E+06	8.60E+06	9.40E+06	8.33E+06	1.22E+06	1.38E+06
312	6.40E+06	8.20E+06	9.00E+06	7.87E+06	1.33E+06	1.51E+06
336	5.80E+06	7.80E+06	8.40E+06	7.33E+06	1.36E+06	1.54E+06
360	5.60E+06	8.00E+06	8.60E+06	7.40E+06	1.59E+06	1.80E+06
384	5.20E+06	8.00E+06	8.40E+06	7.20E+06	1.74E+06	1.97E+06
408	4.80E+06	7.80E+06	8.20E+06	6.93E+06	1.86E+06	2.10E+06

Table F.15. BC13 cell concentrations (cells mL^{-1}) during mixotrophic growth on 50 μM malate, 10 mM potassium tetrathionate, and ambient carbon dioxide.

Elapsed Time (h)	Trial 1	Trial 2	Trial 3	Average	STDEV	95% CI
0	5.40E+07	5.36E+07	5.50E+07	5.42E+07	7.21E+05	8.16E+05
24	4.66E+07	4.46E+07	4.68E+07	4.60E+07	1.23E+06	1.39E+06
48	3.60E+07	3.70E+07	3.66E+07	3.65E+07	5.03E+05	5.70E+05
72	3.02E+07	3.20E+07	3.04E+07	3.09E+07	9.87E+05	1.12E+06
96	2.66E+07	2.80E+07	2.70E+07	2.72E+07	7.21E+05	8.16E+05
120	2.20E+07	2.30E+07	2.22E+07	2.24E+07	5.29E+05	5.99E+05
144	1.98E+07	2.10E+07	1.78E+07	1.95E+07	1.62E+06	1.83E+06
168	1.78E+07	1.66E+07	1.72E+07	1.72E+07	6.00E+05	6.79E+05
192	1.28E+07	1.40E+07	1.50E+07	1.39E+07	1.10E+06	1.25E+06
216	1.04E+07	1.18E+07	1.22E+07	1.15E+07	9.45E+05	1.07E+06
240	9.60E+06	1.12E+07	1.16E+07	1.08E+07	1.06E+06	1.20E+06
264	8.00E+06	9.60E+06	8.20E+06	8.60E+06	8.72E+05	9.86E+05
288	5.00E+06	6.60E+06	7.40E+06	6.33E+06	1.22E+06	1.38E+06
312	4.80E+06	6.60E+06	7.40E+06	6.27E+06	1.33E+06	1.51E+06
336	5.20E+06	7.00E+06	6.00E+06	6.07E+06	9.02E+05	1.02E+06
360	5.00E+06	6.40E+06	5.60E+06	5.67E+06	7.02E+05	7.95E+05
384	4.80E+06	6.20E+06	5.00E+06	5.33E+06	7.57E+05	8.57E+05
408	5.40E+06	6.60E+06	4.80E+06	5.60E+06	9.17E+05	1.04E+06

Table F.16. Steady state concentrations of organic acids (μM) during mixotrophic growth of BC13 in the presence of ambient carbon dioxide.

	Influent		Effluent				
	Trial 1	Trial 1	Trial 2	Trial 3	AVERAGE	STDEV	95% CI
Pyruvate	48.3	0.0	0.0	0.0	0.0	0.0	0.0
Acetate	48.7	40.7	38.8	46.8	42.1	4.2	4.7
Citrate	49.8	40.1	40.9	47.5	42.8	4.1	4.6
2-ketoglutarate	50.7	41.7	43.7	50.8	45.4	4.7	5.4
Succinate	51.4	40.6	48.6	41.8	43.7	4.3	4.9
Malate	50.4	45.6	45.6	44.0	45.1	0.9	1.0

Table F.17. Steady state concentrations of dissolved oxygen (μM) during mixotrophic growth of BC13 on 50 μM of various organic acids and ambient carbon dioxide.

	Influent		Effluent				
	Trial 1	Trial 1	Trial 2	Trial 3	AVERAGE	STDEV	95% CI
Pyruvate	194.4	98.4	95.1	92.8	95.4	2.8	3.2
Acetate	193.8	154.4	140.7	141.0	145.4	7.8	8.9
Citrate	194.7	145.9	142.3	142.6	143.6	2.0	2.3
2-ketoglutarate	194.4	139.1	133.5	136.9	136.5	2.8	3.2
Succinate	194.4	150.6	147.3	144.8	147.6	2.9	3.3
Malate	194.7	149.4	136.8	147.3	144.5	6.8	7.6

Cell Growth using Pyruvate as the Sole Carbon Source under Batch Conditions

BC13 cell and pyruvate concentrations during batch growth when pyruvate supplied the sole carbon source. Experiments were repeated in triplicate and average values, standard deviations (STDEV), and 95% confidence intervals (95% CI) are shown.

Table F.18. BC13 cell concentrations (cells mL^{-1}) growin on 10 mM potassium tetrathionate in a pyruvate and inorganic carbon-free control.

Elapsed Time (h)	Trial 1	Trial 2	Trial 3	Average	STDEV	95% CI
0	2.31E+06	2.03E+06	2.06E+06	2.13E+06	1.51E+05	1.71E+05
12	2.11E+06	2.29E+06	1.97E+06	2.12E+06	1.60E+05	1.81E+05
24	2.26E+06	2.25E+06	2.50E+06	2.34E+06	1.41E+05	1.59E+05
36	2.36E+06	2.19E+06	1.97E+06	2.17E+06	1.93E+05	2.18E+05
48	2.46E+06	2.27E+06	2.22E+06	2.32E+06	1.24E+05	1.40E+05
60	2.46E+06	2.73E+06	2.78E+06	2.65E+06	1.73E+05	1.96E+05
72	2.56E+06	2.90E+06	3.13E+06	2.86E+06	2.89E+05	3.28E+05
84	2.76E+06	2.66E+06	2.56E+06	2.66E+06	9.59E+04	1.09E+05
96	2.86E+06	2.73E+06	2.28E+06	2.62E+06	3.03E+05	3.43E+05

Table F.19. BC13 cell concentrations (cells mL^{-1}) grown on 20 μM pyruvate in a potassium tetrathionate free control in a medium free of inorganic carbon.

Elapsed Time (h)	Trial 1	Trial 2	Trial 3	Average	STDEV	95% CI
0	2.31E+06	2.73E+06	2.93E+06	2.65E+06	3.16E+05	3.58E+05
12	2.01E+06	2.47E+06	2.04E+06	2.17E+06	2.61E+05	2.96E+05
24	2.66E+06	2.77E+06	2.96E+06	2.80E+06	1.52E+05	1.72E+05
36	2.14E+06	2.27E+06	1.76E+06	2.05E+06	2.66E+05	3.01E+05
48	2.06E+06	2.11E+06	1.94E+06	2.04E+06	8.63E+04	9.77E+04
60	2.05E+06	1.85E+06	1.51E+06	1.80E+06	2.73E+05	3.09E+05
72	2.01E+06	2.44E+06	2.10E+06	2.18E+06	2.26E+05	2.56E+05
84	2.21E+06	2.49E+06	2.51E+06	2.40E+06	1.70E+05	1.92E+05
96	2.31E+06	1.90E+06	2.26E+06	2.16E+06	2.24E+05	2.53E+05

Table F.20. Pyruvate concentrations (cells mL^{-1}) in a potassium tetrathionate and inorganic carbon free control.

	Trail 1	Trial 2	Trial 3	Average	STDEV	95% CI
Initial concentration	16.55	20.28	24.87	20.57	4.17	4.72
Final pconcentration	20.72	18.37	14.07	17.72	3.37	3.82
Consumed	-4.18	1.91	10.80	2.84	7.53	8.52
Required for cell growth	na	na	na	na	na	na
Carbon efficiency	na	na	na	na	na	na

Table F.21. BC13 cell concentrations (cells mL^{-1}) in a control containing 10 mM potassium tetrathionate, 20 μM pyruvate, and a head space pressurized to 1 atmosphere carbon dioxide.

Elapsed Time (h)	Trial 1	Trial 2	Trial 3	Average	STDEV	95% CI
0	2.18E+07	2.26E+07	1.71E+07	2.05E+07	2.95E+06	3.34E+06
12	2.25E+07	2.38E+07	1.64E+07	2.09E+07	3.96E+06	4.48E+06
24	3.10E+07	3.92E+07	4.00E+07	3.67E+07	5.02E+06	5.68E+06
36	3.87E+07	2.52E+07	2.93E+07	3.11E+07	6.91E+06	7.82E+06
48	6.57E+07	6.24E+07	6.64E+07	6.48E+07	2.14E+06	2.43E+06
60	1.22E+08	1.29E+08	1.37E+08	1.29E+08	7.11E+06	8.05E+06
72	1.82E+08	1.84E+08	1.64E+08	1.77E+08	1.09E+07	1.23E+07
84	2.52E+08	2.32E+08	2.04E+08	2.30E+08	2.43E+07	2.75E+07
96	2.82E+08	2.69E+08	2.51E+08	2.68E+08	1.56E+07	1.77E+07
108	3.12E+08	2.49E+08	2.81E+08	2.81E+08	3.16E+07	3.57E+07
120	3.05E+08	2.39E+08	3.01E+08	2.82E+08	3.70E+07	4.19E+07

Table F.22. Pyruvate concentrations (μM) in medium containing 10 mM potassium tetrathionate, 20 μM pyruvate, and a head space pressurized to 1 atmosphere carbon dioxide.

	Trail 1	Trial 2	Trial 3	Average	STDEV	95% CI
Initial concentration	22.75	20.04	18.04	20.28	2.36	2.68
Final pconcentration	7.24	5.68	5.68	6.20	0.91	1.02
Consumed	15.51	14.36	12.37	14.08	1.59	1.80
Required for cell growth	na	na	na	na	na	na
Carbon efficiency	na	na	na	na	na	na

Table F.23. BC13 cell concentrations (cells mL^{-1}) grown on 10 mM potassium tetrathionate and 5 μM pyruvate in medium free of inorganic carbon.

Elapsed Time (h)	Trial 1	Trial 2	Trial 3	Average	STDEV	95% CI
0	2.24E+06	2.16E+06	2.23E+06	2.21E+06	4.69E+04	5.30E+04
12	2.39E+06	2.33E+06	2.36E+06	2.36E+06	3.15E+04	3.57E+04
24	2.79E+06	3.22E+06	2.77E+06	2.93E+06	2.51E+05	2.84E+05
36	3.81E+06	3.99E+06	4.01E+06	3.94E+06	1.12E+05	1.27E+05
48	4.01E+06	3.83E+06	3.85E+06	3.90E+06	9.79E+04	1.11E+05
60	4.14E+06	4.08E+06	4.01E+06	4.08E+06	6.36E+04	7.20E+04
72	4.24E+06	4.19E+06	4.18E+06	4.20E+06	3.25E+04	3.68E+04
84	4.14E+06	4.16E+06	4.28E+06	4.19E+06	7.66E+04	8.67E+04
96	3.84E+06	3.82E+06	4.01E+06	3.89E+06	1.02E+05	1.16E+05

Table F.24. Pyruvate concentrations (μM) in medium containing 10 mM potassium tetrathionate, 5 μM pyruvate, and no inorganic carbon.

	Trail 1	Trial 2	Trial 3	Average	STDEV	95% CI
Initial concentration	4.60	6.00	5.65	5.42	0.73	0.82
Final pconcentration	0.00	0.00	0.00	0.00	0.00	0.00
Consumed	4.60	6.00	5.65	5.42	0.73	0.82
Required for cell growth	3.30	3.43	3.66	3.46	0.18	0.20
Carbon efficiency	72%	57%	65%	65%	7%	8%

Table F.25. BC13 cell concentrations (cells mL^{-1}) grown on 10 mM potassium tetrathionate and 10 μM pyruvate in medium free of inorganic carbon.

Elapsed Time (h)	Trial 1	Trial 2	Trial 3	Average	STDEV	95% CI
0	2.07E+06	2.18E+06	2.23E+06	2.16E+06	8.05E+04	9.11E+04
12	2.40E+06	2.46E+06	2.56E+06	2.47E+06	7.99E+04	9.05E+04
24	3.23E+06	3.13E+06	3.28E+06	3.21E+06	7.63E+04	8.64E+04
36	3.57E+06	3.57E+06	3.40E+06	3.51E+06	9.93E+04	1.12E+05
48	4.28E+06	4.28E+06	4.45E+06	4.33E+06	9.99E+04	1.13E+05
60	4.83E+06	5.29E+06	4.76E+06	4.96E+06	2.88E+05	3.26E+05
72	5.59E+06	5.75E+06	5.72E+06	5.68E+06	8.52E+04	9.64E+04
84	5.79E+06	6.01E+06	6.29E+06	6.03E+06	2.53E+05	2.86E+05
96	5.89E+06	5.64E+06	5.55E+06	5.69E+06	1.74E+05	1.97E+05

Table F.26. Pyruvate concentrations (μM) in medium containing 10 mM potassium tetrathionate, 10 μM pyruvate, and no inorganic carbon.

	Trail 1	Trial 2	Trial 3	Average	STDEV	95% CI
Initial concentration	9.78	9.35	9.22	9.45	0.29	0.33
Final pconcentration	0.00	0.00	0.00	0.00	0.00	0.00
Consumed	9.78	9.35	9.22	9.45	0.29	0.33
Required for cell growth	7.86	7.15	6.84	7.29	0.52	0.59
Carbon efficiency	80%	76%	74%	77%	3%	4%

Table F.27. BC13 cell concentrations (cells mL^{-1}) grown on 10 mM potassium tetrathionate and 15 μM pyruvate in medium free of inorganic carbon.

Elapsed Time (h)	Trial 1	Trial 2	Trial 3	Average	STDEV	95% CI
0	2.25E+06	2.28E+06	2.28E+06	2.27E+06	1.74E+04	1.97E+04
12	2.51E+06	2.60E+06	3.07E+06	2.73E+06	2.98E+05	3.37E+05
24	2.65E+06	3.68E+06	3.30E+06	3.21E+06	5.22E+05	5.90E+05
36	3.73E+06	4.58E+06	4.11E+06	4.14E+06	4.25E+05	4.81E+05
48	5.15E+06	5.78E+06	6.10E+06	5.68E+06	4.86E+05	5.50E+05
60	6.35E+06	6.60E+06	6.99E+06	6.65E+06	3.26E+05	3.69E+05
72	6.81E+06	6.41E+06	6.02E+06	6.41E+06	3.92E+05	4.43E+05
84	6.71E+06	7.27E+06	7.27E+06	7.08E+06	3.25E+05	3.68E+05
96	6.31E+06	7.07E+06	6.87E+06	6.75E+06	3.96E+05	4.48E+05

Table F.28. Pyruvate concentrations (μM) in medium containing 10 mM potassium tetrathionate, 15 μM pyruvate, and no inorganic carbon.

	Trail 1	Trial 2	Trial 3	Average	STDEV	95% CI
Initial concentration	15.61	16.41	15.86	15.96	0.41	0.46
Final pconcentration	4.03	5.38	3.18	4.20	1.11	1.26
Consumed	11.58	11.03	12.68	11.77	0.84	0.95
Required for cell growth	8.37	9.89	9.46	9.24	0.78	0.89
Carbon efficiency	72%	90%	75%	79%	9%	11%

Table F.29. BC13 cell concentrations (cells mL^{-1}) grown on 10 mM potassium tetrathionate and 20 μM pyruvate in medium free of inorganic carbon.

Elapsed Time (h)	Trial 1	Trial 2	Trial 3	Average	STDEV	95% CI
0	2.46E+06	2.50E+06	2.44E+06	2.46E+06	3.00E+04	3.40E+04
12	2.67E+06	2.70E+06	2.67E+06	2.68E+06	1.85E+04	2.10E+04
24	3.28E+06	3.35E+06	3.29E+06	3.31E+06	4.06E+04	4.59E+04
36	5.26E+06	5.16E+06	5.21E+06	5.21E+06	4.80E+04	5.43E+04
48	7.18E+06	7.13E+06	7.40E+06	7.24E+06	1.44E+05	1.63E+05
60	8.61E+06	8.28E+06	8.44E+06	8.44E+06	1.66E+05	1.87E+05
72	9.08E+06	8.68E+06	8.77E+06	8.84E+06	2.07E+05	2.35E+05
84	9.18E+06	8.79E+06	8.38E+06	8.78E+06	4.00E+05	4.53E+05
96	8.98E+06	8.79E+06	8.42E+06	8.73E+06	2.84E+05	3.21E+05

Table F.30. Pyruvate concentrations (μM) in medium containing 10 mM potassium tetrathionate, 20 μM pyruvate, and no inorganic carbon.

	Trail 1	Trial 2	Trial 3	Average	STDEV	95% CI
Initial concentration	20.16	23.54	22.28	22.00	1.71	1.94
Final pconcentration	6.33	5.53	5.95	5.94	0.40	0.45
Consumed	13.83	18.02	16.34	16.06	2.11	2.38
Required for cell growth	13.44	12.99	12.33	12.92	0.56	0.63
Carbon efficiency	97%	72%	76%	82%	14%	15%

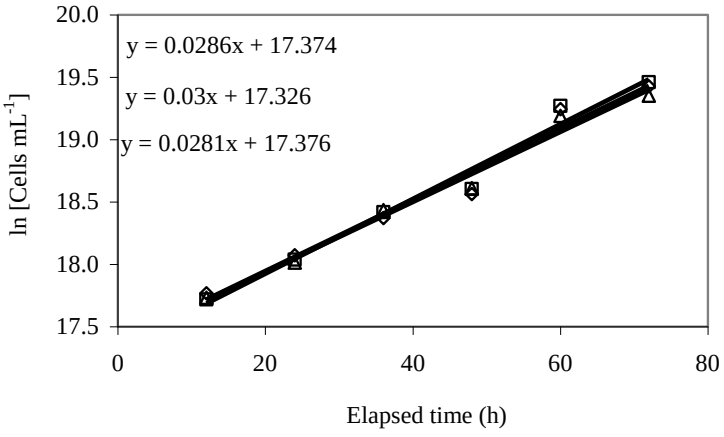
Toxicity of Organic Acids at Lower Concentrations (≤50 μM)

BC13 cell concentrations with time when grown in the presence of varying concentrations of different organic acids. Experiments were repeated in triplicate and average values, standard deviations (STDEV), and 95% confidence intervals (95% CI) are shown. Specific growth rates were calculated using linear regressions and are shown along with the corresponding STDEV and 95% CI to the right of the plots.

Pyruvate

Table F.31. BC13 growth in the presence of 5 μM pyruvate.

	Cells mL^{-1}						ln (Cells mL^{-1})		
Elapsed Time (h)	Trial 1	Trial 2	Trial 3	Average	STDEV	95% CI	Trial 1	Trial 2	Trial 3
0	5.00E+07	5.13E+07	4.98E+07	5.04E+07	8.03E+05	9.09E+05	17.73	17.75	17.72
12	5.21E+07	4.96E+07	5.03E+07	5.07E+07	1.30E+06	1.47E+06	17.77	17.72	17.73
24	7.06E+07	6.82E+07	6.67E+07	6.85E+07	1.97E+06	2.23E+06	18.07	18.04	18.02
36	9.52E+07	9.96E+07	1.01E+08	9.87E+07	3.20E+06	3.63E+06	18.37	18.42	18.43
48	1.15E+08	1.20E+08	1.21E+08	1.19E+08	2.94E+06	3.32E+06	18.56	18.60	18.61
60	2.28E+08	2.34E+08	2.16E+08	2.26E+08	9.04E+06	1.02E+07	19.24	19.27	19.19
72	2.74E+08	2.83E+08	2.54E+08	2.70E+08	1.48E+07	1.67E+07	19.43	19.46	19.35
84	3.04E+08	2.95E+08	2.98E+08	2.99E+08	4.70E+06	5.32E+06	19.53	19.50	19.51
96	3.31E+08	2.85E+08	3.14E+08	3.10E+08	2.30E+07	2.60E+07	19.62	19.47	19.57
108	3.02E+08	2.65E+08	3.24E+08	2.97E+08	2.98E+07	3.37E+07	19.52	19.40	19.60
120	3.00E+08	2.90E+08	3.18E+08	3.03E+08	1.41E+07	1.59E+07	19.52	19.49	19.58



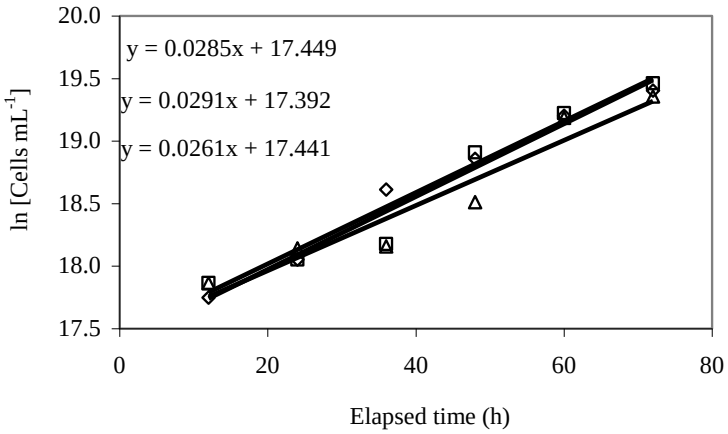
Specific growth rate (h^{-1})

Trial 1	0.029
Trial 2	0.030
Trial 3	0.028
Average	0.029
STDEV	0.001
95% CI	0.001

Figure F.1. Specific growth rate calculations for Trial 1 (open circles), Trial 2 (open squares), and Trial 3 (open triangles).

Table F.32. BC13 growth in the presence of 10 μM pyruvate.

	Cells mL^{-1}						ln (Cells mL^{-1})		
Elapsed Time (h)	Trial 1	Trial 2	Trial 3	Average	STDEV	95% CI	Trial 1	Trial 2	Trial 3
0	5.13E+07	5.42E+07	5.42E+07	5.32E+07	1.64E+06	1.86E+06	17.75	17.81	17.81
12	5.10E+07	5.74E+07	5.73E+07	5.52E+07	3.66E+06	4.14E+06	17.75	17.87	17.86
24	6.92E+07	6.92E+07	7.57E+07	7.14E+07	3.73E+06	4.22E+06	18.05	18.05	18.14
36	1.21E+08	7.83E+07	7.69E+07	9.21E+07	2.51E+07	2.84E+07	18.61	18.18	18.16
48	1.55E+08	1.63E+08	1.10E+08	1.42E+08	2.88E+07	3.25E+07	18.86	18.91	18.51
60	2.18E+08	2.23E+08	2.15E+08	2.19E+08	4.17E+06	4.72E+06	19.20	19.22	19.19
72	2.67E+08	2.83E+08	2.55E+08	2.68E+08	1.40E+07	1.58E+07	19.40	19.46	19.36
84	2.93E+08	2.96E+08	3.02E+08	2.97E+08	4.79E+06	5.42E+06	19.50	19.51	19.53
96	3.20E+08	3.23E+08	3.59E+08	3.34E+08	2.15E+07	2.43E+07	19.58	19.59	19.70
108	3.27E+08	3.31E+08	3.58E+08	3.39E+08	1.71E+07	1.93E+07	19.61	19.62	19.70
120	3.11E+08	3.03E+08	3.21E+08	3.11E+08	9.08E+06	1.03E+07	19.55	19.53	19.59

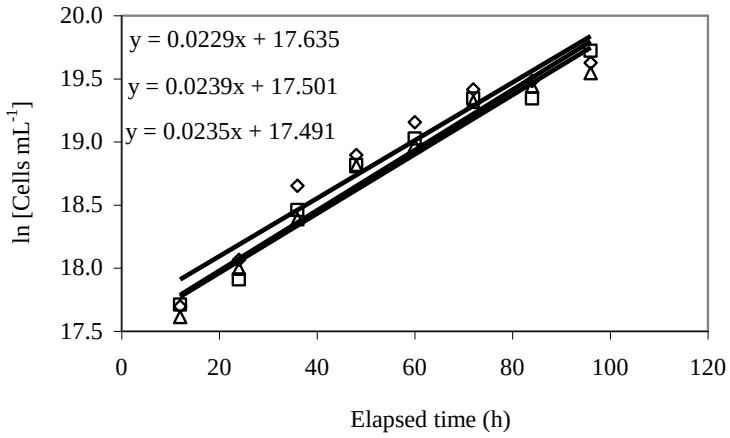


Specific growth rate (h^{-1})	
Trial 1	0.029
Trial 2	0.029
Trial 3	0.026
Average	0.028
STDEV	0.002
95% CI	0.002

Figure F.2. Specific growth rate calculations for Trial 1 (open circles), Trial 2 (open squares), and Trial 3 (open triangles).

Table F.33. BC13 growth in the presence of 20 μM pyruvate.

	Cells mL^{-1}						ln (Cells mL^{-1})		
Elapsed Time (h)	Trial 1	Trial 2	Trial 3	Average	STDEV	95% CI	Trial 1	Trial 2	Trial 3
0	5.00E+07	5.82E+07	5.73E+07	5.52E+07	4.48E+06	5.06E+06	17.73	17.88	17.86
12	4.85E+07	4.92E+07	4.46E+07	4.75E+07	2.48E+06	2.81E+06	17.70	17.71	17.61
24	7.01E+07	6.00E+07	6.55E+07	6.52E+07	5.07E+06	5.74E+06	18.07	17.91	18.00
36	1.26E+08	1.04E+08	9.69E+07	1.09E+08	1.52E+07	1.72E+07	18.65	18.46	18.39
48	1.61E+08	1.49E+08	1.47E+08	1.52E+08	7.38E+06	8.35E+06	18.90	18.82	18.81
60	2.08E+08	1.83E+08	1.73E+08	1.88E+08	1.81E+07	2.04E+07	19.15	19.03	18.97
72	2.70E+08	2.52E+08	2.45E+08	2.56E+08	1.30E+07	1.47E+07	19.41	19.34	19.32
84	2.89E+08	2.51E+08	2.77E+08	2.72E+08	1.93E+07	2.19E+07	19.48	19.34	19.44
96	3.34E+08	3.67E+08	3.08E+08	3.36E+08	2.94E+07	3.33E+07	19.63	19.72	19.55
108	3.30E+08	3.17E+08	3.16E+08	3.21E+08	7.50E+06	8.49E+06	19.61	19.57	19.57
120	3.12E+08	3.22E+08	3.21E+08	3.19E+08	5.29E+06	5.99E+06	19.56	19.59	19.59

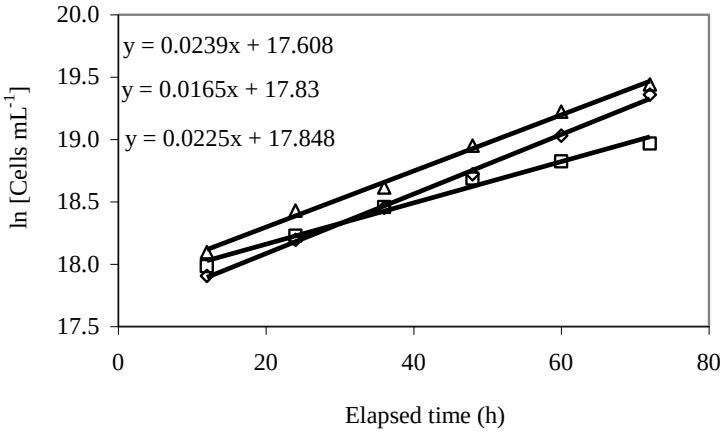


Specific growth rate (h^{-1})	
Trial 1	0.023
Trial 2	0.024
Trial 3	0.025
Average	0.024
STDEV	0.001
95% CI	0.001

Figure F.3. Specific growth rate calculations for Trial 1 (open circles), Trial 2 (open squares), and Trial 3 (open triangles).

Table F.34. BC13 growth in the presence of 30 μM pyruvate.

	Cells mL^{-1}						ln (Cells mL^{-1})		
Elapsed Time (h)	Trial 1	Trial 2	Trial 3	Average	STDEV	95% CI	Trial 1	Trial 2	Trial 3
0	5.50E+07	5.90E+07	5.71E+07	5.71E+07	2.00E+06	2.26E+06	17.82	17.89	17.86
12	5.98E+07	6.45E+07	7.23E+07	6.55E+07	6.29E+06	7.12E+06	17.91	17.98	18.10
24	7.98E+07	8.24E+07	1.01E+08	8.77E+07	1.15E+07	1.30E+07	18.20	18.23	18.43
36	1.03E+08	1.04E+08	1.21E+08	1.10E+08	1.03E+07	1.16E+07	18.45	18.46	18.61
48	1.35E+08	1.30E+08	1.70E+08	1.45E+08	2.17E+07	2.45E+07	18.72	18.69	18.95
60	1.84E+08	1.50E+08	2.23E+08	1.86E+08	3.67E+07	4.16E+07	19.03	18.82	19.22
72	2.55E+08	1.73E+08	2.78E+08	2.35E+08	5.53E+07	6.25E+07	19.36	18.97	19.44
84	2.80E+08	2.10E+08	2.79E+08	2.56E+08	4.05E+07	4.58E+07	19.45	19.16	19.45
96	2.95E+08	2.15E+08	2.92E+08	2.67E+08	4.52E+07	5.11E+07	19.50	19.19	19.49
108	3.01E+08	2.08E+08	2.68E+08	2.59E+08	4.74E+07	5.37E+07	19.52	19.15	19.41
120	2.80E+08	1.97E+08	3.12E+08	2.63E+08	5.99E+07	6.77E+07	19.45	19.10	19.56

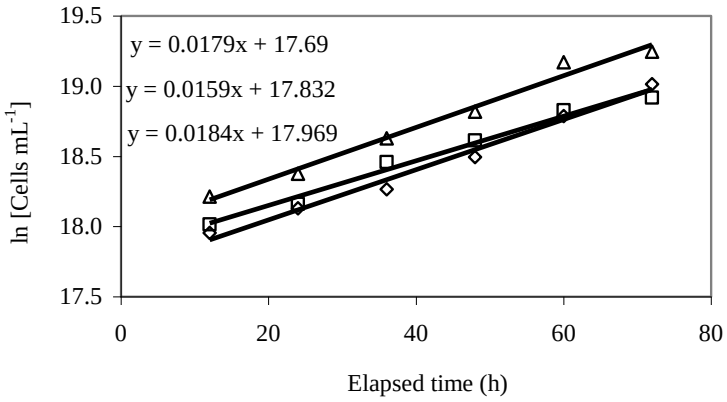


Specific growth rate (h^{-1})	
Trial 1	0.024
Trial 2	0.017
Trial 3	0.023
Average	0.021
STDEV	0.004
95% CI	0.004

Figure F.4. Specific growth rate calculations for Trial 1 (open circles), Trial 2 (open squares), and Trial 3 (open triangles).

Table F.35. BC13 growth in the presence of 50 μM pyruvate.

	Cells mL^{-1}						ln (Cells mL^{-1})		
Elapsed Time (h)	Trial 1	Trial 2	Trial 3	Average	STDEV	95% CI	Trial 1	Trial 2	Trial 3
0	5.56E+07	5.31E+07	5.50E+07	5.46E+07	1.34E+06	1.52E+06	17.83	17.79	17.82
12	6.27E+07	6.67E+07	8.13E+07	7.02E+07	9.81E+06	1.11E+07	17.95	18.02	18.21
24	7.47E+07	7.71E+07	9.57E+07	8.25E+07	1.15E+07	1.30E+07	18.13	18.16	18.38
36	8.56E+07	1.04E+08	1.23E+08	1.04E+08	1.87E+07	2.12E+07	18.27	18.46	18.63
48	1.08E+08	1.21E+08	1.49E+08	1.26E+08	2.10E+07	2.37E+07	18.49	18.61	18.82
60	1.44E+08	1.50E+08	2.12E+08	1.69E+08	3.73E+07	4.22E+07	18.79	18.83	19.17
72	1.81E+08	1.65E+08	2.28E+08	1.91E+08	3.31E+07	3.74E+07	19.01	18.92	19.25
84	2.06E+08	2.13E+08	2.50E+08	2.23E+08	2.36E+07	2.68E+07	19.15	19.18	19.34
96	2.07E+08	2.10E+08	2.84E+08	2.34E+08	4.35E+07	4.93E+07	19.15	19.16	19.46
108	2.26E+08	2.49E+08	2.67E+08	2.47E+08	2.04E+07	2.31E+07	19.24	19.33	19.40
120	2.57E+08	2.69E+08	2.77E+08	2.68E+08	1.02E+07	1.16E+07	19.36	19.41	19.44



Specific growth rate (h^{-1})

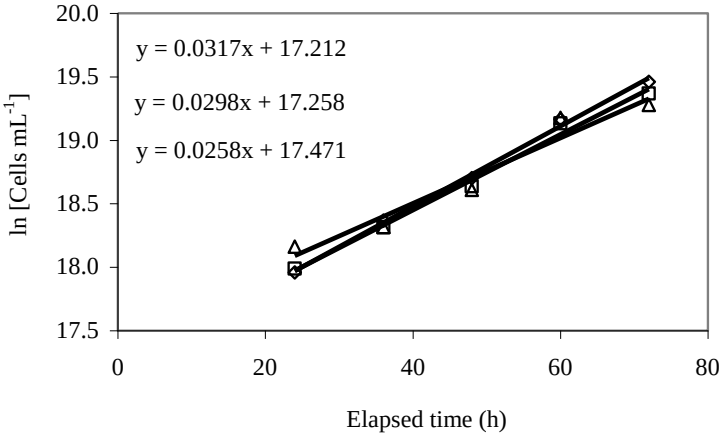
Trial 1	0.018
Trial 2	0.016
Trial 3	0.018
Average	0.017
STDEV	0.001
95% CI	0.001

Figure F.5. Specific growth rate calculations for Trial 1 (open circles), Trial 2 (open squares), and Trial 3 (open triangles).

Acetate

Table F.36. BC13 growth in the presence of 5 μM acetate.

	Cells mL^{-1}						ln (Cells mL^{-1})		
Elapsed Time (h)	Trial 1	Trial 2	Trial 3	Average	STDEV	95% CI	Trial 1	Trial 2	Trial 3
0	5.55E+07	5.10E+07	5.29E+07	5.31E+07	2.27E+06	2.57E+06	17.83	17.75	17.78
12	5.59E+07	5.28E+07	5.44E+07	5.44E+07	1.53E+06	1.73E+06	17.84	17.78	17.81
24	6.31E+07	6.50E+07	7.71E+07	6.84E+07	7.63E+06	8.64E+06	17.96	17.99	18.16
36	9.49E+07	8.99E+07	9.01E+07	9.16E+07	2.80E+06	3.16E+06	18.37	18.31	18.32
48	1.32E+08	1.24E+08	1.21E+08	1.26E+08	5.98E+06	6.77E+06	18.70	18.64	18.61
60	2.11E+08	2.04E+08	2.13E+08	2.09E+08	4.56E+06	5.16E+06	19.17	19.13	19.18
72	2.83E+08	2.58E+08	2.36E+08	2.59E+08	2.36E+07	2.67E+07	19.46	19.37	19.28
84	2.90E+08	2.77E+08	2.90E+08	2.86E+08	7.51E+06	8.50E+06	19.49	19.44	19.49
96	3.21E+08	2.98E+08	3.08E+08	3.09E+08	1.13E+07	1.28E+07	19.59	19.51	19.55
108	3.18E+08	2.97E+08	2.90E+08	3.01E+08	1.44E+07	1.63E+07	19.58	19.51	19.48
120	3.30E+08	3.09E+08	3.23E+08	3.21E+08	1.08E+07	1.22E+07	19.61	19.55	19.59



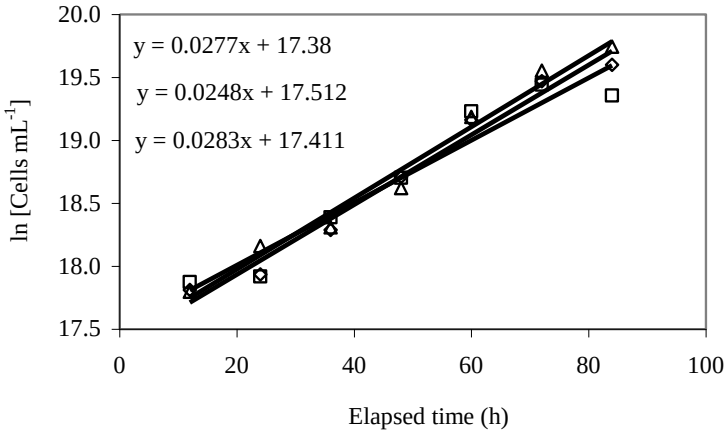
Specific growth rate (h^{-1})

Trial 1	0.032
Trial 2	0.030
Trial 3	0.026
Average	0.029
STDEV	0.003
95% CI	0.003

Figure F.6. Specific growth rate calculations for Trial 1 (open circles), Trial 2 (open squares), and Trial 3 (open triangles).

Table F.37. BC13 growth in the presence of 10 μM acetate.

	Cells mL^{-1}						ln (Cells mL^{-1})		
Elapsed Time (h)	Trial 1	Trial 2	Trial 3	Average	STDEV	95% CI	Trial 1	Trial 2	Trial 3
0	5.29E+07	4.66E+07	5.34E+07	5.10E+07	3.79E+06	4.29E+06	17.78	17.66	17.79
12	5.43E+07	5.80E+07	5.37E+07	5.53E+07	2.31E+06	2.61E+06	17.81	17.88	17.80
24	6.15E+07	6.05E+07	7.71E+07	6.64E+07	9.31E+06	1.05E+07	17.93	17.92	18.16
36	8.75E+07	9.68E+07	8.94E+07	9.12E+07	4.93E+06	5.57E+06	18.29	18.39	18.31
48	1.33E+08	1.33E+08	1.22E+08	1.29E+08	6.18E+06	6.99E+06	18.71	18.70	18.62
60	2.10E+08	2.25E+08	2.15E+08	2.17E+08	7.60E+06	8.60E+06	19.16	19.23	19.19
72	2.85E+08	2.78E+08	3.10E+08	2.91E+08	1.71E+07	1.94E+07	19.47	19.44	19.55
84	3.25E+08	2.55E+08	3.75E+08	3.19E+08	6.06E+07	6.85E+07	19.60	19.36	19.74
96	3.21E+08	2.89E+08	3.55E+08	3.22E+08	3.31E+07	3.74E+07	19.59	19.48	19.69
108	2.85E+08	3.00E+08	3.30E+08	3.05E+08	2.31E+07	2.62E+07	19.47	19.52	19.62
120	3.41E+08	3.45E+08	3.27E+08	3.38E+08	9.02E+06	1.02E+07	19.65	19.66	19.61



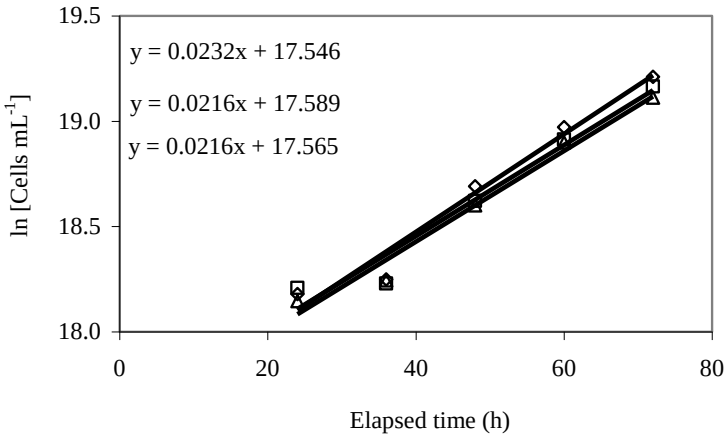
Specific growth rate (h^{-1})

Trial 1	0.028
Trial 2	0.025
Trial 3	0.028
Average	0.027
STDEV	0.002
95% CI	0.002

Figure F.7. Specific growth rate calculations for Trial 1 (open circles), Trial 2 (open squares), and Trial 3 (open triangles).

Table F.38. BC13 growth in the presence of 20 μM acetate.

	Cells mL^{-1}						ln (Cells mL^{-1})		
Elapsed Time (h)	Trial 1	Trial 2	Trial 3	Average	STDEV	95% CI	Trial 1	Trial 2	Trial 3
0	6.05E+07	6.45E+07	6.52E+07	6.34E+07	2.53E+06	2.87E+06	17.92	17.98	17.99
12	6.65E+07	6.60E+07	6.36E+07	6.54E+07	1.54E+06	1.75E+06	18.01	18.00	17.97
24	7.85E+07	8.09E+07	7.60E+07	7.84E+07	2.44E+06	2.76E+06	18.18	18.21	18.15
36	8.42E+07	8.26E+07	8.39E+07	8.36E+07	8.48E+05	9.60E+05	18.25	18.23	18.24
48	1.31E+08	1.22E+08	1.20E+08	1.24E+08	5.98E+06	6.76E+06	18.69	18.62	18.60
60	1.73E+08	1.64E+08	1.61E+08	1.66E+08	6.36E+06	7.20E+06	18.97	18.91	18.90
72	2.20E+08	2.10E+08	2.00E+08	2.10E+08	1.03E+07	1.17E+07	19.21	19.16	19.11
84	2.55E+08	2.55E+08	2.46E+08	2.52E+08	5.07E+06	5.73E+06	19.36	19.36	19.32
96	3.10E+08	3.25E+08	3.04E+08	3.13E+08	1.07E+07	1.21E+07	19.55	19.60	19.53
108	2.86E+08	2.93E+08	2.98E+08	2.92E+08	5.98E+06	6.77E+06	19.47	19.50	19.51
120	3.55E+08	3.40E+08	3.32E+08	3.42E+08	1.13E+07	1.28E+07	19.69	19.65	19.62

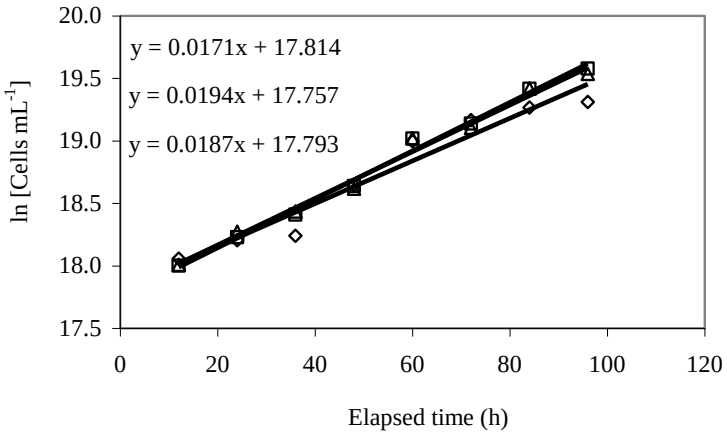


Specific growth rate (h^{-1})	
Trial 1	0.023
Trial 2	0.022
Trial 3	0.022
Average	0.022
STDEV	0.001
95% CI	0.001

Figure F.8. Specific growth rate calculations for Trial 1 (open circles), Trial 2 (open squares), and Trial 3 (open triangles).

Table F.39. BC13 growth in the presence of 30 μM acetate.

	Cells mL^{-1}						ln (Cells mL^{-1})		
Elapsed Time (h)	Trial 1	Trial 2	Trial 3	Average	STDEV	95% CI	Trial 1	Trial 2	Trial 3
0	6.18E+07	6.48E+07	6.47E+07	6.37E+07	1.71E+06	1.93E+06	17.94	17.99	17.98
12	6.95E+07	6.57E+07	6.62E+07	6.72E+07	2.07E+06	2.34E+06	18.06	18.00	18.01
24	8.06E+07	8.25E+07	8.62E+07	8.31E+07	2.86E+06	3.23E+06	18.20	18.23	18.27
36	8.35E+07	9.89E+07	1.01E+08	9.46E+07	9.70E+06	1.10E+07	18.24	18.41	18.44
48	1.25E+08	1.24E+08	1.22E+08	1.24E+08	1.82E+06	2.06E+06	18.65	18.64	18.62
60	1.78E+08	1.82E+08	1.82E+08	1.81E+08	2.37E+06	2.69E+06	19.00	19.02	19.02
72	2.11E+08	2.05E+08	1.98E+08	2.05E+08	6.31E+06	7.14E+06	19.17	19.14	19.10
84	2.33E+08	2.70E+08	2.71E+08	2.58E+08	2.19E+07	2.48E+07	19.27	19.42	19.42
96	2.44E+08	3.18E+08	3.05E+08	2.89E+08	3.97E+07	4.49E+07	19.31	19.58	19.54
108	2.99E+08	3.05E+08	3.15E+08	3.06E+08	8.00E+06	9.06E+06	19.52	19.53	19.57
120	3.69E+08	3.56E+08	3.40E+08	3.55E+08	1.45E+07	1.64E+07	19.73	19.69	19.64

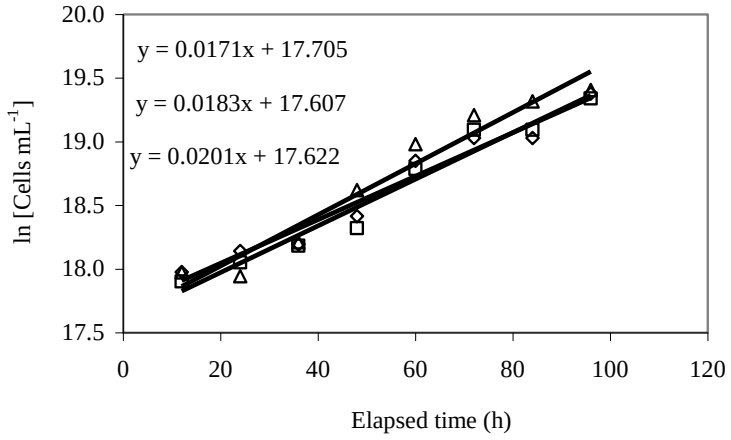


Specific growth rate (h^{-1})	
Trial 1	0.017
Trial 2	0.020
Trial 3	0.019
Average	0.019
STDEV	0.001
95% CI	0.002

Figure F.9. Specific growth rate calculations for Trial 1 (open circles), Trial 2 (open squares), and Trial 3 (open triangles).

Table F.40. BC13 growth in the presence of 50 μM acetate.

	Cells mL^{-1}						ln (Cells mL^{-1})		
Elapsed Time (h)	Trial 1	Trial 2	Trial 3	Average	STDEV	95% CI	Trial 1	Trial 2	Trial 3
0	5.11E+07	5.25E+07	6.30E+07	5.55E+07	6.51E+06	7.37E+06	17.75	17.78	17.96
12	6.41E+07	5.96E+07	6.40E+07	6.26E+07	2.57E+06	2.91E+06	17.98	17.90	17.97
24	7.56E+07	6.92E+07	6.20E+07	6.89E+07	6.78E+06	7.67E+06	18.14	18.05	17.94
36	7.97E+07	7.89E+07	8.10E+07	7.99E+07	1.07E+06	1.21E+06	18.19	18.18	18.21
48	9.96E+07	9.05E+07	1.22E+08	1.04E+08	1.62E+07	1.84E+07	18.42	18.32	18.62
60	1.54E+08	1.44E+08	1.75E+08	1.58E+08	1.60E+07	1.81E+07	18.85	18.78	18.98
72	1.84E+08	1.96E+08	2.20E+08	2.00E+08	1.85E+07	2.10E+07	19.03	19.09	19.21
84	1.84E+08	1.96E+08	2.45E+08	2.08E+08	3.25E+07	3.68E+07	19.03	19.09	19.32
96	2.61E+08	2.51E+08	2.68E+08	2.60E+08	8.63E+06	9.76E+06	19.38	19.34	19.41
108	2.64E+08	2.47E+08	2.57E+08	2.56E+08	8.80E+06	9.96E+06	19.39	19.32	19.37
120	2.46E+08	2.42E+08	2.50E+08	2.46E+08	3.89E+06	4.40E+06	19.32	19.31	19.34



Specific growth rate (h^{-1})

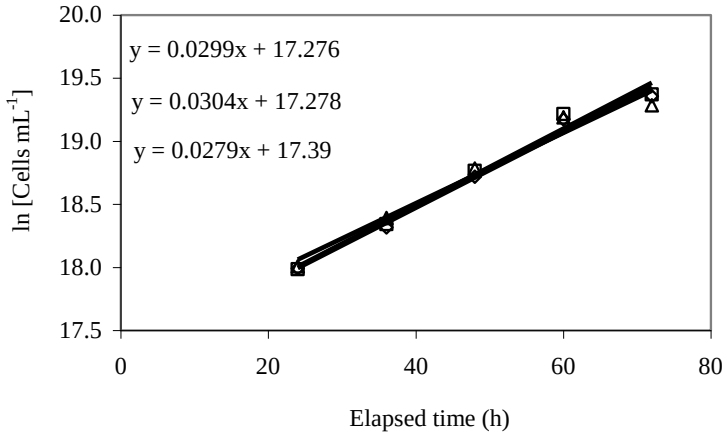
Trial 1	0.017
Trial 2	0.018
Trial 3	0.018
Average	0.017
STDEV	0.001
95% CI	0.001

Figure F.10. Specific growth rate calculations for Trial 1 (open circles), Trial 2 (open squares), and Trial 3 (open triangles).

Citrate

Table F.41. BC13 growth in the presence of 5 μM citrate.

	Cells mL^{-1}						ln (Cells mL^{-1})		
Elapsed Time (h)	Trial 1	Trial 2	Trial 3	Average	STDEV	95% CI	Trial 1	Trial 2	Trial 3
0	5.36E+07	5.34E+07	5.51E+07	5.40E+07	9.60E+05	1.09E+06	17.80	17.79	17.83
12	5.48E+07	5.73E+07	5.71E+07	5.64E+07	1.40E+06	1.58E+06	17.82	17.86	17.86
24	6.51E+07	6.46E+07	6.62E+07	6.53E+07	8.11E+05	9.18E+05	17.99	17.98	18.01
36	9.01E+07	9.25E+07	9.70E+07	9.32E+07	3.51E+06	3.97E+06	18.32	18.34	18.39
48	1.35E+08	1.41E+08	1.44E+08	1.40E+08	4.61E+06	5.22E+06	18.72	18.76	18.78
60	2.13E+08	2.21E+08	2.16E+08	2.17E+08	4.46E+06	5.05E+06	19.17	19.22	19.19
72	2.55E+08	2.58E+08	2.37E+08	2.50E+08	1.13E+07	1.28E+07	19.36	19.37	19.29
84	2.97E+08	3.06E+08	3.11E+08	3.05E+08	6.91E+06	7.82E+06	19.51	19.54	19.56
96	3.23E+08	3.24E+08	3.18E+08	3.22E+08	3.57E+06	4.03E+06	19.59	19.60	19.58
108	3.25E+08	3.18E+08	3.16E+08	3.20E+08	4.93E+06	5.58E+06	19.60	19.58	19.57
120	3.17E+08	3.04E+08	3.00E+08	3.07E+08	8.68E+06	9.82E+06	19.57	19.53	19.52



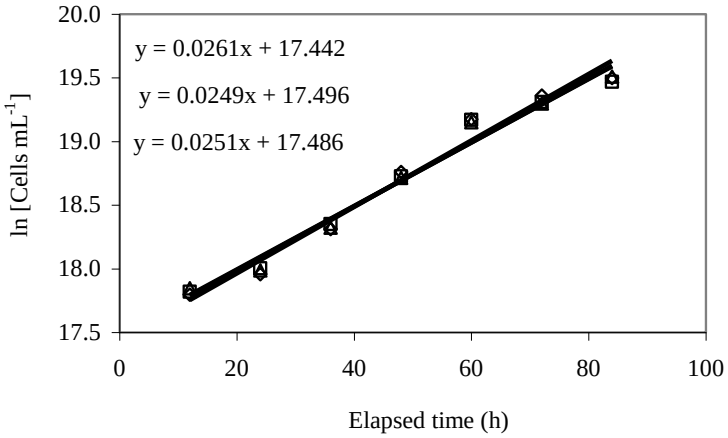
Specific growth rate (h^{-1})

Trial 1	0.030
Trial 2	0.030
Trial 3	0.028
Average	0.029
STDEV	0.001
95% CI	0.001

Figure F.11. Specific growth rate calculations for Trial 1 (open circles), Trial 2 (open squares), and Trial 3 (open triangles).

Table F.42. BC13 growth in the presence of 10 μM citrate.

	Cells mL^{-1}						ln (Cells mL^{-1})		
Elapsed Time (h)	Trial 1	Trial 2	Trial 3	Average	STDEV	95% CI	Trial 1	Trial 2	Trial 3
0	5.60E+07	5.70E+07	5.66E+07	5.65E+07	5.17E+05	5.85E+05	17.84	17.86	17.85
12	5.36E+07	5.49E+07	5.64E+07	5.50E+07	1.39E+06	1.58E+06	17.80	17.82	17.85
24	6.30E+07	6.60E+07	6.49E+07	6.46E+07	1.49E+06	1.69E+06	17.96	18.00	17.99
36	8.96E+07	9.32E+07	9.08E+07	9.12E+07	1.83E+06	2.07E+06	18.31	18.35	18.32
48	1.40E+08	1.36E+08	1.34E+08	1.37E+08	3.22E+06	3.64E+06	18.76	18.73	18.71
60	2.12E+08	2.11E+08	2.08E+08	2.11E+08	2.40E+06	2.71E+06	19.17	19.17	19.15
72	2.56E+08	2.44E+08	2.41E+08	2.47E+08	8.16E+06	9.23E+06	19.36	19.31	19.30
84	2.94E+08	2.85E+08	2.97E+08	2.92E+08	6.08E+06	6.88E+06	19.50	19.47	19.51
96	3.38E+08	3.32E+08	3.15E+08	3.29E+08	1.18E+07	1.34E+07	19.64	19.62	19.57
108	3.25E+08	3.30E+08	3.35E+08	3.30E+08	4.90E+06	5.54E+06	19.60	19.61	19.63
120	3.20E+08	3.12E+08	3.26E+08	3.19E+08	6.80E+06	7.70E+06	19.58	19.56	19.60



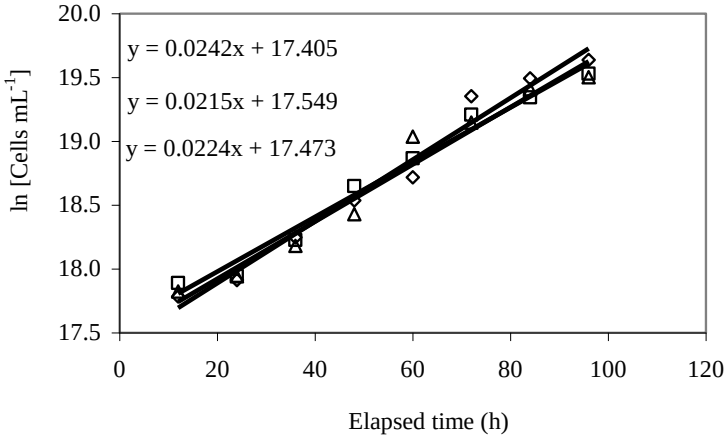
Specific growth rate (h^{-1})

Trial 1	0.026
Trial 2	0.025
Trial 3	0.025
Average	0.025
STDEV	0.001
95% CI	0.001

Figure F.12. Specific growth rate calculations for Trial 1 (open circles), Trial 2 (open squares), and Trial 3 (open triangles).

Table F.43. BC13 growth in the presence of 20 μM citrate.

	Cells mL^{-1}						ln (Cells mL^{-1})		
Elapsed Time (h)	Trial 1	Trial 2	Trial 3	Average	STDEV	95% CI	Trial 1	Trial 2	Trial 3
0	5.60E+07	5.54E+07	5.49E+07	5.54E+07	5.30E+05	6.00E+05	17.84	17.83	17.82
12	5.30E+07	5.89E+07	5.50E+07	5.56E+07	3.00E+06	3.39E+06	17.79	17.89	17.82
24	6.02E+07	6.22E+07	6.20E+07	6.14E+07	1.11E+06	1.26E+06	17.91	17.95	17.94
36	8.40E+07	8.23E+07	7.86E+07	8.17E+07	2.76E+06	3.12E+06	18.25	18.23	18.18
48	1.12E+08	1.26E+08	1.01E+08	1.13E+08	1.24E+07	1.40E+07	18.54	18.65	18.43
60	1.35E+08	1.56E+08	1.85E+08	1.59E+08	2.53E+07	2.86E+07	18.72	18.87	19.04
72	2.54E+08	2.20E+08	2.07E+08	2.27E+08	2.44E+07	2.76E+07	19.35	19.21	19.15
84	2.92E+08	2.52E+08	2.69E+08	2.71E+08	2.03E+07	2.30E+07	19.49	19.34	19.41
96	3.38E+08	3.03E+08	2.95E+08	3.12E+08	2.29E+07	2.60E+07	19.64	19.53	19.50
108	3.18E+08	3.03E+08	3.01E+08	3.07E+08	9.20E+06	1.04E+07	19.58	19.53	19.52
120	3.24E+08	3.30E+08	3.22E+08	3.25E+08	4.04E+06	4.57E+06	19.60	19.61	19.59

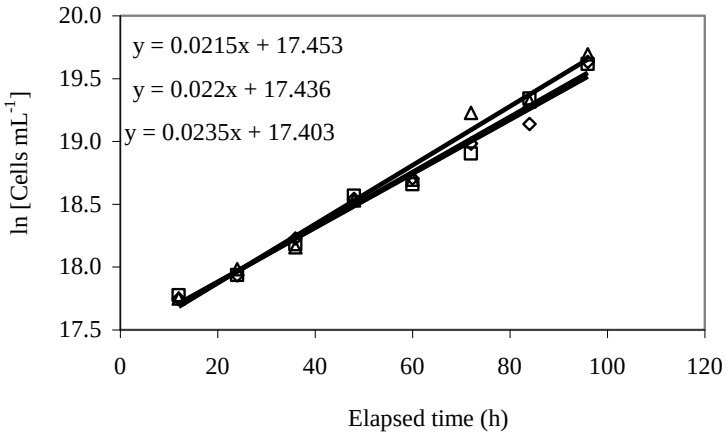


Specific growth rate (h^{-1})	
Trial 1	0.024
Trial 2	0.022
Trial 3	0.022
Average	0.023
STDEV	0.001
95% CI	0.002

Figure F.13. Specific growth rate calculations for Trial 1 (open circles), Trial 2 (open squares), and Trial 3 (open triangles).

Table F.44. BC13 growth in the presence of 30 μM citrate.

	Cells mL^{-1}						ln (Cells mL^{-1})		
Elapsed Time (h)	Trial 1	Trial 2	Trial 3	Average	STDEV	95% CI	Trial 1	Trial 2	Trial 3
0	5.16E+07	4.96E+07	4.90E+07	5.00E+07	1.36E+06	1.54E+06	17.76	17.72	17.71
12	5.10E+07	5.25E+07	5.11E+07	5.15E+07	8.23E+05	9.31E+05	17.75	17.78	17.75
24	6.15E+07	6.16E+07	6.46E+07	6.26E+07	1.75E+06	1.99E+06	17.93	17.94	17.98
36	8.23E+07	7.87E+07	7.69E+07	7.93E+07	2.77E+06	3.13E+06	18.23	18.18	18.16
48	1.13E+08	1.16E+08	1.11E+08	1.13E+08	2.27E+06	2.56E+06	18.54	18.57	18.53
60	1.33E+08	1.27E+08	1.32E+08	1.30E+08	3.21E+06	3.63E+06	18.70	18.66	18.70
72	1.75E+08	1.62E+08	2.24E+08	1.87E+08	3.27E+07	3.70E+07	18.98	18.90	19.23
84	2.05E+08	2.51E+08	2.45E+08	2.34E+08	2.50E+07	2.83E+07	19.14	19.34	19.32
96	3.36E+08	3.30E+08	3.56E+08	3.41E+08	1.37E+07	1.56E+07	19.63	19.61	19.69
108	3.17E+08	3.09E+08	3.40E+08	3.22E+08	1.64E+07	1.86E+07	19.58	19.55	19.65
120	3.32E+08	3.40E+08	3.39E+08	3.37E+08	4.47E+06	5.06E+06	19.62	19.64	19.64

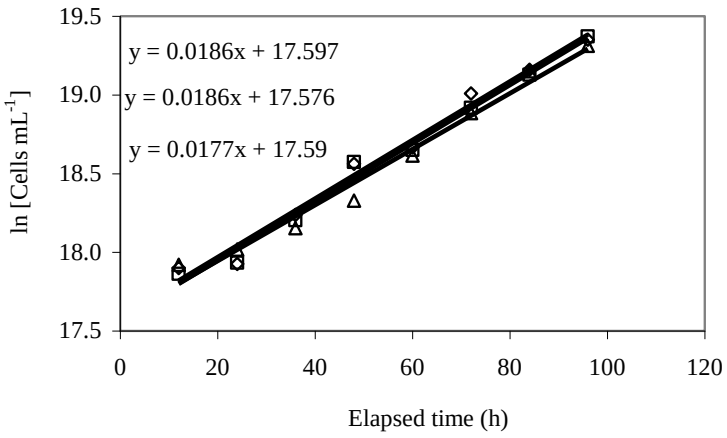


Specific growth rate (h^{-1})	
Trial 1	0.022
Trial 2	0.022
Trial 3	0.024
Average	0.022
STDEV	0.001
95% CI	0.001

Figure F.14. Specific growth rate calculations for Trial 1 (open circles), Trial 2 (open squares), and Trial 3 (open triangles).

Table F.45. BC13 growth in the presence of 50 μM citrate.

	Cells mL^{-1}						ln (Cells mL^{-1})		
Elapsed Time (h)	Trial 1	Trial 2	Trial 3	Average	STDEV	95% CI	Trial 1	Trial 2	Trial 3
0	5.27E+07	5.35E+07	5.42E+07	5.35E+07	7.40E+05	8.37E+05	17.78	17.79	17.81
12	5.94E+07	5.73E+07	6.06E+07	5.91E+07	1.69E+06	1.92E+06	17.90	17.86	17.92
24	6.10E+07	6.15E+07	6.69E+07	6.31E+07	3.25E+06	3.67E+06	17.93	17.93	18.02
36	8.31E+07	8.05E+07	7.66E+07	8.01E+07	3.30E+06	3.74E+06	18.24	18.20	18.15
48	1.15E+08	1.17E+08	9.12E+07	1.08E+08	1.43E+07	1.61E+07	18.56	18.57	18.33
60	1.28E+08	1.26E+08	1.21E+08	1.25E+08	3.23E+06	3.65E+06	18.67	18.65	18.61
72	1.80E+08	1.64E+08	1.59E+08	1.68E+08	1.09E+07	1.24E+07	19.01	18.92	18.88
84	2.10E+08	2.03E+08	2.07E+08	2.06E+08	3.50E+06	3.96E+06	19.16	19.13	19.15
96	2.54E+08	2.59E+08	2.44E+08	2.52E+08	7.58E+06	8.58E+06	19.35	19.37	19.31
108	2.46E+08	2.37E+08	2.58E+08	2.47E+08	1.07E+07	1.21E+07	19.32	19.28	19.37
120	2.36E+08	2.59E+08	2.45E+08	2.47E+08	1.14E+07	1.29E+07	19.28	19.37	19.32



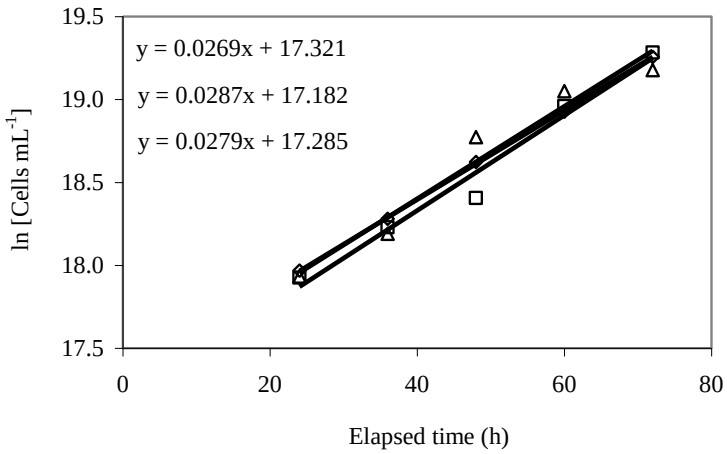
Specific growth rate (h^{-1})	
Trial 1	0.019
Trial 2	0.019
Trial 3	0.018
Average	0.018
STDEV	0.001
95% CI	0.001

Figure F.15. Specific growth rate calculations for Trial 1 (open circles), Trial 2 (open squares), and Trial 3 (open triangles).

2-ketoglutarate

Table F.46. BC13 growth in the presence of 5 μM 2-ketoglutarate.

	Cells mL^{-1}						ln (Cells mL^{-1})		
Elapsed Time (h)	Trial 1	Trial 2	Trial 3	Average	STDEV	95% CI	Trial 1	Trial 2	Trial 3
0	5.04E+07	5.02E+07	5.12E+07	5.06E+07	5.09E+05	5.76E+05	17.74	17.73	17.75
12	5.36E+07	5.29E+07	5.24E+07	5.30E+07	5.98E+05	6.76E+05	17.80	17.78	17.77
24	6.36E+07	6.10E+07	6.13E+07	6.20E+07	1.40E+06	1.59E+06	17.97	17.93	17.93
36	8.69E+07	8.26E+07	7.95E+07	8.30E+07	3.71E+06	4.20E+06	18.28	18.23	18.19
48	1.22E+08	9.84E+07	1.42E+08	1.21E+08	2.19E+07	2.48E+07	18.62	18.40	18.77
60	1.66E+08	1.71E+08	1.87E+08	1.75E+08	1.13E+07	1.28E+07	18.93	18.96	19.05
72	2.31E+08	2.37E+08	2.13E+08	2.27E+08	1.25E+07	1.41E+07	19.26	19.28	19.18
84	2.74E+08	2.63E+08	2.44E+08	2.60E+08	1.55E+07	1.75E+07	19.43	19.39	19.31
96	2.86E+08	2.65E+08	2.57E+08	2.69E+08	1.47E+07	1.67E+07	19.47	19.40	19.36
108	2.90E+08	3.03E+08	3.16E+08	3.03E+08	1.31E+07	1.48E+07	19.49	19.53	19.57
120	2.75E+08	2.78E+08	2.85E+08	2.79E+08	5.25E+06	5.94E+06	19.43	19.44	19.47

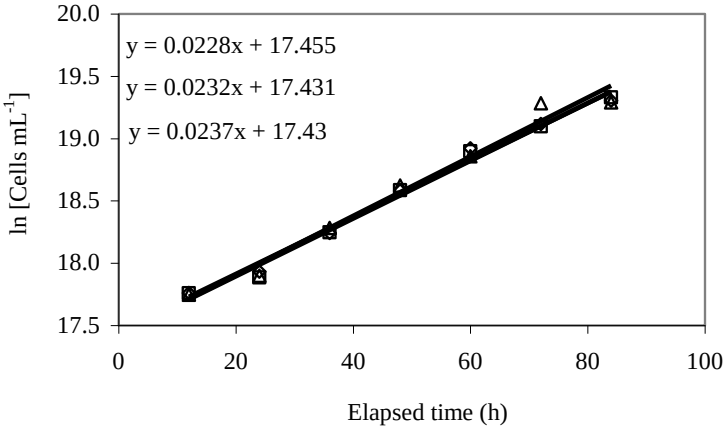


Specific growth rate (h^{-1})	
Trial 1	0.027
Trial 2	0.029
Trial 3	0.028
Average	0.028
STDEV	0.001
95% CI	0.001

Figure F.16. Specific growth rate calculations for Trial 1 (open circles), Trial 2 (open squares), and Trial 3 (open triangles).

Table F.47. BC13 growth in the presence of 10 μM 2-ketoglutarate.

	Cells mL^{-1}						ln (Cells mL^{-1})		
Elapsed Time (h)	Trial 1	Trial 2	Trial 3	Average	STDEV	95% CI	Trial 1	Trial 2	Trial 3
0	5.16E+07	5.39E+07	5.48E+07	5.34E+07	1.66E+06	1.88E+06	17.76	17.80	17.82
12	5.17E+07	5.16E+07	5.10E+07	5.15E+07	4.09E+05	4.63E+05	17.76	17.76	17.75
24	6.14E+07	5.86E+07	5.93E+07	5.98E+07	1.48E+06	1.67E+06	17.93	17.89	17.90
36	8.36E+07	8.41E+07	8.72E+07	8.49E+07	1.93E+06	2.19E+06	18.24	18.25	18.28
48	1.18E+08	1.18E+08	1.22E+08	1.19E+08	2.69E+06	3.05E+06	18.58	18.59	18.62
60	1.65E+08	1.61E+08	1.55E+08	1.60E+08	5.04E+06	5.70E+06	18.92	18.90	18.86
72	2.00E+08	1.97E+08	2.37E+08	2.11E+08	2.22E+07	2.51E+07	19.12	19.10	19.28
84	2.42E+08	2.48E+08	2.39E+08	2.43E+08	4.83E+06	5.47E+06	19.31	19.33	19.29
96	2.72E+08	2.64E+08	2.66E+08	2.67E+08	4.24E+06	4.79E+06	19.42	19.39	19.40
108	3.03E+08	3.10E+08	2.99E+08	3.04E+08	5.33E+06	6.03E+06	19.53	19.55	19.52
120	2.72E+08	2.69E+08	2.70E+08	2.70E+08	1.22E+06	1.38E+06	19.42	19.41	19.41



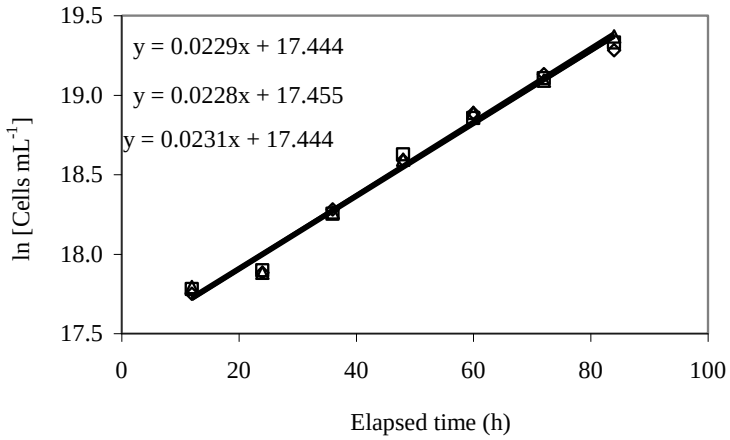
Specific growth rate (h^{-1})

Trial 1	0.023
Trial 2	0.023
Trial 3	0.024
Average	0.023
STDEV	0.000
95% CI	0.001

Figure F.17. Specific growth rate calculations for Trial 1 (open circles), Trial 2 (open squares), and Trial 3 (open triangles).

Table F.48. BC13 growth in the presence of 20 μM 2-ketoglutarate.

	Cells mL^{-1}						ln (Cells mL^{-1})		
Elapsed Time (h)	Trial 1	Trial 2	Trial 3	Average	STDEV	95% CI	Trial 1	Trial 2	Trial 3
0	5.41E+07	5.24E+07	5.50E+07	5.38E+07	1.30E+06	1.47E+06	17.81	17.78	17.82
12	5.12E+07	5.27E+07	5.33E+07	5.24E+07	1.12E+06	1.26E+06	17.75	17.78	17.79
24	5.84E+07	5.93E+07	5.84E+07	5.87E+07	4.80E+05	5.43E+05	17.88	17.90	17.88
36	8.70E+07	8.46E+07	8.54E+07	8.57E+07	1.20E+06	1.36E+06	18.28	18.25	18.26
48	1.18E+08	1.23E+08	1.19E+08	1.20E+08	2.46E+06	2.78E+06	18.59	18.63	18.59
60	1.59E+08	1.54E+08	1.60E+08	1.58E+08	2.96E+06	3.35E+06	18.89	18.85	18.89
72	2.04E+08	1.98E+08	1.96E+08	1.99E+08	4.08E+06	4.62E+06	19.13	19.11	19.09
84	2.37E+08	2.48E+08	2.58E+08	2.48E+08	1.06E+07	1.20E+07	19.28	19.33	19.37
96	2.43E+08	2.30E+08	2.52E+08	2.42E+08	1.09E+07	1.23E+07	19.31	19.25	19.34
108	2.59E+08	2.26E+08	2.43E+08	2.43E+08	1.66E+07	1.87E+07	19.37	19.24	19.31
120	2.34E+08	2.58E+08	2.49E+08	2.47E+08	1.25E+07	1.42E+07	19.27	19.37	19.33

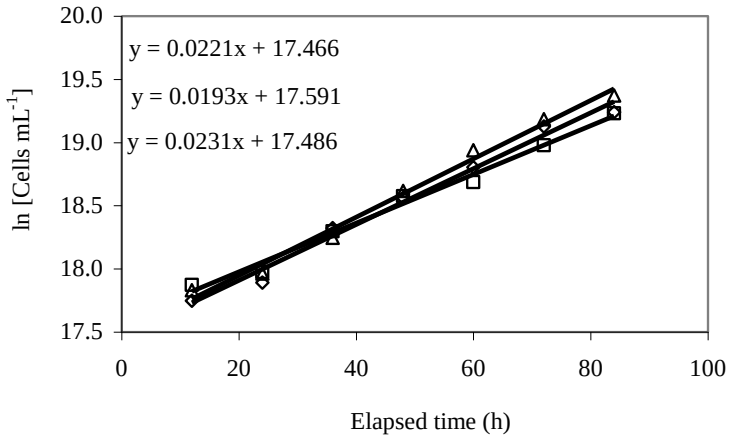


Specific growth rate (h^{-1})	
Trial 1	0.023
Trial 2	0.023
Trial 3	0.023
Average	0.023
STDEV	0.000
95% CI	0.000

Figure F.18. Specific growth rate calculations for Trial 1 (open circles), Trial 2 (open squares), and Trial 3 (open triangles).

Table F.49. BC13 growth in the presence of 30 μM 2-ketoglutarate.

	Cells mL^{-1}						ln (Cells mL^{-1})		
Elapsed Time (h)	Trial 1	Trial 2	Trial 3	Average	STDEV	95% CI	Trial 1	Trial 2	Trial 3
0	5.17E+07	5.23E+07	5.18E+07	5.19E+07	3.45E+05	3.91E+05	17.76	17.77	17.76
12	5.10E+07	5.78E+07	5.55E+07	5.48E+07	3.46E+06	3.91E+06	17.75	17.87	17.83
24	5.89E+07	6.41E+07	6.33E+07	6.21E+07	2.77E+06	3.14E+06	17.89	17.98	17.96
36	9.06E+07	8.84E+07	8.41E+07	8.77E+07	3.32E+06	3.76E+06	18.32	18.30	18.25
48	1.15E+08	1.17E+08	1.22E+08	1.18E+08	3.48E+06	3.94E+06	18.56	18.57	18.62
60	1.47E+08	1.30E+08	1.68E+08	1.48E+08	1.89E+07	2.14E+07	18.80	18.69	18.94
72	2.03E+08	1.75E+08	2.15E+08	1.97E+08	2.05E+07	2.32E+07	19.13	18.98	19.19
84	2.27E+08	2.25E+08	2.59E+08	2.37E+08	1.91E+07	2.16E+07	19.24	19.23	19.37
96	2.43E+08	2.51E+08	2.43E+08	2.46E+08	4.87E+06	5.51E+06	19.31	19.34	19.31
108	2.60E+08	2.50E+08	2.42E+08	2.51E+08	8.94E+06	1.01E+07	19.38	19.34	19.31
120	2.25E+08	2.34E+08	2.44E+08	2.34E+08	9.84E+06	1.11E+07	19.23	19.27	19.31



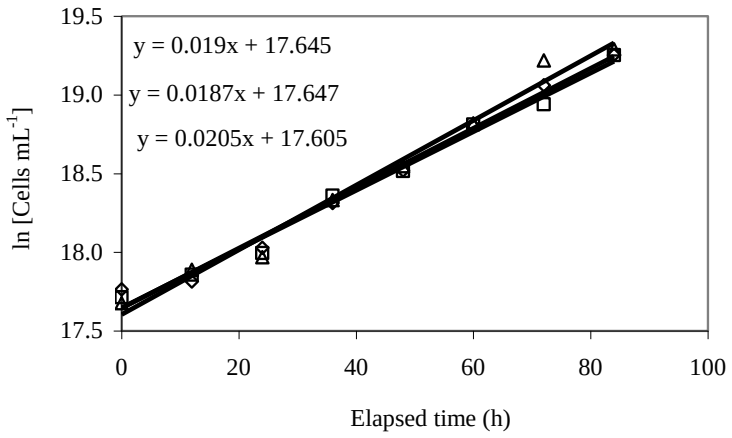
Specific growth rate (h^{-1})

Trial 1	0.022
Trial 2	0.019
Trial 3	0.023
Average	0.022
STDEV	0.002
95% CI	0.002

Figure F.19. Specific growth rate calculations for Trial 1 (open circles), Trial 2 (open squares), and Trial 3 (open triangles).

Table F.50. BC13 growth in the presence of 50 μM 2-ketoglutarate.

	Cells mL^{-1}						ln (Cells mL^{-1})		
Elapsed Time (h)	Trial 1	Trial 2	Trial 3	Average	STDEV	95% CI	Trial 1	Trial 2	Trial 3
0	5.19E+07	4.93E+07	4.75E+07	4.96E+07	2.20E+06	2.49E+06	17.76	17.71	17.68
12	5.45E+07	5.69E+07	5.88E+07	5.67E+07	2.15E+06	2.43E+06	17.81	17.86	17.89
24	6.76E+07	6.53E+07	6.36E+07	6.55E+07	2.01E+06	2.28E+06	18.03	17.99	17.97
36	8.98E+07	9.41E+07	9.15E+07	9.18E+07	2.16E+06	2.44E+06	18.31	18.36	18.33
48	1.10E+08	1.10E+08	1.13E+08	1.11E+08	1.89E+06	2.14E+06	18.52	18.52	18.55
60	1.47E+08	1.48E+08	1.49E+08	1.48E+08	1.00E+06	1.14E+06	18.81	18.81	18.82
72	1.90E+08	1.68E+08	2.22E+08	1.93E+08	2.73E+07	3.09E+07	19.06	18.94	19.22
84	2.30E+08	2.30E+08	2.39E+08	2.33E+08	4.89E+06	5.54E+06	19.25	19.25	19.29
96	2.34E+08	2.38E+08	2.29E+08	2.34E+08	4.67E+06	5.29E+06	19.27	19.29	19.25
108	2.66E+08	2.54E+08	2.52E+08	2.57E+08	7.65E+06	8.66E+06	19.40	19.35	19.34
120	2.31E+08	2.36E+08	2.29E+08	2.32E+08	3.33E+06	3.77E+06	19.26	19.28	19.25



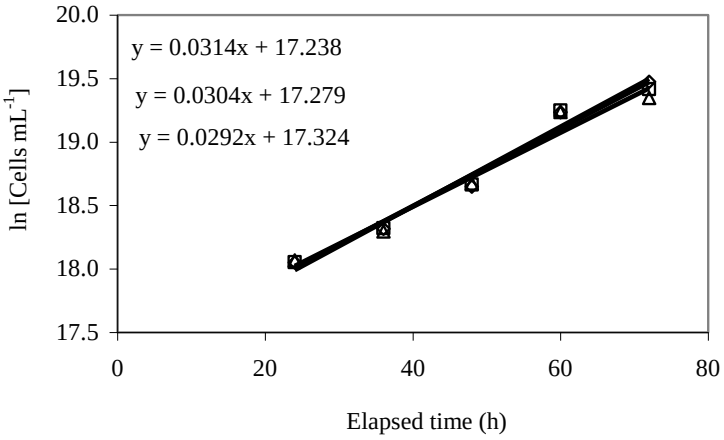
Specific growth rate (h^{-1})	
Trial 1	0.019
Trial 2	0.019
Trial 3	0.021
Average	0.019
STDEV	0.001
95% CI	0.001

Figure F.20. Specific growth rate calculations for Trial 1 (open circles), Trial 2 (open squares), and Trial 3 (open triangles).

Succinate

Table F.51. BC13 growth in the presence of 5 μM succinate.

	Cells mL^{-1}						ln (Cells mL^{-1})		
Elapsed Time (h)	Trial 1	Trial 2	Trial 3	Average	STDEV	95% CI	Trial 1	Trial 2	Trial 3
0	5.62E+07	5.41E+07	5.43E+07	5.49E+07	1.15E+06	1.31E+06	17.84	17.81	17.81
12	5.85E+07	5.68E+07	5.79E+07	5.77E+07	8.38E+05	9.49E+05	17.88	17.86	17.87
24	6.91E+07	6.93E+07	7.03E+07	6.95E+07	6.52E+05	7.38E+05	18.05	18.05	18.07
36	9.01E+07	9.04E+07	8.82E+07	8.96E+07	1.20E+06	1.36E+06	18.32	18.32	18.29
48	1.25E+08	1.28E+08	1.29E+08	1.27E+08	1.70E+06	1.93E+06	18.65	18.66	18.67
60	2.26E+08	2.29E+08	2.26E+08	2.27E+08	1.82E+06	2.05E+06	19.23	19.25	19.24
72	2.87E+08	2.70E+08	2.53E+08	2.70E+08	1.71E+07	1.93E+07	19.47	19.42	19.35
84	2.95E+08	3.10E+08	2.89E+08	2.98E+08	1.09E+07	1.24E+07	19.50	19.55	19.48
96	3.31E+08	3.34E+08	3.19E+08	3.28E+08	7.67E+06	8.68E+06	19.62	19.63	19.58
108	3.36E+08	3.52E+08	3.47E+08	3.45E+08	8.21E+06	9.29E+06	19.63	19.68	19.66
120	3.27E+08	3.40E+08	3.39E+08	3.35E+08	7.30E+06	8.26E+06	19.61	19.65	19.64



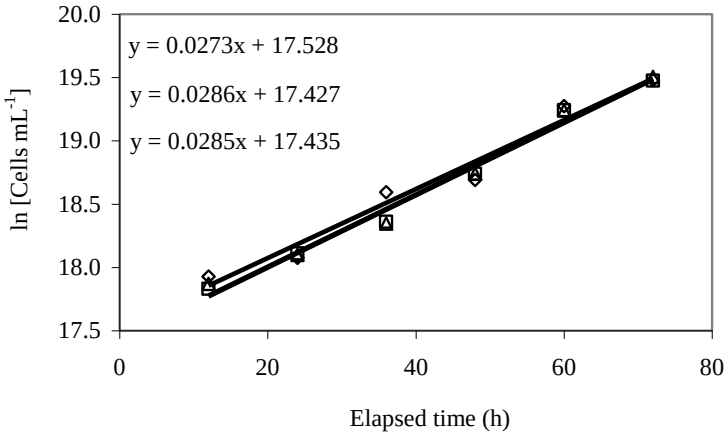
Specific growth rate (h^{-1})

Trial 1	0.031
Trial 2	0.030
Trial 3	0.029
Average	0.030
STDEV	0.001
95% CI	0.001

Figure F.21. Specific growth rate calculations for Trial 1 (open circles), Trial 2 (open squares), and Trial 3 (open triangles).

Table F.52. BC13 growth in the presence of 10 μM succinate.

	Cells mL^{-1}						ln (Cells mL^{-1})		
Elapsed Time (h)	Trial 1	Trial 2	Trial 3	Average	STDEV	95% CI	Trial 1	Trial 2	Trial 3
0	5.48E+07	5.48E+07	5.67E+07	5.54E+07	1.11E+06	1.25E+06	17.82	17.82	17.85
12	6.10E+07	5.54E+07	5.77E+07	5.80E+07	2.82E+06	3.19E+06	17.93	17.83	17.87
24	7.08E+07	7.34E+07	7.25E+07	7.22E+07	1.33E+06	1.51E+06	18.07	18.11	18.10
36	1.19E+08	9.42E+07	9.27E+07	1.02E+08	1.47E+07	1.67E+07	18.59	18.36	18.35
48	1.31E+08	1.38E+08	1.37E+08	1.35E+08	3.68E+06	4.16E+06	18.69	18.74	18.74
60	2.35E+08	2.27E+08	2.26E+08	2.30E+08	4.64E+06	5.25E+06	19.27	19.24	19.24
72	2.88E+08	2.87E+08	2.96E+08	2.90E+08	4.50E+06	5.09E+06	19.48	19.48	19.50
84	3.01E+08	2.87E+08	2.83E+08	2.90E+08	9.17E+06	1.04E+07	19.52	19.47	19.46
96	3.34E+08	3.27E+08	3.14E+08	3.25E+08	1.02E+07	1.15E+07	19.63	19.60	19.56
108	3.21E+08	3.10E+08	3.23E+08	3.18E+08	6.77E+06	7.66E+06	19.59	19.55	19.59
120	3.17E+08	3.17E+08	3.07E+08	3.14E+08	6.15E+06	6.96E+06	19.58	19.57	19.54



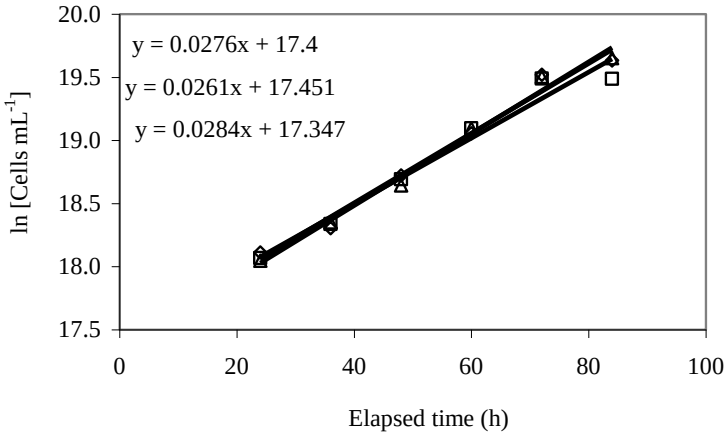
Specific growth rate (h^{-1})

Trial 1	0.027
Trial 2	0.029
Trial 3	0.029
Average	0.028
STDEV	0.001
95% CI	0.001

Figure F.22. Specific growth rate calculations for Trial 1 (open circles), Trial 2 (open squares), and Trial 3 (open triangles).

Table F.53. BC13 growth in the presence of 20 μM succinate.

	Cells mL^{-1}						ln (Cells mL^{-1})		
Elapsed Time (h)	Trial 1	Trial 2	Trial 3	Average	STDEV	95% CI	Trial 1	Trial 2	Trial 3
0	5.64E+07	5.66E+07	5.74E+07	5.68E+07	5.38E+05	6.08E+05	17.85	17.85	17.87
12	6.19E+07	6.16E+07	6.13E+07	6.16E+07	3.29E+05	3.72E+05	17.94	17.94	17.93
24	7.34E+07	7.02E+07	6.88E+07	7.08E+07	2.34E+06	2.65E+06	18.11	18.07	18.05
36	8.90E+07	9.19E+07	9.32E+07	9.14E+07	2.18E+06	2.46E+06	18.30	18.34	18.35
48	1.35E+08	1.31E+08	1.25E+08	1.30E+08	5.11E+06	5.78E+06	18.72	18.69	18.64
60	1.89E+08	1.96E+08	1.97E+08	1.94E+08	4.33E+06	4.89E+06	19.06	19.10	19.10
72	3.00E+08	2.91E+08	2.95E+08	2.96E+08	4.48E+06	5.07E+06	19.52	19.49	19.50
84	3.37E+08	2.91E+08	3.43E+08	3.23E+08	2.84E+07	3.22E+07	19.63	19.49	19.65
96	3.37E+08	3.34E+08	3.39E+08	3.37E+08	2.89E+06	3.27E+06	19.64	19.63	19.64
108	3.33E+08	3.27E+08	3.28E+08	3.29E+08	2.98E+06	3.37E+06	19.62	19.61	19.61
120	3.09E+08	2.98E+08	3.04E+08	3.04E+08	5.45E+06	6.17E+06	19.55	19.51	19.53



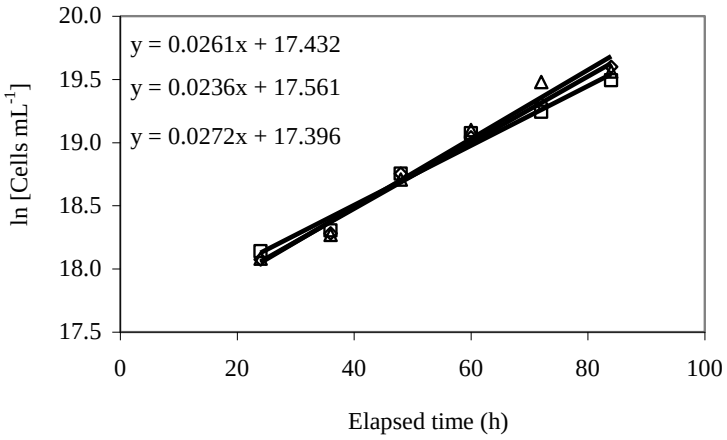
Specific growth rate (h^{-1})

Trial 1	0.028
Trial 2	0.026
Trial 3	0.028
Average	0.027
STDEV	0.001
95% CI	0.001

Figure F.23. Specific growth rate calculations for Trial 1 (open circles), Trial 2 (open squares), and Trial 3 (open triangles).

Table F.54. BC13 growth in the presence of 30 μM succinate.

	Cells mL^{-1}						ln (Cells mL^{-1})		
Elapsed Time (h)	Trial 1	Trial 2	Trial 3	Average	STDEV	95% CI	Trial 1	Trial 2	Trial 3
0	5.59E+07	6.91E+07	5.35E+07	5.95E+07	8.35E+06	9.45E+06	17.84	18.05	17.80
12	6.30E+07	7.27E+07	6.32E+07	6.63E+07	5.56E+06	6.29E+06	17.96	18.10	17.96
24	7.08E+07	7.55E+07	7.12E+07	7.25E+07	2.62E+06	2.96E+06	18.08	18.14	18.08
36	8.70E+07	8.89E+07	8.58E+07	8.73E+07	1.56E+06	1.76E+06	18.28	18.30	18.27
48	1.39E+08	1.40E+08	1.33E+08	1.37E+08	3.67E+06	4.15E+06	18.75	18.75	18.71
60	1.86E+08	1.92E+08	1.97E+08	1.92E+08	5.67E+06	6.41E+06	19.04	19.07	19.10
72	2.42E+08	2.27E+08	2.88E+08	2.52E+08	3.17E+07	3.59E+07	19.30	19.24	19.48
84	3.25E+08	2.92E+08	3.13E+08	3.10E+08	1.64E+07	1.86E+07	19.60	19.49	19.56
96	3.28E+08	3.42E+08	3.50E+08	3.40E+08	1.16E+07	1.31E+07	19.61	19.65	19.67
108	3.22E+08	3.18E+08	3.06E+08	3.15E+08	7.98E+06	9.03E+06	19.59	19.58	19.54
120	3.19E+08	3.19E+08	3.32E+08	3.23E+08	7.83E+06	8.86E+06	19.58	19.58	19.62



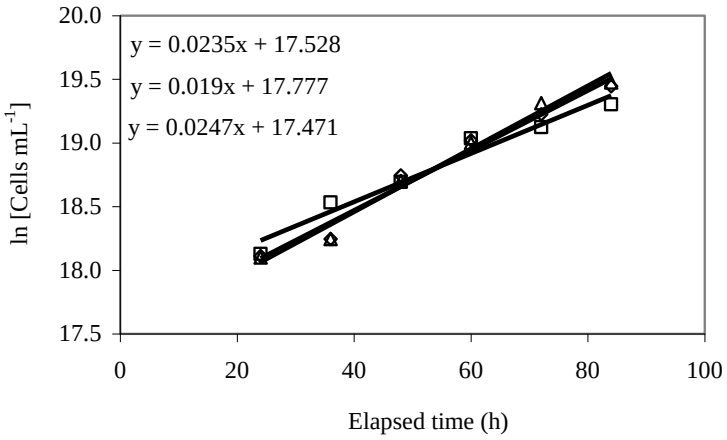
Specific growth rate (h^{-1})

Trial 1	0.026
Trial 2	0.024
Trial 3	0.027
Average	0.026
STDEV	0.002
95% CI	0.002

Figure F.24. Specific growth rate calculations for Trial 1 (open circles), Trial 2 (open squares), and Trial 3 (open triangles).

Table F.55. BC13 growth in the presence of 50 μM succinate.

	Cells mL^{-1}						ln (Cells mL^{-1})		
Elapsed Time (h)	Trial 1	Trial 2	Trial 3	Average	STDEV	95% CI	Trial 1	Trial 2	Trial 3
0	5.63E+07	5.51E+07	5.60E+07	5.58E+07	6.07E+05	6.87E+05	17.85	17.83	17.84
12	6.35E+07	6.33E+07	6.02E+07	6.23E+07	1.83E+06	2.07E+06	17.97	17.96	17.91
24	7.35E+07	7.47E+07	7.26E+07	7.36E+07	1.06E+06	1.20E+06	18.11	18.13	18.10
36	8.39E+07	1.12E+08	8.38E+07	9.32E+07	1.62E+07	1.84E+07	18.25	18.53	18.24
48	1.38E+08	1.31E+08	1.32E+08	1.34E+08	3.66E+06	4.15E+06	18.74	18.69	18.70
60	1.82E+08	1.85E+08	1.78E+08	1.82E+08	3.36E+06	3.80E+06	19.02	19.04	19.00
72	2.24E+08	2.02E+08	2.44E+08	2.23E+08	2.10E+07	2.37E+07	19.23	19.12	19.31
84	2.79E+08	2.41E+08	2.87E+08	2.69E+08	2.43E+07	2.75E+07	19.45	19.30	19.48
96	2.64E+08	2.79E+08	2.62E+08	2.68E+08	9.03E+06	1.02E+07	19.39	19.45	19.39
108	2.34E+08	2.56E+08	2.59E+08	2.50E+08	1.37E+07	1.55E+07	19.27	19.36	19.37
120	2.45E+08	2.68E+08	2.78E+08	2.64E+08	1.67E+07	1.90E+07	19.32	19.40	19.44



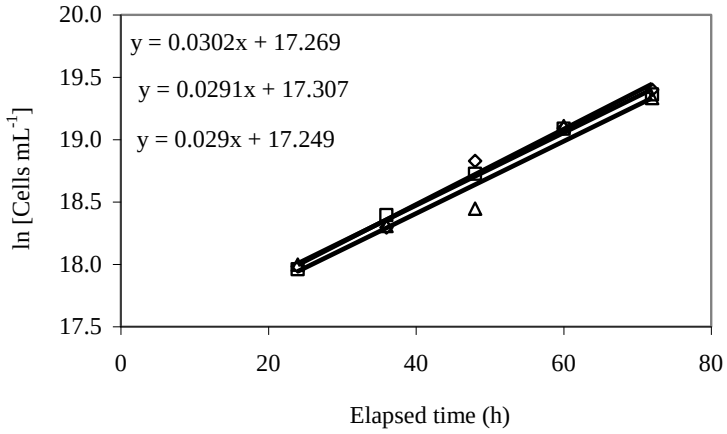
Specific growth rate (h^{-1})	
Trial 1	0.024
Trial 2	0.019
Trial 3	0.025
Average	0.022
STDEV	0.003
95% CI	0.003

Figure F.25. Specific growth rate calculations for Trial 1 (open circles), Trial 2 (open squares), and Trial 3 (open triangles).

Malate

Table F.56. BC13 growth in the presence of 5 μM malate.

	Cells mL^{-1}						ln (Cells mL^{-1})		
Elapsed Time (h)	Trial 1	Trial 2	Trial 3	Average	STDEV	95% CI	Trial 1	Trial 2	Trial 3
0	5.05E+07	5.23E+07	5.31E+07	5.20E+07	1.35E+06	1.53E+06	17.74	17.77	17.79
12	5.25E+07	5.14E+07	5.64E+07	5.34E+07	2.64E+06	2.99E+06	17.78	17.76	17.85
24	6.46E+07	6.30E+07	6.54E+07	6.43E+07	1.22E+06	1.38E+06	17.98	17.96	18.00
36	8.83E+07	9.75E+07	8.94E+07	9.17E+07	5.04E+06	5.71E+06	18.30	18.40	18.31
48	1.50E+08	1.36E+08	1.03E+08	1.30E+08	2.45E+07	2.77E+07	18.83	18.72	18.45
60	1.96E+08	1.95E+08	1.99E+08	1.96E+08	2.23E+06	2.52E+06	19.09	19.09	19.11
72	2.66E+08	2.56E+08	2.49E+08	2.57E+08	8.33E+06	9.43E+06	19.40	19.36	19.33
84	2.84E+08	2.84E+08	2.93E+08	2.87E+08	5.18E+06	5.86E+06	19.47	19.46	19.50
96	3.26E+08	3.20E+08	3.08E+08	3.18E+08	8.96E+06	1.01E+07	19.60	19.58	19.55
108	3.31E+08	2.93E+08	3.05E+08	3.09E+08	1.90E+07	2.16E+07	19.62	19.50	19.53
120	3.40E+08	3.27E+08	3.21E+08	3.30E+08	9.48E+06	1.07E+07	19.64	19.61	19.59



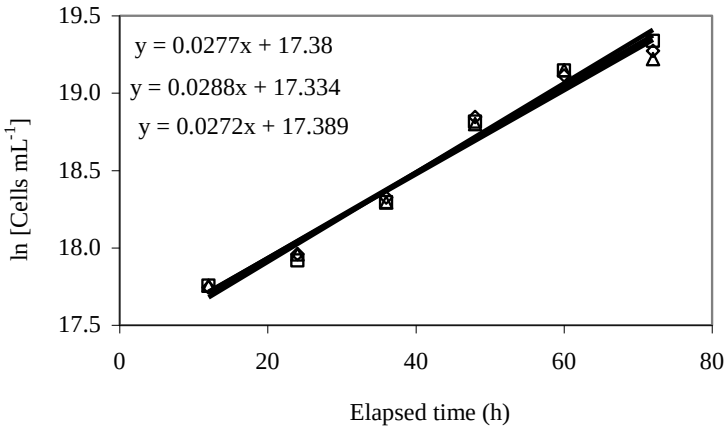
Specific growth rate (h^{-1})

Trial 1	0.030
Trial 2	0.029
Trial 3	0.029
Average	0.029
STDEV	0.001
95% CI	0.001

Figure F.26. Specific growth rate calculations for Trial 1 (open circles), Trial 2 (open squares), and Trial 3 (open triangles).

Table F.57. BC13 growth in the presence of 10 μM malate.

	Cells mL^{-1}						ln (Cells mL^{-1})		
Elapsed Time (h)	Trial 1	Trial 2	Trial 3	Average	STDEV	95% CI	Trial 1	Trial 2	Trial 3
0	5.03E+07	4.79E+07	5.00E+07	4.94E+07	1.30E+06	1.47E+06	17.73	17.69	17.73
12	5.08E+07	5.15E+07	5.14E+07	5.12E+07	3.71E+05	4.20E+05	17.74	17.76	17.76
24	6.30E+07	6.05E+07	6.29E+07	6.21E+07	1.44E+06	1.63E+06	17.96	17.92	17.96
36	9.08E+07	8.82E+07	8.80E+07	8.90E+07	1.59E+06	1.80E+06	18.32	18.30	18.29
48	1.53E+08	1.48E+08	1.46E+08	1.49E+08	3.47E+06	3.93E+06	18.85	18.82	18.80
60	2.00E+08	2.06E+08	2.07E+08	2.04E+08	3.94E+06	4.46E+06	19.11	19.15	19.15
72	2.34E+08	2.50E+08	2.23E+08	2.36E+08	1.37E+07	1.55E+07	19.27	19.34	19.22
84	2.49E+08	2.68E+08	2.41E+08	2.53E+08	1.39E+07	1.57E+07	19.33	19.41	19.30
96	2.55E+08	2.70E+08	2.42E+08	2.56E+08	1.39E+07	1.57E+07	19.36	19.41	19.31
108	2.44E+08	2.64E+08	2.40E+08	2.49E+08	1.30E+07	1.47E+07	19.31	19.39	19.30
120	2.27E+08	2.31E+08	2.39E+08	2.32E+08	6.20E+06	7.01E+06	19.24	19.26	19.29



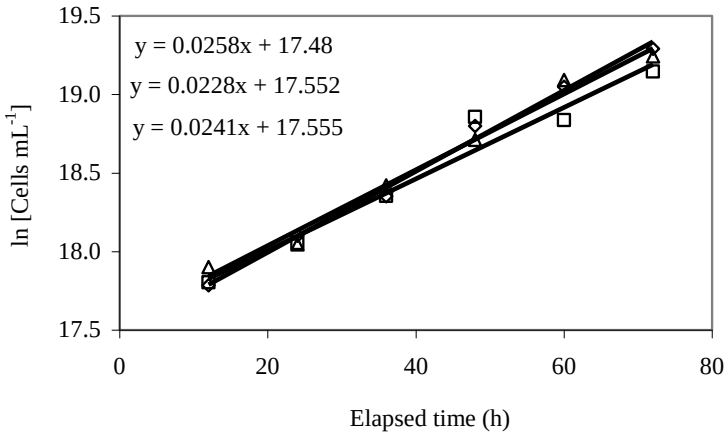
Specific growth rate (h^{-1})

Trial 1	0.028
Trial 2	0.029
Trial 3	0.027
Average	0.028
STDEV	0.001
95% CI	0.001

Figure F.27. Specific growth rate calculations for Trial 1 (open circles), Trial 2 (open squares), and Trial 3 (open triangles).

Table F.58. BC13 growth in the presence of 20 μM malate.

	Cells mL^{-1}						ln (Cells mL^{-1})		
Elapsed Time (h)	Trial 1	Trial 2	Trial 3	Average	STDEV	95% CI	Trial 1	Trial 2	Trial 3
0	4.98E+07	5.05E+07	5.24E+07	5.09E+07	1.34E+06	1.51E+06	17.72	17.74	17.78
12	5.30E+07	5.40E+07	5.95E+07	5.55E+07	3.52E+06	3.98E+06	17.78	17.80	17.90
24	7.26E+07	6.92E+07	6.88E+07	7.02E+07	2.10E+06	2.37E+06	18.10	18.05	18.05
36	9.34E+07	9.35E+07	1.00E+08	9.56E+07	3.76E+06	4.26E+06	18.35	18.35	18.42
48	1.46E+08	1.55E+08	1.34E+08	1.45E+08	1.05E+07	1.19E+07	18.80	18.86	18.71
60	1.88E+08	1.51E+08	1.96E+08	1.78E+08	2.35E+07	2.66E+07	19.05	18.84	19.09
72	2.39E+08	2.06E+08	2.28E+08	2.24E+08	1.65E+07	1.86E+07	19.29	19.15	19.24
84	2.57E+08	2.46E+08	2.36E+08	2.46E+08	1.04E+07	1.18E+07	19.36	19.32	19.28
96	2.45E+08	2.39E+08	2.53E+08	2.45E+08	7.16E+06	8.11E+06	19.32	19.29	19.35
108	2.40E+08	2.23E+08	2.24E+08	2.29E+08	9.39E+06	1.06E+07	19.30	19.22	19.23
120	2.18E+08	2.32E+08	2.39E+08	2.30E+08	1.07E+07	1.21E+07	19.20	19.26	19.29



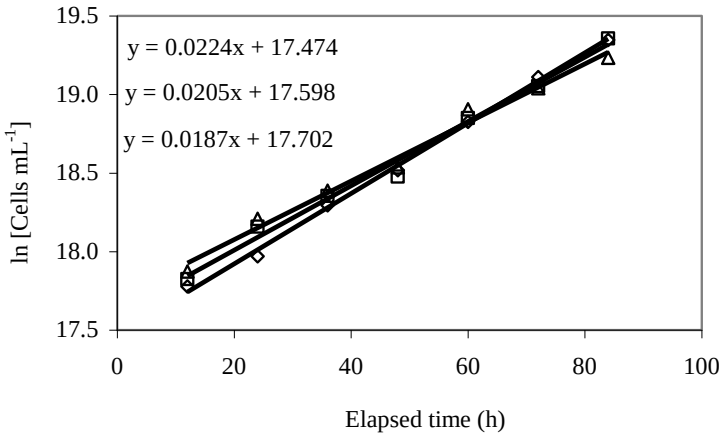
Specific growth rate (h^{-1})

Trial 1	0.026
Trial 2	0.023
Trial 3	0.024
Average	0.024
STDEV	0.002
95% CI	0.002

Figure F.28. Specific growth rate calculations for Trial 1 (open circles), Trial 2 (open squares), and Trial 3 (open triangles).

Table F.59. BC13 growth in the presence of 30 μM malate.

	Cells mL^{-1}						ln (Cells mL^{-1})		
Elapsed Time (h)	Trial 1	Trial 2	Trial 3	Average	STDEV	95% CI	Trial 1	Trial 2	Trial 3
0	5.56E+07	4.69E+07	5.19E+07	5.15E+07	4.40E+06	4.98E+06	17.83	17.66	17.77
12	5.25E+07	5.50E+07	5.78E+07	5.51E+07	2.62E+06	2.97E+06	17.78	17.82	17.87
24	6.37E+07	7.69E+07	8.09E+07	7.38E+07	9.02E+06	1.02E+07	17.97	18.16	18.21
36	8.81E+07	9.35E+07	9.67E+07	9.28E+07	4.35E+06	4.93E+06	18.29	18.35	18.39
48	1.10E+08	1.06E+08	1.12E+08	1.09E+08	3.28E+06	3.72E+06	18.52	18.48	18.54
60	1.50E+08	1.53E+08	1.62E+08	1.55E+08	6.44E+06	7.29E+06	18.82	18.85	18.90
72	1.99E+08	1.88E+08	1.86E+08	1.91E+08	7.30E+06	8.26E+06	19.11	19.05	19.04
84	2.53E+08	2.55E+08	2.25E+08	2.44E+08	1.64E+07	1.86E+07	19.35	19.36	19.23
96	2.33E+08	2.19E+08	2.24E+08	2.25E+08	6.87E+06	7.77E+06	19.26	19.20	19.23
108	2.45E+08	2.42E+08	2.37E+08	2.41E+08	4.01E+06	4.54E+06	19.32	19.30	19.29
120	2.26E+08	2.38E+08	2.43E+08	2.35E+08	8.74E+06	9.89E+06	19.23	19.29	19.31

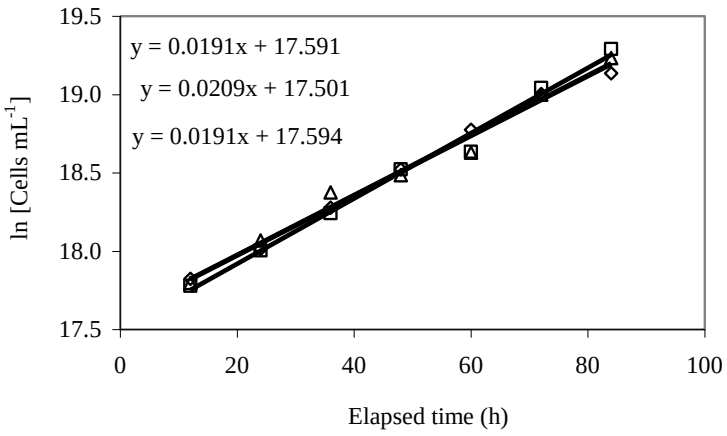


Specific growth rate (h^{-1})	
Trial 1	0.022
Trial 2	0.021
Trial 3	0.019
Average	0.021
STDEV	0.002
95% CI	0.002

Figure F.29. Specific growth rate calculations for Trial 1 (open circles), Trial 2 (open squares), and Trial 3 (open triangles).

Table F.60. BC13 growth in the presence of 50 μM malate.

	Cells mL^{-1}						ln (Cells mL^{-1})		
Elapsed Time (h)	Trial 1	Trial 2	Trial 3	Average	STDEV	95% CI	Trial 1	Trial 2	Trial 3
0	5.58E+07	5.44E+07	5.58E+07	5.53E+07	8.08E+05	9.14E+05	17.84	17.81	17.84
12	5.50E+07	5.26E+07	5.36E+07	5.37E+07	1.24E+06	1.40E+06	17.82	17.78	17.80
24	6.66E+07	6.60E+07	7.03E+07	6.76E+07	2.32E+06	2.62E+06	18.01	18.00	18.07
36	8.66E+07	8.37E+07	9.55E+07	8.86E+07	6.12E+06	6.93E+06	18.28	18.24	18.37
48	1.11E+08	1.11E+08	1.07E+08	1.09E+08	2.35E+06	2.66E+06	18.52	18.52	18.48
60	1.42E+08	1.24E+08	1.23E+08	1.30E+08	1.09E+07	1.24E+07	18.77	18.63	18.63
72	1.79E+08	1.86E+08	1.78E+08	1.81E+08	4.45E+06	5.04E+06	19.00	19.04	19.00
84	2.04E+08	2.39E+08	2.25E+08	2.23E+08	1.73E+07	1.95E+07	19.14	19.29	19.23
96	2.26E+08	2.30E+08	2.11E+08	2.23E+08	1.02E+07	1.16E+07	19.24	19.26	19.17
108	2.17E+08	2.04E+08	2.11E+08	2.11E+08	6.88E+06	7.78E+06	19.20	19.13	19.17
120	2.04E+08	1.95E+08	2.02E+08	2.00E+08	5.09E+06	5.76E+06	19.14	19.09	19.12



Specific growth rate (h^{-1})

Trial 1	0.019
Trial 2	0.021
Trial 3	0.019
Average	0.020
STDEV	0.001
95% CI	0.001

Figure F.30. Specific growth rate calculations for Trial 1 (open circles), Trial 2 (open squares), and Trial 3 (open triangles).

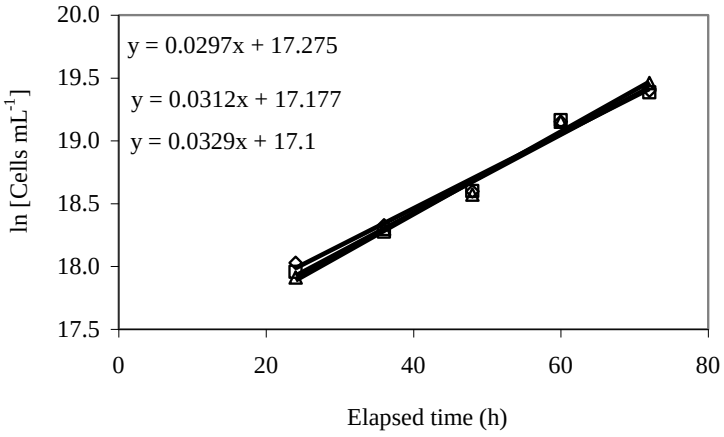
Toxicity of Organic Acids Following Pre-Adaptation through Subsequent Culturing

BC13 cell concentrations with time when grown in the presence of varying concentrations of different organic acids after pre-adaptation via subsequent culturing at the organic acid concentrations tested. Experiments were repeated in triplicate and average values, standard deviations (STDEV), and 95% confidence intervals (95% CI) are shown. Specific growth rates were calculated using linear regressions and are shown along with the corresponding STDEV and 95% CI to the right of the plots.

Pyruvate

Table F.61. BC13 growth in the presence of 5 μM pyruvate following pre-adaptation.

	Cells mL^{-1}						ln (Cells mL^{-1})		
Elapsed Time (h)	Trial 1	Trial 2	Trial 3	Average	STDEV	95% CI	Trial 1	Trial 2	Trial 3
0	6.20E+07	5.22E+07	5.22E+07	5.55E+07	5.64E+06	6.38E+06	17.94	17.77	17.77
12	6.35E+07	5.59E+07	5.52E+07	5.82E+07	4.62E+06	5.23E+06	17.97	17.84	17.83
24	6.76E+07	6.28E+07	6.01E+07	6.35E+07	3.76E+06	4.26E+06	18.03	17.96	17.91
36	9.11E+07	8.65E+07	8.86E+07	8.87E+07	2.27E+06	2.57E+06	18.33	18.28	18.30
48	1.19E+08	1.19E+08	1.16E+08	1.18E+08	1.78E+06	2.02E+06	18.60	18.60	18.57
60	2.08E+08	2.10E+08	2.08E+08	2.09E+08	1.50E+06	1.69E+06	19.15	19.16	19.15
72	2.66E+08	2.62E+08	2.83E+08	2.70E+08	1.08E+07	1.22E+07	19.40	19.39	19.46
84	2.84E+08	2.89E+08	2.85E+08	2.86E+08	2.73E+06	3.09E+06	19.47	19.48	19.47
96	3.06E+08	3.01E+08	3.01E+08	3.03E+08	2.68E+06	3.04E+06	19.54	19.52	19.52
108	3.06E+08	2.92E+08	2.83E+08	2.94E+08	1.11E+07	1.26E+07	19.54	19.49	19.46
120	3.13E+08	3.17E+08	3.06E+08	3.12E+08	5.78E+06	6.54E+06	19.56	19.58	19.54



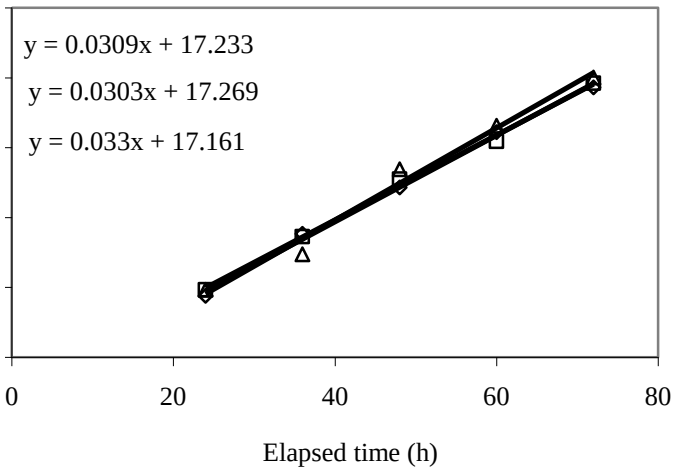
Specific growth rate (h^{-1})

Trial 1	0.030
Trial 2	0.031
Trial 3	0.033
Average	0.031
STDEV	0.002
95% CI	0.002

Figure F.31. Specific growth rate calculations for Trial 1 (open circles), Trial 2 (open squares), and Trial 3 (open triangles).

Table F.62. BC13 growth in the presence of 10 μM pyruvate following pre-adaptation.

	Cells mL^{-1}						ln (Cells mL^{-1})		
Elapsed Time (h)	Trial 1	Trial 2	Trial 3	Average	STDEV	95% CI	Trial 1	Trial 2	Trial 3
0	6.14E+08	5.88E+07	6.08E+07	2.45E+08	3.20E+08	3.62E+08	20.24	17.89	17.92
12	6.29E+07	6.22E+07	6.03E+07	6.18E+07	1.34E+06	1.52E+06	17.96	17.95	17.92
24	6.18E+07	6.45E+07	6.46E+07	6.36E+07	1.57E+06	1.77E+06	17.94	17.98	17.98
36	9.64E+07	9.43E+07	8.32E+07	9.13E+07	7.11E+06	8.05E+06	18.38	18.36	18.24
48	1.34E+08	1.42E+08	1.53E+08	1.43E+08	9.38E+06	1.06E+07	18.71	18.77	18.85
60	1.99E+08	1.87E+08	2.09E+08	1.98E+08	1.11E+07	1.25E+07	19.11	19.04	19.16
72	2.75E+08	2.83E+08	2.95E+08	2.84E+08	1.03E+07	1.16E+07	19.43	19.46	19.50
84	2.78E+08	2.70E+08	2.81E+08	2.76E+08	5.48E+06	6.20E+06	19.44	19.41	19.45
96	3.05E+08	3.05E+08	3.05E+08	3.05E+08	1.14E+05	1.29E+05	19.54	19.54	19.54
108	3.17E+08	3.13E+08	3.06E+08	3.12E+08	5.21E+06	5.89E+06	19.57	19.56	19.54
120	3.14E+08	3.11E+08	3.24E+08	3.16E+08	6.57E+06	7.43E+06	19.56	19.56	19.59



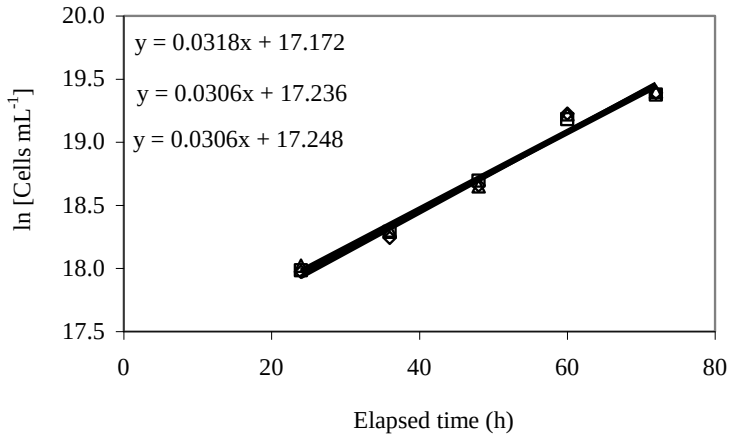
Specific growth rate (h^{-1})

Trial 1	0.031
Trial 2	0.030
Trial 3	0.033
Average	0.031
STDEV	0.001
95% CI	0.002

Figure F.32. Specific growth rate calculations for Trial 1 (open circles), Trial 2 (open squares), and Trial 3 (open triangles).

Table F.63. BC13 growth in the presence of 20 μM pyruvate following pre-adaptation.

	Cells mL^{-1}						ln (Cells mL^{-1})		
Elapsed Time (h)	Trial 1	Trial 2	Trial 3	Average	STDEV	95% CI	Trial 1	Trial 2	Trial 3
0	5.18E+07	5.31E+07	5.45E+07	5.31E+07	1.33E+06	1.51E+06	17.76	17.79	17.81
12	5.25E+07	5.31E+07	5.12E+07	5.23E+07	9.86E+05	1.12E+06	17.78	17.79	17.75
24	6.40E+07	6.47E+07	6.71E+07	6.53E+07	1.63E+06	1.84E+06	17.97	17.99	18.02
36	8.37E+07	8.77E+07	8.87E+07	8.67E+07	2.66E+06	3.00E+06	18.24	18.29	18.30
48	1.27E+08	1.31E+08	1.26E+08	1.28E+08	3.04E+06	3.44E+06	18.66	18.69	18.65
60	2.24E+08	2.14E+08	2.23E+08	2.20E+08	5.40E+06	6.11E+06	19.23	19.18	19.22
72	2.64E+08	2.60E+08	2.66E+08	2.63E+08	3.03E+06	3.43E+06	19.39	19.38	19.40
84	2.80E+08	2.89E+08	2.96E+08	2.88E+08	7.92E+06	8.96E+06	19.45	19.48	19.50
96	3.07E+08	3.07E+08	3.13E+08	3.09E+08	3.32E+06	3.76E+06	19.54	19.54	19.56
108	3.02E+08	3.17E+08	3.17E+08	3.12E+08	8.46E+06	9.57E+06	19.53	19.57	19.57
120	3.23E+08	3.37E+08	3.33E+08	3.31E+08	6.92E+06	7.83E+06	19.59	19.64	19.62



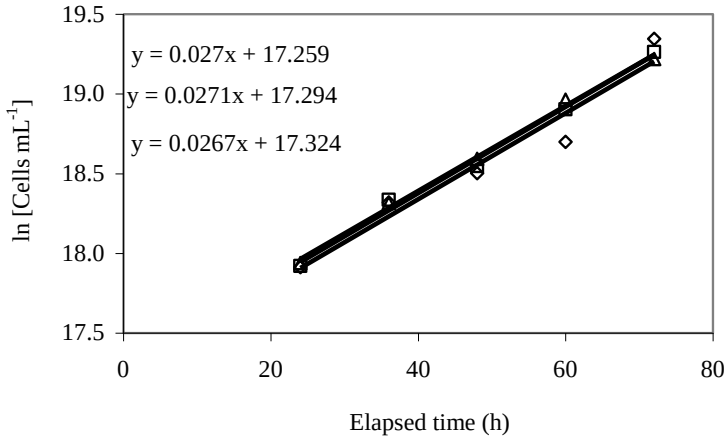
Specific growth rate (h^{-1})

Trial 1	0.031
Trial 2	0.032
Trial 3	0.033
Average	0.032
STDEV	0.001
95% CI	0.001

Figure F.33. Specific growth rate calculations for Trial 1 (open circles), Trial 2 (open squares), and Trial 3 (open triangles).

Table F.64. BC13 growth in the presence of 30 μM pyruvate following pre-adaptation.

	Cells mL^{-1}						ln (Cells mL^{-1})		
Elapsed Time (h)	Trial 1	Trial 2	Trial 3	Average	STDEV	95% CI	Trial 1	Trial 2	Trial 3
0	5.27E+07	5.32E+07	5.38E+07	5.32E+07	5.20E+05	5.89E+05	17.78	17.79	17.80
12	5.46E+07	5.72E+07	5.69E+07	5.63E+07	1.41E+06	1.59E+06	17.82	17.86	17.86
24	6.02E+07	6.07E+07	6.18E+07	6.09E+07	8.26E+05	9.35E+05	17.91	17.92	17.94
36	9.03E+07	9.19E+07	9.00E+07	9.07E+07	9.97E+05	1.13E+06	18.32	18.34	18.32
48	1.09E+08	1.13E+08	1.19E+08	1.14E+08	5.07E+06	5.74E+06	18.50	18.55	18.59
60	1.32E+08	1.62E+08	1.72E+08	1.55E+08	2.08E+07	2.36E+07	18.70	18.90	18.96
72	2.52E+08	2.32E+08	2.22E+08	2.35E+08	1.53E+07	1.73E+07	19.34	19.26	19.22
84	2.15E+08	2.12E+08	2.03E+08	2.10E+08	6.36E+06	7.19E+06	19.19	19.17	19.13
96	2.45E+08	2.39E+08	2.51E+08	2.45E+08	5.87E+06	6.65E+06	19.32	19.29	19.34
108	2.35E+08	2.44E+08	2.47E+08	2.42E+08	6.08E+06	6.89E+06	19.28	19.31	19.32
120	2.20E+08	2.15E+08	2.07E+08	2.14E+08	6.70E+06	7.58E+06	19.21	19.18	19.15

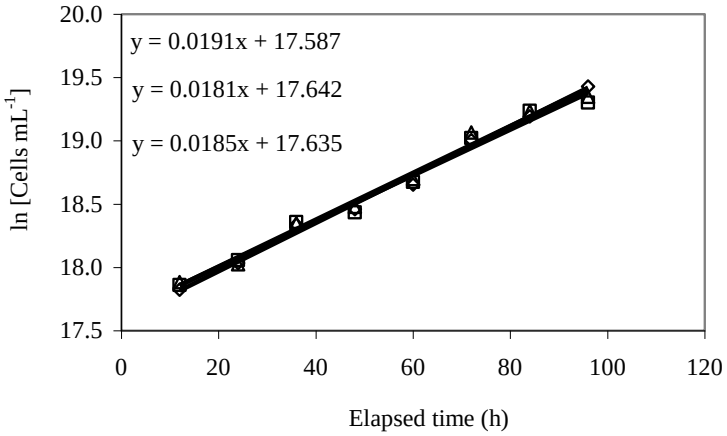


Specific growth rate (h^{-1})	
Trial 1	0.027
Trial 2	0.027
Trial 3	0.027
Average	0.027
STDEV	0.000
95% CI	0.000

Figure F.34. Specific growth rate calculations for Trial 1 (open circles), Trial 2 (open squares), and Trial 3 (open triangles).

Table F.65. BC13 growth in the presence of 50 μM pyruvate following pre-adaptation.

	Cells mL^{-1}						ln (Cells mL^{-1})		
Elapsed Time (h)	Trial 1	Trial 2	Trial 3	Average	STDEV	95% CI	Trial 1	Trial 2	Trial 3
0	5.38E+07	5.36E+07	5.63E+07	5.46E+07	1.49E+06	1.69E+06	17.80	17.80	17.85
12	5.51E+07	5.71E+07	5.84E+07	5.69E+07	1.71E+06	1.93E+06	17.82	17.86	17.88
24	6.79E+07	6.96E+07	6.73E+07	6.83E+07	1.17E+06	1.33E+06	18.03	18.06	18.02
36	9.20E+07	9.38E+07	9.32E+07	9.30E+07	9.32E+05	1.05E+06	18.34	18.36	18.35
48	1.04E+08	1.01E+08	1.06E+08	1.04E+08	2.34E+06	2.65E+06	18.46	18.43	18.48
60	1.26E+08	1.29E+08	1.32E+08	1.29E+08	2.78E+06	3.14E+06	18.65	18.67	18.70
72	1.79E+08	1.83E+08	1.90E+08	1.84E+08	5.69E+06	6.44E+06	19.01	19.02	19.06
84	2.17E+08	2.26E+08	2.26E+08	2.23E+08	5.42E+06	6.14E+06	19.19	19.24	19.23
96	2.74E+08	2.41E+08	2.53E+08	2.56E+08	1.67E+07	1.89E+07	19.43	19.30	19.35
108	2.40E+08	2.50E+08	2.44E+08	2.45E+08	5.32E+06	6.01E+06	19.29	19.34	19.31
120	2.28E+08	2.30E+08	2.34E+08	2.30E+08	2.92E+06	3.30E+06	19.24	19.25	19.27



Specific growth rate (h^{-1})

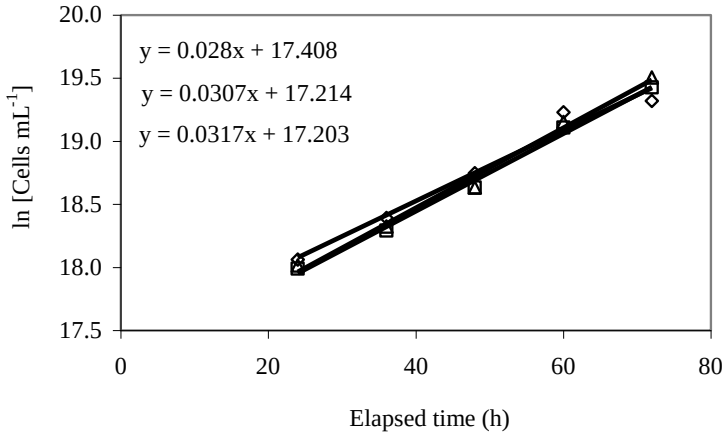
Trial 1	0.019
Trial 2	0.018
Trial 3	0.019
Average	0.019
STDEV	0.001
95% CI	0.001

Figure F.35. Specific growth rate calculations for Trial 1 (open circles), Trial 2 (open squares), and Trial 3 (open triangles).

Acetate

Table F.66. BC13 growth in the presence of 5 μM acetate following pre-adaptation.

	Cells mL^{-1}						ln (Cells mL^{-1})		
Elapsed Time (h)	Trial 1	Trial 2	Trial 3	Average	STDEV	95% CI	Trial 1	Trial 2	Trial 3
0	5.50E+07	5.01E+07	5.05E+07	5.19E+07	2.71E+06	3.07E+06	17.82	17.73	17.74
12	5.74E+07	5.46E+07	5.26E+07	5.49E+07	2.42E+06	2.74E+06	17.87	17.82	17.78
24	6.99E+07	6.50E+07	6.67E+07	6.72E+07	2.44E+06	2.77E+06	18.06	17.99	18.02
36	9.71E+07	8.79E+07	9.07E+07	9.19E+07	4.71E+06	5.33E+06	18.39	18.29	18.32
48	1.38E+08	1.24E+08	1.24E+08	1.29E+08	8.58E+06	9.71E+06	18.75	18.63	18.63
60	2.25E+08	1.99E+08	2.08E+08	2.11E+08	1.31E+07	1.48E+07	19.23	19.11	19.15
72	2.46E+08	2.74E+08	2.96E+08	2.72E+08	2.50E+07	2.83E+07	19.32	19.43	19.51
84	2.99E+08	2.79E+08	2.72E+08	2.83E+08	1.44E+07	1.63E+07	19.52	19.45	19.42
96	3.28E+08	2.99E+08	2.99E+08	3.08E+08	1.67E+07	1.89E+07	19.61	19.52	19.51
108	3.32E+08	3.04E+08	3.18E+08	3.18E+08	1.37E+07	1.55E+07	19.62	19.53	19.58
120	3.46E+08	3.27E+08	3.32E+08	3.35E+08	9.69E+06	1.10E+07	19.66	19.61	19.62



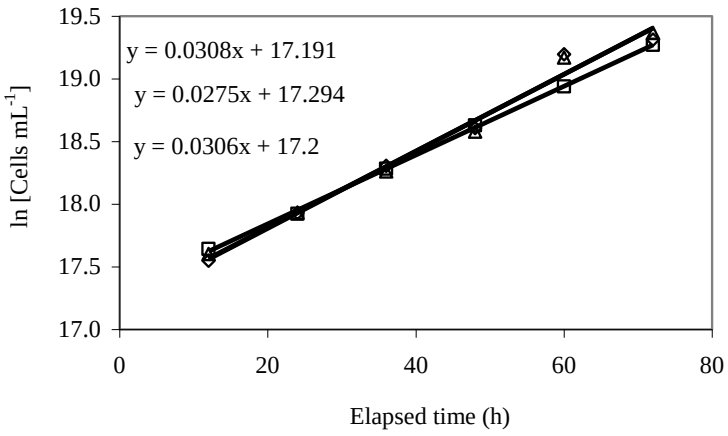
Specific growth rate (h^{-1})

Trial 1	0.028
Trial 2	0.031
Trial 3	0.032
Average	0.030
STDEV	0.002
95% CI	0.002

Figure F.36. Specific growth rate calculations for Trial 1 (open circles), Trial 2 (open squares), and Trial 3 (open triangles).

Table F.67. BC13 growth in the presence of 10 μM acetate following pre-adaptation.

	Cells mL^{-1}						ln (Cells mL^{-1})		
Elapsed Time (h)	Trial 1	Trial 2	Trial 3	Average	STDEV	95% CI	Trial 1	Trial 2	Trial 3
0	4.48E+07	4.49E+07	4.48E+07	4.48E+07	3.42E+04	3.87E+04	17.62	17.62	17.62
12	4.18E+07	4.59E+07	4.41E+07	4.40E+07	2.08E+06	2.35E+06	17.55	17.64	17.60
24	6.11E+07	6.08E+07	6.14E+07	6.11E+07	3.01E+05	3.40E+05	17.93	17.92	17.93
36	8.91E+07	8.71E+07	8.54E+07	8.72E+07	1.85E+06	2.10E+06	18.31	18.28	18.26
48	1.21E+08	1.23E+08	1.17E+08	1.20E+08	2.92E+06	3.30E+06	18.61	18.63	18.58
60	2.17E+08	1.68E+08	2.12E+08	1.99E+08	2.70E+07	3.06E+07	19.20	18.94	19.17
72	2.44E+08	2.34E+08	2.58E+08	2.45E+08	1.19E+07	1.34E+07	19.31	19.27	19.37
84	2.73E+08	2.55E+08	2.76E+08	2.68E+08	1.17E+07	1.32E+07	19.42	19.36	19.44
96	2.97E+08	2.61E+08	2.84E+08	2.80E+08	1.82E+07	2.06E+07	19.51	19.38	19.46
108	3.13E+08	2.55E+08	3.03E+08	2.90E+08	3.08E+07	3.49E+07	19.56	19.36	19.53
120	3.08E+08	2.90E+08	3.07E+08	3.01E+08	1.02E+07	1.15E+07	19.55	19.48	19.54



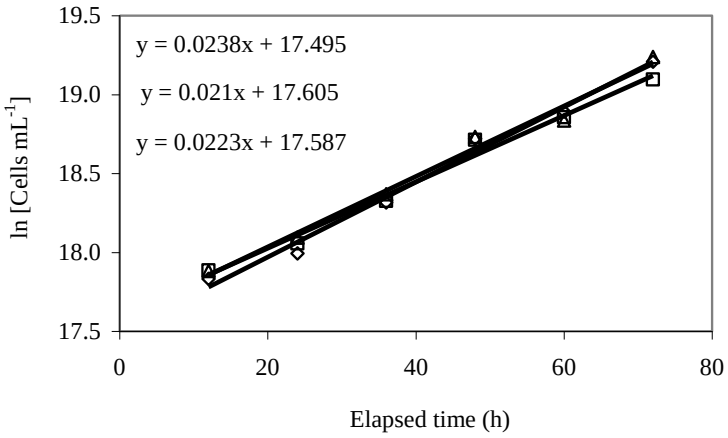
Specific growth rate (h^{-1})

Trial 1	0.031
Trial 2	0.028
Trial 3	0.031
Average	0.030
STDEV	0.002
95% CI	0.002

Figure F.37. Specific growth rate calculations for Trial 1 (open circles), Trial 2 (open squares), and Trial 3 (open triangles).

Table F.68. BC13 growth in the presence of 20 μM acetate following pre-adaptation.

	Cells mL^{-1}						ln (Cells mL^{-1})		
Elapsed Time (h)	Trial 1	Trial 2	Trial 3	Average	STDEV	95% CI	Trial 1	Trial 2	Trial 3
0	5.45E+07	5.51E+07	5.60E+07	5.52E+07	7.70E+05	8.71E+05	17.81	17.82	17.84
12	5.55E+07	5.86E+07	5.84E+07	5.75E+07	1.73E+06	1.96E+06	17.83	17.89	17.88
24	6.52E+07	6.95E+07	7.21E+07	6.89E+07	3.47E+06	3.93E+06	17.99	18.06	18.09
36	9.01E+07	9.09E+07	9.48E+07	9.19E+07	2.54E+06	2.88E+06	18.32	18.32	18.37
48	1.35E+08	1.34E+08	1.36E+08	1.35E+08	1.30E+06	1.47E+06	18.72	18.71	18.73
60	1.60E+08	1.55E+08	1.52E+08	1.55E+08	4.34E+06	4.91E+06	18.89	18.86	18.84
72	2.20E+08	1.97E+08	2.27E+08	2.14E+08	1.58E+07	1.79E+07	19.21	19.10	19.24
84	2.75E+08	2.79E+08	2.67E+08	2.73E+08	6.10E+06	6.91E+06	19.43	19.45	19.40
96	2.99E+08	3.03E+08	3.17E+08	3.06E+08	9.40E+06	1.06E+07	19.52	19.53	19.57
108	3.04E+08	2.92E+08	2.79E+08	2.92E+08	1.26E+07	1.42E+07	19.53	19.49	19.45
120	3.02E+08	3.04E+08	3.29E+08	3.11E+08	1.50E+07	1.69E+07	19.52	19.53	19.61



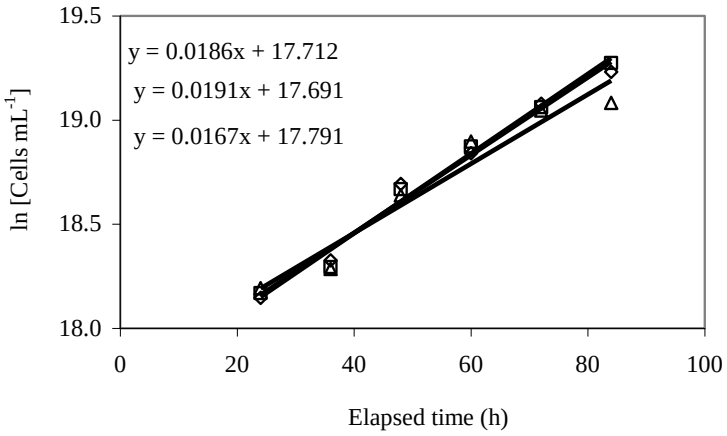
Specific growth rate (h^{-1})

Trial 1	0.024
Trial 2	0.021
Trial 3	0.022
Average	0.022
STDEV	0.001
95% CI	0.002

Figure F.38. Specific growth rate calculations for Trial 1 (open circles), Trial 2 (open squares), and Trial 3 (open triangles).

Table F.69. BC13 growth in the presence of 30 μM acetate following pre-adaptation.

	Cells mL^{-1}						ln (Cells mL^{-1})		
Elapsed Time (h)	Trial 1	Trial 2	Trial 3	Average	STDEV	95% CI	Trial 1	Trial 2	Trial 3
0	5.92E+07	6.07E+07	6.22E+07	6.07E+07	1.48E+06	1.67E+06	17.90	17.92	17.95
12	6.84E+07	7.04E+07	7.00E+07	6.96E+07	1.04E+06	1.18E+06	18.04	18.07	18.06
24	7.60E+07	7.77E+07	7.96E+07	7.78E+07	1.80E+06	2.03E+06	18.15	18.17	18.19
36	9.10E+07	8.81E+07	8.73E+07	8.88E+07	1.91E+06	2.16E+06	18.33	18.29	18.28
48	1.31E+08	1.28E+08	1.24E+08	1.28E+08	3.52E+06	3.98E+06	18.69	18.67	18.64
60	1.52E+08	1.57E+08	1.61E+08	1.57E+08	4.43E+06	5.01E+06	18.84	18.87	18.90
72	1.93E+08	1.90E+08	1.87E+08	1.90E+08	3.02E+06	3.42E+06	19.08	19.06	19.05
84	2.25E+08	2.35E+08	1.94E+08	2.18E+08	2.13E+07	2.41E+07	19.23	19.27	19.08
96	2.90E+08	2.97E+08	3.03E+08	2.97E+08	6.13E+06	6.93E+06	19.49	19.51	19.53
108	2.89E+08	2.93E+08	2.90E+08	2.91E+08	2.27E+06	2.57E+06	19.48	19.50	19.48
120	2.90E+08	2.91E+08	2.81E+08	2.87E+08	5.81E+06	6.58E+06	19.49	19.49	19.45



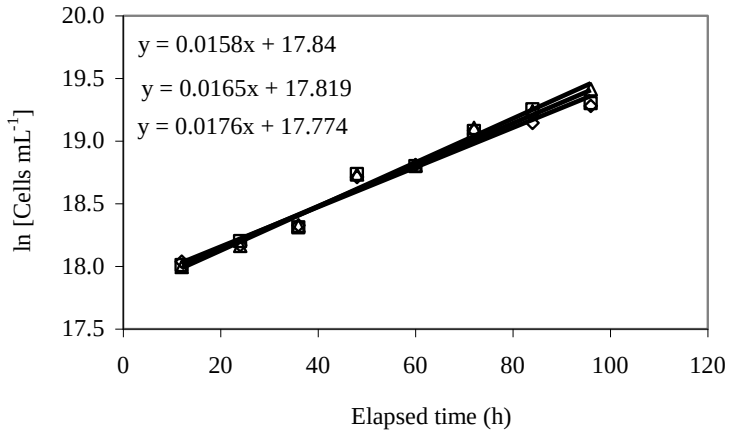
Specific growth rate (h^{-1})

Trial 1	0.019
Trial 2	0.019
Trial 3	0.017
Average	0.018
STDEV	0.001
95% CI	0.001

Figure F.39. Specific growth rate calculations for Trial 1 (open circles), Trial 2 (open squares), and Trial 3 (open triangles).

Table F.70. BC13 growth in the presence of 50 μM acetate following pre-adaptation.

	Cells mL^{-1}						ln (Cells mL^{-1})		
Elapsed Time (h)	Trial 1	Trial 2	Trial 3	Average	STDEV	95% CI	Trial 1	Trial 2	Trial 3
0	5.51E+07	5.92E+07	5.72E+07	5.72E+07	2.07E+06	2.35E+06	17.82	17.90	17.86
12	6.81E+07	6.63E+07	6.54E+07	6.66E+07	1.38E+06	1.56E+06	18.04	18.01	18.00
24	7.76E+07	8.03E+07	7.74E+07	7.85E+07	1.62E+06	1.84E+06	18.17	18.20	18.16
36	9.10E+07	8.97E+07	9.09E+07	9.05E+07	7.36E+05	8.33E+05	18.33	18.31	18.33
48	1.34E+08	1.37E+08	1.37E+08	1.36E+08	1.60E+06	1.81E+06	18.71	18.73	18.73
60	1.47E+08	1.46E+08	1.47E+08	1.47E+08	6.54E+05	7.41E+05	18.81	18.80	18.81
72	1.94E+08	1.93E+08	1.98E+08	1.95E+08	2.61E+06	2.96E+06	19.08	19.08	19.10
84	2.07E+08	2.30E+08	2.27E+08	2.21E+08	1.26E+07	1.43E+07	19.15	19.25	19.24
96	2.36E+08	2.41E+08	2.70E+08	2.49E+08	1.83E+07	2.07E+07	19.28	19.30	19.41
108	2.36E+08	2.76E+08	2.86E+08	2.66E+08	2.64E+07	2.99E+07	19.28	19.44	19.47
120	2.41E+08	2.85E+08	2.89E+08	2.71E+08	2.67E+07	3.02E+07	19.30	19.47	19.48



Specific growth rate (h^{-1})

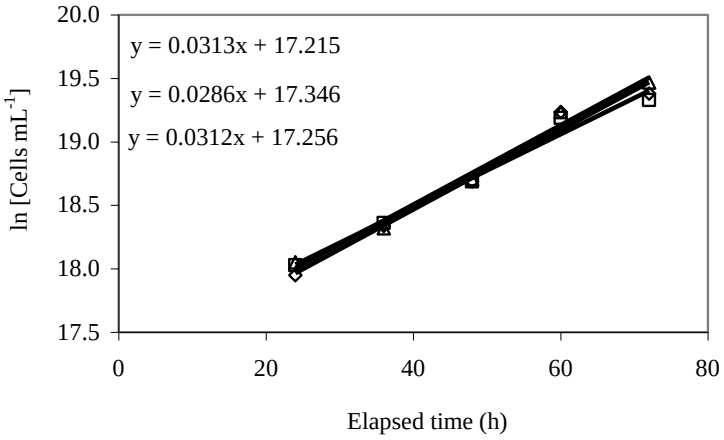
Trial 1	0.016
Trial 2	0.017
Trial 3	0.018
Average	0.017
STDEV	0.001
95% CI	0.001

Figure F.40. Specific growth rate calculations for Trial 1 (open circles), Trial 2 (open squares), and Trial 3 (open triangles).

Citrate

Table F.71. BC13 growth in the presence of 5 μM citrate following pre-adaptation.

	Cells mL^{-1}						ln (Cells mL^{-1})		
Elapsed Time (h)	Trial 1	Trial 2	Trial 3	Average	STDEV	95% CI	Trial 1	Trial 2	Trial 3
0	6.10E+06	6.20E+06	5.80E+06	6.03E+06	2.07E+05	2.35E+05	15.62	15.64	15.57
12	5.90E+07	5.87E+07	5.96E+07	5.91E+07	4.40E+05	4.98E+05	17.89	17.89	17.90
24	6.25E+07	6.75E+07	6.90E+07	6.63E+07	3.43E+06	3.89E+06	17.95	18.03	18.05
36	9.20E+07	9.41E+07	9.04E+07	9.21E+07	1.83E+06	2.07E+06	18.34	18.36	18.32
48	1.30E+08	1.31E+08	1.33E+08	1.31E+08	1.48E+06	1.68E+06	18.69	18.69	18.71
60	2.26E+08	2.15E+08	2.26E+08	2.22E+08	6.02E+06	6.81E+06	19.23	19.19	19.23
72	2.61E+08	2.48E+08	2.85E+08	2.64E+08	1.88E+07	2.12E+07	19.38	19.33	19.47
84	2.90E+08	3.02E+08	2.95E+08	2.96E+08	5.85E+06	6.62E+06	19.49	19.53	19.50
96	3.21E+08	3.22E+08	3.09E+08	3.17E+08	6.88E+06	7.79E+06	19.59	19.59	19.55
108	3.22E+08	3.32E+08	3.30E+08	3.28E+08	5.60E+06	6.33E+06	19.59	19.62	19.61
120	3.25E+08	3.13E+08	3.04E+08	3.14E+08	1.04E+07	1.18E+07	19.60	19.56	19.53



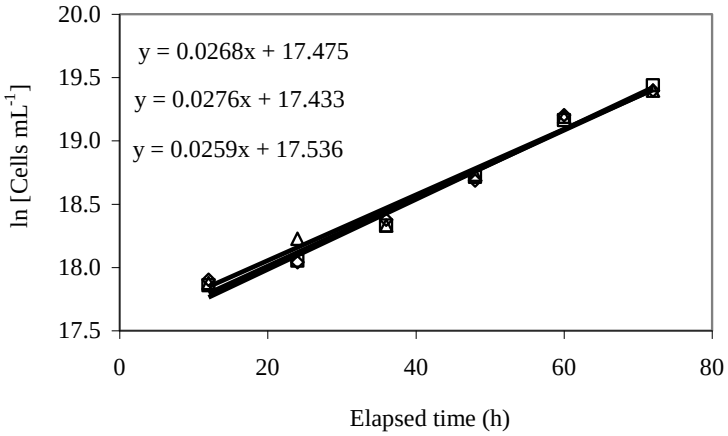
Specific growth rate (h^{-1})

Trial 1	0.031
Trial 2	0.029
Trial 3	0.031
Average	0.030
STDEV	0.002
95% CI	0.002

Figure F.41. Specific growth rate calculations for Trial 1 (open circles), Trial 2 (open squares), and Trial 3 (open triangles).

Table F.72. BC13 growth in the presence of 10 μM citrate following pre-adaptation.

	Cells mL^{-1}						ln (Cells mL^{-1})		
Elapsed Time (h)	Trial 1	Trial 2	Trial 3	Average	STDEV	95% CI	Trial 1	Trial 2	Trial 3
0	5.99E+06	5.70E+06	5.55E+06	5.75E+06	2.22E+05	2.51E+05	15.61	15.56	15.53
12	5.96E+07	5.71E+07	5.81E+07	5.82E+07	1.29E+06	1.46E+06	17.90	17.86	17.88
24	6.84E+07	6.93E+07	8.23E+07	7.33E+07	7.80E+06	8.82E+06	18.04	18.05	18.23
36	9.58E+07	9.14E+07	9.13E+07	9.28E+07	2.56E+06	2.90E+06	18.38	18.33	18.33
48	1.30E+08	1.34E+08	1.37E+08	1.34E+08	3.13E+06	3.54E+06	18.69	18.71	18.73
60	2.19E+08	2.10E+08	2.16E+08	2.15E+08	4.43E+06	5.01E+06	19.20	19.16	19.19
72	2.65E+08	2.77E+08	2.65E+08	2.69E+08	6.59E+06	7.46E+06	19.40	19.44	19.40
84	2.79E+08	2.65E+08	2.64E+08	2.69E+08	8.24E+06	9.32E+06	19.45	19.40	19.39
96	3.28E+08	3.32E+08	3.29E+08	3.30E+08	2.06E+06	2.34E+06	19.61	19.62	19.61
108	3.24E+08	3.18E+08	3.03E+08	3.15E+08	1.05E+07	1.19E+07	19.60	19.58	19.53
120	3.34E+08	3.43E+08	3.30E+08	3.36E+08	6.64E+06	7.51E+06	19.63	19.65	19.61



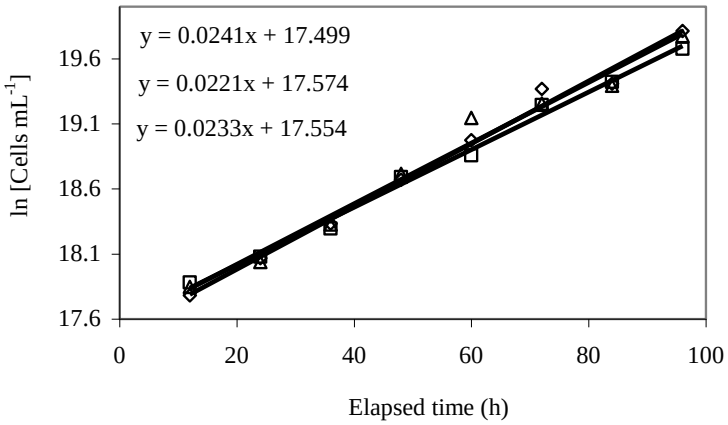
Specific growth rate (h^{-1})

Trial 1	0.027
Trial 2	0.028
Trial 3	0.026
Average	0.027
STDEV	0.001
95% CI	0.001

Figure F.42. Specific growth rate calculations for Trial 1 (open circles), Trial 2 (open squares), and Trial 3 (open triangles).

Table F.73. BC13 growth in the presence of 20 μM citrate following pre-adaptation.

	Cells mL^{-1}						ln (Cells mL^{-1})		
Elapsed Time (h)	Trial 1	Trial 2	Trial 3	Average	STDEV	95% CI	Trial 1	Trial 2	Trial 3
0	6.18E+06	6.05E+06	6.33E+06	6.19E+06	1.39E+05	1.57E+05	15.64	15.62	15.66
12	5.28E+07	5.83E+07	5.63E+07	5.58E+07	2.76E+06	3.12E+06	17.78	17.88	17.85
24	7.03E+07	7.10E+07	6.82E+07	6.98E+07	1.46E+06	1.65E+06	18.07	18.08	18.04
36	9.16E+07	8.83E+07	9.11E+07	9.03E+07	1.79E+06	2.02E+06	18.33	18.30	18.33
48	1.28E+08	1.31E+08	1.34E+08	1.31E+08	2.88E+06	3.26E+06	18.67	18.69	18.71
60	1.74E+08	1.55E+08	2.07E+08	1.78E+08	2.61E+07	2.96E+07	18.97	18.86	19.15
72	2.58E+08	2.28E+08	2.31E+08	2.39E+08	1.67E+07	1.89E+07	19.37	19.24	19.26
84	2.69E+08	2.72E+08	2.64E+08	2.69E+08	4.01E+06	4.54E+06	19.41	19.42	19.39
96	4.02E+08	3.51E+08	3.87E+08	3.80E+08	2.65E+07	3.00E+07	19.81	19.68	19.77
108	3.14E+08	3.26E+08	3.19E+08	3.20E+08	5.97E+06	6.76E+06	19.57	19.60	19.58
120	3.25E+08	3.13E+08	3.28E+08	3.22E+08	7.77E+06	8.79E+06	19.60	19.56	19.61

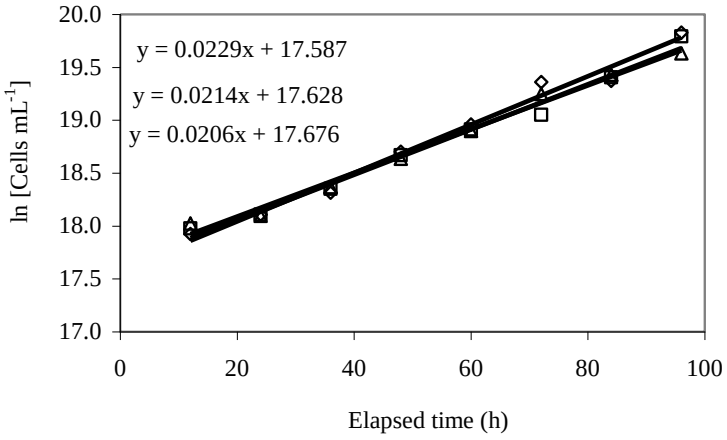


Specific growth rate (h^{-1})	
Trial 1	0.024
Trial 2	0.022
Trial 3	0.023
Average	0.023
STDEV	0.001
95% CI	0.001

Figure F.43. Specific growth rate calculations for Trial 1 (open circles), Trial 2 (open squares), and Trial 3 (open triangles).

Table F.74. BC13 growth in the presence of 30 μM citrate following pre-adaptation.

	Cells mL^{-1}						ln (Cells mL^{-1})		
Elapsed Time (h)	Trial 1	Trial 2	Trial 3	Average	STDEV	95% CI	Trial 1	Trial 2	Trial 3
0	6.05E+06	6.27E+06	6.35E+06	6.22E+06	1.55E+05	1.75E+05	15.62	15.65	15.66
12	6.09E+07	6.41E+07	6.73E+07	6.41E+07	3.21E+06	3.64E+06	17.92	17.98	18.02
24	7.32E+07	7.30E+07	7.23E+07	7.28E+07	4.72E+05	5.34E+05	18.11	18.11	18.10
36	9.00E+07	9.31E+07	9.47E+07	9.26E+07	2.37E+06	2.68E+06	18.32	18.35	18.37
48	1.32E+08	1.28E+08	1.24E+08	1.28E+08	4.16E+06	4.70E+06	18.70	18.67	18.64
60	1.71E+08	1.63E+08	1.61E+08	1.65E+08	5.34E+06	6.05E+06	18.96	18.91	18.90
72	2.56E+08	1.88E+08	2.28E+08	2.24E+08	3.43E+07	3.89E+07	19.36	19.05	19.25
84	2.59E+08	2.68E+08	2.74E+08	2.67E+08	7.69E+06	8.70E+06	19.37	19.40	19.43
96	4.09E+08	3.94E+08	3.35E+08	3.80E+08	3.90E+07	4.41E+07	19.83	19.79	19.63
108	3.05E+08	3.19E+08	3.14E+08	3.13E+08	7.49E+06	8.48E+06	19.53	19.58	19.57
120	3.22E+08	3.35E+08	3.43E+08	3.33E+08	1.05E+07	1.18E+07	19.59	19.63	19.65

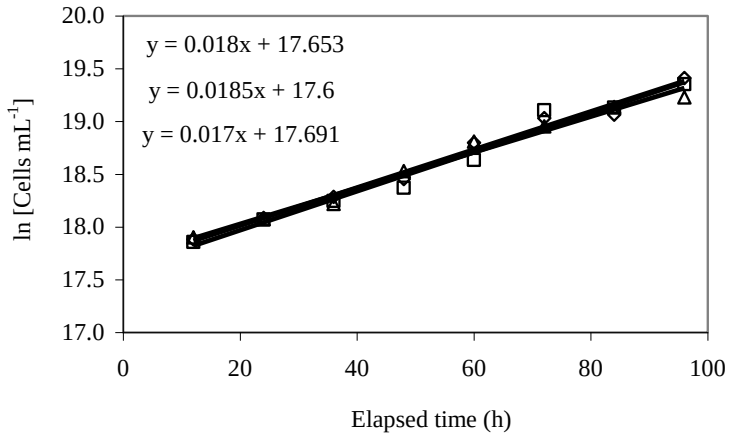


Specific growth rate (h^{-1})	
Trial 1	0.023
Trial 2	0.021
Trial 3	0.021
Average	0.022
STDEV	0.001
95% CI	0.001

Figure F.44. Specific growth rate calculations for Trial 1 (open circles), Trial 2 (open squares), and Trial 3 (open triangles).

Table F.75. BC13 growth in the presence of 50 μM citrate following pre-adaptation.

	Cells mL^{-1}						ln (Cells mL^{-1})		
Elapsed Time (h)	Trial 1	Trial 2	Trial 3	Average	STDEV	95% CI	Trial 1	Trial 2	Trial 3
0	6.30E+06	6.15E+06	6.42E+06	6.29E+06	1.38E+05	1.56E+05	15.66	15.63	15.68
12	5.84E+07	5.70E+07	5.95E+07	5.83E+07	1.24E+06	1.40E+06	17.88	17.86	17.90
24	7.15E+07	7.06E+07	7.07E+07	7.09E+07	5.22E+05	5.91E+05	18.09	18.07	18.07
36	8.73E+07	8.40E+07	8.18E+07	8.44E+07	2.77E+06	3.14E+06	18.28	18.25	18.22
48	1.03E+08	9.52E+07	1.11E+08	1.03E+08	8.12E+06	9.19E+06	18.45	18.37	18.53
60	1.46E+08	1.24E+08	1.47E+08	1.39E+08	1.33E+07	1.50E+07	18.80	18.63	18.81
72	1.84E+08	1.99E+08	1.70E+08	1.84E+08	1.41E+07	1.59E+07	19.03	19.11	18.95
84	1.90E+08	2.04E+08	2.04E+08	1.99E+08	7.96E+06	9.01E+06	19.06	19.13	19.14
96	2.69E+08	2.54E+08	2.24E+08	2.49E+08	2.29E+07	2.59E+07	19.41	19.35	19.23
108	2.80E+08	2.61E+08	2.70E+08	2.70E+08	9.34E+06	1.06E+07	19.45	19.38	19.41
120	2.80E+08	2.51E+08	2.69E+08	2.67E+08	1.47E+07	1.66E+07	19.45	19.34	19.41



Specific growth rate (h^{-1})

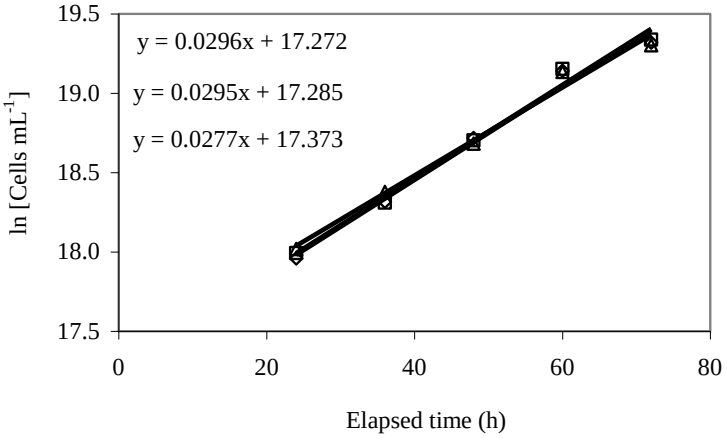
Trial 1	0.018
Trial 2	0.019
Trial 3	0.017
Average	0.018
STDEV	0.001
95% CI	0.001

Figure F.45. Specific growth rate calculations for Trial 1 (open circles), Trial 2 (open squares), and Trial 3 (open triangles).

2-ketoglutarate

Table F.76. BC13 growth in the presence of 5 μM 2-ketoglutarate following pre-adaptation.

	Cells mL^{-1}						ln (Cells mL^{-1})		
Elapsed Time (h)	Trial 1	Trial 2	Trial 3	Average	STDEV	95% CI	Trial 1	Trial 2	Trial 3
0	5.40E+07	5.65E+07	5.42E+07	5.49E+07	1.41E+06	1.59E+06	17.80	17.85	17.81
12	5.95E+07	6.03E+07	6.00E+07	5.99E+07	3.91E+05	4.42E+05	17.90	17.91	17.91
24	6.31E+07	6.51E+07	6.68E+07	6.50E+07	1.89E+06	2.14E+06	17.96	17.99	18.02
36	9.01E+07	8.95E+07	9.59E+07	9.18E+07	3.51E+06	3.98E+06	18.32	18.31	18.38
48	1.34E+08	1.33E+08	1.30E+08	1.32E+08	2.23E+06	2.53E+06	18.72	18.70	18.68
60	2.06E+08	2.08E+08	2.04E+08	2.06E+08	1.93E+06	2.18E+06	19.14	19.15	19.13
72	2.46E+08	2.50E+08	2.42E+08	2.46E+08	4.26E+06	4.82E+06	19.32	19.34	19.30
84	2.64E+08	2.62E+08	2.49E+08	2.58E+08	8.08E+06	9.14E+06	19.39	19.38	19.33
96	2.96E+08	2.88E+08	2.85E+08	2.89E+08	5.41E+06	6.13E+06	19.50	19.48	19.47
108	3.21E+08	3.25E+08	3.29E+08	3.25E+08	4.23E+06	4.79E+06	19.59	19.60	19.61
120	3.30E+08	3.29E+08	3.24E+08	3.28E+08	3.35E+06	3.79E+06	19.61	19.61	19.60



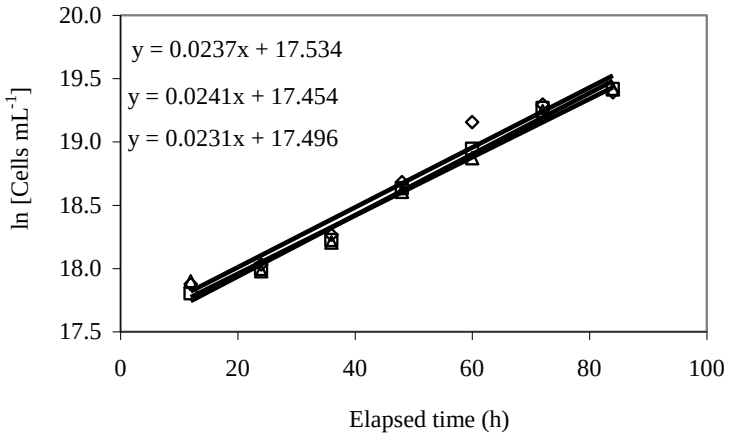
Specific growth rate (h^{-1})

Trial 1	0.030
Trial 2	0.030
Trial 3	0.028
Average	0.029
STDEV	0.001
95% CI	0.001

Figure F.46. Specific growth rate calculations for Trial 1 (open circles), Trial 2 (open squares), and Trial 3 (open triangles).

Table F.77. BC13 growth in the presence of 10 μM 2-ketoglutarate following pre-adaptation.

	Cells mL^{-1}						ln (Cells mL^{-1})		
Elapsed Time (h)	Trial 1	Trial 2	Trial 3	Average	STDEV	95% CI	Trial 1	Trial 2	Trial 3
0	5.63E+07	5.56E+07	5.74E+07	5.64E+07	9.11E+05	1.03E+06	17.85	17.83	17.87
12	5.81E+07	5.39E+07	5.93E+07	5.71E+07	2.85E+06	3.22E+06	17.88	17.80	17.90
24	6.77E+07	6.53E+07	6.43E+07	6.58E+07	1.79E+06	2.02E+06	18.03	18.00	17.98
36	8.57E+07	8.22E+07	8.06E+07	8.28E+07	2.58E+06	2.92E+06	18.27	18.22	18.21
48	1.30E+08	1.24E+08	1.20E+08	1.25E+08	4.76E+06	5.39E+06	18.68	18.63	18.61
60	2.09E+08	1.69E+08	1.57E+08	1.78E+08	2.71E+07	3.07E+07	19.16	18.95	18.87
72	2.40E+08	2.33E+08	2.27E+08	2.33E+08	6.12E+06	6.93E+06	19.29	19.27	19.24
84	2.64E+08	2.71E+08	2.70E+08	2.68E+08	3.85E+06	4.35E+06	19.39	19.42	19.42
96	2.91E+08	2.91E+08	2.97E+08	2.93E+08	3.34E+06	3.78E+06	19.49	19.49	19.51
108	3.00E+08	3.16E+08	3.04E+08	3.07E+08	8.20E+06	9.28E+06	19.52	19.57	19.53
120	2.89E+08	3.15E+08	3.07E+08	3.04E+08	1.32E+07	1.49E+07	19.48	19.57	19.54

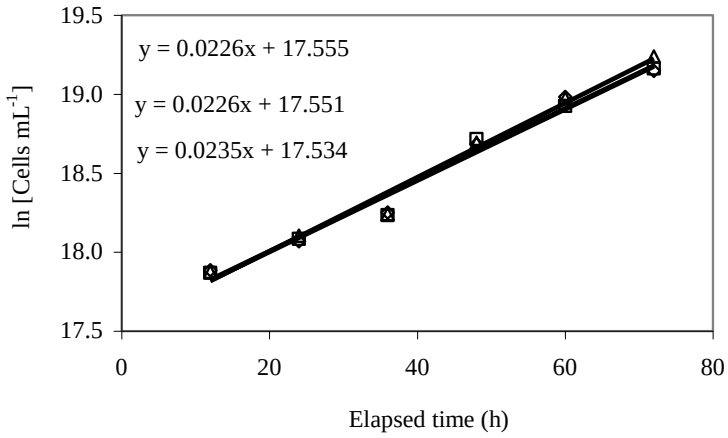


Specific growth rate (h^{-1})	
Trial 1	0.024
Trial 2	0.024
Trial 3	0.023
Average	0.024
STDEV	0.001
95% CI	0.001

Figure F.47. Specific growth rate calculations for Trial 1 (open circles), Trial 2 (open squares), and Trial 3 (open triangles).

Table F.78. BC13 growth in the presence of 20 μM 2-ketoglutarate following pre-adaptation.

	Cells mL^{-1}						ln (Cells mL^{-1})		
Elapsed Time (h)	Trial 1	Trial 2	Trial 3	Average	STDEV	95% CI	Trial 1	Trial 2	Trial 3
0	5.37E+07	5.51E+07	5.48E+07	5.45E+07	7.51E+05	8.49E+05	17.80	17.82	17.82
12	5.86E+07	5.75E+07	5.80E+07	5.81E+07	5.30E+05	6.00E+05	17.89	17.87	17.88
24	7.04E+07	7.15E+07	7.29E+07	7.16E+07	1.26E+06	1.43E+06	18.07	18.08	18.10
36	8.43E+07	8.30E+07	8.35E+07	8.36E+07	6.57E+05	7.44E+05	18.25	18.23	18.24
48	1.30E+08	1.34E+08	1.31E+08	1.32E+08	2.13E+06	2.41E+06	18.68	18.72	18.69
60	1.75E+08	1.66E+08	1.74E+08	1.72E+08	5.20E+06	5.88E+06	18.98	18.93	18.97
72	2.07E+08	2.10E+08	2.27E+08	2.15E+08	1.05E+07	1.19E+07	19.15	19.16	19.24
84	2.71E+08	2.65E+08	2.69E+08	2.69E+08	3.44E+06	3.89E+06	19.42	19.39	19.41
96	2.82E+08	2.74E+08	2.68E+08	2.75E+08	7.16E+06	8.10E+06	19.46	19.43	19.41
108	2.88E+08	2.73E+08	2.91E+08	2.84E+08	9.50E+06	1.07E+07	19.48	19.43	19.49
120	2.65E+08	2.81E+08	2.83E+08	2.76E+08	9.65E+06	1.09E+07	19.40	19.45	19.46

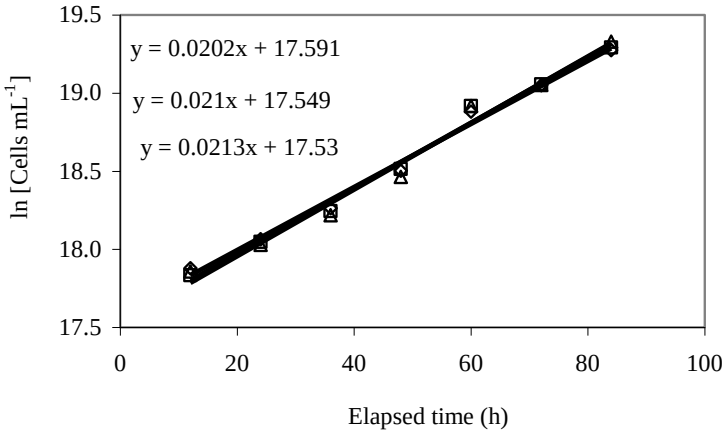


Specific growth rate (h^{-1})	
Trial 1	0.023
Trial 2	0.023
Trial 3	0.024
Average	0.023
STDEV	0.001
95% CI	0.001

Figure F.48. Specific growth rate calculations for Trial 1 (open circles), Trial 2 (open squares), and Trial 3 (open triangles).

Table F.79. BC13 growth in the presence of 30 μM 2-ketoglutarate following pre-adaptation.

	Cells mL^{-1}						ln (Cells mL^{-1})		
Elapsed Time (h)	Trial 1	Trial 2	Trial 3	Average	STDEV	95% CI	Trial 1	Trial 2	Trial 3
0	5.43E+07	5.51E+07	5.58E+07	5.51E+07	7.24E+05	8.19E+05	17.81	17.83	17.84
12	5.81E+07	5.56E+07	5.69E+07	5.69E+07	1.26E+06	1.42E+06	17.88	17.83	17.86
24	7.00E+07	6.89E+07	6.76E+07	6.88E+07	1.22E+06	1.38E+06	18.06	18.05	18.03
36	8.54E+07	8.38E+07	8.16E+07	8.36E+07	1.89E+06	2.14E+06	18.26	18.24	18.22
48	1.09E+08	1.10E+08	1.04E+08	1.08E+08	2.80E+06	3.17E+06	18.50	18.51	18.46
60	1.59E+08	1.64E+08	1.64E+08	1.62E+08	3.32E+06	3.76E+06	18.88	18.92	18.92
72	1.88E+08	1.89E+08	1.88E+08	1.88E+08	5.73E+05	6.49E+05	19.05	19.06	19.05
84	2.35E+08	2.39E+08	2.48E+08	2.41E+08	6.72E+06	7.60E+06	19.28	19.29	19.33
96	2.46E+08	2.31E+08	2.44E+08	2.41E+08	8.17E+06	9.25E+06	19.32	19.26	19.31
108	2.88E+08	2.28E+08	2.55E+08	2.57E+08	2.96E+07	3.35E+07	19.48	19.25	19.36
120	2.18E+08	2.45E+08	2.33E+08	2.32E+08	1.36E+07	1.54E+07	19.20	19.32	19.27

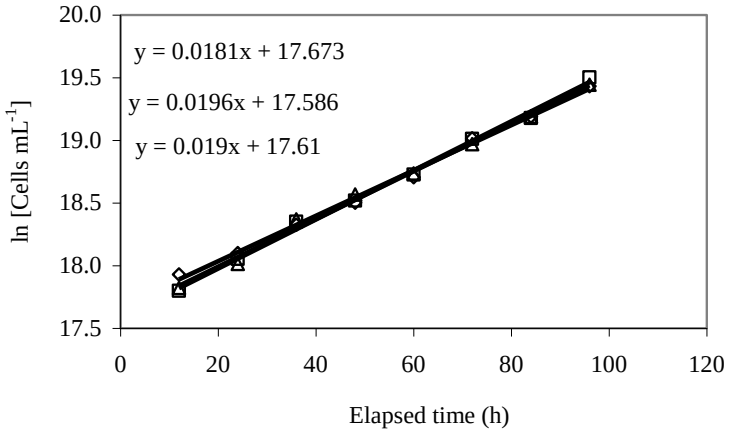


Specific growth rate (h^{-1})	
Trial 1	0.020
Trial 2	0.021
Trial 3	0.021
Average	0.021
STDEV	0.001
95% CI	0.001

Figure F.49. Specific growth rate calculations for Trial 1 (open circles), Trial 2 (open squares), and Trial 3 (open triangles).

Table F.80. BC13 growth in the presence of 50 μM 2-ketoglutarate following pre-adaptation.

	Cells mL^{-1}						ln (Cells mL^{-1})		
Elapsed Time (h)	Trial 1	Trial 2	Trial 3	Average	STDEV	95% CI	Trial 1	Trial 2	Trial 3
0	6.02E+07	5.18E+07	5.18E+07	5.46E+07	4.86E+06	5.50E+06	17.91	17.76	17.76
12	6.12E+07	5.38E+07	5.49E+07	5.66E+07	3.98E+06	4.51E+06	17.93	17.80	17.82
24	7.25E+07	6.93E+07	6.66E+07	6.95E+07	2.96E+06	3.35E+06	18.10	18.05	18.01
36	9.12E+07	9.31E+07	9.51E+07	9.31E+07	1.96E+06	2.22E+06	18.33	18.35	18.37
48	1.09E+08	1.10E+08	1.16E+08	1.12E+08	3.77E+06	4.26E+06	18.50	18.52	18.57
60	1.33E+08	1.36E+08	1.37E+08	1.35E+08	2.03E+06	2.30E+06	18.71	18.73	18.74
72	1.81E+08	1.80E+08	1.73E+08	1.78E+08	4.43E+06	5.01E+06	19.02	19.01	18.97
84	2.16E+08	2.13E+08	2.16E+08	2.15E+08	1.54E+06	1.74E+06	19.19	19.18	19.19
96	2.75E+08	2.95E+08	2.78E+08	2.83E+08	1.07E+07	1.21E+07	19.43	19.50	19.44
108	2.70E+08	2.45E+08	2.45E+08	2.53E+08	1.41E+07	1.60E+07	19.41	19.32	19.32
120	2.24E+08	2.35E+08	2.13E+08	2.24E+08	1.07E+07	1.21E+07	19.23	19.27	19.18



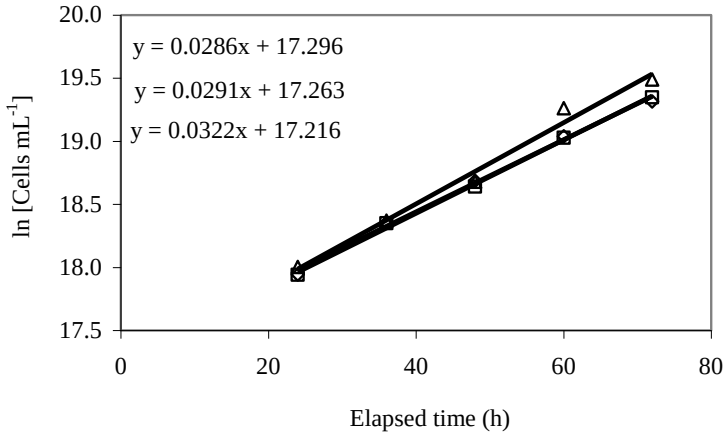
Specific growth rate (h^{-1})	
Trial 1	0.018
Trial 2	0.020
Trial 3	0.019
Average	0.019
STDEV	0.001
95% CI	0.001

Figure F.50. Specific growth rate calculations for Trial 1 (open circles), Trial 2 (open squares), and Trial 3 (open triangles).

Succinate

Table F.81. BC13 growth in the presence of 5 μM succinate following pre-adaptation.

	Cells mL^{-1}						ln (Cells mL^{-1})		
Elapsed Time (h)	Trial 1	Trial 2	Trial 3	Average	STDEV	95% CI	Trial 1	Trial 2	Trial 3
0	5.85E+07	5.67E+07	5.76E+07	5.76E+07	9.15E+05	1.04E+06	17.88	17.85	17.87
12	6.10E+07	5.02E+07	5.85E+07	5.65E+07	5.66E+06	6.40E+06	17.93	17.73	17.88
24	6.21E+07	6.19E+07	6.59E+07	6.33E+07	2.25E+06	2.55E+06	17.94	17.94	18.00
36	9.36E+07	9.31E+07	9.51E+07	9.39E+07	1.04E+06	1.18E+06	18.35	18.35	18.37
48	1.30E+08	1.24E+08	1.30E+08	1.28E+08	3.27E+06	3.70E+06	18.69	18.64	18.68
60	1.86E+08	1.83E+08	2.32E+08	2.00E+08	2.73E+07	3.09E+07	19.04	19.03	19.26
72	2.45E+08	2.53E+08	2.91E+08	2.63E+08	2.46E+07	2.78E+07	19.32	19.35	19.49
84	2.90E+08	2.76E+08	2.79E+08	2.82E+08	7.41E+06	8.38E+06	19.49	19.44	19.45
96	3.16E+08	3.23E+08	3.19E+08	3.19E+08	3.89E+06	4.40E+06	19.57	19.59	19.58
108	3.01E+08	2.97E+08	3.02E+08	3.00E+08	2.49E+06	2.81E+06	19.52	19.51	19.53
120	3.00E+08	2.96E+08	3.08E+08	3.02E+08	5.99E+06	6.77E+06	19.52	19.51	19.55



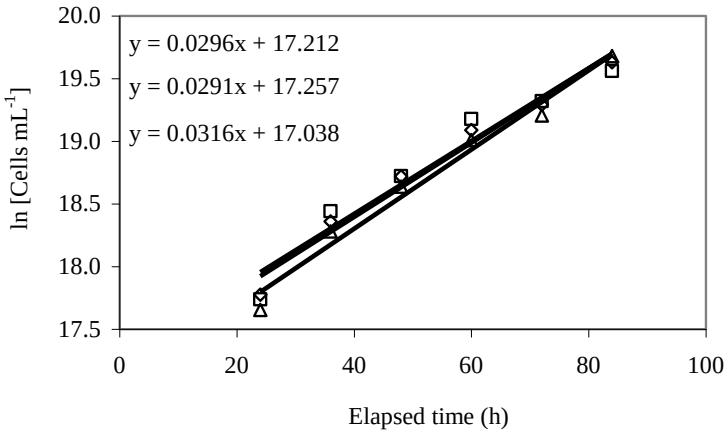
Specific growth rate (h^{-1})

Trial 1	0.029
Trial 2	0.029
Trial 3	0.032
Average	0.030
STDEV	0.002
95% CI	0.002

Figure F.51. Specific growth rate calculations for Trial 1 (open circles), Trial 2 (open squares), and Trial 3 (open triangles).

Table F.82. BC13 growth in the presence of 10 μM succinate following pre-adaptation.

	Cells mL^{-1}						ln (Cells mL^{-1})		
Elapsed Time (h)	Trial 1	Trial 2	Trial 3	Average	STDEV	95% CI	Trial 1	Trial 2	Trial 3
0	4.76E+07	4.53E+07	4.64E+07	4.64E+07	1.15E+06	1.30E+06	17.68	17.63	17.65
12	5.10E+07	5.34E+07	5.80E+07	5.41E+07	3.58E+06	4.05E+06	17.75	17.79	17.88
24	5.25E+07	5.06E+07	4.64E+07	4.98E+07	3.09E+06	3.50E+06	17.78	17.74	17.65
36	9.42E+07	1.02E+08	8.69E+07	9.44E+07	7.59E+06	8.59E+06	18.36	18.44	18.28
48	1.35E+08	1.35E+08	1.24E+08	1.31E+08	6.15E+06	6.96E+06	18.72	18.72	18.64
60	1.95E+08	2.13E+08	1.80E+08	1.96E+08	1.65E+07	1.86E+07	19.09	19.18	19.01
72	2.39E+08	2.46E+08	2.19E+08	2.35E+08	1.39E+07	1.58E+07	19.29	19.32	19.20
84	3.36E+08	3.13E+08	3.52E+08	3.34E+08	1.98E+07	2.24E+07	19.63	19.56	19.68
96	3.09E+08	3.38E+08	2.82E+08	3.10E+08	2.79E+07	3.16E+07	19.55	19.64	19.46
108	2.88E+08	3.02E+08	2.98E+08	2.96E+08	7.23E+06	8.19E+06	19.48	19.53	19.51
120	3.10E+08	3.37E+08	3.11E+08	3.19E+08	1.55E+07	1.75E+07	19.55	19.64	19.55



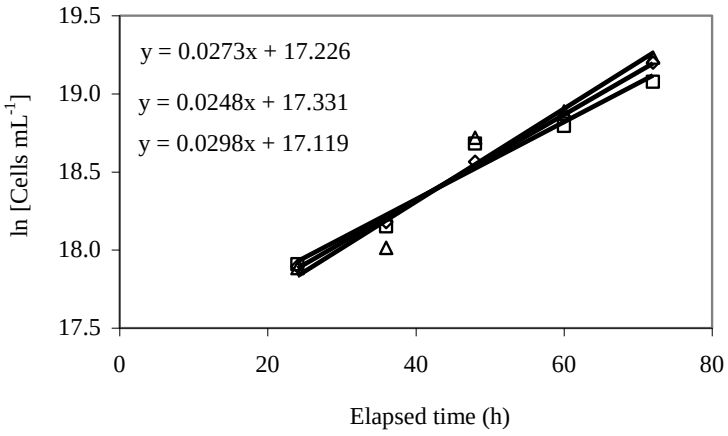
Specific growth rate (h^{-1})

Trial 1	0.030
Trial 2	0.029
Trial 3	0.032
Average	0.030
STDEV	0.001
95% CI	0.001

Figure F.52. Specific growth rate calculations for Trial 1 (open circles), Trial 2 (open squares), and Trial 3 (open triangles).

Table F.83. BC13 growth in the presence of 20 μM succinate following pre-adaptation.

	Cells mL^{-1}						ln (Cells mL^{-1})		
Elapsed Time (h)	Trial 1	Trial 2	Trial 3	Average	STDEV	95% CI	Trial 1	Trial 2	Trial 3
0	5.80E+07	5.65E+07	5.77E+07	5.74E+07	7.74E+05	8.76E+05	17.88	17.85	17.87
12	5.57E+07	5.02E+07	4.78E+07	5.13E+07	4.06E+06	4.59E+06	17.84	17.73	17.68
24	5.91E+07	6.00E+07	5.85E+07	5.92E+07	7.62E+05	8.63E+05	17.90	17.91	17.88
36	7.86E+07	7.63E+07	6.66E+07	7.38E+07	6.35E+06	7.19E+06	18.18	18.15	18.01
48	1.16E+08	1.30E+08	1.35E+08	1.27E+08	9.93E+06	1.12E+07	18.56	18.68	18.72
60	1.54E+08	1.45E+08	1.60E+08	1.53E+08	7.29E+06	8.25E+06	18.85	18.79	18.89
72	2.18E+08	1.93E+08	2.25E+08	2.12E+08	1.70E+07	1.93E+07	19.20	19.08	19.23
84	2.28E+08	2.23E+08	2.63E+08	2.38E+08	2.17E+07	2.46E+07	19.25	19.22	19.39
96	2.55E+08	2.47E+08	2.31E+08	2.45E+08	1.20E+07	1.35E+07	19.36	19.33	19.26
108	2.19E+08	2.66E+08	2.46E+08	2.43E+08	2.36E+07	2.67E+07	19.20	19.40	19.32
120	2.18E+08	2.20E+08	2.60E+08	2.33E+08	2.35E+07	2.66E+07	19.20	19.21	19.37



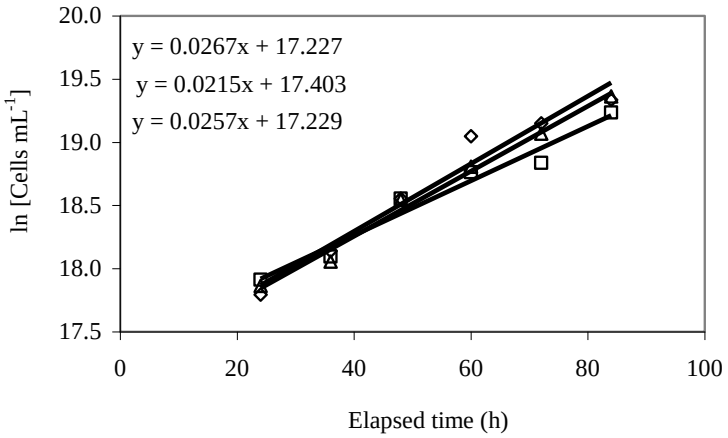
Specific growth rate (h^{-1})

Trial 1	0.027
Trial 2	0.025
Trial 3	0.030
Average	0.027
STDEV	0.003
95% CI	0.003

Figure F.53. Specific growth rate calculations for Trial 1 (open circles), Trial 2 (open squares), and Trial 3 (open triangles).

Table F.84. BC13 growth in the presence of 30 μM succinate following pre-adaptation.

	Cells mL^{-1}						ln (Cells mL^{-1})		
Elapsed Time (h)	Trial 1	Trial 2	Trial 3	Average	STDEV	95% CI	Trial 1	Trial 2	Trial 3
0	5.81E+07	5.73E+07	5.68E+07	5.74E+07	6.80E+05	7.70E+05	17.88	17.86	17.85
12	5.29E+07	5.90E+07	6.07E+07	5.76E+07	4.11E+06	4.65E+06	17.78	17.89	17.92
24	5.34E+07	6.02E+07	5.73E+07	5.70E+07	3.39E+06	3.84E+06	17.79	17.91	17.86
36	7.55E+07	7.22E+07	6.95E+07	7.24E+07	3.00E+06	3.40E+06	18.14	18.09	18.06
48	1.14E+08	1.14E+08	1.13E+08	1.14E+08	6.53E+05	7.39E+05	18.55	18.55	18.54
60	1.87E+08	1.41E+08	1.47E+08	1.58E+08	2.52E+07	2.85E+07	19.05	18.76	18.81
72	2.07E+08	1.52E+08	1.91E+08	1.84E+08	2.87E+07	3.24E+07	19.15	18.84	19.07
84	2.49E+08	2.26E+08	2.57E+08	2.44E+08	1.61E+07	1.82E+07	19.33	19.24	19.36
96	2.31E+08	2.48E+08	2.38E+08	2.39E+08	8.85E+06	1.00E+07	19.26	19.33	19.29
108	2.18E+08	2.29E+08	2.21E+08	2.23E+08	5.67E+06	6.41E+06	19.20	19.25	19.21
120	2.25E+08	2.27E+08	2.25E+08	2.26E+08	1.40E+06	1.58E+06	19.23	19.24	19.23



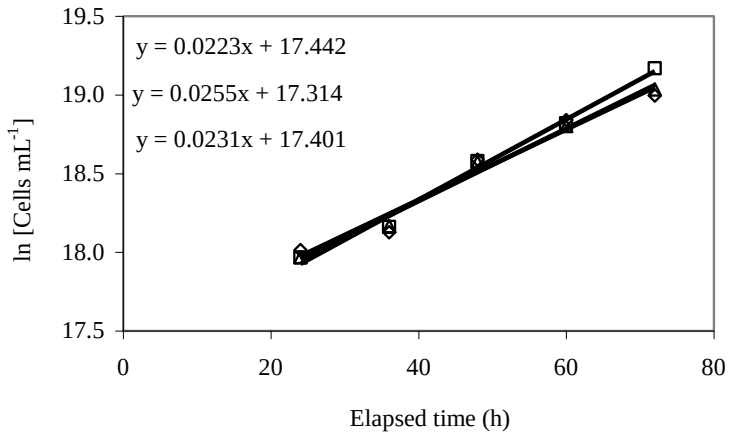
Specific growth rate (h^{-1})

Trial 1	0.027
Trial 2	0.022
Trial 3	0.026
Average	0.025
STDEV	0.003
95% CI	0.003

Figure F.54. Specific growth rate calculations for Trial 1 (open circles), Trial 2 (open squares), and Trial 3 (open triangles).

Table F.85. BC13 growth in the presence of 50 μM succinate following pre-adaptation.

	Cells mL^{-1}						ln (Cells mL^{-1})		
Elapsed Time (h)	Trial 1	Trial 2	Trial 3	Average	STDEV	95% CI	Trial 1	Trial 2	Trial 3
0	5.67E+07	5.45E+07	5.70E+07	5.61E+07	1.36E+06	1.54E+06	17.85	17.81	17.86
12	5.91E+07	5.99E+07	5.81E+07	5.90E+07	9.27E+05	1.05E+06	17.89	17.91	17.88
24	6.65E+07	6.35E+07	6.36E+07	6.46E+07	1.69E+06	1.91E+06	18.01	17.97	17.97
36	7.46E+07	7.70E+07	7.76E+07	7.64E+07	1.59E+06	1.80E+06	18.13	18.16	18.17
48	1.18E+08	1.17E+08	1.16E+08	1.17E+08	8.78E+05	9.94E+05	18.59	18.58	18.57
60	1.52E+08	1.49E+08	1.46E+08	1.49E+08	2.79E+06	3.16E+06	18.84	18.82	18.80
72	1.78E+08	2.11E+08	1.85E+08	1.91E+08	1.76E+07	2.00E+07	19.00	19.17	19.04
84	2.10E+08	2.19E+08	2.17E+08	2.15E+08	4.85E+06	5.48E+06	19.16	19.20	19.20
96	2.00E+08	2.22E+08	2.28E+08	2.17E+08	1.46E+07	1.65E+07	19.12	19.22	19.25
108	2.10E+08	2.22E+08	2.17E+08	2.16E+08	6.11E+06	6.92E+06	19.16	19.22	19.19
120	2.28E+08	2.42E+08	2.10E+08	2.27E+08	1.57E+07	1.78E+07	19.25	19.30	19.16



Specific growth rate (h^{-1})

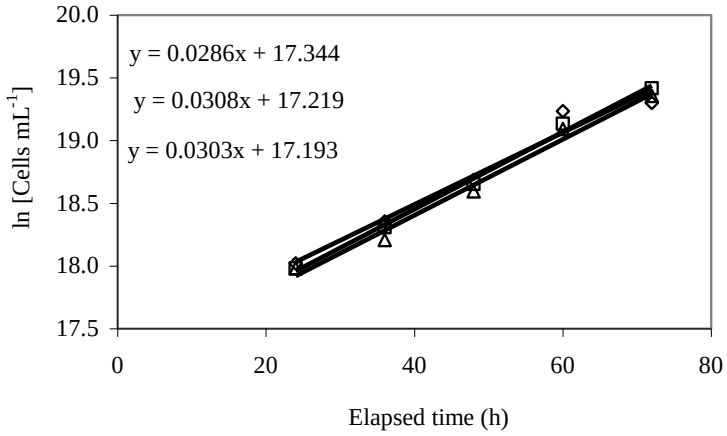
Trial 1	0.022
Trial 2	0.026
Trial 3	0.023
Average	0.024
STDEV	0.002
95% CI	0.002

Figure F.55. Specific growth rate calculations for Trial 1 (open circles), Trial 2 (open squares), and Trial 3 (open triangles).

Malate

Table F.86. BC13 growth in the presence of 5 μM malate following pre-adaptation.

	Cells mL^{-1}						ln (Cells mL^{-1})		
Elapsed Time (h)	Trial 1	Trial 2	Trial 3	Average	STDEV	95% CI	Trial 1	Trial 2	Trial 3
0	5.10E+07	5.30E+07	5.22E+07	5.21E+07	1.01E+06	1.14E+06	17.75	17.79	17.77
12	5.20E+07	5.90E+07	5.97E+07	5.69E+07	4.26E+06	4.82E+06	17.77	17.89	17.90
24	6.71E+07	6.44E+07	6.45E+07	6.53E+07	1.52E+06	1.72E+06	18.02	17.98	17.98
36	9.36E+07	8.94E+07	8.09E+07	8.79E+07	6.47E+06	7.32E+06	18.35	18.31	18.21
48	1.30E+08	1.26E+08	1.19E+08	1.25E+08	5.82E+06	6.58E+06	18.69	18.65	18.59
60	2.26E+08	2.04E+08	1.96E+08	2.09E+08	1.54E+07	1.75E+07	19.23	19.13	19.09
72	2.41E+08	2.71E+08	2.55E+08	2.55E+08	1.50E+07	1.70E+07	19.30	19.42	19.36
84	2.60E+08	3.12E+08	2.80E+08	2.84E+08	2.63E+07	2.97E+07	19.38	19.56	19.45
96	3.01E+08	3.23E+08	3.17E+08	3.14E+08	1.16E+07	1.31E+07	19.52	19.59	19.58
108	3.22E+08	3.62E+08	3.05E+08	3.29E+08	2.96E+07	3.35E+07	19.59	19.71	19.53
120	3.56E+08	3.32E+08	3.49E+08	3.45E+08	1.25E+07	1.42E+07	19.69	19.62	19.67



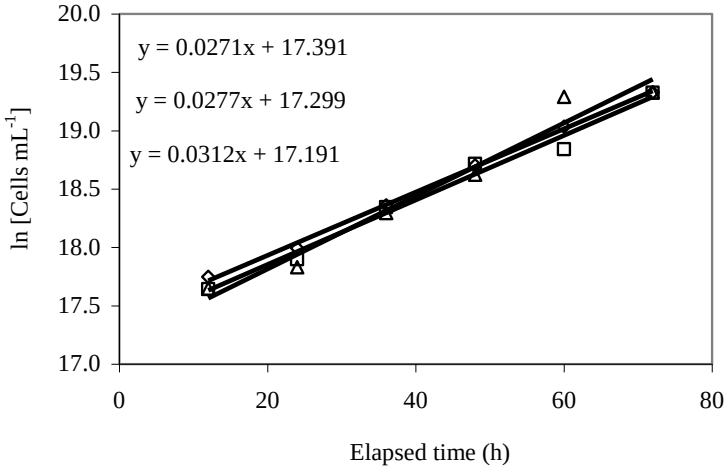
Specific growth rate (h^{-1})

Trial 1	0.029
Trial 2	0.031
Trial 3	0.030
Average	0.030
STDEV	0.001
95% CI	0.001

Figure F.56. Specific growth rate calculations for Trial 1 (open circles), Trial 2 (open squares), and Trial 3 (open triangles).

Table F.87. BC13 growth in the presence of 10 μM malate following pre-adaptation.

	Cells mL^{-1}						ln (Cells mL^{-1})		
Elapsed Time (h)	Trial 1	Trial 2	Trial 3	Average	STDEV	95% CI	Trial 1	Trial 2	Trial 3
0	4.98E+07	4.48E+07	4.42E+07	4.63E+07	3.04E+06	3.44E+06	17.72	17.62	17.60
12	5.10E+07	4.59E+07	4.61E+07	4.77E+07	2.88E+06	3.26E+06	17.75	17.64	17.65
24	6.52E+07	5.93E+07	5.54E+07	6.00E+07	4.91E+06	5.55E+06	17.99	17.90	17.83
36	9.41E+07	9.26E+07	8.81E+07	9.16E+07	3.14E+06	3.55E+06	18.36	18.34	18.29
48	1.33E+08	1.34E+08	1.23E+08	1.30E+08	6.44E+06	7.29E+06	18.70	18.72	18.62
60	1.85E+08	1.52E+08	2.39E+08	1.92E+08	4.37E+07	4.95E+07	19.03	18.84	19.29
72	2.48E+08	2.47E+08	2.48E+08	2.48E+08	3.08E+05	3.49E+05	19.33	19.33	19.33
84	2.62E+08	2.44E+08	2.57E+08	2.54E+08	9.39E+06	1.06E+07	19.39	19.31	19.36
96	3.08E+08	3.30E+08	3.00E+08	3.13E+08	1.54E+07	1.74E+07	19.55	19.62	19.52
108	3.26E+08	3.23E+08	3.51E+08	3.34E+08	1.54E+07	1.74E+07	19.60	19.59	19.68
120	3.40E+08	3.25E+08	3.52E+08	3.39E+08	1.35E+07	1.53E+07	19.64	19.60	19.68



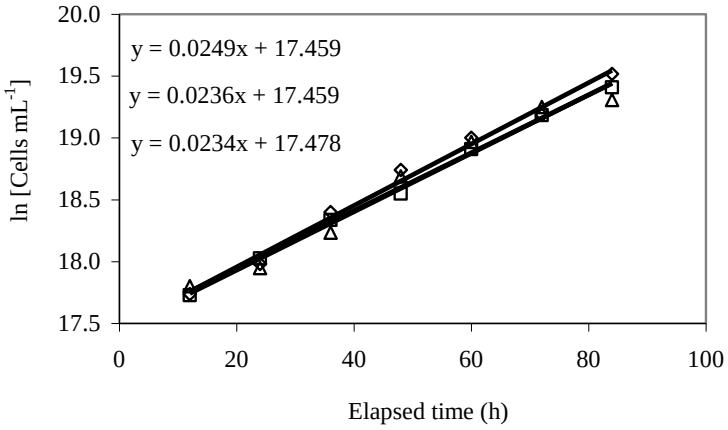
Specific growth rate (h^{-1})

Trial 1	0.027
Trial 2	0.028
Trial 3	0.031
Average	0.029
STDEV	0.002
95% CI	0.003

Figure F.57. Specific growth rate calculations for Trial 1 (open circles), Trial 2 (open squares), and Trial 3 (open triangles).

Table F.88. BC13 growth in the presence of 20 μM malate following pre-adaptation.

	Cells mL^{-1}						ln (Cells mL^{-1})		
Elapsed Time (h)	Trial 1	Trial 2	Trial 3	Average	STDEV	95% CI	Trial 1	Trial 2	Trial 3
0	5.16E+07	4.70E+07	4.91E+07	4.92E+07	2.33E+06	2.64E+06	17.76	17.67	17.71
12	5.05E+07	5.00E+07	5.38E+07	5.14E+07	2.10E+06	2.37E+06	17.74	17.73	17.80
24	6.44E+07	6.74E+07	6.23E+07	6.47E+07	2.53E+06	2.87E+06	17.98	18.03	17.95
36	9.79E+07	9.19E+07	8.31E+07	9.10E+07	7.48E+06	8.47E+06	18.40	18.34	18.24
48	1.38E+08	1.14E+08	1.31E+08	1.27E+08	1.24E+07	1.40E+07	18.74	18.55	18.69
60	1.79E+08	1.63E+08	1.73E+08	1.71E+08	8.03E+06	9.09E+06	19.00	18.91	18.97
72	2.15E+08	2.14E+08	2.29E+08	2.19E+08	8.41E+06	9.52E+06	19.19	19.18	19.25
84	2.99E+08	2.68E+08	2.43E+08	2.70E+08	2.84E+07	3.22E+07	19.52	19.41	19.31
96	3.40E+08	3.01E+08	2.99E+08	3.13E+08	2.33E+07	2.63E+07	19.65	19.52	19.51
108	3.13E+08	3.18E+08	3.18E+08	3.16E+08	3.15E+06	3.56E+06	19.56	19.58	19.58
120	3.16E+08	2.90E+08	3.21E+08	3.09E+08	1.68E+07	1.90E+07	19.57	19.48	19.59

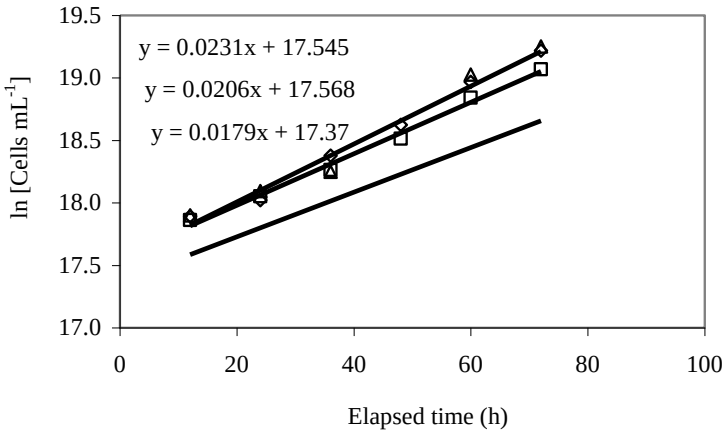


Specific growth rate (h^{-1})	
Trial 1	0.025
Trial 2	0.024
Trial 3	0.023
Average	0.024
STDEV	0.001
95% CI	0.001

Figure F.58. Specific growth rate calculations for Trial 1 (open circles), Trial 2 (open squares), and Trial 3 (open triangles).

Table F.89. BC13 growth in the presence of 30 μM malate following pre-adaptation.

	Cells mL^{-1}						ln (Cells mL^{-1})		
Elapsed Time (h)	Trial 1	Trial 2	Trial 3	Average	STDEV	95% CI	Trial 1	Trial 2	Trial 3
0	5.99E+07	5.28E+07	5.90E+07	5.72E+07	3.85E+06	4.36E+06	17.91	17.78	17.89
12	5.89E+07	5.72E+07	5.95E+07	5.85E+07	1.19E+06	1.35E+06	17.89	17.86	17.90
24	6.70E+07	6.91E+07	7.21E+07	6.94E+07	2.56E+06	2.90E+06	18.02	18.05	18.09
36	9.59E+07	8.54E+07	8.42E+07	8.85E+07	6.45E+06	7.29E+06	18.38	18.26	18.25
48	1.23E+08	1.10E+08	1.09E+07	8.11E+07	6.11E+07	6.91E+07	18.62	18.51	16.20
60	1.73E+08	1.52E+08	1.83E+08	1.69E+08	1.57E+07	1.78E+07	18.97	18.84	19.03
72	2.22E+08	1.91E+08	2.29E+08	2.14E+08	2.02E+07	2.29E+07	19.22	19.07	19.25
84	2.69E+08	2.52E+08	2.44E+08	2.55E+08	1.24E+07	1.41E+07	19.41	19.35	19.31
96	2.55E+08	2.27E+08	2.87E+08	2.56E+08	2.98E+07	3.37E+07	19.36	19.24	19.47
108	2.97E+08	2.58E+08	2.78E+08	2.78E+08	1.97E+07	2.23E+07	19.51	19.37	19.44
120	2.71E+08	2.48E+08	3.01E+08	2.73E+08	2.65E+07	3.00E+07	19.42	19.33	19.52

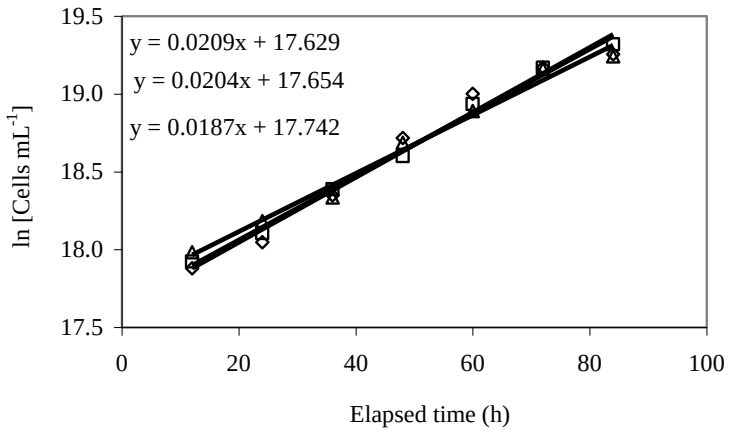


Specific growth rate (h^{-1})	
Trial 1	0.023
Trial 2	0.021
Trial 3	0.018
Average	0.021
STDEV	0.003
95% CI	0.003

Figure F.59. Specific growth rate calculations for Trial 1 (open circles), Trial 2 (open squares), and Trial 3 (open triangles).

Table F.90. BC13 growth in the presence of 50 μM malate following pre-adaptation.

	Cells mL^{-1}						ln (Cells mL^{-1})		
Elapsed Time (h)	Trial 1	Trial 2	Trial 3	Average	STDEV	95% CI	Trial 1	Trial 2	Trial 3
0	5.53E+07	5.10E+07	5.19E+07	5.27E+07	2.28E+06	2.57E+06	17.83	17.75	17.77
12	5.83E+07	6.08E+07	6.46E+07	6.12E+07	3.18E+06	3.60E+06	17.88	17.92	17.98
24	6.89E+07	7.30E+07	7.89E+07	7.36E+07	5.03E+06	5.69E+06	18.05	18.11	18.18
36	9.30E+07	9.68E+07	9.18E+07	9.39E+07	2.60E+06	2.94E+06	18.35	18.39	18.34
48	1.35E+08	1.20E+08	1.30E+08	1.28E+08	7.60E+06	8.61E+06	18.72	18.60	18.69
60	1.79E+08	1.67E+08	1.60E+08	1.69E+08	9.42E+06	1.07E+07	19.00	18.93	18.89
72	2.12E+08	2.11E+08	2.10E+08	2.11E+08	1.04E+06	1.17E+06	19.17	19.17	19.16
84	2.30E+08	2.46E+08	2.27E+08	2.35E+08	9.82E+06	1.11E+07	19.26	19.32	19.24
96	2.23E+08	2.42E+08	2.62E+08	2.43E+08	1.96E+07	2.21E+07	19.22	19.31	19.39
108	2.27E+08	2.35E+08	2.53E+08	2.39E+08	1.33E+07	1.51E+07	19.24	19.28	19.35
120	2.18E+08	2.31E+08	2.30E+08	2.26E+08	7.44E+06	8.42E+06	19.20	19.26	19.25



Specific growth rate (h^{-1})

Trial 1	0.021
Trial 2	0.020
Trial 3	0.019
Average	0.020
STDEV	0.001
95% CI	0.001

Figure F.60. Specific growth rate calculations for Trial 1 (open circles), Trial 2 (open squares), and Trial 3 (open triangles).

APPENDIX G

CHAPTER FOUR RAW DATA

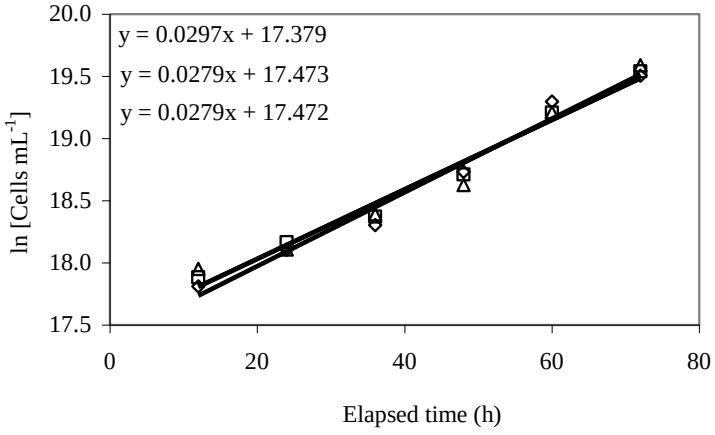
Toxicity of Heavy Metals when Presented Singly

BC13 cell concentrations in batch cultures containing varying concentrations of lead, zinc, or copper sulfates. Experiments were repeated in triplicate and average values, standard deviations (STDEV), and 95% confidence intervals (95% CI) are shown.

Lead

Table G.1. BC13 growth in the presence of 50 μM lead.

	Cells mL^{-1}						ln (Cells mL^{-1})		
Elapsed Time (h)	Trial 1	Trial 2	Trial 3	Average	STDEV	95% CI	Trial 1	Trial 2	Trial 3
0	4.88E+07	5.25E+07	5.34E+07	5.16E+07	2.40E+06	2.72E+06	17.70	17.78	17.79
12	5.44E+07	5.84E+07	6.25E+07	5.84E+07	4.07E+06	4.61E+06	17.81	17.88	17.95
24	7.30E+07	7.76E+07	7.31E+07	7.46E+07	2.60E+06	2.94E+06	18.11	18.17	18.11
36	8.89E+07	9.52E+07	9.70E+07	9.37E+07	4.25E+06	4.81E+06	18.30	18.37	18.39
48	1.36E+08	1.34E+08	1.23E+08	1.31E+08	7.11E+06	8.05E+06	18.73	18.71	18.63
60	2.40E+08	2.20E+08	2.20E+08	2.27E+08	1.17E+07	1.33E+07	19.30	19.21	19.21
72	2.96E+08	3.06E+08	3.22E+08	3.08E+08	1.32E+07	1.50E+07	19.50	19.54	19.59
84	3.26E+08	3.44E+08	3.44E+08	3.38E+08	1.03E+07	1.17E+07	19.60	19.66	19.66
96	3.20E+08	3.26E+08	2.97E+08	3.15E+08	1.51E+07	1.71E+07	19.58	19.60	19.51
108	2.96E+08	3.19E+08	3.34E+08	3.16E+08	1.94E+07	2.20E+07	19.51	19.58	19.63
120	3.11E+08	3.06E+08	3.05E+08	3.07E+08	3.05E+06	3.45E+06	19.55	19.54	19.54

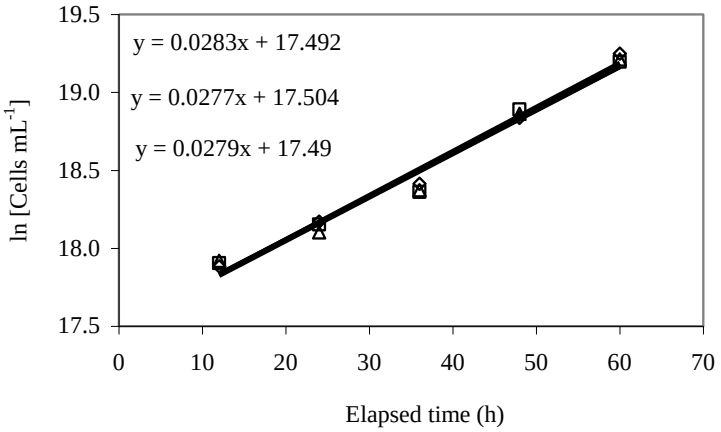


Specific growth rate (h^{-1})	
Trial 1	0.030
Trial 2	0.028
Trial 3	0.028
Average	0.029
STDEV	0.001
95% CI	0.001

Figure G.1. Specific growth rate calculations for Trial 1 (open circles), Trial 2 (open squares), and Trial 3 (open triangles).

Table G.2. BC13 growth in the presence of 100 μM lead.

	Cells mL^{-1}						ln (Cells mL^{-1})		
Elapsed Time (h)	Trial 1	Trial 2	Trial 3	Average	STDEV	95% CI	Trial 1	Trial 2	Trial 3
0	4.59E+07	4.80E+07	4.83E+07	4.74E+07	1.31E+06	1.48E+06	17.64	17.69	17.69
12	5.85E+07	5.96E+07	6.05E+07	5.95E+07	1.05E+06	1.18E+06	17.88	17.90	17.92
24	7.79E+07	7.64E+07	7.28E+07	7.57E+07	2.66E+06	3.02E+06	18.17	18.15	18.10
36	9.93E+07	9.42E+07	9.52E+07	9.62E+07	2.69E+06	3.05E+06	18.41	18.36	18.37
48	1.51E+08	1.60E+08	1.56E+08	1.56E+08	4.20E+06	4.75E+06	18.84	18.89	18.86
60	2.29E+08	2.17E+08	2.20E+08	2.22E+08	6.17E+06	6.98E+06	19.25	19.20	19.21
72	3.16E+08	2.90E+08	2.78E+08	2.95E+08	1.97E+07	2.23E+07	19.57	19.49	19.44
84	3.05E+08	3.35E+08	3.26E+08	3.22E+08	1.56E+07	1.77E+07	19.53	19.63	19.60
96	3.37E+08	3.41E+08	3.61E+08	3.46E+08	1.29E+07	1.46E+07	19.64	19.65	19.70
108	3.14E+08	2.87E+08	3.15E+08	3.05E+08	1.57E+07	1.78E+07	19.56	19.47	19.57
120	3.27E+08	3.39E+08	3.67E+08	3.44E+08	2.04E+07	2.30E+07	19.61	19.64	19.72



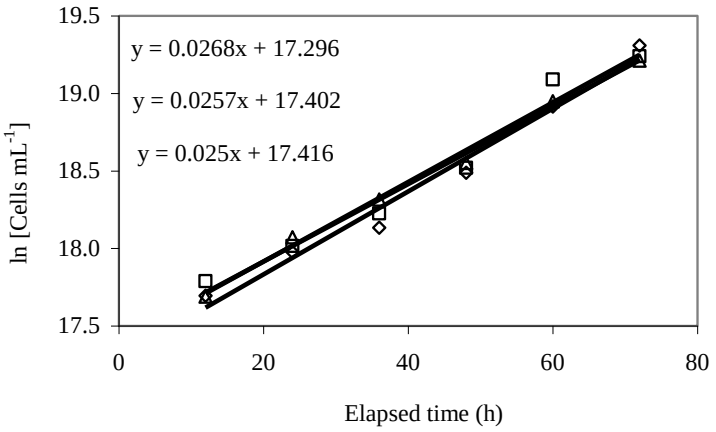
Specific growth rate (h^{-1})

Trial 1	0.028
Trial 2	0.028
Trial 3	0.028
Average	0.028
STDEV	0.000
95% CI	0.000

Figure G.2. Specific growth rate calculations for Trial 1 (open circles), Trial 2 (open squares), and Trial 3 (open triangles).

Table G.3. BC13 growth in the presence of 150 μM lead.

	Cells mL^{-1}						ln (Cells mL^{-1})		
Elapsed Time (h)	Trial 1	Trial 2	Trial 3	Average	STDEV	95% CI	Trial 1	Trial 2	Trial 3
0	4.30E+07	4.11E+07	3.84E+07	4.08E+07	2.34E+06	2.65E+06	17.58	17.53	17.46
12	4.84E+07	5.31E+07	4.81E+07	4.99E+07	2.79E+06	3.16E+06	17.70	17.79	17.69
24	6.41E+07	6.66E+07	7.06E+07	6.71E+07	3.24E+06	3.67E+06	17.98	18.01	18.07
36	7.51E+07	8.23E+07	8.99E+07	8.24E+07	7.42E+06	8.40E+06	18.13	18.23	18.31
48	1.07E+08	1.10E+08	1.14E+08	1.10E+08	3.48E+06	3.94E+06	18.49	18.52	18.55
60	1.64E+08	1.95E+08	1.70E+08	1.76E+08	1.67E+07	1.89E+07	18.92	19.09	18.95
72	2.43E+08	2.27E+08	2.21E+08	2.30E+08	1.16E+07	1.31E+07	19.31	19.24	19.21
84	2.52E+08	2.53E+08	2.57E+08	2.54E+08	2.67E+06	3.02E+06	19.34	19.35	19.36
96	2.84E+08	3.07E+08	2.77E+08	2.89E+08	1.57E+07	1.78E+07	19.47	19.54	19.44
108	2.26E+08	2.39E+08	2.38E+08	2.34E+08	7.33E+06	8.29E+06	19.24	19.29	19.29
120	2.43E+08	2.65E+08	2.42E+08	2.50E+08	1.29E+07	1.46E+07	19.31	19.39	19.30



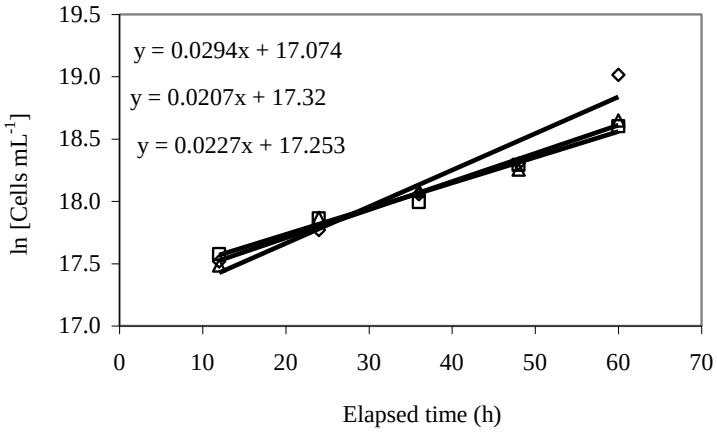
Specific growth rate (h^{-1})

Trial 1	0.027
Trial 2	0.026
Trial 3	0.025
Average	0.026
STDEV	0.001
95% CI	0.001

Figure G.3. Specific growth rate calculations for Trial 1 (open circles), Trial 2 (open squares), and Trial 3 (open triangles).

Table G.4. BC13 growth in the presence of 200 μM lead.

	Cells mL^{-1}						ln (Cells mL^{-1})		
Elapsed Time (h)	Trial 1	Trial 2	Trial 3	Average	STDEV	95% CI	Trial 1	Trial 2	Trial 3
0	4.26E+07	4.18E+07	4.18E+07	4.21E+07	5.08E+05	5.75E+05	17.57	17.55	17.55
12	4.05E+07	4.30E+07	3.92E+07	4.09E+07	1.90E+06	2.15E+06	17.52	17.58	17.48
24	5.22E+07	5.72E+07	5.75E+07	5.56E+07	2.98E+06	3.37E+06	17.77	17.86	17.87
36	6.95E+07	6.52E+07	7.15E+07	6.87E+07	3.21E+06	3.63E+06	18.06	17.99	18.08
48	8.90E+07	8.79E+07	8.47E+07	8.72E+07	2.23E+06	2.52E+06	18.30	18.29	18.25
60	1.81E+08	1.20E+08	1.26E+08	1.42E+08	3.38E+07	3.83E+07	19.01	18.60	18.65
72	2.24E+08	2.14E+08	2.17E+08	2.18E+08	5.34E+06	6.04E+06	19.23	19.18	19.20
84	2.24E+08	2.19E+08	2.26E+08	2.23E+08	3.56E+06	4.03E+06	19.23	19.21	19.24
96	2.62E+08	2.87E+08	2.62E+08	2.70E+08	1.42E+07	1.60E+07	19.39	19.47	19.38
108	2.16E+08	2.01E+08	1.84E+08	2.00E+08	1.58E+07	1.79E+07	19.19	19.12	19.03
120	2.15E+08	2.27E+08	2.22E+08	2.21E+08	6.33E+06	7.16E+06	19.19	19.24	19.22

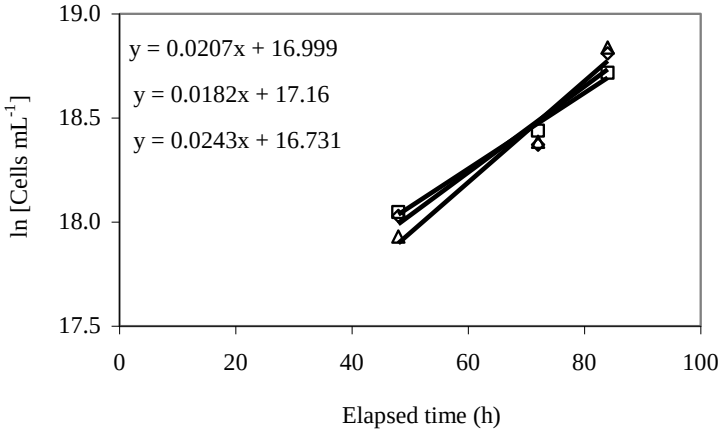


Specific growth rate (h^{-1})	
Trial 1	0.029
Trial 2	0.021
Trial 3	0.023
Average	0.024
STDEV	0.005
95% CI	0.005

Figure G.4. Specific growth rate calculations for Trial 1 (open circles), Trial 2 (open squares), and Trial 3 (open triangles).

Table G.5. BC13 growth in the presence of 500 μM lead.

	Cells mL^{-1}						ln (Cells mL^{-1})		
Elapsed Time (h)	Trial 1	Trial 2	Trial 3	Average	STDEV	95% CI	Trial 1	Trial 2	Trial 3
0	5.78E+07	5.82E+07	5.30E+07	5.63E+07	2.92E+06	3.31E+06	17.87	17.88	17.79
12	5.41E+07	5.37E+07	5.83E+07	5.54E+07	2.54E+06	2.87E+06	17.81	17.80	17.88
24	5.83E+07	5.43E+07	5.88E+07	5.71E+07	2.48E+06	2.81E+06	17.88	17.81	17.89
36	6.05E+07	6.23E+07	6.00E+07	6.09E+07	1.23E+06	1.39E+06	17.92	17.95	17.91
48	6.76E+07	6.89E+07	6.13E+07	6.59E+07	4.06E+06	4.60E+06	18.03	18.05	17.93
72	9.51E+07	1.02E+08	9.65E+07	9.78E+07	3.49E+06	3.95E+06	18.37	18.44	18.38
84	1.48E+08	1.34E+08	1.52E+08	1.45E+08	9.10E+06	1.03E+07	18.81	18.72	18.84
108	2.14E+08	2.15E+08	1.94E+08	2.08E+08	1.19E+07	1.35E+07	19.18	19.19	19.08
120	2.11E+08	2.30E+08	2.17E+08	2.19E+08	1.01E+07	1.15E+07	19.17	19.26	19.20
144	2.45E+08	2.39E+08	2.51E+08	2.45E+08	6.03E+06	6.82E+06	19.32	19.29	19.34
151	1.97E+08	1.98E+08	2.10E+08	2.02E+08	7.25E+06	8.21E+06	19.10	19.10	19.16



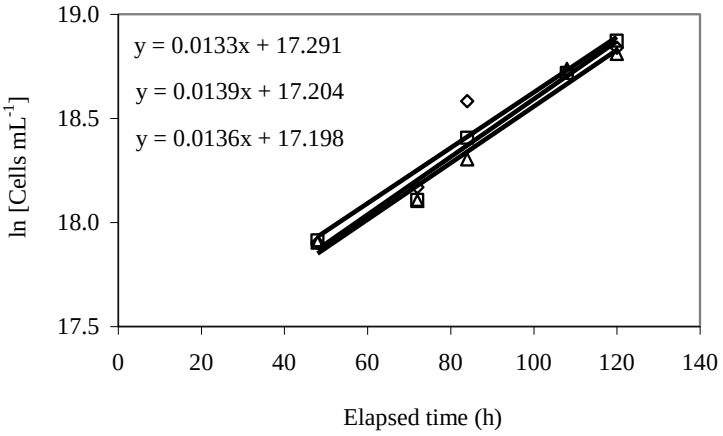
Specific growth rate (h^{-1})

Trial 1	0.021
Trial 2	0.018
Trial 3	0.024
Average	0.021
STDEV	0.003
95% CI	0.003

Figure G.5. Specific growth rate calculations for Trial 1 (open circles), Trial 2 (open squares), and Trial 3 (open triangles).

Table G.6. BC13 growth in the presence of 1 mM lead.

	Cells mL^{-1}						ln (Cells mL^{-1})		
Elapsed Time (h)	Trial 1	Trial 2	Trial 3	Average	STDEV	95% CI	Trial 1	Trial 2	Trial 3
0	5.52E+07	5.85E+07	5.38E+07	5.59E+07	2.40E+06	2.72E+06	17.83	17.88	17.80
12	5.79E+07	6.02E+07	6.27E+07	6.03E+07	2.37E+06	2.68E+06	17.87	17.91	17.95
24	5.31E+07	5.58E+07	5.29E+07	5.39E+07	1.61E+06	1.83E+06	17.79	17.84	17.78
36	6.38E+07	6.24E+07	5.99E+07	6.20E+07	1.96E+06	2.21E+06	17.97	17.95	17.91
48	5.95E+07	6.02E+07	5.96E+07	5.98E+07	3.77E+05	4.27E+05	17.90	17.91	17.90
72	7.77E+07	7.32E+07	7.29E+07	7.46E+07	2.72E+06	3.07E+06	18.17	18.11	18.10
84	1.18E+08	9.86E+07	8.89E+07	1.02E+08	1.46E+07	1.65E+07	18.58	18.41	18.30
108	1.35E+08	1.35E+08	1.37E+08	1.36E+08	1.41E+06	1.60E+06	18.72	18.72	18.74
120	1.52E+08	1.57E+08	1.48E+08	1.52E+08	4.76E+06	5.39E+06	18.84	18.87	18.81
144	1.57E+08	1.64E+08	1.58E+08	1.60E+08	3.71E+06	4.20E+06	18.87	18.92	18.88
151	1.38E+08	1.46E+08	1.42E+08	1.42E+08	4.03E+06	4.56E+06	18.75	18.80	18.77

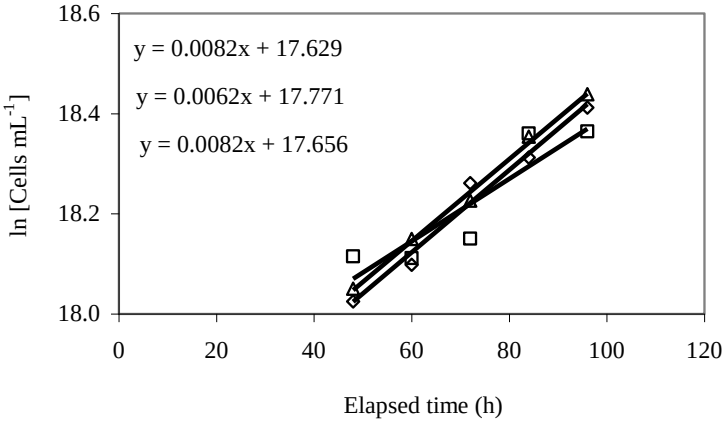


Specific growth rate (h^{-1})	
Trial 1	0.013
Trial 2	0.014
Trial 3	0.014
Average	0.014
STDEV	0.000
95% CI	0.000

Figure G.6. Specific growth rate calculations for Trial 1 (open circles), Trial 2 (open squares), and Trial 3 (open triangles).

Table G.7. BC13 growth in the presence of 3 mM lead.

	Cells mL^{-1}						ln (Cells mL^{-1})		
Elapsed Time (h)	Trial 1	Trial 2	Trial 3	Average	STDEV	95% CI	Trial 1	Trial 2	Trial 3
0	6.36E+07	5.92E+07	6.12E+07	6.13E+07	2.24E+06	2.53E+06	17.97	17.90	17.93
12	6.34E+07	6.78E+07	6.98E+07	6.70E+07	3.24E+06	3.67E+06	17.97	18.03	18.06
24	6.13E+07	6.68E+07	6.54E+07	6.45E+07	2.86E+06	3.24E+06	17.93	18.02	18.00
36	6.37E+07	6.23E+07	6.56E+07	6.39E+07	1.63E+06	1.85E+06	17.97	17.95	18.00
48	6.73E+07	7.36E+07	6.91E+07	7.00E+07	3.26E+06	3.69E+06	18.02	18.11	18.05
60	7.24E+07	7.34E+07	7.63E+07	7.40E+07	2.00E+06	2.26E+06	18.10	18.11	18.15
72	8.53E+07	7.63E+07	8.24E+07	8.13E+07	4.58E+06	5.18E+06	18.26	18.15	18.23
84	8.97E+07	9.41E+07	9.36E+07	9.25E+07	2.41E+06	2.72E+06	18.31	18.36	18.35
96	9.91E+07	9.45E+07	1.02E+08	9.85E+07	3.67E+06	4.16E+06	18.41	18.36	18.44
108	1.02E+08	1.05E+08	1.03E+08	1.03E+08	1.73E+06	1.96E+06	18.44	18.47	18.45
120	9.06E+07	8.54E+07	9.36E+07	8.99E+07	4.17E+06	4.71E+06	18.32	18.26	18.35
151	8.70E+07	8.49E+07	8.94E+07	8.71E+07	2.25E+06	2.54E+06	18.28	18.26	18.31

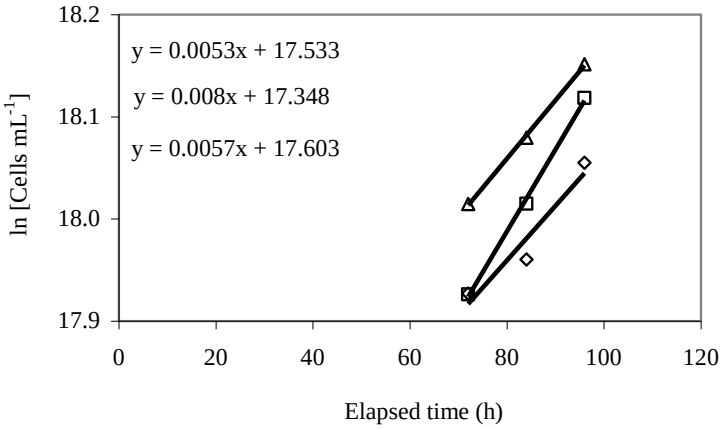


Specific growth rate (h^{-1})	
Trial 1	0.008
Trial 2	0.006
Trial 3	0.008
Average	0.008
STDEV	0.001
95% CI	0.001

Figure G.7. Specific growth rate calculations for Trial 1 (open circles), Trial 2 (open squares), and Trial 3 (open triangles).

Table G.8. BC13 growth in the presence of 5 mM lead.

	Cells mL^{-1}						ln (Cells mL^{-1})		
Elapsed Time (h)	Trial 1	Trial 2	Trial 3	Average	STDEV	95% CI	Trial 1	Trial 2	Trial 3
0	5.72E+07	5.61E+07	5.54E+07	5.62E+07	9.12E+05	1.03E+06	17.86	17.84	17.83
12	5.52E+07	5.57E+07	5.24E+07	5.44E+07	1.74E+06	1.97E+06	17.85	17.84	17.78
24	5.64E+07	5.82E+07	5.29E+07	5.59E+07	2.68E+06	3.03E+06	17.85	17.88	17.78
36	5.83E+07	5.67E+07	5.75E+07	5.75E+07	7.97E+05	9.01E+05	17.88	17.85	17.87
48	5.15E+07	6.46E+07	6.08E+07	5.90E+07	6.75E+06	7.64E+06	17.76	17.98	17.92
60	5.98E+07	6.29E+07	6.16E+07	6.14E+07	1.57E+06	1.78E+06	17.91	17.96	17.94
72	6.10E+07	6.10E+07	6.66E+07	6.29E+07	3.24E+06	3.67E+06	17.93	17.93	18.01
84	6.31E+07	6.67E+07	7.11E+07	6.69E+07	4.00E+06	4.53E+06	17.96	18.02	18.08
96	6.94E+07	7.39E+07	7.64E+07	7.32E+07	3.57E+06	4.03E+06	18.05	18.12	18.15
108	7.05E+07	7.87E+07	7.55E+07	7.49E+07	4.13E+06	4.67E+06	18.07	18.18	18.14
120	7.81E+07	7.24E+07	7.69E+07	7.58E+07	2.97E+06	3.36E+06	18.17	18.10	18.16
151	7.95E+07	7.43E+07	8.04E+07	7.81E+07	3.31E+06	3.75E+06	18.19	18.12	18.20
170	7.44E+07	7.60E+07	8.11E+07	7.72E+07	3.49E+06	3.95E+06	18.13	18.15	18.21

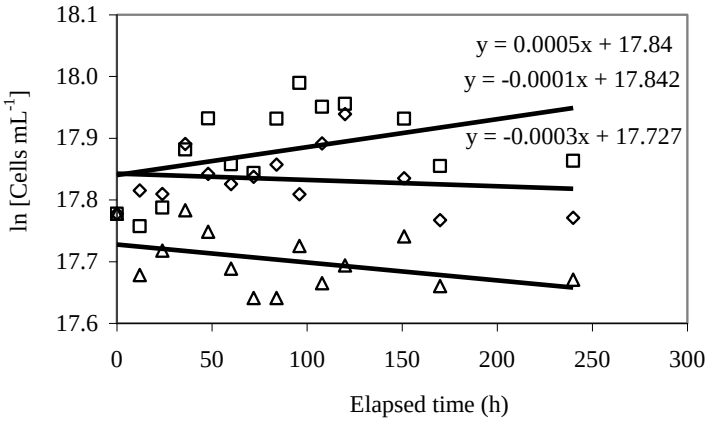


Specific growth rate (h^{-1})	
Trial 1	0.005
Trial 2	0.008
Trial 3	0.006
Average	0.006
STDEV	0.001
95% CI	0.002

Figure G.8. Specific growth rate calculations for Trial 1 (open circles), Trial 2 (open squares), and Trial 3 (open triangles).

Table G.9. BC13 growth in the presence of 7.5 mM lead.

	Cells mL^{-1}						ln (Cells mL^{-1})		
Elapsed Time (h)	Trial 1	Trial 2	Trial 3	Average	STDEV	95% CI	Trial 1	Trial 2	Trial 3
0	5.26E+07	5.26E+07	5.26E+07	5.26E+07	1.00E+00	1.13E+00	17.78	17.78	17.78
12	5.46E+07	5.15E+07	4.76E+07	5.12E+07	3.51E+06	3.97E+06	17.82	17.76	17.68
24	5.43E+07	5.31E+07	4.95E+07	5.23E+07	2.48E+06	2.81E+06	17.81	17.79	17.72
36	5.89E+07	5.83E+07	5.29E+07	5.67E+07	3.32E+06	3.76E+06	17.89	17.88	17.78
48	5.61E+07	6.13E+07	5.10E+07	5.61E+07	5.14E+06	5.82E+06	17.84	17.93	17.75
60	5.52E+07	5.69E+07	4.81E+07	5.34E+07	4.68E+06	5.30E+06	17.83	17.86	17.69
72	5.58E+07	5.61E+07	4.58E+07	5.26E+07	5.85E+06	6.62E+06	17.84	17.84	17.64
84	5.69E+07	6.13E+07	4.58E+07	5.47E+07	7.97E+06	9.02E+06	17.86	17.93	17.64
96	5.42E+07	6.50E+07	4.99E+07	5.64E+07	7.77E+06	8.79E+06	17.81	17.99	17.73
108	5.89E+07	6.25E+07	4.70E+07	5.61E+07	8.13E+06	9.20E+06	17.89	17.95	17.67
120	6.18E+07	6.28E+07	4.83E+07	5.76E+07	8.07E+06	9.13E+06	17.94	17.96	17.69
151	5.57E+07	6.13E+07	5.07E+07	5.59E+07	5.33E+06	6.03E+06	17.83	17.93	17.74
170	5.20E+07	5.68E+07	4.67E+07	5.18E+07	5.02E+06	5.68E+06	17.77	17.85	17.66
240	5.22E+07	5.73E+07	4.72E+07	5.22E+07	5.01E+06	5.67E+06	17.77	17.86	17.67



Specific growth rate (h^{-1})

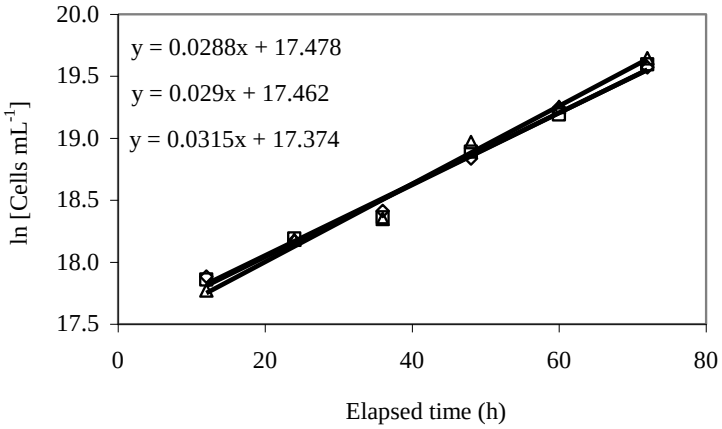
Trial 1	0.000
Trial 2	0.000
Trial 3	0.000
Average	0.000
STDEV	0.000
95% CI	0.000

Figure G.9. Specific growth rate calculations for Trial 1 (open circles), Trial 2 (open squares), and Trial 3 (open triangles).

Zinc

Table G.10. BC13 growth in the presence of 1 mM zinc.

	Cells mL^{-1}						ln (Cells mL^{-1})		
Elapsed Time (h)	Trial 1	Trial 2	Trial 3	Average	STDEV	95% CI	Trial 1	Trial 2	Trial 3
0	5.09E+07	5.51E+07	5.50E+07	5.36E+07	2.40E+06	2.71E+06	17.74	17.82	17.82
12	5.85E+07	5.71E+07	5.22E+07	5.59E+07	3.28E+06	3.71E+06	17.88	17.86	17.77
24	7.79E+07	7.95E+07	7.87E+07	7.87E+07	8.08E+05	9.14E+05	18.17	18.19	18.18
36	9.93E+07	9.42E+07	9.31E+07	9.55E+07	3.27E+06	3.70E+06	18.41	18.36	18.35
48	1.51E+08	1.60E+08	1.73E+08	1.61E+08	1.08E+07	1.22E+07	18.84	18.89	18.97
60	2.29E+08	2.16E+08	2.30E+08	2.25E+08	7.78E+06	8.80E+06	19.25	19.19	19.25
72	3.16E+08	3.24E+08	3.41E+08	3.27E+08	1.25E+07	1.42E+07	19.57	19.60	19.65
84	3.05E+08	3.01E+08	3.05E+08	3.03E+08	2.49E+06	2.82E+06	19.53	19.52	19.54
96	3.37E+08	3.64E+08	3.43E+08	3.48E+08	1.40E+07	1.59E+07	19.64	19.71	19.65
108	3.14E+08	3.09E+08	3.10E+08	3.11E+08	2.31E+06	2.61E+06	19.56	19.55	19.55
120	3.27E+08	3.36E+08	3.67E+08	3.44E+08	2.09E+07	2.36E+07	19.61	19.63	19.72



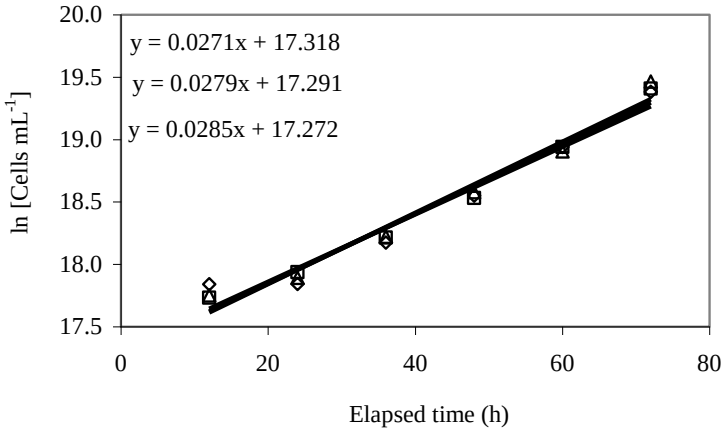
Specific growth rate (h^{-1})

Trial 1	0.029
Trial 2	0.029
Trial 3	0.032
Average	0.030
STDEV	0.002
95% CI	0.002

Figure G.10. Specific growth rate calculations for Trial 1 (open circles), Trial 2 (open squares), and Trial 3 (open triangles).

Table G.11. BC13 growth in the presence of 3 mM zinc.

	Cells mL^{-1}						ln (Cells mL^{-1})		
Elapsed Time (h)	Trial 1	Trial 2	Trial 3	Average	STDEV	95% CI	Trial 1	Trial 2	Trial 3
0	5.35E+07	5.88E+07	6.44E+07	5.89E+07	5.41E+06	6.13E+06	17.80	17.89	17.98
12	5.60E+07	5.03E+07	5.12E+07	5.25E+07	3.05E+06	3.45E+06	17.84	17.73	17.75
24	5.61E+07	6.17E+07	5.89E+07	5.89E+07	2.79E+06	3.16E+06	17.84	17.94	17.89
36	7.82E+07	8.13E+07	8.19E+07	8.05E+07	1.99E+06	2.26E+06	18.17	18.21	18.22
48	1.14E+08	1.12E+08	1.17E+08	1.14E+08	2.66E+06	3.01E+06	18.55	18.53	18.58
60	1.68E+08	1.68E+08	1.62E+08	1.66E+08	3.41E+06	3.86E+06	18.94	18.94	18.90
72	2.61E+08	2.69E+08	2.84E+08	2.71E+08	1.15E+07	1.30E+07	19.38	19.41	19.46
84	2.61E+08	2.44E+08	2.45E+08	2.50E+08	9.76E+06	1.10E+07	19.38	19.31	19.32
96	2.75E+08	2.83E+08	2.71E+08	2.76E+08	6.18E+06	6.99E+06	19.43	19.46	19.42
108	2.28E+08	2.38E+08	2.40E+08	2.35E+08	6.67E+06	7.55E+06	19.24	19.29	19.30
120	2.44E+08	2.59E+08	2.39E+08	2.47E+08	1.00E+07	1.13E+07	19.31	19.37	19.29



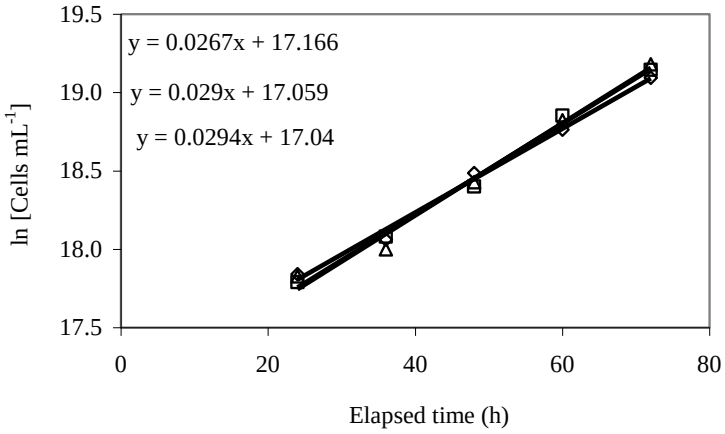
Specific growth rate (h^{-1})

Trial 1	0.027
Trial 2	0.028
Trial 3	0.029
Average	0.028
STDEV	0.001
95% CI	0.001

Figure G.11. Specific growth rate calculations for Trial 1 (open circles), Trial 2 (open squares), and Trial 3 (open triangles).

Table G.12. BC13 growth in the presence of 5 mM zinc.

	Cells mL^{-1}						ln (Cells mL^{-1})		
Elapsed Time (h)	Trial 1	Trial 2	Trial 3	Average	STDEV	95% CI	Trial 1	Trial 2	Trial 3
0	5.41E+07	5.55E+07	5.99E+07	5.65E+07	3.04E+06	3.44E+06	17.81	17.83	17.91
12	5.23E+07	5.72E+07	5.50E+07	5.48E+07	2.48E+06	2.81E+06	17.77	17.86	17.82
24	5.60E+07	5.32E+07	5.52E+07	5.48E+07	1.44E+06	1.63E+06	17.84	17.79	17.83
36	6.98E+07	7.11E+07	6.57E+07	6.88E+07	2.81E+06	3.18E+06	18.06	18.08	18.00
48	1.07E+08	9.79E+07	1.01E+08	1.02E+08	4.56E+06	5.16E+06	18.49	18.40	18.43
60	1.41E+08	1.54E+08	1.50E+08	1.48E+08	6.75E+06	7.64E+06	18.76	18.85	18.82
72	1.96E+08	2.06E+08	2.14E+08	2.05E+08	8.81E+06	9.97E+06	19.09	19.15	19.18
84	2.51E+08	2.40E+08	2.39E+08	2.43E+08	6.94E+06	7.86E+06	19.34	19.30	19.29
96	2.72E+08	2.66E+08	2.87E+08	2.75E+08	1.08E+07	1.22E+07	19.42	19.40	19.48
108	1.87E+08	1.79E+08	1.91E+08	1.85E+08	6.16E+06	6.98E+06	19.05	19.00	19.07
120	2.30E+08	2.40E+08	2.42E+08	2.37E+08	6.08E+06	6.88E+06	19.26	19.30	19.30



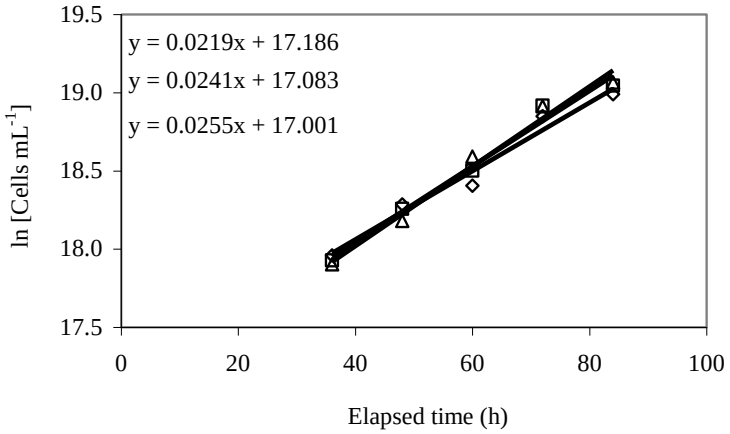
Specific growth rate (h^{-1})

Trial 1	0.027
Trial 2	0.029
Trial 3	0.029
Average	0.028
STDEV	0.001
95% CI	0.002

Figure G.12. Specific growth rate calculations for Trial 1 (open circles), Trial 2 (open squares), and Trial 3 (open triangles).

Table G.13. BC13 growth in the presence of 10 mM zinc.

	Cells mL^{-1}						ln (Cells mL^{-1})		
Elapsed Time (h)	Trial 1	Trial 2	Trial 3	Average	STDEV	95% CI	Trial 1	Trial 2	Trial 3
0	5.52E+07	5.69E+07	5.28E+07	5.50E+07	2.02E+06	2.28E+06	17.83	17.86	17.78
12	5.70E+07	6.24E+07	6.44E+07	6.12E+07	3.81E+06	4.31E+06	17.86	17.95	17.98
24	5.78E+07	5.63E+07	5.96E+07	5.79E+07	1.64E+06	1.85E+06	17.87	17.85	17.90
36	6.31E+07	6.10E+07	5.96E+07	6.12E+07	1.77E+06	2.00E+06	17.96	17.93	17.90
48	8.74E+07	8.50E+07	7.86E+07	8.37E+07	4.52E+06	5.11E+06	18.29	18.26	18.18
60	9.86E+07	1.08E+08	1.19E+08	1.08E+08	9.97E+06	1.13E+07	18.41	18.50	18.59
72	1.54E+08	1.64E+08	1.64E+08	1.61E+08	5.94E+06	6.72E+06	18.85	18.92	18.91
84	1.77E+08	1.87E+08	1.90E+08	1.85E+08	7.09E+06	8.02E+06	18.99	19.04	19.06
96	2.03E+08	2.12E+08	2.25E+08	2.13E+08	1.09E+07	1.24E+07	19.13	19.17	19.23
108	1.41E+08	1.40E+08	1.41E+08	1.40E+08	6.59E+05	7.45E+05	18.76	18.75	18.76
120	1.74E+08	1.86E+08	2.04E+08	1.88E+08	1.53E+07	1.73E+07	18.97	19.04	19.14



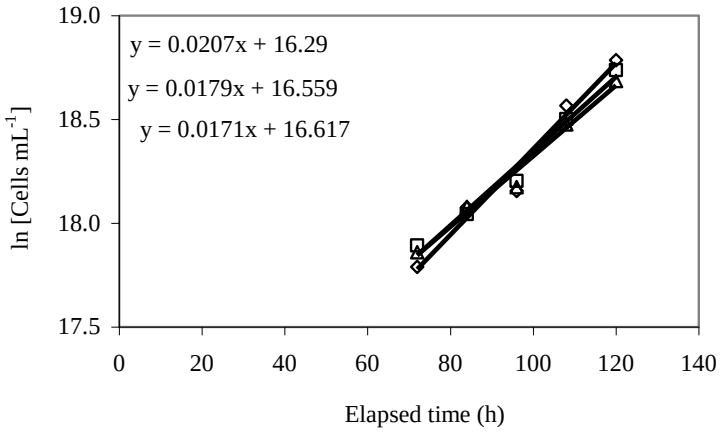
Specific growth rate (h^{-1})

Trial 1	0.022
Trial 2	0.024
Trial 3	0.026
Average	0.024
STDEV	0.002
95% CI	0.002

Figure G.13. Specific growth rate calculations for Trial 1 (open circles), Trial 2 (open squares), and Trial 3 (open triangles).

Table G.14. BC13 growth in the presence of 20 mM zinc.

	Cells mL^{-1}						ln (Cells mL^{-1})		
Elapsed Time (h)	Trial 1	Trial 2	Trial 3	Average	STDEV	95% CI	Trial 1	Trial 2	Trial 3
0	4.54E+07	5.00E+07	5.46E+07	5.00E+07	4.57E+06	5.18E+06	17.63	17.73	17.82
12	4.92E+07	4.85E+07	4.78E+07	4.85E+07	6.93E+05	7.84E+05	17.71	17.70	17.68
24	5.16E+07	4.83E+07	4.54E+07	4.84E+07	3.09E+06	3.50E+06	17.76	17.69	17.63
72	5.32E+07	5.90E+07	5.71E+07	5.64E+07	2.95E+06	3.34E+06	17.79	17.89	17.86
84	7.09E+07	6.86E+07	7.10E+07	7.02E+07	1.38E+06	1.57E+06	18.08	18.04	18.08
96	7.67E+07	8.05E+07	7.81E+07	7.84E+07	1.95E+06	2.21E+06	18.15	18.20	18.17
108	1.16E+08	1.08E+08	1.06E+08	1.10E+08	5.13E+06	5.81E+06	18.57	18.50	18.48
120	1.44E+08	1.37E+08	1.30E+08	1.37E+08	6.91E+06	7.82E+06	18.79	18.74	18.68
144	1.48E+08	1.61E+08	1.77E+08	1.62E+08	1.47E+07	1.66E+07	18.81	18.90	18.99
168	1.19E+08	1.12E+08	1.07E+08	1.13E+08	6.18E+06	6.99E+06	18.59	18.54	18.49



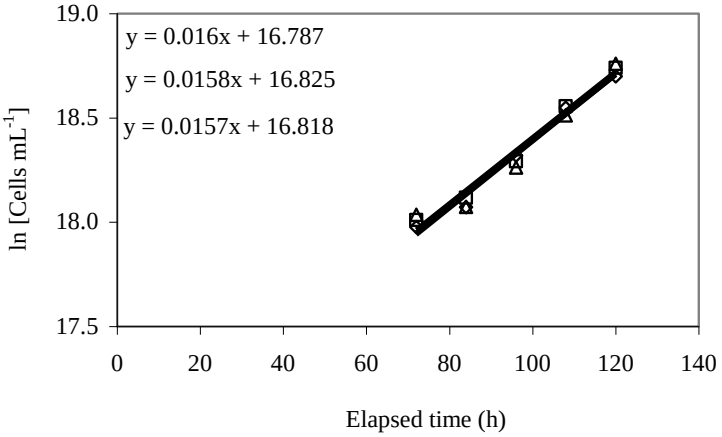
Specific growth rate (h^{-1})

Trial 1	0.021
Trial 2	0.018
Trial 3	0.017
Average	0.019
STDEV	0.002
95% CI	0.002

Figure G.14. Specific growth rate calculations for Trial 1 (open circles), Trial 2 (open squares), and Trial 3 (open triangles).

Table G.15. BC13 growth in the presence of 35 mM zinc.

	Cells mL^{-1}						ln (Cells mL^{-1})		
Elapsed Time (h)	Trial 1	Trial 2	Trial 3	Average	STDEV	95% CI	Trial 1	Trial 2	Trial 3
0	5.68E+07	5.78E+07	5.49E+07	5.65E+07	1.44E+06	1.63E+06	17.85	17.87	17.82
12	5.68E+07	5.53E+07	5.61E+07	5.61E+07	7.64E+05	8.64E+05	17.86	17.83	17.84
24	5.40E+07	5.07E+07	4.82E+07	5.10E+07	2.90E+06	3.28E+06	17.80	17.74	17.69
72	6.42E+07	6.64E+07	6.80E+07	6.62E+07	1.92E+06	2.17E+06	17.98	18.01	18.04
84	7.06E+07	7.38E+07	7.06E+07	7.17E+07	1.85E+06	2.09E+06	18.07	18.12	18.07
96	9.04E+07	8.79E+07	8.53E+07	8.79E+07	2.53E+06	2.86E+06	18.32	18.29	18.26
108	1.14E+08	1.14E+08	1.10E+08	1.13E+08	2.64E+06	2.98E+06	18.55	18.56	18.51
120	1.32E+08	1.38E+08	1.40E+08	1.37E+08	4.19E+06	4.74E+06	18.70	18.74	18.76
144	1.51E+08	1.47E+08	1.48E+08	1.49E+08	2.02E+06	2.28E+06	18.83	18.81	18.82
168	1.57E+08	1.58E+08	1.56E+08	1.57E+08	1.22E+06	1.38E+06	18.87	18.88	18.86

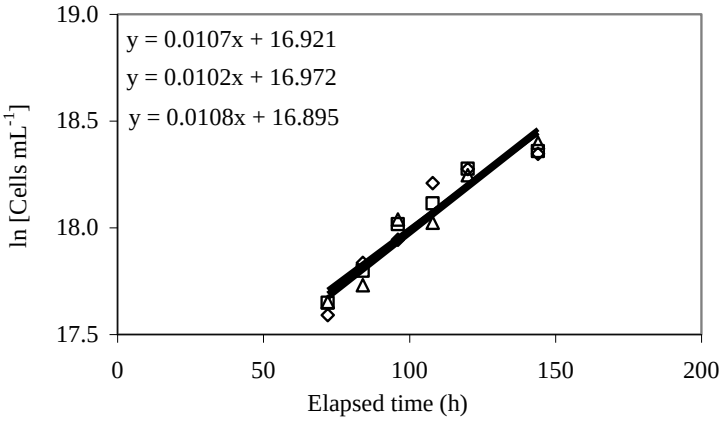


Specific growth rate (h^{-1})	
Trial 1	0.016
Trial 2	0.016
Trial 3	0.016
Average	0.016
STDEV	0.000
95% CI	0.000

Figure G.15. Specific growth rate calculations for Trial 1 (open circles), Trial 2 (open squares), and Trial 3 (open triangles).

Table G.16. BC13 growth in the presence of 50 mM zinc.

	Trial 1	Trial 2	Trial 3	Average	STDEV	95% CI	ln (Cells mL^{-1})		
0	5.23E+07	4.86E+07	5.00E+07	5.03E+07	1.86E+06	2.10E+06	17.77	17.70	17.73
12	5.16E+07	5.00E+07	4.84E+07	5.00E+07	1.62E+06	1.83E+06	17.76	17.73	17.69
24	4.88E+07	5.15E+07	5.26E+07	5.09E+07	1.96E+06	2.22E+06	17.70	17.76	17.78
72	4.36E+07	4.62E+07	4.64E+07	4.54E+07	1.56E+06	1.76E+06	17.59	17.65	17.65
84	5.57E+07	5.37E+07	5.01E+07	5.32E+07	2.82E+06	3.19E+06	17.84	17.80	17.73
96	6.21E+07	6.68E+07	6.82E+07	6.57E+07	3.22E+06	3.65E+06	17.94	18.02	18.04
108	8.09E+07	7.36E+07	6.72E+07	7.39E+07	6.86E+06	7.76E+06	18.21	18.11	18.02
120	8.64E+07	8.65E+07	8.39E+07	8.56E+07	1.47E+06	1.67E+06	18.27	18.28	18.25
144	9.29E+07	9.39E+07	9.78E+07	9.49E+07	2.61E+06	2.95E+06	18.35	18.36	18.40
168	9.09E+07	8.42E+07	8.86E+07	8.79E+07	3.42E+06	3.87E+06	18.33	18.25	18.30

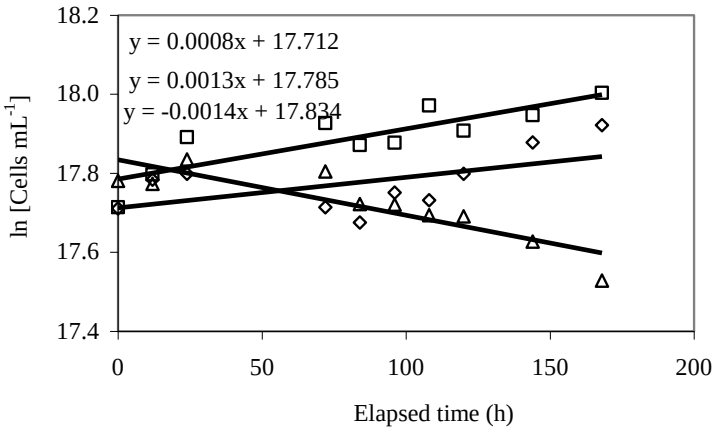


Specific growth rate (h^{-1})	
Trial 2	0.011
Trial 3	0.010
Average	0.011
STDEV	0.000
95% CI	0.000

Figure G.16. Specific growth rate calculations for Trial 1 (open circles), Trial 2 (open squares), and Trial 3 (open triangles).

Table G.17. BC13 growth in the presence of 75 mM zinc.

	Cells mL^{-1}						ln (Cells mL^{-1})		
Elapsed Time (h)	Trial 1	Trial 2	Trial 3	Average	STDEV	95% CI	Trial 1	Trial 2	Trial 3
0	4.92E+07	4.93E+07	5.27E+07	5.04E+07	2.01E+06	2.27E+06	17.71	17.71	17.78
12	5.29E+07	5.36E+07	5.23E+07	5.29E+07	6.24E+05	7.06E+05	17.78	17.80	17.77
24	5.37E+07	5.89E+07	5.57E+07	5.61E+07	2.62E+06	2.97E+06	17.80	17.89	17.83
72	4.93E+07	6.10E+07	5.40E+07	5.48E+07	5.89E+06	6.66E+06	17.71	17.93	17.80
84	4.75E+07	5.77E+07	4.97E+07	5.16E+07	5.40E+06	6.11E+06	17.68	17.87	17.72
96	5.12E+07	5.81E+07	4.97E+07	5.30E+07	4.47E+06	5.06E+06	17.75	17.88	17.72
108	5.02E+07	6.38E+07	4.83E+07	5.41E+07	8.45E+06	9.56E+06	17.73	17.97	17.69
120	5.37E+07	5.99E+07	4.82E+07	5.39E+07	5.84E+06	6.60E+06	17.80	17.91	17.69
144	5.81E+07	6.23E+07	4.52E+07	5.52E+07	8.89E+06	1.01E+07	17.88	17.95	17.63
168	6.07E+07	6.59E+07	4.10E+07	5.59E+07	1.32E+07	1.49E+07	17.92	18.00	17.53



Specific growth rate (h^{-1})

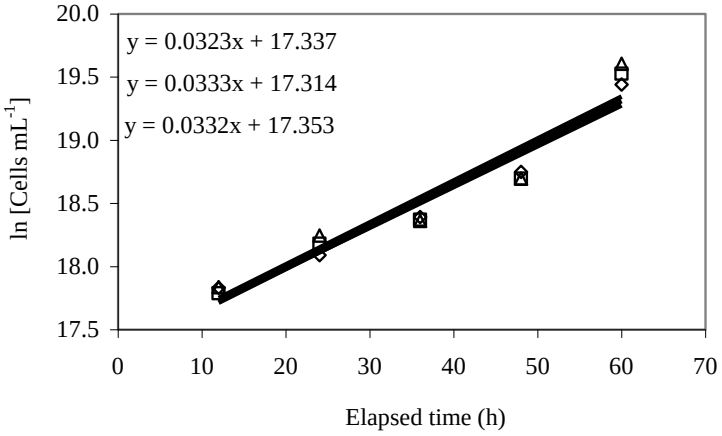
Trial 1	0.000
Trial 2	0.000
Trial 3	0.000
Average	0.000
STDEV	0.000
95% CI	0.000

Figure G.17. Specific growth rate calculations for Trial 1 (open circles), Trial 2 (open squares), and Trial 3 (open triangles).

Copper

Table G.18. BC13 growth in the presence of 1 mM copper.

	Cells mL^{-1}						ln (Cells mL^{-1})		
Elapsed Time (h)	Trial 1	Trial 2	Trial 3	Average	STDEV	95% CI	Trial 1	Trial 2	Trial 3
0	4.68E+07	5.04E+07	4.55E+07	4.76E+07	2.51E+06	2.84E+06	17.66	17.74	17.63
12	5.55E+07	5.31E+07	5.58E+07	5.48E+07	1.48E+06	1.67E+06	17.83	17.79	17.84
24	7.18E+07	7.85E+07	8.40E+07	7.81E+07	6.08E+06	6.88E+06	18.09	18.18	18.25
36	9.71E+07	9.51E+07	9.41E+07	9.54E+07	1.51E+06	1.70E+06	18.39	18.37	18.36
48	1.39E+08	1.32E+08	1.32E+08	1.34E+08	4.12E+06	4.66E+06	18.75	18.69	18.70
60	2.77E+08	3.02E+08	3.27E+08	3.02E+08	2.49E+07	2.82E+07	19.44	19.53	19.61
72	3.38E+08	3.07E+08	2.90E+08	3.12E+08	2.47E+07	2.79E+07	19.64	19.54	19.48
84	2.93E+08	3.22E+08	3.47E+08	3.20E+08	2.71E+07	3.07E+07	19.49	19.59	19.66
96	2.87E+08	3.14E+08	3.31E+08	3.10E+08	2.21E+07	2.50E+07	19.47	19.56	19.62
108	3.02E+08	2.85E+08	2.84E+08	2.90E+08	1.02E+07	1.15E+07	19.53	19.47	19.47
120	3.14E+08	2.90E+08	3.17E+08	3.07E+08	1.51E+07	1.71E+07	19.57	19.48	19.57



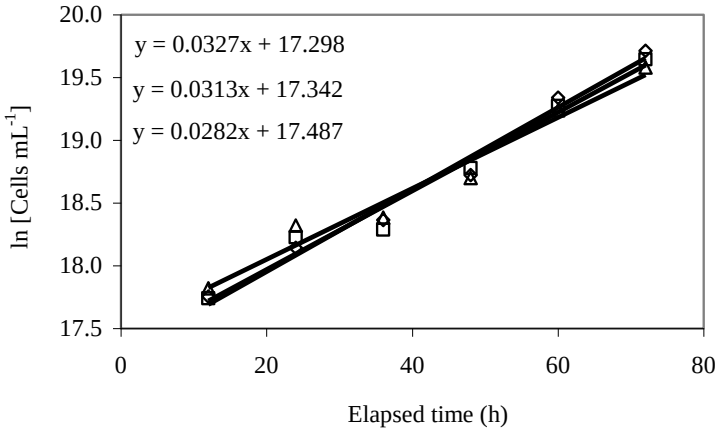
Specific growth rate (h^{-1})

Trial 1	0.032
Trial 2	0.033
Trial 3	0.033
Average	0.033
STDEV	0.001
95% CI	0.001

Figure G.18. Specific growth rate calculations for Trial 1 (open circles), Trial 2 (open squares), and Trial 3 (open triangles).

Table G.19. BC13 growth in the presence of 3 mM copper.

	Cells mL^{-1}						ln (Cells mL^{-1})		
Elapsed Time (h)	Trial 1	Trial 2	Trial 3	Average	STDEV	95% CI	Trial 1	Trial 2	Trial 3
0	4.90E+07	4.88E+07	4.99E+07	4.92E+07	5.89E+05	6.67E+05	17.71	17.70	17.73
12	5.13E+07	5.06E+07	5.48E+07	5.23E+07	2.27E+06	2.57E+06	17.75	17.74	17.82
24	7.58E+07	8.24E+07	9.05E+07	8.29E+07	7.38E+06	8.36E+06	18.14	18.23	18.32
36	9.46E+07	8.76E+07	9.62E+07	9.28E+07	4.60E+06	5.20E+06	18.36	18.29	18.38
48	1.35E+08	1.43E+08	1.32E+08	1.37E+08	5.70E+06	6.45E+06	18.72	18.78	18.70
60	2.51E+08	2.35E+08	2.27E+08	2.37E+08	1.23E+07	1.39E+07	19.34	19.27	19.24
72	3.64E+08	3.41E+08	3.18E+08	3.41E+08	2.28E+07	2.58E+07	19.71	19.65	19.58
84	3.19E+08	3.47E+08	3.31E+08	3.32E+08	1.43E+07	1.62E+07	19.58	19.67	19.62
96	2.75E+08	2.82E+08	2.84E+08	2.81E+08	4.73E+06	5.35E+06	19.43	19.46	19.46
108	2.91E+08	2.95E+08	2.85E+08	2.91E+08	5.17E+06	5.85E+06	19.49	19.50	19.47
120	3.15E+08	3.11E+08	3.34E+08	3.20E+08	1.25E+07	1.42E+07	19.57	19.56	19.63



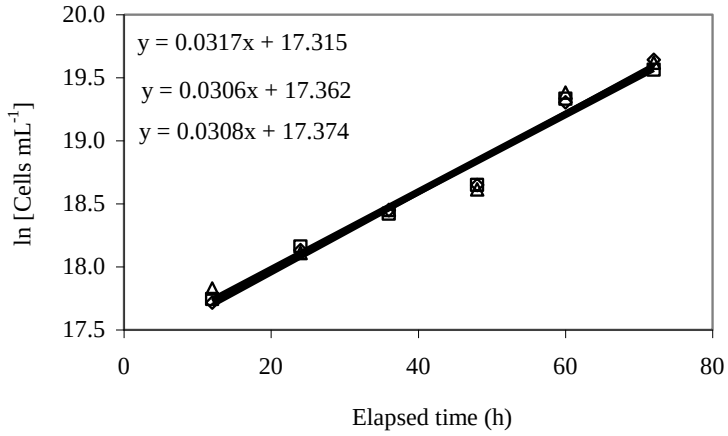
Specific growth rate (h^{-1})

Trial 1	0.033
Trial 2	0.031
Trial 3	0.028
Average	0.031
STDEV	0.002
95% CI	0.003

Figure G.19. Specific growth rate calculations for Trial 1 (open circles), Trial 2 (open squares), and Trial 3 (open triangles).

Table G.20. BC13 growth in the presence of 5 mM copper.

	Cells mL^{-1}						ln (Cells mL^{-1})		
Elapsed Time (h)	Trial 1	Trial 2	Trial 3	Average	STDEV	95% CI	Trial 1	Trial 2	Trial 3
0	4.99E+07	4.56E+07	4.60E+07	4.72E+07	2.37E+06	2.68E+06	17.73	17.64	17.64
12	4.95E+07	5.09E+07	5.52E+07	5.19E+07	3.02E+06	3.41E+06	17.72	17.74	17.83
24	7.51E+07	7.71E+07	7.33E+07	7.52E+07	1.92E+06	2.17E+06	18.13	18.16	18.11
36	1.03E+08	1.00E+08	1.03E+08	1.02E+08	1.67E+06	1.89E+06	18.45	18.42	18.45
48	1.26E+08	1.26E+08	1.21E+08	1.24E+08	2.41E+06	2.73E+06	18.65	18.65	18.61
60	2.42E+08	2.49E+08	2.61E+08	2.51E+08	9.87E+06	1.12E+07	19.30	19.33	19.38
72	3.39E+08	3.14E+08	3.31E+08	3.28E+08	1.29E+07	1.46E+07	19.64	19.56	19.62
84	3.10E+08	3.17E+08	2.97E+08	3.08E+08	9.84E+06	1.11E+07	19.55	19.57	19.51
96	2.87E+08	3.12E+08	3.36E+08	3.12E+08	2.46E+07	2.78E+07	19.48	19.56	19.63
108	2.84E+08	2.57E+08	2.32E+08	2.58E+08	2.60E+07	2.94E+07	19.47	19.37	19.26
120	3.01E+08	3.26E+08	3.27E+08	3.18E+08	1.47E+07	1.67E+07	19.52	19.60	19.61



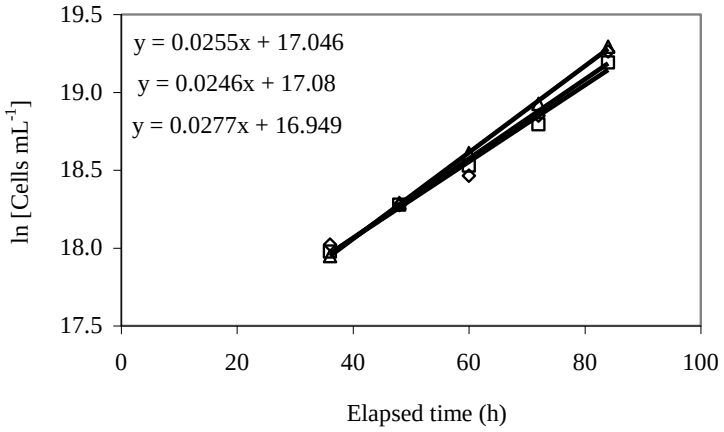
Specific growth rate (h^{-1})

Trial 1	0.032
Trial 2	0.031
Trial 3	0.031
Average	0.031
STDEV	0.001
95% CI	0.001

Figure G.20. Specific growth rate calculations for Trial 1 (open circles), Trial 2 (open squares), and Trial 3 (open triangles).

Table G.21. BC13 growth in the presence of 10 mM copper.

	Cells mL^{-1}						ln (Cells mL^{-1})		
Elapsed Time (h)	Trial 1	Trial 2	Trial 3	Average	STDEV	95% CI	Trial 1	Trial 2	Trial 3
0	5.18E+07	5.16E+07	4.80E+07	5.05E+07	2.13E+06	2.41E+06	17.76	17.76	17.69
12	5.66E+07	5.48E+07	5.23E+07	5.46E+07	2.18E+06	2.46E+06	17.85	17.82	17.77
24	6.09E+07	5.98E+07	6.31E+07	6.13E+07	1.70E+06	1.93E+06	17.92	17.91	17.96
36	6.71E+07	6.41E+07	6.24E+07	6.45E+07	2.38E+06	2.70E+06	18.02	17.98	17.95
48	8.65E+07	8.67E+07	8.76E+07	8.69E+07	5.94E+05	6.72E+05	18.28	18.28	18.29
60	1.04E+08	1.11E+08	1.21E+08	1.12E+08	8.18E+06	9.25E+06	18.46	18.53	18.61
72	1.54E+08	1.45E+08	1.66E+08	1.55E+08	1.03E+07	1.17E+07	18.85	18.79	18.93
84	2.32E+08	2.16E+08	2.39E+08	2.29E+08	1.18E+07	1.34E+07	19.26	19.19	19.29
96	2.62E+08	2.84E+08	2.59E+08	2.68E+08	1.35E+07	1.52E+07	19.39	19.46	19.37
108	2.36E+08	2.29E+08	2.29E+08	2.32E+08	3.74E+06	4.24E+06	19.28	19.25	19.25
120	2.17E+08	2.28E+08	2.06E+08	2.17E+08	1.10E+07	1.24E+07	19.19	19.24	19.14

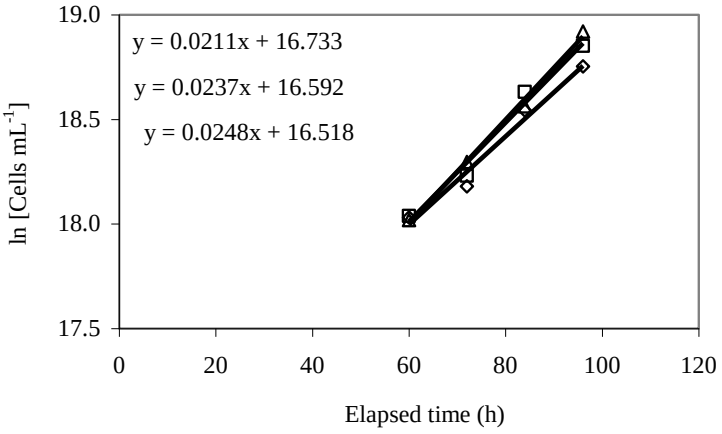


Specific growth rate (h^{-1})	
Trial 1	0.026
Trial 2	0.025
Trial 3	0.028
Average	0.026
STDEV	0.002
95% CI	0.002

Figure G.21. Specific growth rate calculations for Trial 1 (open circles), Trial 2 (open squares), and Trial 3 (open triangles).

Table G.22. BC13 growth in the presence of 20 mM copper.

	Cells mL^{-1}						ln (Cells mL^{-1})		
Elapsed Time (h)	Trial 1	Trial 2	Trial 3	Average	STDEV	95% CI	Trial 1	Trial 2	Trial 3
0	5.63E+07	5.65E+07	5.76E+07	5.68E+07	7.07E+05	8.00E+05	17.85	17.85	17.87
12	5.33E+07	4.93E+07	4.93E+07	5.06E+07	2.34E+06	2.64E+06	17.79	17.71	17.71
24	5.70E+07	5.63E+07	5.42E+07	5.58E+07	1.43E+06	1.61E+06	17.86	17.85	17.81
36	4.98E+07	5.47E+07	5.56E+07	5.34E+07	3.12E+06	3.53E+06	17.72	17.82	17.83
48	5.41E+07	5.71E+07	5.44E+07	5.52E+07	1.67E+06	1.89E+06	17.81	17.86	17.81
60	6.78E+07	6.82E+07	6.69E+07	6.76E+07	6.77E+05	7.66E+05	18.03	18.04	18.02
72	7.86E+07	8.27E+07	8.83E+07	8.32E+07	4.87E+06	5.51E+06	18.18	18.23	18.30
84	1.13E+08	1.23E+08	1.15E+08	1.17E+08	5.46E+06	6.18E+06	18.54	18.63	18.56
96	1.40E+08	1.54E+08	1.65E+08	1.53E+08	1.27E+07	1.44E+07	18.75	18.85	18.92
108	2.37E+08	2.36E+08	2.28E+08	2.34E+08	5.16E+06	5.84E+06	19.28	19.28	19.24
120	2.39E+08	2.58E+08	2.57E+08	2.51E+08	1.05E+07	1.19E+07	19.29	19.37	19.36
151	2.18E+08	2.39E+08	2.45E+08	2.34E+08	1.39E+07	1.58E+07	19.20	19.29	19.32
170	2.35E+08	2.16E+08	2.01E+08	2.17E+08	1.73E+07	1.95E+07	19.28	19.19	19.12

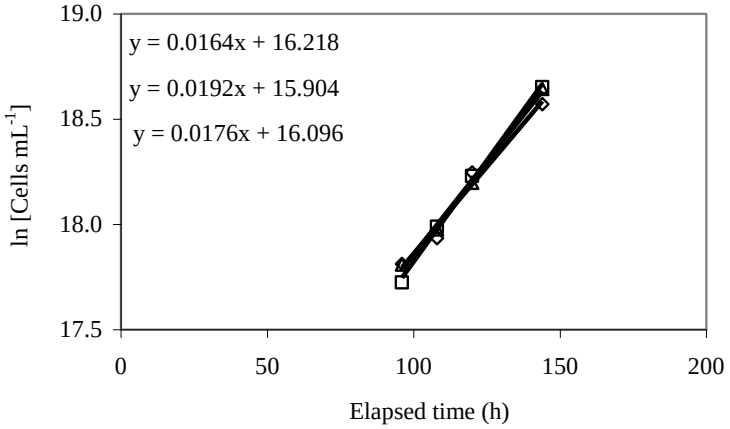


Specific growth rate (h^{-1})	
Trial 1	0.021
Trial 2	0.024
Trial 3	0.025
Average	0.023
STDEV	0.002
95% CI	0.002

Figure G.22. Specific growth rate calculations for Trial 1 (open circles), Trial 2 (open squares), and Trial 3 (open triangles).

Table G.23. BC13 growth in the presence of 50 mM copper.

	Cells mL^{-1}						ln (Cells mL^{-1})		
Elapsed Time (h)	Trial 1	Trial 2	Trial 3	Average	STDEV	95% CI	Trial 1	Trial 2	Trial 3
0	6.16E+07	6.63E+07	6.20E+07	6.33E+07	2.63E+06	2.98E+06	17.94	18.01	17.94
12	5.76E+07	5.19E+07	5.33E+07	5.43E+07	2.97E+06	3.36E+06	17.87	17.77	17.79
24	6.22E+07	6.49E+07	6.13E+07	6.28E+07	1.86E+06	2.11E+06	17.95	17.99	17.93
72	5.03E+07	4.98E+07	5.13E+07	5.05E+07	7.29E+05	8.25E+05	17.73	17.72	17.75
84	5.17E+07	5.21E+07	5.35E+07	5.24E+07	9.00E+05	1.02E+06	17.76	17.77	17.79
96	5.44E+07	4.99E+07	5.42E+07	5.28E+07	2.57E+06	2.90E+06	17.81	17.72	17.81
108	6.15E+07	6.50E+07	6.41E+07	6.35E+07	1.79E+06	2.02E+06	17.94	17.99	17.98
120	8.40E+07	8.26E+07	8.00E+07	8.22E+07	2.06E+06	2.33E+06	18.25	18.23	18.20
144	1.16E+08	1.26E+08	1.25E+08	1.22E+08	5.36E+06	6.06E+06	18.57	18.65	18.64
168	1.47E+08	1.36E+08	1.49E+08	1.44E+08	6.90E+06	7.81E+06	18.80	18.73	18.82

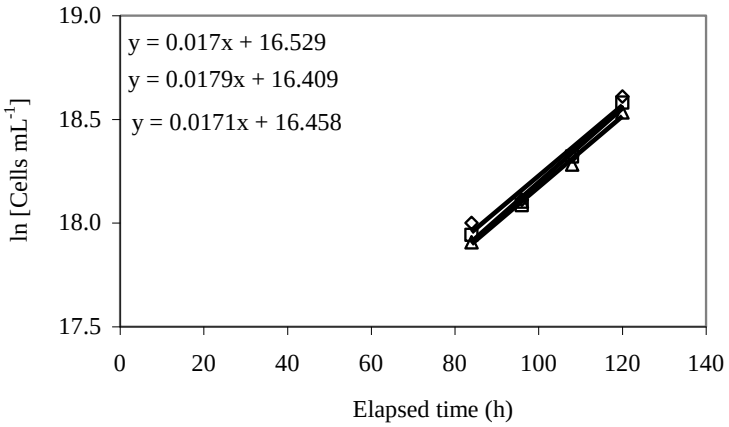


Specific growth rate (h^{-1})	
Trial 1	0.016
Trial 2	0.019
Trial 3	0.018
Average	0.018
STDEV	0.001
95% CI	0.002

Figure G.23. Specific growth rate calculations for Trial 1 (open circles), Trial 2 (open squares), and Trial 3 (open triangles).

Table G.24. BC13 growth in the presence of 100 mM copper.

	Cells mL^{-1}						ln (Cells mL^{-1})		
Elapsed Time (h)	Trial 1	Trial 2	Trial 3	Average	STDEV	95% CI	Trial 1	Trial 2	Trial 3
0	5.25E+07	5.03E+07	5.38E+07	5.22E+07	1.79E+06	2.02E+06	17.78	17.73	17.80
12	5.29E+07	5.04E+07	5.42E+07	5.25E+07	1.91E+06	2.16E+06	17.78	17.74	17.81
24	5.36E+07	5.11E+07	5.22E+07	5.23E+07	1.22E+06	1.38E+06	17.80	17.75	17.77
72	5.80E+07	5.75E+07	5.14E+07	5.56E+07	3.70E+06	4.19E+06	17.88	17.87	17.75
84	6.57E+07	6.20E+07	5.99E+07	6.25E+07	2.97E+06	3.37E+06	18.00	17.94	17.91
96	7.34E+07	7.15E+07	7.29E+07	7.26E+07	9.71E+05	1.10E+06	18.11	18.09	18.10
108	9.07E+07	9.04E+07	8.70E+07	8.93E+07	2.04E+06	2.31E+06	18.32	18.32	18.28
120	1.21E+08	1.17E+08	1.12E+08	1.17E+08	4.46E+06	5.05E+06	18.61	18.58	18.53
144	1.56E+08	1.48E+08	1.53E+08	1.52E+08	3.78E+06	4.28E+06	18.86	18.81	18.84
168	1.48E+08	1.47E+08	1.36E+08	1.44E+08	6.51E+06	7.36E+06	18.81	18.80	18.73

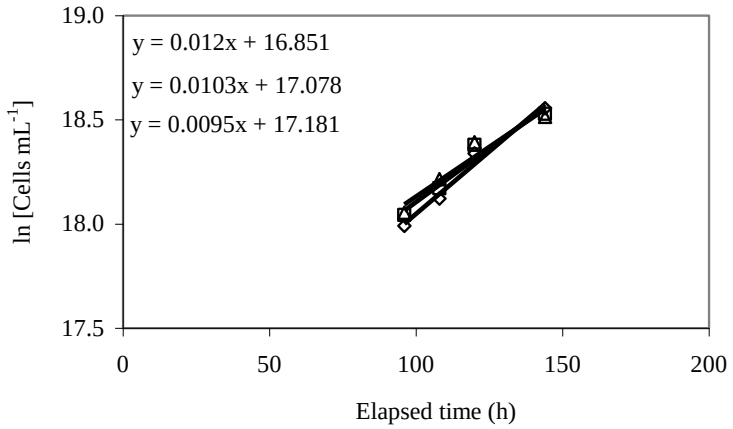


Specific growth rate (h^{-1})	
Trial 1	0.017
Trial 2	0.018
Trial 3	0.017
Average	0.017
STDEV	0.000
95% CI	0.001

Figure G.24. Specific growth rate calculations for Trial 1 (open circles), Trial 2 (open squares), and Trial 3 (open triangles).

Table G.25. BC13 growth in the presence of 150 mM copper.

	Cells mL^{-1}						ln (Cells mL^{-1})		
Elapsed Time (h)	Trial 1	Trial 2	Trial 3	Average	STDEV	95% CI	Trial 1	Trial 2	Trial 3
0	5.25E+07	4.90E+07	4.70E+07	4.95E+07	2.81E+06	3.18E+06	17.78	17.71	17.66
12	5.05E+07	4.81E+07	4.69E+07	4.85E+07	1.83E+06	2.07E+06	17.74	17.69	17.66
24	5.32E+07	5.12E+07	5.39E+07	5.28E+07	1.39E+06	1.57E+06	17.79	17.75	17.80
72	5.69E+07	5.89E+07	6.32E+07	5.97E+07	3.21E+06	3.63E+06	17.86	17.89	17.96
84	5.92E+07	6.16E+07	6.36E+07	6.15E+07	2.17E+06	2.45E+06	17.90	17.94	17.97
96	6.51E+07	6.85E+07	6.94E+07	6.77E+07	2.27E+06	2.57E+06	17.99	18.04	18.06
108	7.42E+07	7.80E+07	8.14E+07	7.78E+07	3.58E+06	4.05E+06	18.12	18.17	18.21
120	9.21E+07	9.59E+07	9.72E+07	9.51E+07	2.65E+06	3.00E+06	18.34	18.38	18.39
144	1.14E+08	1.11E+08	1.10E+08	1.12E+08	2.30E+06	2.60E+06	18.55	18.53	18.51
168	1.08E+08	1.02E+08	1.00E+08	1.04E+08	4.28E+06	4.84E+06	18.50	18.44	18.43

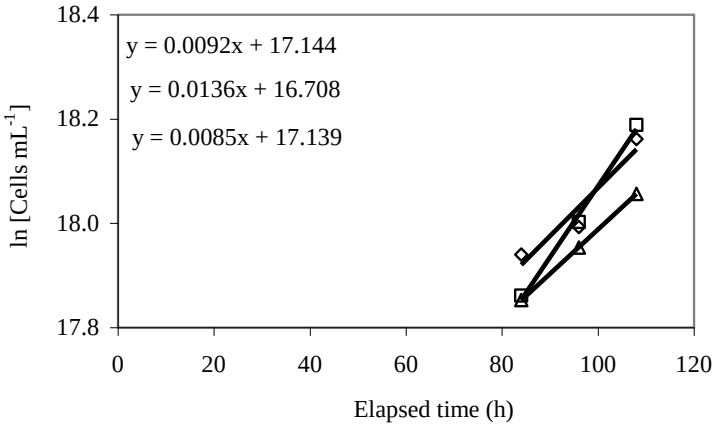


Specific growth rate (h^{-1})	
Trial 1	0.012
Trial 2	0.010
Trial 3	0.010
Average	0.011
STDEV	0.001
95% CI	0.001

Figure G.25. Specific growth rate calculations for Trial 1 (open circles), Trial 2 (open squares), and Trial 3 (open triangles).

Table G.26. BC13 growth in the presence of 200 mM copper.

	Cells mL^{-1}						ln (Cells mL^{-1})		
Elapsed Time (h)	Trial 1	Trial 2	Trial 3	Average	STDEV	95% CI	Trial 1	Trial 2	Trial 3
0	4.75E+07	4.54E+07	4.21E+07	4.50E+07	2.72E+06	3.08E+06	17.68	17.63	17.56
12	5.06E+07	5.26E+07	5.34E+07	5.22E+07	1.44E+06	1.63E+06	17.74	17.78	17.79
24	5.19E+07	5.08E+07	5.51E+07	5.26E+07	2.20E+06	2.49E+06	17.76	17.74	17.82
72	5.66E+07	5.37E+07	5.00E+07	5.34E+07	3.28E+06	3.71E+06	17.85	17.80	17.73
84	6.18E+07	5.71E+07	5.67E+07	5.85E+07	2.85E+06	3.22E+06	17.94	17.86	17.85
96	6.52E+07	6.58E+07	6.27E+07	6.46E+07	1.64E+06	1.86E+06	17.99	18.00	17.95
108	7.72E+07	7.93E+07	6.95E+07	7.53E+07	5.15E+06	5.83E+06	18.16	18.19	18.06
120	8.30E+07	8.93E+07	8.07E+07	8.43E+07	4.46E+06	5.04E+06	18.23	18.31	18.21
144	9.08E+07	9.03E+07	8.90E+07	9.01E+07	9.12E+05	1.03E+06	18.32	18.32	18.30
168	1.07E+08	1.13E+08	1.08E+08	1.09E+08	3.42E+06	3.87E+06	18.49	18.54	18.49



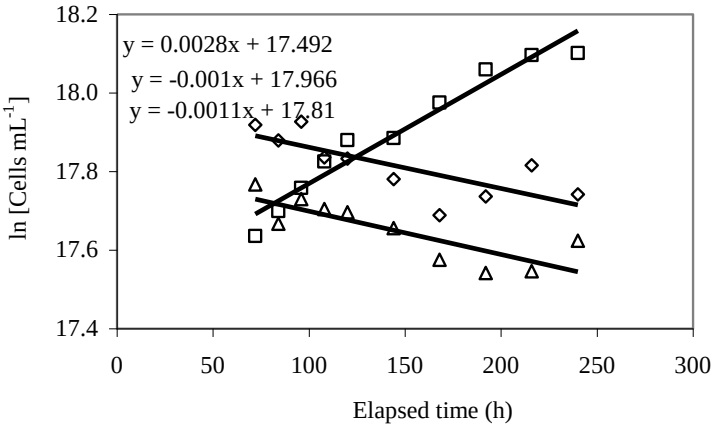
Specific growth rate (h^{-1})

Trial 1	0.009
Trial 2	0.014
Trial 3	0.009
Average	0.010
STDEV	0.003
95% CI	0.003

Figure G.26. Specific growth rate calculations for Trial 1 (open circles), Trial 2 (open squares), and Trial 3 (open triangles).

Table G.27. BC13 growth in the presence of 250 mM copper.

	Cells mL^{-1}						ln (Cells mL^{-1})		
Elapsed Time (h)	Trial 1	Trial 2	Trial 3	Average	STDEV	95% CI	Trial 1	Trial 2	Trial 3
0	5.20E+07	5.39E+07	5.74E+07	5.44E+07	2.76E+06	3.13E+06	17.77	17.80	17.87
12	5.34E+07	5.05E+07	5.87E+07	5.42E+07	4.17E+06	4.71E+06	17.79	17.74	17.89
24	5.76E+07	4.61E+07	5.45E+07	5.28E+07	5.95E+06	6.73E+06	17.87	17.65	17.81
72	6.05E+07	4.56E+07	5.20E+07	5.27E+07	7.48E+06	8.46E+06	17.92	17.64	17.77
84	5.82E+07	4.86E+07	4.71E+07	5.13E+07	6.02E+06	6.81E+06	17.88	17.70	17.67
96	6.11E+07	5.16E+07	5.01E+07	5.42E+07	5.93E+06	6.72E+06	17.93	17.76	17.73
108	5.57E+07	5.51E+07	4.88E+07	5.32E+07	3.81E+06	4.31E+06	17.84	17.83	17.70
120	5.55E+07	5.82E+07	4.85E+07	5.41E+07	5.04E+06	5.71E+06	17.83	17.88	17.70
144	5.27E+07	5.85E+07	4.66E+07	5.26E+07	5.98E+06	6.77E+06	17.78	17.88	17.66
168	4.81E+07	6.41E+07	4.29E+07	5.17E+07	1.10E+07	1.25E+07	17.69	17.98	17.58
192	5.05E+07	6.97E+07	4.15E+07	5.39E+07	1.44E+07	1.63E+07	17.74	18.06	17.54
216	5.46E+07	7.23E+07	4.17E+07	5.62E+07	1.54E+07	1.74E+07	17.82	18.10	17.55
240	5.07E+07	7.27E+07	4.51E+07	5.62E+07	1.46E+07	1.65E+07	17.74	18.10	17.62
264	4.62E+07	7.00E+07	4.22E+07	5.28E+07	1.50E+07	1.70E+07	17.65	18.06	17.56



Specific growth rate (h^{-1})

Trial 1	0.003
Trial 2	0.000
Trial 3	0.000
Average	0.001
STDEV	0.002
95% CI	0.002

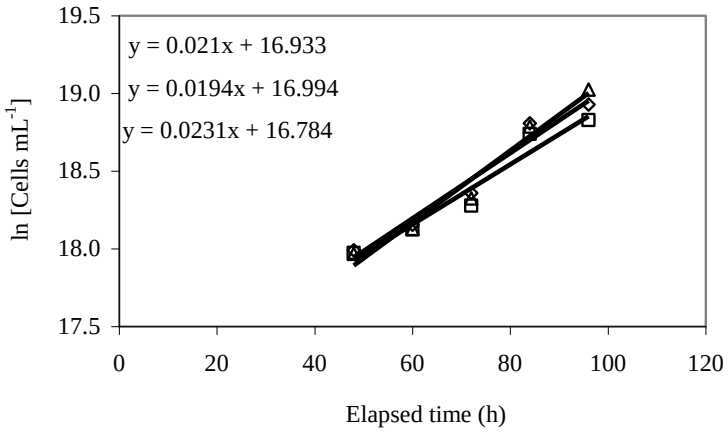
Figure G.27. Specific growth rate calculations for Trial 1 (open circles), Trial 2 (open squares), and Trial 3 (open triangles).

Toxicity of Heavy Metals when Combined

Lead and Zinc

Table G.28. BC13 growth in the presence of 0.125 x Pb_{MIC} + 0.125 x Zn_{MIC}.

	Cells mL^{-1}						ln (Cells mL^{-1})		
Elapsed Time (h)	Trial 1	Trial 2	Trial 3	Average	STDEV	95% CI	Trial 1	Trial 2	Trial 3
0	5.77E+07	6.01E+07	5.63E+07	5.81E+07	1.93E+06	2.18E+06	17.87	17.91	17.85
12	5.65E+07	5.62E+07	5.65E+07	5.64E+07	1.58E+05	1.78E+05	17.85	17.85	17.85
24	4.93E+07	4.97E+07	5.44E+07	5.11E+07	2.85E+06	3.22E+06	17.71	17.72	17.81
36	6.10E+07	6.06E+07	6.13E+07	6.10E+07	3.48E+05	3.94E+05	17.93	17.92	17.93
48	6.50E+07	6.39E+07	6.36E+07	6.42E+07	7.74E+05	8.76E+05	17.99	17.97	17.97
60	7.67E+07	7.44E+07	7.47E+07	7.53E+07	1.26E+06	1.42E+06	18.16	18.13	18.13
72	9.39E+07	8.67E+07	9.09E+07	9.05E+07	3.64E+06	4.12E+06	18.36	18.28	18.33
84	1.47E+08	1.37E+08	1.44E+08	1.43E+08	4.95E+06	5.60E+06	18.81	18.74	18.79
96	1.66E+08	1.50E+08	1.83E+08	1.66E+08	1.63E+07	1.84E+07	18.93	18.83	19.02
108	1.93E+08	1.64E+08	1.86E+08	1.81E+08	1.51E+07	1.71E+07	19.08	18.92	19.04
120	2.18E+08	1.32E+08	1.26E+08	1.59E+08	5.13E+07	5.80E+07	19.20	18.70	18.65
144	2.28E+08	1.47E+08	1.41E+08	1.72E+08	4.88E+07	5.53E+07	19.25	18.81	18.76

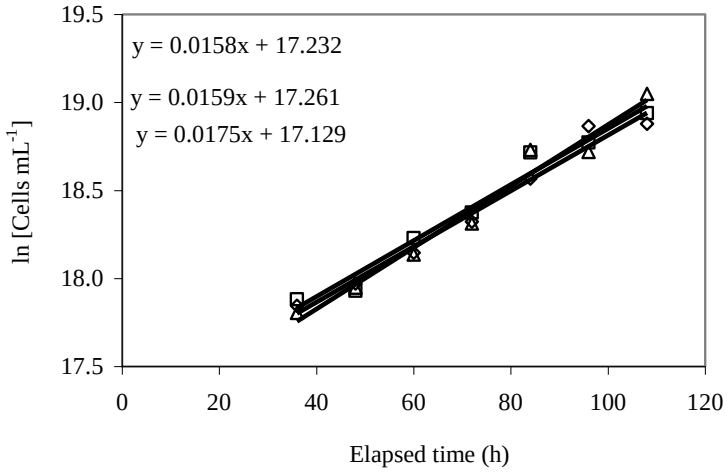


Specific growth rate (h^{-1})	
Trial 1	0.021
Trial 2	0.019
Trial 3	0.023
Average	0.021
STDEV	0.002
95% CI	0.002

.Figure G.28. Specific growth rate calculations for Trial 1 (open circles), Trial 2 (open squares), and Trial 3 (open triangles).

Table G.29. BC13 growth in the presence of 0.25 x Pb_{MIC} + 0.25 x Zn_{MIC}.

	Cells mL^{-1}						ln (Cells mL^{-1})		
Elapsed Time (h)	Trial 1	Trial 2	Trial 3	Average	STDEV	95% CI	Trial 1	Trial 2	Trial 3
0	5.26E+07	5.35E+07	5.55E+07	5.39E+07	1.45E+06	1.65E+06	17.78	17.79	17.83
12	5.56E+07	5.78E+07	5.68E+07	5.67E+07	1.09E+06	1.24E+06	17.83	17.87	17.85
24	5.48E+07	5.84E+07	6.17E+07	5.83E+07	3.47E+06	3.92E+06	17.82	17.88	17.94
36	5.62E+07	5.83E+07	5.40E+07	5.62E+07	2.15E+06	2.43E+06	17.84	17.88	17.81
48	6.38E+07	6.12E+07	6.23E+07	6.24E+07	1.26E+06	1.43E+06	17.97	17.93	17.95
60	7.60E+07	8.25E+07	7.53E+07	7.79E+07	4.01E+06	4.54E+06	18.15	18.23	18.14
72	9.07E+07	9.55E+07	8.97E+07	9.20E+07	3.09E+06	3.50E+06	18.32	18.37	18.31
84	1.16E+08	1.34E+08	1.36E+08	1.29E+08	1.13E+07	1.28E+07	18.57	18.71	18.73
96	1.56E+08	1.42E+08	1.35E+08	1.44E+08	1.09E+07	1.23E+07	18.87	18.77	18.72
108	1.58E+08	1.68E+08	1.87E+08	1.71E+08	1.49E+07	1.69E+07	18.88	18.94	19.05
120	1.79E+08	1.50E+08	1.74E+08	1.67E+08	1.57E+07	1.78E+07	19.00	18.82	18.97
144	1.86E+08	1.41E+08	1.79E+08	1.69E+08	2.41E+07	2.73E+07	19.04	18.77	19.00
168	1.95E+08	1.31E+08	1.63E+08	1.63E+08	3.23E+07	3.65E+07	19.09	18.69	18.91

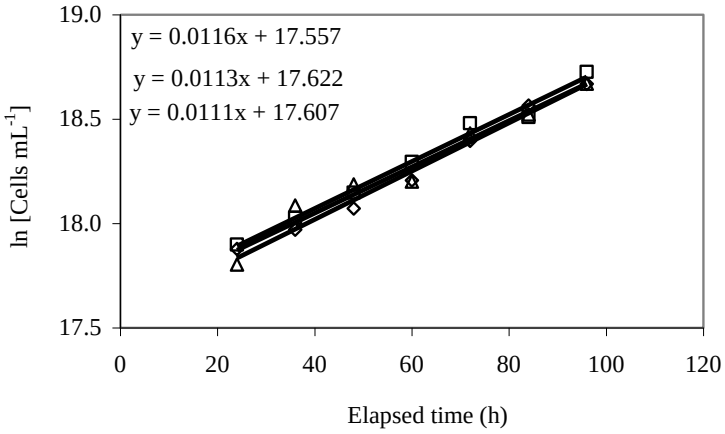


Specific growth rate (h^{-1})	
Trial 1	0.016
Trial 2	0.016
Trial 3	0.018
Average	0.016
STDEV	0.001
95% CI	0.001

Figure G.29. Specific growth rate calculations for Trial 1 (open circles), Trial 2 (open squares), and Trial 3 (open triangles).

Table G.30. BC13 growth in the presence of 0.375 x Pb_{MIC} + 0.375 x Zn_{MIC}.

	Cells mL^{-1}						ln (Cells mL^{-1})		
Elapsed Time (h)	Trial 1	Trial 2	Trial 3	Average	STDEV	95% CI	Trial 1	Trial 2	Trial 3
0	5.52E+07	5.71E+07	5.49E+07	5.57E+07	1.15E+06	1.31E+06	17.83	17.86	17.82
12	5.79E+07	5.75E+07	5.90E+07	5.81E+07	7.77E+05	8.79E+05	17.87	17.87	17.89
24	5.81E+07	5.94E+07	5.39E+07	5.71E+07	2.85E+06	3.22E+06	17.88	17.90	17.80
36	6.38E+07	6.74E+07	7.15E+07	6.76E+07	3.87E+06	4.38E+06	17.97	18.03	18.09
48	7.05E+07	7.61E+07	7.92E+07	7.53E+07	4.39E+06	4.97E+06	18.07	18.15	18.19
60	8.07E+07	8.81E+07	8.02E+07	8.30E+07	4.44E+06	5.03E+06	18.21	18.29	18.20
72	9.76E+07	1.06E+08	1.01E+08	1.02E+08	4.32E+06	4.88E+06	18.40	18.48	18.43
84	1.15E+08	1.09E+08	1.11E+08	1.12E+08	3.26E+06	3.69E+06	18.56	18.51	18.52
96	1.28E+08	1.36E+08	1.28E+08	1.31E+08	4.39E+06	4.96E+06	18.67	18.73	18.67
108	1.37E+08	1.30E+08	1.37E+08	1.35E+08	4.16E+06	4.70E+06	18.74	18.68	18.73
120	1.38E+08	1.48E+08	1.46E+08	1.44E+08	4.97E+06	5.62E+06	18.75	18.81	18.80
144	1.34E+08	1.24E+08	1.36E+08	1.31E+08	6.33E+06	7.17E+06	18.72	18.64	18.73
168	1.36E+08	1.29E+08	1.40E+08	1.35E+08	5.65E+06	6.39E+06	18.73	18.68	18.76

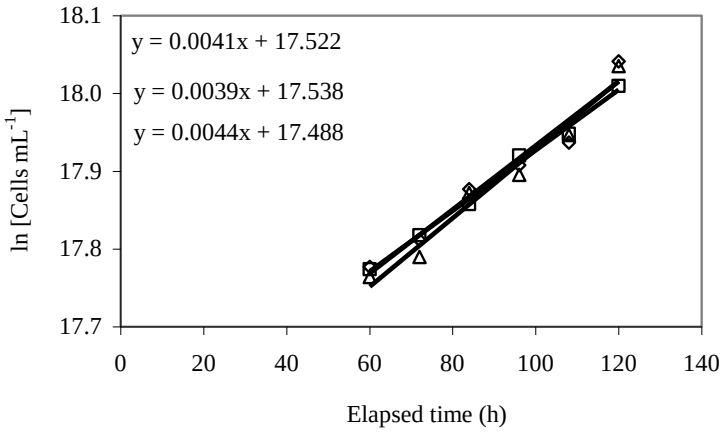


Specific growth rate (h^{-1})	
Trial 1	0.012
Trial 2	0.011
Trial 3	0.011
Average	0.011
STDEV	0.000
95% CI	0.000

Figure G.30. Specific growth rate calculations for Trial 1 (open circles), Trial 2 (open squares), and Trial 3 (open triangles).

Table G.31. BC13 growth in the presence of 0.50 x Pb_{MIC} + 0.50 x Zn_{MIC}.

	Cells mL^{-1}						ln (Cells mL^{-1})		
Elapsed Time (h)	Trial 1	Trial 2	Trial 3	Average	STDEV	95% CI	Trial 1	Trial 2	Trial 3
0	4.94E+07	4.84E+07	4.77E+07	4.85E+07	8.54E+05	9.66E+05	17.72	17.69	17.68
12	5.13E+07	5.00E+07	5.12E+07	5.09E+07	7.20E+05	8.15E+05	17.75	17.73	17.75
24	5.29E+07	5.22E+07	5.37E+07	5.29E+07	7.33E+05	8.30E+05	17.78	17.77	17.80
36	5.38E+07	5.45E+07	5.27E+07	5.37E+07	8.97E+05	1.01E+06	17.80	17.81	17.78
48	5.17E+07	5.27E+07	5.26E+07	5.23E+07	5.82E+05	6.59E+05	17.76	17.78	17.78
60	5.25E+07	5.24E+07	5.19E+07	5.23E+07	3.51E+05	3.98E+05	17.78	17.77	17.76
72	5.44E+07	5.47E+07	5.32E+07	5.41E+07	7.91E+05	8.95E+05	17.81	17.82	17.79
84	5.81E+07	5.69E+07	5.78E+07	5.76E+07	5.76E+05	6.52E+05	17.88	17.86	17.87
96	5.99E+07	6.06E+07	5.91E+07	5.99E+07	7.52E+05	8.51E+05	17.91	17.92	17.90
108	6.16E+07	6.23E+07	6.22E+07	6.21E+07	3.78E+05	4.28E+05	17.94	17.95	17.95
120	6.84E+07	6.63E+07	6.80E+07	6.76E+07	1.13E+06	1.27E+06	18.04	18.01	18.04
144	6.94E+07	6.96E+07	6.86E+07	6.92E+07	5.06E+05	5.73E+05	18.06	18.06	18.04
168	7.04E+07	7.04E+07	6.84E+07	6.97E+07	1.16E+06	1.31E+06	18.07	18.07	18.04



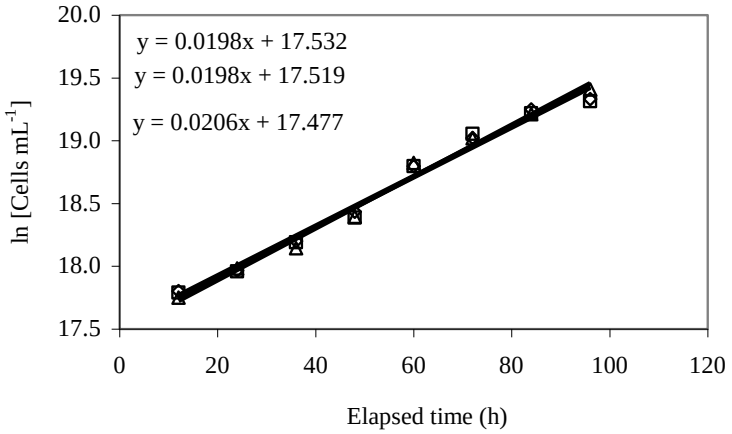
Specific growth rate (h^{-1})	
Trial 1	0.004
Trial 2	0.004
Trial 3	0.004
Average	0.0041
STDEV	0.0003
95% CI	0.0003

Figure G.31. Specific growth rate calculations for Trial 1 (open circles), Trial 2 (open squares), and Trial 3 (open triangles).

Lead and Copper

Table G.32. BC13 growth in the presence of 0.125 x Pb_{MIC} + 0.125 x Cu_{MIC}.

	Cells mL^{-1}						ln (Cells mL^{-1})		
Elapsed Time (h)	Trial 1	Trial 2	Trial 3	Average	STDEV	95% CI	Trial 1	Trial 2	Trial 3
0	5.20E+07	5.24E+07	5.47E+07	5.30E+07	1.45E+06	1.64E+06	17.77	17.77	17.82
12	5.39E+07	5.33E+07	5.12E+07	5.28E+07	1.44E+06	1.62E+06	17.80	17.79	17.75
24	6.35E+07	6.29E+07	6.44E+07	6.36E+07	7.58E+05	8.58E+05	17.97	17.96	17.98
36	8.01E+07	7.95E+07	7.58E+07	7.85E+07	2.34E+06	2.65E+06	18.20	18.19	18.14
48	1.01E+08	9.67E+07	9.74E+07	9.85E+07	2.52E+06	2.85E+06	18.43	18.39	18.39
60	1.46E+08	1.46E+08	1.50E+08	1.47E+08	2.22E+06	2.52E+06	18.80	18.80	18.82
72	1.82E+08	1.88E+08	1.82E+08	1.84E+08	3.66E+06	4.15E+06	19.02	19.05	19.02
84	2.29E+08	2.22E+08	2.20E+08	2.24E+08	4.49E+06	5.08E+06	19.25	19.22	19.21
96	2.48E+08	2.45E+08	2.68E+08	2.54E+08	1.28E+07	1.44E+07	19.33	19.32	19.41
108	2.01E+08	2.10E+08	2.18E+08	2.10E+08	8.62E+06	9.75E+06	19.12	19.16	19.20
120	2.18E+08	2.20E+08	2.09E+08	2.15E+08	5.71E+06	6.46E+06	19.20	19.21	19.16
144	2.44E+08	2.53E+08	2.64E+08	2.54E+08	1.03E+07	1.17E+07	19.31	19.35	19.39



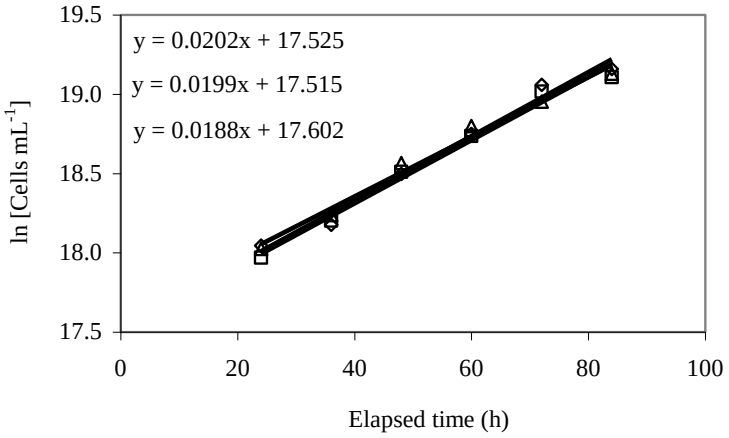
Specific growth rate (h^{-1})

Trial 1	0.020
Trial 2	0.020
Trial 3	0.021
Average	0.020
STDEV	0.000
95% CI	0.001

Figure G.32. Specific growth rate calculations for Trial 1 (open circles), Trial 2 (open squares), and Trial 3 (open triangles).

Table G.33. BC13 growth in the presence of 0.25 x Pb_{MIC} + 0.25 x Cu_{MIC}.

	Cells mL^{-1}						ln (Cells mL^{-1})		
Elapsed Time (h)	Trial 1	Trial 2	Trial 3	Average	STDEV	95% CI	Trial 1	Trial 2	Trial 3
0	5.00E+07	4.52E+07	4.44E+07	4.65E+07	3.01E+06	3.41E+06	17.73	17.63	17.61
12	5.45E+07	5.89E+07	6.17E+07	5.84E+07	3.62E+06	4.10E+06	17.81	17.89	17.94
24	6.87E+07	6.36E+07	6.73E+07	6.65E+07	2.61E+06	2.96E+06	18.04	17.97	18.02
36	7.83E+07	8.04E+07	8.33E+07	8.07E+07	2.48E+06	2.81E+06	18.18	18.20	18.24
48	1.08E+08	1.09E+08	1.16E+08	1.11E+08	4.10E+06	4.63E+06	18.50	18.51	18.57
60	1.39E+08	1.37E+08	1.46E+08	1.41E+08	4.67E+06	5.28E+06	18.75	18.74	18.80
72	1.89E+08	1.81E+08	1.70E+08	1.80E+08	9.59E+06	1.08E+07	19.06	19.02	18.95
84	2.09E+08	1.99E+08	2.03E+08	2.04E+08	5.34E+06	6.04E+06	19.16	19.11	19.13
96	2.42E+08	2.25E+08	2.35E+08	2.34E+08	8.75E+06	9.90E+06	19.30	19.23	19.27
108	1.94E+08	2.13E+08	2.30E+08	2.12E+08	1.82E+07	2.06E+07	19.08	19.18	19.25
120	2.14E+08	2.04E+08	2.16E+08	2.11E+08	6.32E+06	7.15E+06	19.18	19.13	19.19
144	2.57E+08	2.69E+08	2.58E+08	2.61E+08	6.43E+06	7.27E+06	19.37	19.41	19.37
168	2.50E+08	2.52E+08	2.60E+08	2.54E+08	5.42E+06	6.13E+06	19.34	19.34	19.38

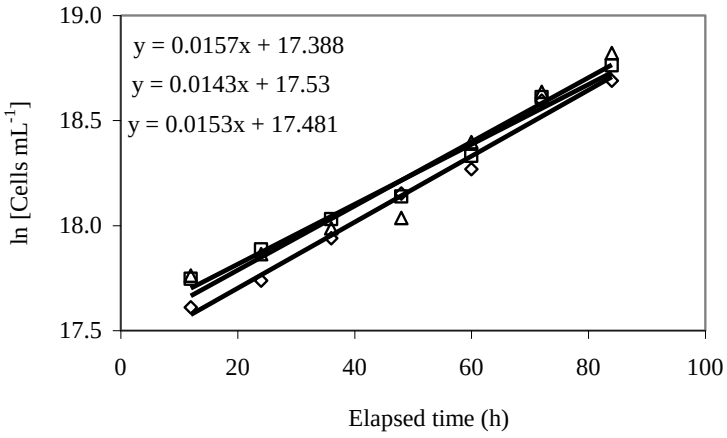


Specific growth rate (h^{-1})	
Trial 1	0.020
Trial 2	0.020
Trial 3	0.019
Average	0.020
STDEV	0.001
95% CI	0.001

Figure G.33. Specific growth rate calculations for Trial 1 (open circles), Trial 2 (open squares), and Trial 3 (open triangles).

Table G.34. BC13 growth in the presence of 0.375 x Pb_{MIC} + 0.375 x Cu_{MIC}.

	Cells mL^{-1}						ln (Cells mL^{-1})		
Elapsed Time (h)	Trial 1	Trial 2	Trial 3	Average	STDEV	95% CI	Trial 1	Trial 2	Trial 3
0	4.52E+07	4.52E+07	4.44E+07	4.49E+07	4.72E+05	5.34E+05	17.63	17.63	17.61
12	4.45E+07	5.09E+07	5.17E+07	4.90E+07	3.97E+06	4.49E+06	17.61	17.75	17.76
24	5.05E+07	5.86E+07	5.73E+07	5.55E+07	4.35E+06	4.93E+06	17.74	17.89	17.86
36	6.18E+07	6.77E+07	6.48E+07	6.48E+07	2.95E+06	3.34E+06	17.94	18.03	17.99
48	7.65E+07	7.54E+07	6.81E+07	7.33E+07	4.59E+06	5.19E+06	18.15	18.14	18.04
60	8.58E+07	9.15E+07	9.76E+07	9.17E+07	5.90E+06	6.68E+06	18.27	18.33	18.40
72	1.19E+08	1.21E+08	1.24E+08	1.21E+08	2.60E+06	2.94E+06	18.59	18.61	18.64
84	1.31E+08	1.41E+08	1.49E+08	1.40E+08	9.19E+06	1.04E+07	18.69	18.76	18.82
96	1.44E+08	1.41E+08	1.27E+08	1.37E+08	8.91E+06	1.01E+07	18.78	18.76	18.66
108	1.17E+08	1.14E+08	1.14E+08	1.15E+08	1.66E+06	1.87E+06	18.57	18.55	18.55
120	1.15E+08	1.16E+08	1.11E+08	1.14E+08	2.33E+06	2.63E+06	18.56	18.57	18.53
144	1.07E+08	1.09E+08	1.06E+08	1.08E+08	1.73E+06	1.96E+06	18.49	18.51	18.48
168	1.16E+08	1.14E+08	1.15E+08	1.15E+08	1.12E+06	1.26E+06	18.57	18.55	18.56



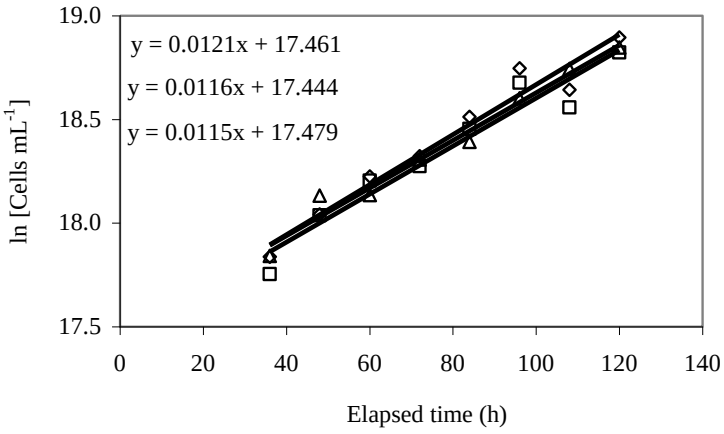
Specific growth rate (h^{-1})

Trial 1	0.016
Trial 2	0.014
Trial 3	0.015
Average	0.015
STDEV	0.001
95% CI	0.001

Figure G.34. Specific growth rate calculations for Trial 1 (open circles), Trial 2 (open squares), and Trial 3 (open triangles).

Table G.35. BC13 growth in the presence of 0.50 x Pb_{MIC} + 0.50 x Cu_{MIC}.

	Cells mL^{-1}						ln (Cells mL^{-1})		
Elapsed Time (h)	Trial 1	Trial 2	Trial 3	Average	STDEV	95% CI	Trial 1	Trial 2	Trial 3
0	5.51E+07	6.01E+07	6.58E+07	6.03E+07	5.34E+06	6.05E+06	17.82	17.91	18.00
12	5.44E+07	5.16E+07	4.83E+07	5.14E+07	3.04E+06	3.44E+06	17.81	17.76	17.69
24	5.59E+07	5.18E+07	4.91E+07	5.23E+07	3.40E+06	3.85E+06	17.84	17.76	17.71
36	5.58E+07	5.13E+07	5.60E+07	5.44E+07	2.65E+06	3.00E+06	17.84	17.75	17.84
48	6.84E+07	6.81E+07	7.49E+07	7.05E+07	3.83E+06	4.34E+06	18.04	18.04	18.13
60	8.21E+07	8.06E+07	7.52E+07	7.93E+07	3.67E+06	4.15E+06	18.22	18.20	18.14
72	9.06E+07	8.63E+07	8.92E+07	8.87E+07	2.19E+06	2.48E+06	18.32	18.27	18.31
84	1.10E+08	1.03E+08	9.71E+07	1.03E+08	6.24E+06	7.06E+06	18.51	18.45	18.39
96	1.39E+08	1.29E+08	1.20E+08	1.29E+08	9.32E+06	1.05E+07	18.75	18.68	18.60
108	1.25E+08	1.15E+08	1.38E+08	1.26E+08	1.18E+07	1.33E+07	18.64	18.56	18.74
120	1.61E+08	1.49E+08	1.53E+08	1.54E+08	5.75E+06	6.51E+06	18.90	18.82	18.85
144	1.59E+08	1.60E+08	1.56E+08	1.58E+08	1.79E+06	2.02E+06	18.89	18.89	18.87
168	1.47E+08	1.45E+08	1.51E+08	1.48E+08	2.66E+06	3.01E+06	18.81	18.79	18.83



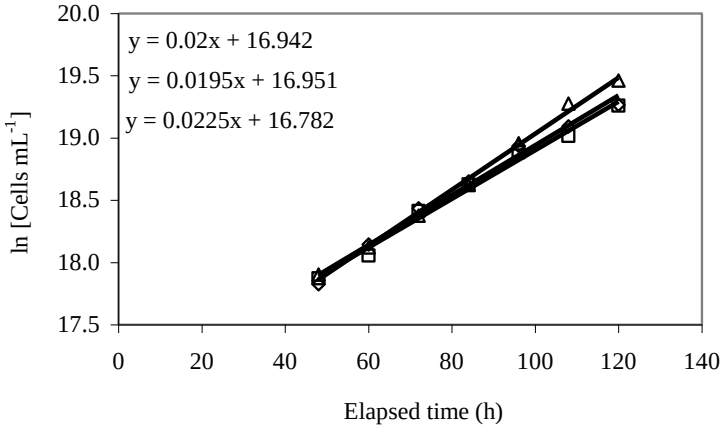
Specific growth rate (h^{-1})	
Trial 1	0.012
Trial 2	0.012
Trial 3	0.012
Average	0.012
STDEV	0.000
95% CI	0.000

Figure G.35. Specific growth rate calculations for Trial 1 (open circles), Trial 2 (open squares), and Trial 3 (open triangles).

Zinc and Copper

Table G.36. BC13 growth in the presence of 0.125 x Zn_{MIC} + 0.125 x Cu_{MIC}.

	Cells mL^{-1}						ln (Cells mL^{-1})		
Elapsed Time (h)	Trial 1	Trial 2	Trial 3	Average	STDEV	95% CI	Trial 1	Trial 2	Trial 3
0	5.62E+07	5.10E+07	4.64E+07	5.12E+07	4.86E+06	5.50E+06	17.84	17.75	17.65
12	5.33E+07	5.65E+07	5.88E+07	5.62E+07	2.77E+06	3.13E+06	17.79	17.85	17.89
24	5.37E+07	5.60E+07	5.34E+07	5.43E+07	1.41E+06	1.59E+06	17.80	17.84	17.79
36	5.43E+07	5.21E+07	5.31E+07	5.32E+07	1.10E+06	1.24E+06	17.81	17.77	17.79
48	5.52E+07	5.78E+07	5.95E+07	5.75E+07	2.20E+06	2.49E+06	17.83	17.87	17.90
60	7.58E+07	6.93E+07	7.41E+07	7.31E+07	3.37E+06	3.81E+06	18.14	18.05	18.12
72	1.01E+08	9.94E+07	9.57E+07	9.88E+07	2.87E+06	3.25E+06	18.43	18.41	18.38
84	1.26E+08	1.23E+08	1.22E+08	1.24E+08	1.95E+06	2.21E+06	18.65	18.63	18.62
96	1.67E+08	1.59E+08	1.71E+08	1.66E+08	5.99E+06	6.78E+06	18.94	18.89	18.96
108	1.96E+08	1.81E+08	2.35E+08	2.04E+08	2.80E+07	3.17E+07	19.09	19.02	19.28
120	2.33E+08	2.31E+08	2.83E+08	2.49E+08	2.94E+07	3.33E+07	19.27	19.26	19.46
144	2.18E+08	2.39E+08	3.00E+08	2.52E+08	4.26E+07	4.82E+07	19.20	19.29	19.52

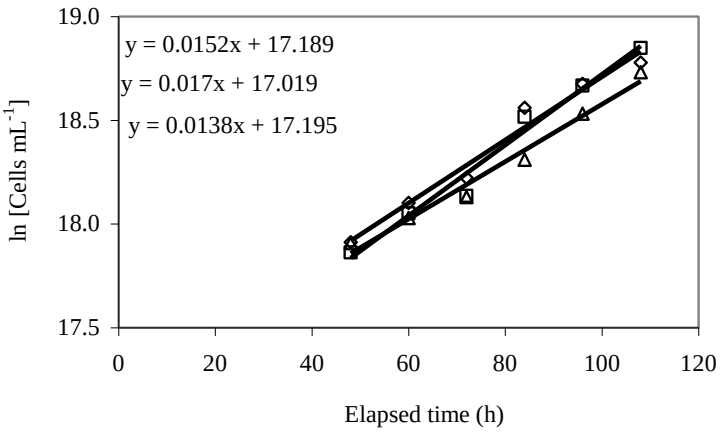


Specific growth rate (h^{-1})	
Trial 1	0.020
Trial 2	0.020
Trial 3	0.023
Average	0.021
STDEV	0.002
95% CI	0.002

Figure G.36. Specific growth rate calculations for Trial 1 (open circles), Trial 2 (open squares), and Trial 3 (open triangles).

Table G.37. BC13 growth in the presence of 0.25 x Zn_{MIC} + 0.25 x Cu_{MIC}.

	Cells mL^{-1}						ln (Cells mL^{-1})		
Elapsed Time (h)	Trial 1	Trial 2	Trial 3	Average	STDEV	95% CI	Trial 1	Trial 2	Trial 3
0	5.20E+07	5.26E+07	5.71E+07	5.39E+07	2.75E+06	3.11E+06	17.77	17.78	17.86
12	5.60E+07	5.32E+07	5.83E+07	5.58E+07	2.58E+06	2.92E+06	17.84	17.79	17.88
24	5.85E+07	5.79E+07	5.42E+07	5.69E+07	2.35E+06	2.66E+06	17.88	17.87	17.81
36	5.57E+07	5.57E+07	5.59E+07	5.58E+07	1.21E+05	1.37E+05	17.84	17.84	17.84
48	6.02E+07	5.73E+07	5.99E+07	5.91E+07	1.59E+06	1.80E+06	17.91	17.86	17.91
60	7.27E+07	6.91E+07	6.76E+07	6.98E+07	2.64E+06	2.99E+06	18.10	18.05	18.03
72	8.20E+07	7.52E+07	7.48E+07	7.73E+07	4.05E+06	4.59E+06	18.22	18.14	18.13
84	1.15E+08	1.10E+08	8.95E+07	1.05E+08	1.35E+07	1.53E+07	18.56	18.52	18.31
96	1.29E+08	1.28E+08	1.12E+08	1.23E+08	9.65E+06	1.09E+07	18.67	18.67	18.53
108	1.43E+08	1.53E+08	1.36E+08	1.44E+08	8.58E+06	9.71E+06	18.78	18.85	18.73
120	1.89E+08	1.71E+08	1.55E+08	1.72E+08	1.74E+07	1.97E+07	19.06	18.96	18.86
144	1.71E+08	1.80E+08	1.82E+08	1.78E+08	5.96E+06	6.75E+06	18.96	19.01	19.02
168	1.86E+08	1.80E+08	1.62E+08	1.76E+08	1.22E+07	1.38E+07	19.04	19.01	18.90

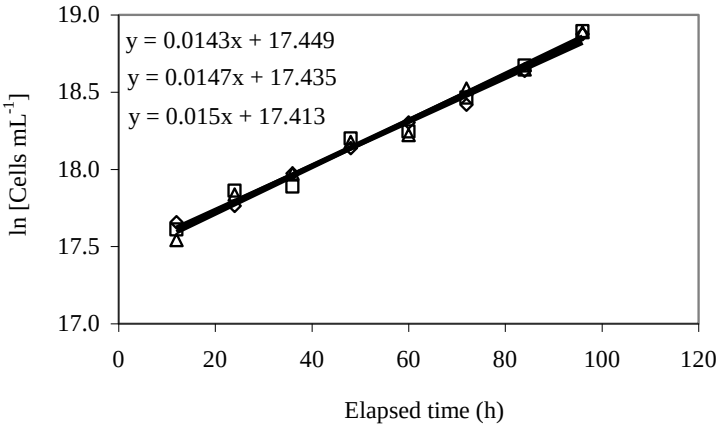


Specific growth rate (h^{-1})	
Trial 1	0.015
Trial 2	0.017
Trial 3	0.014
Average	0.015
STDEV	0.002
95% CI	0.002

Figure G.37. Specific growth rate calculations for Trial 1 (open circles), Trial 2 (open squares), and Trial 3 (open triangles).

Table G.38. BC13 growth in the presence of 0.375 x Zn_{MIC} + 0.375 x Cu_{MIC}.

	Cells mL^{-1}						ln (Cells mL^{-1})		
Elapsed Time (h)	Trial 1	Trial 2	Trial 3	Average	STDEV	95% CI	Trial 1	Trial 2	Trial 3
0	4.69E+07	4.78E+07	4.44E+07	4.63E+07	1.77E+06	2.00E+06	17.66	17.68	17.61
12	4.66E+07	4.44E+07	4.16E+07	4.42E+07	2.53E+06	2.87E+06	17.66	17.61	17.54
24	5.18E+07	5.71E+07	5.58E+07	5.49E+07	2.76E+06	3.13E+06	17.76	17.86	17.84
36	6.39E+07	5.87E+07	6.39E+07	6.22E+07	3.00E+06	3.40E+06	17.97	17.89	17.97
48	7.53E+07	8.01E+07	7.83E+07	7.79E+07	2.41E+06	2.73E+06	18.14	18.20	18.18
60	8.89E+07	8.39E+07	8.20E+07	8.49E+07	3.56E+06	4.03E+06	18.30	18.25	18.22
72	9.98E+07	1.04E+08	1.11E+08	1.05E+08	5.46E+06	6.18E+06	18.42	18.46	18.52
84	1.24E+08	1.29E+08	1.25E+08	1.26E+08	2.23E+06	2.52E+06	18.64	18.67	18.65
96	1.58E+08	1.60E+08	1.60E+08	1.59E+08	1.46E+06	1.66E+06	18.88	18.89	18.89
108	1.27E+08	1.29E+08	1.32E+08	1.29E+08	2.55E+06	2.89E+06	18.66	18.68	18.70
120	1.23E+08	1.26E+08	1.14E+08	1.21E+08	6.18E+06	6.99E+06	18.63	18.66	18.56
144	1.13E+08	1.17E+08	1.24E+08	1.18E+08	5.52E+06	6.25E+06	18.54	18.58	18.63
168	1.24E+08	1.31E+08	1.19E+08	1.25E+08	5.83E+06	6.60E+06	18.63	18.69	18.59

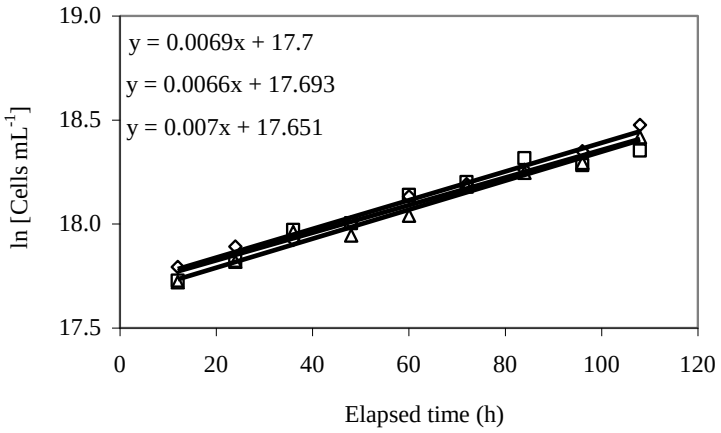


Specific growth rate (h^{-1})	
Trial 1	0.014
Trial 2	0.015
Trial 3	0.015
Average	0.015
STDEV	0.000
95% CI	0.000

Figure G.38. Specific growth rate calculations for Trial 1 (open circles), Trial 2 (open squares), and Trial 3 (open triangles).

Table G.39. BC13 growth in the presence of 0.50 x Zn_{MIC} + 0.50 x Cu_{MIC}.

	Cells mL^{-1}						ln (Cells mL^{-1})		
Elapsed Time (h)	Trial 1	Trial 2	Trial 3	Average	STDEV	95% CI	Trial 1	Trial 2	Trial 3
0	5.42E+07	5.78E+07	5.80E+07	5.67E+07	2.11E+06	2.39E+06	17.81	17.87	17.88
12	5.34E+07	5.00E+07	4.97E+07	5.10E+07	2.08E+06	2.35E+06	17.79	17.73	17.72
24	5.89E+07	5.50E+07	5.48E+07	5.62E+07	2.32E+06	2.63E+06	17.89	17.82	17.82
36	6.08E+07	6.38E+07	6.32E+07	6.26E+07	1.58E+06	1.79E+06	17.92	17.97	17.96
48	6.61E+07	6.58E+07	6.21E+07	6.47E+07	2.22E+06	2.51E+06	18.01	18.00	17.94
60	7.50E+07	7.55E+07	6.83E+07	7.29E+07	3.99E+06	4.52E+06	18.13	18.14	18.04
72	7.95E+07	8.03E+07	7.86E+07	7.95E+07	8.09E+05	9.16E+05	18.19	18.20	18.18
84	8.52E+07	9.01E+07	8.39E+07	8.64E+07	3.25E+06	3.68E+06	18.26	18.32	18.25
96	9.31E+07	8.71E+07	8.80E+07	8.94E+07	3.26E+06	3.69E+06	18.35	18.28	18.29
108	1.06E+08	9.34E+07	9.96E+07	9.95E+07	6.09E+06	6.89E+06	18.48	18.35	18.42
120	1.45E+08	1.02E+08	9.92E+07	1.16E+08	2.58E+07	2.92E+07	18.79	18.44	18.41
144	1.51E+08	1.20E+08	1.07E+08	1.26E+08	2.26E+07	2.56E+07	18.83	18.61	18.49
168	1.55E+08	1.29E+08	1.17E+08	1.34E+08	1.92E+07	2.18E+07	18.86	18.68	18.58



Specific growth rate (h^{-1})	
Trial 1	0.007
Trial 2	0.007
Trial 3	0.007
Average	0.0068
STDEV	0.0002
95% CI	0.0002

Figure G.39. Specific growth rate calculations for Trial 1 (open circles), Trial 2 (open squares), and Trial 3 (open triangles).

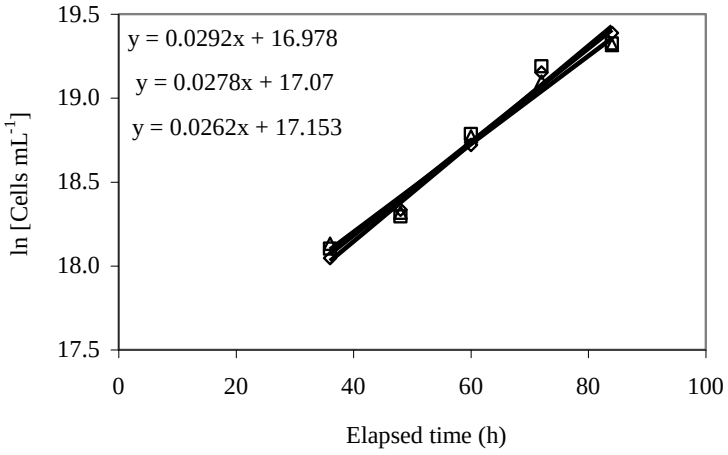
Effect of Ferrous Iron on Heavy-Metal Toxicity

BC13 cell concentrations with time when grown in the presence of lead, zinc, and copper IC_{50}s with ferrous iron added to a concentration of 25, 50, 75, or 100 mM. Experiments were repeated in triplicate and average values, standard deviations (STDEV), and 95% confidence intervals (95% CI) are shown. Specific growth rates were calculated using linear regressions and are shown along with the corresponding STDEV and 95% CI to the right of the plots.

Lead Toxicity in the Presence of Ferrous Iron

Table G.40. BC13 growth in the presence of the lead IC_{50} and 25 mM ferrous iron.

	Cells mL^{-1}						ln (Cells mL^{-1})		
Elapsed Time (h)	Trial 1	Trial 2	Trial 3	Average	STDEV	95% CI	Trial 1	Trial 2	Trial 3
0	4.71E+07	4.40E+07	4.40E+07	4.50E+07	1.82E+06	2.06E+06	17.67	17.60	17.60
12	5.05E+07	5.06E+07	5.09E+07	5.07E+07	2.09E+05	2.36E+05	17.74	17.74	17.75
24	5.78E+07	5.72E+07	5.95E+07	5.82E+07	1.17E+06	1.33E+06	17.87	17.86	17.90
36	6.88E+07	7.28E+07	7.50E+07	7.22E+07	3.17E+06	3.58E+06	18.05	18.10	18.13
48	9.19E+07	8.82E+07	9.02E+07	9.01E+07	1.83E+06	2.07E+06	18.34	18.30	18.32
60	1.35E+08	1.44E+08	1.42E+08	1.40E+08	4.76E+06	5.38E+06	18.72	18.79	18.77
72	2.08E+08	2.16E+08	1.97E+08	2.07E+08	9.50E+06	1.08E+07	19.15	19.19	19.10
84	2.63E+08	2.47E+08	2.45E+08	2.52E+08	9.81E+06	1.11E+07	19.39	19.33	19.32
96	2.88E+08	2.98E+08	3.01E+08	2.96E+08	7.10E+06	8.04E+06	19.48	19.51	19.52
108	2.58E+08	2.38E+08	2.33E+08	2.43E+08	1.34E+07	1.51E+07	19.37	19.29	19.26
120	2.69E+08	2.57E+08	2.65E+08	2.63E+08	6.26E+06	7.08E+06	19.41	19.36	19.39



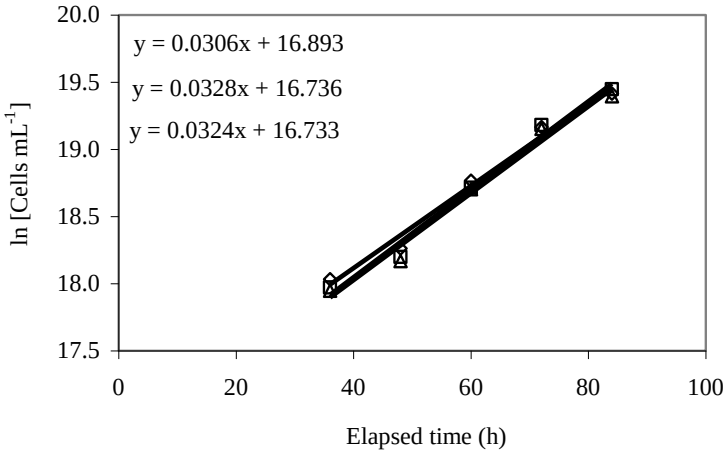
Specific growth rate (h^{-1})

Trial 1	0.029
Trial 2	0.028
Trial 3	0.026
Average	0.028
STDEV	0.002
95% CI	0.002

Figure G.40. Specific growth rate calculations for Trial 1 (open circles), Trial 2 (open squares), and Trial 3 (open triangles).

Table G.41. BC13 growth in the presence of the lead IC_{50} and 50 mM ferrous iron.

	Cells mL^{-1}						ln (Cells mL^{-1})		
Elapsed Time (h)	Trial 1	Trial 2	Trial 3	Average	STDEV	95% CI	Trial 1	Trial 2	Trial 3
0	4.23E+07	4.34E+07	4.31E+07	4.29E+07	5.84E+05	6.60E+05	17.56	17.59	17.58
12	5.31E+07	5.03E+07	5.27E+07	5.20E+07	1.52E+06	1.72E+06	17.79	17.73	17.78
24	5.57E+07	5.70E+07	5.95E+07	5.74E+07	1.93E+06	2.19E+06	17.83	17.86	17.90
36	6.78E+07	6.38E+07	6.23E+07	6.46E+07	2.82E+06	3.19E+06	18.03	17.97	17.95
48	8.53E+07	8.02E+07	7.76E+07	8.10E+07	3.91E+06	4.42E+06	18.26	18.20	18.17
60	1.41E+08	1.34E+08	1.33E+08	1.36E+08	4.64E+06	5.25E+06	18.77	18.71	18.70
72	2.11E+08	2.14E+08	2.08E+08	2.11E+08	2.94E+06	3.33E+06	19.17	19.18	19.15
84	2.70E+08	2.79E+08	2.65E+08	2.72E+08	7.12E+06	8.06E+06	19.41	19.45	19.40
96	2.67E+08	2.61E+08	2.76E+08	2.68E+08	7.73E+06	8.74E+06	19.40	19.38	19.44
108	2.31E+08	2.21E+08	2.27E+08	2.26E+08	5.32E+06	6.01E+06	19.26	19.21	19.24
120	2.51E+08	2.35E+08	2.37E+08	2.41E+08	8.41E+06	9.51E+06	19.34	19.28	19.28



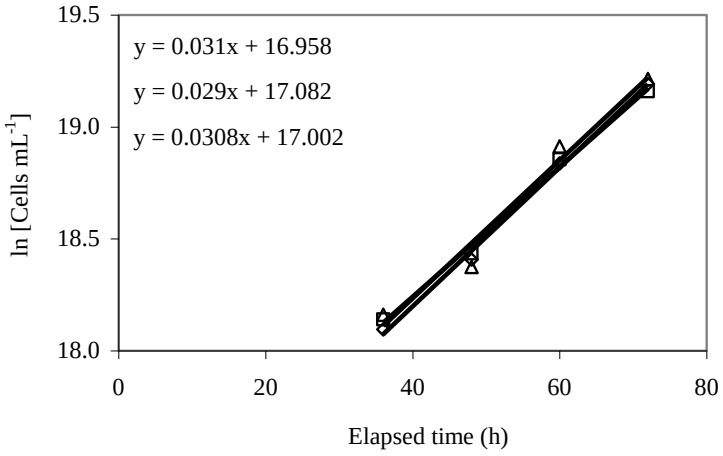
Specific growth rate (h^{-1})

Trial 1	0.031
Trial 2	0.033
Trial 3	0.032
Average	0.032
STDEV	0.001
95% CI	0.001

Figure G.41. Specific growth rate calculations for Trial 1 (open circles), Trial 2 (open squares), and Trial 3 (open triangles).

Table G.42. BC13 growth in the presence of the lead IC_{50} and 75 mM ferrous iron.

	Cells mL^{-1}						ln (Cells mL^{-1})		
Elapsed Time (h)	Trial 1	Trial 2	Trial 3	Average	STDEV	95% CI	Trial 1	Trial 2	Trial 3
0	4.55E+07	4.77E+07	5.00E+07	4.77E+07	2.28E+06	2.58E+06	17.63	17.68	17.73
12	5.25E+07	5.38E+07	5.24E+07	5.29E+07	8.06E+05	9.12E+05	17.78	17.80	17.77
24	5.96E+07	5.94E+07	5.77E+07	5.89E+07	1.07E+06	1.21E+06	17.90	17.90	17.87
36	7.22E+07	7.55E+07	7.72E+07	7.50E+07	2.51E+06	2.85E+06	18.10	18.14	18.16
48	9.87E+07	1.01E+08	9.56E+07	9.86E+07	2.95E+06	3.34E+06	18.41	18.44	18.38
60	1.52E+08	1.55E+08	1.64E+08	1.57E+08	6.20E+06	7.02E+06	18.84	18.86	18.91
72	2.16E+08	2.09E+08	2.21E+08	2.16E+08	6.01E+06	6.80E+06	19.19	19.16	19.22
84	2.54E+08	2.41E+08	2.38E+08	2.44E+08	8.14E+06	9.21E+06	19.35	19.30	19.29
96	2.85E+08	3.02E+08	3.18E+08	3.02E+08	1.62E+07	1.83E+07	19.47	19.53	19.58
108	2.34E+08	2.40E+08	2.39E+08	2.38E+08	3.23E+06	3.65E+06	19.27	19.30	19.29
120	2.48E+08	2.48E+08	2.58E+08	2.51E+08	5.59E+06	6.33E+06	19.33	19.33	19.37

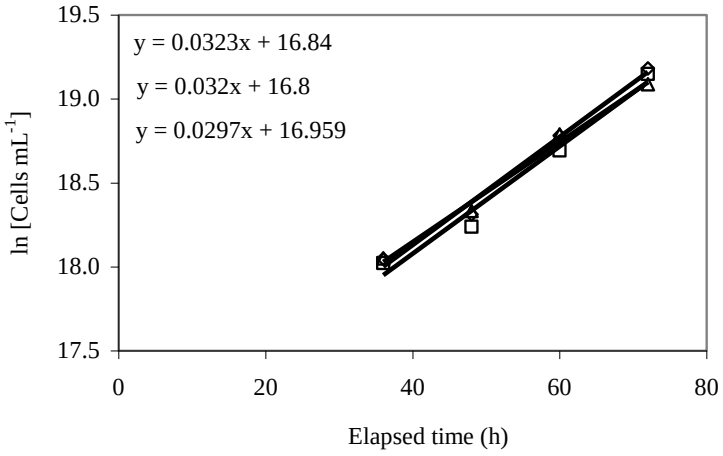


Specific growth rate (h^{-1})	
Trial 1	0.031
Trial 2	0.029
Trial 3	0.031
Average	0.030
STDEV	0.001
95% CI	0.001

Figure G.42. Specific growth rate calculations for Trial 1 (open circles), Trial 2 (open squares), and Trial 3 (open triangles).

Table G.43. BC13 growth in the presence of the lead IC_{50} and 100 mM ferrous iron.

	Cells mL^{-1}						ln (Cells mL^{-1})		
Elapsed Time (h)	Trial 1	Trial 2	Trial 3	Average	STDEV	95% CI	Trial 1	Trial 2	Trial 3
0	4.46E+07	4.25E+07	4.19E+07	4.30E+07	1.39E+06	1.57E+06	17.61	17.56	17.55
12	5.06E+07	4.70E+07	5.03E+07	4.93E+07	1.97E+06	2.23E+06	17.74	17.67	17.73
24	5.91E+07	5.34E+07	5.75E+07	5.67E+07	2.95E+06	3.34E+06	17.89	17.79	17.87
36	6.90E+07	6.71E+07	6.91E+07	6.84E+07	1.08E+06	1.22E+06	18.05	18.02	18.05
48	8.97E+07	8.33E+07	9.16E+07	8.82E+07	4.30E+06	4.87E+06	18.31	18.24	18.33
60	1.44E+08	1.31E+08	1.44E+08	1.40E+08	7.29E+06	8.25E+06	18.78	18.69	18.79
72	2.14E+08	2.07E+08	1.95E+08	2.05E+08	9.72E+06	1.10E+07	19.18	19.15	19.09
84	2.70E+08	2.63E+08	2.64E+08	2.65E+08	3.94E+06	4.46E+06	19.41	19.39	19.39
96	2.73E+08	2.83E+08	2.58E+08	2.72E+08	1.24E+07	1.40E+07	19.43	19.46	19.37
108	2.47E+08	2.61E+08	2.56E+08	2.55E+08	7.43E+06	8.40E+06	19.32	19.38	19.36
120	2.62E+08	2.39E+08	2.54E+08	2.52E+08	1.16E+07	1.31E+07	19.38	19.29	19.35



Specific growth rate (h^{-1})

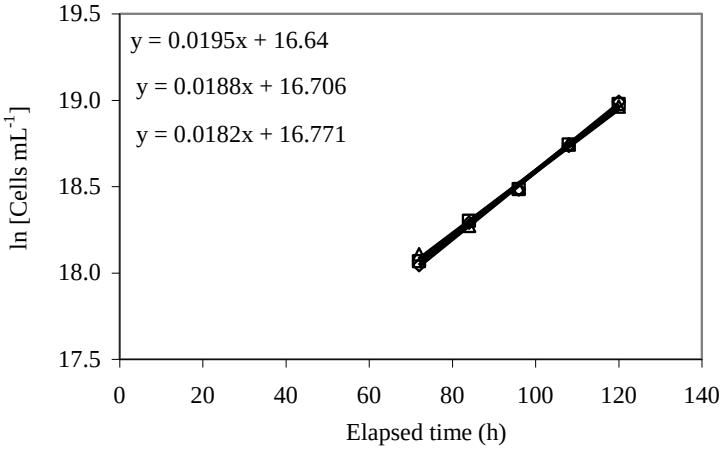
Trial 1	0.032
Trial 2	0.032
Trial 3	0.030
Average	0.031
STDEV	0.001
95% CI	0.002

Figure G.43. Specific growth rate calculations for Trial 1 (open circles), Trial 2 (open squares), and Trial 3 (open triangles).

Zinc Toxicity in the Presence of Ferrous Iron

Table G.44. BC13 growth in the presence of the zinc IC_{50} and 25 mM ferrous iron.

	Cells mL^{-1}			**25 mM**			ln (Cells mL^{-1})		
Elapsed Time (h)	Trial 1	Trial 2	Trial 3	Average	STDEV	95% CI	Trial 1	Trial 2	Trial 3
0	5.14E+07	5.05E+07	4.87E+07	5.02E+07	1.38E+06	1.56E+06	17.76	17.74	17.70
12	5.59E+07	5.28E+07	4.96E+07	5.28E+07	3.13E+06	3.54E+06	17.84	17.78	17.72
24	6.08E+07	5.85E+07	5.86E+07	5.93E+07	1.31E+06	1.48E+06	17.92	17.89	17.89
72	6.87E+07	7.03E+07	7.32E+07	7.07E+07	2.30E+06	2.60E+06	18.04	18.07	18.11
84	8.78E+07	8.88E+07	8.62E+07	8.76E+07	1.29E+06	1.46E+06	18.29	18.30	18.27
96	1.07E+08	1.07E+08	1.07E+08	1.07E+08	4.35E+05	4.92E+05	18.48	18.48	18.49
108	1.37E+08	1.38E+08	1.38E+08	1.38E+08	5.90E+05	6.68E+05	18.74	18.74	18.74
120	1.77E+08	1.75E+08	1.72E+08	1.74E+08	2.32E+06	2.62E+06	18.99	18.98	18.96
144	1.86E+08	1.76E+08	1.81E+08	1.81E+08	4.82E+06	5.45E+06	19.04	18.99	19.02
168	1.54E+08	1.48E+08	1.56E+08	1.53E+08	4.07E+06	4.61E+06	18.86	18.81	18.86

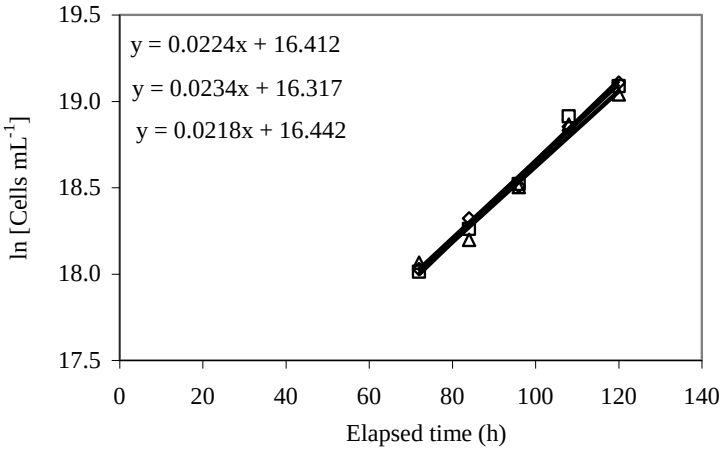


Specific growth rate (h^{-1})	
Trial 1	0.020
Trial 2	0.019
Trial 3	0.018
Average	0.019
STDEV	0.001
95% CI	0.001

Figure G.44. Specific growth rate calculations for Trial 1 (open circles), Trial 2 (open squares), and Trial 3 (open triangles).

Table G.45. BC13 growth in the presence of the zinc IC_{50} and 50 mM ferrous iron.

	Cells mL^{-1}						ln (Cells mL^{-1})		
Elapsed Time (h)	Trial 1	Trial 2	Trial 3	Average	STDEV	95% CI	Trial 1	Trial 2	Trial 3
0	4.82E+07	5.02E+07	4.73E+07	4.86E+07	1.48E+06	1.67E+06	17.69	17.73	17.67
12	5.49E+07	5.45E+07	5.12E+07	5.36E+07	2.04E+06	2.31E+06	17.82	17.81	17.75
24	6.35E+07	6.52E+07	6.31E+07	6.39E+07	1.14E+06	1.29E+06	17.97	17.99	17.96
72	6.76E+07	6.65E+07	7.01E+07	6.81E+07	1.86E+06	2.11E+06	18.03	18.01	18.07
84	9.05E+07	8.52E+07	8.01E+07	8.53E+07	5.22E+06	5.90E+06	18.32	18.26	18.20
96	1.09E+08	1.10E+08	1.09E+08	1.09E+08	9.59E+05	1.09E+06	18.51	18.52	18.50
108	1.54E+08	1.64E+08	1.56E+08	1.58E+08	5.01E+06	5.67E+06	18.85	18.91	18.87
120	1.99E+08	1.95E+08	1.86E+08	1.93E+08	6.63E+06	7.51E+06	19.11	19.09	19.04
144	1.82E+08	1.75E+08	1.72E+08	1.76E+08	5.28E+06	5.98E+06	19.02	18.98	18.96
168	1.58E+08	1.51E+08	1.53E+08	1.54E+08	3.72E+06	4.20E+06	18.88	18.83	18.85



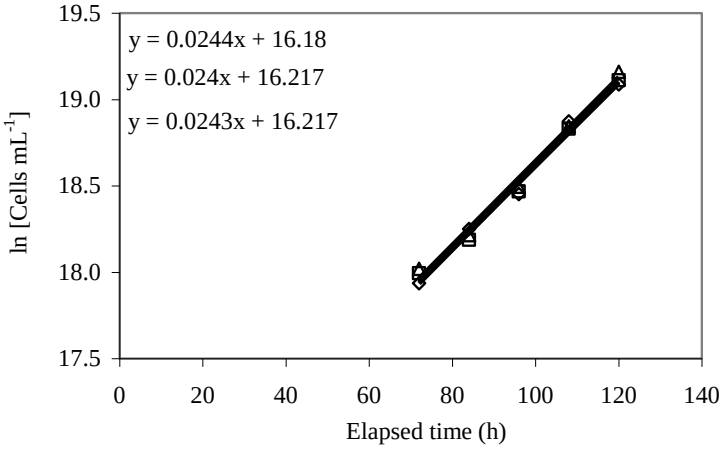
Specific growth rate (h^{-1})

Trial 1	0.022
Trial 2	0.023
Trial 3	0.022
Average	0.023
STDEV	0.001
95% CI	0.001

Figure G.45. Specific growth rate calculations for Trial 1 (open circles), Trial 2 (open squares), and Trial 3 (open triangles).

Table G.46. BC13 growth in the presence of the zinc IC_{50} and 75 mM ferrous iron.

	Cells mL^{-1}						ln (Cells mL^{-1})		
Elapsed Time (h)	Trial 1	Trial 2	Trial 3	Average	STDEV	95% CI	Trial 1	Trial 2	Trial 3
0	4.81E+07	5.05E+07	4.78E+07	4.88E+07	1.47E+06	1.67E+06	17.69	17.74	17.68
12	6.11E+07	6.26E+07	6.39E+07	6.25E+07	1.41E+06	1.60E+06	17.93	17.95	17.97
24	5.90E+07	5.72E+07	5.51E+07	5.71E+07	1.92E+06	2.17E+06	17.89	17.86	17.82
72	6.16E+07	6.53E+07	6.69E+07	6.46E+07	2.74E+06	3.10E+06	17.94	17.99	18.02
84	8.44E+07	7.93E+07	8.14E+07	8.17E+07	2.56E+06	2.90E+06	18.25	18.19	18.22
96	1.03E+08	1.05E+08	1.08E+08	1.05E+08	2.22E+06	2.51E+06	18.45	18.47	18.49
108	1.57E+08	1.51E+08	1.53E+08	1.54E+08	3.32E+06	3.76E+06	18.87	18.83	18.85
120	1.95E+08	2.00E+08	2.09E+08	2.01E+08	7.52E+06	8.50E+06	19.09	19.11	19.16
144	1.93E+08	2.03E+08	1.96E+08	1.97E+08	5.09E+06	5.75E+06	19.08	19.13	19.09
168	1.51E+08	1.55E+08	1.57E+08	1.54E+08	2.88E+06	3.25E+06	18.83	18.86	18.87



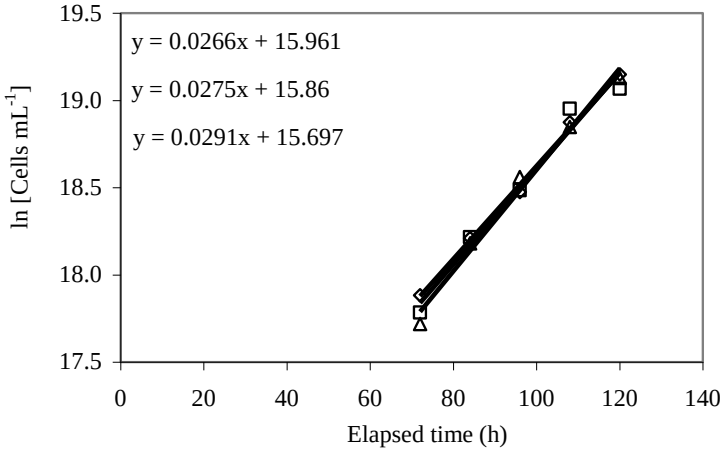
Specific growth rate (h^{-1})

Trial 1	0.024
Trial 2	0.024
Trial 3	0.024
Average	0.024
STDEV	0.000
95% CI	0.000

Figure G.46. Specific growth rate calculations for Trial 1 (open circles), Trial 2 (open squares), and Trial 3 (open triangles).

Table G.47. BC13 growth in the presence of the zinc IC_{50} and 100 mM ferrous iron.

	Cells mL^{-1}						ln (Cells mL^{-1})		
Elapsed Time (h)	Trial 1	Trial 2	Trial 3	Average	STDEV	95% CI	Trial 1	Trial 2	Trial 3
0	5.06E+07	5.52E+07	5.03E+07	5.20E+07	2.77E+06	3.14E+06	17.74	17.83	17.73
12	5.78E+07	5.40E+07	5.38E+07	5.52E+07	2.24E+06	2.53E+06	17.87	17.80	17.80
24	6.16E+07	5.86E+07	5.53E+07	5.85E+07	3.14E+06	3.55E+06	17.94	17.89	17.83
72	5.84E+07	5.29E+07	4.95E+07	5.36E+07	4.47E+06	5.05E+06	17.88	17.78	17.72
84	8.11E+07	8.15E+07	7.87E+07	8.04E+07	1.52E+06	1.72E+06	18.21	18.22	18.18
96	1.06E+08	1.07E+08	1.15E+08	1.09E+08	5.17E+06	5.85E+06	18.48	18.48	18.56
108	1.57E+08	1.70E+08	1.53E+08	1.60E+08	8.81E+06	9.97E+06	18.87	18.95	18.85
120	2.07E+08	1.91E+08	2.03E+08	2.00E+08	8.63E+06	9.77E+06	19.15	19.07	19.13
144	1.85E+08	1.95E+08	2.09E+08	1.96E+08	1.23E+07	1.39E+07	19.04	19.09	19.16
168	1.50E+08	1.35E+08	1.24E+08	1.36E+08	1.27E+07	1.44E+07	18.82	18.72	18.64



Specific growth rate (h^{-1})

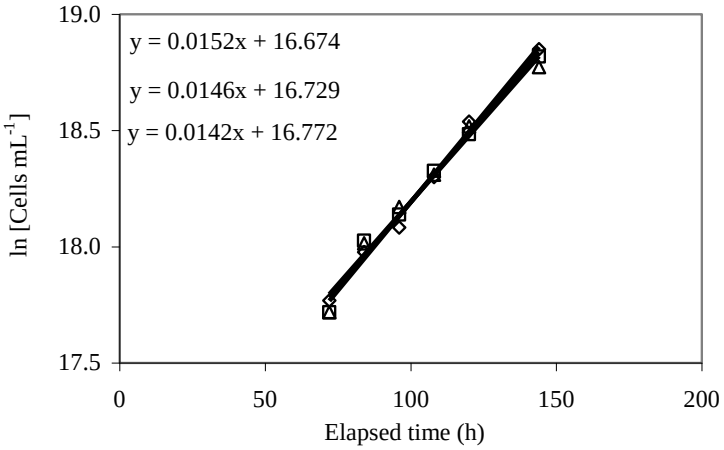
Trial 1	0.027
Trial 2	0.028
Trial 3	0.029
Average	0.028
STDEV	0.001
95% CI	0.001

Figure G.47. Specific growth rate calculations for Trial 1 (open circles), Trial 2 (open squares), and Trial 3 (open triangles).

Copper Toxicity in the Presence of Ferrous Iron

Table G.48. BC13 growth in the presence of the copper IC_{50} and 25 mM ferrous iron.

	Cells mL^{-1}						ln (Cells mL^{-1})		
Elapsed Time (h)	Trial 1	Trial 2	Trial 3	Average	STDEV	95% CI	Trial 1	Trial 2	Trial 3
0	5.36E+07	5.10E+07	5.12E+07	5.19E+07	1.47E+06	1.66E+06	17.80	17.75	17.75
12	4.58E+07	4.45E+07	4.27E+07	4.43E+07	1.55E+06	1.75E+06	17.64	17.61	17.57
24	5.88E+07	5.92E+07	6.25E+07	6.02E+07	2.01E+06	2.28E+06	17.89	17.90	17.95
72	5.21E+07	4.95E+07	4.96E+07	5.04E+07	1.47E+06	1.66E+06	17.77	17.72	17.72
84	6.42E+07	6.74E+07	6.67E+07	6.61E+07	1.67E+06	1.89E+06	17.98	18.03	18.02
96	7.14E+07	7.54E+07	7.79E+07	7.49E+07	3.28E+06	3.71E+06	18.08	18.14	18.17
108	8.86E+07	9.10E+07	8.95E+07	8.97E+07	1.18E+06	1.33E+06	18.30	18.33	18.31
120	1.12E+08	1.07E+08	1.10E+08	1.10E+08	2.98E+06	3.37E+06	18.54	18.48	18.52
144	1.54E+08	1.49E+08	1.42E+08	1.48E+08	5.75E+06	6.51E+06	18.85	18.82	18.77
168	1.32E+08	1.34E+08	1.26E+08	1.31E+08	4.03E+06	4.56E+06	18.70	18.71	18.65



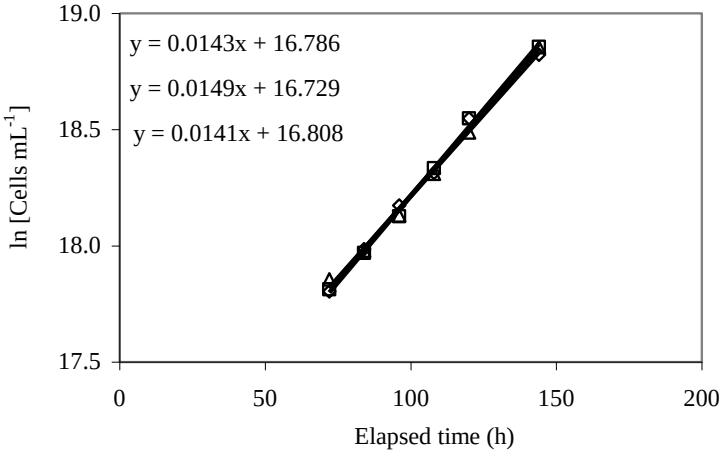
Specific growth rate (h^{-1})

Trial 1	0.015
Trial 2	0.015
Trial 3	0.014
Average	0.015
STDEV	0.001
95% CI	0.001

Figure G.48. Specific growth rate calculations for Trial 1 (open circles), Trial 2 (open squares), and Trial 3 (open triangles).

Table G.49. BC13 growth in the presence of the copper IC_{50} and 50 mM ferrous iron.

	Cells mL^{-1}						ln (Cells mL^{-1})		
Elapsed Time (h)	Trial 1	Trial 2	Trial 3	Average	STDEV	95% CI	Trial 1	Trial 2	Trial 3
0	5.05E+07	4.80E+07	4.72E+07	4.86E+07	1.71E+06	1.93E+06	17.74	17.69	17.67
12	4.49E+07	4.49E+07	4.27E+07	4.41E+07	1.28E+06	1.45E+06	17.62	17.62	17.57
24	5.75E+07	5.89E+07	6.08E+07	5.91E+07	1.65E+06	1.86E+06	17.87	17.89	17.92
72	5.40E+07	5.44E+07	5.69E+07	5.51E+07	1.55E+06	1.75E+06	17.80	17.81	17.86
84	6.47E+07	6.37E+07	6.43E+07	6.42E+07	5.25E+05	5.94E+05	17.99	17.97	17.98
96	7.82E+07	7.46E+07	7.48E+07	7.59E+07	2.00E+06	2.26E+06	18.17	18.13	18.13
108	8.98E+07	9.17E+07	8.95E+07	9.04E+07	1.20E+06	1.36E+06	18.31	18.33	18.31
120	1.14E+08	1.14E+08	1.07E+08	1.11E+08	3.85E+06	4.36E+06	18.55	18.55	18.49
144	1.49E+08	1.55E+08	1.54E+08	1.53E+08	2.92E+06	3.30E+06	18.82	18.86	18.86
168	1.49E+08	1.45E+08	1.49E+08	1.48E+08	1.99E+06	2.25E+06	18.82	18.79	18.82

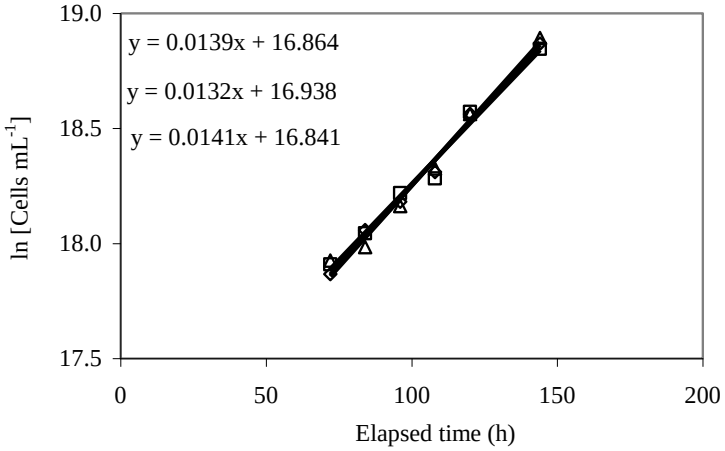


Specific growth rate (h^{-1})	
Trial 1	0.014
Trial 2	0.015
Trial 3	0.014
Average	0.014
STDEV	0.000
95% CI	0.000

Figure G.49. Specific growth rate calculations for Trial 1 (open circles), Trial 2 (open squares), and Trial 3 (open triangles).

Table G.50. BC13 growth in the presence of the copper IC_{50} and 75 mM ferrous iron.

	Cells mL^{-1}						ln (Cells mL^{-1})		
Elapsed Time (h)	Trial 1	Trial 2	Trial 3	Average	STDEV	95% CI	Trial 1	Trial 2	Trial 3
0	5.51E+07	5.77E+07	5.65E+07	5.65E+07	1.30E+06	1.47E+06	17.83	17.87	17.85
12	4.81E+07	5.06E+07	5.37E+07	5.08E+07	2.78E+06	3.15E+06	17.69	17.74	17.80
24	5.67E+07	5.75E+07	6.02E+07	5.81E+07	1.85E+06	2.09E+06	17.85	17.87	17.91
72	5.75E+07	6.00E+07	6.09E+07	5.95E+07	1.77E+06	2.00E+06	17.87	17.91	17.93
84	6.96E+07	6.86E+07	6.47E+07	6.76E+07	2.59E+06	2.93E+06	18.06	18.04	17.98
96	7.87E+07	8.17E+07	7.73E+07	7.92E+07	2.25E+06	2.55E+06	18.18	18.22	18.16
108	8.96E+07	8.70E+07	9.10E+07	8.92E+07	1.99E+06	2.25E+06	18.31	18.28	18.33
120	1.15E+08	1.16E+08	1.15E+08	1.16E+08	6.02E+05	6.81E+05	18.56	18.57	18.56
144	1.57E+08	1.53E+08	1.60E+08	1.57E+08	3.67E+06	4.16E+06	18.87	18.85	18.89
168	1.34E+08	1.36E+08	1.32E+08	1.34E+08	1.79E+06	2.03E+06	18.72	18.72	18.70



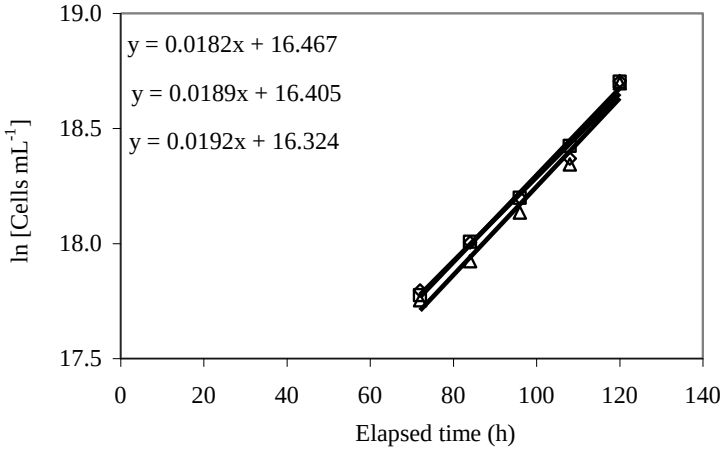
Specific growth rate (h^{-1})

Trial 1	0.014
Trial 2	0.013
Trial 3	0.014
Average	0.014
STDEV	0.000
95% CI	0.001

Figure G.50. Specific growth rate calculations for Trial 1 (open circles), Trial 2 (open squares), and Trial 3 (open triangles).

Table G.51. BC13 growth in the presence of the copper IC_{50} and 100 mM ferrous iron.

	Cells mL^{-1}						ln (Cells mL^{-1})		
Elapsed Time (h)	Trial 1	Trial 2	Trial 3	Average	STDEV	95% CI	Trial 1	Trial 2	Trial 3
0	5.37E+07	5.62E+07	6.06E+07	5.68E+07	3.46E+06	3.91E+06	17.80	17.84	17.92
12	4.78E+07	4.71E+07	4.74E+07	4.74E+07	3.78E+05	4.28E+05	17.68	17.67	17.67
24	5.97E+07	6.02E+07	6.39E+07	6.12E+07	2.30E+06	2.60E+06	17.90	17.91	17.97
72	5.35E+07	5.25E+07	5.13E+07	5.25E+07	1.11E+06	1.25E+06	17.80	17.78	17.75
84	6.59E+07	6.61E+07	6.08E+07	6.43E+07	3.04E+06	3.44E+06	18.00	18.01	17.92
96	8.01E+07	8.00E+07	7.51E+07	7.84E+07	2.84E+06	3.21E+06	18.20	18.20	18.13
108	9.50E+07	1.00E+08	9.26E+07	9.60E+07	3.93E+06	4.44E+06	18.37	18.42	18.34
120	1.33E+08	1.33E+08	1.32E+08	1.32E+08	6.13E+05	6.94E+05	18.71	18.70	18.70
144	1.50E+08	1.51E+08	1.50E+08	1.50E+08	1.01E+06	1.15E+06	18.82	18.84	18.83
168	1.41E+08	1.48E+08	1.58E+08	1.49E+08	8.64E+06	9.78E+06	18.76	18.82	18.88



Specific growth rate (h^{-1})

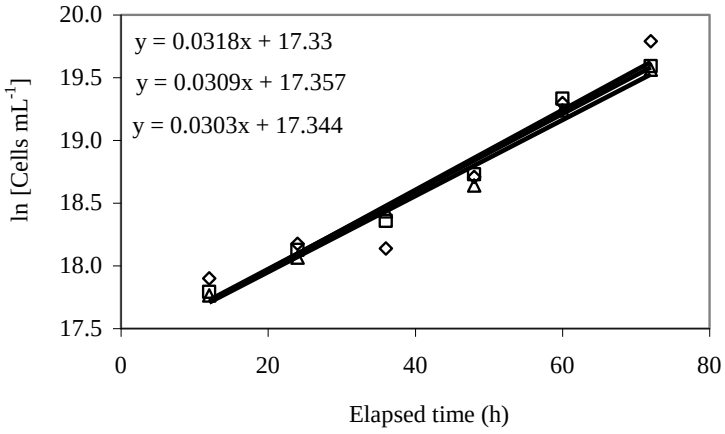
Trial 1	0.018
Trial 2	0.019
Trial 3	0.019
Average	0.019
STDEV	0.001
95% CI	0.001

Figure G.51. Specific growth rate calculations for Trial 1 (open circles), Trial 2 (open squares), and Trial 3 (open triangles).

Effect of Ferrous Iron on the Growth of BC13

Table G.52. BC13 growth in the presence of 25 mM ferrous iron.

	Cells mL^{-1}						ln (Cells mL^{-1})		
Elapsed Time (h)	Trial 1	Trial 2	Trial 3	Average	STDEV	9.50E-01	Trial 1	Trial 2	Trial 3
0	4.73E+07	4.82E+07	4.42E+07	4.66E+07	2.08E+06	2.36E+06	17.66	17.69	17.60
12	5.01E+07	5.33E+07	5.18E+07	5.17E+07	1.59E+06	1.79E+06	17.90	17.79	17.76
24	7.71E+07	7.45E+07	7.00E+07	7.39E+07	3.59E+06	4.06E+06	18.18	18.13	18.06
36	1.03E+08	9.40E+07	1.01E+08	9.96E+07	4.97E+06	5.63E+06	18.14	18.36	18.43
48	1.30E+08	1.36E+08	1.24E+08	1.30E+08	5.84E+06	6.61E+06	18.71	18.73	18.64
60	2.40E+08	2.48E+08	2.27E+08	2.38E+08	1.09E+07	1.24E+07	19.30	19.33	19.24
72	3.15E+08	3.22E+08	3.13E+08	3.17E+08	4.54E+06	5.14E+06	19.79	19.59	19.56
84	3.73E+08	3.81E+08	3.54E+08	3.69E+08	1.37E+07	1.54E+07	19.75	19.76	19.69
96	2.72E+08	2.71E+08	2.78E+08	2.74E+08	3.78E+06	4.28E+06	19.40	19.42	19.44
108	2.96E+08	2.87E+08	2.79E+08	2.87E+08	8.46E+06	9.57E+06	19.56	19.48	19.45
120	3.09E+08	2.97E+08	3.15E+08	3.07E+08	8.92E+06	1.01E+07	19.44	19.51	19.57



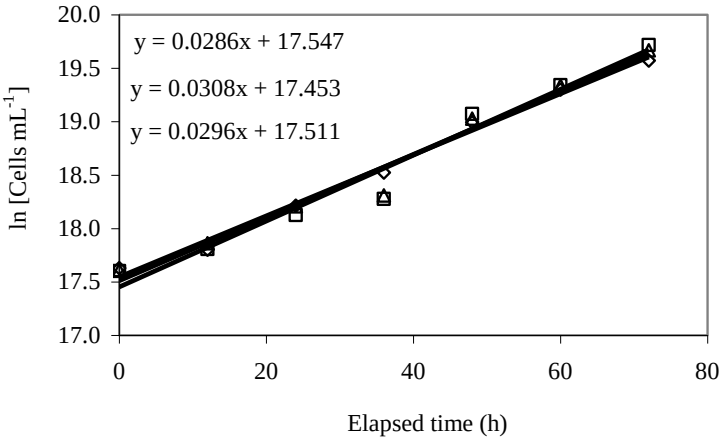
Specific growth rate (h^{-1})

Trial 1	0.032
Trial 2	0.031
Trial 3	0.030
Average	0.031
STDEV	0.001
95% CI	0.001

Figure G.52. Specific growth rate calculations for Trial 1 (open circles), Trial 2 (open squares), and Trial 3 (open triangles).

Table G.53. BC13 growth in the presence of 50 mM ferrous iron.

	Cells mL^{-1}						ln (Cells mL^{-1})		
Elapsed Time (h)	Trial 1	Trial 2	Trial 3	Average	STDEV	9.50E-01	Trial 1	Trial 2	Trial 3
0	4.53E+07	4.41E+07	4.46E+07	4.47E+07	6.07E+05	6.87E+05	17.63	17.60	17.61
12	5.38E+07	5.42E+07	5.72E+07	5.51E+07	1.87E+06	2.12E+06	17.80	17.81	17.86
24	8.13E+07	7.45E+07	8.09E+07	7.89E+07	3.81E+06	4.32E+06	18.21	18.13	18.21
36	1.11E+08	8.66E+07	8.94E+07	9.56E+07	1.32E+07	1.50E+07	18.52	18.28	18.31
48	1.78E+08	1.92E+08	1.84E+08	1.84E+08	7.14E+06	8.08E+06	19.00	19.07	19.03
60	2.41E+08	2.51E+08	2.50E+08	2.48E+08	5.63E+06	6.37E+06	19.30	19.34	19.34
72	3.16E+08	3.66E+08	3.48E+08	3.43E+08	2.52E+07	2.85E+07	19.57	19.72	19.67
84	3.55E+08	3.74E+08	3.87E+08	3.72E+08	1.60E+07	1.81E+07	19.69	19.74	19.77
96	2.86E+08	3.11E+08	3.29E+08	3.09E+08	2.14E+07	2.42E+07	19.47	19.56	19.61
108	2.89E+08	2.83E+08	2.90E+08	2.87E+08	3.81E+06	4.31E+06	19.48	19.46	19.48
120	3.00E+08	2.82E+08	2.87E+08	2.90E+08	9.63E+06	1.09E+07	19.52	19.46	19.47



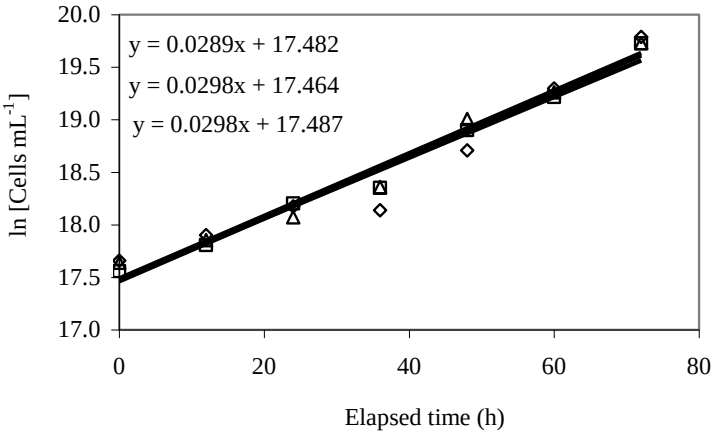
Specific growth rate (h^{-1})

Trial 1	0.029
Trial 2	0.031
Trial 3	0.030
Average	0.030
STDEV	0.001
95% CI	0.001

Figure G.53. Specific growth rate calculations for Trial 1 (open circles), Trial 2 (open squares), and Trial 3 (open triangles).

Table G.54. BC13 growth in the presence of 75 mM ferrous iron.

	Cells mL^{-1}						ln (Cells mL^{-1})		
Elapsed Time (h)	Trial 1	Trial 2	Trial 3	Average	STDEV	9.50E-01	Trial 1	Trial 2	Trial 3
0	4.66E+07	4.22E+07	4.57E+07	4.49E+07	2.34E+06	2.65E+06	17.66	17.56	17.64
12	5.94E+07	5.42E+07	5.68E+07	5.68E+07	2.63E+06	2.98E+06	17.90	17.81	17.86
24	7.82E+07	8.05E+07	7.06E+07	7.64E+07	5.18E+06	5.86E+06	18.18	18.20	18.07
36	7.54E+07	9.33E+07	9.40E+07	8.75E+07	1.05E+07	1.19E+07	18.14	18.35	18.36
48	1.33E+08	1.62E+08	1.80E+08	1.58E+08	2.35E+07	2.66E+07	18.71	18.90	19.01
60	2.40E+08	2.22E+08	2.32E+08	2.31E+08	9.18E+06	1.04E+07	19.30	19.22	19.26
72	3.93E+08	3.69E+08	3.70E+08	3.77E+08	1.35E+07	1.53E+07	19.79	19.73	19.73
84	3.79E+08	3.54E+08	3.48E+08	3.60E+08	1.63E+07	1.84E+07	19.75	19.68	19.67
96	2.66E+08	2.74E+08	2.96E+08	2.78E+08	1.57E+07	1.78E+07	19.40	19.43	19.51
108	3.13E+08	3.08E+08	2.93E+08	3.05E+08	1.07E+07	1.21E+07	19.56	19.55	19.50
120	2.77E+08	2.57E+08	2.48E+08	2.61E+08	1.48E+07	1.67E+07	19.44	19.37	19.33



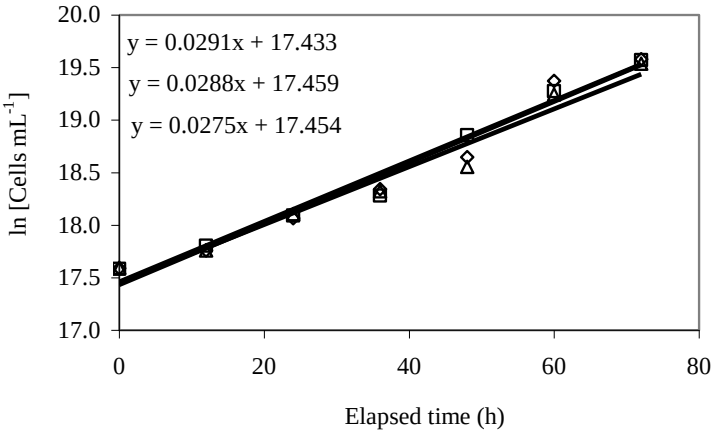
Specific growth rate (h^{-1})

Trial 1	0.029
Trial 2	0.030
Trial 3	0.030
Average	0.030
STDEV	0.001
95% CI	0.001

Figure G.54. Specific growth rate calculations for Trial 1 (open circles), Trial 2 (open squares), and Trial 3 (open triangles).

Table G.55. BC13 growth in the presence of 100 mM ferrous iron.

	Cells mL^{-1}						ln (Cells mL^{-1})		
Elapsed Time (h)	Trial 1	Trial 2	Trial 3	Average	STDEV	9.50E-01	Trial 1	Trial 2	Trial 3
0	4.36E+07	4.33E+07	4.38E+07	4.36E+07	2.26E+05	2.56E+05	17.59	17.58	17.59
12	5.17E+07	5.39E+07	5.16E+07	5.24E+07	1.32E+06	1.50E+06	17.76	17.80	17.76
24	7.01E+07	7.20E+07	7.29E+07	7.17E+07	1.42E+06	1.61E+06	18.07	18.09	18.10
36	9.26E+07	8.70E+07	9.06E+07	9.01E+07	2.82E+06	3.19E+06	18.34	18.28	18.32
48	1.25E+08	1.55E+08	1.14E+08	1.31E+08	2.09E+07	2.37E+07	18.65	18.86	18.55
60	2.59E+08	2.35E+08	2.28E+08	2.40E+08	1.63E+07	1.84E+07	19.37	19.27	19.24
72	3.18E+08	3.16E+08	3.05E+08	3.13E+08	6.72E+06	7.60E+06	19.58	19.57	19.54
84	3.93E+08	4.02E+08	3.86E+08	3.94E+08	7.79E+06	8.82E+06	19.79	19.81	19.77
96	2.45E+08	2.31E+08	2.45E+08	2.40E+08	8.39E+06	9.49E+06	19.32	19.26	19.32
108	3.25E+08	3.40E+08	3.11E+08	3.25E+08	1.48E+07	1.67E+07	19.60	19.65	19.55
120	2.82E+08	2.94E+08	3.23E+08	3.00E+08	2.14E+07	2.42E+07	19.46	19.50	19.59



Specific growth rate (h^{-1})

Trial 1	0.029
Trial 2	0.029
Trial 3	0.028
Average	0.028
STDEV	0.001
95% CI	0.001

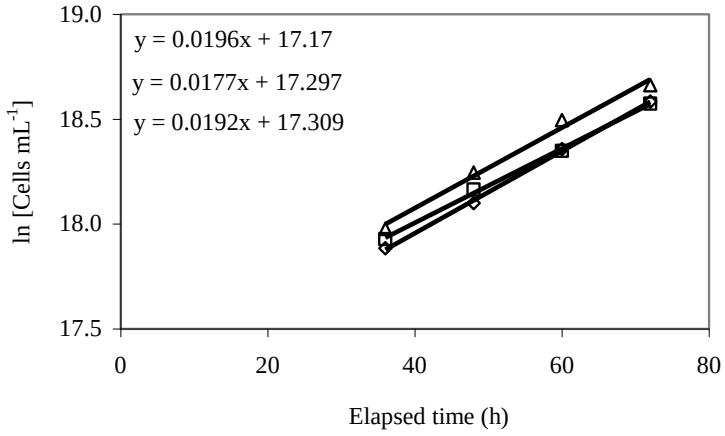
Figure G.55. Specific growth rate calculations for Trial 1 (open circles), Trial 2 (open squares), and Trial 3 (open triangles).

Toxicity of Heavy Metals Following Pre-Adaptation through Subsequent Culturing

BC13 cell concentrations with time when grown in the presence of varying concentrations of lead, zinc, and copper after pre-adaptation via subsequent culturing at the respective IC_{50}. Experiments were repeated in triplicate and average values, standard deviations (STDEV), and 95% confidence intervals (95% CI) are shown. Specific growth rates were calculated using linear regressions and are shown along with the corresponding STDEV and 95% CI to the right of the plots.

Table G.56. BC13 growth in the presence of the lead IC_{50} following pre-adaptation.

	Cells mL^{-1}						ln (Cells mL^{-1})		
Elapsed Time (h)	Trial 1	Trial 2	Trial 3	Average	STDEV	9.50E-01	Trial 1	Trial 2	Trial 3
0	5.17E+07	5.13E+07	5.12E+07	5.14E+07	2.62E+05	2.96E+05	17.76	17.75	17.75
12	6.22E+07	6.81E+07	7.35E+07	6.79E+07	5.61E+06	6.34E+06	17.95	18.04	18.11
24	5.23E+07	5.00E+07	5.07E+07	5.10E+07	1.14E+06	1.29E+06	17.77	17.73	17.74
36	5.85E+07	6.10E+07	6.42E+07	6.12E+07	2.87E+06	3.24E+06	17.88	17.93	17.98
48	7.25E+07	7.73E+07	8.39E+07	7.79E+07	5.74E+06	6.49E+06	18.10	18.16	18.25
60	9.38E+07	9.31E+07	1.08E+08	9.82E+07	8.26E+06	9.35E+06	18.36	18.35	18.50
72	1.18E+08	1.17E+08	1.27E+08	1.20E+08	5.87E+06	6.65E+06	18.58	18.57	18.66
84	1.38E+08	1.27E+08	1.33E+08	1.32E+08	5.51E+06	6.24E+06	18.74	18.66	18.71
96	1.59E+08	1.38E+08	1.35E+08	1.44E+08	1.27E+07	1.43E+07	18.88	18.75	18.72
108	1.49E+08	1.51E+08	1.42E+08	1.47E+08	4.77E+06	5.40E+06	18.82	18.83	18.77

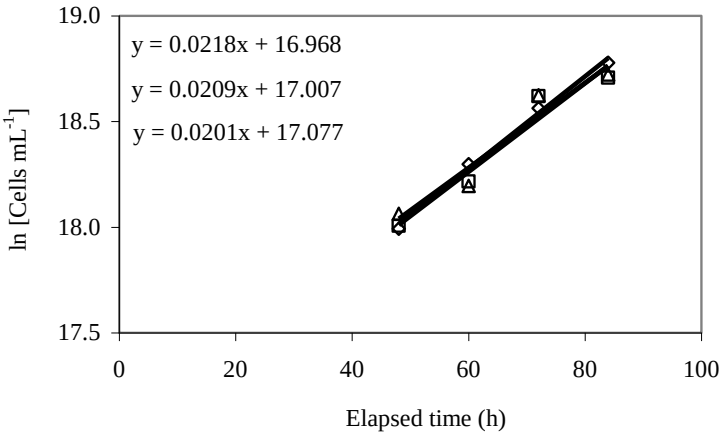


Specific growth rate (h^{-1})	
Trial 1	0.020
Trial 2	0.018
Trial 3	0.019
Average	0.019
STDEV	0.001
95% CI	0.001

Figure G.56. Specific growth rate calculations for Trial 1 (open circles), Trial 2 (open squares), and Trial 3 (open triangles).

Table G.57. BC13 growth in the presence of the zinc IC_{50} following pre-adaptation.

	Cells mL^{-1}						ln (Cells mL^{-1})		
Elapsed Time (h)	Trial 1	Trial 2	Trial 3	Average	STDEV	9.50E-01	Trial 1	Trial 2	Trial 3
0	5.42E+07	5.96E+07	6.09E+07	5.82E+07	3.54E+06	4.00E+06	17.81	17.90	17.92
12	5.15E+07	5.84E+07	5.94E+07	5.64E+07	4.27E+06	4.83E+06	17.76	17.88	17.90
24	5.56E+07	5.18E+07	5.02E+07	5.25E+07	2.76E+06	3.13E+06	17.83	17.76	17.73
36	6.29E+07	6.78E+07	7.05E+07	6.71E+07	3.88E+06	4.39E+06	17.96	18.03	18.07
48	6.52E+07	6.61E+07	6.99E+07	6.71E+07	2.51E+06	2.85E+06	17.99	18.01	18.06
60	8.85E+07	8.15E+07	7.99E+07	8.33E+07	4.58E+06	5.19E+06	18.30	18.22	18.20
72	1.15E+08	1.22E+08	1.23E+08	1.20E+08	4.12E+06	4.66E+06	18.56	18.62	18.62
84	1.43E+08	1.33E+08	1.35E+08	1.37E+08	5.12E+06	5.80E+06	18.78	18.71	18.72
96	1.43E+08	1.56E+08	1.58E+08	1.52E+08	8.06E+06	9.12E+06	18.78	18.87	18.88
108	1.57E+08	1.50E+08	1.60E+08	1.56E+08	4.79E+06	5.42E+06	18.87	18.83	18.89

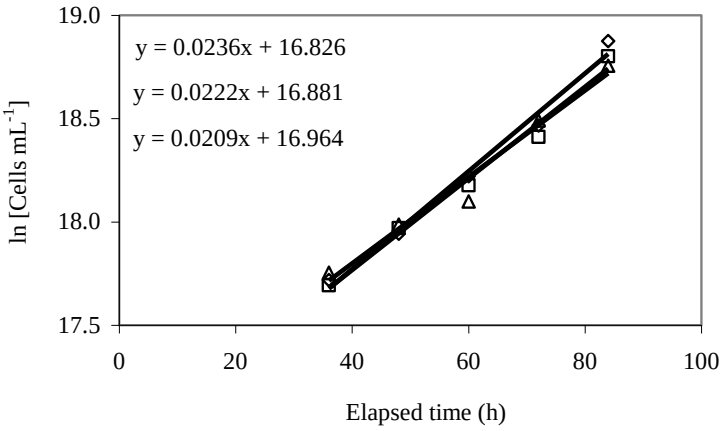


Specific growth rate (h^{-1})	
Trial 1	0.022
Trial 2	0.021
Trial 3	0.020
Average	0.021
STDEV	0.001
95% CI	0.001

Figure G.57. Specific growth rate calculations for Trial 1 (open circles), Trial 2 (open squares), and Trial 3 (open triangles).

Table G.58. BC13 growth in the presence of the copper IC_{50} following pre-adaptation.

	Cells mL^{-1}						ln (Cells mL^{-1})		
Elapsed Time (h)	Trial 1	Trial 2	Trial 3	Average	STDEV	9.50E-01	Trial 1	Trial 2	Trial 3
0	5.54E+07	5.77E+07	5.73E+07	5.68E+07	1.22E+06	1.38E+06	17.83	17.87	17.86
12	5.37E+07	5.01E+07	4.60E+07	4.99E+07	3.87E+06	4.38E+06	17.80	17.73	17.64
24	5.32E+07	5.09E+07	5.60E+07	5.33E+07	2.54E+06	2.87E+06	17.79	17.75	17.84
36	4.96E+07	4.83E+07	5.13E+07	4.97E+07	1.53E+06	1.73E+06	17.72	17.69	17.75
48	6.20E+07	6.37E+07	6.48E+07	6.35E+07	1.43E+06	1.62E+06	17.94	17.97	17.99
60	8.19E+07	7.83E+07	7.25E+07	7.76E+07	4.72E+06	5.34E+06	18.22	18.18	18.10
72	1.05E+08	9.90E+07	1.07E+08	1.04E+08	4.22E+06	4.77E+06	18.47	18.41	18.49
84	1.58E+08	1.46E+08	1.40E+08	1.48E+08	8.97E+06	1.01E+07	18.88	18.80	18.76
96	1.62E+08	1.43E+08	1.51E+08	1.52E+08	9.56E+06	1.08E+07	18.90	18.78	18.83
108	1.60E+08	1.38E+08	1.34E+08	1.44E+08	1.43E+07	1.61E+07	18.89	18.74	18.71



Specific growth rate (h^{-1})

Trial 1	0.024
Trial 2	0.022
Trial 3	0.021
Average	0.022
STDEV	0.001
95% CI	0.002

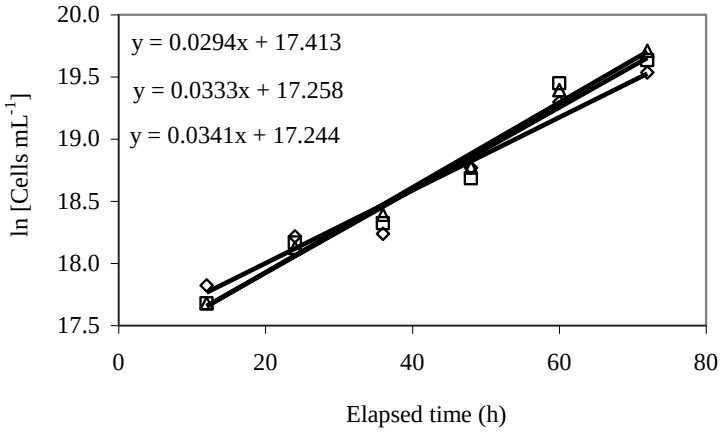
Figure G.58. Specific growth rate calculations for Trial 1 (open circles), Trial 2 (open squares), and Trial 3 (open triangles).

Resuscitation of BC13 Following Exposure to Heavy Metal MICs

BC13 cell concentrations with time when grown in metal free medium after being harvested from medium containing an MIC of lead, zinc, or copper. Experiments were repeated in triplicate and average values, standard deviations (STDEV), and 95% confidence intervals (95% CI) are shown. Specific growth rates were calculated using linear regressions and are shown along with the corresponding STDEV and 95% CI to the right of the plots.

Table G.59. BC13 growth in metal free medium following exposure to the lead MIC.

	Cells mL^{-1}						ln (Cells mL^{-1})		
Elapsed Time (h)	Trial 1	Trial 2	Trial 3	Average	STDEV	95% CI	Trial 1	Trial 2	Trial 3
0	4.77E+07	5.04E+07	4.78E+07	4.86E+07	1.54E+06	1.74E+06	17.68	17.74	17.68
12	5.50E+07	4.76E+07	4.76E+07	5.01E+07	4.26E+06	4.83E+06	17.82	17.68	17.68
24	8.15E+07	7.76E+07	7.43E+07	7.78E+07	3.59E+06	4.06E+06	18.22	18.17	18.12
36	8.33E+07	9.07E+07	9.71E+07	9.04E+07	6.88E+06	7.79E+06	18.24	18.32	18.39
48	1.42E+08	1.30E+08	1.42E+08	1.38E+08	6.73E+06	7.62E+06	18.77	18.68	18.77
60	2.40E+08	2.79E+08	2.64E+08	2.61E+08	1.96E+07	2.22E+07	19.30	19.45	19.39
72	3.05E+08	3.36E+08	3.63E+08	3.35E+08	2.92E+07	3.30E+07	19.53	19.63	19.71
84	3.37E+08	2.92E+08	2.99E+08	3.09E+08	2.39E+07	2.71E+07	19.63	19.49	19.51
96	3.03E+08	3.21E+08	3.18E+08	3.14E+08	9.82E+06	1.11E+07	19.53	19.59	19.58
108	3.21E+08	2.88E+08	2.68E+08	2.92E+08	2.66E+07	3.01E+07	19.59	19.48	19.41
120	3.29E+08	2.91E+08	3.14E+08	3.11E+08	1.92E+07	2.18E+07	19.61	19.49	19.56

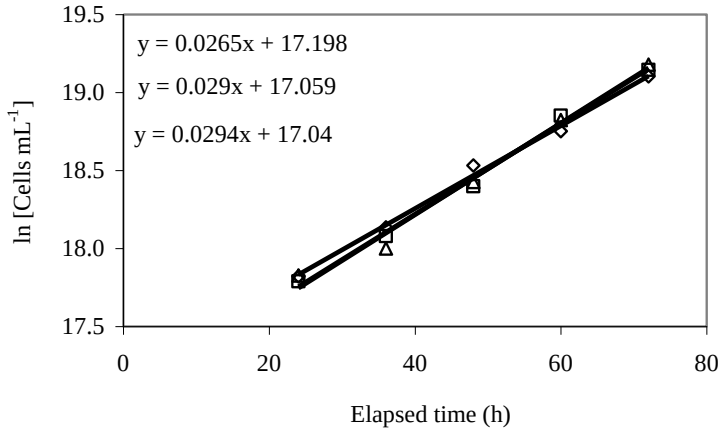


Specific growth rate (h^{-1})	
Trial 1	0.029
Trial 2	0.033
Trial 3	0.034
Average	0.032
STDEV	0.003
95% CI	0.003

Figure G.59. Specific growth rate calculations for Trial 1 (open circles), Trial 2 (open squares), and Trial 3 (open triangles).

Table G.60. BC13 growth in metal free medium following exposure to the zinc MIC.

	Cells mL^{-1}						ln (Cells mL^{-1})		
Elapsed Time (h)	Trial 1	Trial 2	Trial 3	Average	STDEV	95% CI	Trial 1	Trial 2	Trial 3
0	5.07E+07	5.55E+07	5.99E+07	5.54E+07	4.62E+06	5.23E+06	17.74	17.83	17.91
12	5.15E+07	5.72E+07	5.50E+07	5.46E+07	2.87E+06	3.25E+06	17.76	17.86	17.82
24	5.50E+07	5.32E+07	5.52E+07	5.45E+07	1.10E+06	1.24E+06	17.82	17.79	17.83
36	7.52E+07	7.11E+07	6.57E+07	7.07E+07	4.77E+06	5.40E+06	18.14	18.08	18.00
48	1.12E+08	9.79E+07	1.01E+08	1.03E+08	7.36E+06	8.33E+06	18.53	18.40	18.43
60	1.39E+08	1.54E+08	1.50E+08	1.48E+08	7.51E+06	8.50E+06	18.75	18.85	18.82
72	1.98E+08	2.06E+08	2.14E+08	2.06E+08	7.81E+06	8.84E+06	19.10	19.15	19.18
84	2.32E+08	2.40E+08	2.39E+08	2.37E+08	3.98E+06	4.50E+06	19.26	19.30	19.29
96	2.60E+08	2.66E+08	2.87E+08	2.71E+08	1.42E+07	1.61E+07	19.38	19.40	19.48
108	2.51E+08	2.79E+08	2.51E+08	2.60E+08	1.61E+07	1.82E+07	19.34	19.45	19.34
120	2.37E+08	2.40E+08	2.42E+08	2.40E+08	2.27E+06	2.57E+06	19.28	19.30	19.30



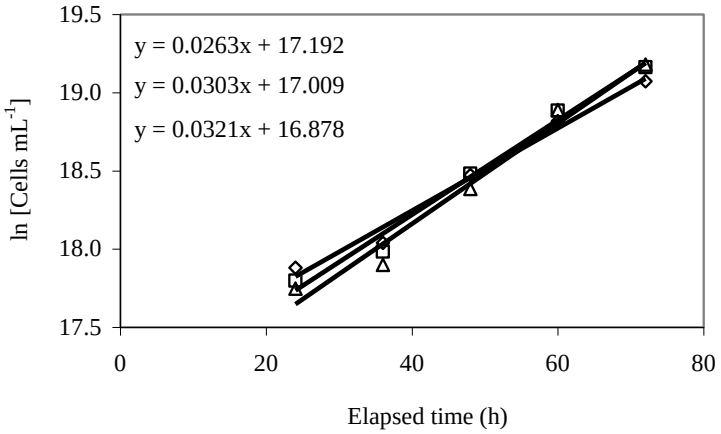
Specific growth rate (h^{-1})

Trial 1	0.027
Trial 2	0.029
Trial 3	0.029
Average	0.028
STDEV	0.002
95% CI	0.002

Figure G.60. Specific growth rate calculations for Trial 1 (open circles), Trial 2 (open squares), and Trial 3 (open triangles).

Table G.61. BC13 growth in metal free medium following exposure to the copper MIC.

	Cells mL^{-1}						ln (Cells mL^{-1})		
Elapsed Time (h)	Trial 1	Trial 2	Trial 3	Average	STDEV	95% CI	Trial 1	Trial 2	Trial 3
0	5.12E+07	5.44E+07	5.29E+07	5.28E+07	1.60E+06	1.82E+06	17.75	17.81	17.78
12	5.26E+07	4.85E+07	5.23E+07	5.12E+07	2.27E+06	2.57E+06	17.78	17.70	17.77
24	5.83E+07	5.36E+07	5.10E+07	5.43E+07	3.69E+06	4.18E+06	17.88	17.80	17.75
36	6.83E+07	6.46E+07	5.93E+07	6.41E+07	4.51E+06	5.10E+06	18.04	17.98	17.90
48	1.05E+08	1.06E+08	9.65E+07	1.03E+08	5.41E+06	6.12E+06	18.47	18.48	18.38
60	1.49E+08	1.59E+08	1.60E+08	1.56E+08	6.21E+06	7.02E+06	18.82	18.88	18.89
72	1.92E+08	2.10E+08	2.13E+08	2.05E+08	1.15E+07	1.31E+07	19.07	19.16	19.18
84	2.63E+08	2.84E+08	2.58E+08	2.68E+08	1.37E+07	1.55E+07	19.39	19.46	19.37
96	2.56E+08	2.55E+08	2.57E+08	2.56E+08	8.37E+05	9.47E+05	19.36	19.36	19.36
108	2.56E+08	2.79E+08	2.96E+08	2.77E+08	2.05E+07	2.32E+07	19.36	19.45	19.51
120	2.12E+08	3.09E+08	2.04E+08	2.42E+08	5.83E+07	6.59E+07	19.17	19.55	19.13



Specific growth rate (h^{-1})

Trial 1	0.026
Trial 2	0.030
Trial 3	0.032
Average	0.030
STDEV	0.003
95% CI	0.003

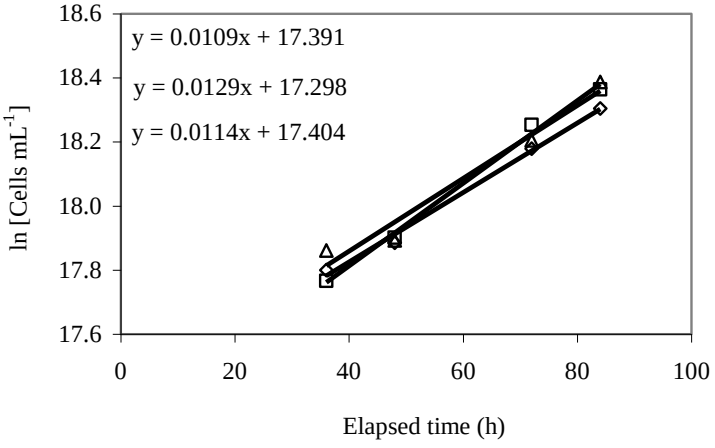
Figure G.61. Specific growth rate calculations for Trial 1 (open circles), Trial 2 (open squares), and Trial 3 (open triangles).

Toxicity of Heavy-Metal Chlorides

BC13 cell concentrations with time when grown in the presence of lead, zinc, and copper chlorides added to a concentration equal to the previously calculated IC_{50}s of lead, zinc, and copper sulfates, respectively. BC13 was also grown in the presence of the previously calculated metal sulfate IC_{50}s for comparison. Experiments were repeated in triplicate and average values, standard deviations (STDEV), and 95% confidence intervals (95% CI) are shown. Specific growth rates were calculated using linear regressions and are shown along with the corresponding STDEV and 95% CI to the right of the plots.

Table G.62. BC13 growth in medium containing lead chloride at a concentration equal to the previously calculated IC_{50} of lead sulfate.

	Cells mL^{-1}						ln (Cells mL^{-1})		
Elapsed Time (h)	Trial 1	Trial 2	Trial 3	Average	STDEV	95% CI	Trial 1	Trial 2	Trial 3
0	5.36E+07	5.61E+07	5.94E+07	5.64E+07	2.95E+06	3.34E+06	17.80	17.84	17.90
12	5.26E+07	5.40E+07	5.77E+07	5.48E+07	2.61E+06	2.96E+06	17.78	17.80	17.87
24	5.07E+07	5.51E+07	5.54E+07	5.37E+07	2.65E+06	3.00E+06	17.74	17.83	17.83
36	5.38E+07	5.20E+07	5.71E+07	5.43E+07	2.61E+06	2.95E+06	17.80	17.77	17.86
48	5.86E+07	5.95E+07	5.90E+07	5.90E+07	4.53E+05	5.12E+05	17.89	17.90	17.89
72	7.85E+07	8.46E+07	8.06E+07	8.12E+07	3.09E+06	3.50E+06	18.18	18.25	18.21
84	8.91E+07	9.45E+07	9.67E+07	9.34E+07	3.93E+06	4.45E+06	18.30	18.36	18.39
108	9.18E+07	8.67E+07	9.36E+07	9.07E+07	3.55E+06	4.02E+06	18.33	18.28	18.35
120	9.94E+07	1.06E+08	1.10E+08	1.05E+08	5.11E+06	5.79E+06	18.42	18.48	18.51
144	8.61E+07	9.41E+07	1.01E+08	9.36E+07	7.33E+06	8.29E+06	18.27	18.36	18.43
151	9.75E+07	1.00E+08	1.02E+08	9.99E+07	2.36E+06	2.67E+06	18.40	18.42	18.44

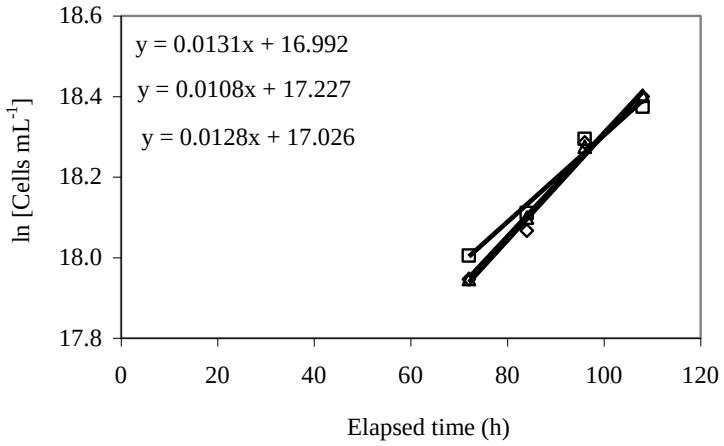


Specific growth rate (h^{-1})	
Trial 1	0.011
Trial 2	0.013
Trial 3	0.011
Average	0.012
STDEV	0.001
95% CI	0.001

Figure G.62. Specific growth rate calculations for Trial 1 (open circles), Trial 2 (open squares), and Trial 3 (open triangles).

Table G.63. BC13 growth in medium containing zinc chloride at a concentration equal to the previously calculated IC_{50} of zinc sulfate.

	Cells mL^{-1}						ln (Cells mL^{-1})		
Elapsed Time (h)	Trial 1	Trial 2	Trial 3	Average	STDEV	95% CI	Trial 1	Trial 2	Trial 3
0	5.20E+07	5.38E+07	5.36E+07	5.31E+07	9.81E+05	1.11E+06	17.77	17.80	17.80
12	5.15E+07	5.42E+07	5.16E+07	5.24E+07	1.57E+06	1.77E+06	17.76	17.81	17.76
24	5.47E+07	5.29E+07	5.34E+07	5.37E+07	9.35E+05	1.06E+06	17.82	17.78	17.79
72	6.23E+07	6.60E+07	6.23E+07	6.35E+07	2.15E+06	2.43E+06	17.95	18.00	17.95
84	7.02E+07	7.34E+07	7.25E+07	7.20E+07	1.64E+06	1.86E+06	18.07	18.11	18.10
96	8.74E+07	8.82E+07	8.65E+07	8.74E+07	8.41E+05	9.52E+05	18.29	18.29	18.28
108	9.79E+07	9.55E+07	9.81E+07	9.72E+07	1.47E+06	1.67E+06	18.40	18.37	18.40
120	1.04E+08	1.10E+08	1.16E+08	1.10E+08	6.06E+06	6.86E+06	18.46	18.51	18.57
144	1.09E+08	1.16E+08	1.15E+08	1.14E+08	3.64E+06	4.12E+06	18.51	18.57	18.56
168	1.00E+08	1.02E+08	1.01E+08	1.01E+08	9.46E+05	1.07E+06	18.42	18.44	18.43

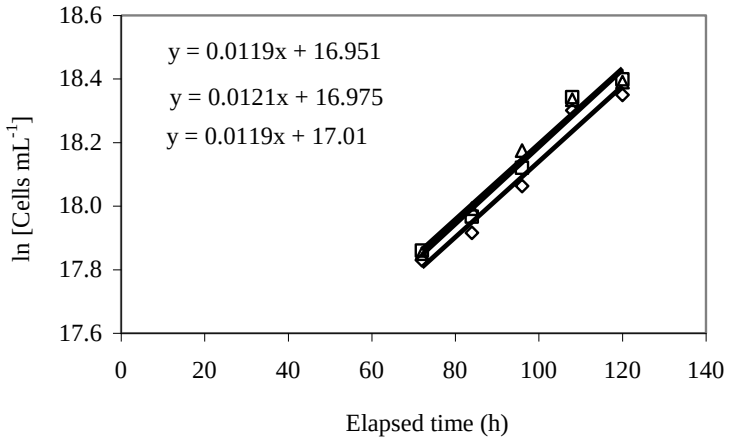


Specific growth rate (h^{-1})	
Trial 1	0.013
Trial 2	0.011
Trial 3	0.013
Average	0.012
STDEV	0.001
95% CI	0.001

Figure G.63. Specific growth rate calculations for Trial 1 (open circles), Trial 2 (open squares), and Trial 3 (open triangles).

Table G.64. BC13 growth in medium containing copper chloride at a concentration equal to the previously calculated IC_{50} of copper sulfate.

	Cells mL^{-1}						ln (Cells mL^{-1})		
Elapsed Time (h)	Trial 1	Trial 2	Trial 3	Average	STDEV	95% CI	Trial 1	Trial 2	Trial 3
0	4.83E+07	4.82E+07	4.93E+07	4.86E+07	6.11E+05	6.91E+05	17.69	17.69	17.71
12	5.47E+07	5.55E+07	5.66E+07	5.56E+07	9.44E+05	1.07E+06	17.82	17.83	17.85
24	5.26E+07	5.09E+07	5.12E+07	5.15E+07	9.11E+05	1.03E+06	17.78	17.74	17.75
72	5.54E+07	5.71E+07	5.65E+07	5.63E+07	8.74E+05	9.89E+05	17.83	17.86	17.85
84	6.04E+07	6.35E+07	6.51E+07	6.30E+07	2.40E+06	2.71E+06	17.92	17.97	17.99
96	6.99E+07	7.40E+07	7.82E+07	7.40E+07	4.12E+06	4.66E+06	18.06	18.12	18.17
108	8.88E+07	9.25E+07	9.17E+07	9.10E+07	1.97E+06	2.23E+06	18.30	18.34	18.33
120	9.32E+07	9.78E+07	9.70E+07	9.60E+07	2.46E+06	2.79E+06	18.35	18.40	18.39
144	9.04E+07	8.90E+07	8.73E+07	8.89E+07	1.56E+06	1.76E+06	18.32	18.30	18.28
168	1.16E+08	1.20E+08	1.18E+08	1.18E+08	1.99E+06	2.25E+06	18.57	18.60	18.59



Specific growth rate (h^{-1})

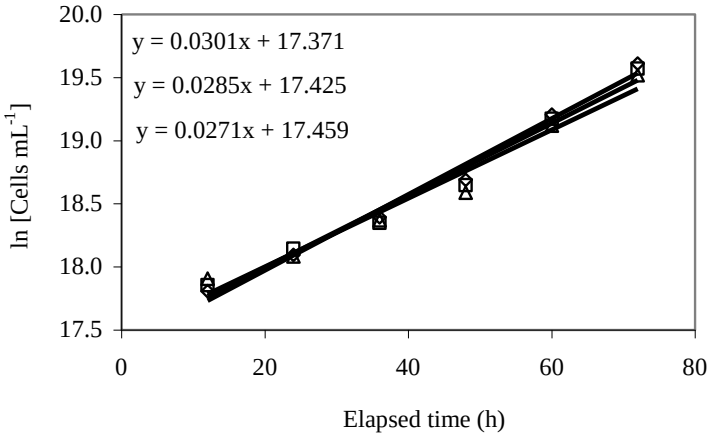
Trial 1	0.012
Trial 2	0.012
Trial 3	0.012
Average	0.012
STDEV	0.000
95% CI	0.000

Figure G.64. Specific growth rate calculations for Trial 1 (open circles), Trial 2 (open squares), and Trial 3 (open triangles).

Toxicity of Heavy-Metal Sulfates at Previously Calculated IC_{50}s

Table G.65. BC13 growth in medium containing lead sulfate at a concentration equal to the previously calculated IC_{50}.

	Cells mL^{-1}						ln (Cells mL^{-1})		
Elapsed Time (h)	Trial 1	Trial 2	Trial 3	Average	STDEV	95% CI	Trial 1	Trial 2	Trial 3
0	5.12E+07	5.07E+07	5.26E+07	5.15E+07	9.65E+05	1.09E+06	17.75	17.74	17.78
12	5.42E+07	5.67E+07	5.99E+07	5.69E+07	2.83E+06	3.20E+06	17.81	17.85	17.91
24	7.22E+07	7.58E+07	7.13E+07	7.31E+07	2.35E+06	2.66E+06	18.10	18.14	18.08
36	9.73E+07	9.29E+07	9.50E+07	9.51E+07	2.19E+06	2.48E+06	18.39	18.35	18.37
48	1.31E+08	1.25E+08	1.18E+08	1.25E+08	6.34E+06	7.17E+06	18.69	18.65	18.59
60	2.19E+08	2.12E+08	2.01E+08	2.11E+08	9.10E+06	1.03E+07	19.20	19.17	19.12
72	3.28E+08	3.16E+08	3.00E+08	3.15E+08	1.42E+07	1.61E+07	19.61	19.57	19.52
84	3.27E+08	3.10E+08	3.07E+08	3.15E+08	1.09E+07	1.23E+07	19.61	19.55	19.54
96	3.13E+08	3.15E+08	3.35E+08	3.21E+08	1.19E+07	1.35E+07	19.56	19.57	19.63
108	3.16E+08	3.31E+08	3.49E+08	3.32E+08	1.66E+07	1.88E+07	19.57	19.62	19.67
120	3.08E+08	3.03E+08	3.03E+08	3.05E+08	2.89E+06	3.27E+06	19.55	19.53	19.53

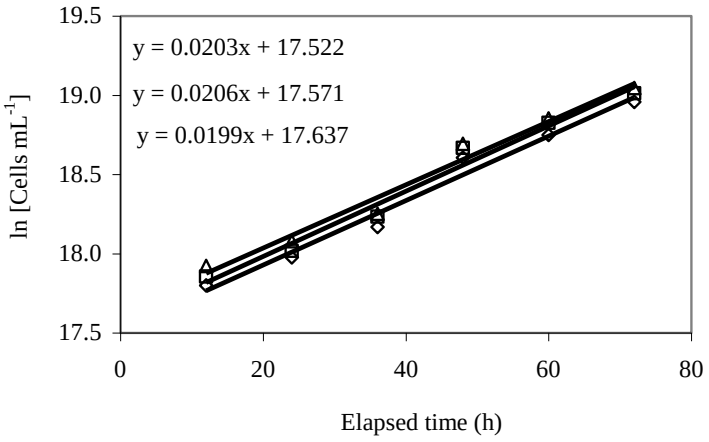


Specific growth rate (h^{-1})	
Trial 1	0.030
Trial 2	0.029
Trial 3	0.027
Average	0.029
STDEV	0.002
95% CI	0.002

Figure G.65. Specific growth rate calculations for Trial 1 (open circles), Trial 2 (open squares), and Trial 3 (open triangles).

Table G.66. BC13 growth in medium containing zinc sulfate at a concentration equal to the previously calculated IC_{50}.

	Cells mL^{-1}						ln (Cells mL^{-1})		
Elapsed Time (h)	Trial 1	Trial 2	Trial 3	Average	STDEV	95% CI	Trial 1	Trial 2	Trial 3
0	5.83E+07	5.54E+07	5.78E+07	5.72E+07	1.53E+06	1.73E+06	17.88	17.83	17.87
12	5.38E+07	5.68E+07	6.08E+07	5.71E+07	3.54E+06	4.01E+06	17.80	17.86	17.92
24	6.42E+07	6.68E+07	7.11E+07	6.73E+07	3.49E+06	3.94E+06	17.98	18.02	18.08
36	7.76E+07	8.30E+07	8.45E+07	8.17E+07	3.59E+06	4.07E+06	18.17	18.23	18.25
48	1.20E+08	1.28E+08	1.31E+08	1.27E+08	5.64E+06	6.38E+06	18.61	18.67	18.69
60	1.39E+08	1.50E+08	1.54E+08	1.48E+08	7.96E+06	9.01E+06	18.75	18.83	18.85
72	1.71E+08	1.81E+08	1.87E+08	1.80E+08	7.80E+06	8.83E+06	18.96	19.01	19.04
84	1.72E+08	1.88E+08	2.04E+08	1.88E+08	1.62E+07	1.83E+07	18.96	19.05	19.13
96	1.64E+08	1.73E+08	1.77E+08	1.71E+08	6.81E+06	7.71E+06	18.91	18.97	18.99
108	1.77E+08	1.74E+08	1.72E+08	1.74E+08	2.75E+06	3.12E+06	18.99	18.98	18.96
120	1.73E+08	1.66E+08	1.69E+08	1.69E+08	3.21E+06	3.64E+06	18.97	18.93	18.95

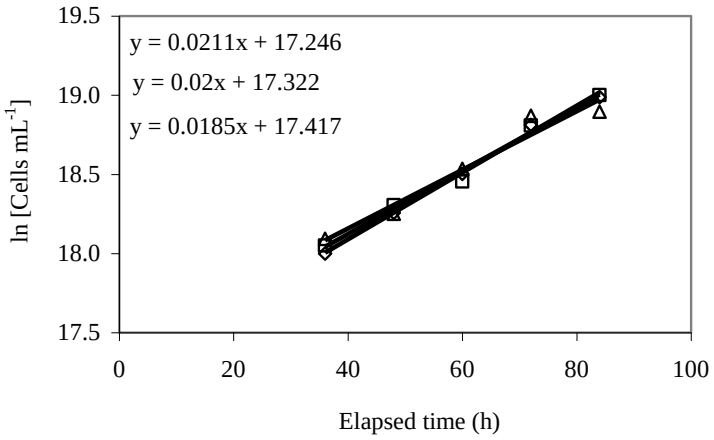


Specific growth rate (h^{-1})	
Trial 1	0.020
Trial 2	0.021
Trial 3	0.020
Average	0.020
STDEV	0.000
95% CI	0.000

Figure G.66. Specific growth rate calculations for Trial 1 (open circles), Trial 2 (open squares), and Trial 3 (open triangles).

Table G.67. BC13 growth in medium containing copper sulfate at a concentration equal to the previously calculated IC_{50}.

	Cells mL^{-1}						ln (Cells mL^{-1})		
Elapsed Time (h)	Trial 1	Trial 2	Trial 3	Average	STDEV	95% CI	Trial 1	Trial 2	Trial 3
0	5.79E+07	6.22E+07	6.12E+07	6.04E+07	2.25E+06	2.54E+06	17.87	17.95	17.93
12	5.73E+07	6.28E+07	6.60E+07	6.20E+07	4.42E+06	5.00E+06	17.86	17.96	18.00
24	6.04E+07	6.52E+07	5.91E+07	6.16E+07	3.24E+06	3.67E+06	17.92	17.99	17.89
36	6.56E+07	6.91E+07	7.21E+07	6.89E+07	3.23E+06	3.65E+06	18.00	18.05	18.09
48	8.48E+07	8.91E+07	8.44E+07	8.61E+07	2.59E+06	2.93E+06	18.26	18.30	18.25
60	1.09E+08	1.03E+08	1.12E+08	1.08E+08	4.30E+06	4.87E+06	18.50	18.45	18.53
72	1.48E+08	1.47E+08	1.57E+08	1.51E+08	5.17E+06	5.85E+06	18.81	18.81	18.87
84	1.76E+08	1.79E+08	1.61E+08	1.72E+08	9.66E+06	1.09E+07	18.99	19.00	18.90
96	1.88E+08	1.90E+08	1.91E+08	1.89E+08	1.44E+06	1.63E+06	19.05	19.06	19.07
108	2.06E+08	1.98E+08	1.80E+08	1.95E+08	1.33E+07	1.50E+07	19.14	19.11	19.01
120	1.73E+08	1.76E+08	1.88E+08	1.79E+08	8.12E+06	9.19E+06	18.97	18.98	19.05



Specific growth rate (h^{-1})	
Trial 1	0.021
Trial 2	0.020
Trial 3	0.019
Average	0.020
STDEV	0.001
95% CI	0.001

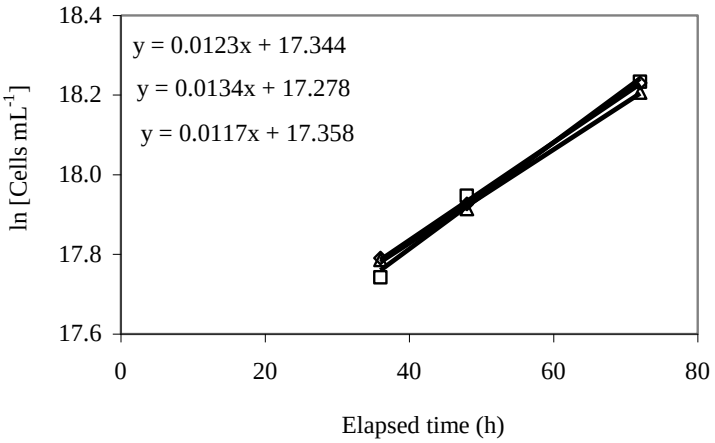
Figure G.67. Specific growth rate calculations for Trial 1 (open circles), Trial 2 (open squares), and Trial 3 (open triangles).

Toxicity of Metal Sulfates + Sodium Chloride

BC13 cell concentrations with time when grown in the presence of lead, zinc, and copper sulfate IC_{50}s with sodium chloride added to a concentration equivalent to that which would be present if metal chlorides were added to the IC_{50}s of lead, zinc, and copper sulfates, respectively. Experiments were repeated in triplicate and average values, standard deviations (STDEV), and 95% confidence intervals (95% CI) are shown. Specific growth rates were calculated using linear regressions and are shown along with the corresponding STDEV and 95% CI to the right of the plots.

Table G.68. BC13 growth in medium containing lead sulfate + sodium chloride.

	Cells mL^{-1}						ln (Cells mL^{-1})		
Elapsed Time (h)	Trial 1	Trial 2	Trial 3	Average	STDEV	95% CI	Trial 1	Trial 2	Trial 3
0	5.60E+07	5.64E+07	5.32E+07	5.52E+07	1.73E+06	1.96E+06	17.84	17.85	17.79
12	5.10E+07	4.82E+07	4.55E+07	4.82E+07	2.75E+06	3.11E+06	17.75	17.69	17.63
24	5.23E+07	5.18E+07	5.31E+07	5.24E+07	6.84E+05	7.74E+05	17.77	17.76	17.79
36	5.33E+07	5.07E+07	5.30E+07	5.23E+07	1.38E+06	1.57E+06	17.79	17.74	17.79
48	6.10E+07	6.22E+07	6.03E+07	6.12E+07	9.99E+05	1.13E+06	17.93	17.95	17.91
72	8.27E+07	8.29E+07	8.07E+07	8.21E+07	1.21E+06	1.36E+06	18.23	18.23	18.21
84	9.25E+07	9.71E+07	9.62E+07	9.53E+07	2.48E+06	2.80E+06	18.34	18.39	18.38
108	8.79E+07	8.46E+07	8.44E+07	8.56E+07	1.95E+06	2.20E+06	18.29	18.25	18.25
120	1.05E+08	1.01E+08	1.05E+08	1.04E+08	2.24E+06	2.54E+06	18.47	18.43	18.47
144	8.36E+07	8.09E+07	8.23E+07	8.23E+07	1.36E+06	1.54E+06	18.24	18.21	18.23
151	9.76E+07	1.00E+08	1.02E+08	9.99E+07	2.27E+06	2.57E+06	18.40	18.42	18.44

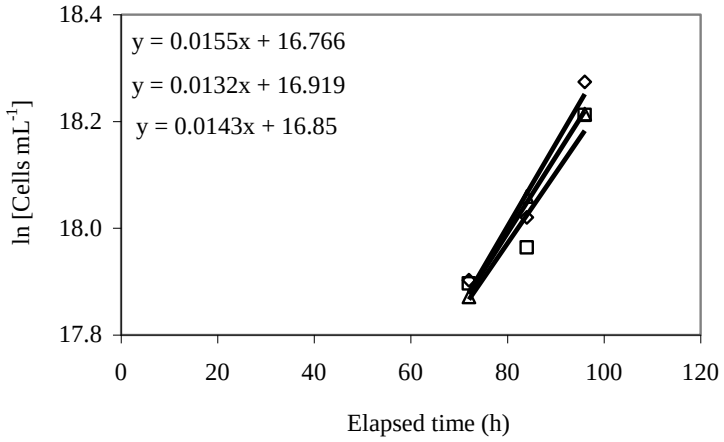


Specific growth rate (h^{-1})	
Trial 1	0.012
Trial 2	0.013
Trial 3	0.012
Average	0.012
STDEV	0.001
95% CI	0.001

Figure G.68. Specific growth rate calculations for Trial 1 (open circles), Trial 2 (open squares), and Trial 3 (open triangles).

Table G.69. BC13 growth in medium containing zinc sulfate + sodium chloride.

	Cells mL^{-1}						ln (Cells mL^{-1})		
Elapsed Time (h)	Trial 1	Trial 2	Trial 3	Average	STDEV	95% CI	Trial 1	Trial 2	Trial 3
0	5.39E+07	5.48E+07	5.38E+07	5.42E+07	5.77E+05	6.53E+05	17.80	17.82	17.80
12	5.21E+07	4.99E+07	5.01E+07	5.07E+07	1.21E+06	1.37E+06	17.77	17.73	17.73
24	5.51E+07	5.18E+07	5.06E+07	5.25E+07	2.32E+06	2.63E+06	17.82	17.76	17.74
72	5.96E+07	5.92E+07	5.77E+07	5.88E+07	9.74E+05	1.10E+06	17.90	17.90	17.87
84	6.70E+07	6.34E+07	6.97E+07	6.67E+07	3.17E+06	3.59E+06	18.02	17.96	18.06
96	8.63E+07	8.12E+07	8.13E+07	8.29E+07	2.95E+06	3.33E+06	18.27	18.21	18.21
108	1.01E+08	9.47E+07	9.43E+07	9.66E+07	3.57E+06	4.05E+06	18.43	18.37	18.36
120	1.02E+08	9.58E+07	9.47E+07	9.75E+07	4.02E+06	4.55E+06	18.44	18.38	18.37
144	1.07E+08	1.13E+08	1.18E+08	1.13E+08	5.40E+06	6.11E+06	18.49	18.55	18.59
168	1.03E+08	1.05E+08	1.03E+08	1.04E+08	1.12E+06	1.27E+06	18.45	18.47	18.45

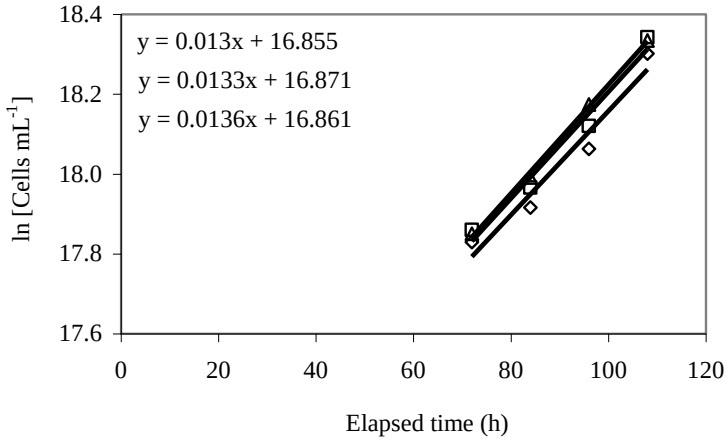


Specific growth rate (h^{-1})	
Trial 1	0.016
Trial 2	0.013
Trial 3	0.014
Average	0.014
STDEV	0.001
95% CI	0.001

Figure G.69. Specific growth rate calculations for Trial 1 (open circles), Trial 2 (open squares), and Trial 3 (open triangles).

Table G.70. BC13 growth in medium containing copper sulfate + sodium chloride.

	Cells mL^{-1}						ln (Cells mL^{-1})		
Elapsed Time (h)	Trial 1	Trial 2	Trial 3	Average	STDEV	95% CI	Trial 1	Trial 2	Trial 3
0	4.95E+07	4.82E+07	4.93E+07	4.86E+07	6.11E+05	6.91E+05	17.69	17.69	17.71
12	5.72E+07	5.55E+07	5.66E+07	5.56E+07	9.44E+05	1.07E+06	17.82	17.83	17.85
24	5.10E+07	5.09E+07	5.12E+07	5.15E+07	9.11E+05	1.03E+06	17.78	17.74	17.75
72	5.21E+07	5.71E+07	5.65E+07	5.63E+07	8.74E+05	9.89E+05	17.83	17.86	17.85
84	5.68E+07	6.35E+07	6.51E+07	6.30E+07	2.40E+06	2.71E+06	17.92	17.97	17.99
96	7.25E+07	7.40E+07	7.82E+07	7.40E+07	4.12E+06	4.66E+06	18.06	18.12	18.17
108	8.53E+07	9.25E+07	9.17E+07	9.10E+07	1.97E+06	2.23E+06	18.30	18.34	18.33
120	9.67E+07	9.78E+07	9.70E+07	9.60E+07	2.46E+06	2.79E+06	18.35	18.40	18.39
144	9.00E+07	8.90E+07	8.73E+07	8.89E+07	1.56E+06	1.76E+06	18.32	18.30	18.28
168	1.23E+08	1.20E+08	1.18E+08	1.18E+08	1.99E+06	2.25E+06	18.57	18.60	18.59



Specific growth rate (h^{-1})

Trial 1	0.013
Trial 2	0.013
Trial 3	0.014
Average	0.013
STDEV	0.000
95% CI	0.000

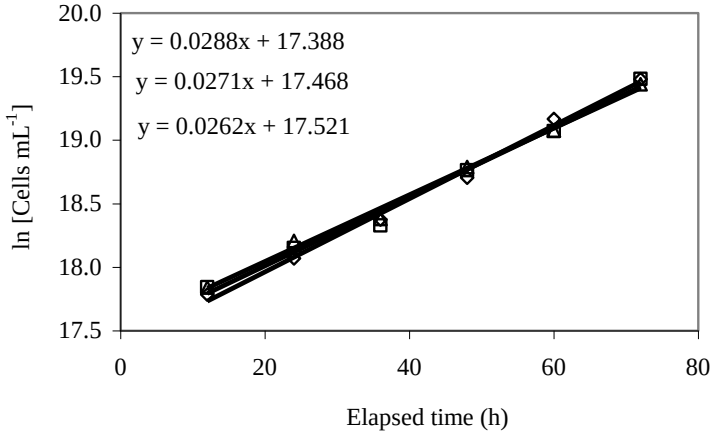
Figure G.70. Specific growth rate calculations for Trial 1 (open circles), Trial 2 (open squares), and Trial 3 (open triangles).

Toxicity of Sodium Chloride

BC13 cell concentrations with time when grown in the presence sodium chloride added to concentrations of 50, 100, and 200 mM. Experiments were repeated in triplicate and average values, standard deviations (STDEV), and 95% confidence intervals (95% CI) are shown. Specific growth rates were calculated using linear regressions and are shown along with the corresponding STDEV and 95% CI to the right of the plots.

Table G.71. BC13 growth in medium containing 50 mM sodium chloride.

	Cells mL^{-1}						ln (Cells mL^{-1})		
Elapsed Time (h)	Trial 1	Trial 2	Trial 3	Average	STDEV	95% CI	Trial 1	Trial 2	Trial 3
0	4.85E+07	5.07E+07	5.19E+07	5.03E+07	1.75E+06	1.98E+06	17.70	17.74	17.77
12	5.30E+07	5.61E+07	5.61E+07	5.51E+07	1.79E+06	2.02E+06	17.79	17.84	17.84
24	7.03E+07	7.64E+07	8.07E+07	7.58E+07	5.21E+06	5.89E+06	18.07	18.15	18.21
36	9.56E+07	9.11E+07	9.59E+07	9.42E+07	2.69E+06	3.04E+06	18.38	18.33	18.38
48	1.33E+08	1.41E+08	1.44E+08	1.39E+08	5.94E+06	6.73E+06	18.70	18.76	18.79
60	2.11E+08	1.92E+08	1.93E+08	1.98E+08	1.07E+07	1.21E+07	19.17	19.07	19.08
72	2.89E+08	2.89E+08	2.77E+08	2.85E+08	6.85E+06	7.75E+06	19.48	19.48	19.44
84	3.06E+08	3.03E+08	2.73E+08	2.94E+08	1.82E+07	2.06E+07	19.54	19.53	19.43
96	3.19E+08	3.09E+08	2.91E+08	3.06E+08	1.38E+07	1.56E+07	19.58	19.55	19.49
108	2.91E+08	3.12E+08	3.04E+08	3.03E+08	1.05E+07	1.19E+07	19.49	19.56	19.53
120	3.12E+08	2.88E+08	2.98E+08	3.00E+08	1.22E+07	1.39E+07	19.56	19.48	19.51



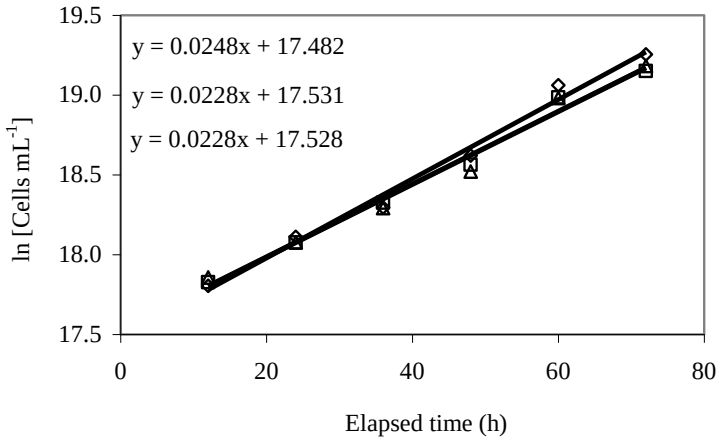
Specific growth rate (h^{-1})

Trial 1	0.029
Trial 2	0.027
Trial 3	0.026
Average	0.027
STDEV	0.001
95% CI	0.001

Figure G.71. Specific growth rate calculations for Trial 1 (open circles), Trial 2 (open squares), and Trial 3 (open triangles).

Table G.72. BC13 growth in medium containing 100 mM sodium chloride.

	Cells mL^{-1}						ln (Cells mL^{-1})		
Elapsed Time (h)	Trial 1	Trial 2	Trial 3	Average	STDEV	95% CI	Trial 1	Trial 2	Trial 3
0	5.30E+07	5.36E+07	5.05E+07	5.24E+07	1.65E+06	1.86E+06	17.79	17.80	17.74
12	5.40E+07	5.53E+07	5.69E+07	5.54E+07	1.47E+06	1.66E+06	17.80	17.83	17.86
24	7.34E+07	7.09E+07	7.09E+07	7.17E+07	1.44E+06	1.63E+06	18.11	18.08	18.08
36	8.82E+07	9.10E+07	8.79E+07	8.90E+07	1.70E+06	1.92E+06	18.29	18.33	18.29
48	1.22E+08	1.15E+08	1.10E+08	1.16E+08	5.90E+06	6.67E+06	18.62	18.56	18.52
60	1.90E+08	1.76E+08	1.75E+08	1.80E+08	8.16E+06	9.24E+06	19.06	18.99	18.98
72	2.30E+08	2.08E+08	2.14E+08	2.17E+08	1.17E+07	1.32E+07	19.26	19.15	19.18
84	2.59E+08	2.82E+08	3.09E+08	2.83E+08	2.49E+07	2.82E+07	19.37	19.46	19.55
96	2.47E+08	2.42E+08	2.52E+08	2.47E+08	4.95E+06	5.60E+06	19.32	19.30	19.34
108	2.62E+08	2.82E+08	2.60E+08	2.68E+08	1.23E+07	1.40E+07	19.39	19.46	19.37
120	2.73E+08	2.96E+08	3.11E+08	2.93E+08	1.94E+07	2.19E+07	19.42	19.50	19.56



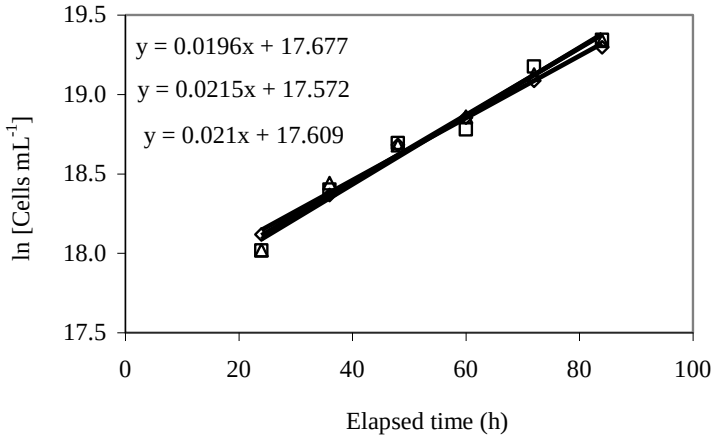
Specific growth rate (h^{-1})

Trial 1	0.025
Trial 2	0.023
Trial 3	0.023
Average	0.023
STDEV	0.001
95% CI	0.001

Figure G.72. Specific growth rate calculations for Trial 1 (open circles), Trial 2 (open squares), and Trial 3 (open triangles).

Table G.73. BC13 growth in medium containing 200 mM sodium chloride.

	Cells mL^{-1}						ln (Cells mL^{-1})		
Elapsed Time (h)	Trial 1	Trial 2	Trial 3	Average	STDEV	95% CI	Trial 1	Trial 2	Trial 3
0	5.00E+07	5.48E+07	5.79E+07	5.42E+07	4.01E+06	4.54E+06	17.73	17.82	17.87
12	5.19E+07	5.07E+07	5.49E+07	5.25E+07	2.18E+06	2.46E+06	17.76	17.74	17.82
24	7.39E+07	6.67E+07	6.69E+07	6.92E+07	4.09E+06	4.63E+06	18.12	18.02	18.02
36	9.47E+07	9.80E+07	1.02E+08	9.83E+07	3.70E+06	4.19E+06	18.37	18.40	18.44
48	1.30E+08	1.31E+08	1.30E+08	1.30E+08	1.03E+06	1.16E+06	18.68	18.69	18.68
60	1.54E+08	1.43E+08	1.55E+08	1.51E+08	6.73E+06	7.62E+06	18.85	18.78	18.86
72	1.94E+08	2.13E+08	2.02E+08	2.03E+08	9.13E+06	1.03E+07	19.09	19.18	19.12
84	2.40E+08	2.52E+08	2.50E+08	2.47E+08	6.41E+06	7.25E+06	19.30	19.34	19.34
96	2.40E+08	2.29E+08	2.34E+08	2.34E+08	5.60E+06	6.33E+06	19.30	19.25	19.27
108	2.29E+08	2.38E+08	2.16E+08	2.28E+08	1.07E+07	1.22E+07	19.25	19.29	19.19
120	2.13E+08	2.05E+08	2.23E+08	2.13E+08	9.10E+06	1.03E+07	19.18	19.14	19.22



Specific growth rate (h^{-1})

Trial 1	0.020
Trial 2	0.022
Trial 3	0.021
Average	0.021
STDEV	0.001
95% CI	0.001

Figure G.73. Specific growth rate calculations for Trial 1 (open circles), Trial 2 (open squares), and Trial 3 (open triangles).

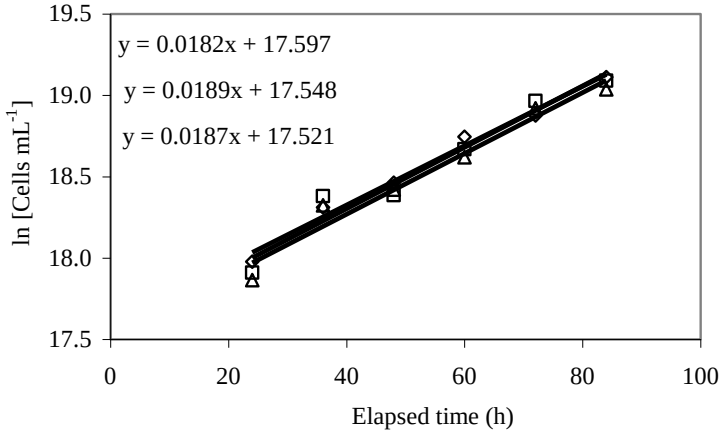
Combined Toxicity of Heavy-Metal Sulfates and Chloride

BC13 cell concentrations with time when grown in the presence lead, zinc, and copper sulfates (at either the 0.5 x IC_{50} or 1.0 x IC_{50}) mixed with sodium chloride added to concentrations of 50, 100, and 200 mM. Experiments were repeated in triplicate and average values, standard deviations (STDEV), and 95% confidence intervals (95% CI) are shown. Specific growth rates were calculated using linear regressions and are shown along with the corresponding STDEV and 95% CI to the right of the plots.

0.5 x IC_{50} Lead Sulfate + Chloride

Table G.74. BC13 growth in medium containing 0.5 x IC_{50} lead sulfate and 50 mM sodium chloride.

	Cells mL^{-1}						ln (Cells mL^{-1})		
Elapsed Time (h)	Trial 1	Trial 2	Trial 3	Average	STDEV	95% CI	Trial 1	Trial 2	Trial 3
0	5.70E+07	5.62E+07	5.72E+07	5.68E+07	5.45E+05	6.17E+05	17.86	17.84	17.86
12	5.78E+07	5.76E+07	5.32E+07	5.62E+07	2.63E+06	2.98E+06	17.87	17.87	17.79
24	6.42E+07	6.01E+07	5.73E+07	6.05E+07	3.46E+06	3.92E+06	17.98	17.91	17.86
36	8.97E+07	9.60E+07	9.08E+07	9.22E+07	3.40E+06	3.84E+06	18.31	18.38	18.32
48	1.04E+08	9.67E+07	1.00E+08	1.00E+08	3.81E+06	4.31E+06	18.46	18.39	18.42
60	1.38E+08	1.28E+08	1.22E+08	1.30E+08	8.34E+06	9.43E+06	18.75	18.67	18.62
72	1.58E+08	1.72E+08	1.65E+08	1.65E+08	7.29E+06	8.24E+06	18.88	18.96	18.92
84	1.99E+08	1.95E+08	1.85E+08	1.93E+08	7.34E+06	8.31E+06	19.11	19.09	19.04
96	1.66E+08	1.56E+08	1.61E+08	1.61E+08	4.99E+06	5.64E+06	18.93	18.87	18.90
108	1.80E+08	1.66E+08	1.64E+08	1.70E+08	8.77E+06	9.92E+06	19.01	18.93	18.92
120	1.74E+08	1.70E+08	1.52E+08	1.65E+08	1.19E+07	1.35E+07	18.97	18.95	18.84



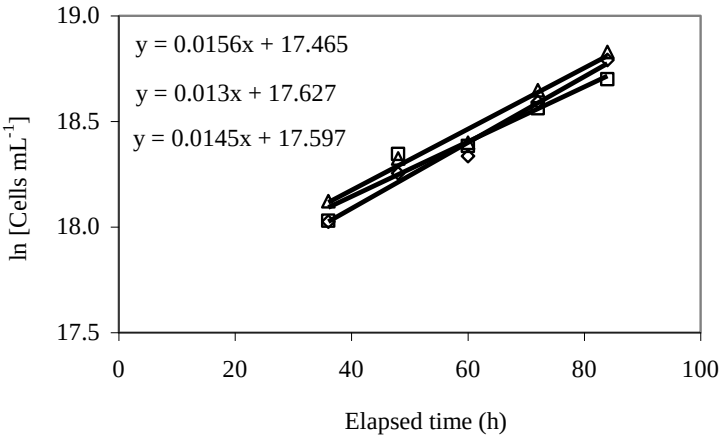
Specific growth rate (h^{-1})

Trial 1	0.018
Trial 2	0.019
Trial 3	0.019
Average	0.019
STDEV	0.000
95% CI	0.000

Figure G.74. Specific growth rate calculations for Trial 1 (open circles), Trial 2 (open squares), and Trial 3 (open triangles).

Table G.75. BC13 growth in medium containing 0.5 x IC_{50} lead sulfate and 100 mM sodium chloride.

	Cells mL^{-1}						ln (Cells mL^{-1})		
Elapsed Time (h)	Trial 1	Trial 2	Trial 3	Average	STDEV	95% CI	Trial 1	Trial 2	Trial 3
0	5.79E+07	5.70E+07	5.54E+07	5.68E+07	1.30E+06	1.47E+06	17.88	17.86	17.83
12	6.01E+07	6.19E+07	6.64E+07	6.28E+07	3.25E+06	3.68E+06	17.91	17.94	18.01
24	6.08E+07	6.42E+07	5.95E+07	6.15E+07	2.44E+06	2.76E+06	17.92	17.98	17.90
36	6.73E+07	6.76E+07	7.41E+07	6.97E+07	3.85E+06	4.35E+06	18.03	18.03	18.12
48	8.47E+07	9.28E+07	9.09E+07	8.95E+07	4.22E+06	4.77E+06	18.25	18.35	18.32
60	9.18E+07	9.63E+07	9.78E+07	9.53E+07	3.14E+06	3.56E+06	18.34	18.38	18.40
72	1.19E+08	1.15E+08	1.25E+08	1.20E+08	5.20E+06	5.89E+06	18.59	18.56	18.65
84	1.45E+08	1.32E+08	1.50E+08	1.42E+08	9.35E+06	1.06E+07	18.79	18.70	18.83
96	1.53E+08	1.41E+08	1.45E+08	1.46E+08	6.18E+06	6.99E+06	18.85	18.76	18.79
108	1.51E+08	1.39E+08	1.30E+08	1.40E+08	1.04E+07	1.17E+07	18.83	18.75	18.68
120	1.65E+08	1.82E+08	1.42E+08	1.63E+08	2.01E+07	2.27E+07	18.92	19.02	18.77



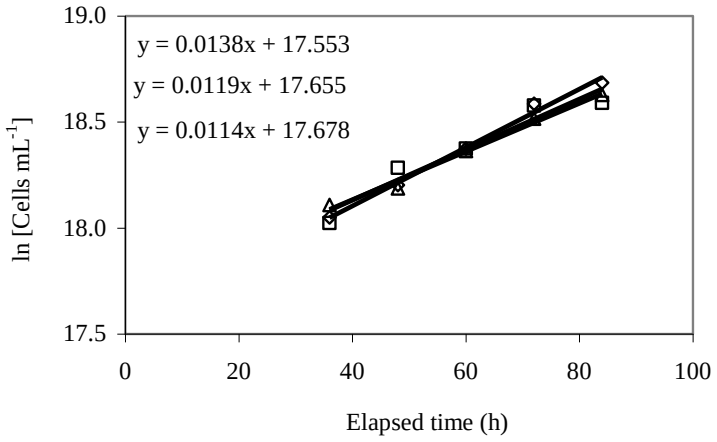
Specific growth rate (h^{-1})

Trial 1	0.016
Trial 2	0.013
Trial 3	0.015
Average	0.014
STDEV	0.001
95% CI	0.001

Figure G.75. Specific growth rate calculations for Trial 1 (open circles), Trial 2 (open squares), and Trial 3 (open triangles).

Table G.76. BC13 growth in medium containing 0.5 x IC_{50} lead sulfate and 200 mM sodium chloride.

	Cells mL^{-1}						ln (Cells mL^{-1})		
Elapsed Time (h)	Trial 1	Trial 2	Trial 3	Average	STDEV	95% CI	Trial 1	Trial 2	Trial 3
0	5.55E+07	5.39E+07	5.07E+07	5.34E+07	2.45E+06	2.77E+06	17.83	17.80	17.74
12	5.57E+07	5.69E+07	6.23E+07	5.83E+07	3.52E+06	3.98E+06	17.84	17.86	17.95
24	6.64E+07	7.30E+07	6.94E+07	6.96E+07	3.31E+06	3.74E+06	18.01	18.11	18.06
36	6.90E+07	6.72E+07	7.32E+07	6.98E+07	3.10E+06	3.51E+06	18.05	18.02	18.11
48	8.04E+07	8.71E+07	7.92E+07	8.22E+07	4.27E+06	4.83E+06	18.20	18.28	18.19
60	9.54E+07	9.54E+07	9.45E+07	9.51E+07	5.56E+05	6.30E+05	18.37	18.37	18.36
72	1.18E+08	1.17E+08	1.10E+08	1.15E+08	4.33E+06	4.90E+06	18.59	18.58	18.52
84	1.30E+08	1.18E+08	1.23E+08	1.24E+08	5.93E+06	6.71E+06	18.68	18.59	18.63
96	1.54E+08	1.49E+08	1.43E+08	1.49E+08	5.54E+06	6.27E+06	18.86	18.82	18.78
108	1.48E+08	1.44E+08	1.47E+08	1.46E+08	1.78E+06	2.02E+06	18.81	18.79	18.80
120	1.37E+08	1.58E+08	1.23E+08	1.39E+08	1.74E+07	1.97E+07	18.73	18.88	18.63



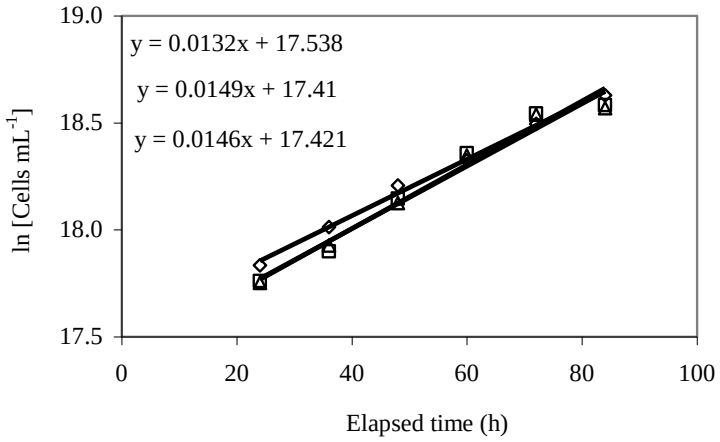
Specific growth rate (h^{-1})	
Trial 1	0.014
Trial 2	0.012
Trial 3	0.011
Average	0.012
STDEV	0.001
95% CI	0.001

Figure G.76. Specific growth rate calculations for Trial 1 (open circles), Trial 2 (open squares), and Trial 3 (open triangles).

1.0 x IC_{50} Lead Sulfate + Chloride

Table G.77. BC13 growth in medium containing 1.0 x IC_{50} lead sulfate and 50 mM sodium chloride.

	Cells mL^{-1}						ln (Cells mL^{-1})		
Elapsed Time (h)	Trial 1	Trial 2	Trial 3	Average	STDEV	95% CI	Trial 1	Trial 2	Trial 3
0	6.05E+07	6.00E+07	5.93E+07	5.99E+07	5.88E+05	6.65E+05	17.92	17.91	17.90
12	5.65E+07	5.44E+07	5.40E+07	5.50E+07	1.38E+06	1.56E+06	17.85	17.81	17.80
24	5.56E+07	5.17E+07	5.12E+07	5.28E+07	2.40E+06	2.72E+06	17.83	17.76	17.75
36	6.65E+07	5.93E+07	6.11E+07	6.23E+07	3.74E+06	4.24E+06	18.01	17.90	17.93
48	8.08E+07	7.60E+07	7.45E+07	7.71E+07	3.29E+06	3.73E+06	18.21	18.15	18.13
60	9.08E+07	9.39E+07	9.29E+07	9.25E+07	1.55E+06	1.76E+06	18.32	18.36	18.35
72	1.08E+08	1.13E+08	1.12E+08	1.11E+08	2.89E+06	3.27E+06	18.50	18.54	18.54
84	1.23E+08	1.18E+08	1.16E+08	1.19E+08	3.68E+06	4.16E+06	18.63	18.58	18.57
96	1.30E+08	1.29E+08	1.22E+08	1.27E+08	4.14E+06	4.68E+06	18.68	18.68	18.62
108	1.29E+08	1.17E+08	1.14E+08	1.20E+08	8.31E+06	9.41E+06	18.68	18.58	18.55
120	1.27E+08	1.25E+08	1.17E+08	1.23E+08	5.67E+06	6.41E+06	18.66	18.65	18.58

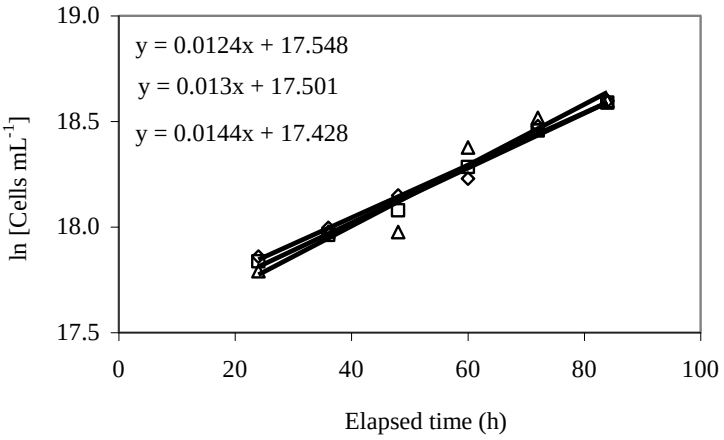


Specific growth rate (h^{-1})	
Trial 1	0.013
Trial 2	0.015
Trial 3	0.015
Average	0.014
STDEV	0.001
95% CI	0.001

Figure G.77. Specific growth rate calculations for Trial 1 (open circles), Trial 2 (open squares), and Trial 3 (open triangles).

Table G.78. BC13 growth in medium containing 1.0 x IC_{50} lead sulfate and 100 mM sodium chloride.

	Cells mL^{-1}						ln (Cells mL^{-1})		
Elapsed Time (h)	Trial 1	Trial 2	Trial 3	Average	STDEV	95% CI	Trial 1	Trial 2	Trial 3
0	6.46E+07	7.03E+07	7.33E+07	6.94E+07	4.46E+06	5.05E+06	17.98	18.07	18.11
12	5.87E+07	5.31E+07	4.95E+07	5.38E+07	4.63E+06	5.24E+06	17.89	17.79	17.72
24	5.71E+07	5.58E+07	5.33E+07	5.54E+07	1.95E+06	2.21E+06	17.86	17.84	17.79
36	6.54E+07	6.32E+07	6.42E+07	6.43E+07	1.10E+06	1.24E+06	18.00	17.96	17.98
48	7.62E+07	7.10E+07	6.41E+07	7.05E+07	6.07E+06	6.87E+06	18.15	18.08	17.98
60	8.26E+07	8.72E+07	9.57E+07	8.85E+07	6.63E+06	7.50E+06	18.23	18.28	18.38
72	1.06E+08	1.04E+08	1.10E+08	1.07E+08	3.24E+06	3.67E+06	18.48	18.46	18.52
84	1.19E+08	1.18E+08	1.19E+08	1.19E+08	5.84E+05	6.61E+05	18.60	18.59	18.60
96	1.35E+08	1.45E+08	1.40E+08	1.40E+08	4.97E+06	5.62E+06	18.72	18.79	18.76
108	1.36E+08	1.32E+08	1.28E+08	1.32E+08	4.23E+06	4.78E+06	18.73	18.70	18.67
120	1.33E+08	1.43E+08	1.37E+08	1.38E+08	4.92E+06	5.57E+06	18.70	18.78	18.74

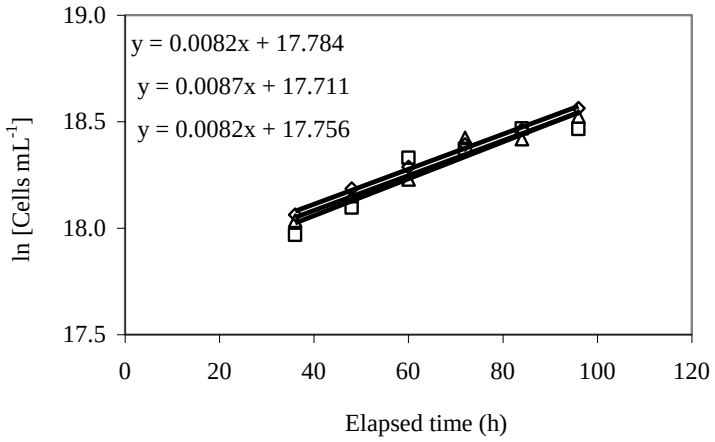


Specific growth rate (h^{-1})	
Trial 1	0.012
Trial 2	0.013
Trial 3	0.014
Average	0.013
STDEV	0.001
95% CI	0.001

Figure G.78. Specific growth rate calculations for Trial 1 (open circles), Trial 2 (open squares), and Trial 3 (open triangles).

Table G.79. BC13 growth in medium containing 1.0 x IC_{50} lead sulfate and 200 mM sodium chloride.

	Cells mL^{-1}						ln (Cells mL^{-1})		
Elapsed Time (h)	Trial 1	Trial 2	Trial 3	Average	STDEV	95% CI	Trial 1	Trial 2	Trial 3
0	5.36E+07	5.24E+07	5.32E+07	5.31E+07	5.83E+05	6.60E+05	17.80	17.77	17.79
12	6.55E+07	6.61E+07	7.05E+07	6.74E+07	2.76E+06	3.12E+06	18.00	18.01	18.07
24	6.73E+07	7.29E+07	7.71E+07	7.24E+07	4.93E+06	5.58E+06	18.02	18.10	18.16
36	6.99E+07	6.36E+07	6.80E+07	6.65E+07	3.23E+06	3.65E+06	18.06	17.97	18.04
48	7.90E+07	7.23E+07	7.63E+07	7.59E+07	3.35E+06	3.79E+06	18.18	18.10	18.15
60	8.75E+07	9.13E+07	8.25E+07	8.71E+07	4.41E+06	4.99E+06	18.29	18.33	18.23
72	9.73E+07	9.53E+07	1.00E+08	9.76E+07	2.51E+06	2.84E+06	18.39	18.37	18.42
84	1.04E+08	1.05E+08	9.97E+07	1.03E+08	2.81E+06	3.18E+06	18.46	18.47	18.42
96	1.15E+08	1.05E+08	1.11E+08	1.10E+08	5.44E+06	6.16E+06	18.56	18.46	18.52
108	1.30E+08	1.25E+08	1.15E+08	1.23E+08	7.99E+06	9.04E+06	18.69	18.64	18.56
120	1.29E+08	1.34E+08	1.37E+08	1.33E+08	3.81E+06	4.31E+06	18.68	18.71	18.73



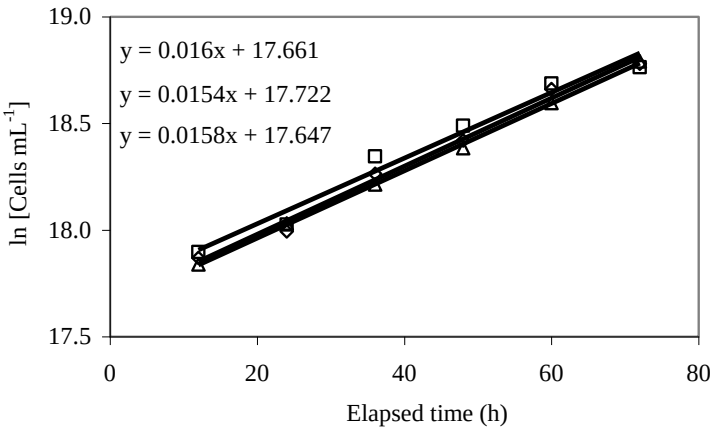
Specific growth rate (h^{-1})	
Trial 1	0.008
Trial 2	0.009
Trial 3	0.008
Average	0.008
STDEV	0.000
95% CI	0.000

Figure G.79. Specific growth rate calculations for Trial 1 (open circles), Trial 2 (open squares), and Trial 3 (open triangles).

0.5 x IC_{50} Zinc Sulfate + Chloride

Table G.80. BC13 growth in medium containing 0.5 x IC_{50} zinc sulfate and 50 mM sodium chloride.

	Cells mL^{-1}						ln (Cells mL^{-1})		
Elapsed Time (h)	Trial 1	Trial 2	Trial 3	Average	STDEV	95% CI	Trial 1	Trial 2	Trial 3
0	5.47E+07	5.13E+07	5.48E+07	5.36E+07	1.97E+06	2.22E+06	17.82	17.75	17.82
12	5.76E+07	5.92E+07	5.59E+07	5.76E+07	1.64E+06	1.86E+06	17.87	17.90	17.84
24	6.53E+07	6.74E+07	6.77E+07	6.68E+07	1.31E+06	1.49E+06	17.99	18.03	18.03
36	8.55E+07	9.27E+07	8.14E+07	8.65E+07	5.75E+06	6.50E+06	18.26	18.35	18.21
48	1.00E+08	1.07E+08	9.65E+07	1.01E+08	5.44E+06	6.16E+06	18.42	18.49	18.38
60	1.27E+08	1.31E+08	1.19E+08	1.26E+08	5.92E+06	6.70E+06	18.66	18.69	18.60
72	1.43E+08	1.41E+08	1.45E+08	1.43E+08	1.99E+06	2.25E+06	18.78	18.76	18.79
84	1.43E+08	1.54E+08	1.52E+08	1.50E+08	5.92E+06	6.70E+06	18.78	18.85	18.84
96	1.56E+08	1.58E+08	1.57E+08	1.57E+08	1.41E+06	1.59E+06	18.86	18.88	18.87
108	1.55E+08	1.76E+08	1.77E+08	1.69E+08	1.26E+07	1.43E+07	18.86	18.99	18.99
120	1.74E+08	1.78E+08	1.65E+08	1.73E+08	6.75E+06	7.64E+06	18.98	19.00	18.92



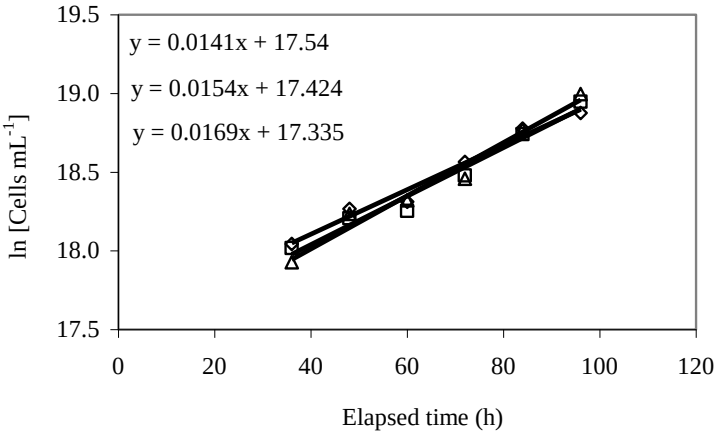
Specific growth rate (h^{-1})

Trial 1	0.016
Trial 2	0.015
Trial 3	0.016
Average	0.016
STDEV	0.000
95% CI	0.000

Figure G.80. Specific growth rate calculations for Trial 1 (open circles), Trial 2 (open squares), and Trial 3 (open triangles).

Table G.81. BC13 growth in medium containing 0.5 x IC_{50} zinc sulfate and 100 mM sodium chloride.

	Cells mL^{-1}						ln (Cells mL^{-1})		
Elapsed Time (h)	Trial 1	Trial 2	Trial 3	Average	STDEV	95% CI	Trial 1	Trial 2	Trial 3
0	5.78E+07	6.19E+07	6.01E+07	5.99E+07	2.04E+06	2.31E+06	17.87	17.94	17.91
12	5.86E+07	5.95E+07	5.90E+07	5.90E+07	4.42E+05	5.00E+05	17.89	17.90	17.89
24	6.18E+07	6.35E+07	6.50E+07	6.34E+07	1.58E+06	1.78E+06	17.94	17.97	17.99
36	6.86E+07	6.69E+07	6.10E+07	6.55E+07	3.99E+06	4.51E+06	18.04	18.02	17.93
48	8.57E+07	8.08E+07	8.30E+07	8.32E+07	2.50E+06	2.82E+06	18.27	18.21	18.23
60	8.97E+07	8.45E+07	9.05E+07	8.82E+07	3.22E+06	3.65E+06	18.31	18.25	18.32
72	1.15E+08	1.06E+08	1.04E+08	1.08E+08	6.22E+06	7.03E+06	18.56	18.48	18.46
84	1.43E+08	1.38E+08	1.42E+08	1.41E+08	2.71E+06	3.06E+06	18.78	18.74	18.77
96	1.58E+08	1.69E+08	1.78E+08	1.68E+08	1.02E+07	1.15E+07	18.88	18.95	19.00
108	1.55E+08	1.58E+08	1.54E+08	1.56E+08	2.06E+06	2.34E+06	18.86	18.88	18.85
120	1.52E+08	1.40E+08	1.44E+08	1.45E+08	5.84E+06	6.61E+06	18.84	18.76	18.78



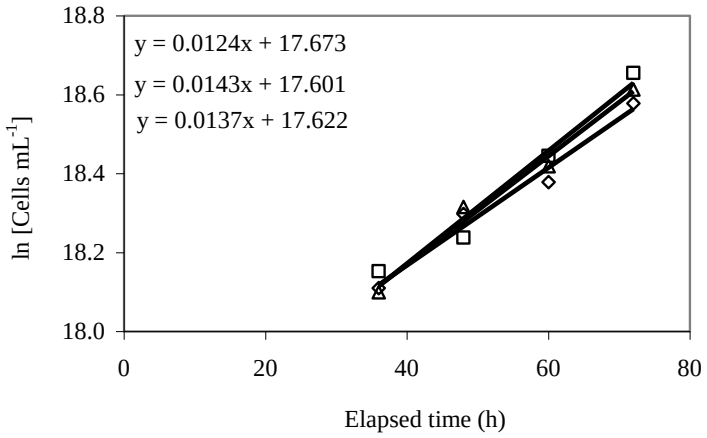
Specific growth rate (h^{-1})

Trial 1	0.014
Trial 2	0.015
Trial 3	0.017
Average	0.015
STDEV	0.001
95% CI	0.002

Figure G.81. Specific growth rate calculations for Trial 1 (open circles), Trial 2 (open squares), and Trial 3 (open triangles).

Table G.82. BC13 growth in medium containing 0.5 x IC_{50} zinc sulfate and 200 mM sodium chloride.

	Cells mL^{-1}						ln (Cells mL^{-1})		
Elapsed Time (h)	Trial 1	Trial 2	Trial 3	Average	STDEV	95% CI	Trial 1	Trial 2	Trial 3
0	5.41E+07	5.62E+07	5.22E+07	5.42E+07	2.03E+06	2.30E+06	17.81	17.84	17.77
12	5.60E+07	6.09E+07	6.35E+07	6.01E+07	3.77E+06	4.26E+06	17.84	17.93	17.97
24	6.72E+07	6.54E+07	6.63E+07	6.63E+07	9.04E+05	1.02E+06	18.02	18.00	18.01
36	7.33E+07	7.65E+07	7.25E+07	7.41E+07	2.08E+06	2.35E+06	18.11	18.15	18.10
48	8.84E+07	8.33E+07	9.00E+07	8.72E+07	3.53E+06	4.00E+06	18.30	18.24	18.32
60	9.58E+07	1.02E+08	9.98E+07	9.94E+07	3.33E+06	3.77E+06	18.38	18.44	18.42
72	1.17E+08	1.26E+08	1.21E+08	1.22E+08	4.70E+06	5.32E+06	18.58	18.66	18.61
84	1.38E+08	1.35E+08	1.31E+08	1.35E+08	3.59E+06	4.06E+06	18.74	18.72	18.69
96	1.42E+08	1.39E+08	1.28E+08	1.36E+08	7.18E+06	8.12E+06	18.77	18.75	18.67
108	1.46E+08	1.40E+08	1.27E+08	1.38E+08	9.51E+06	1.08E+07	18.80	18.75	18.66
120	1.33E+08	1.27E+08	1.31E+08	1.30E+08	2.82E+06	3.19E+06	18.70	18.66	18.69



Specific growth rate (h^{-1})

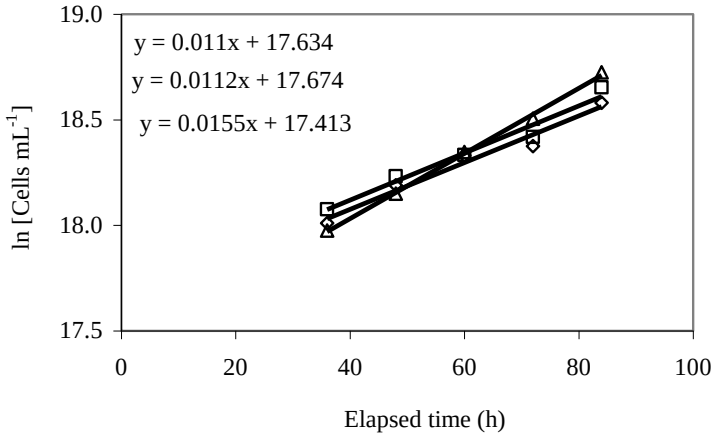
Trial 1	0.012
Trial 2	0.014
Trial 3	0.014
Average	0.013
STDEV	0.001
95% CI	0.001

Figure G.82. Specific growth rate calculations for Trial 1 (open circles), Trial 2 (open squares), and Trial 3 (open triangles).

1.0 x IC_{50} Zinc Sulfate + Chloride

Table G.83. BC13 growth in medium containing 1.0 x IC_{50} zinc sulfate and 50 mM sodium chloride.

	Cells mL^{-1}						ln (Cells mL^{-1})		
Elapsed Time (h)	Trial 1	Trial 2	Trial 3	Average	STDEV	95% CI	Trial 1	Trial 2	Trial 3
0	6.80E+07	6.23E+07	6.64E+07	6.56E+07	2.94E+06	3.33E+06	18.04	17.95	18.01
12	6.75E+07	6.34E+07	6.82E+07	6.64E+07	2.63E+06	2.97E+06	18.03	17.96	18.04
24	6.97E+07	7.02E+07	6.67E+07	6.88E+07	1.87E+06	2.12E+06	18.06	18.07	18.02
36	6.64E+07	7.09E+07	6.40E+07	6.71E+07	3.48E+06	3.94E+06	18.01	18.08	17.97
48	7.93E+07	8.29E+07	7.63E+07	7.95E+07	3.30E+06	3.73E+06	18.19	18.23	18.15
60	9.14E+07	9.17E+07	9.29E+07	9.20E+07	8.23E+05	9.31E+05	18.33	18.33	18.35
72	9.55E+07	9.98E+07	1.09E+08	1.01E+08	6.78E+06	7.67E+06	18.37	18.42	18.50
84	1.17E+08	1.26E+08	1.36E+08	1.26E+08	9.12E+06	1.03E+07	18.58	18.65	18.72
96	1.40E+08	1.32E+08	1.20E+08	1.31E+08	9.66E+06	1.09E+07	18.75	18.70	18.61
108	1.34E+08	1.23E+08	1.33E+08	1.30E+08	6.20E+06	7.02E+06	18.71	18.62	18.70
120	1.19E+08	1.27E+08	1.20E+08	1.22E+08	4.28E+06	4.84E+06	18.59	18.66	18.60

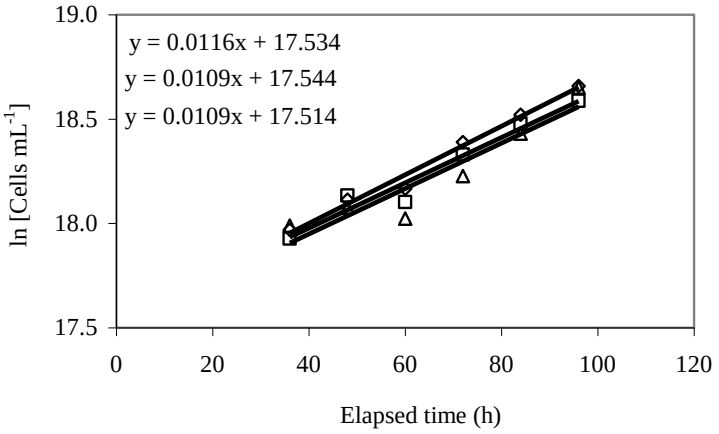


Specific growth rate (h^{-1})	
Trial 1	0.011
Trial 2	0.011
Trial 3	0.016
Average	0.013
STDEV	0.003
95% CI	0.003

Figure G.83. Specific growth rate calculations for Trial 1 (open circles), Trial 2 (open squares), and Trial 3 (open triangles).

Table G.84. BC13 growth in medium containing 1.0 x IC_{50} zinc sulfate and 100 mM sodium chloride.

	Cells mL^{-1}						ln (Cells mL^{-1})		
Elapsed Time (h)	Trial 1	Trial 2	Trial 3	Average	STDEV	95% CI	Trial 1	Trial 2	Trial 3
0	5.98E+07	5.63E+07	5.20E+07	5.60E+07	3.87E+06	4.38E+06	17.91	17.85	17.77
12	5.86E+07	5.87E+07	6.38E+07	6.04E+07	2.96E+06	3.35E+06	17.89	17.89	17.97
24	6.12E+07	5.76E+07	5.83E+07	5.90E+07	1.87E+06	2.11E+06	17.93	17.87	17.88
36	6.36E+07	6.11E+07	6.49E+07	6.32E+07	1.96E+06	2.22E+06	17.97	17.93	17.99
48	7.36E+07	7.50E+07	7.08E+07	7.31E+07	2.14E+06	2.42E+06	18.11	18.13	18.08
60	7.75E+07	7.27E+07	6.72E+07	7.25E+07	5.12E+06	5.79E+06	18.17	18.10	18.02
72	9.70E+07	9.14E+07	8.23E+07	9.02E+07	7.38E+06	8.35E+06	18.39	18.33	18.23
84	1.10E+08	1.06E+08	1.01E+08	1.06E+08	4.80E+06	5.43E+06	18.52	18.48	18.43
96	1.27E+08	1.18E+08	1.26E+08	1.24E+08	4.75E+06	5.38E+06	18.66	18.59	18.65
108	1.23E+08	1.21E+08	1.27E+08	1.23E+08	2.82E+06	3.20E+06	18.63	18.61	18.66
120	1.25E+08	1.36E+08	1.45E+08	1.35E+08	1.01E+07	1.14E+07	18.64	18.73	18.79



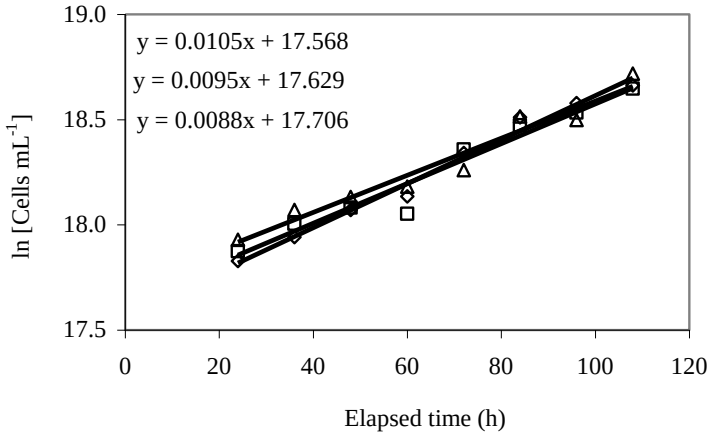
Specific growth rate (h^{-1})

Trial 1	0.012
Trial 2	0.011
Trial 3	0.011
Average	0.011
STDEV	0.000
95% CI	0.000

Figure G.84. Specific growth rate calculations for Trial 1 (open circles), Trial 2 (open squares), and Trial 3 (open triangles).

Table G.85. BC13 growth in medium containing 1.0 x IC_{50} zinc sulfate and 200 mM sodium chloride.

	Cells mL^{-1}						ln (Cells mL^{-1})		
Elapsed Time (h)	Trial 1	Trial 2	Trial 3	Average	STDEV	95% CI	Trial 1	Trial 2	Trial 3
0	5.58E+07	5.07E+07	5.53E+07	5.39E+07	2.78E+06	3.15E+06	17.84	17.74	17.83
12	5.68E+07	5.62E+07	5.49E+07	5.60E+07	9.71E+05	1.10E+06	17.86	17.84	17.82
24	5.53E+07	5.79E+07	6.11E+07	5.81E+07	2.94E+06	3.33E+06	17.83	17.87	17.93
36	6.20E+07	6.59E+07	7.04E+07	6.61E+07	4.23E+06	4.79E+06	17.94	18.00	18.07
48	7.05E+07	7.12E+07	7.50E+07	7.22E+07	2.41E+06	2.72E+06	18.07	18.08	18.13
60	7.51E+07	6.92E+07	7.87E+07	7.43E+07	4.80E+06	5.43E+06	18.13	18.05	18.18
72	9.23E+07	9.39E+07	8.52E+07	9.05E+07	4.64E+06	5.25E+06	18.34	18.36	18.26
84	1.09E+08	1.05E+08	1.10E+08	1.08E+08	2.52E+06	2.85E+06	18.51	18.47	18.52
96	1.17E+08	1.12E+08	1.08E+08	1.12E+08	4.50E+06	5.09E+06	18.58	18.53	18.50
108	1.27E+08	1.25E+08	1.35E+08	1.29E+08	4.86E+06	5.50E+06	18.66	18.65	18.72
120	1.22E+08	1.24E+08	1.15E+08	1.20E+08	4.96E+06	5.61E+06	18.62	18.64	18.56



Specific growth rate (h^{-1})

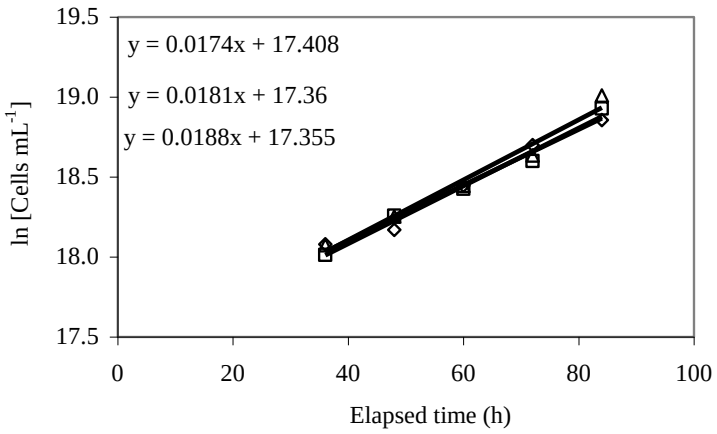
Trial 1	0.011
Trial 2	0.010
Trial 3	0.009
Average	0.010
STDEV	0.001
95% CI	0.001

Figure G.85. Specific growth rate calculations for Trial 1 (open circles), Trial 2 (open squares), and Trial 3 (open triangles).

0.5 x IC_{50} Copper Sulfate + Chloride

Table G.86. BC13 growth in medium containing 0.5 x IC_{50} copper sulfate and 50 mM sodium chloride.

	Cells mL^{-1}						ln (Cells mL^{-1})		
Elapsed Time (h)	Trial 1	Trial 2	Trial 3	Average	STDEV	95% CI	Trial 1	Trial 2	Trial 3
0	5.61E+07	5.83E+07	5.40E+07	5.62E+07	2.18E+06	2.47E+06	17.84	17.88	17.80
12	6.28E+07	6.60E+07	7.13E+07	6.67E+07	4.26E+06	4.82E+06	17.96	18.00	18.08
24	6.69E+07	7.35E+07	6.80E+07	6.95E+07	3.50E+06	3.96E+06	18.02	18.11	18.04
36	7.10E+07	6.65E+07	7.06E+07	6.94E+07	2.52E+06	2.85E+06	18.08	18.01	18.07
48	7.78E+07	8.50E+07	8.45E+07	8.24E+07	4.02E+06	4.55E+06	18.17	18.26	18.25
60	1.03E+08	1.01E+08	1.02E+08	1.02E+08	1.15E+06	1.30E+06	18.45	18.43	18.45
72	1.32E+08	1.20E+08	1.24E+08	1.25E+08	6.43E+06	7.27E+06	18.70	18.60	18.64
84	1.55E+08	1.66E+08	1.80E+08	1.67E+08	1.28E+07	1.45E+07	18.86	18.93	19.01
96	1.66E+08	1.71E+08	1.69E+08	1.69E+08	2.19E+06	2.48E+06	18.93	18.96	18.94
108	1.55E+08	1.41E+08	1.39E+08	1.45E+08	8.77E+06	9.93E+06	18.86	18.77	18.75
120	1.59E+08	1.68E+08	1.71E+08	1.66E+08	6.18E+06	6.99E+06	18.88	18.94	18.96



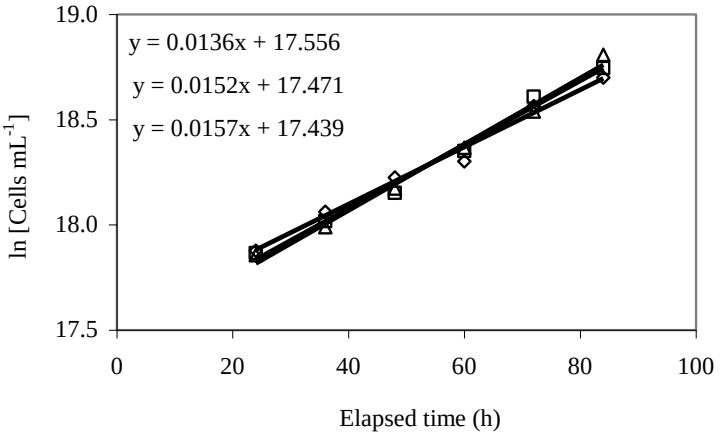
Specific growth rate (h^{-1})

Trial 1	0.017
Trial 2	0.018
Trial 3	0.019
Average	0.018
STDEV	0.001
95% CI	0.001

Figure G.86. Specific growth rate calculations for Trial 1 (open circles), Trial 2 (open squares), and Trial 3 (open triangles).

Table G.87. BC13 growth in medium containing 0.5 x IC_{50} copper sulfate and 100 mM sodium chloride.

	Cells mL^{-1}						ln (Cells mL^{-1})		
Elapsed Time (h)	Trial 1	Trial 2	Trial 3	Average	STDEV	95% CI	Trial 1	Trial 2	Trial 3
0	5.34E+07	5.20E+07	4.89E+07	5.14E+07	2.32E+06	2.63E+06	17.79	17.77	17.71
12	6.00E+07	5.67E+07	5.45E+07	5.70E+07	2.74E+06	3.10E+06	17.91	17.85	17.81
24	5.81E+07	5.74E+07	5.68E+07	5.74E+07	6.09E+05	6.89E+05	17.88	17.87	17.86
36	6.99E+07	6.68E+07	6.49E+07	6.72E+07	2.51E+06	2.84E+06	18.06	18.02	17.99
48	8.22E+07	7.64E+07	7.80E+07	7.89E+07	2.98E+06	3.37E+06	18.22	18.15	18.17
60	8.88E+07	9.32E+07	9.47E+07	9.22E+07	3.04E+06	3.44E+06	18.30	18.35	18.37
72	1.15E+08	1.21E+08	1.13E+08	1.16E+08	4.13E+06	4.67E+06	18.56	18.61	18.54
84	1.32E+08	1.38E+08	1.47E+08	1.39E+08	7.56E+06	8.55E+06	18.70	18.75	18.81
96	1.42E+08	1.32E+08	1.36E+08	1.36E+08	4.96E+06	5.61E+06	18.77	18.70	18.73
108	1.43E+08	1.47E+08	1.48E+08	1.46E+08	2.78E+06	3.14E+06	18.78	18.81	18.81
120	1.52E+08	1.53E+08	1.48E+08	1.51E+08	2.92E+06	3.31E+06	18.84	18.85	18.81



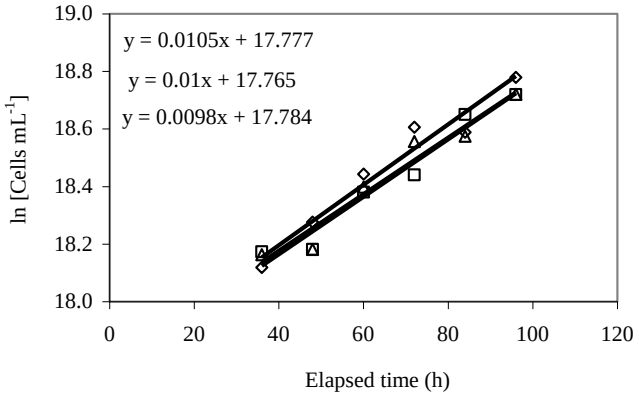
Specific growth rate (h^{-1})

Trial 1	0.014
Trial 2	0.015
Trial 3	0.016
Average	0.015
STDEV	0.001
95% CI	0.001

Figure G.87. Specific growth rate calculations for Trial 1 (open circles), Trial 2 (open squares), and Trial 3 (open triangles).

Table G.88. BC13 growth in medium containing 0.5 x IC_{50} copper sulfate and 200 mM sodium chloride.

	Cells mL^{-1}						ln (Cells mL^{-1})		
Elapsed Time (h)	Trial 1	Trial 2	Trial 3	Average	STDEV	95% CI	Trial 1	Trial 2	Trial 3
0	5.92E+07	5.75E+07	5.66E+07	5.78E+07	1.34E+06	1.52E+06	17.90	17.87	17.85
12	5.79E+07	6.15E+07	5.71E+07	5.89E+07	2.36E+06	2.67E+06	17.87	17.94	17.86
24	6.92E+07	6.59E+07	6.86E+07	6.79E+07	1.75E+06	1.99E+06	18.05	18.00	18.04
36	7.39E+07	7.81E+07	7.73E+07	7.64E+07	2.21E+06	2.50E+06	18.12	18.17	18.16
48	8.66E+07	7.87E+07	7.87E+07	8.13E+07	4.53E+06	5.12E+06	18.28	18.18	18.18
60	1.02E+08	9.60E+07	9.77E+07	9.87E+07	3.20E+06	3.62E+06	18.44	18.38	18.40
72	1.20E+08	1.02E+08	1.15E+08	1.12E+08	9.40E+06	1.06E+07	18.61	18.44	18.56
84	1.18E+08	1.26E+08	1.17E+08	1.20E+08	4.85E+06	5.48E+06	18.59	18.65	18.57
96	1.43E+08	1.35E+08	1.35E+08	1.38E+08	4.76E+06	5.39E+06	18.78	18.72	18.72
108	1.39E+08	1.32E+08	1.36E+08	1.36E+08	3.64E+06	4.11E+06	18.75	18.70	18.73
120	1.48E+08	1.33E+08	1.22E+08	1.34E+08	1.30E+07	1.47E+07	18.81	18.71	18.62



Specific growth rate (h^{-1})

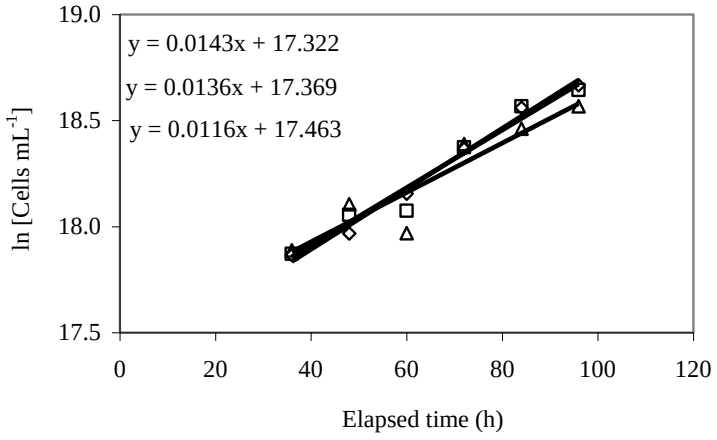
Trial 1	0.011
Trial 2	0.010
Trial 3	0.010
Average	0.010
STDEV	0.000
95% CI	0.000

Figure G.88. Specific growth rate calculations for Trial 1 (open circles), Trial 2 (open squares), and Trial 3 (open triangles).

1.0 x IC_{50} Copper Sulfate + Chloride

Table G.89. BC13 growth in medium containing 1.0 x IC_{50} copper sulfate and 50 mM sodium chloride.

	Cells mL^{-1}						ln (Cells mL^{-1})		
Elapsed Time (h)	Trial 1	Trial 2	Trial 3	Average	STDEV	95% CI	Trial 1	Trial 2	Trial 3
0	6.06E+07	5.73E+07	5.46E+07	5.75E+07	3.00E+06	3.40E+06	17.92	17.86	17.82
12	5.71E+07	6.07E+07	6.33E+07	6.04E+07	3.10E+06	3.50E+06	17.86	17.92	17.96
24	5.53E+07	5.66E+07	5.62E+07	5.60E+07	6.18E+05	6.99E+05	17.83	17.85	17.84
36	5.74E+07	5.78E+07	5.87E+07	5.80E+07	6.89E+05	7.80E+05	17.87	17.87	17.89
48	6.36E+07	6.93E+07	7.30E+07	6.86E+07	4.74E+06	5.37E+06	17.97	18.05	18.11
60	7.67E+07	7.07E+07	6.37E+07	7.04E+07	6.53E+06	7.39E+06	18.16	18.07	17.97
72	9.47E+07	9.54E+07	9.69E+07	9.57E+07	1.15E+06	1.30E+06	18.37	18.37	18.39
84	1.15E+08	1.16E+08	1.04E+08	1.12E+08	6.41E+06	7.25E+06	18.56	18.57	18.46
96	1.28E+08	1.25E+08	1.16E+08	1.23E+08	6.32E+06	7.15E+06	18.67	18.64	18.57
108	1.21E+08	1.13E+08	1.19E+08	1.18E+08	4.10E+06	4.64E+06	18.61	18.54	18.60
120	1.21E+08	1.17E+08	1.24E+08	1.21E+08	3.66E+06	4.14E+06	18.61	18.58	18.64

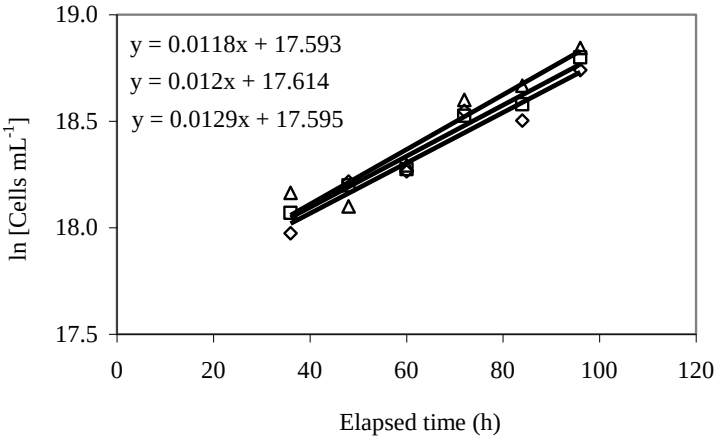


Specific growth rate (h^{-1})	
Trial 1	0.014
Trial 2	0.014
Trial 3	0.012
Average	0.013
STDEV	0.001
95% CI	0.002

Figure G.89. Specific growth rate calculations for Trial 1 (open circles), Trial 2 (open squares), and Trial 3 (open triangles).

Table G.90. BC13 growth in medium containing 1.0 x IC_{50} copper sulfate and 100 mM sodium chloride.

	Cells mL^{-1}						ln (Cells mL^{-1})		
Elapsed Time (h)	Trial 1	Trial 2	Trial 3	Average	STDEV	95% CI	Trial 1	Trial 2	Trial 3
0	5.85E+07	5.31E+07	5.76E+07	5.64E+07	2.88E+06	3.26E+06	17.88	17.79	17.87
12	6.05E+07	6.01E+07	5.49E+07	5.85E+07	3.10E+06	3.50E+06	17.92	17.91	17.82
24	6.20E+07	6.79E+07	7.01E+07	6.67E+07	4.18E+06	4.73E+06	17.94	18.03	18.07
36	6.40E+07	7.04E+07	7.73E+07	7.05E+07	6.65E+06	7.53E+06	17.97	18.07	18.16
48	8.15E+07	8.00E+07	7.26E+07	7.80E+07	4.76E+06	5.38E+06	18.22	18.20	18.10
60	8.56E+07	8.64E+07	8.79E+07	8.66E+07	1.19E+06	1.35E+06	18.27	18.27	18.29
72	1.14E+08	1.11E+08	1.20E+08	1.15E+08	4.43E+06	5.02E+06	18.55	18.52	18.60
84	1.09E+08	1.17E+08	1.28E+08	1.18E+08	9.63E+06	1.09E+07	18.50	18.58	18.67
96	1.38E+08	1.46E+08	1.53E+08	1.45E+08	7.48E+06	8.46E+06	18.74	18.80	18.84
108	1.30E+08	1.19E+08	1.18E+08	1.23E+08	6.30E+06	7.12E+06	18.68	18.60	18.59
120	1.35E+08	1.23E+08	1.15E+08	1.24E+08	9.84E+06	1.11E+07	18.72	18.63	18.56

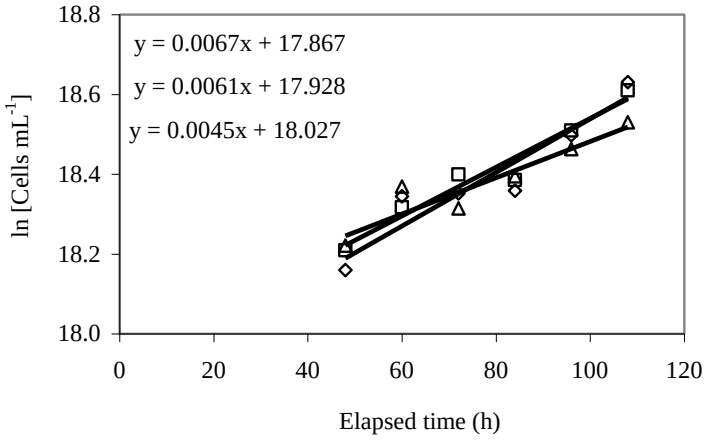


Specific growth rate (h^{-1})	
Trial 1	0.012
Trial 2	0.012
Trial 3	0.013
Average	0.012
STDEV	0.001
95% CI	0.001

Figure G.90. Specific growth rate calculations for Trial 1 (open circles), Trial 2 (open squares), and Trial 3 (open triangles).

Table G.91. BC13 growth in medium containing 1.0 x IC_{50} copper sulfate and 200 mM sodium chloride.

	Cells mL^{-1}						ln (Cells mL^{-1})		
Elapsed Time (h)	Trial 1	Trial 2	Trial 3	Average	STDEV	95% CI	Trial 1	Trial 2	Trial 3
0	6.95E+07	7.47E+07	7.00E+07	7.14E+07	2.84E+06	3.22E+06	18.06	18.13	18.06
12	6.76E+07	7.40E+07	7.43E+07	7.20E+07	3.82E+06	4.32E+06	18.03	18.12	18.12
24	7.10E+07	7.41E+07	6.68E+07	7.06E+07	3.64E+06	4.12E+06	18.08	18.12	18.02
36	7.47E+07	7.66E+07	8.26E+07	7.80E+07	4.15E+06	4.69E+06	18.13	18.15	18.23
48	7.70E+07	8.09E+07	8.19E+07	8.00E+07	2.57E+06	2.91E+06	18.16	18.21	18.22
60	9.27E+07	9.02E+07	9.49E+07	9.26E+07	2.38E+06	2.69E+06	18.34	18.32	18.37
72	9.34E+07	9.79E+07	8.99E+07	9.37E+07	4.00E+06	4.53E+06	18.35	18.40	18.31
84	9.40E+07	9.65E+07	9.74E+07	9.60E+07	1.77E+06	2.01E+06	18.36	18.38	18.39
96	1.08E+08	1.09E+08	1.04E+08	1.07E+08	2.59E+06	2.93E+06	18.50	18.51	18.46
108	1.23E+08	1.21E+08	1.12E+08	1.19E+08	6.22E+06	7.04E+06	18.63	18.61	18.53
120	1.28E+08	1.16E+08	1.14E+08	1.19E+08	7.29E+06	8.25E+06	18.66	18.57	18.55



Specific growth rate (h^{-1})

Trial 1	0.007
Trial 2	0.006
Trial 3	0.005
Average	0.006
STDEV	0.001
95% CI	0.001

Figure G.91. Specific growth rate calculations for Trial 1 (open circles), Trial 2 (open squares), and Trial 3 (open triangles).

Prediction of Heavy Metal Speciation

MINTEQA2 (version 2.53) was used to predict the speciation of lead, zinc, and copper under the various concentrations and conditions tested. The following compositions were predicted based on a pH of 2.50 and a temperature of 45°C.

Individual Heavy Metal Studies using Sulfate Salts

Table G.92. Speciation of lead at concentrations tested in single metal toxicity studies.

	Aqueous concentration (mM)								
Total	0.019	0.021	0.021	0.021	0.022	0.027	0.078	0.180	0.380
Pb^{+2}	1.90E-02	2.05E-02	2.05E-02	2.05E-02	2.05E-02	2.05E-02	2.05E-02	2.05E-02	2.05E-02
$PbCl^{+}$	2.12E-07	8.39E-07	1.89E-06	3.36E-06	2.10E-05	8.39E-05	7.55E-04	2.10E-03	4.72E-03
PbSO4 (aq)	1.36E-05	5.46E-05	1.23E-04	2.18E-04	1.37E-03	5.46E-03	4.92E-02	1.37E-01	3.07E-01
$Pb(SO_4)_2^{-2}$	2.08E-06	8.45E-06	1.90E-05	3.38E-05	2.11E-04	8.45E-04	7.60E-03	2.11E-02	4.75E-02
$PbNO_3^{+}$	5.50E-09	2.10E-08	4.73E-08	8.40E-08	5.25E-07	2.10E-06	1.89E-05	5.25E-05	1.18E-04
$PbH_2PO_4^{+}$	3.20E-08	1.27E-07	2.86E-07	5.08E-07	3.18E-06	1.27E-05	1.14E-04	3.18E-04	7.14E-04

Table G.93. Speciation of zinc at concentrations tested in single metal toxicity studies.

	Aqueous concentration (mM)							
Total	1	3	5	10	20	35	50	75
Zn^{+2}	4.39E-01	1.32E+00	2.19E+00	4.37E+00	8.69E+00	1.51E+01	2.13E+01	3.37E+01
$ZnCl^{+}$	7.20E-04	2.16E-03	3.55E-03	6.90E-03	1.32E-02	2.21E-02	3.00E-02	4.80E-02
$ZnSO_4$ (aq)	3.98E-01	1.20E+00	2.00E+00	4.02E+00	8.07E+00	1.41E+01	2.02E+01	2.96E+01
$Zn(SO4)_2^{-2}$	9.37E-02	2.88E-01	4.91E-01	1.03E+00	2.26E+00	4.38E+00	6.81E+00	9.03E+00
ZnS_4O_6 (aq)	6.83E-02	1.96E-01	3.14E-01	5.70E-01	9.66E-01	1.38E+00	1.68E+00	2.64E+00

Table G.94. Speciation of copper at concentrations tested in single metal toxicity studies.

	Aqueous concentration (mM)									
Total	1	3	5	10	20	50	100	150	200	250
Cu^{+2}	0.53	1.58	2.62	5.18	10.16	24.02	44.17	61.37	76.28	89.37
$CuCl^{+}$	0.00	0.00	0.00	0.01	0.01	0.09	0.04	0.06	0.07	0.08
$CuSO_4$ (aq)	0.47	1.42	2.37	4.80	9.80	25.86	55.58	88.24	123.18	159.93
$CuHSO_4^{+}$	0.00	0.00	0.01	0.02	0.03	0.16	0.20	0.32	0.45	0.59

Multivariate Statistical Analysis of the Effect of Heavy Metal Speciation on Observed Specific Growth Rates of BC13

Lead

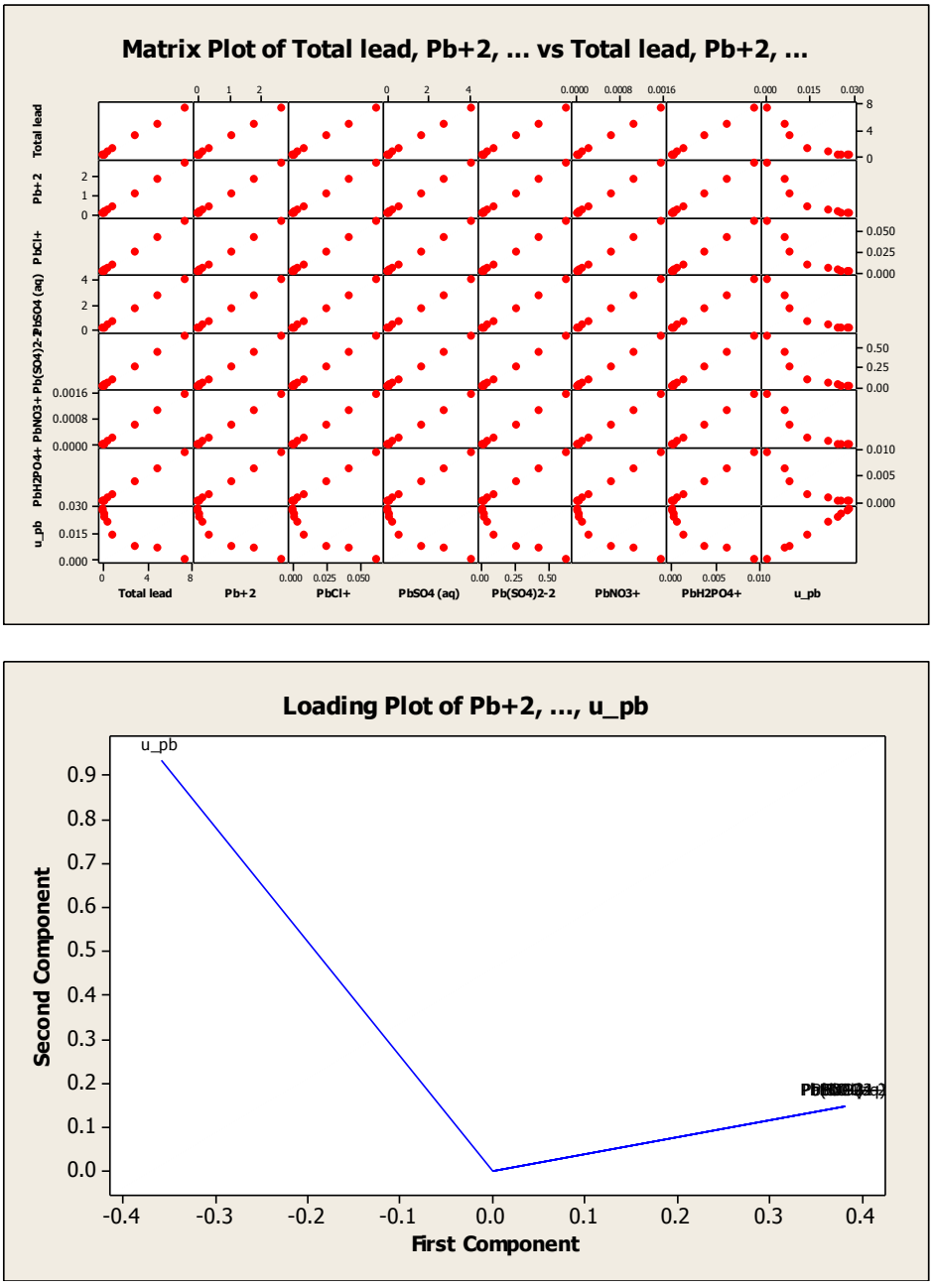


Figure G.92. Matrix plot (top) and primary component analysis of the effects of lead speciation on the observed specific growth rate of BC13.

Zinc

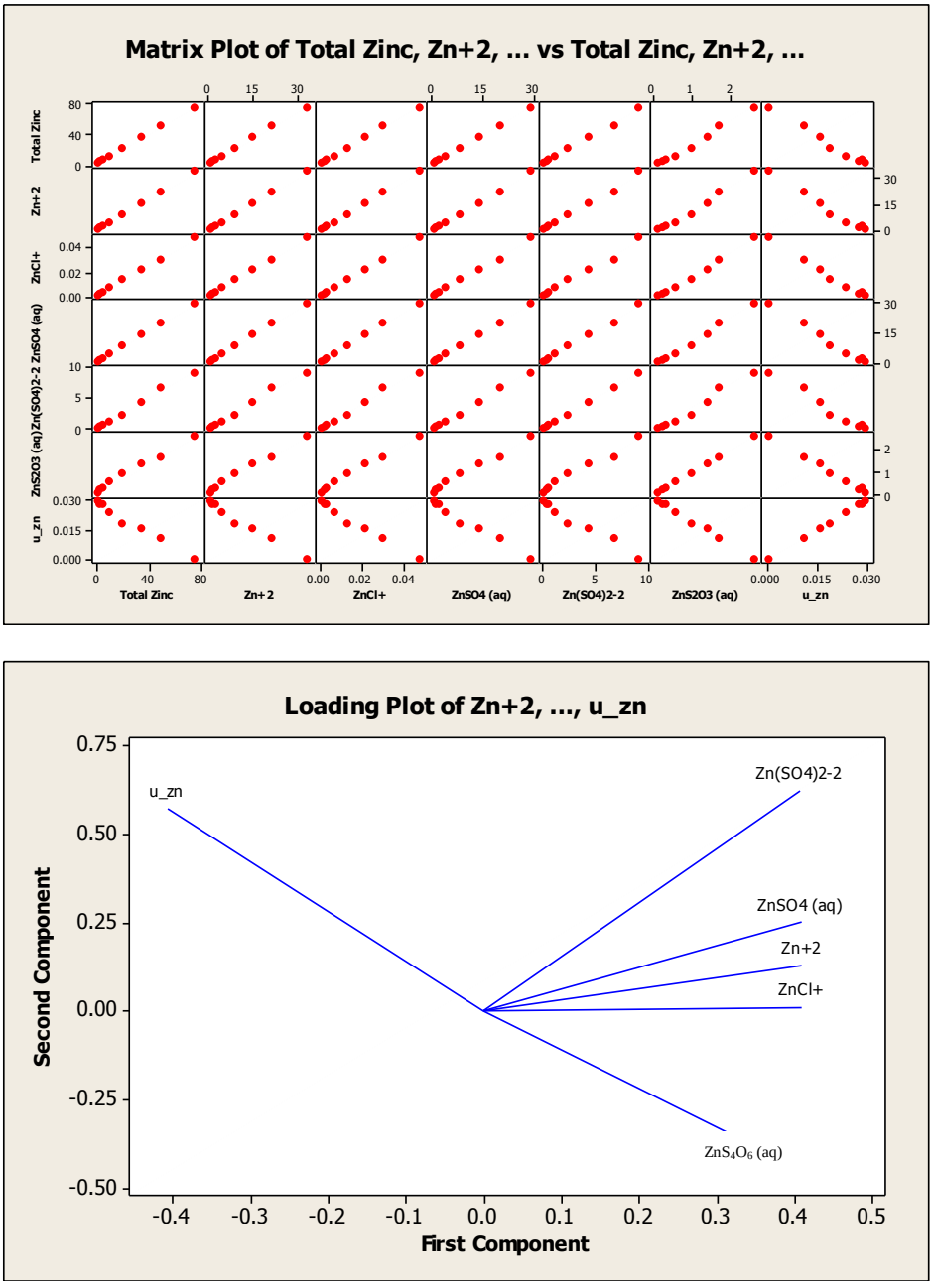


Figure G.93. Matrix plot (top) and primary component analysis of the effects of zinc speciation on the observed specific growth rate of BC13.

Copper

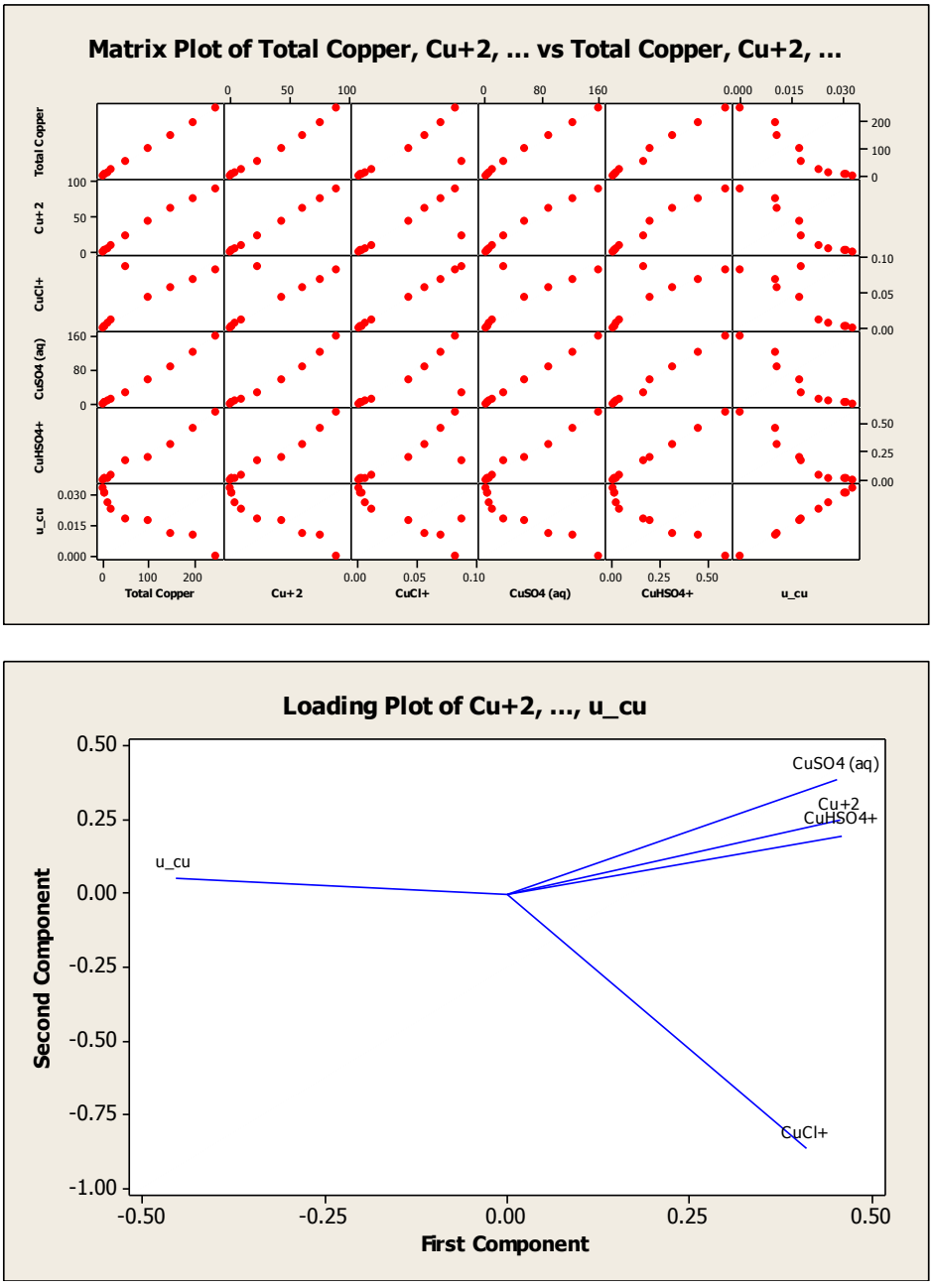


Figure G.94. Matrix plot (top) and primary component analysis of the effects of copper speciation on the observed specific growth rate of BC13.

Combined Heavy Metal Studies using Sulfate Salts

Table G.95. Percent composition of heavy metal species in binary mixtures of lead, zinc, and copper using metal concentrations equal to previously calculated IC_{50}s.

	Pb/Zn	Pb/Cu	Zn/Cu
Pb^{+2}	29.21	33.74	-
$PbCl^{+}$	0.53	0.69	-
$PbSO_4$ (aq)	53.43	53.91	-
$Pb(SO_4)_2^{-2}$	16.74	11.54	-
$PbNO^{3+}$	0.01	0.02	-
PbH_2PO^{4+}	0.08	0.11	-
Zn^{+2}	34.04	-	46.52
$ZnCl^{+}$	0.04	-	0.07
$ZnSO_4$ (aq)	41.19	-	38.86
$Zn(SO_4)_2^{-2}$	21.83	-	10.27
ZnS_4O_6 (aq)	2.90	-	4.29
Cu^{+2}	-	42.45	48.27
$CuCl^{+}$	-	0.04	0.05
$CuSO_4$ (aq)	-	57.30	51.49
$CuHSO^{4+}$	-	0.21	0.18

Heavy Metal Speciation in the Presence of Ferrous Iron

Table G.96. Percent composition of heavy metals when present at their previously calculated IC_{50}s with 100 mM ferrous sulfate.

Pb^{+2}	30.21	Zn^{+2}	40.29	Cu^{+2}	40.97
$PbCl^{+}$	0.60	$ZnCl^{+}$	0.05	$CuCl^{+}$	0.04
$PbSO_4$ (aq)	54.65	$ZnSO_4$ (aq)	40.33	$CuSO_4$ (aq)	58.77
$Pb(SO_4)_2^{-2}$	14.51	$Zn(SO_4)_2^{-2}$	15.99	$CuHSO^{4+}$	0.21
$PbNO^{3+}$	0.02	ZnS_4O_6 (aq)	3.34		
PbH_2PO^{4+}	0.02				

Table G.97. Percent composition of 100 mM ferrous sulfate when present with the previously calculated IC_{50}s of lead, zinc, or copper.

Lead	Zinc	Copper
78.24	68.41	56.39
0.02	0.02	0.01
21.47	31.31	43.34
0.27	0.26	0.26

Heavy Metal Speciation when Added as Chloride Salts

Table G.98. Percent composition of lead, zinc, and copper when added as chloride salts to the previously calculated IC_{50}s of corresponding sulfate salts.

Pb^{+2}	36.35	Zn^{+2}	60.71	Cu^{+2}	71.37
$PbCl^{+}$	1.43	$ZnCl^{+}$	4.27	$CuCl^{+}$	9.12
PbSO4 (aq)	53.96	$ZnSO_4$ (aq)	0.03	$CuSO_4$ (aq)	0.57
$Pb(SO_4)_2^{-2}$	8.10	$Zn(SO4)_2^{-2}$	0.33	$CuHSO_4^{+}$	18.85
$PbNO_3^{+}$	0.02	ZnS_4O_6 (aq)	26.00		
$PbH_2PO_4^{+}$	0.13				

APPENDIX H

CHAPTER FIVE RAW DATA

Effects of pH on Heavy-Metal Sorption to BC13

Lead

Table H.1. Sorption, Q_t, of lead to viable BC13 cells with time at pH 1.5 and 45ºC. Initial concentrations were the highest tested for lead, 0.241 mM.

	Q_t (mmol g^{-1})					
Elapsed Time (min)	Trial 1	Trial 2	Trial 3	Average	STDEV	95% CI
0	0.000	0.000	0.000	0.000	0.000	0.000
1	0.057	0.056	0.053	0.056	0.002	0.003
5	0.065	0.064	0.065	0.065	0.000	0.000
15	0.065	0.065	0.063	0.064	0.002	0.002
30	0.068	0.067	0.067	0.067	0.001	0.001
60	0.072	0.073	0.071	0.072	0.001	0.001

Table H.2. Equilibrium sorption, Q_e, and solution, C_e, concentrations of lead in the presence of viable BC13 cells at pH 1.5 and 45ºC, with varying concentrations, C_o.

	Q_e (mmol g^{-1})			C_e (mmol L^{-1})		
C_o (mmol L^{-1})	Trial 1	Trial 2	Trial 3	Trial 1	Trial 2	Trial 3
0.029	0.027	0.026	0.027	0.026	0.026	0.026
0.039	0.034	0.034	0.035	0.035	0.035	0.035
0.048	0.039	0.039	0.038	0.044	0.044	0.045
0.072	0.053	0.053	0.052	0.067	0.067	0.067
0.121	0.061	0.058	0.061	0.115	0.115	0.115
0.241	0.072	0.073	0.071	0.234	0.234	0.234

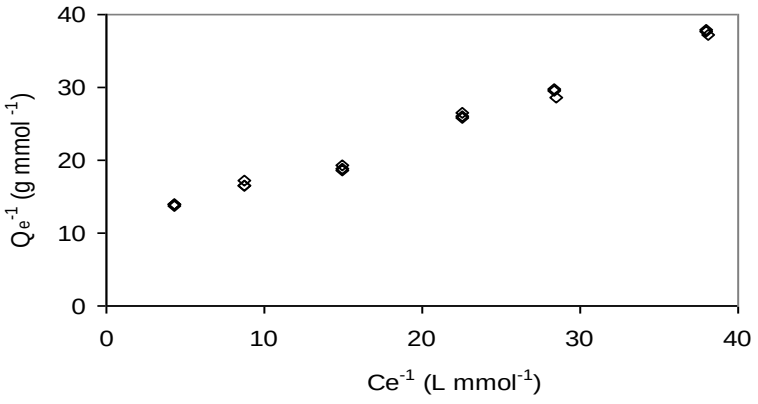


Figure H.1. Lineweaver-Burk plot relating equilibrium lead concentrations.

Table H.3. Sorption, Q_t, of lead to viable BC13 cells with time at pH 2.5 and 45ºC. Initial concentrations were the highest tested for lead, 0.241 mM.

	Q_t (mmol g^{-1})					
Elapsed Time (min)	Trial 1	Trial 2	Trial 3	Average	STDEV	95% CI
0	0.000	0.000	0.000	0.000	0.000	0.000
1	0.122	0.134	0.126	0.127	0.006	0.007
5	0.157	0.172	0.170	0.166	0.008	0.009
15	0.191	0.198	0.188	0.192	0.005	0.006
30	0.199	0.210	0.203	0.204	0.006	0.006
60	0.208	0.212	0.203	0.208	0.004	0.005

Table H.4. Equilibrium sorption, Q_e, and solution, C_e, concentrations of lead in the presence of viable BC13 cells at pH 2.5 and 45ºC, with varying concentrations, C_o.

	Q_e (mmol g^{-1})			C_e (mmol L^{-1})		
C_o (mmol L^{-1})	Trial 1	Trial 2	Trial 3	Trial 1	Trial 2	Trial 3
0.029	0.102	0.099	0.100	0.019	0.019	0.019
0.039	0.128	0.127	0.130	0.026	0.026	0.026
0.048	0.148	0.157	0.153	0.034	0.033	0.033
0.072	0.166	0.173	0.169	0.056	0.055	0.056
0.121	0.186	0.186	0.188	0.102	0.102	0.102
0.241	0.208	0.212	0.203	0.220	0.220	0.221

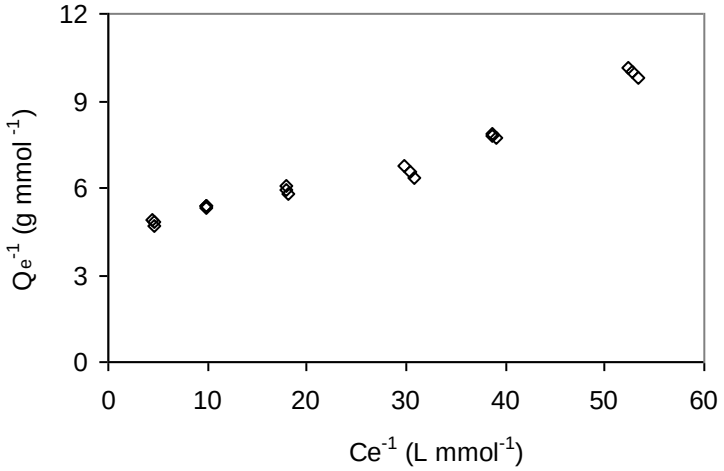


Figure H.2. Lineweaver-Burk plot relating equilibrium lead concentrations.

Table H.5. Sorption, Q_t, of lead to viable BC13 cells with time at pH 4.0 and 45ºC. Initial concentrations were the highest tested for lead, 0.241 mM.

	Q_t (mmol g^{-1})					
Elapsed Time (min)	Trial 1	Trial 2	Trial 3	Average	STDEV	95% CI
0	0.000	0.000	0.000	0.000	0.000	0.000
1	0.166	0.171	0.165	0.167	0.004	0.004
5	0.192	0.194	0.191	0.192	0.002	0.002
15	0.200	0.210	0.206	0.205	0.005	0.006
30	0.210	0.225	0.212	0.216	0.008	0.009
60	0.221	0.225	0.204	0.217	0.011	0.012

Table H.6. Equilibrium sorption, Q_e, and solution, C_e, concentrations of lead in the presence of viable BC13 cells at pH 4.0 and 45ºC, with varying concentrations, C_o.

	Q_e (mmol g^{-1})			C_e (mmol L^{-1})		
C_o (mmol L^{-1})	Trial 1	Trial 2	Trial 3	Trial 1	Trial 2	Trial 3
0.029	0.123	0.124	0.117	0.017	0.017	0.017
0.039	0.151	0.146	0.139	0.023	0.024	0.025
0.048	0.170	0.164	0.172	0.031	0.032	0.031
0.072	0.204	0.198	0.204	0.052	0.053	0.052
0.121	0.209	0.214	0.209	0.100	0.099	0.100
0.241	0.221	0.225	0.214	0.219	0.219	0.220

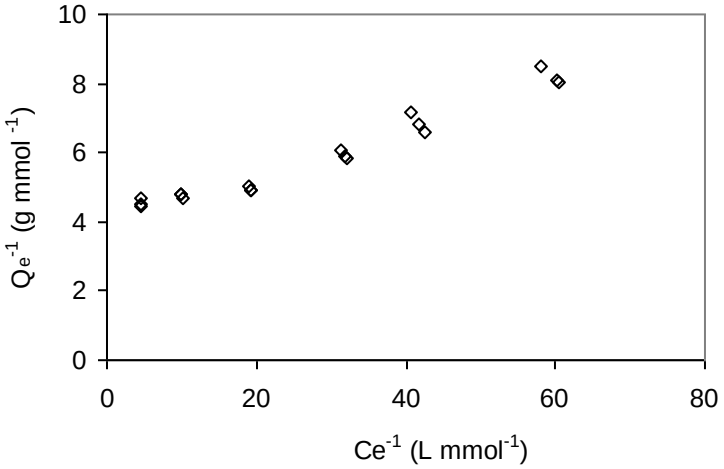


Figure H.3. Lineweaver-Burk plot relating equilibrium lead concentrations.

Table H.7. Sorption, Q_t, of lead to viable BC13 cells with time at pH 5.5 and 45ºC. Initial concentrations were the highest tested for lead, 0.241 mM.

	Q_t (mmol g^{-1})					
Elapsed Time (min)	Trial 1	Trial 2	Trial 3	Average	STDEV	95% CI
0	0.000	0.000	0.000	0.000	0.000	0.000
1	0.262	0.270	0.259	0.264	0.006	0.007
5	0.287	0.307	0.302	0.299	0.010	0.012
15	0.291	0.307	0.299	0.299	0.008	0.009
30	0.296	0.300	0.283	0.293	0.009	0.010
60	0.305	0.325	0.323	0.317	0.011	0.013

Table H.8. Equilibrium sorption, Q_e, and solution, C_e, concentrations of lead in the presence of viable BC13 cells at pH 5.5 and 45ºC, with varying concentrations, C_o.

	Q_e (mmol g^{-1})			C_e (mmol L^{-1})		
C_o (mmol L^{-1})	Trial 1	Trial 2	Trial 3	Trial 1	Trial 2	Trial 3
0.029	0.150	0.149	0.154	0.014	0.014	0.014
0.039	0.178	0.172	0.174	0.021	0.021	0.021
0.048	0.204	0.199	0.207	0.028	0.028	0.028
0.072	0.238	0.236	0.238	0.049	0.049	0.049
0.121	0.277	0.273	0.276	0.093	0.093	0.093
0.241	0.305	0.325	0.323	0.211	0.209	0.209

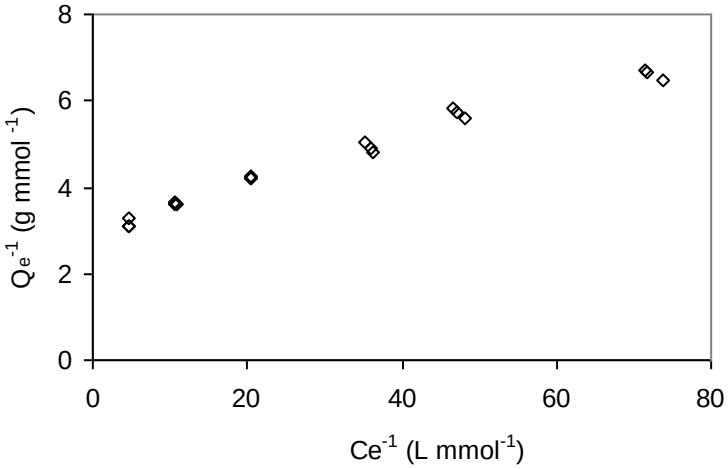


Figure H.4. Lineweaver-Burk plot relating equilibrium lead concentrations.

Table H.9. Sorption, Q_t, of lead to viable BC13 cells with time at pH 7.0 and 45ºC. Initial concentrations were the highest tested for lead, 0.241 mM.

	Q_t (mmol g^{-1})					
Elapsed Time (min)	Trial 1	Trial 2	Trial 3	Average	STDEV	95% CI
0	0.000	0.000	0.000	0.000	0.000	0.000
1	0.258	0.274	0.270	0.267	0.008	0.010
5	0.296	0.305	0.295	0.299	0.005	0.006
15	0.303	0.322	0.305	0.310	0.011	0.012
30	0.306	0.334	0.312	0.317	0.014	0.016
60	0.315	0.330	0.317	0.320	0.008	0.009

Table H.10. Equilibrium sorption, Q_e, and solution, C_e, concentrations of lead in the presence of viable BC13 cells at pH 7.0 and 45ºC, with varying concentrations, C_o.

	Q_e (mmol g^{-1})			C_e (mmol L^{-1})		
C_o (mmol L^{-1})	Trial 1	Trial 2	Trial 3	Trial 1	Trial 2	Trial 3
0.029	0.143	0.145	0.149	0.015	0.014	0.014
0.039	0.181	0.185	0.182	0.021	0.020	0.020
0.048	0.207	0.208	0.206	0.028	0.027	0.028
0.072	0.235	0.229	0.232	0.049	0.049	0.049
0.121	0.284	0.282	0.285	0.092	0.092	0.092
0.241	0.315	0.330	0.317	0.210	0.208	0.210

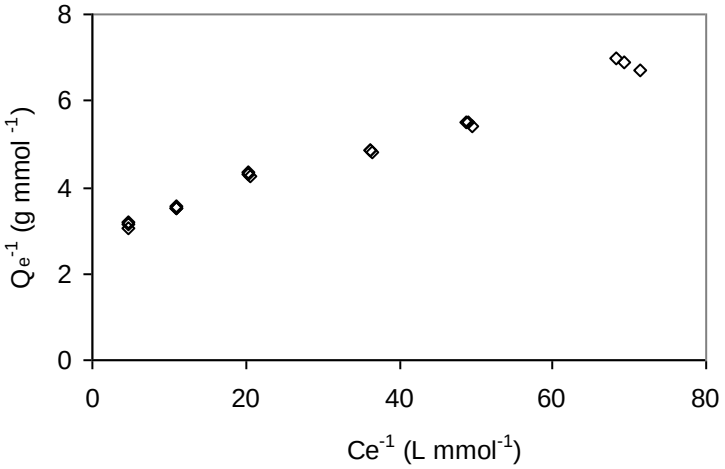


Figure H.5. Lineweaver-Burk plot relating equilibrium lead concentrations.

Table H.11. Sorption, Q_t, of lead to dehydrated BC13 cells with time at pH 1.5 and 45ºC. Initial concentrations were the highest tested for lead, 0.241 mM.

	Q_t (mmol g^{-1})					
Elapsed Time (min)	Trial 1	Trial 2	Trial 3	Average	STDEV	95% CI
0	0.000	0.000	0.000	0.000	0.000	0.000
1	0.026	0.027	0.027	5.581	0.001	0.001
5	0.037	0.039	0.035	7.667	0.002	0.002
15	0.038	0.041	0.039	8.123	0.002	0.002
30	0.039	0.043	0.042	8.588	0.002	0.002
60	0.040	0.042	0.040	8.248	0.001	0.002

Table H.12. Equilibrium sorption, Q_e, and solution, C_e, concentrations of lead in the presence of dehydrated BC13 cells at pH 1.5 and 45ºC, with varying concentrations, C_o.

	Q_e (mmol g^{-1})			C_e (mmol L^{-1})		
C_o (mmol L^{-1})	Trial 1	Trial 2	Trial 3	Trial 1	Trial 2	Trial 3
0.029	0.019	0.018	0.017	0.027	0.027	0.027
0.039	0.023	0.023	0.022	0.036	0.036	0.036
0.048	0.027	0.027	0.026	0.046	0.046	0.046
0.072	0.032	0.031	0.031	0.069	0.069	0.069
0.121	0.036	0.035	0.035	0.117	0.117	0.117
0.241	0.040	0.042	0.040	0.237	0.237	0.237

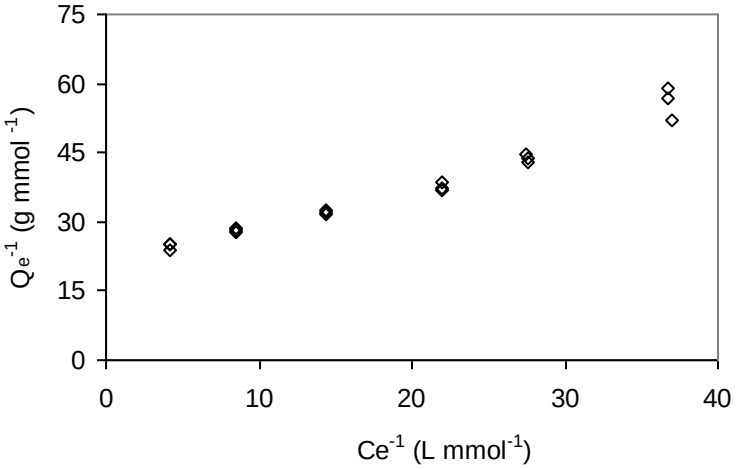


Figure H.6. Lineweaver-Burk plot relating equilibrium lead concentrations.

Table H.13. Sorption, Q_t, of lead to dehydrated BC13 cells with time at pH 2.5 and 45ºC. Initial concentrations were the highest tested for lead, 0.241 mM.

	Q_t (mmol g^{-1})					
Elapsed Time (min)	Trial 1	Trial 2	Trial 3	Average	STDEV	95% CI
0	0.000	0.000	0.000	0.000	0.000	0.000
1	0.107	0.116	0.115	0.113	0.005	0.006
5	0.120	0.124	0.117	0.121	0.004	0.004
15	0.121	0.133	0.121	0.125	0.007	0.008
30	0.123	0.125	0.118	0.122	0.004	0.004
60	0.128	0.136	0.127	0.131	0.005	0.006

Table H.14. Equilibrium sorption, Q_e, and solution, C_e, concentrations of lead in the presence of dehydrated BC13 cells at pH 2.5 and 45ºC, with varying concentrations, C_o.

	Q_e (mmol g^{-1})			C_e (mmol L^{-1})		
C_o (mmol L^{-1})	Trial 1	Trial 2	Trial 3	Trial 1	Trial 2	Trial 3
0.029	0.075	0.074	0.073	0.021	0.022	0.022
0.039	0.082	0.084	0.082	0.030	0.030	0.030
0.048	0.088	0.087	0.083	0.039	0.040	0.040
0.072	0.104	0.101	0.098	0.062	0.062	0.063
0.121	0.116	0.116	0.114	0.109	0.109	0.109
0.241	0.128	0.136	0.127	0.229	0.228	0.229

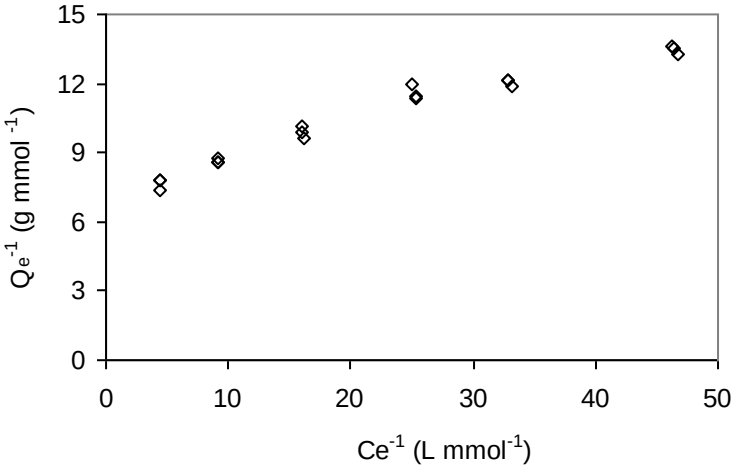


Figure H.7. Lineweaver-Burk plot relating equilibrium lead concentrations.

Table H.15. Sorption, Q_t, of lead to dehydrated BC13 cells with time at pH 4.0 and 45ºC. Initial concentrations were the highest tested for lead, 0.241 mM.

	Q_t (mmol g^{-1})					
Elapsed Time (min)	Trial 1	Trial 2	Trial 3	Average	STDEV	95% CI
0	0.000	0.000	0.000	0.000	0.000	0.000
1	0.163	0.179	0.177	0.173	0.009	0.010
5	0.181	0.196	0.188	0.188	0.008	0.009
15	0.186	0.200	0.188	0.192	0.008	0.009
30	0.190	0.194	0.179	0.187	0.008	0.009
60	0.199	0.204	0.190	0.198	0.007	0.008

Table H.16. Equilibrium sorption, Q_e, and solution, C_e, concentrations of lead in the presence of dehydrated BC13 cells at pH 4.0 and 45ºC, with varying concentrations, C_o.

	Q_e (mmol g^{-1})			C_e (mmol L^{-1})		
C_o (mmol L^{-1})	Trial 1	Trial 2	Trial 3	Trial 1	Trial 2	Trial 3
0.029	0.113	0.107	0.110	0.018	0.018	0.018
0.039	0.130	0.133	0.136	0.026	0.025	0.025
0.048	0.146	0.152	0.150	0.034	0.033	0.033
0.072	0.170	0.169	0.169	0.055	0.056	0.056
0.121	0.180	0.179	0.178	0.103	0.103	0.103
0.241	0.199	0.204	0.190	0.221	0.221	0.222

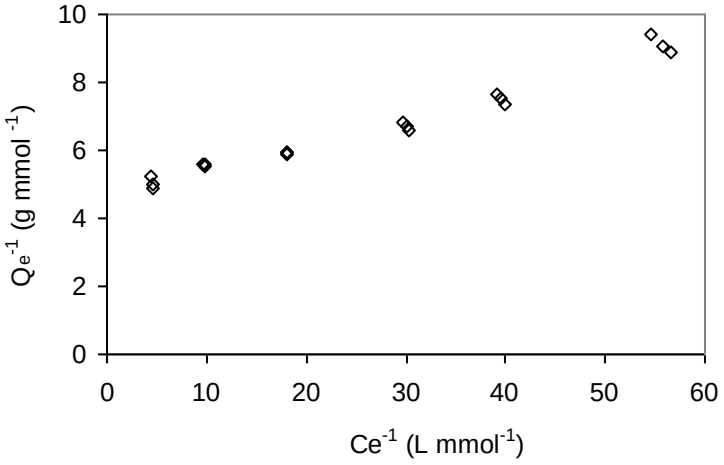


Figure H.8. Lineweaver-Burk plot relating equilibrium lead concentrations.

Table H.17. Sorption, Q_t, of lead to dehydrated BC13 cells with time at pH 5.5 and 45ºC. Initial concentrations were the highest tested for lead, 0.241 mM.

	Q_t (mmol g^{-1})					
Elapsed Time (min)	Trial 1	Trial 2	Trial 3	Average	STDEV	95% CI
0	0.000	0.000	0.000	0.000	0.000	0.000
1	0.242	0.250	0.234	0.242	0.008	0.009
5	0.249	0.253	0.229	0.244	0.013	0.015
15	0.255	0.263	0.243	0.254	0.010	0.011
30	0.260	0.263	0.258	0.260	0.003	0.003
60	0.269	0.271	0.252	0.264	0.010	0.012

Table H.18. Equilibrium sorption, Q_e, and solution, C_e, concentrations of lead in the presence of dehydrated BC13 cells at pH 5.5 and 45ºC, with varying concentrations, C_o.

	Q_e (mmol g^{-1})			C_e (mmol L^{-1})		
C_o (mmol L^{-1})	Trial 1	Trial 2	Trial 3	Trial 1	Trial 2	Trial 3
0.029	0.136	0.135	0.135	0.015	0.015	0.015
0.039	0.167	0.163	0.163	0.022	0.022	0.022
0.048	0.191	0.188	0.191	0.029	0.029	0.029
0.072	0.214	0.213	0.217	0.051	0.051	0.051
0.121	0.237	0.241	0.233	0.097	0.097	0.097
0.241	0.269	0.271	0.252	0.214	0.214	0.216

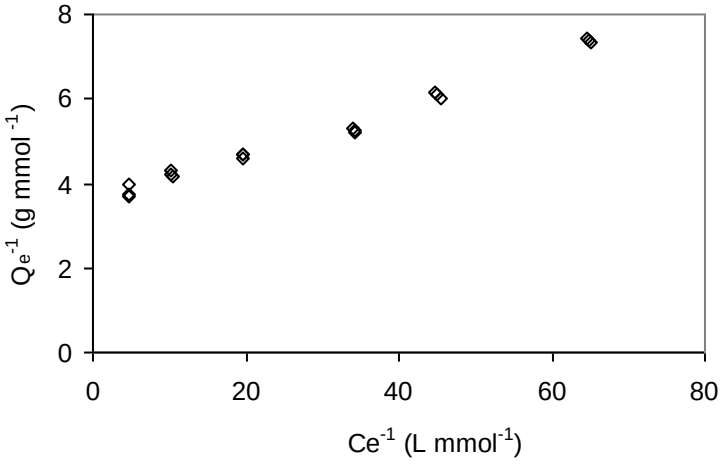


Figure H.9. Lineweaver-Burk plot relating equilibrium lead concentrations.

Table H.19. Sorption, Q_t, of lead to dehydrated BC13 cells with time at pH 7.0 and 45ºC. Initial concentrations were the highest tested for lead, 0.241 mM.

	Q_t (mmol g^{-1})					
Elapsed Time (min)	Trial 1	Trial 2	Trial 3	Average	STDEV	95% CI
0	0.000	0.000	0.000	0.000	0.000	0.000
1	0.193	0.208	0.198	0.200	0.008	0.009
5	0.200	0.214	0.210	0.208	0.007	0.008
15	0.206	0.214	0.197	0.206	0.009	0.010
30	0.214	0.217	0.214	0.215	0.001	0.002
60	0.220	0.227	0.216	0.221	0.006	0.006

Table H.20. Equilibrium sorption, Q_e, and solution, C_e, concentrations of lead in the presence of dehydrated BC13 cells at pH 7.0 and 45ºC, with varying concentrations, C_o.

	Q_e (mmol g^{-1})			C_e (mmol L^{-1})		
C_o (mmol L^{-1})	Trial 1	Trial 2	Trial 3	Trial 1	Trial 2	Trial 3
0.029	0.117	0.121	0.124	0.017	0.017	0.017
0.039	0.145	0.151	0.155	0.024	0.023	0.023
0.048	0.176	0.169	0.171	0.031	0.031	0.031
0.072	0.194	0.199	0.205	0.053	0.053	0.052
0.121	0.231	0.241	0.231	0.098	0.097	0.098
0.241	0.220	0.227	0.216	0.219	0.219	0.220

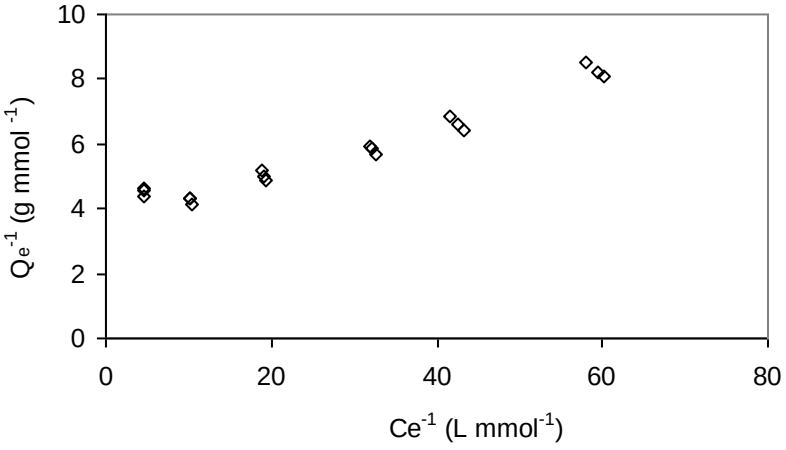


Figure H.10. Lineweaver-Burk plot relating equilibrium lead concentrations.

Zinc

Table H.21. Sorption, Q_t, of zinc to viable BC13 cells with time at pH 1.5 and 45ºC. Initial concentrations were the highest tested for zinc, 0.918 mM.

	Q_t (mmol g^{-1})					
Elapsed Time (min)	Trial 1	Trial 2	Trial 3	Average	STDEV	95% CI
0	0.000	0.000	0.000	0.000	0.000	0.000
1	0.329	0.360	0.335	0.342	0.017	0.019
5	0.373	0.403	0.381	0.385	0.016	0.018
15	0.392	0.399	0.370	0.387	0.015	0.017
30	0.426	0.426	0.390	0.414	0.021	0.024
60	0.477	0.491	0.455	0.474	0.018	0.020

Table H.22. Equilibrium sorption, Q_e, and solution, C_e, concentrations of zinc in the presence of viable BC13 cells at pH 1.5 and 45ºC, with varying concentrations, C_o.

	Q_e (mmol g^{-1})			C_e (mmol L^{-1})		
C_o (mmol L^{-1})	Trial 1	Trial 2	Trial 3	Trial 1	Trial 2	Trial 3
0.122	0.276	0.261	0.268	0.095	0.096	0.096
0.184	0.336	0.363	0.370	0.150	0.147	0.146
0.229	0.390	0.393	0.395	0.190	0.190	0.190
0.306	0.418	0.423	0.414	0.264	0.264	0.265
0.459	0.446	0.456	0.438	0.414	0.413	0.415
0.918	0.491	0.519	0.487	0.869	0.866	0.869

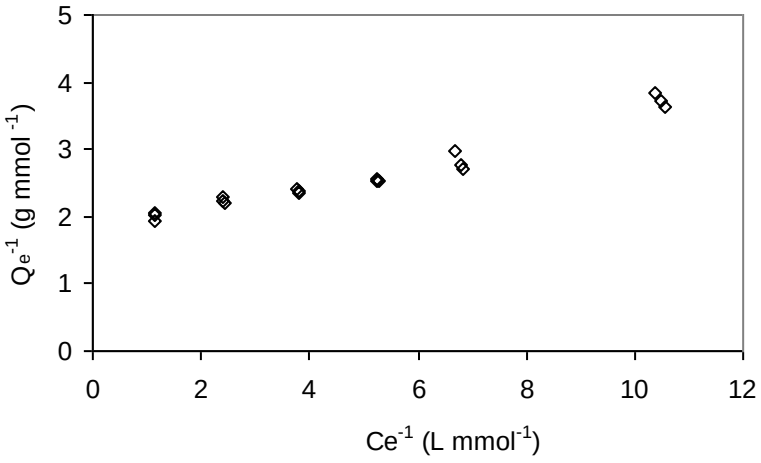


Figure H.11. Lineweaver-Burk plot relating equilibrium zinc concentrations.

Table H.23. Sorption, Q_t, of zinc to viable BC13 cells with time at pH 2.5 and 45ºC. Initial concentrations were the highest tested for zinc, 0.918 mM.

	Q_t (mmol g^{-1})					
Elapsed Time (min)	Trial 1	Trial 2	Trial 3	Average	STDEV	95% CI
0	0.000	0.000	0.000	0.000	0.000	0.000
1	0.836	0.884	0.803	0.841	0.041	0.046
5	1.079	1.169	1.141	1.129	0.046	0.052
15	1.227	1.280	1.173	1.227	0.053	0.060
30	1.336	1.366	1.300	1.334	0.033	0.037
60	1.414	1.460	1.438	1.437	0.023	0.026

Table H.24. Equilibrium sorption, Q_e, and solution, C_e, concentrations of zinc in the presence of viable BC13 cells at pH 2.5 and 45ºC, with varying concentrations, C_o.

	Q_e (mmol g^{-1})			C_e (mmol L^{-1})		
C_o (mmol L^{-1})	Trial 1	Trial 2	Trial 3	Trial 1	Trial 2	Trial 3
0.122	0.705	0.666	0.706	0.052	0.056	0.052
0.184	0.897	0.910	0.928	0.094	0.093	0.091
0.229	1.037	1.012	0.979	0.126	0.128	0.132
0.306	1.147	1.159	1.170	0.191	0.190	0.189
0.459	1.296	1.271	1.283	0.329	0.332	0.331
0.918	1.455	1.502	1.479	0.772	0.768	0.770

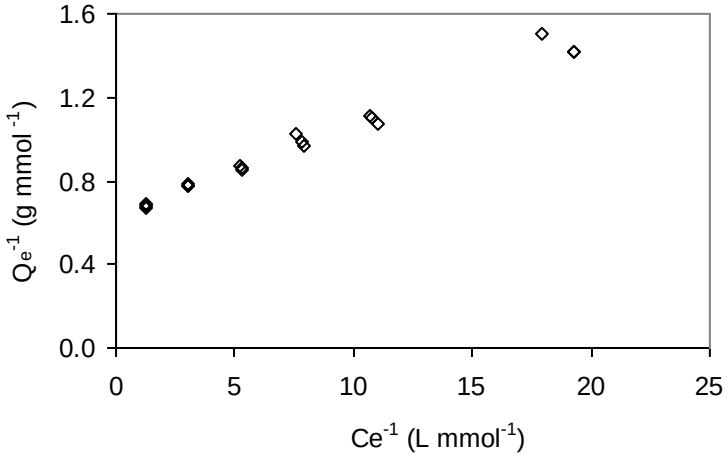


Figure H.12. Lineweaver-Burk plot relating equilibrium zinc concentrations.

Table H.25. Sorption, Q_t, of zinc to viable BC13 cells with time at pH 4.0 and 45ºC. Initial concentrations were the highest tested for zinc, 0.918 mM.

	Q_t (mmol g^{-1})					
Elapsed Time (min)	Trial 1	Trial 2	Trial 3	Average	STDEV	95% CI
0	0.000	0.000	0.000	0.000	0.000	0.000
1	0.922	1.006	0.979	0.969	0.043	0.048
5	1.273	1.284	1.263	1.274	0.011	0.012
15	1.371	1.441	1.338	1.383	0.052	0.059
30	1.543	1.630	1.542	1.572	0.050	0.057
60	1.568	1.699	1.551	1.606	0.081	0.091

Table H.26. Equilibrium sorption, Q_e, and solution, C_e, concentrations of zinc in the presence of viable BC13 cells at pH 4.0 and 45ºC, with varying concentrations, C_o.

	Q_e (mmol g^{-1})			C_e (mmol L^{-1})		
C_o (mmol L^{-1})	Trial 1	Trial 2	Trial 3	Trial 1	Trial 2	Trial 3
0.122	0.745	0.718	0.728	0.048	0.051	0.050
0.184	0.924	0.891	0.928	0.091	0.094	0.091
0.229	1.007	0.991	0.997	0.129	0.130	0.130
0.306	1.175	1.188	1.141	0.188	0.187	0.192
0.459	1.278	1.299	1.275	0.331	0.329	0.331
0.918	1.614	1.598	1.595	0.756	0.758	0.758

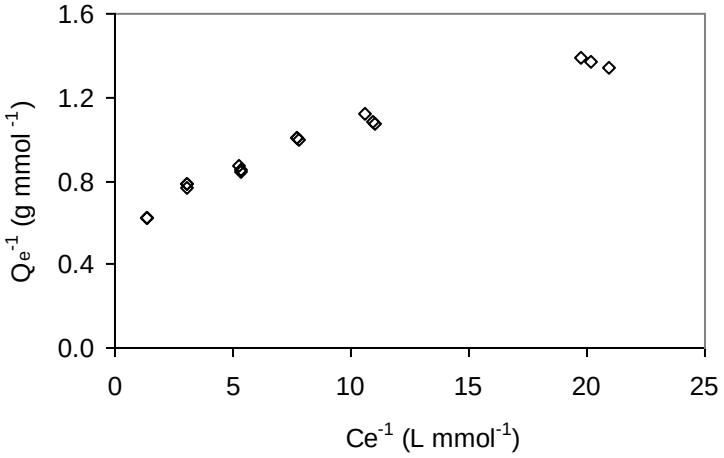


Figure H.13. Lineweaver-Burk plot relating equilibrium zinc concentrations.

Table H.27. Sorption, Q_t, of zinc to viable BC13 cells with time at pH 5.5 and 45ºC. Initial concentrations were the highest tested for zinc, 0.918 mM.

	Q_t (mmol g^{-1})					
Elapsed Time (min)	Trial 1	Trial 2	Trial 3	Average	STDEV	95% CI
0	0.000	0.000	0.000	0.000	0.000	0.000
1	1.234	1.298	1.293	1.275	0.036	0.041
5	1.357	1.435	1.379	1.390	0.040	0.045
15	1.412	1.456	1.390	1.420	0.034	0.038
30	1.491	1.509	1.433	1.478	0.040	0.045
60	1.611	1.709	1.657	1.659	0.049	0.056

Table H.28. Equilibrium sorption, Q_e, and solution, C_e, concentrations of zinc in the presence of viable BC13 cells at pH 5.5 and 45ºC, with varying concentrations, C_o.

	Q_e (mmol g^{-1})			C_e (mmol L^{-1})		
C_o (mmol L^{-1})	Trial 1	Trial 2	Trial 3	Trial 1	Trial 2	Trial 3
0.122	0.759	0.746	0.755	0.046	0.048	0.047
0.184	0.976	0.951	0.962	0.086	0.088	0.087
0.229	1.091	1.034	1.016	0.120	0.126	0.128
0.306	1.181	1.217	1.204	0.188	0.184	0.185
0.459	1.464	1.456	1.472	0.312	0.313	0.312
0.918	1.657	1.758	1.705	0.752	0.742	0.747

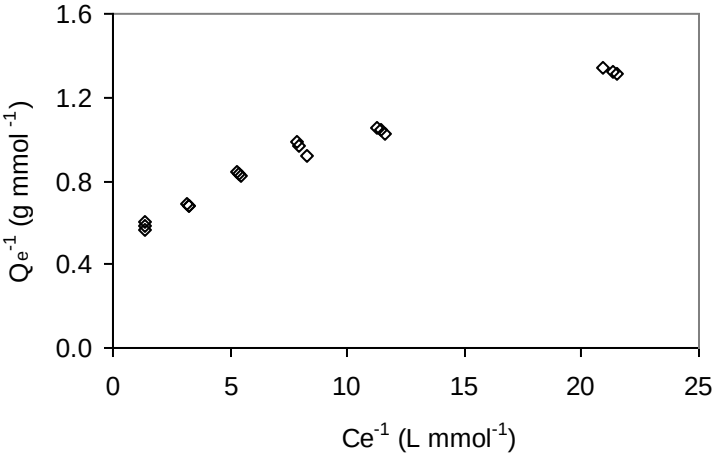


Figure H.14. Lineweaver-Burk plot relating equilibrium zinc concentrations.

Table H.29. Sorption, Q_t, of zinc to viable BC13 cells with time at pH 7.0 and 45ºC. Initial concentrations were the highest tested for zinc, 0.918 mM.

	Q_t (mmol g^{-1})					
Elapsed Time (min)	Trial 1	Trial 2	Trial 3	Average	STDEV	95% CI
0	0.000	0.000	0.000	0.000	0.000	0.000
1	0.840	0.885	0.880	0.868	0.025	0.028
5	0.868	0.942	0.906	0.906	0.037	0.042
15	1.070	1.173	1.075	1.106	0.058	0.065
30	1.076	1.148	1.061	1.095	0.047	0.053
60	1.078	1.113	1.077	1.089	0.021	0.023

Table H.30. Equilibrium sorption, Q_e, and solution, C_e, concentrations of zinc in the presence of viable BC13 cells at pH 7.0 and 45ºC, with varying concentrations, C_o.

	Q_e (mmol g^{-1})			C_e (mmol L^{-1})		
C_o (mmol L^{-1})	Trial 1	Trial 2	Trial 3	Trial 1	Trial 2	Trial 3
0.122	0.583	0.582	0.586	0.064	0.064	0.064
0.184	0.781	0.773	0.791	0.105	0.106	0.104
0.229	0.874	0.873	0.886	0.142	0.142	0.141
0.306	0.936	0.948	0.974	0.212	0.211	0.209
0.459	1.000	1.011	1.023	0.359	0.358	0.357
0.918	1.109	1.145	1.108	0.807	0.803	0.807

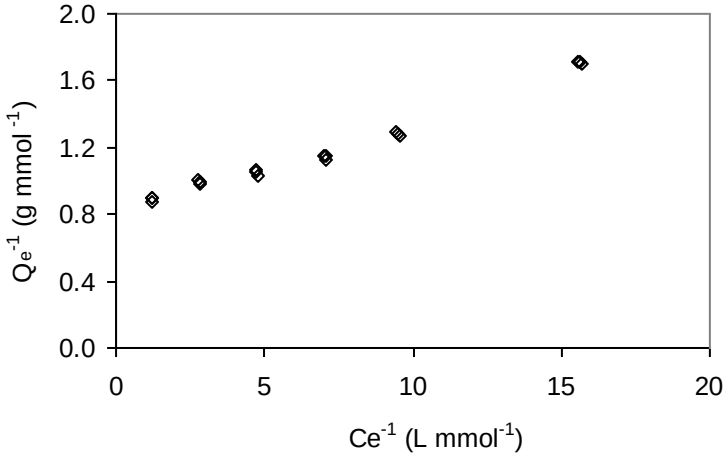


Figure H.15. Lineweaver-Burk plot relating equilibrium zinc concentrations.

Table H.31. Sorption, Q_t, of zinc to dehydrated BC13 cells with time at pH 1.5 and 45ºC. Initial concentrations were the highest tested for zinc, 0.918 mM.

	Q_t (mmol g^{-1})					
Elapsed Time (min)	Trial 1	Trial 2	Trial 3	Average	STDEV	95% CI
0	0.000	0.000	0.000	0.000	0.000	0.000
1	0.148	0.150	0.148	0.149	0.001	0.001
5	0.168	0.177	0.177	0.174	0.005	0.006
15	0.184	0.194	0.186	0.188	0.005	0.006
30	0.180	0.181	0.176	0.179	0.002	0.003
60	0.189	0.204	0.198	0.197	0.008	0.009

Table H.32. Equilibrium sorption, Q_e, and solution, C_e, concentrations of zinc in the presence of dehydrated BC13 cells at pH 1.5 and 45ºC, with varying concentrations, C_o.

	Q_e (mmol g^{-1})			C_e (mmol L^{-1})		
C_o (mmol L^{-1})	Trial 1	Trial 2	Trial 3	Trial 1	Trial 2	Trial 3
0.122	0.103	0.102	0.104	0.112	0.112	0.112
0.184	0.121	0.117	0.119	0.171	0.172	0.172
0.229	0.133	0.134	0.134	0.216	0.216	0.216
0.306	0.147	0.149	0.151	0.291	0.291	0.291
0.459	0.161	0.170	0.163	0.443	0.442	0.443
0.918	0.194	0.210	0.203	0.898	0.897	0.897

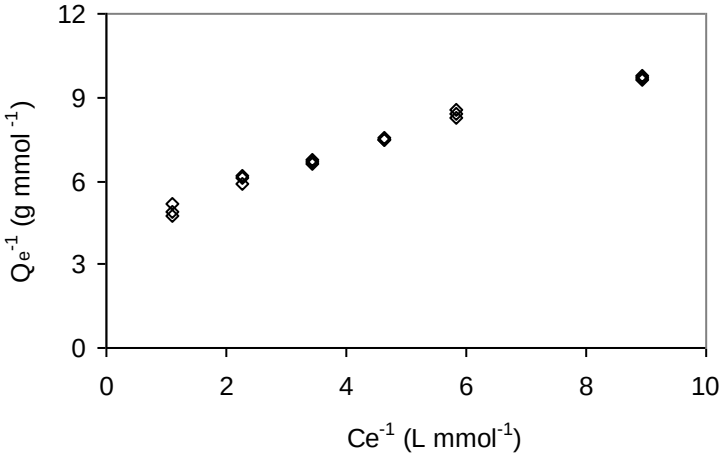


Figure H.16. Lineweaver-Burk plot relating equilibrium zinc concentrations.

Table H.33. Sorption, Q_t, of zinc to dehydrated BC13 cells with time at pH 2.5 and 45ºC. Initial concentrations were the highest tested for zinc, 0.918 mM.

	Q_t (mmol g^{-1})					
Elapsed Time (min)	Trial 1	Trial 2	Trial 3	Average	STDEV	95% CI
0	0.000	0.000	0.000	0.000	0.000	0.000
1	0.435	0.444	0.415	0.431	0.015	0.017
5	0.428	0.467	0.427	0.441	0.023	0.026
15	0.439	0.479	0.478	0.465	0.023	0.026
30	0.492	0.512	0.500	0.501	0.010	0.011
60	0.516	0.549	0.546	0.537	0.018	0.021

Table H.34. Equilibrium sorption, Q_e, and solution, C_e, concentrations of zinc in the presence of dehydrated BC13 cells at pH 2.5 and 45ºC, with varying concentrations, C_o.

	Q_e (mmol g^{-1})			C_e (mmol L^{-1})		
C_o (mmol L^{-1})	Trial 1	Trial 2	Trial 3	Trial 1	Trial 2	Trial 3
0.122	0.330	0.339	0.329	0.089	0.088	0.089
0.184	0.383	0.383	0.380	0.145	0.145	0.146
0.229	0.404	0.419	0.416	0.189	0.188	0.188
0.306	0.438	0.445	0.440	0.262	0.261	0.262
0.459	0.457	0.451	0.471	0.413	0.414	0.412
0.918	0.531	0.565	0.562	0.865	0.861	0.862

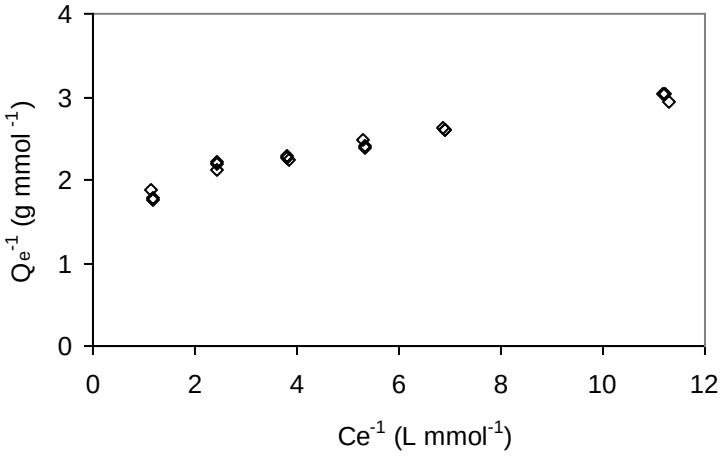


Figure H.17. Lineweaver-Burk plot relating equilibrium zinc concentrations.

Table H.35. Sorption, Q_t, of zinc to dehydrated BC13 cells with time at pH 4.0 and 45ºC. Initial concentrations were the highest tested for zinc, 0.918 mM.

	Q_t (mmol g^{-1})					
Elapsed Time (min)	Trial 1	Trial 2	Trial 3	Average	STDEV	95% CI
0	0.000	0.000	0.000	0.000	0.000	0.000
1	0.617	0.629	0.568	0.605	0.032	0.037
5	0.652	0.680	0.660	0.664	0.014	0.016
15	0.731	0.786	0.724	0.747	0.034	0.039
30	0.791	0.856	0.837	0.828	0.033	0.038
60	0.786	0.852	0.847	0.828	0.037	0.042

Table H.36. Equilibrium sorption, Q_e, and solution, C_e, concentrations of zinc in the presence of dehydrated BC13 cells at pH 4.0 and 45ºC, with varying concentrations, C_o.

	Q_e (mmol g^{-1})			C_e (mmol L^{-1})		
C_o (mmol L^{-1})	Trial 1	Trial 2	Trial 3	Trial 1	Trial 2	Trial 3
0.122	0.514	0.511	0.535	0.071	0.071	0.069
0.184	0.648	0.664	0.661	0.119	0.117	0.117
0.229	0.716	0.725	0.740	0.158	0.157	0.155
0.306	0.779	0.790	0.808	0.228	0.227	0.225
0.459	0.816	0.824	0.813	0.377	0.376	0.378
0.918	0.808	0.876	0.871	0.837	0.830	0.831

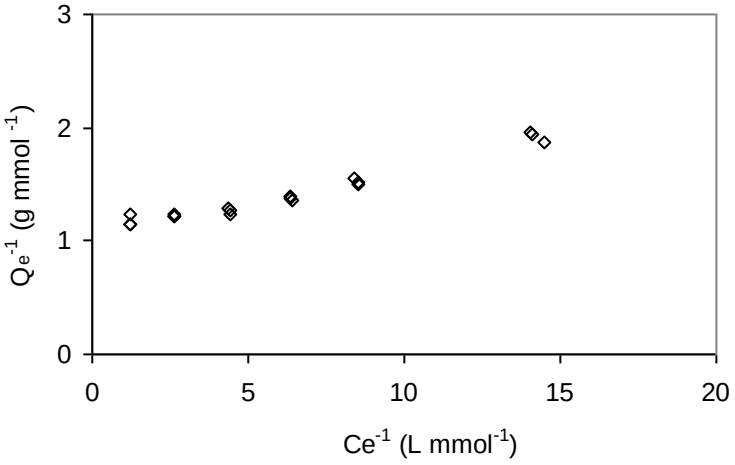


Figure H.18. Lineweaver-Burk plot relating equilibrium zinc concentrations.

Table H.37. Sorption, Q_t, of zinc to dehydrated BC13 cells with time at pH 5.5 and 45ºC. Initial concentrations were the highest tested for zinc, 0.918 mM.

	Q_t (mmol g^{-1})					
Elapsed Time (min)	Trial 1	Trial 2	Trial 3	Average	STDEV	95% CI
0	0.000	0.000	0.000	0.000	0.000	0.000
1	0.729	0.776	0.770	0.758	0.026	0.030
5	0.764	0.766	0.716	0.749	0.028	0.032
15	0.772	0.781	0.707	0.753	0.041	0.046
30	0.785	0.814	0.748	0.783	0.033	0.037
60	0.802	0.855	0.813	0.823	0.028	0.031

Table H.38. Equilibrium sorption, Q_e, and solution, C_e, concentrations of zinc in the presence of dehydrated BC13 cells at pH 5.5 and 45ºC, with varying concentrations, C_o.

	Q_e (mmol g^{-1})			C_e (mmol L^{-1})		
C_o (mmol L^{-1})	Trial 1	Trial 2	Trial 3	Trial 1	Trial 2	Trial 3
0.122	0.512	0.507	0.513	0.071	0.072	0.071
0.184	0.632	0.642	0.630	0.120	0.119	0.121
0.229	0.722	0.724	0.743	0.157	0.157	0.155
0.306	0.760	0.748	0.735	0.230	0.231	0.232
0.459	0.803	0.785	0.808	0.379	0.380	0.378
0.918	0.825	0.880	0.837	0.835	0.830	0.834

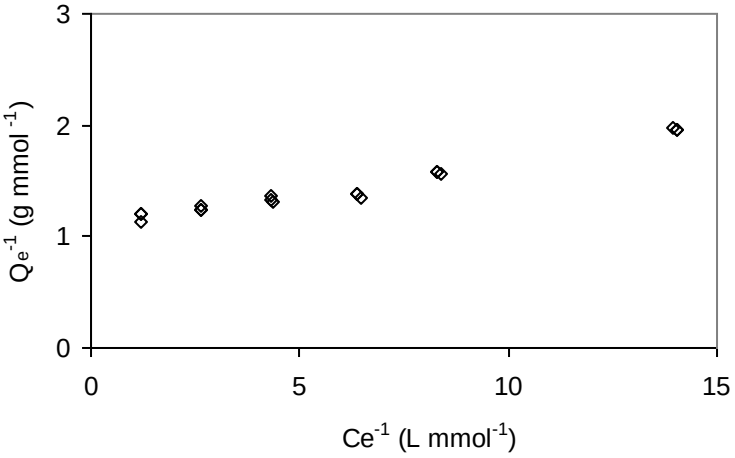


Figure H.19. Lineweaver-Burk plot relating equilibrium zinc concentrations.

Table H.39. Sorption, Q_t, of zinc to dehydrated BC13 cells with time at pH 7.0 and 45ºC. Initial concentrations were the highest tested for zinc, 0.918 mM.

	Q_t (mmol g^{-1})					
Elapsed Time (min)	Trial 1	Trial 2	Trial 3	Average	STDEV	95% CI
0	0.000	0.000	0.000	0.000	0.000	0.000
1	0.592	0.621	0.595	0.603	0.016	0.018
5	0.671	0.730	0.722	0.708	0.032	0.036
15	0.787	0.801	0.788	0.792	0.008	0.009
30	0.848	0.857	0.782	0.829	0.041	0.047
60	0.848	0.848	0.828	0.842	0.011	0.013

Table H.40. Equilibrium sorption, Q_e, and solution, C_e, concentrations of zinc in the presence of dehydrated BC13 cells at pH 7.0 and 45ºC, with varying concentrations, C_o.

	Q_e (mmol g^{-1})			C_e (mmol L^{-1})		
C_o (mmol L^{-1})	Trial 1	Trial 2	Trial 3	Trial 1	Trial 2	Trial 3
0.122	0.492	0.504	0.487	0.073	0.072	0.074
0.184	0.657	0.641	0.650	0.118	0.119	0.119
0.229	0.700	0.682	0.685	0.159	0.161	0.161
0.306	0.760	0.753	0.679	0.230	0.231	0.238
0.459	0.839	0.831	0.814	0.375	0.376	0.377
0.918	0.873	0.873	0.852	0.830	0.830	0.832

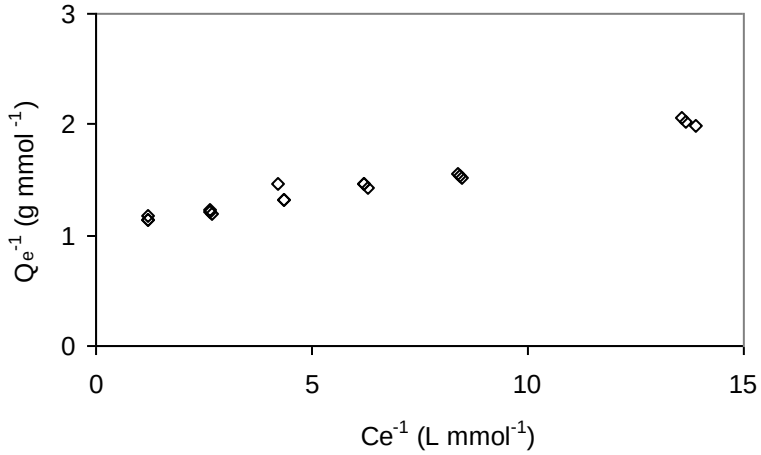


Figure H.20. Lineweaver-Burk plot relating equilibrium zinc concentrations.

Copper

Table H.41. Sorption, Q_t, of copper to viable BC13 cells with time at pH 1.5 and 45ºC. Initial concentrations were the highest tested for copper, 1.574 mM.

	Q_t (mmol g^{-1})					
Elapsed Time (min)	Trial 1	Trial 2	Trial 3	Average	STDEV	95% CI
0	0.000	0.000	0.000	0.000	0.000	0.000
1	1.112	1.197	1.120	1.143	0.047	0.053
5	1.280	1.360	1.321	1.320	0.040	0.045
15	1.361	1.370	1.256	1.329	0.064	0.072
30	1.428	1.458	1.344	1.410	0.059	0.067
60	1.484	1.627	1.545	1.552	0.072	0.081

Table H.42. Equilibrium sorption, Q_e, and solution, C_e, concentrations of copper in the presence of viable BC13 cells at pH 1.5 and 45ºC, with varying concentrations, C_o.

	Q_e (mmol g^{-1})			C_e (mmol L^{-1})		
C_o (mmol L^{-1})	Trial 1	Trial 2	Trial 3	Trial 1	Trial 2	Trial 3
0.189	0.956	0.944	0.924	0.093	0.094	0.096
0.236	1.110	1.123	1.094	0.125	0.124	0.127
0.315	1.241	1.170	1.190	0.191	0.198	0.196
0.393	1.271	1.277	1.307	0.266	0.266	0.263
0.787	1.392	1.399	1.375	0.648	0.647	0.649
1.574	1.484	1.514	1.504	1.425	1.422	1.423

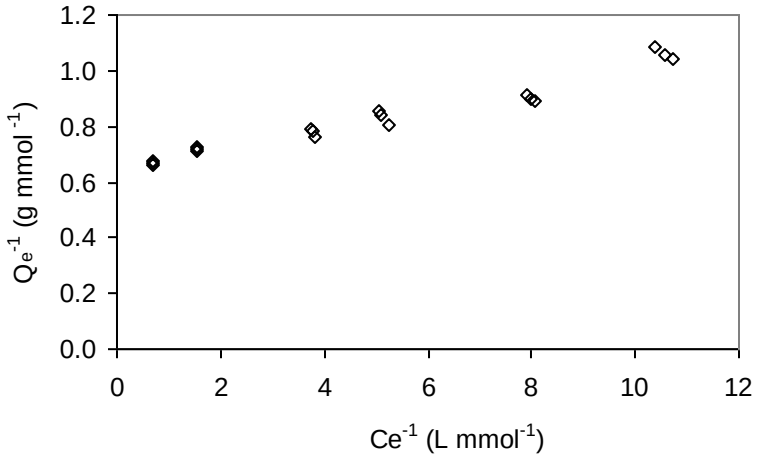


Figure H.21. Lineweaver-Burk plot relating equilibrium copper concentrations.

Table H.43. Sorption, Q_t, of copper to viable BC13 cells with time at pH 2.5 and 45ºC. Initial concentrations were the highest tested for copper, 1.574 mM.

	Q_t (mmol g^{-1})					
Elapsed Time (min)	Trial 1	Trial 2	Trial 3	Average	STDEV	95% CI
0	0.000	0.000	0.000	0.000	0.000	0.000
1	1.337	1.436	1.398	1.390	0.050	0.057
5	2.280	2.493	2.390	2.387	0.106	0.120
15	2.731	2.746	2.677	2.718	0.036	0.041
30	2.836	2.959	2.943	2.913	0.067	0.076
60	2.888	2.894	2.732	2.838	0.092	0.104

Table H.44. Equilibrium sorption, Q_e, and solution, C_e, concentrations of copper in the presence of viable BC13 cells at pH 2.5 and 45ºC, with varying concentrations, C_o.

	Q_e (mmol g^{-1})			C_e (mmol L^{-1})		
C_o (mmol L^{-1})	Trial 1	Trial 2	Trial 3	Trial 1	Trial 2	Trial 3
0.189	1.542	1.528	1.521	0.035	0.036	0.037
0.236	1.786	1.804	1.811	0.057	0.056	0.055
0.315	2.102	2.132	2.114	0.104	0.102	0.103
0.393	2.272	2.220	2.236	0.166	0.171	0.170
0.787	2.684	2.763	2.285	0.518	0.510	0.558
1.574	2.888	2.850	2.732	1.285	1.289	1.300

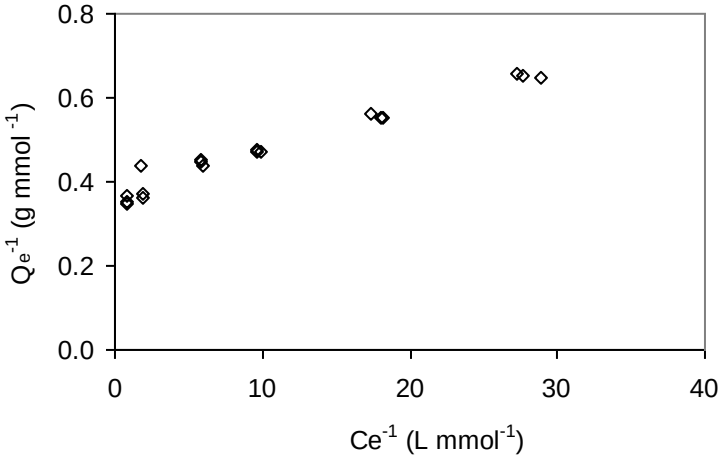


Figure H.22. Lineweaver-Burk plot relating equilibrium copper concentrations.

Table H.45. Sorption, Q_t, of copper to viable BC13 cells with time at pH 4.0 and 45ºC. Initial concentrations were the highest tested for copper, 1.574 mM.

	Q_t (mmol g^{-1})					
Elapsed Time (min)	Trial 1	Trial 2	Trial 3	Average	STDEV	95% CI
0	0.000	0.000	0.000	0.000	0.000	0.000
1	3.647	3.546	3.318	3.036	0.169	0.191
5	4.153	3.951	4.039	3.825	0.101	0.114
15	4.701	4.571	4.372	4.286	0.166	0.188
30	4.872	4.722	4.553	4.487	0.159	0.180
60	4.964	4.915	4.898	4.628	0.034	0.039

Table H.46. Equilibrium sorption, Q_e, and solution, C_e, concentrations of copper in the presence of viable BC13 cells at pH 4.0 and 45ºC, with varying concentrations, C_o.

	Q_e (mmol g^{-1})			C_e (mmol L^{-1})		
C_o (mmol L^{-1})	Trial 1	Trial 2	Trial 3	Trial 1	Trial 2	Trial 3
0.189	1.740	1.731	1.744	0.015	0.016	0.014
0.236	2.130	2.101	2.098	0.023	0.026	0.026
0.315	2.744	2.696	2.665	0.040	0.045	0.048
0.393	3.389	3.264	3.310	0.055	0.067	0.062
0.787	4.663	4.724	4.741	0.320	0.314	0.313
1.574	4.964	4.915	4.898	1.077	1.082	1.084

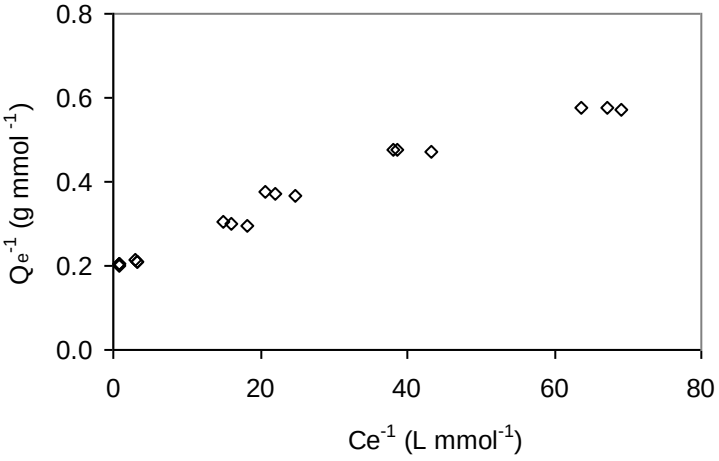


Figure H.23. Lineweaver-Burk plot relating equilibrium copper concentrations.

Table H.47. Sorption, Q_t, of copper to viable BC13 cells with time at pH 5.5 and 45ºC. Initial concentrations were the highest tested for copper, 1.574 mM.

	Q_t (mmol g^{-1})					
Elapsed Time (min)	Trial 1	Trial 2	Trial 3	Average	STDEV	95% CI
0	0.000	0.000	0.000	0.000	0.000	0.000
1	4.098	4.290	4.078	4.155	0.117	0.132
5	4.181	4.572	4.558	4.437	0.222	0.251
15	4.270	4.353	3.950	4.191	0.213	0.241
30	4.526	4.651	4.608	4.595	0.063	0.071
60	4.723	4.991	4.512	4.742	0.240	0.271

Table H.48. Equilibrium sorption, Q_e, and solution, C_e, concentrations of copper in the presence of viable BC13 cells at pH 5.5 and 45ºC, with varying concentrations, C_o.

	Q_e (mmol g^{-1})			C_e (mmol L^{-1})		
C_o (mmol L^{-1})	Trial 1	Trial 2	Trial 3	Trial 1	Trial 2	Trial 3
0.189	1.657	1.649	1.642	0.023	0.024	0.025
0.236	2.115	2.067	2.065	0.025	0.029	0.030
0.315	2.679	2.656	2.604	0.047	0.049	0.054
0.393	3.154	3.109	3.094	0.078	0.083	0.084
0.787	4.270	4.446	4.348	0.360	0.342	0.352
1.574	4.553	4.522	4.393	1.118	1.122	1.134

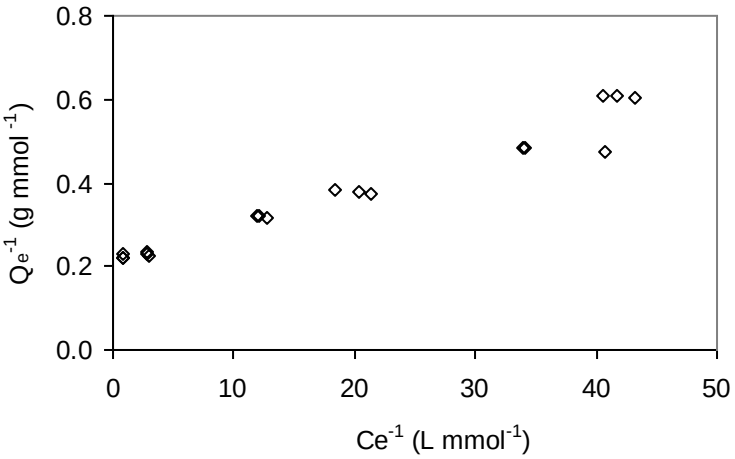


Figure H.24. Lineweaver-Burk plot relating equilibrium copper concentrations.

Table H.49. Sorption, Q_t, of copper to viable BC13 cells with time at pH 7.0 and 45ºC. Initial concentrations were the highest tested for copper, 1.574 mM.

	Q_t (mmol g^{-1})					
Elapsed Time (min)	Trial 1	Trial 2	Trial 3	Average	STDEV	95% CI
0	0.000	0.000	0.000	0.000	0.000	0.000
1	3.342	3.625	3.581	3.516	0.152	0.173
5	3.942	4.053	3.917	3.970	0.073	0.082
15	4.151	4.477	4.447	4.358	0.180	0.204
30	4.410	4.445	4.411	4.422	0.020	0.022
60	4.380	4.776	4.585	4.580	0.198	0.224

Table H.50. Equilibrium sorption, Q_e, and solution, C_e, concentrations of copper in the presence of viable BC13 cells at pH 7.0 and 45ºC, with varying concentrations, C_o.

	Q_e (mmol g^{-1})			C_e (mmol L^{-1})		
C_o (mmol L^{-1})	Trial 1	Trial 2	Trial 3	Trial 1	Trial 2	Trial 3
0.189	1.598	1.587	1.610	0.029	0.030	0.028
0.236	1.973	1.988	1.909	0.039	0.037	0.045
0.315	2.604	2.635	2.621	0.054	0.051	0.053
0.393	2.979	2.774	2.887	0.096	0.116	0.105
0.787	4.074	3.829	3.955	0.379	0.404	0.391
1.574	4.380	4.776	4.585	1.136	1.096	1.115

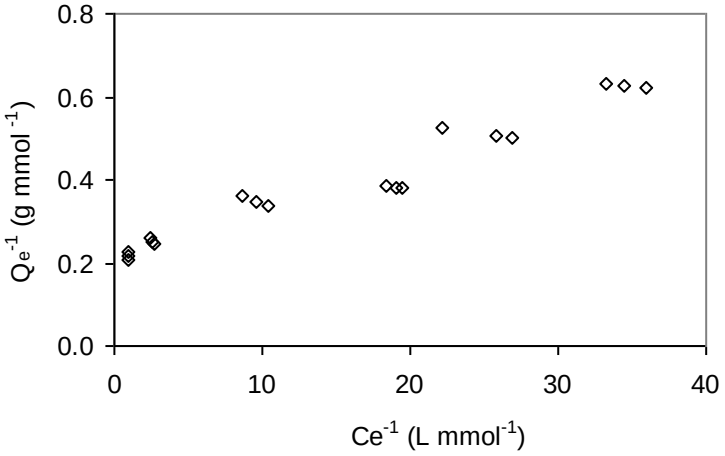


Figure H.25. Lineweaver-Burk plot relating equilibrium copper concentrations.

Table H.51. Sorption, Q_t, of copper to dehydrated BC13 cells with time at pH 1.5 and 45ºC. Initial concentrations were the highest tested for copper, 1.574 mM.

	Q_t (mmol g^{-1})					
Elapsed Time (min)	Trial 1	Trial 2	Trial 3	Average	STDEV	95% CI
0	0.000	0.000	0.000	0.000	0.000	0.000
1	0.559	0.609	0.593	0.555	0.025	0.029
5	0.587	0.620	0.640	0.630	0.026	0.030
15	0.622	0.647	0.648	0.586	0.015	0.017
30	0.640	0.640	0.682	0.626	0.024	0.027
60	0.651	0.669	0.645	0.641	0.012	0.014

Table H.52. Equilibrium sorption, Q_e, and solution, C_e, concentrations of copper in the presence of dehydrated BC13 cells at pH 1.5 and 45ºC, with varying concentrations, C_o.

	Q_e (mmol g^{-1})			C_e (mmol L^{-1})		
C_o (mmol L^{-1})	Trial 1	Trial 2	Trial 3	Trial 1	Trial 2	Trial 3
0.189	0.384	0.403	0.377	0.150	0.149	0.151
0.236	0.411	0.409	0.388	0.195	0.195	0.197
0.315	0.455	0.438	0.422	0.269	0.271	0.273
0.393	0.488	0.471	0.453	0.345	0.346	0.348
0.787	0.570	0.563	0.551	0.730	0.731	0.732
1.574	0.651	0.669	0.645	1.509	1.507	1.509

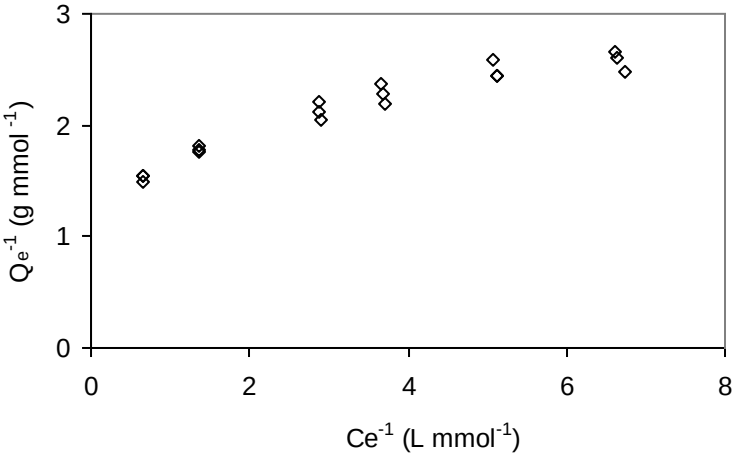


Figure H.26. Lineweaver-Burk plot relating equilibrium copper concentrations.

Table H.53. Sorption, Q_t, of copper to dehydrated BC13 cells with time at pH 2.5 and 45ºC. Initial concentrations were the highest tested for copper, 1.574 mM.

	Q_t (mmol g^{-1})					
Elapsed Time (min)	Trial 1	Trial 2	Trial 3	Average	STDEV	95% CI
0	0.000	0.000	0.000	0.000	0.000	0.000
1	1.735	1.843	1.715	1.764	0.069	0.078
5	1.788	1.809	1.751	1.783	0.029	0.033
15	1.835	1.952	1.858	1.882	0.062	0.070
30	1.815	1.943	1.912	1.890	0.067	0.076
60	1.851	1.986	1.821	1.886	0.088	0.099

Table H.54. Equilibrium sorption, Q_e, and solution, C_e, concentrations of copper in the presence of dehydrated BC13 cells at pH 2.5 and 45ºC, with varying concentrations, C_o.

	Q_e (mmol g^{-1})			C_e (mmol L^{-1})		
C_o (mmol L^{-1})	Trial 1	Trial 2	Trial 3	Trial 1	Trial 2	Trial 3
0.189	1.257	1.217	1.236	0.063	0.067	0.065
0.236	1.383	1.395	1.330	0.098	0.097	0.103
0.315	1.499	1.490	1.505	0.165	0.166	0.164
0.393	1.578	1.598	1.626	0.236	0.234	0.231
0.787	1.768	1.734	1.731	0.610	0.613	0.614
1.574	1.851	1.986	1.821	1.389	1.375	1.392

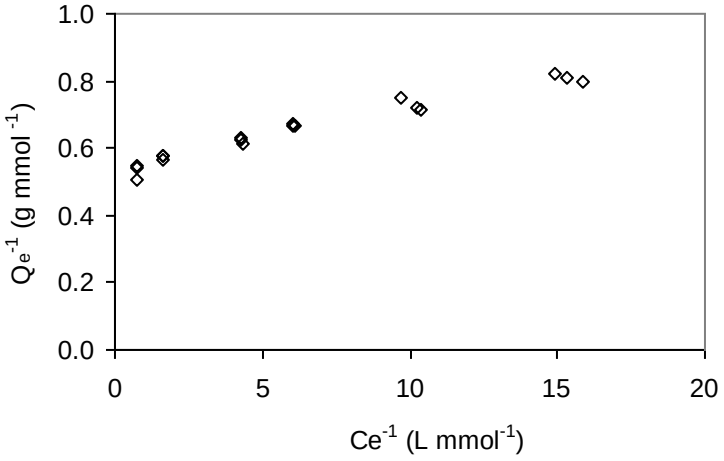


Figure H.27. Lineweaver-Burk plot relating equilibrium copper concentrations.

Table H.55. Sorption, Q_t, of copper to dehydrated BC13 cells with time at pH 4.0 and 45ºC. Initial concentrations were the highest tested for copper, 1.574 mM.

	Q_t (mmol g^{-1})					
Elapsed Time (min)	Trial 1	Trial 2	Trial 3	Average	STDEV	95% CI
0	0.000	0.000	0.000	0.000	0.000	0.000
1	2.097	2.302	2.269	2.223	0.110	0.125
5	2.308	2.490	2.340	2.380	0.098	0.110
15	2.380	2.568	2.466	2.471	0.094	0.107
30	2.532	2.607	2.379	2.506	0.116	0.132
60	2.492	2.527	2.421	2.480	0.054	0.061

Table H.56. Equilibrium sorption, Q_e, and solution, C_e, concentrations of copper in the presence of dehydrated BC13 cells at pH 4.0 and 45ºC, with varying concentrations, C_o.

	Q_e (mmol g^{-1})			C_e (mmol L^{-1})		
C_o (mmol L^{-1})	Trial 1	Trial 2	Trial 3	Trial 1	Trial 2	Trial 3
0.189	1.469	1.437	1.469	0.042	0.045	0.042
0.236	1.658	1.678	1.610	0.070	0.068	0.075
0.315	1.909	1.896	1.960	0.124	0.125	0.119
0.393	2.102	2.066	2.121	0.183	0.187	0.181
0.787	2.362	2.413	2.427	0.551	0.546	0.544
1.574	2.492	2.527	2.421	1.324	1.321	1.332

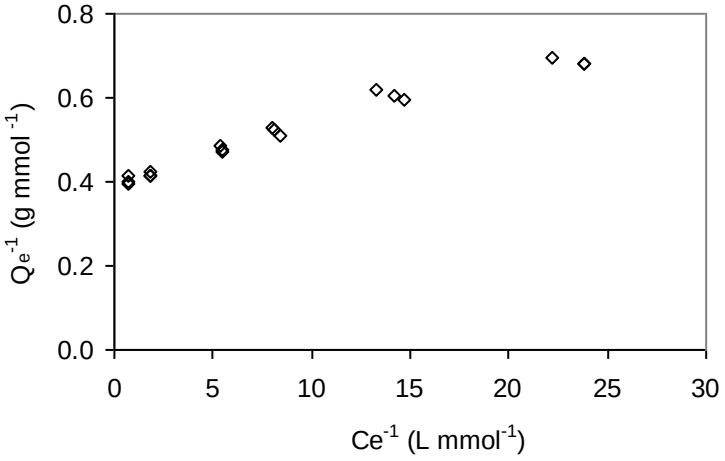


Figure H.28. Lineweaver-Burk plot relating equilibrium copper concentrations.

Table H.57. Sorption, Q_t, of copper to dehydrated BC13 cells with time at pH 5.5 and 45ºC. Initial concentrations were the highest tested for copper, 1.574 mM.

	Q_t (mmol g^{-1})					
Elapsed Time (min)	Trial 1	Trial 2	Trial 3	Average	STDEV	95% CI
0	0.000	0.000	0.000	0.000	0.000	0.000
1	2.885	3.152	3.022	3.020	0.134	0.151
5	3.058	3.353	3.228	3.213	0.148	0.167
15	3.158	3.433	3.161	3.251	0.158	0.179
30	3.316	3.605	3.305	3.408	0.170	0.193
60	3.231	3.308	3.242	3.261	0.041	0.047

Table H.58. Equilibrium sorption, Q_e, and solution, C_e, concentrations of copper in the presence of dehydrated BC13 cells at pH 5.5 and 45ºC, with varying concentrations, C_o.

	Q_e (mmol g^{-1})			C_e (mmol L^{-1})		
C_o (mmol L^{-1})	Trial 1	Trial 2	Trial 3	Trial 1	Trial 2	Trial 3
0.189	1.551	1.559	1.560	0.034	0.033	0.033
0.236	1.822	1.799	1.778	0.054	0.056	0.058
0.315	2.255	2.065	2.161	0.089	0.108	0.099
0.393	2.472	2.303	2.447	0.146	0.163	0.149
0.787	3.042	2.993	3.074	0.483	0.488	0.479
1.574	3.231	3.308	3.242	1.251	1.243	1.249

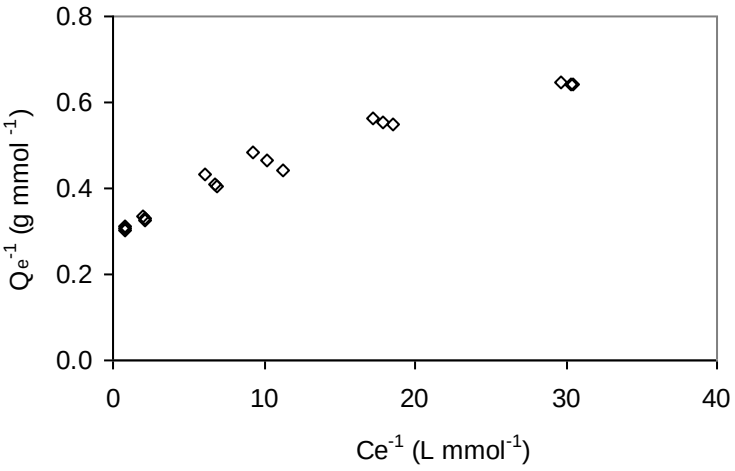


Figure H.29. Lineweaver-Burk plot relating equilibrium copper concentrations.

Table H.59. Sorption, Q_t, of copper to dehydrated BC13 cells with time at pH 7.0 and 45ºC. Initial concentrations were the highest tested for copper, 1.574 mM.

	Q_t (mmol g^{-1})					
Elapsed Time (min)	Trial 1	Trial 2	Trial 3	Average	STDEV	95% CI
0	0.000	0.000	0.000	0.000	0.000	0.000
1	1.982	2.128	2.012	2.041	0.077	0.087
5	2.088	2.269	2.259	2.205	0.102	0.115
15	2.421	2.474	2.261	2.385	0.111	0.125
30	2.524	2.596	2.347	2.489	0.128	0.145
60	2.493	2.505	2.444	2.481	0.032	0.036

Table H.60. Equilibrium sorption, Q_e, and solution, C_e, concentrations of copper in the presence of dehydrated BC13 cells at pH 7.0 and 45ºC, with varying concentrations, C_o.

	Q_e (mmol g^{-1})			C_e (mmol L^{-1})		
C_o (mmol L^{-1})	Trial 1	Trial 2	Trial 3	Trial 1	Trial 2	Trial 3
0.189	1.346	1.324	1.341	0.054	0.056	0.055
0.236	1.657	1.641	1.575	0.070	0.072	0.079
0.315	1.846	1.828	1.925	0.130	0.132	0.122
0.393	2.066	2.021	1.976	0.187	0.191	0.196
0.787	2.214	2.292	2.224	0.565	0.558	0.564
1.574	2.493	2.505	2.444	1.324	1.323	1.329

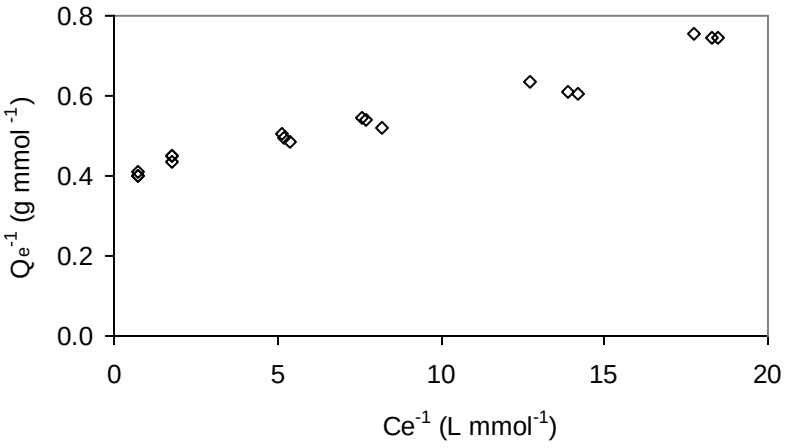


Figure H.30. Lineweaver-Burk plot relating equilibrium copper concentrations.

Summary of pH Effects on Heavy-Metal Sorption to BC13

Table H.61. Sorption affinity, k_L, and capacity, Q_o, for lead to BC13 at 45ºC calculated from Lineweaver-Burk plots using the LINEST function in Microsoft Excel. The corresponding R^2 values are shown, as well as the ratio of protons to complexed metals for the given pH. This ratio was predicted using MINTEQ thermodynamic modeling software.

Sorption of Lead to Viable Cells

pH	k_L (L mmol^{-1})	Q_o (mmol g^{-1})	Goodness of fit (R^2)	LN{[H^+][complexed ion]$^{-1}$}
1.5	14.50 ± 0.49	0.10 ± 0.01	0.986	9.26
2.5	41.43 ± 2.73	0.24 ± 0.01	0.949	6.68
4.0	58.03 ± 3.55	0.25 ± 0.01	0.955	3.12
5.5	60.12 ± 2.48	0.33 ± 0.01	0.979	-0.76
7.0	53.72 ± 2.01	0.34 ± 0.01	0.983	-6.27

Sorption of Lead to Dehydrated Cells

pH	k_L (L mmol^{-1})	Q_o (mmol g^{-1})	Goodness of fit (R^2)	LN{[H^+][complexed ion]$^{-1}$}
1.5	21.11 ± 1.18	0.05 ± 0.0	0.962	9.26
2.5	54.24 ± 3.25	0.13 ± 0.0	0.957	6.68
4.0	61.24 ± 2.98	0.22 ± 0.01	0.971	3.12
5.5	60.76 ± 1.96	0.29 ± 0.01	0.987	-0.76
7.0	52.80 ± 3.41	0.27 ± 0.01	0.950	-6.27

Table H.62. Table H.61. Sorption affinity, k_L, and capacity, Q_o, for zinc to BC13 at 45ºC calculated from Lineweaver-Burk plots using the LINEST function in Microsoft Excel. The corresponding R^2 values are shown, as well as the ratio of protons to complexed metals for the given pH. This ratio was predicted using MINTEQ thermodynamic modeling software.

Sorption of Zinc to Viable Cells

pH	k_L (L mmol^{-1})	Q_o (mmol g^{-1})	Goodness of fit (R^2)	LN{[H^+][complexed ion]$^{-1}$}
1.5	9.74 ± 0.62	0.58 ± 0.02	0.952	9.14
2.5	14.93 ± 0.57	1.56 ± 0.04	0.982	6.67
4.0	17.47 ± 1.07	1.53 ± 0.06	0.955	3.14
5.5	16.56 ± 0.99	1.67 ± 0.07	0.957	-1.31
7.0	14.31 ± 0.62	1.25 ± 0.03	0.977	-7.19

Sorption of Zinc to Dehydrated Cells

pH	k_L (L mmol^{-1})	Q_o (mmol g^{-1})	Goodness of fit (R^2)	LN{[H^+][complexed ion]$^{-1}$}
1.5	7.63 ± 0.34	0.22 ± 0.01	0.975	9.14
2.5	16.47 ± 1.05	0.55 ± 0.01	0.951	6.67
4.0	17.94 ± 1.05	0.95 ± 0.02	0.959	3.14
5.5	17.69 ± 0.93	0.93 ± 0.02	0.967	-1.31
7.0	15.32 ± 0.87	0.96 ± 0.03	0.961	-7.19

Table H.63. Table H.61. Sorption affinity, k_L, and capacity, Q_o, for copper to BC13 at 45ºC calculated from Lineweaver-Burk plots using the LINEST function in Microsoft Excel. The corresponding R^2 values are shown, as well as the ratio of protons to complexed metals for the given pH. This ratio was predicted using MINTEQ thermodynamic modeling software.

Sorption of Copper to Viable Cells

pH	k_L (L mmol^{-1})	Q_o (mmol g^{-1})	Goodness of fit (R^2)	LN{[H^+][complexed ion]$^{-1}$}
1.5	17.48 ± 0.98	1.55 ± 0.03	0.962	7.26
2.5	35.20 ± 1.93	2.72 ± 0.06	0.964	4.84
4.0	36.11 ± 1.89	4.75 ± 0.02	0.955	1.12
5.5	24.60 ± 1.45	4.76 ± 0.03	0.959	-4.64
7.0	18.93 ± 1.16	4.63 ± 0.03	0.955	-9.42

Sorption of Copper to Dehydrated Cells

pH	k_L (L mmol^{-1})	Q_o (mmol g^{-1})	Goodness of fit (R^2)	LN{[H^+][complexed ion]$^{-1}$}
1.5	8.78 ± 0.76	0.65 ± 0.03	0.914	7.26
2.5	29.59 ± 1.75	1.85 ± 0.03	0.958	4.84
4.0	31.60 ± 1.63	2.47 ± 0.05	0.968	1.12
5.5	28.35 ± 1.88	3.09 ± 0.11	0.948	-4.64
7.0	22.04 ± 1.20	2.51 ± 0.06	0.964	-9.42

Heavy-Metal Speciation under Experimental Conditions Tested

Table H.64. Speciation of lead at various pH and 45ºC predicted using MINTEQ thermodynamic modeling at the highest concentrations tested in sorption experiments (0.241 mM).

			pH		
Lead speciation	7.0	5.5	4.0	2.5	1.5
Pb^{+2}	76.27	97.85	98.99	99.19	96.58
$PbOH^{+}$	19.27	0.78	0.03	-	-
$PbHPO_4$ (aq)	3.82	0.36	0.01	-	-
$PbCl^{+}$	0.23	0.29	0.30	0.30	3.19
$PbH_2PO_4^{+}$	0.19	0.56	0.53	0.37	-
$PbNO_3^{+}$	0.09	0.12	0.12	0.12	-
Pb_2OH^{+3}	0.04	0.03	0.03	-	-
$Pb_3(OH)_4^{+2}$	0.04	-	-	-	-
$Pb(OH)_2$ (aq)	0.03	-	-	-	-
$PbSO_4$ (aq)	0.03	-	-	0.03	-

Table H.65. Speciation of zinc at various pH and 45ºC predicted using MINTEQ thermodynamic modeling at the highest concentrations tested in sorption experiments (0.918 mM).

			pH		
Zinc Speciation	7.0	5.5	4.0	2.5	1.5
Zn^{+2}	81.31	98.78	99.80	99.84	99.73
$ZnOH^{+}$	1.92	0.07	-	-	-
$Zn(OH)_2$ (aq)	0.05	-	-	-	-
$ZnCl^{+}$	0.09	0.11	0.11	0.11	-
$ZnSO_4$ (aq)	0.02	0.02	0.02	0.02	-
ZnS_4O_6 (aq)	0.02	0.02	0.02	0.02	-
$Zn(NH_3)_3^{+2}$	0.13	-	-	-	-
$Zn(NH_3)_2^{+2}$	1.01	-	-	-	-
$ZnNH_3^{+2}$	8.67	0.34	0.01	-	-
$ZnNO3^{+}$	0.02	0.02	0.02	0.02	-
$ZnHPO_4$ (aq)	6.77	0.64	0.02	-	-

Table H.66. Speciation of copper at various pH and 45ºC predicted using MINTEQ thermodynamic modeling at the highest concentrations tested in sorption experiments (1.574 mM).

			pH		
Copper Speciation	7.0	5.5	4.0	2.5	1.5
Cu^{+2}	5.32	79.19	98.75	99.43	99.29
$CuOH^{+}$	2.34	1.09	0.04	-	
$Cu(OH)_2$ (aq)	0.15	-	-	-	
$Cu_2(OH)_2^{+2}$	12.69	2.78	-	-	
$Cu_3(OH)_4^{+2}$	12.90	0.04	-	-	
$CuCl^{+}$	0.03	0.42	0.52	0.51	0.68
$Cu(NH_3)_4^{+2}$	0.45	-	-	-	
$Cu(NH_3)_3^{+2}$	8.58	-	-	-	
$Cu(NH_3)_2^{+2}$	28.42	0.48	-	-	
$CuNH_3^{+2}$	26.71	13.39	0.53	0.02	
$CuHPO^4$ (aq)	2.40	2.52	0.11	-	
$CuSO_4$ (aq)	-	0.02	0.02	0.02	
Cu_2OH^{+3}	-	0.04	-	-	
$CuNO_3^{+}$	-	0.02	0.02	0.02	0.02

Effects of Temperature on Heavy-Metal Sorption to BC13

Lead

Table H.67. Equilibrium sorption, Q_e, and solution, C_e, concentrations of lead in the presence of viable BC13 cells at pH 2.5 and 25ºC, with varying concentrations, C_o.

	Q_e (mmol g^{-1})			C_e (mmol L^{-1})		
C_o (mmol L^{-1})	Trial 1	Trial 2	Trial 3	Trial 1	Trial 2	Trial 3
0.029	0.123	0.125	0.125	0.017	0.016	0.016
0.039	0.152	0.151	0.150	0.023	0.024	0.024
0.048	0.164	0.159	0.163	0.032	0.032	0.032
0.072	0.191	0.193	0.194	0.053	0.053	0.053
0.121	0.205	0.199	0.200	0.100	0.101	0.101
0.241	0.224	0.228	0.234	0.219	0.219	0.218

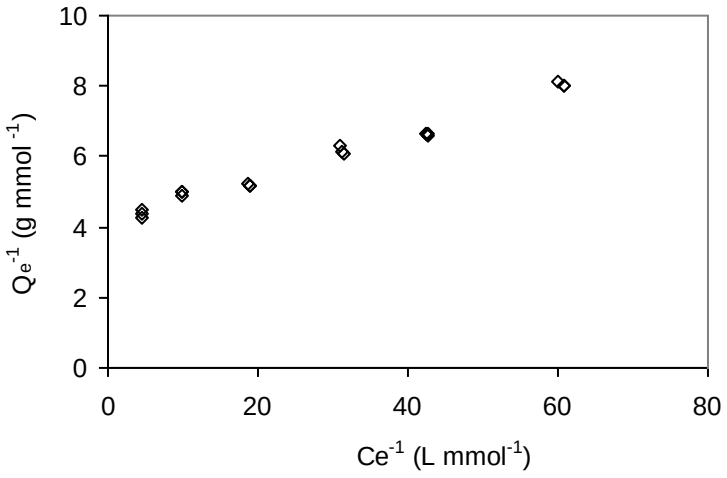


Figure H.31. Lineweaver-Burk plot relating equilibrium lead concentrations.

Table H.68. Equilibrium sorption, Q_e, and solution, C_e, concentrations of lead in the presence of dehydrated BC13 cells at pH 2.5 and 25ºC, with varying concentrations, C_o.

	Q_e (mmol g^{-1})			C_e (mmol L^{-1})		
C_o (mmol L^{-1})	Trial 1	Trial 2	Trial 3	Trial 1	Trial 2	Trial 3
0.029	0.087	0.086	0.085	0.020	0.020	0.020
0.039	0.093	0.094	0.096	0.029	0.029	0.029
0.048	0.099	0.098	0.095	0.038	0.038	0.039
0.072	0.107	0.105	0.106	0.062	0.062	0.062
0.121	0.113	0.120	0.111	0.109	0.109	0.110
0.241	0.120	0.125	0.126	0.229	0.229	0.229

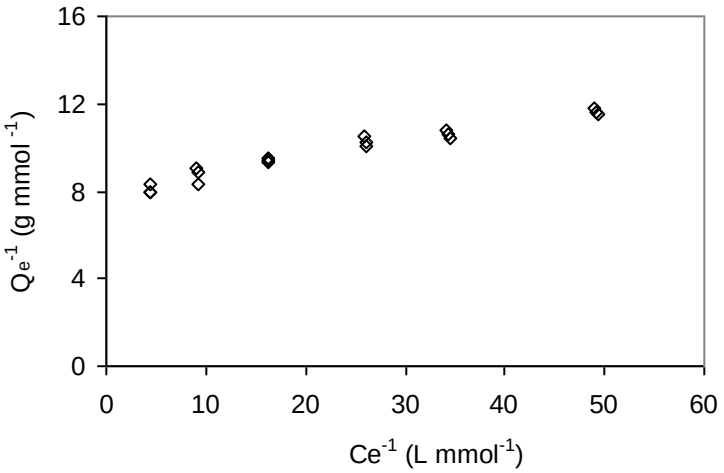


Figure H.32. Lineweaver-Burk plot relating equilibrium lead concentrations.

Table H.69. Equilibrium sorption, Q_e, and solution, C_e, concentrations of lead in the presence of viable BC13 cells at pH 2.5 and 35ºC, with varying concentrations, C_o.

	Q_e (mmol g^{-1})			C_e (mmol L^{-1})		
C_o (mmol L^{-1})	Trial 1	Trial 2	Trial 3	Trial 1	Trial 2	Trial 3
0.029	0.121	0.120	0.123	0.017	0.017	0.017
0.039	0.154	0.149	0.154	0.023	0.024	0.023
0.048	0.167	0.162	0.165	0.032	0.032	0.032
0.072	0.194	0.188	0.190	0.053	0.054	0.053
0.121	0.210	0.206	0.205	0.100	0.100	0.100
0.241	0.228	0.232	0.230	0.219	0.218	0.218

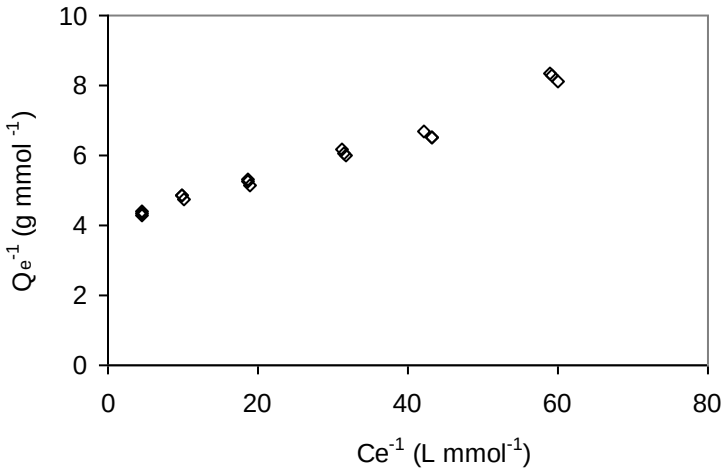


Figure H.33. Lineweaver-Burk plot relating equilibrium lead concentrations.

Table H.70. Equilibrium sorption, Q_e, and solution, C_e, concentrations of lead in the presence of dehydrated BC13 cells at pH 2.5 and 35ºC, with varying concentrations, C_o.

	Q_e (mmol g^{-1})			C_e (mmol L^{-1})		
C_o (mmol L^{-1})	Trial 1	Trial 2	Trial 3	Trial 1	Trial 2	Trial 3
0.029	0.079	0.081	0.082	0.021	0.021	0.021
0.039	0.090	0.086	0.088	0.030	0.030	0.030
0.048	0.094	0.093	0.095	0.039	0.039	0.039
0.072	0.107	0.105	0.096	0.062	0.062	0.063
0.121	0.113	0.120	0.111	0.109	0.109	0.110
0.241	0.124	0.130	0.135	0.229	0.228	0.228

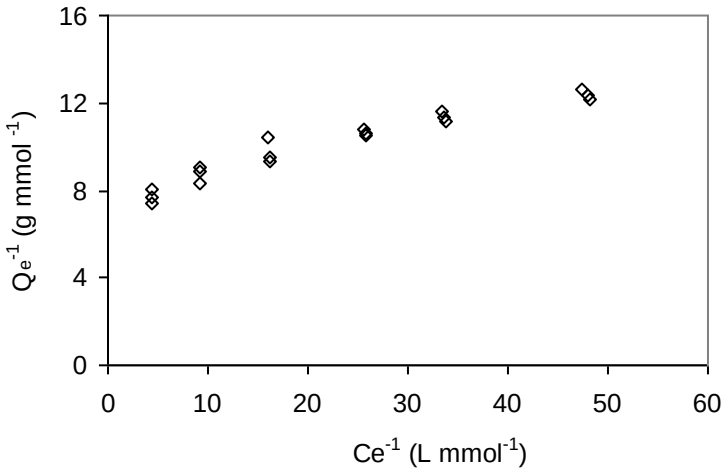


Figure H.34. Lineweaver-Burk plot relating equilibrium lead concentrations.

Zinc

Table H.71. Equilibrium sorption, Q_e, and solution, C_e, concentrations of zinc in the presence of viable BC13 cells at pH 2.5 and 25ºC, with varying concentrations, C_o.

	Q_e (mmol g^{-1})			C_e (mmol L^{-1})		
C_o (mmol L^{-1})	Trial 1	Trial 2	Trial 3	Trial 1	Trial 2	Trial 3
0.122	0.863	0.871	0.855	0.036	0.035	0.037
0.184	1.094	1.052	1.075	0.074	0.078	0.076
0.229	1.157	1.169	1.152	0.114	0.113	0.114
0.306	1.320	1.291	1.300	0.174	0.177	0.176
0.459	1.460	1.455	1.496	0.313	0.313	0.309
0.918	1.523	1.517	1.510	0.765	0.766	0.767

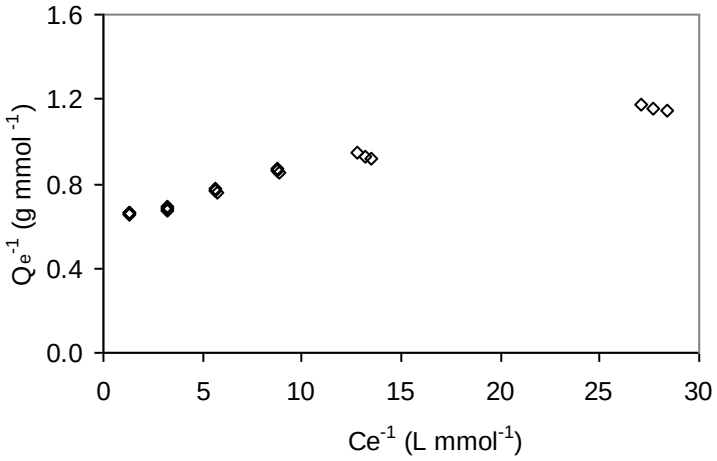


Figure H.35. Lineweaver-Burk plot relating equilibrium zinc concentrations.

Table H.72. Equilibrium sorption, Q_e, and solution, C_e, concentrations of zinc in the presence of dehydrated BC13 cells at pH 2.5 and 25ºC, with varying concentrations, C_o.

	Q_e (mmol g^{-1})			C_e (mmol L^{-1})		
C_o (mmol L^{-1})	Trial 1	Trial 2	Trial 3	Trial 1	Trial 2	Trial 3
0.122	0.412	0.422	0.410	0.081	0.080	0.081
0.184	0.440	0.435	0.431	0.140	0.140	0.140
0.229	0.465	0.462	0.470	0.183	0.183	0.182
0.306	0.480	0.471	0.463	0.258	0.259	0.260
0.459	0.523	0.515	0.515	0.407	0.407	0.407
0.918	0.543	0.552	0.524	0.863	0.863	0.865

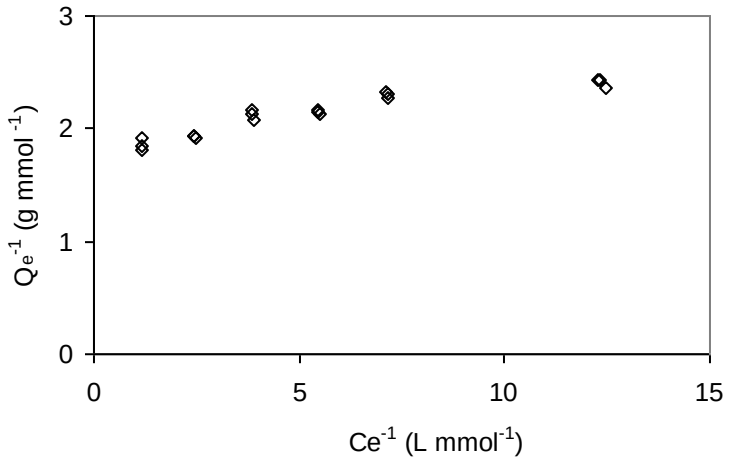


Figure H.36. Lineweaver-Burk plot relating equilibrium zinc concentrations.

Table H.73. Equilibrium sorption, Q_e, and solution, C_e, concentrations of zinc in the presence of viable BC13 cells at pH 2.5 and 35ºC, with varying concentrations, C_o.

	Q_e (mmol g^{-1})			C_e (mmol L^{-1})		
C_o (mmol L^{-1})	Trial 1	Trial 2	Trial 3	Trial 1	Trial 2	Trial 3
0.122	0.802	0.815	0.823	0.042	0.041	0.040
0.184	1.054	0.974	0.992	0.078	0.086	0.084
0.229	1.203	1.154	1.160	0.109	0.114	0.113
0.306	1.301	1.258	1.277	0.176	0.180	0.178
0.459	1.497	1.450	1.462	0.309	0.314	0.313
0.918	1.590	1.543	1.556	0.759	0.763	0.762

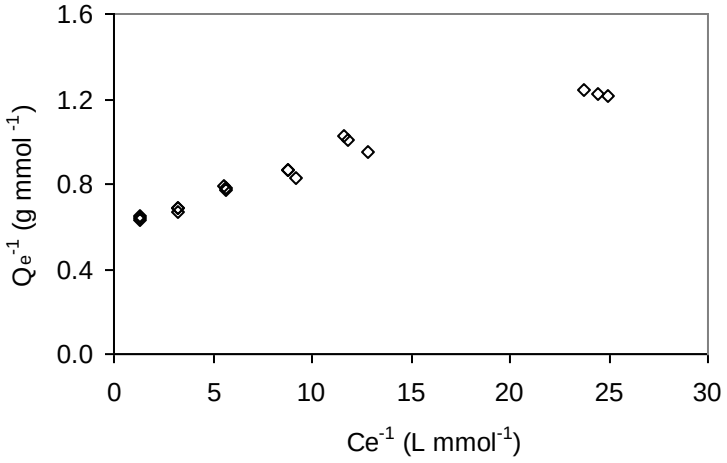


Figure H.37. Lineweaver-Burk plot relating equilibrium zinc concentrations.

Table H.74. Equilibrium sorption, Q_e, and solution, C_e, concentrations of zinc in the presence of dehydrated BC13 cells at pH 2.5 and 35ºC, with varying concentrations, C_o.

	Q_e (mmol g^{-1})			C_e (mmol L^{-1})		
C_o (mmol L^{-1})	Trial 1	Trial 2	Trial 3	Trial 1	Trial 2	Trial 3
0.122	0.384	0.367	0.379	0.084	0.086	0.084
0.184	0.423	0.440	0.425	0.141	0.140	0.141
0.229	0.451	0.449	0.440	0.184	0.185	0.185
0.306	0.456	0.461	0.452	0.260	0.260	0.261
0.459	0.490	0.482	0.493	0.410	0.411	0.410
0.918	0.543	0.550	0.533	0.863	0.863	0.864

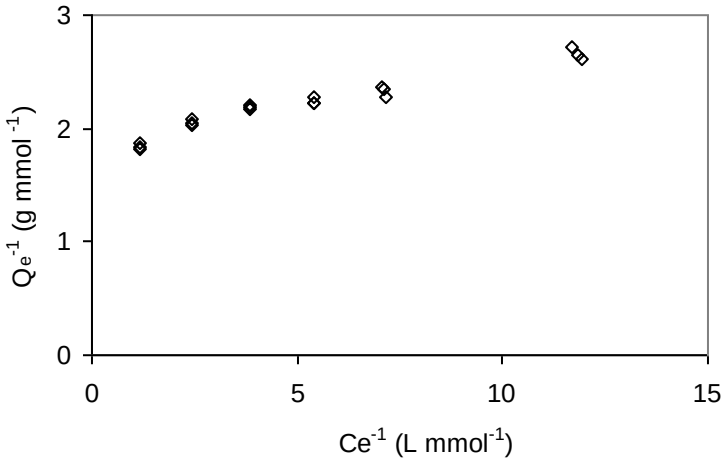


Figure H.38. Lineweaver-Burk plot relating equilibrium zinc concentrations.

Copper

Table H.75. Equilibrium sorption, Q_e, and solution, C_e, concentrations of copper in the presence of viable BC13 cells at pH 2.5 and 25ºC, with varying concentrations, C_o.

	Q_e (mmol g^{-1})			C_e (mmol L^{-1})		
C_o (mmol L^{-1})	Trial 1	Trial 2	Trial 3	Trial 1	Trial 2	Trial 3
0.189	1.644	1.650	1.647	0.024	0.024	0.024
0.236	2.052	2.040	2.022	0.031	0.032	0.034
0.315	2.564	2.514	2.499	0.058	0.063	0.065
0.393	2.662	2.590	2.531	0.127	0.134	0.140
0.787	3.045	3.036	3.027	0.482	0.483	0.484
1.574	3.153	3.180	3.210	1.258	1.256	1.253

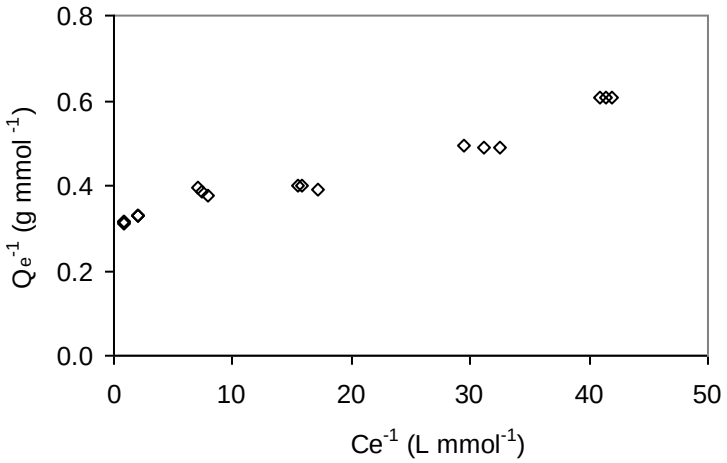


Figure H.39. Lineweaver-Burk plot relating equilibrium copper concentrations.

Table H.76. Equilibrium sorption, Q_e, and solution, C_e, concentrations of copper in the presence of dehydrated BC13 cells at pH 2.5 and 25ºC, with varying concentrations, C_o.

	Q_e (mmol g^{-1})			C_e (mmol L^{-1})		
C_o (mmol L^{-1})	Trial 1	Trial 2	Trial 3	Trial 1	Trial 2	Trial 3
0.189	1.423	1.389	1.424	0.047	0.050	0.046
0.236	1.523	1.547	1.564	0.084	0.081	0.080
0.315	1.623	1.640	1.605	0.152	0.151	0.154
0.393	1.731	1.754	1.704	0.220	0.218	0.223
0.787	1.791	1.802	1.892	0.608	0.607	0.598
1.574	1.810	1.823	1.842	1.393	1.391	1.389

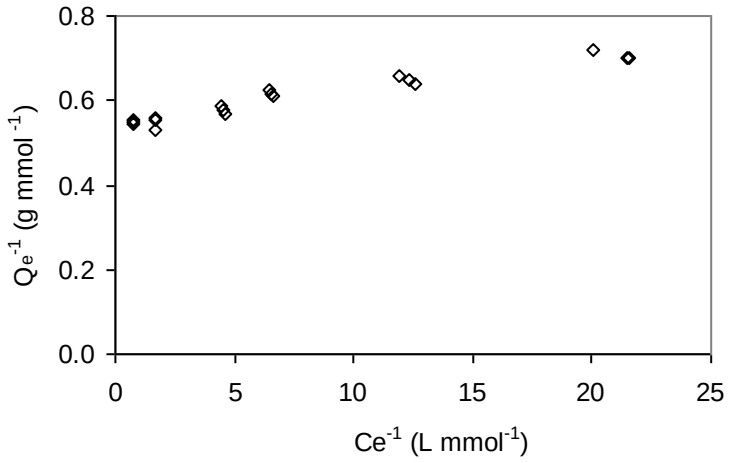


Figure H.40. Specific growth rate calculations for Trial 1 (open circles), Trial 2 (open squares), and Trial 3 (open triangles).

Table H.77. Equilibrium sorption, Q_e, and solution, C_e, concentrations of copper in the presence of viable BC13 cells at pH 2.5 and 35ºC, with varying concentrations, C_o.

	Q_e (mmol g^{-1})			C_e (mmol L^{-1})		
C_o (mmol L^{-1})	Trial 1	Trial 2	Trial 3	Trial 1	Trial 2	Trial 3
0.189	1.634	1.611	1.650	0.025	0.028	0.024
0.236	1.921	1.847	1.923	0.044	0.051	0.044
0.315	2.309	2.313	2.415	0.084	0.083	0.073
0.393	2.654	2.599	2.601	0.128	0.134	0.133
0.787	3.030	3.054	3.052	0.484	0.481	0.482
1.574	3.218	3.457	3.334	1.252	1.228	1.240

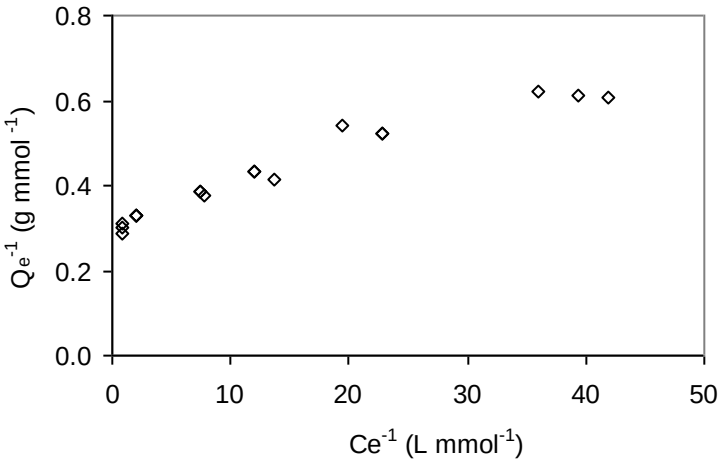


Figure H.41. Lineweaver-Burk plot relating equilibrium copper concentrations.

Table H.78. Equilibrium sorption, Q_e, and solution, C_e, concentrations of copper in the presence of dehydrated BC13 cells at pH 2.5 and 35ºC, with varying concentrations, C_o.

	Q_e (mmol g^{-1})			C_e (mmol L^{-1})		
C_o (mmol L^{-1})	Trial 1	Trial 2	Trial 3	Trial 1	Trial 2	Trial 3
0.189	1.320	1.365	1.354	0.057	0.052	0.053
0.236	1.450	1.425	1.456	0.091	0.094	0.090
0.315	1.580	1.602	1.596	0.157	0.155	0.155
0.393	1.700	1.623	1.648	0.223	0.231	0.229
0.787	1.791	1.802	1.892	0.608	0.607	0.598
1.574	1.840	1.830	1.825	1.390	1.391	1.391

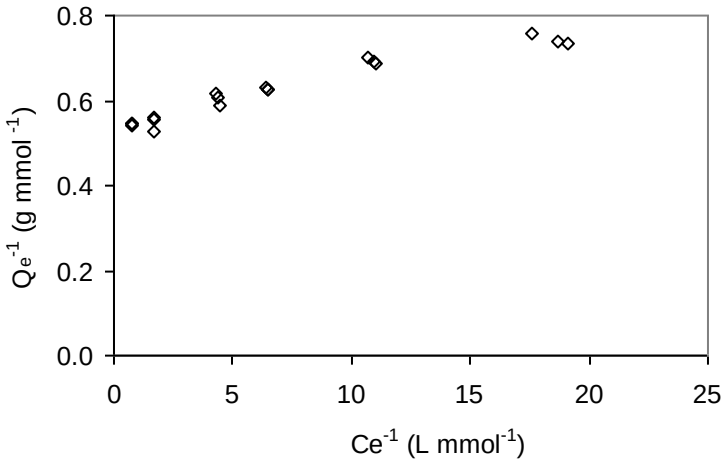


Figure H.42. Lineweaver-Burk plot relating equilibrium copper concentrations.

Summary of Temperature Effects on Heavy-Metal Sorption to BC13

Table H.79. Sorption capacity, Q_o, and affinity, k_L, of lead for BC13 cells with changes in temperature at pH 2.5. The Arrhenius pre-exponential factor, A, and heat of sorption, ΔH, are also shown. R is the universal gas constant, 0.00831 KJ K^{-1} mol^{-1}.

			Viable		
T (C^o)	Q_o (mmol g^{-1})	k_L (L $mmol^{-1}$)	$R^{-1}T^{-1}$ (K^{-1})	ln[k_L(L $mmol^{-1}$)]	A (L $mmol^{-1}$)
25	0.24 ± 0.0	66.24 ± 2.39	0.40	4.19	0.07
35	0.25 ± 0.01	60.15 ± 2.63	0.39	4.10	ΔH (kJ mol^{-1})
45	0.24 ± 0.01	41.43 ± 2.73	0.38	3.72	-18.38

			Freeze-dried		
T (C^o)	Q_o (mmol g^{-1})	k_L (L $mmol^{-1}$)	$R^{-1}T^{-1}$ (K^{-1})	ln[k_L(L $mmol^{-1}$)]	A (L $mmol^{-1}$)
25	0.13 ± 0.0	104.89 ± 6.50	0.40	4.65	0.00
35	0.13 ± 0.0	74.46 ± 5.63	0.39	4.31	ΔH (kJ mol^{-1})
45	0.13 ± 0.0	54.24 ± 3.25	0.38	3.99	-26.01

Table H.80. Sorption capacity, Q_o, and affinity, k_L, of lead for BC13 cells with changes in temperature at pH 2.5. The Arrhenius pre-exponential factor, A, and heat of sorption, ΔH, are also shown. R is the universal gas constant, 0.00831 KJ K^{-1} mol^{-1}.

			Viable		
T (C^o)	Q_o (mmol g^{-1})	k_L (L $mmol^{-1}$)	$R^{-1}T^{-1}$ (K^{-1})	ln[k_L(L $mmol^{-1}$)]	A (L $mmol^{-1}$)
25	1.53 ± 0.03	34.34 ± 1.76	0.40	3.54	0.00
35	1.60 ± 0.04	24.13 ± 1.32	0.39	3.18	ΔH (kJ mol^{-1})
45	1.56 ± 0.04	14.93 ± 0.57	0.38	2.70	-32.79

			Freeze-dried		
T (C^o)	Q_o (mmol g^{-1})	k_L (L $mmol^{-1}$)	$R^{-1}T^{-1}$ (K^{-1})	ln[k_L(L $mmol^{-1}$)]	A (L $mmol^{-1}$)
25	0.54 ± 0.01	37.22 ± 3.87	0.40	3.62	0.00
35	0.54 ± 0.01	26.41 ± 1.82	0.39	3.27	ΔH (kJ mol^{-1})
45	0.55 ± 0.01	16.47 ± 1.05	0.38	2.80	-32.09

Table H.81. Sorption capacity, Q_o, and affinity, k_L, of lead for BC13 cells with changes in temperature at pH 2.5. The Arrhenius pre-exponential factor, A, and heat of sorption, ΔH, are also shown. R is the universal gas constant, 0.00831 KJ K^{-1} mol^{-1}.

			Viable		
T (C°)	Q_o (mmol g^{-1})	k_L (L $mmol^{-1}$)	$R^{-1}T^{-1}$ (K^{-1})	ln[k_L(L $mmol^{-1}$)]	A (L $mmol^{-1}$)
25	3.20 ± 0.09	47.82 ± 2.84	0.40	3.87	0.36
35	3.16 ± 0.10	39.22 ± 2.60	0.39	3.67	ΔH (kJ mol^{-1})
45	2.72 ± 0.06	35.20 ± 1.93	0.38	3.56	-12.12

			Freeze-dried		
T (C°)	Q_o (mmol g^{-1})	k_L (L $mmol^{-1}$)	$R^{-1}T^{-1}$ (K^{-1})	ln[k_L(L $mmol^{-1}$)]	A (L $mmol^{-1}$)
25	1.84 ± 0.02	67.62 ± 4.56	0.40	4.21	0.00
35	1.84 ± 0.03	47.07 ± 3.39	0.39	3.85	ΔH (kJ mol^{-1})
45	1.85 ± 0.03	29.59 ± 1.75	0.38	3.39	-32.54

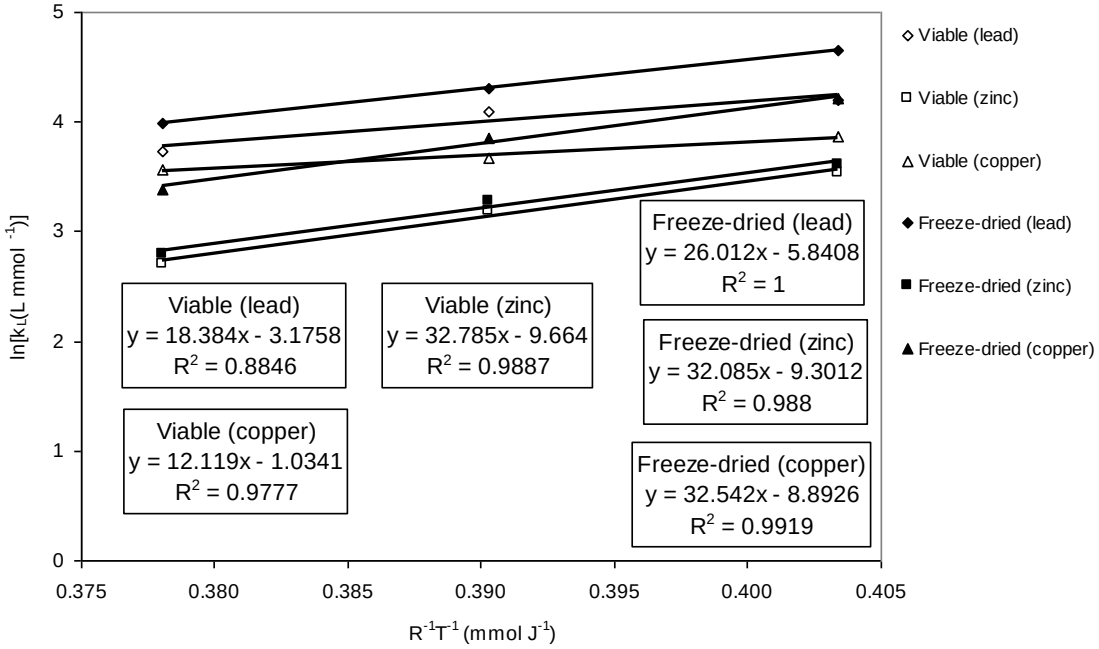


Figure H.43. Arrhenius plot used to calculate the pre-exponential factor (natural logarithm of the y-intercept) and the heat of sorption (negative of the slope).

<u>Zinc</u>

Sorption of Heavy-Metal Mixtures

Table H.82. Equilibrium sorption concentrations, Q_e, of lead, zinc, and copper when added individually to the highest concentrations tested, 0.241, 0.918, and 1.574 mM for lead, zinc, and copper respectively. Experiments were carried out using viable BC13 cells at pH 2.5 and 45ºC.

	Q_e (mmol g^{-1})					
	Trial 1	Trial 2	Trial 3	Average	STDEV	95% CI
Lead	0.208	0.212	0.203	0.208	0.004	0.005
Zinc	1.455	1.502	1.479	1.479	0.023	0.027
Copper	2.888	2.850	2.732	2.823	0.082	0.092

Table H.83. Equilibrium sorption concentrations, Q_e, of lead, zinc, and copper when added as metal mixtures. The concentrations given are for the metals listed outside of parenthesis in the presence of metals listed inside the parenthesis. All metals were added to the highest concentrations tested, 0.241, 0.918, and 1.574 mM for lead, zinc, and copper respectively. Experiments were carried out using viable BC13 cells at pH 2.5 and 45ºC.

	Q_e (mmol g^{-1})				
	Trial 2	Trial 3	Average	STDEV	95% CI
Lead	0.202	0.194	0.198	0.004	0.005
Lead (+Zinc)	0.197	0.187	0.194	0.006	0.007
Lead (+Copper)	0.091	0.099	0.096	0.005	0.006
Zinc	1.408	1.412	1.369	0.071	0.081
Zinc (+Lead)	1.391	1.461	1.413	0.041	0.047
Zinc (+Copper)	0.451	0.467	0.500	0.072	0.081
Copper	2.747	2.668	2.677	0.065	0.074
Copper (+Lead)	2.772	2.716	2.709	0.067	0.075
Copper (+Zinc)	2.806	2.750	2.739	0.073	0.082
Lead (+Zinc, Copper)	0.075	0.084	0.083	0.008	0.009
Zinc (+Lead, Copper)	0.392	0.399	0.424	0.049	0.056
Copper (+Lead, Zinc)	2.659	2.510	2.577	0.076	0.086

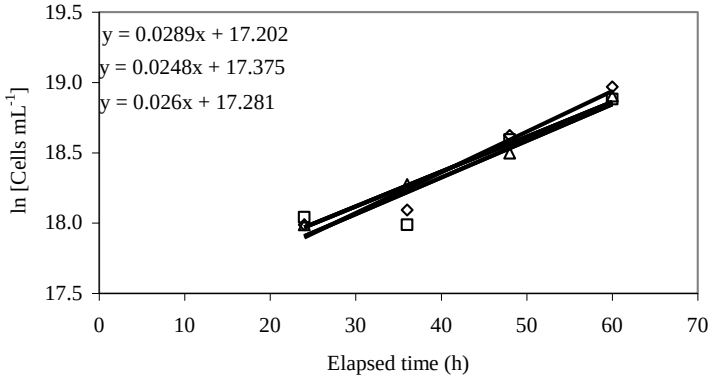
APPENDIX I

CHAPTER SIX RAW DATA

Growth of BC13 in Spent Growth Medium Containing Heavy Metals

Table I.1. BC13 growth in spent medium containing no heavy metals.

	Cells mL^{-1}						ln (Cells mL^{-1})		
Elapsed Time (h)	Trial 1	Trial 2	Trial 3	Average	STDEV	95% CI	Trial 1	Trial 2	Trial 3
0	5.40E+07	5.04E+07	4.32E+07	4.92E+07	5.50E+06	6.22E+06	17.80	17.74	17.58
12	5.76E+07	5.40E+07	4.68E+07	5.28E+07	5.50E+06	6.22E+06	17.87	17.80	17.66
24	6.48E+07	6.84E+07	6.48E+07	6.60E+07	2.08E+06	2.35E+06	17.99	18.04	17.99
36	7.20E+07	6.48E+07	8.64E+07	7.44E+07	1.10E+07	1.24E+07	18.09	17.99	18.27
48	1.22E+08	1.19E+08	1.08E+08	1.16E+08	7.49E+06	8.48E+06	18.62	18.59	18.50
60	1.73E+08	1.58E+08	1.62E+08	1.64E+08	7.49E+06	8.48E+06	18.97	18.88	18.90
72	2.12E+08	2.12E+08	2.09E+08	2.11E+08	2.08E+06	2.35E+06	19.17	19.17	19.16
84	2.27E+08	2.48E+08	2.34E+08	2.36E+08	1.10E+07	1.24E+07	19.24	19.33	19.27
96	2.45E+08	2.56E+08	2.59E+08	2.53E+08	7.49E+06	8.48E+06	19.32	19.36	19.37
108	2.70E+08	2.77E+08	2.70E+08	2.72E+08	4.16E+06	4.70E+06	19.41	19.44	19.41
120	3.02E+08	2.45E+08	2.56E+08	2.68E+08	3.06E+07	3.46E+07	19.53	19.32	19.36

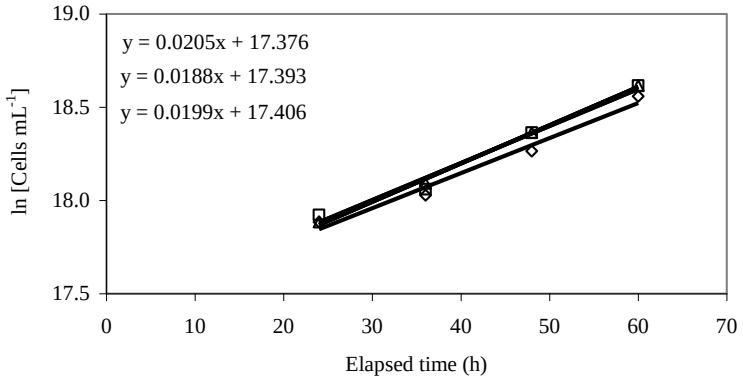


Specific growth rates (h^{-1})	
Trial 1	0.029
Trial 2	0.025
Trial 3	0.026
Average	0.027
STDEV	0.002
95% CI	0.002

Figure I.1. Specific growth rate calculations for Trial 1 (open circles), Trial 2 (open squares), and Trial 3 (open triangles).

Table I.2. BC13 growth in spent medium containing lead.

	Cells mL^{-1}						ln (Cells mL^{-1})		
Elapsed Time (h)	Trial 1	Trial 2	Trial 3	Average	STDEV	95% CI	Trial 1	Trial 2	Trial 3
0	4.5E+07	5.2E+07	4.7E+07	4.80E+07	3.44E+06	3.89E+06	17.62	17.76	17.67
12	4.5E+07	5.2E+07	5.4E+07	5.03E+07	4.68E+06	5.30E+06	17.62	17.76	17.80
24	5.9E+07	6.1E+07	5.9E+07	5.93E+07	1.30E+06	1.47E+06	17.88	17.92	17.88
36	6.8E+07	7.0E+07	7.2E+07	6.98E+07	2.25E+06	2.55E+06	18.03	18.06	18.09
48	8.6E+07	9.5E+07	9.5E+07	9.15E+07	5.20E+06	5.88E+06	18.26	18.36	18.36
60	1.1E+08	1.2E+08	1.2E+08	1.19E+08	3.90E+06	4.41E+06	18.56	18.62	18.62
72	1.3E+08	9.9E+07	1.0E+08	1.11E+08	1.70E+07	1.93E+07	18.68	18.41	18.45
84	1.5E+08	1.3E+08	1.3E+08	1.38E+08	1.30E+07	1.47E+07	18.84	18.68	18.68
96	1.3E+08	1.3E+08	1.2E+08	1.27E+08	9.37E+06	1.06E+07	18.72	18.68	18.57
108	1.5E+08	1.2E+08	1.3E+08	1.29E+08	1.50E+07	1.70E+07	18.80	18.57	18.65
120	1.5E+08	1.1E+08	1.4E+08	1.35E+08	2.04E+07	2.31E+07	18.83	18.53	18.78

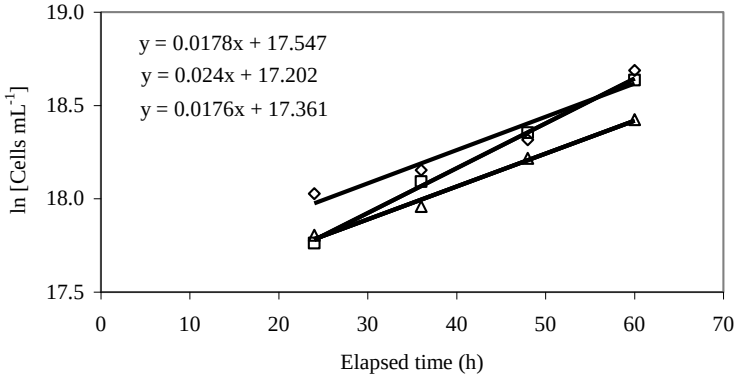


Specific growth rates (h^{-1})	
Trial 1	0.021
Trial 2	0.019
Trial 3	0.020
Average	0.020
STDEV	0.001
95% CI	0.001

Figure I.2. Specific growth rate calculations for Trial 1 (open circles), Trial 2 (open squares), and Trial 3 (open triangles).

Table I.3. BC13 growth in spent medium containing zinc.

	Cells mL^{-1}						ln (Cells mL^{-1})		
Elapsed Time (h)	Trial 1	Trial 2	Trial 3	Average	STDEV	95% CI	Trial 1	Trial 2	Trial 3
0	5.0E+07	4.7E+07	4.5E+07	4.73E+07	2.25E+06	2.55E+06	17.72	17.67	17.62
12	5.0E+07	4.7E+07	4.5E+07	4.73E+07	2.25E+06	2.55E+06	17.72	17.67	17.62
24	6.8E+07	5.2E+07	5.4E+07	5.78E+07	8.52E+06	9.64E+06	18.03	17.76	17.80
36	7.7E+07	7.2E+07	6.3E+07	7.05E+07	6.87E+06	7.78E+06	18.15	18.09	17.96
48	9.0E+07	9.4E+07	8.2E+07	8.83E+07	6.17E+06	6.98E+06	18.32	18.35	18.22
60	1.3E+08	1.2E+08	1.0E+08	1.18E+08	1.59E+07	1.80E+07	18.69	18.64	18.42
72	1.5E+08	4.2E+07	1.6E+08	1.18E+08	6.59E+07	7.45E+07	18.82	17.55	18.90
84	1.6E+08	1.3E+08	1.3E+08	1.41E+08	1.31E+07	1.48E+07	18.87	18.72	18.70
96	1.5E+08	1.6E+08	1.4E+08	1.50E+08	6.28E+06	7.10E+06	18.83	18.86	18.78
108	1.7E+08	1.4E+08	1.5E+08	1.54E+08	1.27E+07	1.44E+07	18.94	18.78	18.83
120	1.5E+08	1.5E+08	1.6E+08	1.52E+08	4.26E+06	4.82E+06	18.84	18.81	18.87

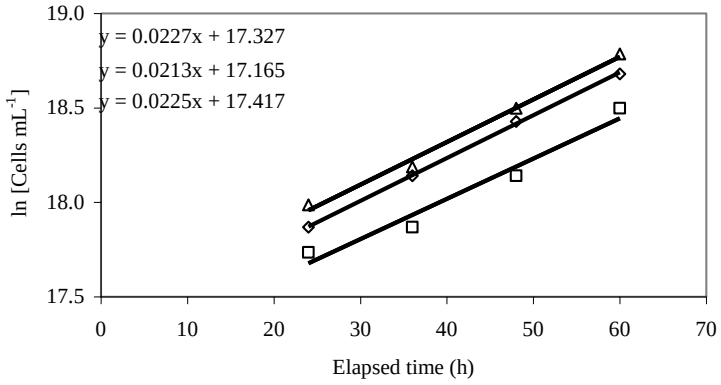


Specific growth rates (h^{-1})	
Trial 1	0.018
Trial 2	0.024
Trial 3	0.018
Average	0.020
STDEV	0.004
95% CI	0.004

Figure I.3. Specific growth rate calculations for Trial 1 (open circles), Trial 2 (open squares), and Trial 3 (open triangles).

Table I.4. BC13 growth in spent medium containing copper.

	Cells mL^{-1}						ln (Cells mL^{-1})		
Elapsed Time (h)	Trial 1	Trial 2	Trial 3	Average	STDEV	95% CI	Trial 1	Trial 2	Trial 3
0	5.76E+07	3.96E+07	5.04E+07	4.92E+07	9.06E+06	1.03E+07	17.87	17.49	17.74
12	5.76E+07	4.68E+07	5.40E+07	5.28E+07	5.50E+06	6.22E+06	17.87	17.66	17.80
24	5.76E+07	5.04E+07	6.48E+07	5.76E+07	7.20E+06	8.15E+06	17.87	17.74	17.99
36	7.56E+07	5.76E+07	7.92E+07	7.08E+07	1.16E+07	1.31E+07	18.14	17.87	18.19
48	1.01E+08	7.56E+07	1.08E+08	9.48E+07	1.70E+07	1.93E+07	18.43	18.14	18.50
60	1.30E+08	1.08E+08	1.44E+08	1.27E+08	1.81E+07	2.05E+07	18.68	18.50	18.79
72	1.37E+08	1.30E+08	1.34E+08	1.34E+08	3.60E+06	4.07E+06	18.74	18.68	18.71
84	1.66E+08	1.23E+08	1.66E+08	1.52E+08	2.49E+07	2.82E+07	18.93	18.63	18.93
96	1.73E+08	1.48E+08	2.02E+08	1.74E+08	2.70E+07	3.06E+07	18.97	18.81	19.12
108	1.84E+08	1.66E+08	2.06E+08	1.85E+08	1.98E+07	2.24E+07	19.03	18.93	19.14
120	1.80E+08	1.77E+08	2.13E+08	1.90E+08	1.98E+07	2.24E+07	19.01	18.99	19.18



Specific growth rates (h^{-1})	
Trial 1	0.023
Trial 2	0.021
Trial 3	0.023
Average	0.022
STDEV	0.001
95% CI	0.001

Figure I.4. Specific growth rate calculations for Trial 1 (open circles), Trial 2 (open squares), and Trial 3 (open triangles).

Heavy Metal Concentrations Remaining in Spent Medium Preceding Re-inoculation

Table I.5. Concentration of lead, zinc, or copper remaining in spent medium following initial exposure to BC13. Concentration is given as a percentage of the previously calculated IC_{50}s, and was used to predict an expected toxicity of the fresh inoculum.

	Percent of IC_{50}	95% CI
Lead	59.26	15.57
Zinc	63.64	1.71
Copper	77.33	1.28

MALDI Whole-Cell Analysis of BC13 in the Presence of Organic Acids and Metals

Table I.6. Counts per second per cell (CPS) of at various molecular weights (MW) during whole-cell MALDI analysis of BC13 cells exposed to different organic acids.

Organic acid free control		Pyruvate		Malate		Fumarate	
MW	CPS	MW	CPS	MW	CPS	MW	CPS
6515	0.40	7205	0.81	11775	1.77	7426	1.56
6517	2.22	7243	0.81	11944	1.06	7430	1.51
6517	0.86	7370	0.80	11968	1.63	7448	1.32
6518	1.74	7462	0.94	16042	1.92	7453	1.37
6518	6.08	7551	0.87	16151	2.05	7554	1.18
6520	6.43	7569	0.79	16171	1.23	7977	2.05
6521	2.12	7664	0.87	16416	1.14	7999	1.51
6522	1.14	7666	0.78	16442	1.49	8055	1.68
6522	1.12	7771	0.95	17242	1.45	8057	1.84
6523	0.95	7798	0.84	17377	1.02	8098	1.71
6524	0.32	7839	0.84	17389	1.20	8169	1.86
7223	0.27	7957	0.88	17404	1.50	8182	1.93
9221	0.29	7972	0.79	17416	1.14	8247	2.39
9222	1.15	8075	0.99	17434	1.30	8289	1.39
9222	0.60	8090	0.82	17438	1.45	8391	1.50
9223	1.73	8094	0.83	17441	1.32	8453	1.23
9223	1.51	8113	0.80	17452	1.02	8602	1.33
9224	2.08	8114	0.80	17465	1.95	9203	1.64
9225	1.32	8120	0.80	17473	1.61	9252	1.80
9226	0.67	8124	0.87	17476	1.32	9257	1.46
9226	1.56	8165	0.81	17487	1.97	9292	1.45
9227	1.06	8181	1.01	17490	1.49	9516	1.67
9227	0.31	8189	1.21	17494	1.07	9547	1.31
9228	0.63	8193	0.81	17496	1.27	9590	1.43
9230	0.31	8204	0.84	17500	1.10	9597	1.19
9577	0.26	8207	0.80	17502	1.49	9811	1.16
9956	0.30	8236	1.00	17518	1.96	9824	1.19
9957	0.41	8271	1.14	17521	2.78	9979	1.28
9959	0.29	8305	1.26	17531	1.21	11599	1.21
9960	0.53	8397	0.77	17534	1.36	11802	1.86
10906	0.26	8613	0.92	17535	1.37	14364	1.32
10906	0.34	8817	0.81	17537	1.46	16172	1.52
10908	0.45	9027	0.78	17539	1.29	16439	1.16
10910	0.32	9179	1.25	17547	1.04	17243	1.33
11595	0.27	9208	0.80	17562	1.07	17273	1.47
11597	0.46	9240	1.52	17569	2.17	17373	1.78
11791	0.31	9242	1.75	17594	1.03	17401	1.43
11795	1.14	9246	1.19	17612	2.21	17418	1.77
11796	0.81	9255	0.79	17629	1.03	17488	1.52
11797	0.37	9258	0.79	17634	1.79	17587	1.84
11798	0.52	9272	0.89	17645	1.71	17653	3.74
11799	0.31	9283	0.82	17653	1.23	17670	1.27
11800	0.58	9576	0.91	17670	1.02	17675	1.35
14340	0.34	9954	1.24	17676	1.47	17679	1.37
16148	0.50	9964	0.92	17689	1.03	17689	1.60
16149	0.39	9968	0.93	17701	1.47	17724	1.48
16150	0.27	10244	1.14	20543	1.05	17785	1.53
16151	0.27	11812	1.02	20611	1.15	17840	1.76
16155	1.11	17534	0.77	23202	1.08	17857	1.16
16156	0.27	25940	1.36	25960	1.10	25960	1.29

Table I.7. Counts per second per cell (CPS) of at various molecular weights (MW) during whole-cell MALDI analysis of BC13 cells exposed to heavy metals.

Metal free control		Lead		Zinc		Copper	
MW	CPS	MW	CPS	MW	CPS	MW	CPS
6515	0.40	6517	0.20	6212	0.84	6515	1.01
6517	2.22	6517	0.13	6519	1.15	6516	0.72
6517	0.86	6518	0.28	6519	2.16	6517	1.15
6518	1.74	6520	0.18	6521	1.30	6518	3.60
6518	6.08	6521	0.41	6522	0.87	6518	14.42
6520	6.43	6523	0.22	8089	0.96	6519	2.38
6521	2.12	8090	0.16	8090	1.12	6520	17.23
6522	1.14	8092	0.23	8091	0.80	6521	3.03
6522	1.12	8846	0.19	9220	2.23	6522	1.08
6523	0.95	9223	0.43	9221	2.40	6522	1.73
6524	0.32	9224	1.94	9222	12.52	6524	1.73
7223	0.27	9226	0.54	9223	8.06	6532	0.72
9221	0.29	9227	0.38	9224	13.12	6535	0.72
9222	1.15	9227	0.23	9225	24.18	6537	0.87
9222	0.60	9229	0.26	9226	11.32	7222	1.21
9223	1.73	9230	0.17	9227	4.46	7224	0.99
9223	1.51	9231	0.21	9228	5.23	7226	0.99
9224	2.08	9576	0.17	9229	1.54	7230	0.76
9225	1.32	9958	0.27	9957	0.89	8087	0.80
9226	0.67	9959	0.19	9958	0.89	8088	0.96
9226	1.56	9960	0.11	9959	2.67	9223	1.37
9227	1.06	9961	0.17	9962	1.43	9224	1.20
9227	0.31	9963	0.19	10906	0.93	9225	1.03
9228	0.63	9964	0.25	10909	1.31	9226	1.20
9230	0.31	10906	0.20	11599	0.96	9229	1.03
9577	0.26	10908	0.16	11600	2.12	9818	0.88
9956	0.30	11600	0.14	11601	0.96	9956	0.89
9957	0.41	11670	0.14	11668	0.77	9958	1.51
9959	0.29	11673	0.13	11672	0.96	9959	1.96
9960	0.53	11794	0.19	11675	0.77	9962	1.60
10906	0.26	11796	0.19	11676	0.77	11793	0.97
10906	0.34	11797	0.27	11795	2.13	11794	2.13
10908	0.45	11799	0.48	11796	1.75	11796	2.33
10910	0.32	11800	0.32	11798	2.33	11797	1.84
11595	0.27	11958	0.27	11798	0.78	11799	1.94
11597	0.46	11959	0.15	11801	0.97	11799	1.16
11791	0.31	11961	0.17	11802	0.97	11801	0.87
11795	1.14	11962	0.27	11958	1.07	11802	1.36
11796	0.81	11963	0.20	11961	0.98	11809	1.36
11797	0.37	12238	0.12	12815	0.91	11817	0.97
11798	0.52	16041	0.11	12819	0.81	14335	0.75
11799	0.31	16073	0.28	12984	1.02	14336	0.75
11800	0.58	16149	0.11	16149	2.61	14337	1.50
14340	0.34	16151	0.41	16151	3.29	14343	0.86
16148	0.50	16152	0.23	16152	1.48	16153	0.91
16149	0.39	16155	0.11	16153	2.84	16154	0.79
16150	0.27	16157	0.11	16156	4.20	16399	0.80
16151	0.27	16159	0.11	16157	1.36	16435	0.92
16155	1.11	16426	0.11	16172	0.91	17518	1.18
16156	0.27	25956	0.76	25957	0.86	25967	0.72

APPENDIX J

PROTOCOLS FOR PROTEIN SEPARATION AND ANALYSIS

Appendix J.1. Recipe for phosphate buffer used in protein separation protocols.

Dissolve the following in 800ml nanopure water (18.4 MΩ)

- 8g of NaCl
- 0.2g of KCl
- 1.44g of Na_2HPO_4
- 0.24g of KH_2PO_4
- Adjust pH to 7.4.
- Adjust volume to 1L with nanopure water (18.4 MΩ)

Sterilize by autoclaving

Appendix J.2. Recipe for denaturing buffer used in protein separation protocols.

- 20 mL glycerol
- 12 mL 1M tris-HCl pH 6.8
- 4 g sodium dodecyl sulfate
- 400 μL of 1% stock bromophenol blue
- Add nanopure water (18.4 MΩ) to 50 mL
- Make 0.5 mL aliquots and store at -20^{o}C
- Add 1M DTT before use (1 μL for each 5 μL buffer)

Appendix J.3. Recipe for rehydration buffer used in protein separation protocols.

- 25 mL of 30 mM tris-HCl (pH 8.5)
- 10.51 g urea
- 3.8 g thiourea
- 1 g CHAPS
- 0.345 g ASB-14
- Mix until proteins are solublized then add:
- Protease inhibitor cocktail (20 μL)
- 100 μL 1% Bromophenol blue
- 2 μL DNase/Rnase

Make 1 mL aliquots and store at -80^{o}C

Appendix J.4. Recipe for equilibration buffer used in protein separation protocols.

Equilibration Buffer

- 72.1 g urea
- 84.2 g glycerine
- 4 g sodium dodecyl sulfate
- 10 mL of 75 mM tris-HCl (pH 8.8)
- 400 μL of 1% stock bromophenol blue

Appendix J.5. Recipe for running buffer used in protein separation protocols.

10X SDS Running Buffer

- 144 g glycine
- 30 g tris base
- Add nanopure water (18.4 MΩ) to 1L and filter
- 10 g sodium dodecyl sulfate

Appendix J.6. Recipe for coomassie blue used in protein separation protocols.

- Dissolve 2g Coomassie Blue in 250 mL nanopure water (18.4 MΩ).
- Add 75 mL of glacial acetic acid
- Add 500 mL of ethanol
- Add nanopure water (18.4 MΩ) to a volume of 1 L

Appendix J.7. Protocol for cell fractionation.

- Spin down cells at 4,700 rpm for 15 minutes
- Remove supernatant and wash cells with 4 mL of 25 mM Phosphate buffer saline
- Spin down cells at 4,700 rpm for 15 minutes
- Remove supernatant and wash cells with 1.5 mL of 25 mM PBS
- Spin down cells at 4,700 rpm for 15 minutes
- Remove supernatant and resuspend pellet in 1.0 mL of 25 mM PBS
- Add 5 μL DNAse/RNAse and 20 μL of protease inhibitor cocktail to each sample.
- Freeze in liquid nitrogen and then thaw, repeat 3 times.
- Transfer samples to 15 mL falcon tubes
- Sonicate samples twice, 1 minutes each, and then incubate at room temperature for 15 minutes
- Spin samples at 15,000 g for 35 minutes at 4°C
- Save supernatant at -80°C (Soluble 1)
- Resuspend pellet in 0.5 M NaCl in 20 mM Sodium Acetate with 20 μL PIC and 5 μL DNAse/RNAse added.
- Spin down sample at 15,000xg for 25 minutes and save supernatant at -80°C (Soluble 2)
- Resuspend pellet in 150-200 μL of 0.4% triton X-100 in 25 mM PBS
- Spin down sample for 25 minutes at 13,000xg
- Save supernatant at -80°C (detergent fraction/ Peripheral proteins)
- Resuspend pellet in 150-200 μL of 25 mM PBS (integral membrane proteins)

Appendix J.8. Protocol for IEF separation.

IEF Strip Loading

- Measuring the sample protein concentration to determine the volume needed
- Add Urea buffer to sample to give desired total volume and protein
- Add DTT to a concentration of 40 mM (19.2 μL of 1 M stock to 450 μL sample)
- Add IPG Buffer to sample. The final conc. should be 0.5% of IPG Buffer
- Mix the sample at room temperature 15 min for complete solubilization
- Spin the sample at 15,000 RPM @ 20°C for 10 min
- Load the desired volume onto the IEF strip, being careful to avoid any unsolubilized particulate at the bottom of the tube (even if you don't see one)
- Load your IEF strip into ceramic strip holder with the gel facing down and cover with 3 ml of mineral oil
- Cover the strip holder with its plastic cover and load it onto the IEF instrument
- Cover the instrument with black sheet to prevent light if you are using Cydye or Zedye in your sample
- Follow the IEF focusing progress by monitoring the movement of the bromophenol blue dye towered the anode side (+). The blue dye should be at the end of the strip by the end of the focusing protocol
- Remove the strip from the holder and proceed with equilibration steps or freeze your strips at -80°C

IEF Strip Equilibration

- Place strips in plastic holders, gel side facing up
- Set-aside two aliquots of equilibration buffers
    - Add 100 mg/ 10 mL DTT to the first and 250 mg/10 mL iodoacitimide to the second
    - Mix each solution until it dissolves
- Add 3 mL of first equilibration solution to each strip, cover and shake for 15 minutes
- Decant first equilibration solution and add 3 mL of the second equilibration solution and cover and shake another 15 minutes before carefully decanting this solution. Strips are now ready for second dimension

Appendix J.9. Protocol for 2nd dimension separation.

2nd Dimension Preparation

- Acrylamide from the refrigerator ~ 1 hour before use
- Collect necessary gel plates and spacers and rinse with nanopure water
- Place identification labels between gel plates as you load them into the Amersham casting box. Be sure to leave a plastic spacer between each plate
- Adjust the lower drain on the casting box so that it is facing upwards and cover it with parafilm
- Fill casting box with water to the "fill line" to determine the necessary gel volume. Allow water to sit for at least 10 minutes to make sure there are no leaks
- Prepare 1.5 M Tris
    - pH Tris to 8.8 using concentrated HCl
    - Vacuum filter using 0.45 μm filters
    - Prepare 10% SDS (by weight) in nanopure water
    - Prepare 10% APS (by weight) in nanopure, this should be fresh
    - Mix Tris, 10% SDS, acrylmide, and nanopure using the volumes for the desired % gel listed below

	Per 100 mL			
	10%	11%	12%	13%
40% Acrylamide	25	27.5	30	32.5
1.5 M Tris-HCl pH 8.8	25	25	25	25
10% SDS	1	1	1	1
nanopure water	48.5	46	43.5	41
TEMED	0.05	0.05	0.05	0.05
10% APS	0.5	0.5	0.5	0.5
Total	100.05	100.05	100.05	100.05

- Degas mixture using vacuum for at least 5 minutes
- Empty water from casting box and re-seal drain using parafilm
- Add APS to gel solution
- Add TEMED to gel solution
- Pour gel into casting box using a glass funnel
- Use spray bottle to evenly cover each gel with 1-2 mL of water
- Cover and allow gels to polymerize overnight
- Fill Daltwelve box with 10 L nanopure water
- Re-fill box with 9 L of nanopure water
- Add 1 L of 10 x sodium dodecyl sulfate running buffer

- Add 1x SDS running buffer to the top of the gel
- Insert IEF strips
- Insert marker paper at end of strips, dotted with 200 μL of a molecular weight marker
- Add 0.75% agarose in 1xSDS running buffer smoothly to the top of the gel, being careful to avoid bubbles
- Turn on pump and powersource (4W per gel) and run until the blue line migrates out of the gel

Appendix J.10. Protocol for trypsin digest.

- Stain gel
- Excise bands of interest using sterile techniques
- Wash samples 3 x 10 minutes with 25 mM ammonium bicarbonate in 50% acetonitrile
- Dry samples in a vacuum centrifuge for 10 minutes at 30°C
- Reduce samples for 40 minutes at 56°C using a solution of 10 mM DTT, 25 mM ammonium bicarbonate in 50% acetonitrile
- Dehydrate samples for 5 minutes using 50/50 methanol/acetonitrile
- Alkylate samples for 30 minutes at room temperuature in a 25 mM solution of ammonium bicarbonate containing 55 mM iodoacetimide
- Wash samples using 25 mM ammonium bicarbonate for 10 minutes, and then dehydrate using 50/50 methanol/acetonitrile and repeat three times
- Dry samples in a vacuum centrifuge for 10 minutes at 30°C
- Rehydrate cells on ice for 30 minutes with a 40 ng μL^{-1} tyrpsin solution in 25 mM ammonium bicarbonate. Then incubate for 24 hours at 37°C

Appendix J.11. Gradients used in mass-spectrometry analysis.

Nano Pump

Time (min)	Percent B
0	0
1	0
23	100
27	100
29	0

Capillary Pump

Time (min)	Percent B
0	0
9	100
10	100
12	0

APPENDIX K

16S rRNA GENE SEQUENCE

Table K.1. 16S rRNA gene sequence for strain used in experiments.

gatctggaggaacaccagtggcgaaggcggtcacctggcccaatactgacgttgaggcgcgaaagcgtggggagcaaacag
gattagataccctggtagtccacgccctaaacgatggatactggatgtttggcgccttaggtgctgagtgtcgtagctaacgcgat
aagtatcccgcctgggaagtacggccgcaaggttaaaactcaaaggaattgacgggggcccgcacaagcggtggagcatgtg
gtttaattcgatgcaacgcgaagaaccttacctgggcttgacatgtccggaaccctgcagagatgtgggggtgcccttcgggga
atcggaacacaggtgctgcatggctgtcgtcagctcgtgtcgtgagatgttgggttaagtcccgcaacgagcgcaacccttgttc
ctagttgccagcggttcggccgggcactctagggagactgccggtgacaaaccggaggaaggtggggatgacgtcaagtcct
catggcctttatgtccagggctacacacgtgctacaatggcgcgtacagagggaagccaagccgcgaggtcgcgagcagacc
ccagaaagcgcgtcgtagttcggattgcagtctgcaactcgactgcatgaagtcggaatcgctagtaatcgcggatcagcatgc
cgcggtgaatacgttcccgggccttgtacacaccgcccgtaagaccatgggagtggatgg

Sequencing results: > 99% similarity to multiple *Acidithobacillus* caldus strains.